Investigations into new methods for the efficient and environmentally benign catalytic asymmetric epoxidation of alkenes

A thesis submitted for the degree of Doctor of Philosophy

Giorgio De Faveri

Queen Mary
University of London

I always loved reading dedications on books, and never thought one day it would be my turn to write one. Dedicating a book to someone is a splendid act of love and a sign of respect and admiration. I love, admire and respect too many persons to choose one to represent them all, so I dedicate this thesis to you, without saying your name, because I am sure you recognised yourself in these words.

Thank you, my dearest friend.

Table of Contents

Declaration

I declare that the work presented in this thesis is my own and that no part of it has been submitted in support of an application for another degree or qualification of this or any other university or other institution of learning

Signature..... Date.....

Acknowledgements

Many people have been essential in the process of writing this thesis and in the much longer, painstaking, learning process that we call “doing our PhD”. If it wasn`t for their help, guidance and support, nobody would be reading these words right now.
What follows is in a completely sparse order, following only the flow of my reminiscences and memories; so please don`t get offended if you are not on top of the page.

To my supervisors, Prof. Michael Watkinson and Dr. Marina Resmini, for their suggestions, support, guidance and directions throughout my PhD. Mike, it was a real pleasure to work with you. A special thanks to Dr. Resmini for giving me the chance to participate to an international conference in the United States, it was the journey of a lifetime.

To my mum and dad. Your full, unreserved, sincere love and support have been my very lifeblood, without mentioning your financial support when things got difficult. Thank you from the bottom of my heart.

A big thank you goes to Pietro and Giampaolo back in Italy; without your mentoring I could not be the chemist I am today. The period spent working with you gave me essential skills to survive my PhD. Also I want to thank you for supporting me through the difficult decision of leaving the country and start a new life in London.

To Gennadiy and Shirin for their great help in the last couple of months of experimental work, a big thank you guys, I am thankful for everything.

A big thank you to Ludovic, a good friend and a great colleague. It was a pleasure working with you even if for a short time. You are a good man.

To Cristina Gentilini, Franz Ravalico, Giovanni Birarda, Rita De Zorzi and Nicola Demitri for being such good friends despite the distances and for being my always reliable source of hard-to-find journals (a big thank you to your institutions too...).

To the original STOMP group and all its additions over the years (Rita, Farid, Jules, Mario, Josep and the others). I owe you so much gratitude to you guys, for always being there and for being on my side when I needed it and for telling me off when I deserved it. These years would not have been the same without you.

To all the friends that came and went during these years. Emiliano and Eileen among many. I want to thank you for your friendship and to wish you all the best in life.

To Kevin, for those long weekends and our friendship, my liver and my brain will hate you forever, but my heart will always thank you.

To Rita, once more, for showing me how to look at the world with new eyes.

Many thanks to the technical staff of the department. To Alan Bradshaw for the help, the incredible service, the tea and the songs. To Greg Coumbarides for the help with the NMR, to John, Jalal and Janet for their helpfulness and the fun talk when demonstrating.

To all the friends in the department, the fellow PhDs and the students that I met over the years.

To John Cowley for his exceptional glassblowing skills. To Majid Motevally for the X-Ray service. To Ian Saunders and Alan Scott for the analytical services.

To all the people that had a part big or small in my life during these years. To Alexandra, Patricia, Rui, Grazvydas, Luca, Susan, Lisa, Gary, Thomas, Mary, Jim, Simon, Carlos, the guy of the GymBox, Troy Alves, Tiesto, Miki the sweeper and his silent friend.

There is still so many of you; I cannot fit you all in these two pages but there is enough space in my heart for all of you.

Once again, Thank you.

List of abbreviations

^{13}C	carbon, isotope 13 in NMR
^{1}H	proton in NMR
^{19}F	fluorine, isotope 19 in NMR
Å	angstrom
AcO	acetate
AcOH	acetic acid
ACN	acetonitrile
Ar	Aryl
ATR	attenuated total reflection
Binol	1, 1`-bi-2-naphthol
boc	*tert*-butoxycarbonyl
Bn	benzyl
br	broad (IR spectroscopy)
^{n}Bu	*n*-butyl
^{sec}Bu	*sec*-butyl
^{t}Bu	*tert*-butyl
ca.	circa
c.f.	*conferre* (Latin, compare)
m-CPBA	*m*-chloro perbenzoic acid
conc.	concentration
config.	configuration
conv.	conversion
d	doublet
DCM	dichloromethane
de	diastereomeric excess $\left(\frac{\%major - \%minor}{\%major + \%minor}\right) \times 100$
dec.	decomposed (in melting point measurements)
DHN	dihydronaphtalene
DIC	N, N`-diisopropylcarbodiimide
DMAP	dimethyalaminopyridine
DMF	dimethylformamide
DMG	directed metalation group
DMSO	dimethulsulfoxide
DMSO-d_6	deuterated DMSO
dr	diastereomeric ratio
ee	enantiomeric excess $\left(\frac{\%major - \%minor}{\%major + \%minor}\right) \times 100$
e.g.	exempli gratia (Latin, for example)
ESI	electron-spray ionisation
eq	equivalent/equivalents
E_{pa}	potential of the anodic peak
E_{pc}	potential of the cathodic peak
Et	ethyl
et al.	et alii (Latin, and others)
Et_2O	diethyl ether

EtOAc	ethyl acetate
EtOH	ethanol
ESI	electron spry ionisation
G	generic substituent
GC	gas chromatography
h	hour/hours
HPLC	high performance liquid chromatography
HRMS	high resolution mass spectroscopy
IPA	propan-2-ol
IR	infrared radiation
L	ligand
LAH	lithium aluminium hydride
LDA	lithium diisopropylamine
lit.	literature value
m	multiplet
M	molarity
Me	methyl
MEM	methoxyethyl ether
MeOH	methanol
min	minute
mol %	molar %
mol	mole (moles)
mol eq.	molar equivalents
MTO	methyloxorhenium
m/z	mass-to-charge ratio
NMR	nuclear magnetic resonance
Nu	nucleophile
OMe	methoxy
OTf	trifluoromethanesulfonate
oxaH	oxalic acid
oxaNa	sodium oxalate
P.A.	phthalic anhydride
PAA_r	commercial peracetic acid
PAA_c	peracetic acid prepared on acidic resin
Ph	phenyl
PIFA	phenyliodine bis(trifluoroacetate)
POHP	triphenylphosphine hydrogen peroxide
ppm	parts per million
^{i}Pr	isopropyl
PTC	phase transfer catalyst
py	pyridine
pybox	bis(oxazolinyl)pyridine
pydic	pyridine-2,6-dicarboxylate
H_2pydic	pyridine-2,6-dicarboxylic acid
pyboxazine	2,2’-pyridine-2,6-dily bi(5,6-dihydron-4h-1,3-oxazine)
q	quartet

R	alkyl substituent
RT	room temperature
s	singlet (NMR) or second
sc	single crystal
S_N1	type one nucleophilic substitution
S_N2	type two nucleophilic substitution
t	triplet
T	temperature
TACN	triazacyclononane
TE	total substituent effect coefficients
TEA	triethylamine
THF	tetrahydrofuran
TLC	thin layer chromatography
TMEDA	tetramethylethylenediamine
TMS	tetramethylsylane
TMSBr	tetramethylsilylbromide
TMTACN	1,4,7-trimethyl-1,4,7-triazacyclononane
Ton	turnover numbers $\frac{moles\ product}{moles\ catalyst}$
TS	transition state
Ts	tosyl
UHP	urea hydrogen peroxide
UV	ultraviolet radiation
w.r.t.	with respect to

Abstract

This thesis presents our investigations into the catalytic asymmetric epoxidation of alkenes.

An introductory chapter highlights the importance of chirality in nature and industry. It focuses on a few relevant examples of syntheses in which the use of optically pure epoxides as building blocks is fundamental to the overall stereochemistry of the product. The introduction then continues describing the advances in the field of asymmetric epoxidation of olefins; it contains a review of a wide range of the ligands and metals employed in the recent literature together with a range of different oxidants. A section on organocatalytic epoxidations concludes this chapter.

A second chapter presents attempts to impart enantioselectivity in the epoxidation of olefins by employing chiral additives (BINOL derivatives) in conjunction with a known oxidising system, TMTACN/manganese with hydrogen peroxide as the oxidant. A brief electrochemical study of the redox potential of the catalytic systems described in this chapter and a study of the effect of the electronic properties of the substrates on the reaction is also reported.

The third and fourth chapters describe the synthesis of a series of tri- tetra- and pentadentate ligands based on the backbone of L-proline and *trans*-diaminocyclohexane. The chapters contain the results of the screening of the above mentioned ligands in the epoxidation of alkenes with a number of metal salts using either hydrogen peroxide or peracetic acid as the oxidant. Single crystal X-ray structures of some of the new ligands are also presented herein.

A final experimental chapter presents the supporting characterisation data associated with the compounds synthesised.

Chapter 1 - Introduction

1.1 The impact of chirality

It is clear to see, just by taking a look at our body and at our surroundings, that the environment in which we live is chiral. Chirality shows up in our everyday life. Just think of the hands and feet of the human body and its external symmetry. This combination of symmetric yet non superimposable parts is found everywhere in the natural world. When we move to the microscopic world, the importance of chirality becomes even more apparent. The sugars in our DNA, its helical structure, the amino acids that make up our muscles and tissues all could exist in their current form and their mirror image form, but the latter structures are not observed in nature. Essentially only L-amino acids, and D-sugars are present in living organisms, their mirror images are not metabolised and are not used in biology. Somewhere, when life originated, something happened that made the world "turn" as we know it and it has remained that way ever since. Evolution considered chirality an essential aspect of life that had to be preserved.

In organic chemistry, chirality generally arises when an atom bears four different substituents; that atom is called a stereogenic centre. Other forms of chirality do not derive from the substituents on a single atom, as in 1, 1'-2, 2'-binaphthols, which have axial chirality due to the hindered rotation around a bond that forces them into a specific configuration.

At the molecular level, chirality is essential for the life of all organisms. An example is given by the chemical communication between insects and animals. This is mediated by pheromones, which are often chiral molecules with a specific stereochemistry.[1] In Figure 1.1 two important insect pheromones are represented, **1** a sex pheromone of the gypsy moth (*Porthetria dispar*) and **2** the mosquito oviposition attractant for *Culex pipiens fatigens*, a molecule secreted by the eggs of this species that attracts other females to deposit their eggs at the same spot.[2, 3]

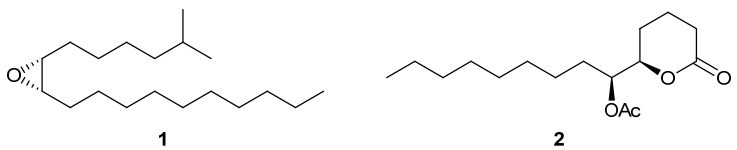

1 2

Figure 1.1 Examples of optically active pheromones.

The specific stereochemistry of these molecules is needed for them to be recognised uniquely by the insect receptor to trigger a precise response. Moreover, their molecular structure makes them only active for some species and not for others, so that the message they carry is received only by the right individuals.

Chiral recognition in the human species is also critical, an example lays in the interaction between drugs and receptors inside our bodies. A well documented example of its importance is that of Thalidomide (Figure 1.2, **3**). Thalidomide, a sedative-hypnotic, was used as an anti-nausea drug for pregnant women in the 1960s. The drug was administered as a racemate, a 50:50 mixture of the enantiomer **3a** and **3b**, with disastrous effects.

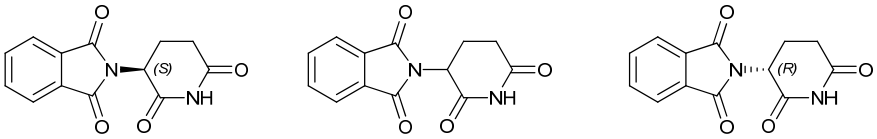

Figure 1.2 Enantiomers of Thalidomide.

Only one of the enantiomers is in fact active as an anti-nausea medication (**3b**), while the other (**3a**), if taken during pregnancy, caused birth defects like phocomelia.[4] Thousands of victims of the drug were counted worldwide before the connection between **3** and birth defects was made. In this case, switching to the pure enantiomer did not bring any benefit, since it has been proven that even single enantiomers racemise *in vivo*, restoring the toxicity.[5]

1.2 Optically active epoxides in chemistry

1.2.1 The nature of epoxides

Epoxides are cyclic oxygenated structures related to ethers, made of two carbon atoms and an oxygen atom linked together by single bonds. The two C-O bonds are polarised because of the electronegativity of the oxygen atom. The simplest structure of this family is oxirane (or ethylene oxide, Figure 1.3). Epoxides are useful reagents in synthetic chemistry because of their reliable and predictable reactivity, being susceptible to nucleophilc attack which causes them to ring open.

Weak nucleophiles (R-OH, H_2O) can react with epoxides under acidic conditions, as protonation of the oxygen makes the epoxide more electrophilic. The reaction has partial S_N1 character because in the transition state, bond cleavage slightly precedes bond formation (Figure 1.3).

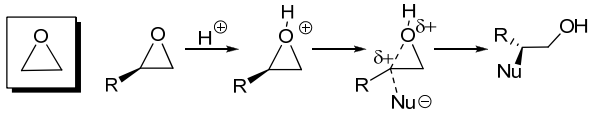

Figure 1.3 Structure of oxirane (left) and reactivity of epoxides towards weak nucleophiles (right).

Reactive nucleophiles react with epoxides in an S_N2 type reaction, without the need for protonation; these strong nucleophiles are usually anions, and the reaction conditions are generally basic. Nucleophiles like organolithium compounds, Grignard reagents, metallic hydrides and hydroxide are good examples.[6]

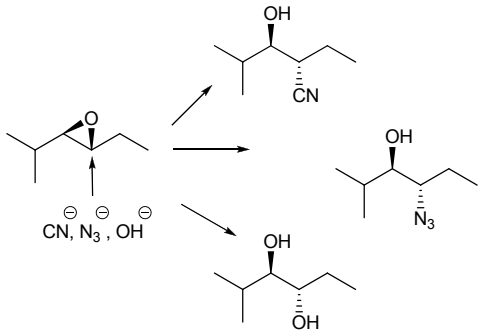

Figure 1.4 Reaction of epoxides with strong nucleophiles.

When dealing with substituted epoxides, the regioselectivity of the nucleophilic attack depends again on the nature of nucleophile and on the reaction conditions. Unsymmetrically substituted epoxides, in fact, react with anionic nucleophiles at the less hindered carbon of the ring, while under acid catalysis (with the oxygen protonated), the more highly substituted carbon is attacked. This happens because in the transition state (TS), the carbocation is located on the carbon that better supports the positive charge (Figure 1.5).

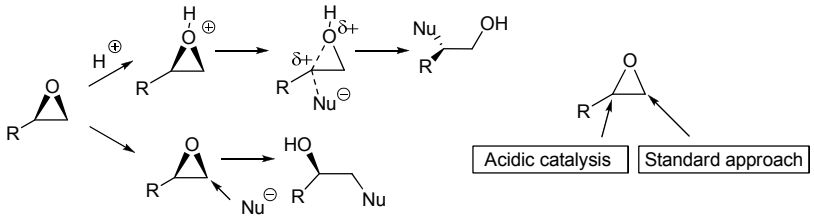

Figure 1.5 Summary of the ring opening mechanisms of epoxides.

Even if the reaction occurs in an S_N1 fashion, the participation of the nucleophile in the transition state is enough relevant to force inversion of configuration.

1.2.2 Optically active epoxides in asymmetric synthesis

As stressed previously, the stereochemistry of a molecule is often fundamental for its biological activity. In recent years, the use of molecules extracted from natural sources has been largely replaced by the preparation of synthetic analogues. Alongside the use of natural molecules, the chemical, pharmaceutical and agrochemical industries have developed an enormous number of chiral compounds to be used as drugs,[7, 8] pesticides [9] and herbicides.[10]

Nature has extremely complex enzyme-mediated synthetic pathways to produce optically pure compounds; to obtain these molecules with a specific stereochemistry, chemistry resorts to asymmetric syntheses.

Asymmetric synthesis is based either on the use of optically pure starting materials, that are then subject to a series of chemical transformations that preserve their original chirality, use chiral reagents (from the chiral pool) or rely on stereoselective reactions which can introduce stereocenters (with a specific configuration) into prochiral molecules. It is also possible to use the chiral induction given by any existing stereochemistry to favour one product over its diastereo- or enantiomer.

Asymmetric epoxidations are used to generate optically active epoxides, as these can be implemented as building blocks in total synthesis. An enantiomerically pure epoxide can be used to introduce up to two new stereocentres into a molecule in a single reaction step. To better understand their importance in total synthesis, two relevant examples of their applications are given.

Rifamycin S is one of the antibiotics of the ansamycin family, and active in the treatment of tuberculosis and leprosy among other therapeutic uses. Figure 1.6 highlights how the precise sequence of stereocentres on the alkyl chain has been obtained starting from an enantiomerically pure epoxide, generated by asymmetric epoxidation of the corresponding alkene by a Sharpless epoxidation. The stereospecific ring opening of the epoxide yields the desired precursor.[11]

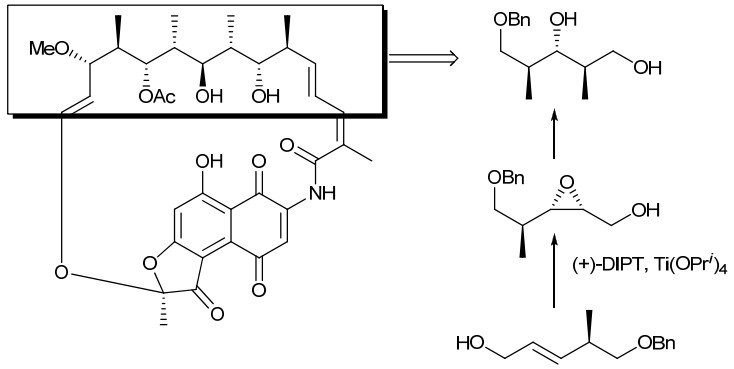

Figure 1.6 Rifamycin S (left), highlighted is the segment deriving from the ring-opening of a chiral epoxide.

(+)-Brefeldin A (Figure 1.7) is an antibiotic of lactonic structure of fungal origin. Its structure contains five stereocentres which are needed for its activity. In one total synthesis of its core, two stereocentres are introduced *via* intramolecular ring opening of an enantiomerically pure epoxide.[12]

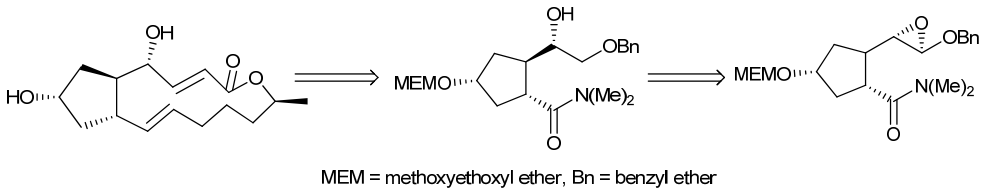

Figure 1.7 Some retrosynthetic steps from a possible total synthesis of Brefeldin A (left), showing the use of a chiral epoxide.

1.3 Non-catalysed asymmetric synthesis of epoxides

Using chiral auxiliaries to induce a preferential conformation in the products is a widely used strategy that often allows high levels of enantioselectivity to be achieved and this has been exploited in the synthesis of enantiomerically active epoxides. Chiral sulfides like the one in Figure 1.8 are used in the synthesis of epoxides starting from aldehydes.[13, 14] The synthesis involves the formation of a chiral ylide that then reacts stereospecifically with the desired aldehyde. Another example of a sulfur containing chiral auxiliary[15] is reported in brackets (Figure 1.8)

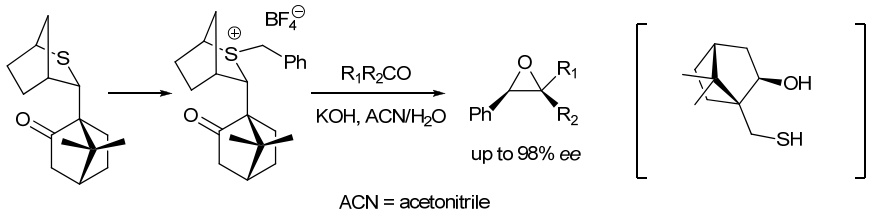

Figure 1.8 Use of chiral auxiliaries in the ylide mediated synthesis of epoxides from aldehydes.

Another strategy for obtaining epoxide rings with high diastereoselectivity is to exploit the chirality already present in a molecule, like in the ring closures of halohydrins[16] and their derivatives such as acetyl-chlorohydrins[17] (Figure 1.9), where the stereochemistry of the substrate drives the reaction without the need for a catalyst.

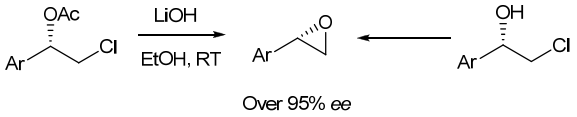

Figure 1.9 Examples of asymmetric synthesis of epoxides via ring-closure reactions.

Another way to generate an oxirane ring is through the oxidation of a double bond with a peracid, a peroxide or other sources of oxygen. This reaction is generally not stereoselective but in some cases asymmetry can be obtained if a chiral centre or sterically hindered groups are already present in the vicinity of the alkene. Epoxidations with *m*-chloroperbenzoic acid are generally not selective, but when the substrate is optically active and is able to stabilise a specific conformation of the transition state *via* hydrogen bonding the reaction can become stereoselective.[18, 19] Another case in which this reaction is stereoselective is found when a bulky group is present in the vicinity of the double bond and the latter is substituted. In this case, the favoured approach is the one that minimises repulsions (Figure 1.10). [20]

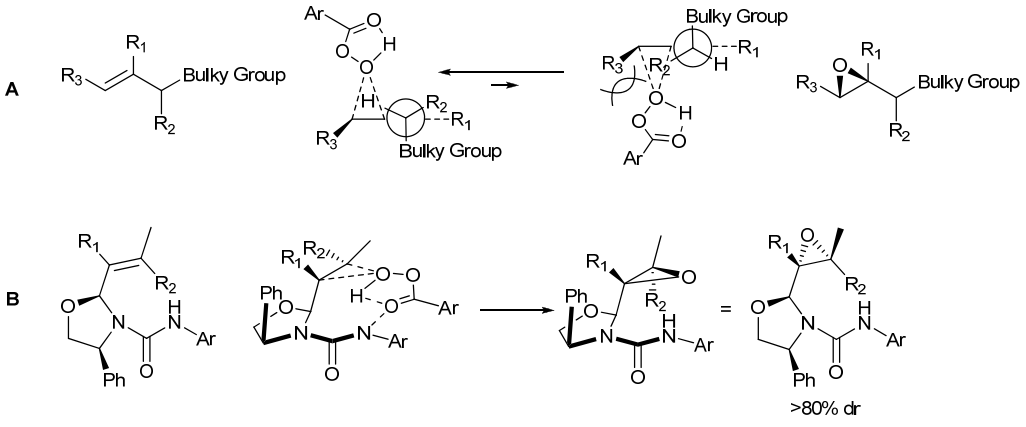

Figure 1.10 A) effect of substitution on the stereoselectivity of the reaction; B) effect of hydrogen bonding on the stereoselectivity of the reaction.

The most widespread procedures for the asymmetric epoxidation of alkenes employ a chiral catalyst. This approach by-passes the need for pre-existing chirality on the substrate and can generate optically active epoxides from unfunctionalised alkenes. Catalysed reactions allow the use of a wide range of oxidants like molecular oxygen, hydrogen peroxide, bleach, peracetic acid, alkyl-hydroperoxides and iodosylbenzene; the substrate scope of these reactions is extremely wide and diverse. Over the past thirty years, many catalytic systems have been developed and studied in the continuing struggle towards finding a combination of catalyst and conditions active towards the largest number of alkenes possible, but to date no universal system has been developed.[21-24]

The advantages of metal-catalysed reactions over traditional procedures become evident when moving from laboratory-based chemistry to the industrial scale, where yields, enantiomeric excess, side products, solvents and waste materials are crucial issues. Catalysis reduces the production of waste materials and often allows the use of stoichiometric amounts of reagents where an excess was needed before.

An example is the industrial synthesis of propylene oxide, which is still mainly obtained by reacting propylene with chlorine to generate the corresponding chlorhydrin which is then converted into propylene oxide. To obtain a ton of pure epoxide, two tons of NaCl and 0.1 ton of 1,2-dichloropropane are generated and need to be eliminated. A greener, more efficient metal catalysed epoxidation of propene with a more environmentally benign oxidant that generates a less toxic by-product, like the Halcon-Arco process, brought an improvement. This process involves the preparation of an alkyl hydroperoxide by reaction with molecular oxygen at high temperatures. The oxidant then reacts with propene in the presence of metal oxides of groups 4 to 7, yielding the epoxide and an alcohol as side-product.

The ideal catalyst would be atom economic, thus using an oxidant with a high oxygen content and producing fewer and non-toxic side-products. In this regard, molecular oxygen is considered to be the most environmentally benign oxidant. Unfortunately molecular oxygen can cause oxidative damage to the catalysts, causing inactivation and the systems often require a sacrificial oxygen acceptor like an aldehyde to circumvent this process. In recent years, though, several examples of efficient use of dioxygen as the oxidant have appeared. [25-27]

Following oxygen in the list of the desirable oxidants, we find hydrogen peroxide, with an oxygen content of 47% which produces only water as a by-product, NaOCl (bleach) and peracetic acid. The use of hydrogen peroxide and peracetic acid as the terminal oxidant has found wide application recently.

1.4 Metal-catalysed asymmetric epoxidation of alkenes using hydrogen peroxide and peracetic acid.

A large number of catalysts based on transition metals and organic ligands have been developed to allow their use in the asymmetric epoxidation of alkenes with these two environmentally friendly oxidants. Different complexes tend to be active with a different family of olefins, and their selectivity changes depending on the combination of ligand, metal and oxidant used. Here follows a short review of the major advances in the field of asymmetric epoxidation with hydrogen peroxide and peracetic acid (potentially generated *in situ* from acetic acid and hydrogen peroxide), organised by the metal centre of the complex focusing mainly on manganese and iron, as well as a brief introduction to another promising field, asymmetric organocatalytic epoxidation.

1.4.1 Manganese

Manganese is involved in several biochemical processes; it is an essential co-factor in several ubiquitous enzymes like peroxidises,[28] catalases,[29] enolases and phosphoesterases[30] just to mention a few. It is also present in photosystem II of the photosynthetic apparatus in a tetranuclear cluster, where it facilitates the oxidation of water to dioxygen.[31] Its low toxicity and commercial availability, together with its biological relevance in oxidoreductive processes quickly identified it as an ideal candidate for the metal centre in epoxidation catalysts.

1.4.1.1 TMTACN and derivatives

The first reported structures of manganese-1,4,7-triaza-1,4,7-trimethylcyclononane (TMTACN, **4**) complexes go back to the 1960`s, especially from the work of Wieghardt[32] and co-workers, who synthesised an oxo-bridged dimeric complex of TMTACN and manganese. Its use in oxidative chemistry came some years later when Hage[33] reported its activity as a bleaching agent and as an efficient catalyst for the epoxidation of alkenes and polyphenols with hydrogen peroxide as the oxidant. Although extremely active, this system was not enantioselective. It was not until 1997 with the work of Bolm *et al*.[34] that chiral derivatives of TMTACN were proven to be effective in asymmetric epoxidation. Bolm reported the first asymmetric epoxidation of olefins using C_2-symmetric derivatives bearing chiral arms at the nitrogen atoms (Figure 1.11, **5a, b**).

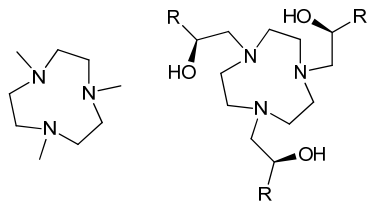

4 **5a** R = Me
5b R = ^{i}Pr

Figure 1.11 TMTACN and examples of Bolm's derivatives.

Styrene was converted into the corresponding epoxide using 30 % H_2O_2 (2 eq.) in methanol; the complex was generated *in situ* by addition of manganese(II) acetate (3 %) and **5a** in a 1:1.5 ratio. The (*R*)-enantiomer of styrene oxide was obtained in an encouraging 43 % *ee* although the conversion remained about 15 %. It was found that longer reaction times increased the conversion but negatively affected the *ee*. When **5b** was used, the enantioselectivity was reversed and the (*S*)-enantiomer formed with *ee*s in the range 13-38 %.

When *cis*-β-methylstyrene was used as the substrate under the same conditions but with one extra equivalent of oxidant, it was completely converted over 3 h, into a mixture of isomeric epoxides in a 7:1 ratio. The major (*R*,*R*)-*trans*-isomer was obtained with an enantiomeric excess of 55 %, while the other component was identified as the *cis*-isomer with an *ee* of 13 %. The last screened alkene in this study was chromene. Using the previous conditions, **5a** gave the (*R*, *R*) epoxide with a 40 % *ee*, while **5b** produced the (*S*, *S*) enantiomer with 38 % *ee*. For both, the conversion was about 50 % after 15 h.

Bolm and co-workers followed another route to introduce asymmetry by making the TMTACN backbone chiral.[35] Their derivative (Figure 1.12, **6**) derived from the cyclisation of an L-proline tripeptide. The ligand was used to prepare the dimeric manganese complex **7**. Complex **7** in 2 % catalyst loading with hydrogen peroxide as the oxidant (the amount was not reported by the authors) was able to epoxidise styrene, resulting in 28 % conversion (23 % *ee*, (*S*)-enantiomer) over 2 h. The group also realised that longer reaction times positively influenced the conversion, which increased to *ca.* 88 % over 8 h, but at the expense of enantioselectivity, which dropped to 15 %. Other substrates in this study included 4-chlorostyrene and 3-nitrostyrene which gave products in 21 % and 26 % *ee* respectively.

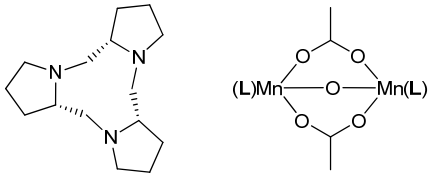

6 **7** (L = **6**)

Figure 1.12 Chiral TMTACN and its complex synthesised by Bolm.

New chiral versions of TMTACN were later designed and tested by Gibson as well as by Watkinson.[36-39] The groups focused on modifying the ring and developed a synthetic procedure based on the use of chiral tosylazides derived from aminoacids. Several novel chiral macrocycles were synthesised (Figure 1.13).

The epoxidation tests were carried out using an *in situ* generated complex, utilising 0.16-0.2 mol% of the macrocycles **8** and 0.1-0.13 mol% of manganese(II) acetate or sulfate with and without ascorbic acid/sodium ascorbate as a co-ligand to increase the activity of the system as suggested by Berkessel and Sklorz.[40] Ligand **8a** proved inactive in the epoxidation of styrene in all the conditions tested. The ^{i}-Pr-derivative **8b** afforded (*R*)-styrene epoxide in 31 % yield and 16 % *ee*. The most successful conditions were found in acetonitrile, with manganese(II) acetate in 0.1 mol%, 0.21 mol% ascorbate, 0.05 mol% ascorbic acid and 0.16 mol% of ligand. The oxidant was a mixture of hydrogen peroxide (2 eq.) and acetone, to prevent disproportionation to water and oxygen.[41] The last derivative **8c** was found to be most active in the absence of ascorbate/ascorbic acid, higher amounts of ligand (0.2 mol%) and manganese sulfate (0.13 mol%). The solvent-oxidant system employed was again hydrogen peroxide (2 eq.) in acetone. These conditions provided (*R*)-styrene epoxide in 16 % yield and 23 % *ee*.

Süss-Fink *et al.* subsequently synthesised another series of chiral TACN derivatives (Figure 1.13, **9**, **10**), whose design was clearly inspired by **5**, and these were tested in the epoxidation of alkenes as well as the oxidation of alcohols and alkanes. The group also reported a successful application of **11** in the epoxidation of alkenes. Although structure **11** had already been reported and tested by Beller[42] in a patent which claimed high yield and enantioselectivity for a number of substrates, they found the system to be essentially ineffective providing very low yields and *ee*s.

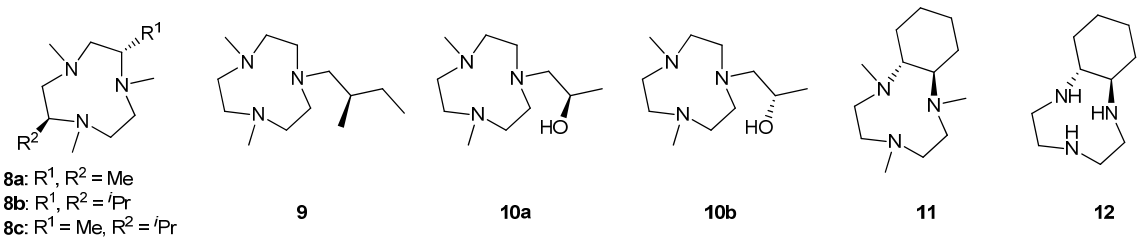

Figure 1.13 Examples of chiral derivatives of TMTACN presented in the work of Gibson, Watkinson, Beller and Golding.

Ligands **10a** and **10b** were used to obtain dimeric manganese complexes (**13a**, **13b**) and these were tested in the epoxidation of indene with hydrogen peroxide in different solvents, with and without a co-catalyst (Table 1.1).

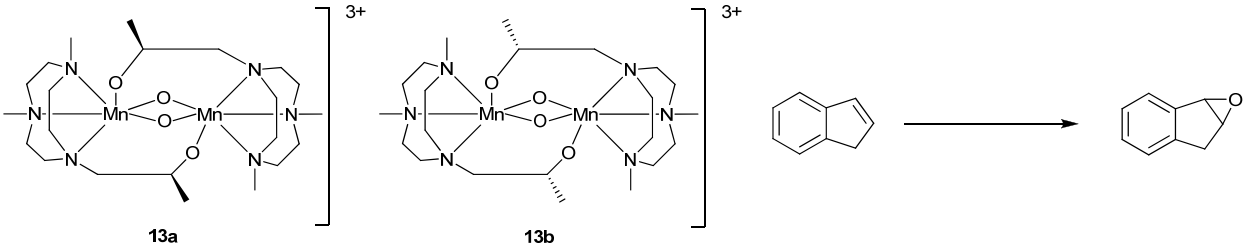

Entry	Complex	acetone, no additive		ACN, additive		H_2O/ACN (50/50 v) no additive		H_2O/ACN (50/50 v) oxalate		H_2O/ACN (50/50 v) ascorbate	
		ee (%),	Conv.[a]	*ee* (%)	Conv.[a]	*ee* (%)	Conv.[a]	*ee* (%)	Conv.[a]	*ee* (%)	Conv.[a] (%)
1	**13b**	7 (1*R*, 2*S*)	6.4	7 (1*S*, 2*R*)	2.1	13 (1*S*, 2*R*)	2.9	4.4 (1*S*, 2*R*)	10.5	11 (1*S*, 2*R*)	6.2
2	**13a**	7 (1*S*, 2*R*)	6.4	7 (1*R*, 2*S*)	2.1	13 (1*R*, 2*S*)	2.9	4.2 (1*R*, 2*S*)	10.4	11 (1*R*, 2*S*)	6.2

Table 1.1 Epoxidation of indene with pre-formed complexes 13a and 13b, 2 h reaction. Conv. = conversion. Ascorbic buffer 0.3 mM (30 eq., 0.15 mM ascH + 0.15 mM ascNa); oxalate buffer 0.3 mM (30 eq., 0.15 mM oxaH + 0.15 mM oxaNa); H_2O_2 2 eq.; complexes 0.1 mol%; configuration of the major product in brackets. a) Substrate conversion (%).

When the same substrate was epoxidised generating the catalyst *in situ* in water/acetonitrile 50:50 v/v (Table 1.2) lower yields and *ee* were obtained.

Entry	Ligand	no co-catalyst		oxalate		ascorbate	
		ee (%)	Conv.[a] (%)	*ee* (%)	Conv. (%)	*ee* (%)	Conv. (%)
1	**9**	5.9 (1*S*, 2*R*)	1.46	4.1 (1*S*, 2*R*)	6.0	10 (1*S*, 2*R*)	0.55
2	**10a**	17 (1*R*, 2*S*)	4.2	3.5 (1*R*, 2*S*)	15.9	3.3 (1*R*, 2*S*)	0.51
3	**10b**	17 (1*S*, 2*R*)	4.2	3.5 (1*S*, 2*R*)	3.5	3.3 (1*S*, 2*R*)	0.49
4	**11**	13 (1*S*, 2*R*)	0.68	1.4 (1*S*, 2*R*)	1.26	10 (1*S*, 2*R*)	0.54

Table 1.2 Epoxidation of indene with *in situ* generation of the active complex, 2 h reaction. Metal: $MnSO_4$ 0.1 mol %; ligands 0.15 mol %; ascorbic buffer 0.3 mM (30 eq., 0.15 mM ascH + 0.15 mM ascNa); oxalate buffer 0.3 mM (30 eq., 0.15 nM oxaH + 0.15 mM oxaNa); H_2O_2 2 eq.; configuration of the major product in brackets. a) Substrate conversion.

Several other examples of chiral derivatives of TMTACN have been reported by Hall and Kopac.[43] Their group developed an efficient solid-phase synthesis that allowed a library of interesting structures to be produced (Figure 1.14) that remain at the present time untested in asymmetric epoxidation.

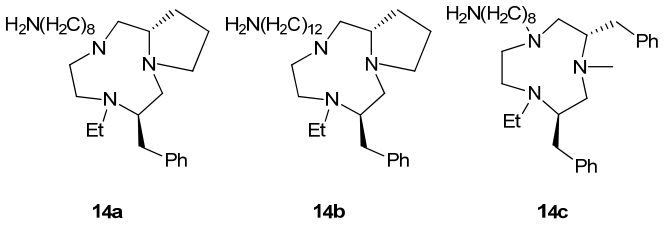

Figure 1.14 Some of the chiral derivatives synthesised by Hall and Kopac.

The use of chiral additives and their effect on the activity of Mn/TMTACN systems have also been extensively explored, disclosing a series of interesting properties. Additives were found to change the rate of the reaction and the selectivity of the system for different classes of alkenes,[40, 44, 45] but no reports of enantioselective processes has yet appeared.

1.4.1.2 Salen and derivatives

Salen owes its success to the relative ease of its synthesis and the large number of sites on its structure that can be modified to tune the electronic effect of the ligand, introduce higher asymmetry, more chiral centres, bulky groups or polymerisable units.

The basic Salen ligand (Figure 1.15, **15**, $R^{1\text{-}8}$ = H) was first synthesised by Pfeiffer[46] in 1933 although the activity of its manganese complexes in the asymmetric epoxidation of alkenes was first reported by Jacobsen and Katsuki concurrently in 1990.[47, 48] The original oxidant chosen in the studies was iodosylbenzene, and for some substrates tested the *ee*s were generally over 50 % and sometimes as high as 93 %. The most active in the series of ligands was **15c**, suggesting that

bulkiness of the substituents on the aromatic rings was a decisive parameter in controlling the asymmetric induction of the complex.

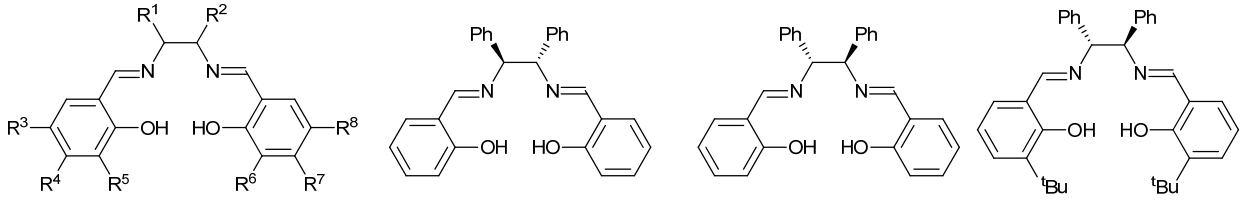

Figure 1.15 Salen backbone with potential sites for modification highlighted (15) and structures used in Jacobsen's original study (15a, b and c).

In the following years after the initial discovery, most of the applications of salen related structures in the asymmetric epoxidation of alkenes involved the use of bleach, iodosylbenzene, or hydroperoxide as oxidants.

One of the first applications of hydrogen peroxide came again from Katsuki,[49] who used a chiral salen incorporating a cyclohexanediamine ring (**16**) in the epoxidation of chromene derivatives. It was found that the presence of a second ligand, coordinating axially, increased both yields and *ee*. Adding a soluble ammonium salt as a source of protons also affected the outcome of the reaction. A series of different solvents were screened to determine the best conditions; acetonitrile and ethanol being the most successful media. The concentration of the substrate was found to be a critical issue too; with higher concentrations giving the best results (0.3 M). The best results and the final conditions are reported in Table 1.3.

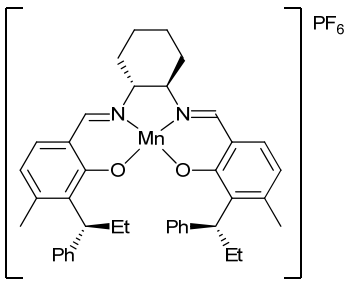

Entry	Substrate [a, c, d]	Yield (%)	*ee* (%)
1	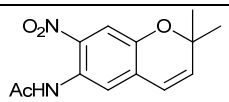	98	95
2	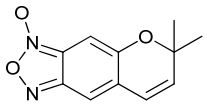	79	93
3	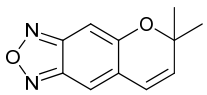	68	92
4	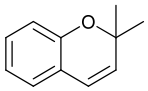	55	88

Table 1.3 Epoxidation of various chromene derivatives with hydrogen peroxide and 16. Substrate 0.1 M, catalyst loading 0.02 eq., 1 eq. oxidant, acetonitrile; a) 0.1 eq. *N*-methylimidazole; b) 0.1 eq. NH_4PF_6; c) 10 eq. H_2O_2 added dropwise; d) substrate 0.3 M, 1 h reaction time.

In an attempt to exploit the chiral properties of bisnaphthols, Meunier *et al.* synthesised a series of salen ligands incorporating the bisnaphthyl motif (Figure 1.16).[50] The group synthesised five ligands with different substituents on the aromatic rings (**17-21**) and a novel cyclohexanediamine derivative (**22**) and prepared manganese, copper, zinc and iron complexes of them. The manganese(III) complexes were tested in the epoxidation of dihydronaphthalene and styrene using H_2O_2 and NaOCl.

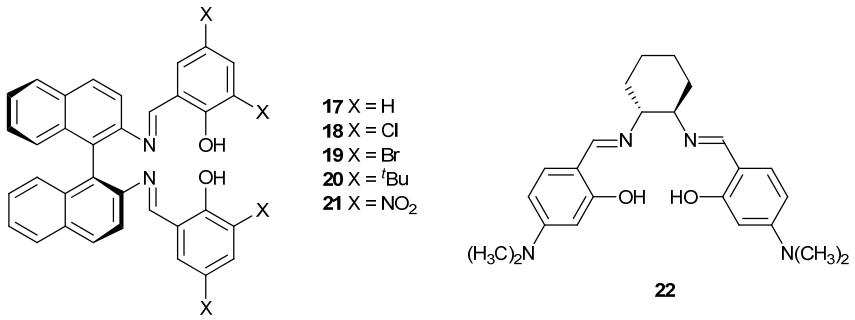

Figure 1.16 Novel salen-like structures presented by Meunier.

The respective manganese complexes **17-Mn**, **18-Mn**, **19-Mn**, **20-Mn** were tested alongside Jacobsen`s ligand (**23**) as a reference. The conditions were: 12 mol% catalyst loading, in the presence of 0.14 mmol of 1,4-dibromobenzene, 0.25 mmol of imidazole, 0.5 mmol of dihydronaphthalene and 2 eq. of hydrogen peroxide added over 45 minutes. The solvent was a 1:1 mixture of methanol and dichloromethane. All the complexes tested gave a conversion of about 6 % over 1 h, not significantly different from the conversion obtained for the blank experiments and *ee*s were not measured. When **23** was used in the same conditions, though, it gave complete conversion and an encouraging 61 % *ee*.

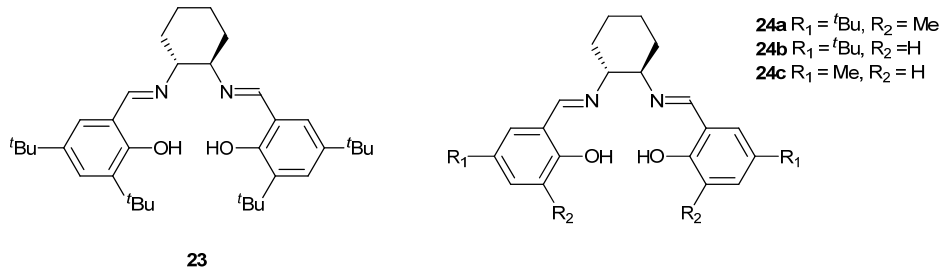

23

Figure 1.17 Jacobsen`s and Brun`s ligands.

Brun and Garcia[51] later employed a manganese(III) complex of **23** and of three other salen derivatives (Figure 1.17, **24a**, **b** and **c**) in the regio- and enantioselective epoxidation of geraniol derivatives. The study initially used NaOCl as the oxidant, but due to the very low yields obtained, this was replaced with H_2O_2. The regioselectivity obtained was quite high, favouring the 6,7 isomer (9:1) and with reasonable epoxide yields. Several solvents were tested to assess the best conditions. A selection of the result obtained by the group is reported in Table 1.4.

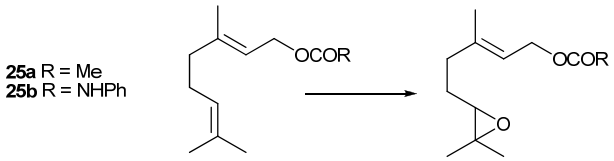

Entry	Substrate	Solvent	Catalyst	Yield (%)	*ee* (%)[a]	Entry	Substrate	Solvent	Catalyst	Yield (%)	*ee* (%)[a]
1	**25a**	CH_3OH	**24b-Mn**	45	53	**5**	**25b**	CH_3OH	**24b-Mn**	50	48
2		CH_3CN	**24b-Mn**	40	52	**6**		CH_3CN	**23-Mn**	12	48
3	**25b**	CH_3OH	**23-Mn**	40	50	**7**			**24a-Mn**	30	51
4			**24a-Mn**	31	52	**8**			**24b-Mn**	45	52

Table 1.4 Epoxidation of geraniol derivatives. Conditions: substrate 1 mmol, 0.023 mmol catalyst, 0.7 mL H_2O_2 (50 %) a) determined by GC on the trifluoroacetyl ester of the deprototeced alcohol.

In an attempt to mimic the activity of an iron peroxidase, where the metal centre is surrounded by the four nitrogen atoms of a haem group and also coordinates to an axial imidazole residue, Berkessel *et al.*[52] synthesised a novel series of pentadentate salen-based ligands in both racemic and enantiopure forms, together with a reference racemic structure lacking the extra coordinating capabilities (Figure 1.18, **26**, **27** and **28** respectively). Their manganese(III) complexes were then tested on styrene, 1,2-dihydronaphthalene and 6,8-dimethyl-dihydronaphthalene with hydrogen peroxide (Table 1.5) in acetonitrile or in a biphasic system (dichloromethane/H_2O_2). Interestingly, pentacoordinate manganese(III) proved to be an essential pre-requisite for peroxidise activity; removal of the extra coordinating arm changes the reactivity of the complex.

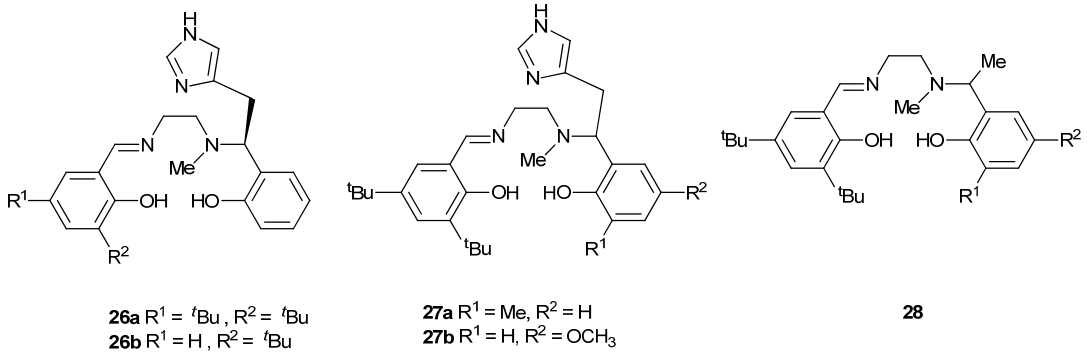

26a R^1 = ^{t}Bu , R^2 = ^{t}Bu
26b R^1 = H , R^2 = ^{t}Bu

27a R^1 = Me, R^2 = H
27b R^1 = H, R^2 = OCH_3

28

Figure 1.18 Tetra- and pentadentate ligands presented in Berkessel's work.

Entry	Substrate	Reaction time (h)	Olefin consumption (%)	Epoxide yield (%)[b, c]	*ee* (%)[b]
1	1,2 dihydronaphthalene[a]	12[d, f]	87	60 (69)	34
2		1[d, g]	93	73 (78)	45
3		1[f]	92	77 (84)	48
4		1[f, g]	91	65 (71)	50
5		1[e, g]	93	72 (77)	64[h]
6	1,2 dihydronaphthalene[i]	1[e, g]	71	47 (66)	66[h]
7	1,2 dihydronaphthalene[l]	4[e, g]	0	0	0
8	styrene[a]	2[e, g]	51	52	46

Table 1.5 Biphasic epoxidation. Olefin:oxidant:catalyst ratio 10:100:1; a) complex was 26a-Mn; b) determined by GC, c) values in brackets represent the yields corrected for the actual conversion of substrate, d) oxidant from 30 % solution, e) oxidant from 1% solution, f) solvent was acetonitrile, oxidant added as acetonitrile solution over 12 h, g) reaction at 0 °C, h) *ee* of ligand used > 98 %, otherwise 81 %; i) complex was 26b-Mn; l) complex was 28-Mn.

In the same period, Katsuki published an interesting discovery, an asymmetric epoxidation using a salen ligand with no chiral centres in conjunction with a chiral additive.[53] It was found that achiral salen complexes of manganese exist in a mixture of two enantiomeric conformers in equilibrium.

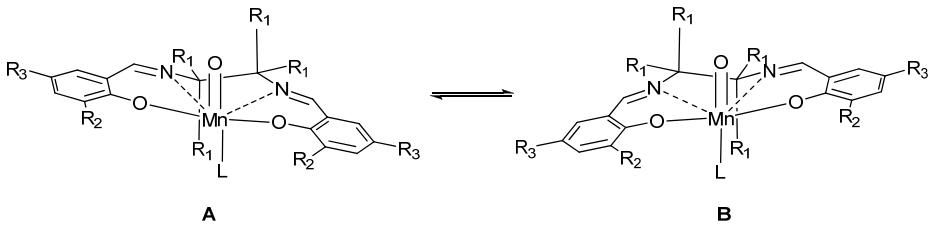

A **B**

Both catalyse epoxidation of alkenes giving a racemic mixture of products. However, the use of chiral amines, such as sparteine, that can axially coordinate to the metal centre moves this

equilibrium to favour only one of the conformers, resulting in asymmetry in the system and *ee*s as high as 34 %.

Katsuki introduced the use of methylimidazole and ammonium salts as axial ligands[49] to promote the formation of a metal oxo-species (Figure 1.19) over homolytic dissociation of the O-O bond in hydrogen peroxide, but the limitations of this system derive from oxidative degradation of the co-catalyst. In an attempt to replicate and improve the performance of this system, Pietkäinen[54] tested carboxylate salts, less sensitive to oxidation, as co-catalysts.

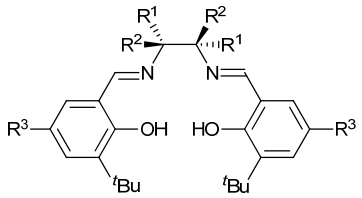

(*S, S*)-29 R^1 = Ph, R^2 = H, R^3 = Me
(*S, S*)-30 R^1 = Ph, R^2 = H, R^3 = OSi(^{i}Pr)$_3$
(*R, R*)-31 R^1 = H, R^2 = Ph, R^3 = Br
(*R, R*)-32 R^1 = H, R^2 = -$(CH_2)_4$-, R^3 = OSi(^{i}Pr)$_3$

Figure 1.19 Structures employed in Pietkäinen`s study.

The study included a preliminary screen of co-catalysts in the epoxidation of dihydronaphthalene to select the optimal conditions and the most active additive. The catalyst chosen for the screening was **(*S*, *S*)-29-Mn** (Table 1.6).

Entry	Additive (mol. eq.)[a]	T (°C)	Time (h)	Yield (%)[b]	*ee* (%)[c]	Entry	Additive (mol. eq.)[a]	T (°C)	Time (h)	Yield (%)[b]	*ee*(%)[c]
1	*N*-MeIm (0.6)	2	1.25	51	64 (60)[d]	**7**	NH_4OAc (0.4)[f]	2	1	68	67
2	^{t}BuPy (0.6)	2	1.5	60	59	**8**	NH_4OAc (0.4)	-18	4	73	68
3	NMO (0.4)	2	2	74	69	**9**	NH_4O_2CH (0.4)	2	1.25	65	68
4	PPMO (0.4)	2	1.5	61	69	**10**	NaOAc (0.4)	2	1	68	69
5	NH_4OAc (0.4)	RT	1.25	73	61	**11**	NaO_2CPh (0.4)	2	1.25	69	67
6	NH_4OAc (0.4)	2	1.25	73 (70)[e]	67 (66)[e]	**12**	$NaHCO_3$ (0.2)	2	1	62	66

Table 1.6 Screening of co-catalysts in the epoxidation of dihydronaphthalene. Conditions: substrate 0.5 mmol, catalyst 5 mol%, ratio of substrate:H_2O_2:co-catalyst:salen 1:2.5:0.2-0.6:0.05, CH_2Cl_2:CH_3OH 1:1. a) *N*-MeIm = *N*-methylimidazole, ^{t}BuPy = 4-*tert*-butylpyridine, NMO = *N*-methylmorpholine *N*-oxide, PPNO = 4-phenyl-pyridine *N*-oxide; b) isolated yields; c) determined by NMR; d) in brackets, value obtained at RT; e) value in brackets obtained using 0.2 mol. eq. co-catalyst; f) urea-H_2O_2 as the oxidant (3 eq.).

NH_4OAc was found to be the most active additive even at lower concentrations and it was then used in the epoxidation of a range of other substrates (which included indene and substituted chromenes) resulting in epoxide *ee*s between 80 % and 90 % and yields generally over 70 %.

Pietkäinen proposed some possible roles for the additive in the reaction. The nitrogen heterocycles were proposed to act as both ligands and bases, and to assist the dissociation of μ-oxo dimers of the catalyst into reactive monomeric oxo species. The carboxylates, were proposed to be acting as bases promoting the formation of HO_2^-, which could bind to the salen complex giving the corresponding hydroperoxo complex. Another role they were found to be playing is lowering the pH of the reaction. Finally, they might react with the oxidant first, forming a peroxyacyl species that coordinates to the complex and finally generates the oxo-species. The activity of $NaHCO_3$ also supports that the most relevant effect of the carboxylates is to influence the pH, being an unlikely axial ligand.

Pietkäinen subsequently published new results in the epoxidation of alkenes generating peroxyacids *in situ* with H_2O_2 and other anhydrous sources of hydrogen peroxide. The substrates tested were all cyclic alkenes such as benzocycloheptene, dihydronaphthalene and indene (Table 1.7). Peroxymaleic acid was prepared by reaction of an excess of anhydride (MA) and either urea-H_2O_2 (UHP) or triphenylphospine-H_2O_2 (POHP) in CH_2Cl_2/DMF. The corresponding peracids were also prepared in the same way starting from phthalic anhydride (PA) and acetic anhydride.

Entry	Substrate	catalyst	Oxidant	T (°C)	Time (h)	Yield (%)[a]	*ee* (%)[b]
1	Benzocyclooctene	**(*S*, *S*)-23-Mn**	POHP/MA	2	0.5	81	88
2		**(*R*, *R*)-32-Mn**	POHP/MA	-18	1.5	73	92
3		**(*S*, *S*)-23-Mn**	UHP/Ac_2O	-18	0.5	80	89
4		**(*S*, *S*)-23-Mn**	PLA	-18	2.75	66	91
5	DHN	**(*S*, *S*)-29-Mn**	UHP/MA	-18	1	70	73
6		**(*S*, *S*)-29-Mn**	POHP/MA	-70	1	69	66
7	Indene	**(*S*, *S*)-23-Mn**	UHP/MA	2	0.5	41	73
8		**(*S*, *S*)-30-Mn**	UHP/MA	-18	1.25	40	81

Table 1.7 Epoxidation with salen and *in situ* formation of the peracid, DNH = 1,2-dihydronaphthalene, PLA = peroxylauric acid. a) isolated yield; b) determined by NMR; c) in CH_3OH/DCM 1:1.

To increase the catalytic activity of salen, Kureshy[55] *et al.* designed structure **33**, a dimeric derivative of the known ligand **(*R*, *R*)-23**, on the basis that more active sites should result in higher activity and turnover numbers.

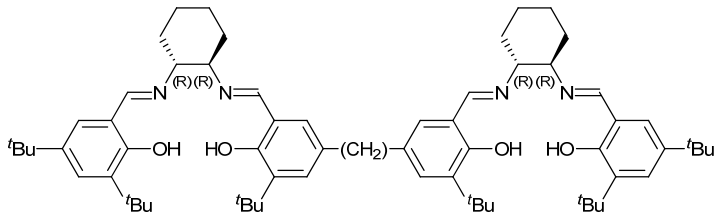

33

Figure 1.20 Dimeric salen ligand synthesised by Kureshy.

The manganese complex of **33** was tested on chromene and some of its derivatives as well as on styrene and indene using UHP as the oxidant. In this case too, ammonium acetate was added as a co-catalyst. Excellent yields and *ee* were obtained for the chromene derivatives with nearly total conversion and *ee*s up to 100 %. Styrene performed disappointingly, with just 23 % *ee*. The amount of catalyst used was 1 %, with about 10 % of co-catalyst. The oxidant was used in slight excess (1.5 eq.) in a mixture of DCM:MeOH 1:1 at 2 °C.

To determine the effect of the co-catalyst, a series of amines were added to the system UHP/**33-Mn** and tested in the epoxidation of 2,2-dimethylchromene (Table 1.8). Some of the additives had already been tested by Pietkäinen[54] and Katsuki.

Entry	Co-catalyst	Conversion (%)	Time (h)	*ee* (%)
1	NMO	>99	8	86
2	4-PhPyNO	>99	7	86
3	4-PPPyNO	>99	6.5	86
4	PyNO	>99	7	86
5	NMeIm	95	7	81

Table 1.8 Enantioselective epoxidation of 2,2-dimethylchromene with UHP/33-Mn. Conditions: catalyst (0.025 mmol), substrate (2.5 mmol), co-catalyst (0.2 mmol), oxidant (3.0 mmol), DCM:MeOH 1:1, 2 °C. 4-PhPyNO = 4-phenylpyridine *N*-oxide, PyNO = pyridine *N*-oxide, 4-PPPyNO = 4-(3-phenyl propyl pyridine *N*-oxide).

Contrary to what was expected, changing the co-catalyst did not significantly affect the activity of the system or asymmetric induction (although a marginal increase in *ee* of about 2 % was observed). Recycling was also investigated, by precipitating **33-Mn** from the reaction mixture and using it in a new reaction. Over five recycling cycles, the conversion reduced drastically from 100 % to 53 % and the reaction time had to be increased to 10 hours for the last run. Interestingly, the *ee* of the product remained stable at 84 % in each cycle. These findings suggested that the loss of activity was due to catalyst degradation and inactivation in each run.

In 2004, Stack[56] published a large study on the effect of ligands and pH on the epoxidation of terminal olefins with manganese complexes and peracetic acid. It was found that most manganese complexes of polyamine ligands showed higher activity under less acidic conditions. The Mn-salen system showed very little activity in the study despite the good record of yields and *ee* with *in situ* formed peracids, indicating little activity with terminal electron deficient alkenes. Stack employed two different peracetic acids, a commercial version (PAAc) with a pH of ca 1 and peracetic acid prepared over acidic resins (PAAr) which has a pH of *ca.* 4. When PAAc was used, with a catalyst loading of 1 %, only 2 % of epoxide was obtained. Switching to the less acidic oxidant raised the value to 15 %. The enantioselectivity of the reaction was not reported.

After Berkessel[52] proved that an extra coordinating arm on the salen structure was positively affecting its activity, Katsuki and Shitama[57] tried to expand his study, screening different coordinating functionalities.

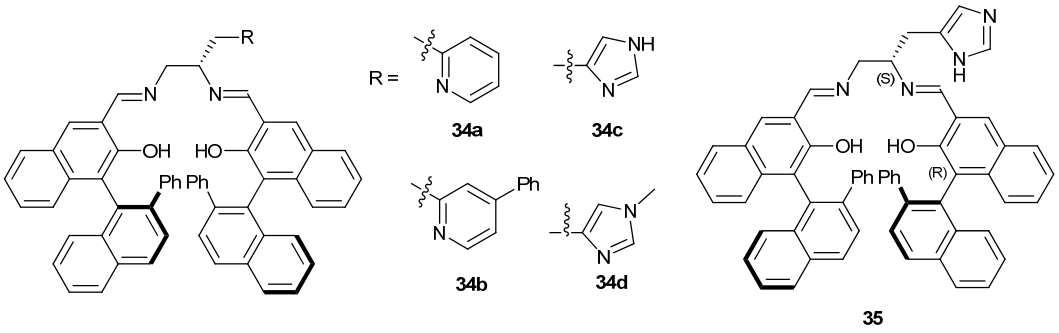

Figure 1.21 Pentadentate salen ligands proposed by Katsuki and Shitama.

The new ligands also included bulkier groups then *tert*-butyl on the structure, in order to increase the asymmetric induction.

The first part of the study focused on the finding the most active catalyst using 2,2-dimethylchromene as the test substrate and hydrogen peroxide as the oxidant (Table 1.9).

Entry	Catalyst	T (°C)	Yield (%)[a]	*ee* (%)[b]	Entry	Catalyst	T (°C)	Yield (%)[a]	*ee* (%)[b]
1	**34a-Mn**	RT	27	95	**7**	**35-Mn**	0	12	83
2	**34a-Mn**	RT	22[c]	92	**8**	**34d-Mn**	0	63	97
3	**34a-Mn**	0	49-60	97	**9**	**34d-Mn**	0	85 [e]	98
4	**34a-Mn**	0	28[d]	90	**10**	**34d-Mn**	0	48 [e,f]	98
5	**34b-Mn**	0	67	96	**11**	**34d-Mn**	0	56 [e-g]	98
6	**34c-Mn**	0	26	95	**12**	**34d-Mn**	0	67 [e, h]	98

Table 1.9 Epoxidation of 2,2-dimethylchromene with pentadentate salen ligands. Conditions: Catalyst (2.5 mol%, PF_6 salt), oxidant (H_2O_2 30 %, 3 eq.), DCM, 24 h. a) isolated yield; b) determined by HPLC; c) UHP as the oxidant, 1eq.; d) solvent was ACN; e) 5 mol% cat. loading; f) 1 eq. H_2O_2 only; g) 48 h reaction; h) 1 eq. H_2O_2 over 8 h, then 62 h reaction time; i) after 24 h, 2 more eq. of oxidant; results after further 24 hours.

Complex **34d-Mn**, bearing a methyl-imidazole coordinating arm, was found to be the most active of the series. It is noteworthy that when the fifth coordinating moiety is present, there is no need for any co-catalyst to achieve high activity. **34d-Mn** was tested with a number of chromene derivatives and other cyclic and electron rich olefins, showing excellent yields and extremely high enantiomeric excess (Table 1.10).

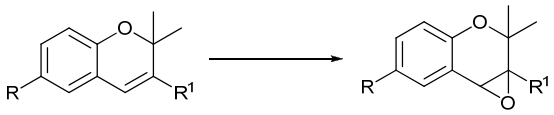

Entry	Substrate	Yield (%)	*ee* (%)	Entry	Substrate	Yield (%)	*ee* (%)
1	R = CN, R^1 = H	95 [a]	99 [b]	**4**	R = Me, R^1 = H	80 [a]	97 [b]
2	R = Br, R^1 = H	98 [a]	98 [b]	**5**	R = OMe, R^1 = H	78 [a]	98 [b]
3	R = NO_2, R^1 = H	85 [a]	99 [b]	**6**	R =H, R^1 = Me	84 [a]	97 [b]

Table 1.10 Asymmetric epoxidation using aqueous hydrogen peroxide. Conditions: catalyst loading (5 mol%, 34d-Mn), oxidant (H_2O_2 30 %, 3 eq.), 0 °C, DCM, 24 h. a) isolated yields; b) determined by chiral HPLC; c) determined by NMR.

Silva[58] *et al.* focused their efforts on the study of the epoxidation of a less common family of substrates, the (*E*,*E*)- cinnamylideneacetophenones. These structures contain two double bonds with different reactivity. The group studied the regio- and diastereoselectivity of the reaction with Jacobsen`s catalyst (**(*R*, *R*)-23-Mn**) and hydrogen peroxide as well as iodosylbenzene. An NMR study of the reaction allowed for assignment of the stereochemistry of each product obtained and precise calculation of respective yields and ratios. Preliminary tests to determine the best conditions were conducted. The epoxidation was performed at RT first, giving disappointingly low yields and conversions but also only enantiopure material. Raising the temperature resulted in higher conversions but in the formation of a second set of products that

were found to be diastereomeric mixtures of double epoxides and in some cases unwanted side-products.

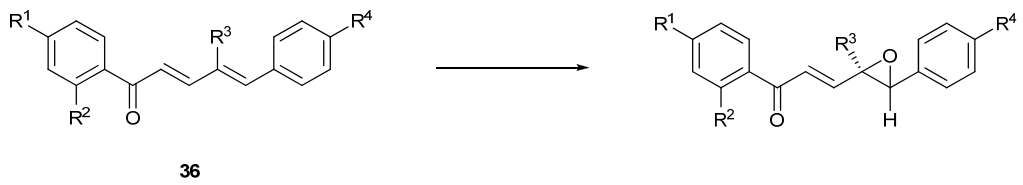

Figure 1.22 General structure of the (*E*,*E*)- cinnamylideneacetophenones used in Silva's study.

In a study following the previously published pentadentate salens,[52, 57, 59] Katsuki and Shitama explored the origin of the inversion of enantioselectivity shown by pentacoordinate salens compared to their other analogues. As reported earlier, the conformation of the salen backbone is the main source of asymmetric induction and it was found that salens with a coordinating arm on the ethylenediamine group have a different preferential conformation (axial, **B**), where the tetra-coordinating derivatives prefer **A** (Figure 1.23).

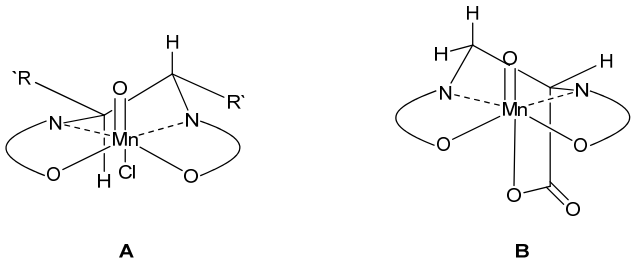

Figure 1.23 Difference in conformation of the salen complexes induced by a fifth coordinating centre.

Salens preferentially assume an equatorial (**A**) conformation when the extra coordinating arm is absent. The enantioselectivity of salen derives from the conformation of the complex, favouring one way of approach of the substrate over the other. Katsuki found that even when the relative stereochemistry on the ethylenediamine group of the two structures corresponds, the extra coordination forces salen in the **B** conformation, thus reversing the selectivity. The catalysts, substrate scope and results exactly matched those previously reported.[57]

1.4.1.3 Other ligands

For many years, the ligands of choice for asymmetric epoxidation of olefins have been chiral salens and derivatives. During those years, though, a parallel line of research developed involving the use of manganese complexes of tri- and tetradentate nitrogen containing ligands. Many structures (Figure 1.24) have been synthesised and tested with hydrogen peroxide and peracetic acid and have proved extremely active in the epoxidation of a large number of

substrates, although strangely enough, no enantioselectivity was reported; a description of the activity of these ligands can be found in Stack's work.[56, 60, 61]

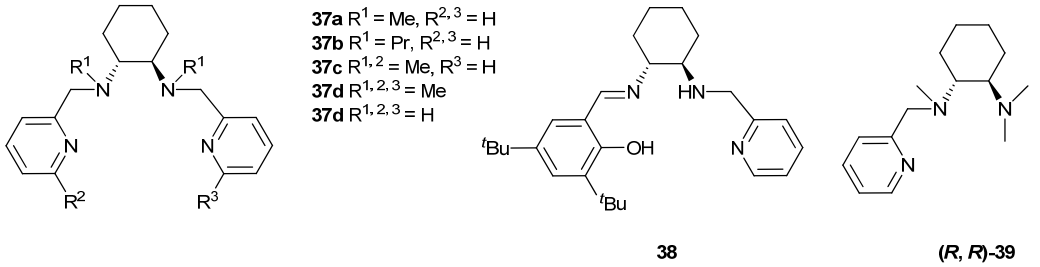

Figure 1.24 Selection of chiral ligands presented by Stack.

In 2007, Costas[62] *et al.* developed a novel tetradentate ligand based on the diaminocyclohexane backbone containing two pinene moieties.

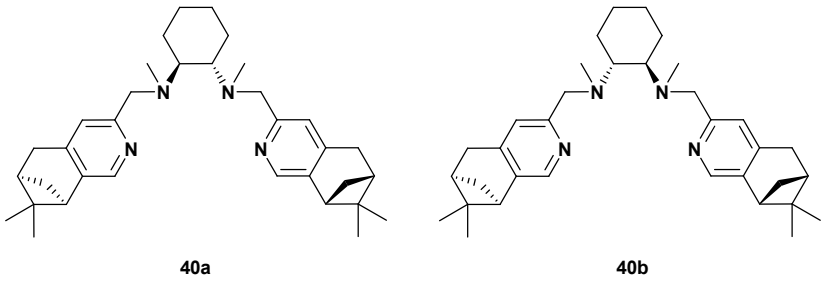

Figure 1.25 New tetradentate ligands from Costas' work.

Costas' ligands included both the wide substrate scope of Stack`s ligands and the stereoselectivity of the salen/salan structure. The group designed ligands **40**, and synthesised the manganese(II) triflate complexes of both. The pinene group was introduced to increase the robustness of the catalyst through an expected electron donating effect which would help stabilise the high oxidation state of the active species.

The complexes were tested in the epoxidation of styrene using the manganese complex of **37a** as reference and of a number of other olefins in order to find the best working conditions; the oxidant was peracetic acid.

The study proved that the enantioselectivity was not related to the stereochemistry of the pinene rings; the bulky substituents, though, potentially contributed to expand the chiral pocket created by the cyclohexanediamine. Several additives were tested but none of them significantly improved yields; increasing the catalyst loading also did not have any appreciable effect on yields and enantioselectivity. The only parameter that affected the *ee*s was temperature. When the temperature was lowered to -20 or -40 °C, the *ee*s increased by as much as 10 % (Table 1.11).

Entry	Substrate	Yield (%)[a]	*ee* (%)	Entry	Substrate	Yield (%)[a]	*ee* (%)
1	*trans*-β-Methylstyrene	93	36	**7**	1-Ph-1-Cyclohexene	37	37
2	Styrene	78[b]	46	**8**	1-Octene	60	0
3	*p*-Chlorostyrene	85	43	**9**	Vinyl cyclohexane	85	15
4	*p*-Methylstyrene	49	34	**10**	*cis*-Cyclooctene	81	0
5	*m*-Nitrostyrene	85	27	**11**	(-)-Carvone	71	42[c, d]
6	*trans*-Chalcone	45	37	**12**	*cis*-2-Heptene	51	5

Table 1.11 Substrate screening in epoxidation with 40a-Mn with optimised conditions. Conditions: substrate (200 eq.), catalyst (1 eq.), oxidant (peracetic acid from 32 %, 200 eq., over 3 min), ACN, 0 °C. a) determined by GC; b) reaction at -40 °C, 220 eq. oxidant; c) diastereomeric excess; d) reaction at -20 °C.

The system proved to be regioselective, with *cis*- and *trans*-olefins being epoxidised with more than 99 % retention of configuration which suggests that the reaction does not follow a radical pathway. Although the *ee*s were modest, the catalyst had a wide substrate scope, being active on aromatic, linear, terminal, electron deficient, electron rich and conjugated olefins.

Watkinson *et al.*, [63] after the work on chiral derivatives of TMTACN, focused on a series of bipyridyl derived ligands and their use in asymmetric epoxidation. The interest in this kind of ligands arose from the work of Stack[56] on similar structures. In their work, six novel ligands were synthesised and several manganese chloride complexes synthesised and characterised.

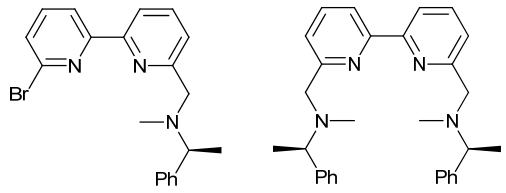

41 **42**

Figure 1.26 A selection of Watkinson`s ligands.

Most of the complexes proved to be inactive with H_2O_2 as the oxidant, catalysing oxidant disproportionation over epoxidation; when commercial peracetic acid was used, its high acidity led to decomposition of the catalyst. Using peracetic acid with a higher pH (either treated on resins or buffered prior use) proved to be the best choice. The manganese complexes derived from ligands **41** and **42** were found to be the most active. The enantioselectivity was unfortunately low, never getting over 21 %. Complex **42-Mn** was employed in the epoxidation of a number of other substrates including cyclohexene, dihydronaphthalene, *trans*-stilbene and others, but no *ee*s was reported for these substrates. The group reported that in a preliminary screen using 10 mol% **41-Mn** in acetone at 0 °C with NaOAc (1 eq.), styrene could be

epoxidised with hydrogen peroxide in 33 % yield with 83 % *ee*s, but this result could not be reproduced.

Following the work of Costas and Stack on biologically inspired tetradentate ligands, Xia and Sun[64] synthesised three novel ligands based on the structure of **37a**. Like Costas, the group considered that introducing more chiral groups on the ligand would increase the enantioselectivity of the catalyst. The extra chirality was introduced in a position closer to the reaction centre than the more remote positions in the pinene derivatives **40.**

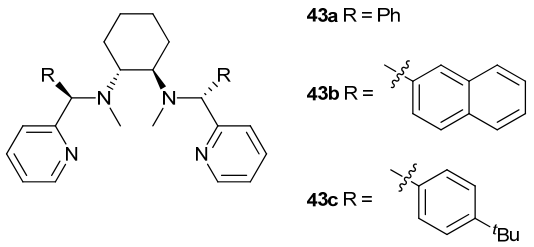

Figure 1.27 Sun's ligands with added stereogenic centres.

The oxidant used was a combination of hydrogen peroxide and acetic acid, to generate peracetic acid *in situ* during the reaction. In a comparative study, the activity of manganese(II) complexes of the novel ligands were compared to the activity of **37a-Mn** and for the first time, its enantioselectivity was disclosed (Table1.12).

Entry	Substrate	Reaction time (h)	Complex	Yield (%)	*ee* (%)	Entry	Substrate	Reaction time (h)	Complex	Yield (%)	*ee* (%)
1	Styrene	1.5	**43c-Mn**	46 [a, c]	44	**5**	Styrene	1.5	**37a-Mn**	30 [a]	26
2		1.5	**43c-Mn**	85 [a]	43	**6**	Chalcone	1	**43a-Mn**	90 [b]	77
3		1.5	**43a-Mn**	89 [a]	46	**7**		1	**43b-Mn**	87 [b]	71
4		1.5	**43b-Mn**	78 [a]	46	**8**		1	**43c-Mn**	91 [b]	78

Table 1.12 Preliminary activity tests with the system H_2O_2/AcOH. Conditions: substrate (0.25 mmol), catalyst (1 mol%), H_2O_2 (6 eq., added last over 3 min), AcOH (5 eq.), ACN, RT. a) determined by GC; b) isolated yield; c) 3 eq. H_2O_2, 5 eq. AcOH.

All the novel complexes proved more effective than **37a-Mn**, both in yields and *ee*s. After the initial screening, **43c-Mn** was chosen as the test catalyst and used in the same conditions in the epoxidation of a large number of substituted α,β-enones and other olefins. The system was not particularly active towards substituted styrenes, with the highest *ee* reported of 43 %. Chalcones were better substrates, with yields and *ee*s almost always over 80 %.

Another interesting development of the bipyridine core came from Romero[65] *et al.*, who reasoned that a catalyst should be easy to obtain and at same time robust and versatile. They

combined the recent findings of Stack[56, 60] and Watkinson[63] with the work of Costas[62] on the effect of pinene groups on enantioselectivity, leading to ligand **44**. With the novel ligand in hand, six complexes with different manganese salts were synthesised and characterised.

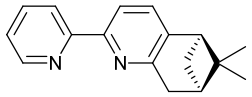

44

Figure 1.28 Romero's most active ligand.

The complexes obtained: $[(MnCl\text{-}L)_2(\mu\text{-}Cl)_2]$ **A,** $[(Mn\text{-}L)_2(\mu\text{-}OAc)_3](PF)_6$ **B**, $[MnCl_2(H_2O)\text{-}L]$ **C**, $[MnCl_2L_2]$ **D**, $[Mn(CF_3SO_3)_2\text{-}L_2]$ **E**, $[Mn(NO_3)(H_2O)\text{-}L_2)](NO_3)$ **F**, where L = **44**,were tested in the catalytic epoxidation of styrene with peracetic acetic as the oxidant. The results are reported in Table 1.13.

Entry	Complex	Conversion (%)	Yield (%)	*ee* (%)	Entry	Complex	Conversion (%)	Yield (%)	*ee* (%)
1	**A**	100	65	10	**5**	**D**	52	30	10
2	**A**	3 [a]	3	21	**6**	**E**	18	6	15
3	**B**	10	10	19	**7**	**F**	19	10	19
4	**C**	10	7	20	**8**	**37a-Mn**	100 [b]	80	40

Table 1.13 Screening for activity and enantioselectivity with peracetic acid as the oxidant. Conditions: substrate (250 μmol), catalyst (2.5 μmol), oxidant (500 μmol, from 32 %), 30 min reaction, ACN. a) T 0 °C; b) oxidant:substrate 1:1.

A new strategy to rapidly create a library of tetradentate ligands with a coordination chemistry similar to those synthesised by Stack and Costas was recently reported by Hao and Wang.[66] Starting from the consideration that the pyridyl rings present on many structures[56, 60] synthesised so far are difficult to modify, they decided to replace them with a different group, with similar coordinating properties, but that was easier to derivatise. Their new structures combined the well established ethylenediamine backbone with triazole rings, easily introduced by the "click" reaction between a propargyl group and an azide (Huisgen cycloaddition).[67] Both required functionalities are easy to generate and allow for a large number of groups to be introduced on the ligand.

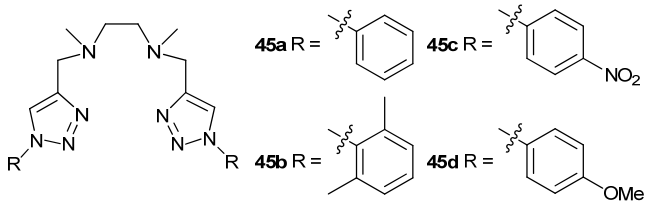

Figure 1.29 "Click" generated tetradentate ligands.

The manganese trifluoromethanesulfonate complexes of these ligands have been tested in the epoxidation of various terminal olefins with peracetic acid and proved quite effective, with yields generally over 80 %. Unfortunately, no chiral version of these structures has been published and tested so far; this entry was included in the review for the novelty of the approach.

1.4.2 Iron

Iron, like manganese, is widely involved as a cofactor in many biological transformations, most of which involve oxygen transfer or transport. The most well known iron-containing biological structure is probably haemoglobin,[68] which is involved in the transport of dioxygen;[69] iron-sulfur proteins like rubredoxin and other ferredoxins[70] are also widespread in the biological world. Of great interest for chemistry is the family of cytochromes P450[71] because of their role in oxidising a wide range of biological substrates. It was probably this very last family of enzymes that has most inspired the design of iron containing catalysts for oxidation reactions like hydroxylations and epoxidations.

1.4.2.1 Porphyrins

Porphyrins are rigid, equatorial ligands constituted by a macrocyclic core and a periphery which can be extensively modified to alter the activity of their complexes. In the iron-catalysed asymmetric epoxidation of olefins they remain the most known and studied family of ligands, affording high yields and good to excellent *ee*s. The oxidants of choice for these systems are generally iodosylbenzene, dichloropyridine-*N*-oxide. A few examples of the use of hydrogen peroxide can be found in the literature, but no one reports any enantiomeric excess appearing. For a more comprehensive review of porphyrin catalysed epoxidation see Xia,[21] Burgess[22] and Rose.[72]

1.4.2.2 Other ligands

In 2001, Que *et al.*[73] investigateted the activity of the iron complexes of one of the ligands later employed by Stack[61] (**46** and **47**) in the hydroxylation of alkenes with hydrogen peroxide. The

substrate, cyclooctene, was converted into the corresponding epoxide by [Fe(**46a**)$(ACN)_2$]$(ClO_4)_2$ in 75 % yield with 9 % of the *cis*-diol also being formed. When [Fe(**46b**)$(CF_3SO_3)_2$] was employed, 15 % epoxide and 64 % diol were obtained. Encouraged by these results, they tested two more iron complexes of known ligands (**(*S*, *S*)-37d** and **37a**) under the same conditions using *trans*-2-heptene as the substrate in acetonitrile with either 10 or 20 equivalents of H_2O_2. Complex **37a-Fe** gave 29 % *ee* for the diol and 12 % for the epoxide, while **(*S*, *S*)-37d-Fe** gave 79 % *ee* for diol but only racemic epoxide. The other enantiomer of **37d** was also tested and gave the same enantiomeric excess but with the opposite configuration, suggesting that the selectivity of the reaction is guided by the configuration of the cyclohexanediamine ring.

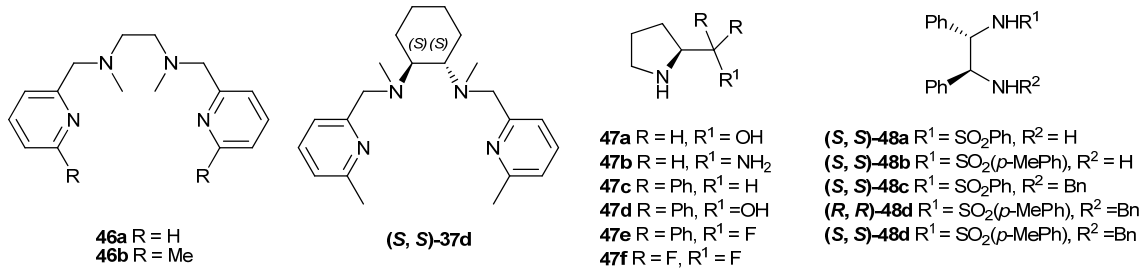

Figure 1.30 Stack and Beller's ligands.

In 2007, Beller[74] *et al.* disclosed a new library of ligands that managed to break the 20 % *ee* barrier for the iron catalysed epoxidation of alkenes with hydrogen peroxide. This work was reported as the first promising iron-catalysed system for the epoxidation of aromatic alkenes that did not use porphyrins. The group's initial investigations were based on ligands derived from the L-proline backbone (**47a-f**, Table 1.14).

Entry	Ligand	Time (h)	Conversion (%)[a]	Yield (%)[a]	*ee* (%)[b]	Entry	Ligand	Time (h)	Conversion (%)[a]	Yield (%)[a]	*ee* (%)[b]
1	**47a**	1	95	73	0	**4**	**47d**	36	78	53	10 (2*R*, 3*R*)[c]
2	**47b**	36	60	58	1 (2*S*, 3*S*) [c]	**5**	**47e**[d]	14	100	98	17 (2*S*, 3*S*) [c]
3	**47c**	60	61	45	0	**6**	**47f**	1	100	93	2 (2*R*, 3*R*) [c]

Table 1.14 Epoxidation of *trans*-stilbene with proline derived ligands and hydrogen peroxide. Conditions: metal ($FeCl_3$ $6H_2O$, 5 mol%), additive (pyridine 2,6-dicarboxylic acid, H_2Pydic, 5 mol%), ligand (12 mol%),oxidant (H_2O_2, 3 eq.), 2-methylbutan-2-ol, RT. a) determined via GC; b) determined by HLPC; c) determined by comparing optical rotation with literature data; d) reaction was carried out at 0 °C.

From their preliminary results it was concluded that the presence of a group capable of intramolecular hydrogen bonding was playing a determining step. Following this consideration,

the group moved to test a series of ligands based on chiral diamine (*S*, *S*)-1,2-diphenylethylenediamine, containing a hydrogen-bond capable sulfonyl group. Again, the group synthesised and tested a number of ligands (**48a-d**) in the epoxidation of *trans*-stilbene (Table 1.15).

Entry	Ligand	Conv. (%) [a]	Yield (%) [a]	*ee* (%) [b]	Entry	Ligand	Conv. (%) [a]	Yield (%) [a]	*ee* (%) [b]
1	**(*S*, *S*)-48a**	100	88	26 (2*S*, 3*S*)	**4**	**(*R*, *R*)-48d**	100	92	41 (2*S*, 3*S*)
2	**(*S*, *S*)-48b**	100	86	28 (2*S*, 3*S*)	**5**	**(*S*, *S*)-48d**	100	87	42 (2*R*, 3*R*)
3	**(*S*, *S*)-48c**	100	98	36 (2*R*, 3*R*)	**6**	**(*S*, *S*)-48d**[d]	100	97	47 (2*R*, 3*R*)

Table 1.15 Epoxidation of *trans*-stylbene with diphenylethylenediamine ligands. Conditions: substrate (0.5 mmol), oxidant (H_2O_2, 1 mmol), metal ($FeCl_3$ $6H_2O$, 5 mol%), H_2Pydic (5 mol%), ligand (12 mol%), 2-methylbuthane-2-ol, RT, 1h. a) determined by GC; b) determined by HPLC; c) determined by comparing optical rotation with literature data; d) reaction at -10 °C, 24 h.

Once **(*S*, *S*)-48d** was identified as the most active of the ligand family, it was tested on a large number of aromatic olefins under similar conditions with very diverse results depending on the substrate, but enantioselectivity was always observed. The approach taken in all of these tests was the *in situ* generation of the catalyst, instead of using a pre-formed complex.

In the same year, Beller released another system for the epoxidation of a wide range of alkenes, based on hydrogen peroxide using iron as the metal.[75] The ligands employed (pyridinebisimidazolines, terpyridines, pyridinebisoxazolines) contained chiral groups but no enantiomeric excess was reported in this study.

Soon after, a catalyst based on chiral bispyridine was presented by Menage.[76] The ligands used (**49a-b**) in conjunction with iron(III) chloride, proved to be good epoxidation catalysts when used with peracetic acid.

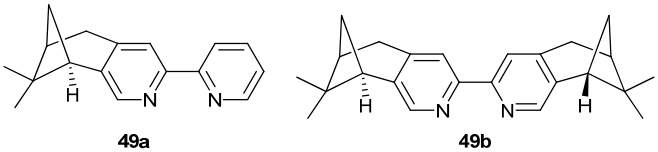

49a **49b**

Figure 1.31 Bispyridine derived chiral ligands.

The complex $[Fe_2O(\mathbf{49a})_2(H_2O)](ClO_4)_4$ was known to oxidise sulfones with *ee*s up to 40 % with H_2O_2 and when used by the group in the epoxidation of *trans*-β-methylstyrene with peracetic

acid, it yielded an encouraging 10 % *ee*. The next optimisation undertaken lead to **49b**, where a second pinene group was introduced on the backbone. A homologous complex ($[Fe_2O(\mathbf{49b})_2(H_2O)](ClO_4)_4$) was synthesised and tested on a range of aromatic alkenes. The results of this study are summarised in Table 1.16.

Entry	Substrate	Conv. (%) [c]	Yield (%) [c]	*ee* (%) [d]	Entry	Substrate	Conv. (%) [c]	Yield (%) [c]	*ee* (%) [d]
1	*trans*-2-Heptene	97 [a]	100	9	**6**	*cis*-β-Methylstyrene	100 [a]	74	15
2	Styrene	84 [b]	73	15 (*R*)	**7**	*trans*-β-Methylcynnamate	70 [b]	49	63
3	*p*-Bromostyrene	100 [b]	82	28	**8**	*trans*-β-Isopropylcynnamate	n.d. [a]	n.d.	19
4	*o*-Bromostyrene	87 [b]	78	15	**9**	*trans*-Chalcone	92 [a]	66	56
5	*trans*-β-Methylstyrene	86 [b]	56	24	**10**	*trans*-Stilbene	67 [a]	67	0

Table 1.16 Epoxidation of aromatic olefins with $[Fe_2O(\mathbf{49b})_2(H_2O)](ClO_4)_4$ and peracetic acid. Conditions: substrate (0.9 M), catalyst (0.2 mol%), oxidant (peracetic acid, from 32 %, 1.15 eq.), reaction time 2 min. a) solvent was ACN; b) solvent was DCM; c) determined by GC; d) determined via HPLC or GC.

When a different oxidant like hydrogen peroxide or an alkyl peroxide were used, no epoxidation was observed. The study also proved that in these conditions, the catalyst was deactivated in the reaction and could not be recovered and recycled.

After the first positive results with mono-*N*-sulfonylated chiral diamines,[74] Beller *et al.* published an expansion of their previous work,[77] including old and novel ligands, and an extensive study of the mechanism of the reaction that lead them to propose the presence of radical intermediates. Again, the test substrate was *trans*-stilbene (Table 1.17) and the screening was then expanded to a large number of aromatic alkenes.

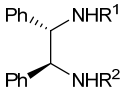

(*S*, *S*)-50a R^1 = 4-PhC_6H_4, R^2 = H
(*S*, *S*)-50b R^1 = 4-^{t}BuC_6H_4, R^2 = H
(*S*, *S*)-50c R^1 = 4-PhC_6H_4, R^2 = Bn
(*S*, *S*)-50d R^1 = 4-^{t}BuC_6H_4, R^2 = Bn
(*S*, *S*)-50e R^1 = 4-MeC_6H_4, R^2 = 4-MeBn

Entry	Ligand	Conv. (%) [a]	Yield (%) [a]	*ee* (%) [b]	Entry	Ligand	Conv. (%) [a]	Yield (%) [a]	*ee* (%) [b]
1	**(*S*, *S*)-48d**	100	87	42 (2*R*, 3*R*)	**4**	**(*S*, *S*)-50c**	100	84	39 (2*R*, 3*R*)
2	**(*S*, *S*)-50a**	100	84	29 (2*S*, 3*S*)	**5**	**(*S*, *S*)-50d**	100	95	40 (2*R*, 3*R*)
3	**(*S*, *S*)-50b**	100	84	29 (2*S*, 3*S*)	**6**	**(*S*, *S*)-50e**	100	92	39 (2*R*, 3*R*)

Table 1.17 Epoxidation of *trans*-stilbene with hydrogen peroxide and chiral diamine derived ligands. Conditions: substrate (0.5 mmol), oxidant (1.0 mmol), metal ($FeCl_3$ $6H_2O$, 5 mol%), H_2Pydic (5 mol%), ligand (12 mol%), *tert*-amyl alcohol, RT, 1h. a) determined by GC; b) determined by HPLC, absolute configurations determined by comparing optical rotation with literature values.

The group found a correlation between the substituents on both nitrogen atoms and enantioselectivity. Steric hindrance on the nitrogen influenced the stereochemistry of the products; when the benzyl group substitutes the free amine, it gave the opposite enantiomer of *trans*-stilbene epoxide. The amount of the catalyst was also found to affect yields and *ee*s, with the best results obtained with an ideal load of ligand of 12 mol%. Higher concentrations lead to increased yields but to a drop in *ee*, while lower concentrations gave disappointing yields but almost maintained the same level of enantioselectivity. With optimised conditions in hand, **(*S*, *S*)-48d** was employed in the epoxidation of a new group of aromatic alkenes (Table 1.18).

Entry	Substrate	Yield (%) [a]	*ee* (%) [b]	Entry	Substrate	Yield (%) [a]	*ee* (%) [b]
1	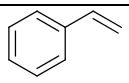	84	8	**7**	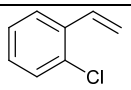	62	14
2	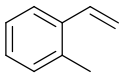	61	8	**8**	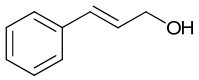	49	48 (2*R*, 3*R*)
3	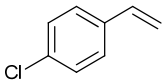	82	21	**9**	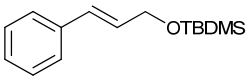	42	29 (2*R*, 3*R*)
4	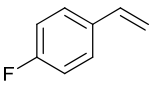	73	11	**10**	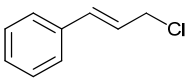	33	23 (2*R*, 3*R*)
5	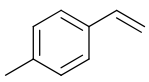	52	26	**11**	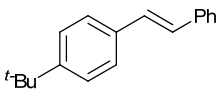	91 [c]	53 (2*R*, 3*R*)

6	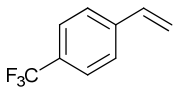	60	20	**12**	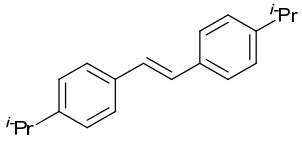	90 [c]	71 (2*R*, 3*R*)

Table 1.187 Screening of (*S*, *S*)-48d in the epoxidation of aromatic alkenes. Conditions: substrate (0.5 mmol), oxidant (1.0 mmol), metal ($FeCl_3$ $6H_2O$, 5 mol%), H_2Pydic (5 mol%), ligand (12 mol%), *tert*-amyl alcohol, RT, 1 h. a) determined by GC; b) determined by HPLC, absolute configurations determined by comparing optical rotation with literature values; c) isolated yields.

Bispyridines bearing chiral groups had already proven to be interesting ligands in the asymmetric epoxidation of olefins,[76] an evolution of this system came in recent years from the work of Kwong *et al.*.[78] The group synthesised an oligopyridine bearing pinene groups at its extremities, and tested it in the iron catalysed epoxidation of aromatic alkenes. An iron complex of the novel ligand (**51**) was prepared, and although no crystal structure could be obtained, other measurements suggested a dimeric μ-oxo iron complex (**52**) with the structure [Fe_2O(**51**)Cl_2].

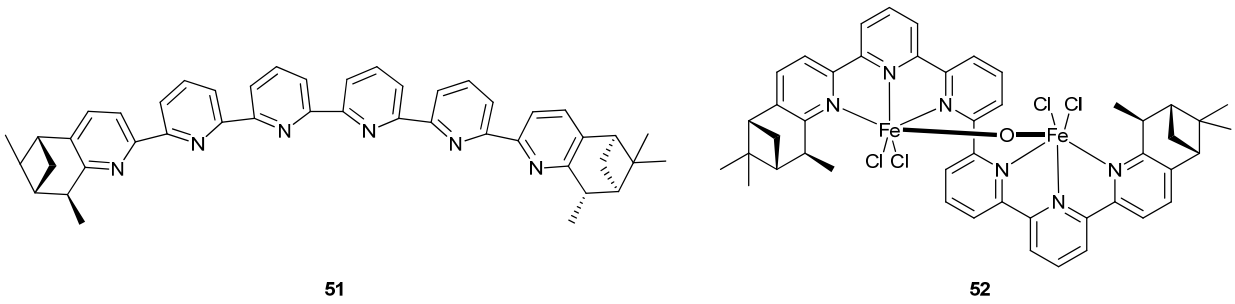

51 **52**

Figure 1.32 Sexipyridine ligand developed by Kwong (left) and its proposed diiron complex (right).

The complex was only active with hydrogen peroxide, attempts to add acetic acid to the mixture did not improve the yields significantly and attempts to employ peracetic acid resulted in no reaction, proving that *in situ* formed peracetic acid is not the terminal oxidant (Table1.19).

Entry	Substrate	Yield (%) [a]	*ee* (%) [b, c]	Entry	Substrate	Yield (%) [a]	*ee* (%) [b, c]
1	Styrene	100	43 (*R*)	**5**	α-Methylstyrene	80	17 (*R*)
2	*p*-Methoxystyrene	100	15 (*R*)	**6**	*trans*-β-Methylstyrene	96	37 (1*R*, 2*S*)
3	*p*-Methylstyrene	100	30 (*R*)	**7**	*cis*-β-Methylstyrene	100	40 (1*S*, 2*R*)
4	*p*-Chlorostyrene	90	42 (*R*)	**8**	1,2-Dihydronaphtalene	50	31 (1*R*, 2*S*)

Table 1.19 Epoxidation of alkenes with complex 52. Conditions: Substrate (0.14 mmol), catalyst (2 mol%), acetic acid (10 eq. to catalyst), oxidant (H_2O_2 from 35 %, 0.21 mmol), ACN, 0 °C, 3 min reaction time. a) determined by GC; b) determined by chiral HPLC or GC; c) absolute configuration was determined by comparing retention times of mixtures with those of original samples.

The best results were obtained with smaller substrates, indicating that the steric hindrance of the proposed complex might be a limiting factor in its applications.

1.4.3 Titanium.

Asymmetric epoxidation of unfunctionalised olefins using hydrogen peroxide and a titanium based catalyst was first reported by Katsuki in 2005.[79] The initial research was based on the salen ligand **53** (giving complex **54**), which was found to catalyse asymmetric sulfoxidation with UHP,[80] would be an excellent starting point.[79] Though the complex was inactive as the catalyst, the results suggested that the ligand needed to be made more flexible in order to stabilise the dimeric species in solution. Hence titanium complex **56** containing the more flexible ligand **55**, was synthesised and tested with great success (Figure 1.33 and Table 1.20)

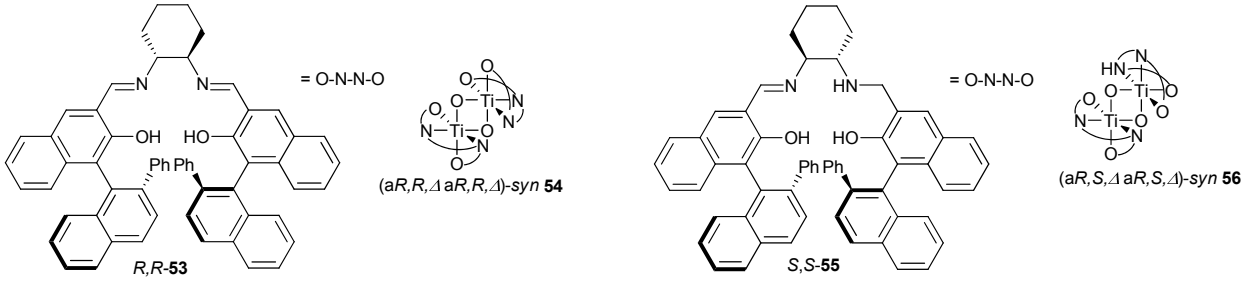

Figure 1.33 Asymmetric epoxidation using aqueous hydrogen peroxide as the terminal oxidant and the structures of complexes 54 and 56 used in the initial study.

Entry	Substrate	Solvent	Time (h)	Yield (%)	*ee* (%)	Config.
1[a]	1,2-Dihydronaphthalene	DCM	24	14	83	1*S*,2*R*
2[b]		DCM	72	>99	>99	1*R*,2*S*
3[c]		DCM	48	92	>99	1*R*,2*S*
4		Toluene	18	>99	>99	1*R*,2*S*
5		EtOAc	18	>99	>99	1*R*,2*S*
6		THF	85	97	97	1*R*,2*S*
7	Indene	EtOAc	24	87	99	1*R*,2*S*
8	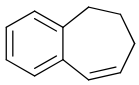	EtOAc	24	85	98	5*R*,6*S*
9	Styrene	DCM	24	90	93	*R*

Table 1.20 Asymmetric epoxidation of selected alkenes by titanium complex 56 using aqueous hydrogen peroxide as terminal oxidant. a) (*R*, *R*)-55 was used as the ligand; b) 0.1 mol% of catalyst used; c) 0.02 mol% of catalyst used.

The epoxidation proceeded in excellent yields and very high stereoselectivity for nearly every substrate. Catalytic loadings as low as 0.02 mol% were successfully employed with a stoichiometric amount of hydrogen peroxide.

A series of papers describing optimisation of the catalyst and the reaction conditions followed shortly after the original publication. The synthesis of the catalyst was simplified by reducing both imine functionalities on the ligand, adding extra flexibility and removing the need for the difficult synthetic step involving a Meerwein-Ponndorf-Verley reaction.[81] The influence of the aromatic substituent Ar on the ligand **57** was then systematically investigated in the epoxidation of styrene (Figure 1.34, Table 1.21).

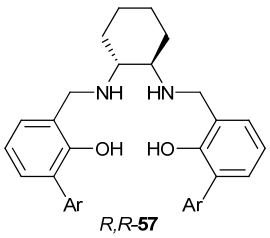

R,R-**57**

Figure 1.34 Novel ligand 57.

Entry	Ar	Yield (%)	*ee* (%)	Config.
1	Ph (**57a**)	27	78	*S*
2	*o*-$MeOC_6H_4$ (**57b**)	62	89	*S*
3	*m*-$MeOC_6H_4$ (**57c**)	39	81	*S*
4	*p*-$MeOC_6H_4$ (**57d**)	28	83	*S*
5	2,6-$(MeO)_2C_6H_3$ (**57e**)	5	67	*S*
6	*o*-MeC_6H_4 (**57f**)	52	85	*S*
7	*o*-$CF_3C_6H_4$ (**57g**)	71	87	*S*
8[a]	*o*-EtC_6H_4 (**57h**)	48	87	*R*
9	*o*-$EtOC_6H_4$ (**57i**)	49	83	*S*
10	*o*-$BnOC_6H_4$ (**57j**)	55	85	*S*

Table 1.21 Asymmetric epoxidation of styrene with different titanium catalysts derived from ligand 57. a) (*S, S)*-57 was used.

The presence of an *ortho*-substituted phenyl group at C3 and C3' resulted in increased effectiveness of the complexes of the salan ligands in terms of both yield and enantioselectivity. Sterically more hindered groups decreased the catalytic activity, but not the selectivity. The enantioselectivity was also not affected by electronic properties of the substituents.[81] It was also demonstrated that alkyl substituent, such as *tert*-butyl, at the position C3/ C3' position reduced the effectiveness of the catalyst.[82]

Further insight into the influence of the substituents at positions C3, C5, C3' and C5' was obtained by Berkessel.[83] A simple stepwise route allowed for the synthesis of ligands with various substituents at the aforementioned positions (Figure 1.35, **58**).

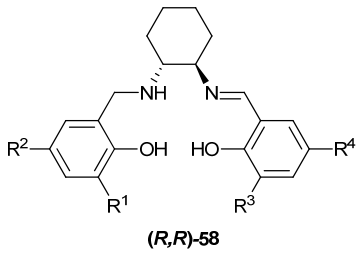

(*R,R*)-58

Figure 1.35 General structure of Berkessel's[83] new ligand with modified sites highlighted.

This set of new salalen ligand was tested in the epoxidation of three different substrates (Table 1.22).

		Substituents				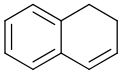		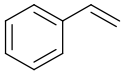		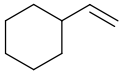	
Entry	**Ligand**	**R^1**	**R^2**	**R^3**	**R^4**	**Yield (%)**	***ee* (%)**	**Yield (%)**	***ee* (%)**	**Yield (%)**	***ee* (%)**
1	**58a**	F	F	H	H	0	-	0	-	0	-
2	**58b**	Cl	Cl	H	H	69	91	23	75	4	66
3	**58c**	I	I	H	H	6	36	1	-	<1	-
4	**58d**	OMe	H	H	H	25	93	2	75	<1	-
5	**58e**	^{t}Bu	^{t}Bu	H	H	45	96	4	74	2	47
6	**58f**	Ph	H	H	H	76	98	24	77	5	73
7	**58g**	Ph	H	F	F	0	-	0	-	0	-
8	**58h**	Ph	H	Cl	Cl	54	98	13	73	3	68
9	**58i**	Ph	H	I	I	26	86	3	59	<1	-
10	**58j**	Ph	H	NO_2	NO_2	12	95	2	73	2	11
11	**58k**	Ph	H	OMe	H	44	96	8	75	2	54
12	**58l**	Ph	H	^{t}Bu	^{t}Bu	<1	-	<1	-	<1	-
13	**58m**	Ph	H	Ph	H	91	35	35	78	8	81

Table 1.22 Positional testing of the "left" and "right" halves of the salalen ligand 58. Typical reaction conditions: 58 (10 mol%), Ti(O-^{i}Pr)$_4$ (10 mol%), 30 % H_2O_2 (1.5 eq.), DCM, RT, 18 h.

The results clearly illustrated that having an aromatic substituent in the C3-position is the most advantageous. All other substituents have proven to be inferior, with Cl being the next best group. The "right" half of the ligand also showed a similar behaviour, with an aromatic substituent at the C3' position producing the best results, suggesting that the catalytic system is highly sensitive to steric congestion around the C3/C3' positions.

Katsuki *et al*. have noted that as the epoxidation reactions were proceeding, measurable amounts of by-products were accumulating with time,[81] so the next logical step was to reduce the reaction

timescale. In order to do this, larger catalytic loadings were required. In the course of these studies it was found that the pH of the reaction was slowly decreasing and the low pH appeared to be the cause of by-product formation.[84] Consequently the reaction was carried out under controlled pH, using a phosphate buffer (pH 7.4 - 8.0).[84] Though the overall conversion and the epoxide yield increased, the rate of the reaction decreased and hence further adjustments were required such as an increased concentration (from 0.1 M to 0.4 M w.r.t. substrate) and temperature (from RT to 40 ^{o}C). Under these conditions the catalytic loadings were decreased to 1 mol% with a reaction time of 6 hours (Table 1.23).[84]

Entry	Product	Time (h)	Conv. (%)	Yield (%)	*ee* (%)	Entry	Product	Time (h)	Conv. (%)	Yield (%)	*ee* (%)
1	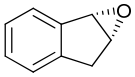	6	99	98	97	**4**	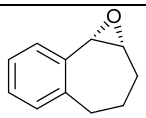	9	88	88	97
2	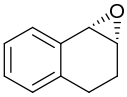	6	99	99	98	**5**	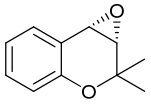	6	92	87	>99
3	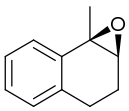	6	97	93	97	**6**	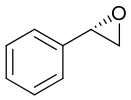	6	66	65	88
						7		18	87	86	88

Table 1.23 Substrate scope in the asymmetric epoxidation using Ti(O-^{i}Pr)$_4$ (1 mol%), ligand 57b (1.3 mol%), 30 % H_2O_2 (1.5 eq.) in DCM and phosphate buffer (pH 7.4) at 40 ^{o}C.[84]

Though the methodology proved to work best on aromatic alkenes, it was successfully extended towards linear, non-activated olefins as well although with inferior *ee*s.[85] Quite importantly, the enantiomeric excesses achieved in this work are the highest reported to date for these types of substrates.[85]

Epoxysilanes are the synthetic equivalent of epoxides,[86] yet there are very few catalytic enantioselective epoxidations of alkenylsilanes.[87] The scope of **56** was extended further in the epoxidation of alkenylsilanes where it showed excellent ability to carry out the transformation under low catalytic loadings (typical 0.5 - 2 mol%) resulting in complete conversions in less then 24 h (Table 1.24).[87] With only one exception (Entry 5), all the substrates were converted to the corresponding epoxysilanes in high yields.

Entry	Product	56 (mol%)	Time (h)	Yield (%)	*ee* (%)
1	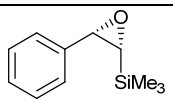	0.5	9	87	>99
2	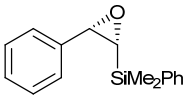	2	9	95	>99
3	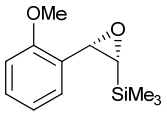	2	18	94	>99
4	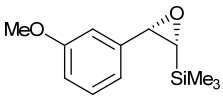	0.5	7	96	>99
5	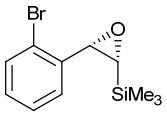	2	24	10	>99
6	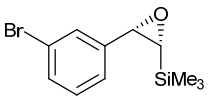	2	4	98	>99
7	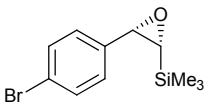	0.5	6	99	>99
8	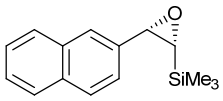	1	9	92	>99
9	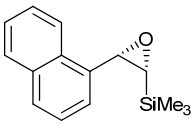	0.5	6	96	>99

Table 1.24 Asymmetric epoxidation of *cis*-alkenylsilanes with titanium (salalen) 56.

Though the epoxidation of alkenylsilanes proceeded in excellent yields and very high *ee*s, it still required the removal of silane group in order to obtain the desired styrene oxide analogue thus reducing the overall efficiency of the catalyst. Hence Katsuki developed novel proline-derived salan ligands **59** which were subsequently screened in the epoxidation of styrenes (Figure 1.36).[88]

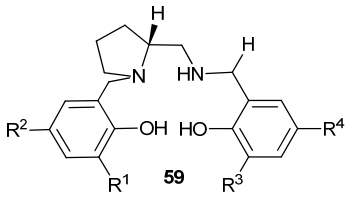

59a $R^1 = {}^t$Bu, $R^2 = {}^t$Bu, $R^3 = {}^t$Bu, $R^4 = {}^t$Bu
59b $R^1 = {}^t$Bu, $R^2 = {}^t$Bu, R^3 = Ph, R^4 = H
59c R^1 = Ph, R^2 = H, $R^3 = {}^t$Bu, $R^4 = {}^t$Bu
59d R^1 = Ph, R^2 = H, R^3 = Ph, R^4 = H

Figure 1.36 Proline-derived salan ligands 59.

All four ligands were then evaluated in the epoxidation of 2-vinylnaphthalene under various conditions (Table 1.25).

Entry	Ligand	T (°C)	Conc. (M)	Conv. (%)	Yield (%)	*ee* (%)	Entry	Ligand	T (°C)	Conc. (M)	Conv. (%)	Yield (%)	*ee* (%)
1[a]	**59a**	25	0.2	13	8	28 (*S*)	**7**[a]	**59c**	-20	0.2	58	52	94 (*S*)
2[a]	**59b**	25	0.2	10	3	1 (*R*)	**8**[a]	**59d**	-20	0.2	52	44	96 (*S*)
3[a]	**59c**	25	0.2	55	32	88 (*S*)	**9**[a]	**59d**	-20	1.0	90	74	96 (*S*)
4[a]	**59d**	25	0.2	38	9	78 (*S*)	**10**[a,b]	**59d**	-20	1.0	96	95	97 (*S*)
5[a]	**59c**	0	0.2	71	64	94 (*S*)	**11**[b,c]	**59d**	-20	1.0	44	43	97 (*S*)
6[a]	**59d**	0	0.2	46	38	92 (*S*)							

Table 1.25 Evaluation of ligands 59 in the asymmetric epoxidation of 2-vinylnaphthalene. a) 10 mol% Ti(O-^{i}Pr)$_4$/Ligand; b) in the presence of brine; c) 2 mol% Ti(O-^{i}Pr)$_4$/Ligand.

The results clearly show that the presence of a phenyl group at C3 and C3' positions is essential for both activity and selectivity; it also appears that the reaction is influenced by both temperature and concentration, with lower temperatures and higher concentrations improving the selectivity and yields. When the catalytic loading was decreased the conversion and yields decreased, albeit without any loss in *ee*. Despite the high catalytic loadings required, this system, containing only one chiral centre, appears to be superior to those already described which contain up to four chiral components and was successfully applied in the asymmetric epoxidation of a variety of styrenes (Table 1.26) and the enantioselectivity of epoxidation was generally very high (96-98 % *ee*).[88]

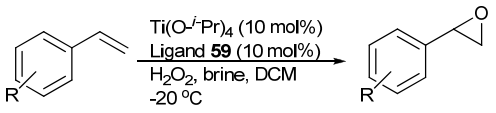

Entry	R	Conv (%)	Yield (%)	*ee* (%)
1	H	73	71	98 (*S*)
2	*o*-Me	70	70	97 (+)
3	*m*-Me	85	84	98 (+)
4	*p*-Me	80	80	98 (*S*)
5	*o*-Cl	21	16	96 (*S*)
6	*m*-Cl	69	66	98 (*S*)
7	*p*-Cl	67	66	98 (*S*)

Table 1.26 Substrate scope with the Ti(O-^{i}Pr)$_4$/ligand 59d system.

More recently Sun *et al.* have reported a synthesis of novel salan and salalen ligands **60** and **61** derived from binaphthol and tested them in the titanium catalysed epoxidation of alkenes.[89] Out of the six ligands tested in the asymmetric epoxidation of styrene, two (**60a** and **61b)** have shown the best catalytic activity and were screened further in the epoxidation of other alkenes (Figure 1.37).

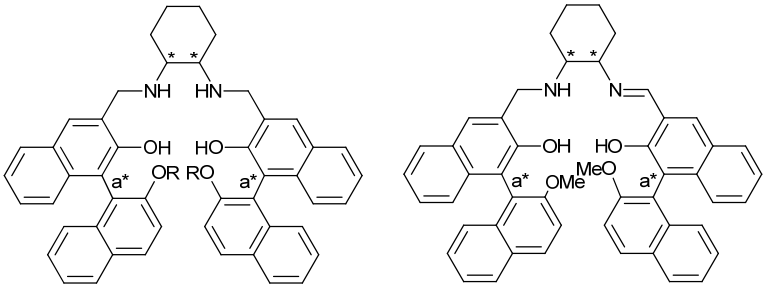

60a (*R*,*R*, S_p,S_p), R = Me
60b (*R*,*R*, S_p,S_p), R = Bn
60c (*R*,*R*, R_p,R_p), R = Me
60d (*S*,*S*, S_p,S_p), R = Me

61a (*R*,*R*, S_p,S_p)
61b (*R*,*R*, R_p,R_p)

Figure 1.37 Structure of ligands 60 and 61 developed and screened by Sun *et al.*

Entry	Substrate	Time (h)	Ligand	Yield (%)	*ee* (%)	Config
1	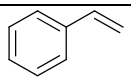	9	**60a**	78	80	(*S*)
2			**61b**	61	79	(*S*)
3	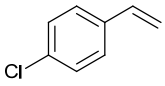	9	**60a**	82	73	(*S*)
4			**61b**	73	76	(*S*)
5	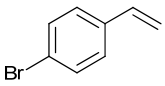	9	**60a**	84	75	(*S*)
6			**61b**	70	71	(*S*)
7	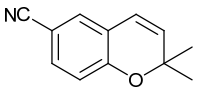	6	**60a**	90	98	(3*S*,4*S*)
8			**61b**	92	99	(3*S*,4*S*)
9	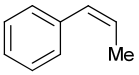	24	**60a**	70	73	(2*R*,3*S*)
10			**61b**	95	80	(2*R*,3*S*)

Table 1.27 Asymmetric epoxidation of various olefins at RT. using ligand/Ti(O-^{i}Pr)$_4$ (10 mol%) and 50 % H_2O_2 (3 eq.).

At present there is no clear mechanism to identify the active species or to explain the origin of the enantioselectivity, however a few interesting facts have emerged. Berkessel has investigated the degradation pathways of the Ti(salalen) complexes such as **62** using mass-spectrometry and kinetic studies.[90] The results (summarised in Figure 1.38) indicate that the Ti(salalen) complex **62** is activated by hydrogen peroxide to form the monomeric peroxo-species **63** which may be the active species. The lifetime of this species is long enough for the epoxidation of electron-rich, conjugated olefins such, as 1,2-dihydronaphthalene. However, it appears to be too short to effectively transfer an oxygen atom to less reactive, electron-poor olefins, such as vinylcyclohexane.[90] The peroxo-species **63** can also decompose by demetallation (pathway A) or by the oxidation of amine functionality following by dehydration resulting in salen complex **66**, which is inactive (pathway B).

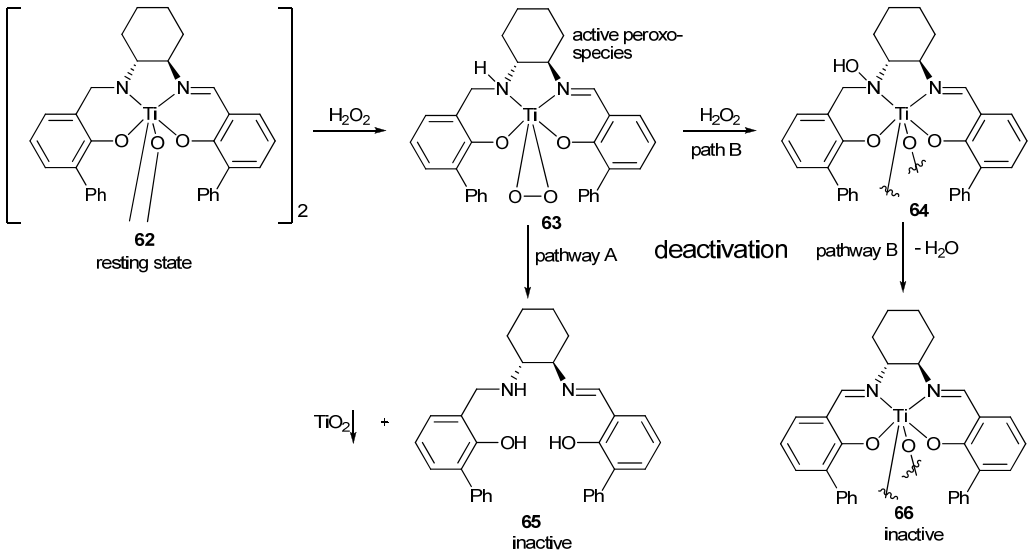

Figure1.38 Decomposition pathways for complex 62.

This is significant as it implicates that the presence of secondary amine functionality is important for successful catalysis. This is supported further by lack of catalytic activity displayed by ligand **59** when the secondary amine is converted to a tertiary amine by methylation.[88]

Based on the decomposition **pathway B** and active peroxo-species **63**, Katsuki proposed that Ti(salan) complexes could react with hydrogen peroxide and oxidise/dehydrate *in situ* resulting in Ti(salalen) type complexes which then undergo further oxidation to give active peroxo-species.[91] However, when ligand **57b** and structurally related ligand **67** were tested under identical reaction conditions different *ee*s were obtained disproving the theory. Thus it appears that although the active species may be similar in both cases, they are not identical.[91]

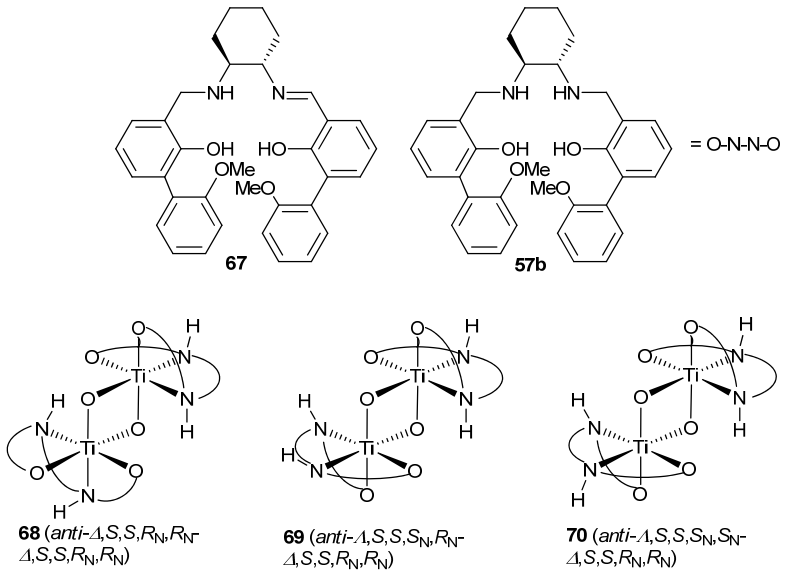

Figure 1.39 Schematic representation of complexes 68-70 synthesised and isolated by Katsuki.[91]

In order to get further insight, Katsuki *et al*. have synthesised and isolated three complexes **68**-**70** arising from ligand **57b**. Complex **68** has a homochiral configuration whereas complexes **69** and **70** are pseudo-heterochiral as the titanium centres in the two units have opposite chirality. Also **69** and **70** are different due to the stereochemistry around the nitrogen atoms. Reaction between complex **68** and hydrogen peroxide resulted in the novel μ-oxo-μ-$\eta^2\eta^2$-peroxo titanium complex **71** which was isolated and crystallised. This novel complex did not react with olefins to give epoxides under stoichiometric reaction conditions. However, when used at catalytic levels in the presence of hydrogen peroxide its reactivity was comparable to that for **68**-**70**. This demonstrated that complex **71** was an intermediate and not the active catalyst. In fact the finding suggests that the active catalyst arises from the dissociation of μ-oxo-μ-$\eta^2\eta^2$-peroxo titanium complexes such as **71** into monomeric species which then catalyse the epoxidation (Figure 1.40).[91]

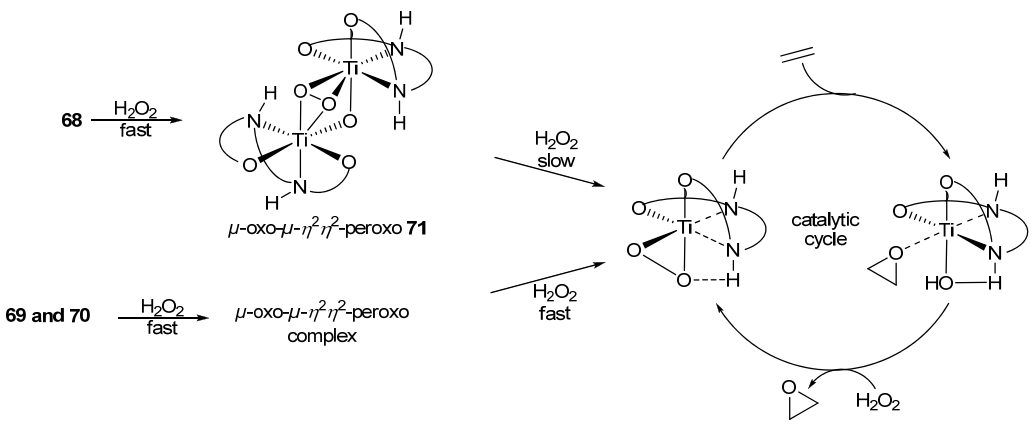

Figure 1.40 A possible reaction pathway.[91]

Though the intrinsic mechanism remains to be clarified and the asymmetric epoxidation of some unfunctionalised olefins still needs to be improved, the titanium/hydrogen peroxide system works very well for the majority of substrates and the high yields and selectivities combined with high atom economy makes this a very useful catalytic system.

1.4.4 Ruthenium

The topic of asymmetric epoxidation of alkenes using chiral ruthenium complexes is well documented and recently was reviewed by Chatterjee.[92] Here the focus will only be on the examples which involve hydrogen peroxide as the terminal oxidant. Such asymmetric epoxidation was first reported by Beller *et al.* in 2004 using Ru(pybox)(pydic) and Ru(pyboxazine)(pydic) complexes (pybox = bis(oxazolinyl)pyridine; pydic = pyridine-2,6-dicarboxylate; and pyboxazine = 2,2'-pyridine-2,6-dily bi(5,6-dihydron-4h-1,3-oxazine)).[92] The choice of ligands was based on both the work reported by Nishiyama *et al.* in the area of ruthenium catalysed epoxidation[93] and the ease with which various chiral variants of the ligands can be obtained from commercially available amino acids.[94] The ruthenium complexes **72-79** were screened for the catalytic activity in the epoxidation of styrene using hydrogen peroxide (Figure 1.41).[94]

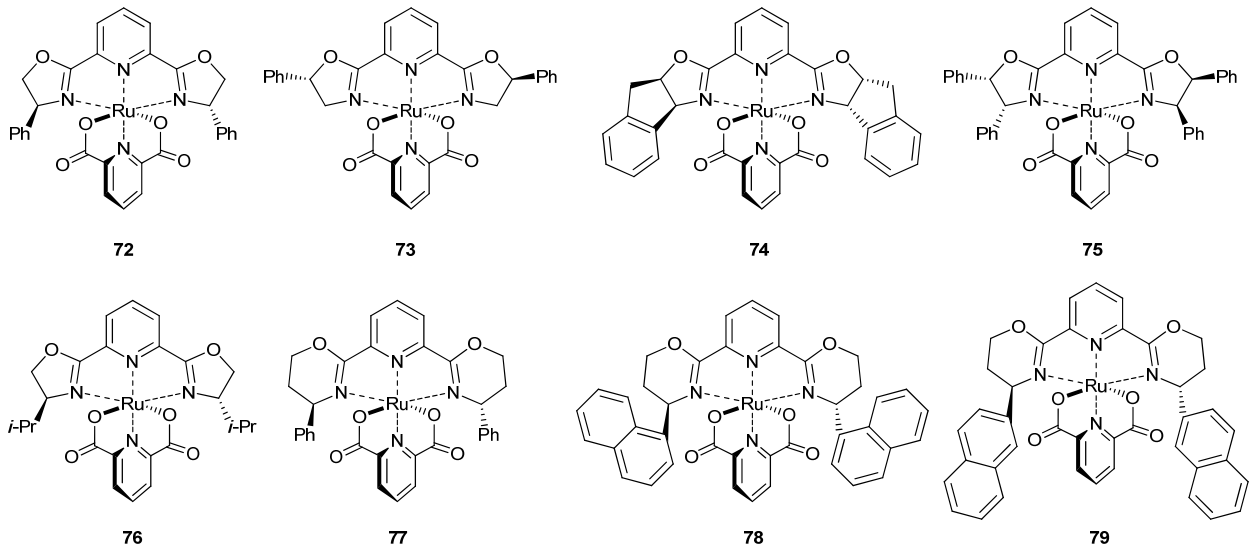

Figure 1.41 Selection of Nishiyama's complexes.

With a catalyst loading of 5 mol% and 3 equivalents of hydrogen peroxide, Nishiyama's ligands afforded yields ranging from 40 to 70 % but with *ee*s never higher than 48 %.

All of the complexes showed different levels of catalytic activity. The pybox complexes gave better yields, however the enantioselectivity was higher with pyboxazine complexes. Complex **79** was judged to be the best screened and was used to carry out the epoxidation of various aromatic olefins, providing yields higher than 90 % with *ee*s values often in the range of 50-70 %. Different aromatic olefins were oxidized in the presence of catalyst **79** in good yields and good *ee*s under mild conditions. Interestingly, the addition of acetic acid as co-catalyst increased

both the yields and the *ee*s. The authors proposed that acetic acid accelerates the rate of the reaction by stabilising the active intermediates against self-degradation.[94]

Since the first report, Beller has reported around 50 structurally related ruthenium complexes.[95-97] All the complexes have shown various degrees of activity in the epoxidation of one or more substrates. Generally, the reported yields for the epoxides were quite high, in some cases reaching >99 %, however the enantioselectivity was not as good and only moderate asymmetric induction (average 50 %) was generally achieved. However, ruthenium complexes such as **80** have shown much better asymmetric induction in the epoxidation of various aromatic alkenes (*ee* up to 71 % and yields up to 100 %).[96, 97]

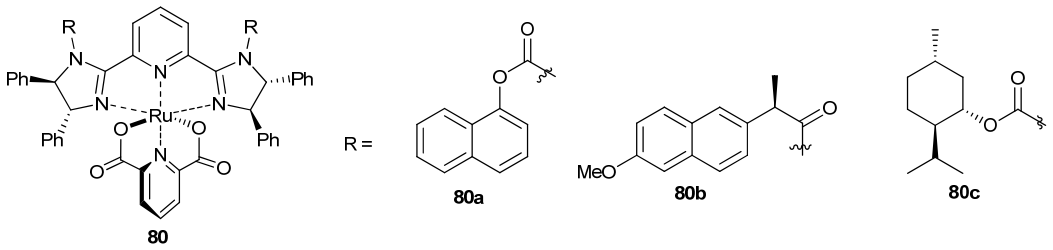

Figure 1.42 Structure of novel Ruthenium complexes 80.

Beller suggested that under the reaction conditions the carboxylate ligand dissociates from the metal centre and thus making its oxidation much faster resulting in a Ru(III) species which then enters the catalytic cycle.[98] Beller *et al*. have also shown that in order to obtain any enantioselectivity the pybox ligand must be C_2-symmetric, as chiral C_1-symmetric ligands do not show any enantioselectivity.[98] Finally, the presence of pydic ligand is also important for the catalytic activity.[98] If pydic is substituted for pyridine-monocarboxylate or bipyridine-monocarboxylate the catalytic activity decreases to <10 %.[98]

1.4.5 Platinum

Michelin and Strukul have carried out a systematic study into the design of platinum complexes which are able to undertake the efficient asymmetric epoxidation of terminal alkenes with hydrogen peroxide. They have shown that the electron-poor platinum complexes containing phosphine and pentafluorobenzene ligands are suitable catalysts, which require only stoichiometric amounts of hydrogen peroxide.[99] They continued to develop the system towards asymmetric epoxidation and in 2006 reported a series of platinum complexes (Figure 1.43) which were capable of transferring chirality.[100]

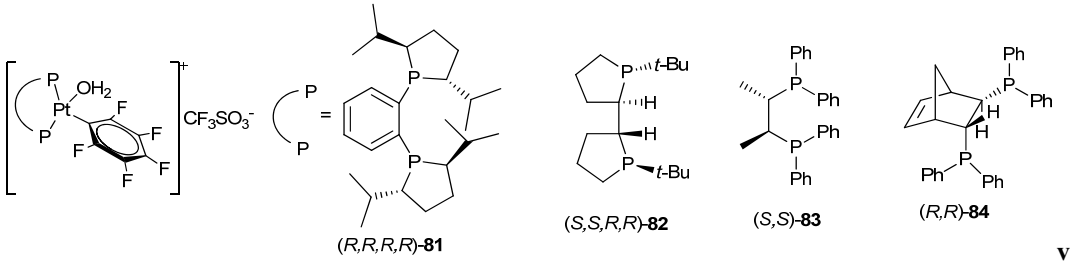

v

Figure 1.43 Asymmetric epoxidation of terminal alkenes with hydrogen peroxide catalysed by Pt(II) chiral complexes.

All four complexes were capable of chirality transfer in the epoxidation of 4-methyl-1-pentene, however complexes derived from ligands **81** and **83** gave epoxides in poor yields (5 %). Since the highest yield (68 %) and *ee* (75 %) were achieved using ligand **83** it was screened further to illustrate its limitations and capabilities in the epoxidation of various terminal alkenes (Table 1.28).

Entry	Substrate	T (^{o}C)	Time (h)	Yield (%)	*ee* (%)	Config
1		-10	24	98	58	(*R*)-(+)
2		-25	24	78	64	(*R*)-(+)
3		-10	24	99	64	(*R*)
4		-10	48	57	72	(*R*)
5[a]		-10	48	63	78	(*R*)
6		-10	20	77	68	(*R*)
7		-10	20	48	83	(*R*)
8		20	5	76	64	(*R*)
9		-10	48	88	79	(*R*)
10		-10	48	81	71	(*R*)
11		20	24	75	66	(*R*)-(-)
12		-10	48	79	75	(*R*)-(-)
13		-10	48	45	76	(*R*)-(-)
14		-10	48	45	82	(*R*)-(-)
15		-10	48	27	84	(*R*)

16	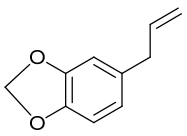	-10	24	64	87	(*R*)
17		-10	24	70	83	(*S*)[b]
18[c]	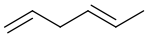	-10	48	93	63	(*R*)

Table 1.28 Catalytic asymmetric epoxidation of terminal alkenes with hydrogen peroxide in dichloroethane mediated by Pt(II) complex (2 mol%) derived from ligand 83. a) reaction carried out in chloroform; b) Pt complex derived from 84 was used; c) 100:0 ratio of terminal:internal epoxide.

In general high yields and good enantioselectivities were achieved for all of the substrates with the exception of Entry 15 where the epoxide yield was low.[100] The length of the alkyl chain has some effect on the selectivity, although *ee*s increased slightly for branched alkenes suggesting that sterics influence the enantioselectivity of the reaction. Alyllic benzene derivatives also proved to be suitable substrates, though styrene was not epoxidized at all.[100] It appears that lower temperatures favour higher enantiomeric excesses. Changing solvent from dichloroethane to chloroform resulted in increased epoxide yield and enantioselectivity.

The epoxidation occurred exclusively at the terminal/less substituted double bond with complete regiocontrol and up to 98 % *ee*.[100] Interestingly this regioselectivity is opposite to that observed in electrophilic oxidations (e.g with *m*-CPBA).[101] Further mechanistic studies revealed that this epoxidation was indeed a rare example of epoxidation of alkenes by means of electrophilic alkene and nucleophilic oxidant activation provided by metal catalysis.[102] Based on the ^{31}P and ^{19}F NMR spectroscopic investigations and kinetic analysis, the mechanism for this platinum-catalysed oxidation can be summarised in Figure 1.44.

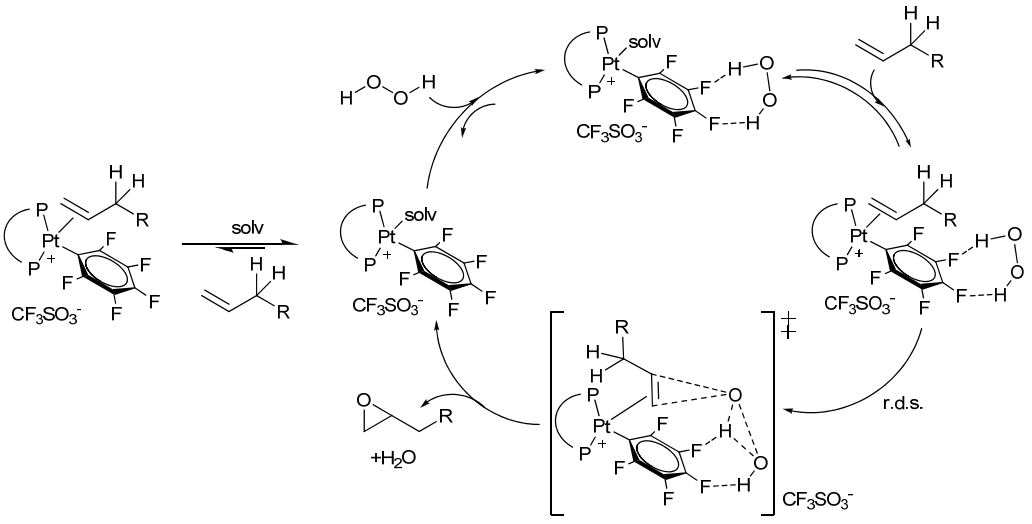

Figure 1.44 Mechanistic hypothesis for the epoxidation of unfunctionalised alkenes catalysed by Pt(II) complexes.

1.4.6 Niobium

Having successfully explored the potential of the Ti(salan) complexes in the epoxidation of unfunctionalised alkenes, Katsuki turned to the asymmetric epoxidation of allylic alcohols with hydrogen peroxide and salan complexes. In order to take advantage of the allylic alcohol functionality, it must be able to coordinate to the metal centre during the oxygen transfer (as in the Sharpless epoxidation system). In the case of titanium salen complexes such coordination is not possible since its coordination sphere is already saturated, hence bigger, group 5, metals were considered. In particular, salan and salalen complexes of niobium and tantalum were prepared and screened for catalytic activity.[103] The initial screening using the UHP adduct showed that the Nb(salan) complex **85** was the best catalyst and it was used for further studies (Table 1.29).[103]

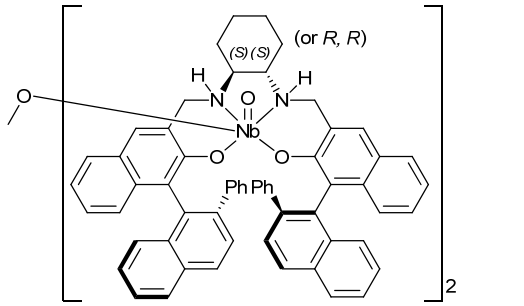

85

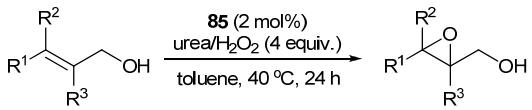

Entry	Substrate	Yield (%)	*ee* (%)	Config.
1	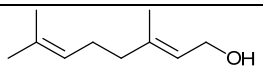	83	81	(2*S*. 3*S*)
2	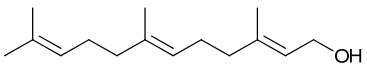	72	80	(2*S*, 3*S*)
3	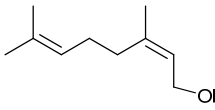	66	80	(2*S*, 3*R*)
4	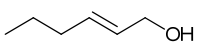	78	80	(2*S*, 3*S*)
5	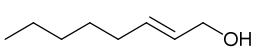	81	79	(2*S*, 3*S*)

Table 1.29 Epoxidation of allylic alcohols with Nb(salan) 85 as catalyst using UHP as terminal oxidant.

The epoxidation of di- and tri-substituted alkenes proceeded with good levels of enantioselectivity irrespective of their geometry;[103] however it was noted that the presence of

geminal substituents diminished the enantioselectivity; also **85** does not catalyse the epoxidation of simple alkenes such as 1,2-dihydronaphthalene, thus showing that presence of an allylic alcohol is required to coordinate to the metal centre.[103]

1.4.7 Rhenium

Methyltrioxorhenium (MTO) is one of the most efficient catalysts in the non-chiral epoxidation of alkenes,[104, 105] but attempts to develop an asymmetric version have met with very limited success. For example, in 1997 Herrman used Troger's base to form chiral MTO complexes, but the epoxidation was completely non-selective.[106] Rudler also failed to obtain any enantioselectivity when MTO and (-)-(4,5)-pinenebipyridine was used as the catalyst.[107] Several other attempts using chiral pyridinamides, bis-amines and bis-oxazolines as ligands in the epoxidation of styrenes gave *ee*s of less than 10 %.[108, 109] The improvement in enantioselectivity was achieved by Corma when the reactions were carried out at -5 or -35 ^{o}C using chiral amines or amides as ligands (Table 1.30) in the epoxidation of unfuctionalised olefins.[110] Though the *ee*s were modest (up to 35 %), the conversions were low, an excess of the alkene was required and the selectivity was also unsatisfactory.

Entry	Substrate	Amine	T (^{o}C)	Conv. (%)[a]	Epoxide (%)	Diol (%)	*ee* (%)
1		L-Prolinamide	-5	12	35	65	4
2		(+)-2-Aminomethyl Ppyrrolidine	-5	18	80	20	5
3		L-Prolinamide	-35	59	96	4	8
4		(+)-2-Aminomethyl pyrrolidine	-35	29	70	30	13
5[b]		L-Prolinamide	-55	15	85	15	9
6[b]		(+)-2-Aminomethyl Pyrrolidine	-55	48	78	22	20
7[b]	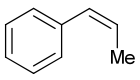	(*R*)-(+)-1-Phenyl ethylamine	-5	10	77	16	35
8[b]	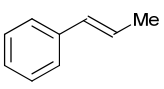	(*R*)-(+)-1-Phenyl ethylamine	-5	10	80	19	20

9 [b]	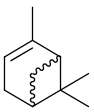	(+)-2-Aminomethyl Pyrrolidine	-5	11	57	25	41 de

Table 1.30 Asymmetric epoxidation of alkenes catalysed by MTO-amine complexes using hydrogen peroxide as terminal oxidant. Reaction conditions: MTO (2.5 mol%) and amine (2.5 mol%) , 8 mmol of substrate and 2 mmol of H_2O_2, DCM (10 mL); time = 7 h at -5 ^oC; 45 h at -35 ^oC and 48 h at -55 ^oC. a) Conversion calculated as percentage of the maximum amount of alkene that can be epoxidised; b) UHP used as oxidant.

Initially the lack of reactivity was explained by intrinsic stereochemical features of the newly formed chiral complexes.[110] Later Herrmann *et al*. proposed that the competing oxidation of coordinated nitrogen to the *N*-oxide reduced the overall yields and diminished the influence of chiral centres on the epoxidation reaction.[111] Hence a number of chiral pyrazoles **86-90**, which are more stable to transformation to their *N*-oxides or other oxidation processes,[112] were synthesised and tested as ligands for the MTO (Table 1.31).[111]

Entry	Ligand	Conv. (%)	*ee* (%)	Entry	Ligand	Conv. (%)	*ee* (%)
1	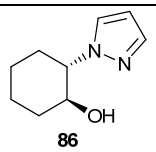 **86**	6	27	**4**	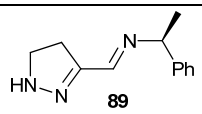 **89**	22	15
2	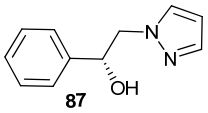 **87**	9	12	**5**	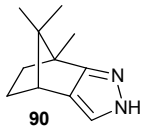 **90**	22	6
3	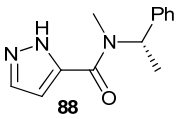 **88**	14	10				

Table 1.31 Epoxidation of *cis-β*-methylstyrene, with MTO (1 mol%) and chiral pyrazole ligands 86-90 (12 mol%) using hydrogen peroxide as the terminal oxidant at -30 ^oC.

Once again, modest levels of enantioselectivity were achieved (up to 27 %), however the conversions were very poor.[111] Prolonging the reaction times or increasing the reaction temperatures increased the yields, albeit at the expenses of enantioselectivity.[111]

Herrmann and co-workers have also attempted to use tartrate derived chiral diols as MTO ligands in order to induce enantioselectivity.[111] However this also resulted in very limited success. The epoxidation of *cis-β*-methylstyrene was carried out between -5 and - 30 ^oC using MTO (1 mol%) and chiral diol (12 mol%), and hydrogen peroxide (1.5 eq.). Out of 10 ligands tested **91-94**, only ligand **92** gave the epoxide with a reasonable level of enantioselectivity(41 % *ee*), albeit with only 5 % conversion.

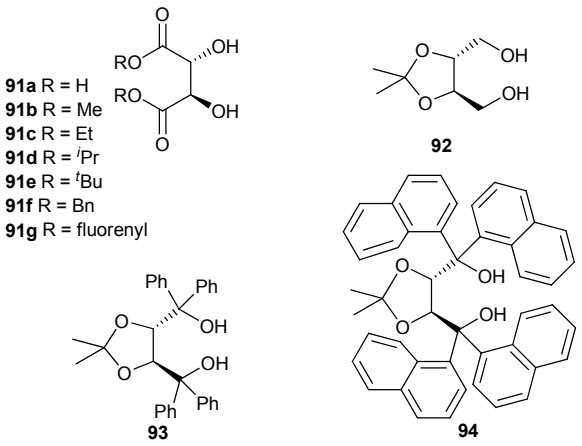

Figure 1.45 Structures of Hermann's ligands.

When ligand **91b** was used no epoxide was produced. The highest conversions were achieved with ligand **91a**, but the *ee*s were the lowest (5 %). All other ligands produced epoxide with *ee*s of 5-18 % and 5-10 % conversions.[111]

Finally, Burke and co-workers, took into consideration the previously reported results and proposed that 2-substituted pyridines, such as **95-100**, would be ideal ligand in the MTO catalysed epoxidations using UHP.[113] The ligands were screened in the epoxidation of various olefins (Figure 1.46).[113]

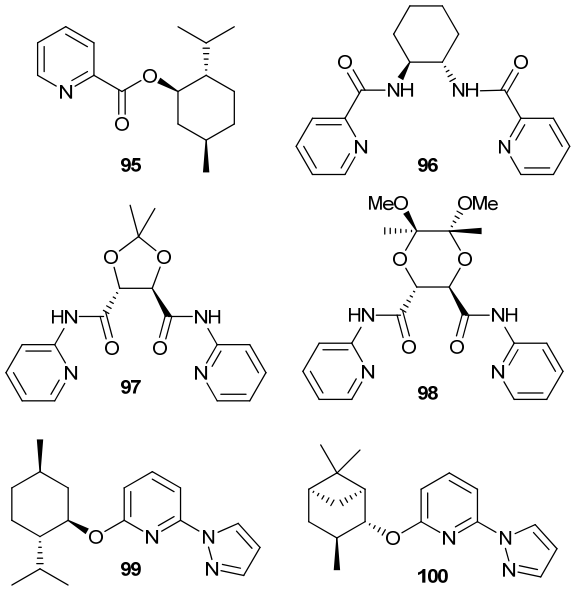

Figure 1.46 Ligands used in the epoxidation of olefins with MTO and UHP.

Although the selectivity for epoxide formation was very good (>98 %) in almost all cases the enantioselectivity of the reactions was very poor, the highest being 12 % in the epoxidation of styrene and 4-methyl styrene. The highest conversions were achieved with ligand **97** in the

epoxidation of 1-methylcyclohexene, though once again the enantioselectivity was very low (7 % *ee*).

1.5 Organocatalytic asymmetric epoxidation

The use of organocatalysts in oxidative transformations has a rich history and has been comprehensively reviewed.[114, 115] The activation of hydrogen peroxide with organic substrates to effect asymmetric epoxidation was first shown with stoichiometric reagents,[116] but it was quickly shown that sub-stoichiometric levels of organocatalysts could be used, for example arenesulfonimidoylimidazoles.[117] Arguably the most effective and widely employed methods that have been developed centre on the use of dioxiranes generated from chiral ketones of which the contributions of Shi and Yang are noteworthy.[118-120] Oxone ($2KHSO_5 \cdot KHSO_4 \cdot K_2SO_4$) was almost exclusively used as the oxygen source for the formation of such dioxiranes until the seminal contribution of Shi who demonstrated that peroxyimidic acid could be formed *in situ* from the reaction of hydrogen peroxide with acetonitrile which effected the formation of the desired dioxirane.[121-123] In addition, the peptide-catalysed asymmetric epoxidation of enones such as the Juliá-Colonna epoxidation is a well established protocol.[124-128] Phase transfer catalysts (PTC) derived from *Chinchona* alkaloids have also been used to great effect.[129-134] A recent innovation in this area has been to add a commercially available surfactant to the PTC system. This was found to improve both reaction rates and enantioselectivties.[132] Herein a summary of recent developments in the area of homogeneous asymmetric organocatalytic epoxidation is presented.

Shi has continued to develop alternative ketone-based organocatalysts to extend the substrate scope of the system.[120] Although the fructose-derived ketone **101** is an effective catalyst for the epoxidation of a wide-ranging set of *trans*- and tri-substituted alkenes, it was somewhat limited for other olefins. Oxazolidinone containing ketones **102** had also been established as excellent catalysts for the epoxidation of *cis*-alkenes, styrenes and some trisubstituted alkenes but it was only recently that the effective application of the RCN-H_2O_2 system was established.[135] A key finding was that ^{n}-BuOH was the most effective solvent and that 3.8 equivalents of ACN and 3 equivalents of H_2O_2 provided optimal results for a range of substrates. Catalyst **102c** was shown to be as effective for a range of substrates in the Oxone system although catalyst decomposition did occur over time which restricts its use to more rapidly reacting substrates. H. Shi has applied this chemistry in an efficient synthesis of the antibiotic (1*R*, 2*S*)-(-)-(1,2)epoxypropylphosphoric acid (fosfomycin) but found that amine **103**, afforded both higher yield and *ee* than the D-fructose derived organocatalyst **101** which was achieved with lower catalyst loading (5 mol% for the

amine *c.f.* 20 mol% for the Shi catalyst). Moreover, the amine was found to be stable under the reaction conditions, whereas the D-fructose derived ligand underwent Baeyer-Villiger oxidation and could not be re-used.[136] The amine was shown to affect the organocatalytic epoxidation of a number of other electron deficient alkenes, although *ee*s were not determined.

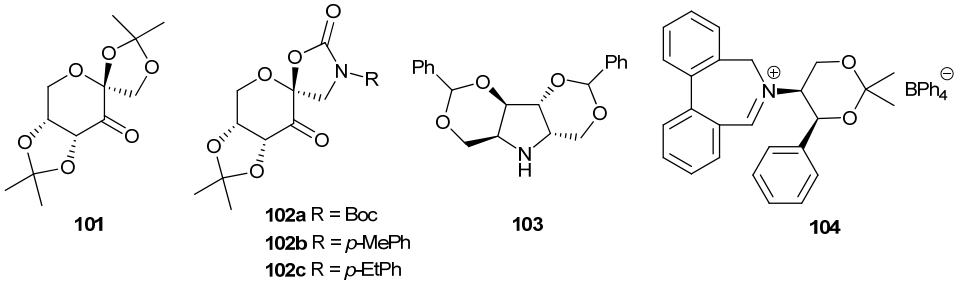

Figure 1.47 Structures of organocatalysts 101-104.

The structurally related oxaziridines, although generally less reactive than dioxiranes, have also found widespread application in asymmetric epoxidation. Standard iminium salt epoxidation conditions employ Oxone as the stoichiometric oxidant, in combination with sodium carbonate in an ACN:H_2O mixture, severely limiting the temperatures that can be used as the mixture freezes at about -10 ^oC and Oxone decomposes under these condition at room temperature. Page *et al*.,[137] elegantly reasoned that although hydrogen peroxide does not induce epoxidation in the presence of iminium salts, by employing a co-catalyst that when oxidised is able to transfer oxygen to the imminium ion, asymmetric epoxidation could be achieved. It was found that biphenylazepinium salt **104** in combination with hydrogen peroxide and a range of hydroxide, hydrogen carbonate and carbonate bases did indeed give epoxidation with moderate ees and optimisation using 1-phenylcyclohexene as the substrate gave an *ee* of 56 %.

α, β-Unsaturated aldehydes, ketones and cyclic enones are suitable targets for organocatalytic epoxidation with hydrogen peroxide due to the reactivity of the intermediate iminium ions formed with amine-based organocatalysts (Figure 1.47). The first report of such catalysis was reported by Jørgensen *et al*.,[138, 139] who showed the efficacy of pyrrolidine **105** in the epoxidation of a range of *α, β*-unsaturated aldehydes in moderate to excellent yield and excellent *d.r.* and *ee* in dichloromethane, and the catalyst was effective in EtOH:H_2O mixtures.

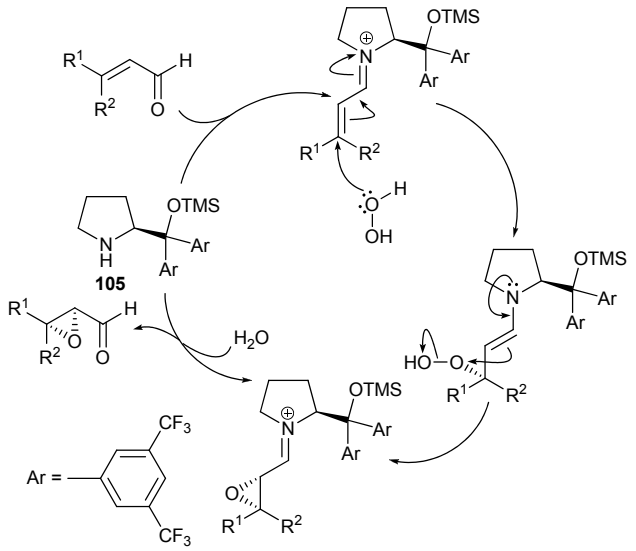

Figure 1.48 The mechanism proposed by Jørgensen *et al.* for the enantioselective epoxidation of *α, β*-unsaturated aldehydes *via* iminium ion intermediates.

Córdova *et al.*,[140-142] followed a similar approach using a number of related pyrrolidines, as well as proline, its analogues and an imidiazolidinone with both H_2O_2, sodium percarbonate and UHP as the oxidants. They also elegantly demonstrated the efficacy of one-pot organocatalytic asymmetric tandem epoxidation-Wittig reaction sequences, the application of iminium/enamine organocatalysis in epoxidation-Mannich cascade reactions,[141] as well as the tandem organocatalytic synthesis of 1,2,3-triols with good *d.r.* and *ee*.[142] List *et al.*,[143] demonstrated the catalytic epoxidation of a broad range of cyclic enones could be achieved with primary amines **106** and **107**. The sense of asymmetric induction was reversed when the pseudoenantiomer quinidine-derived amine **107b** was used. The reaction was proposed to proceed *via* iminium ion **108** in which the second basic nitrogen directs delivery of the peroxide towards one enantioface of the double bond (Figure 1.49).

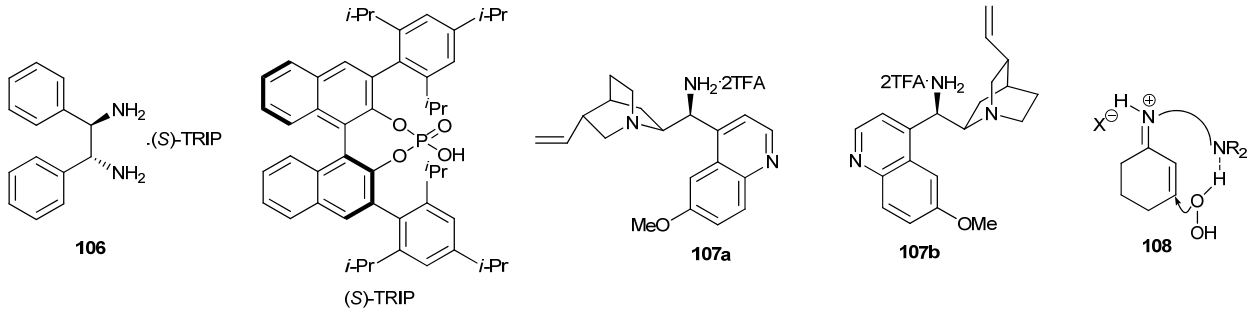

Figure 1.49 Structures of catalysts 106, 107 and proposed iminium ion 108.

In a subsequent study, List *et al.*[144] used **107a** and **107b** in the first example of organocatalytic asymmetric epoxidation of *α, β*-unsaturated ketones using hydrogen peroxide. In this case rather than the direct formation of the epoxide, catalytic asymmetric hydroperoxidation occurred (Figure 1.50). The peroxyhemiketals **109** were formed in reasonable yield with very high

enantioselectivity for linear, branched and cyclic aliphatic side chains, although aromatic and trisubstituted enones were unreactive. The perhemiketals could be converted both to epoxides **110** and aldol-like products **111**, which could also be formed using a one-pot strategy using $P(OEt)_3$. Furthermore the effect of the stereochemistry of the alkene was shown not to affect that of the epoxide, whilst the pseudoenantiomeric catalysts **107a** and **107b** were shown again to give opposite enantiomers.

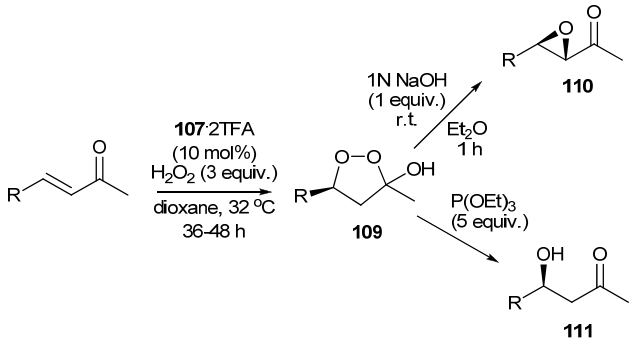

Figure 1.50 The elegant organocatalytic asymmetric hydroperoxidation developed by List *et al.*

Miller *et al*.,[145-147] used *N*-Boc-protected L-aspartate benzyl ester in combination with DCI as a stoichiometric activator, DMAP as an acyl transfer catalysts and hydrogen peroxide to develop optimal reaction conditions using 1-phenylcyclohexene as the substrate. Although there was no enantioselectivity with this system they were able to confirm that the reaction proceeded via the expected pathway and that DMAP-*N*-oxide (which was formed *in situ*) was also as effective as DMAP as an acyl transfer agent. To induce asymmetry in the process a short peptide known to adopt *β*-turn-type structures **112** was introduced together with the introduction of carbamate functionality in the substrate to promote catalyst-substrate interactions though hydrogen bonding. Up to 17 catalytic turnovers could be achieved at 25 °C. The epoxide derived from **113a** (Ar = Ph, n =1) could be obtained in 97 % yield and 89 % *ee* at -10 °C, although the enantioselectivity could be improved by using UHP and running the reaction in toluene (Figure 1.51). The reaction was compatible with both electron-donating and electron-withdrawing *N*-aryl *para*-substituted substrates although homologation of the carbamate function in **113b** (Ar = Ph, n = 2) resulted in complete loss of stereocontrol.

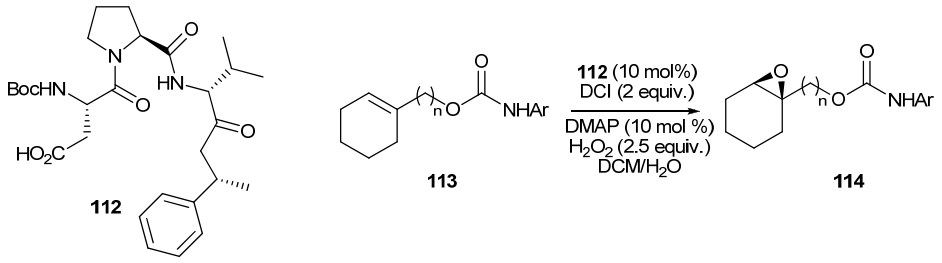

Figure 1.51 Asymmetric epoxidation of carbamate substrates by peptide catalysts 112.

In a follow-up mechanistic study the analogue peptidomimetic **115** was prepared in which the NHBoc of **112** was replaced by a methyl group, and gave **113** (Ar = Ph, n = 1) in an analogous *ee* of 88 % indicating that the group is not involved in hydrogen-bonding interactions. The role of the Pro-D-Val amide group was then probed by its replacement with an alkene isostere, **117**. In this case there was a significant erosion of *ee* and it was shown that **117** existed as 3.5:1 mixture of two distinct catalytic conformers in solution at 23 °C in DMSO-d_6, unlike **116**. In order to include amide-like character in the olefin catalyst **118** was prepared with the anticipation that the fluoroalkene would contribute to a *β*-turn with greater fidelity, which indeed proved to be the case with a 10:1 mixture of conformers under the same conditions. The major conformers for **117** and **118** assigned through extensive 2D-NMR spectroscopy studies appeared consistent with the structure of **115** obtained by single crystal X-ray diffraction. The intermediate *ee* of 52 % with **118** indicates an important role of this residue in stabilising the transition state. Replacement of the C-terminal amide with an olefin in **119** results in poor enantioselectivity (*ee* = 16 %), but the the loss of the *β*-turn structure complicated the analysis.

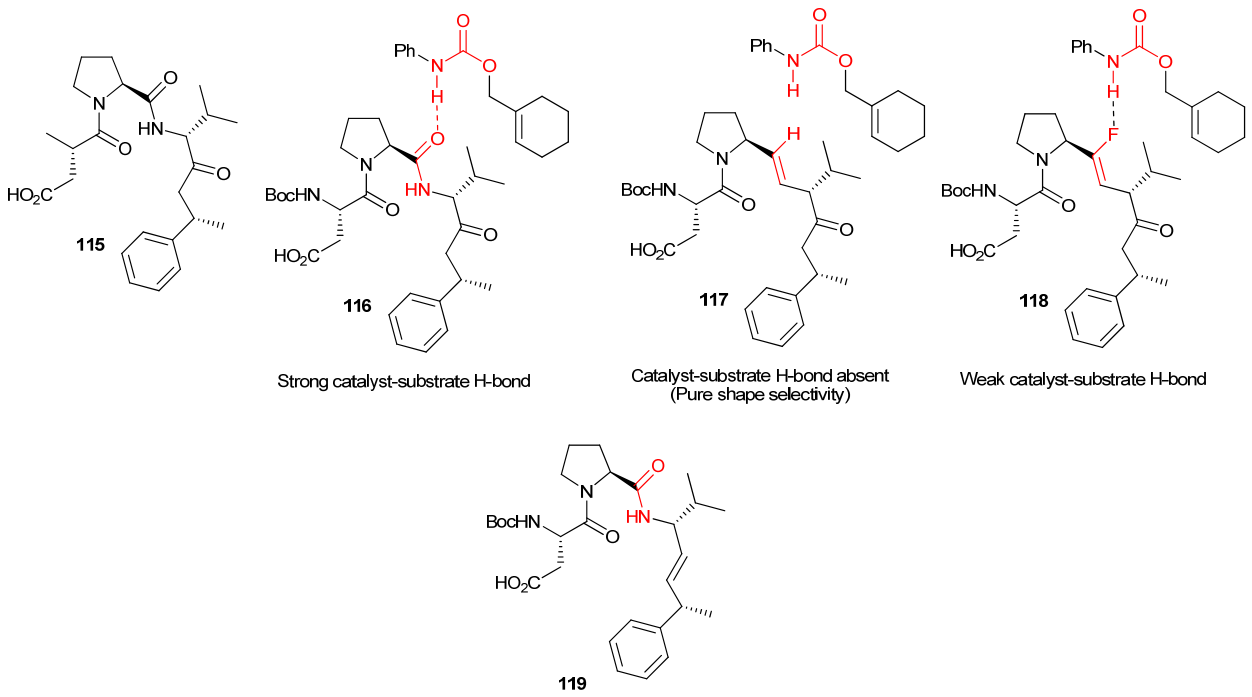

Figure 1.52 Structures of peptide catalysts 115-119.

In a recent report Tanaka and Nagasawa have overcome the moderate to poor *ee*s that have been obtained to date with guanidine organocatalysts by preparing C_2-symmetric bifunctional catalysts which also contain ureas which are capable of hydrogen bonding with both substrate and oxidant (Figure 1.53).[148] A range of catalysts were tested under phase-transfer conditions, including model catalysts lacking either the guanidine or urea, in the epoxidation of *trans*-chalcone. Only catalysts containing both the urea and guanidine groups were effective with **120**

proving to be the best catalyst; the strongly electron withdrawing aryl group was necessary to enhance the interaction of the urea with the reaction substrates. After optimisation of reaction conditions the catalyst was shown to be effective for the conversion of a range of 1,3-diarylenones with both electron withdrawing and/or donating groups in essentially quantitative yield and excellent *ee* (85-96 %).

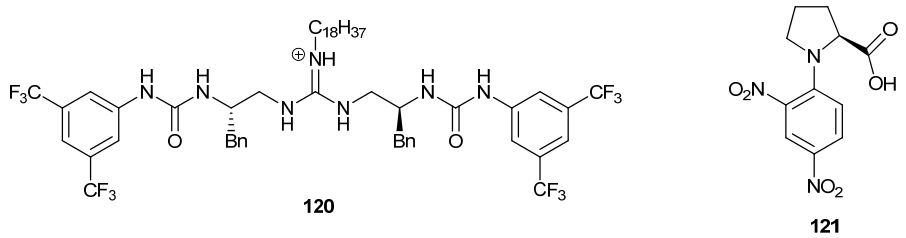

Figure 1.53 Structures of guanidine organocatalyst 120 and proline derived catalyst 121.

Finally Goswami *et al*.,[149] reasoned that sol-gel immobilised *Pseudomonas* lipase G6 could be used as a catalyst to generate peracids *in situ* with hydrogen peroxide and UHP, which in turn could convert alkene susbtrates to epoxides. A series of enantiomerically pure acids were tested for a range of styrene substrates. Proline-derivative **121** proved to be the most effective organocatalyst with good yields and moderate *ee*s reported.

1.6 Concluding remarks

The homogeneous catalysed asymmetric epoxidation of alkenes using hydrogen peroxide and its derivatives as the oxidant has made remarkable steps forward in the last fifteen years, with a large number of new catalytic systems being developed and known catalysts being improved; the developments of the titanium salen/salalen-based complexes have been particularly impressive.

The tendency has been moving towards benign metals, oxidants and solvents, a sign that chemistry is increasingly concerning about environmental issues. Although many of the systems presented in the previous sections were extremely effective in the asymmetric epoxidation of alkenes, providing excellent yields and *ee*s, they are all limited in their application to one or more specific families of alkenes (terminal, electron rich, aromatic, etc.).

The next step in asymmetric catalysis would ideally be the development of a universal system for epoxidation which is active with a larger number of substrates or a system consisting of a ligand that can form catalysts active towards different groups of olefins depending on the metal and oxidant employed. While the ideal catalyst still looks Utopical, remarkable progress has indeed

been seen in asymmetric epoxidation, a field that has definitely left its infancy and moved with big steps towards its golden age.

1.7 References

1. P. A. Brennan and F. Zufall, *Nature*, 2006, **444**, 308-315
2. B. R. Laurence and J. A. Pickett, *J. Chem. Soc., Chem. Commun.*, 1982, 59-60.
3. L. Guo-Qiang, *Pure Appl. Chem.*, 1993, **65**, 1233-1240.
4. C. E. Housecroft and E. C. Constable, *Chemistry: An Introduction to Organic, Inorganic and Physical Chemistry* 2nd edition edn., Pearson Prentice Hall, 2002.
5. T. Eriksson, S. Björkman, B. Roth, A. Fyge and P. Hoglund, *Chirality*, 1995, **7**, 44-52.
6. J. Clayden, S. Warren, N. Greeves and P. Wothers, *Organic Chemistry*, 4 edn., Oxford University Press, 2005, 513-514.
7. J. McConathy and M. J. Owens, *Primary care companion, Journal of Clinic Psychiatry*, 2003, **5**, 70-73.
8. S. C. Stinson, *Chem. Eng. News*, 2000, **78**, 55.
9. W. P. Liu, J. Ye and M. Q. Jin, *J. Agric. Food. Chem.*, 2009, **57**, 2087-2095.
10. N. Karanth, J. Anderson and K. Domsch, *J. Biosci.*, 1984, **6**, 829-837.
11. G. Q. Lin, Y.-M. Li and A. S. C. Chan, *Principles and applications of asymmetric synthesis*, Wiley-Interscience, 2001.
12. A. K. Yudin, *Aziridines and epoxides in organic synthesis*, Wiley-WCH, 2006.
13. J. Zanardi, C. Leriverend, D. Aubert, K. Julienne and P. Metzner, *J. Org. Chem.*, 2001, **66**, 5620-5623.
14. V. K. Aggarwal, H. Abdel-Rahman, R. V. H. Jones, H. Y. Lee and B. D. Reid, *J. Am. Chem. Soc.*, 1994, **116**, 5973-5974.
15. V. K. Aggarwal, J. G. Ford, S. Fonquerna, H. Adams, R. V. H. Jones and R. Fieldhouse, *J. Am. Chem. Soc.*, 1998, **120**, 8328-8339.
16. E. J. Corey, S. Shibata and R. K. Bakshi, *J. Org. Chem.*, 1988, **53**, 2861-2863.
17. A. Traff, K. Bogar, M. Warner and J. E. Backvall, *Org. Lett.*, 2008, **10**, 4807-4810.
18. W. Adam and S. B. Schambony, *Org. Lett.*, 2001, **3**, 79-82.
19. L. Dong and A. K. Sergey, *Angew. Chem. Int. Ed.*, 2001, **40**, 4757-4759.
20. T. Nagase, T. Kawashima and N. Inamoto, *Chem. Lett.*, 1985, 1655-1658.
21. Q. H. Xia, H. Q. Ge, C. P. Ye, Z. M. Liu and K. X. Su, *Chem. Rev.*, 2005, **105**, 1603-1662.
22. B. S. Lane and K. Burgess, *Chem. Rev.*, 2003, **103**, 2457-2474.
23. K. C. Gupta and A. K. Sutar, *Coord. Chem. Rev.*, 2008, **252**, 1420-1450.
24. K. A. Jörgensen, *Chem. Rev.*, 1989, **89**, 431-458.
25. X. T. Zhou, Q. H. Tang and H. B. Ji, *Tetrahedron Lett.*, 2009, **50**, 6601-6605.

26. J. Z. Li, B. Xu, W. D. Jiang, B. Zhou, W. Zeng and S. Y. Qin, *Transition Met. Chem.*, 2008, **33**, 975-979.
27. J. H. Huang, T. Akita, J. Faye, T. Fujitani, T. Takei and M. Haruta, *Angew. Chem. Int. Ed.*, 2009, **48**, 7862-7866.
28. X. B. Cheng, R. Jia, P. S. Li, S. Q. Tu, Q. Zhu, W. Z. Tang and X. D. Li, *Enzyme and Microbial Technology*, 2007, **41**, 258-264.
29. L. Dubois, J. Pécaut, M.-F. Charlot, C. Baffert, M.-N. Collomb, A. Deronzier and J.-M. Latour, *Chem. Eur. J.*, 2008, **14**, 3013-3025.
30. G. C. Dismukes, *Chem. Rev.*, 1996, **96**, 2909-2926.
31. W. Karl, *Angew. Chem. Int. Ed.*, 1994, **33**, 725-728.
32. K. Wieghardt, U. Bossek, B. Nuber, J. Weiss, J. Bonvoisin, M. Corbella, S. E. Vitols and J. J. Girerd, *J. Am. Chem. Soc.*, 1988, **110**, 7398-7411.
33. R. Hage, J. E. Iburg, J. Kerschner, J. H. Koek, E. L. M. Lempers, R. J. Martens, U. S. Racherla, S. W. Russell, T. Swarthoff, M. R. P. Vanvliet, J. B. Warnaar, L. Vanderwolf and B. Krijnen, *Nature*, 1994, **369**, 637-639.
34. C. Bolm, D. Kadereit and M. Valacchi, *Synlett*, 1997, 687-688.
35. C. Bolm, N. Meyer, G. Raabe, T. Weyhermuller and E. Bothe, *Chem. Commun.*, 2000, 2435-2436.
36. J. E. W. Scheuermann, F. Ronketti, M. Motevalli, D. V. Griffiths and M. Watkinson, *New J. Chem.*, 2002, **26**, 1054-1059.
37. S. Pulacchini, K. F. Sibbons, K. Shastri, M. Motevalli, M. Watkinson, H. Wan, A. Whiting and A. P. Lightfoot, *Dalton Trans.*, 2003, 2043–2052.
38. S. Pulacchini and M. Watkinson, *Tetrahedron Lett.*, 1999, **40**, 9363-9365.
39. G. Argouarch, C. L. Gibson, G. Stones and D. C. Sherrington, *Tetrahedron Lett.*, 2002, **43**, 3795-3798.
40. A. Berkessel and C. A. Sklorz, *Tetrahedron Lett.*, 1999, **40**, 7965-7968.
41. D. E. De Vos and T. Bein, *J. Organomet. Chem.*, 1996, **520**, 195-200.
42. K. F. Sibbons, K. Shastri and M. Watkinson, *Dalton Trans.*, 2006, 645-661.
43. D. S. Kopac and D. G. Hall, *J. Comb. Chem.*, 2002, **4**, 251-254.
44. B. C. Gilbert, J. R. Lindsay Smith, A. Mairata i Payeras, J. Oakes and R. Pons y Prats, *J. Mol. Catal. A: Chem.*, 2004, **219**, 265-272.
45. J. R. Lindsay Smith, B. C. Gilbert, A. Mairata i Payeras, J. Murray, T. R. Lowdon, J. Oakes, R. Pons i Prats and P. H. Walton, *J. Mol. Catal. A: Chem.*, 2006, **251**, 114-122.
46. P. Pfeiffer, E. Breith, E. Lübbe and T. Tsumaki, *Justus Liebig's Annalen der Chemie*, 1933, **503**, 84-130.

47. W. Zhang, J. L. Loebach, S. R. Wilson and E. N. Jacobsen, *J. Am. Chem. Soc.*, 1990, **112**, 2801-2803.
48. E. N. Jacobsen, W. Zhang and J. Loebach, *Abstracts of Papers of the American Chemical Society*, 1990, **199**, 241
49. R. Irie, N. Hosoya and T. Katsuki, *Synlett*, 1994, 255-256.
50. K. Bernardo, S. Leppard, A. Robert, G. Commenges, F. Dahan and B. Meunier, *Inorg. Chem.*, 1996, **35**, 387-396.
51. M. A. Garcia, A. Meou and P. Brun, *Synlett*, 1996, 1049.
52. A. Berkessel, M. Frauenkron, T. Schwenkreis, A. Steinmetz, G. Baum and D. Fenske, *J. Mol. Catal. A: Chem.*, 1996, **113**, 321-342.
53. T. Hashihayata, Y. Ito and T. Katsuki, *Tetrahedron*, 1997, **53**, 9541-9552.
54. P. Piëtikainen, *Tetrahedron*, 1998, **54**, 4319-4326.
55. R. I. Kureshy, N.-u. H. Khan, S. H. R. Abdi, S. T. Patel and R. V. Jasra, *Tetrahedron: Asymmetry*, 2001, **12**, 433-437.
56. A. Murphy, A. Pace and T. D. P. Stack, *Org. Lett.*, 2004, **6**, 3119-3122.
57. H. Shitama and T. Katsuki, *Tetrahedron Lett.*, 2006, **47**, 3203-3207.
58. C. M. M. Santos, A. M. S. Silva, J. A. S. Cavaleiro, A. Lévai and T. Patonay, *Eur. J. Org. Chem.*, 2007, 2877-2887.
59. A. Berkessel, M. Frauenkron, T. Schwenkreis and A. Steinmetz, *J. Mol. Catal. A: Chem.*, 1997, **117**, 339-346.
60. A. Murphy, G. Dubois and T. D. P. Stack, *J. Am. Chem. Soc.*, 2003, **125**, 5250-5251.
61. A. Murphy and T. D. P. Stack, *J. Mol. Catal. A: Chem.*, 2006, **251**, 78-88.
62. L. Gomez, I. Garcia-Bosch, A. Company, X. Sala, X. Fontrodona, X. Ribas and M. Costas, *Dalton Trans.*, 2007, 5539-5545.
63. G. Ilyashenko, D. Sale, M. Motevalli and M. Watkinson, *J. Mol. Catal. A: Chem.*, 2008, **296**, 1-8.
64. M. Wu, B. Wang, S. F. Wang, C. G. Xia and W. Sun, *Org. Lett.*, 2009, **11**, 3622-3625.
65. J. Rich, M. Rodriguez, I. Romero, L. Vaquer, X. Sala, A. Llobet, M. Corbella, M. N. Collomb and X. Fontrodona, *Dalton Trans.*, 2009, 8117-8126.
66. E. R. Hao, Z. Y. Wang, L. J. Jiao and S. W. Wang, *Dalton Trans.*, 2010, **39**, 2660-2666.
67. V. V. Rostovtsev, L. G. Green, V. V. Fokin and K. B. Sharpless, *Angew. Chem. Int. Ed.*, 2002, **41**, 2596-2599.
68. M. F. Perutz, *Nature*, 1990, **348**, 583-584.
69. O. A. Karlsen, L. Ramsevik, L. J. Bruseth, O. Larsen, A. Brenner, F. S. Berven, H. B. Jensen and J. R. Lillehaug, *FEBS J.*, 2005, **272**, 2428-2440.

70. S. Ciurli and F. Musiani, *Photosynth. Res.*, 2005, **85**, 115-131.
71. M. J. Coon, *Annu. Rev. Pharmacol. Toxicol.*, 2005, **45**, 1-25.
72. E. Rose, B. Andrioletti, S. Zrig and M. Quelquejeu-Ehteve, *Chem. Soc. Rev.*, 2005, **34**, 573-583.
73. M. Costas, A. K. Tipton, K. Chen, D. H. Jo and L. Que, *J. Am. Chem. Soc.*, 2001, **123**, 6722-6723.
74. F. G. Gelalcha, B. Bitterlich, G. Anilkumar, M. K. Tse and M. Beller, *Angew. Chem. Int. Ed.*, 2007, **46**, 7293-7296.
75. B. Bitterlich, G. Anilkumar, F. G. Gelalcha, B. Spilker, A. Grotevendt, R. Jackstell, M. K. Tse and M. Beller, *Chem. Asian J.*, 2007, **2**, 521-529.
76. C. Marchi-Delapierre, A. Jorge-Robin, A. Thibon and S. Ménage, *Chem. Commun.*, 2007, 1166-1168.
77. F. G. Gelalcha, G. Anilkumar, M. K. Tse, A. Brueckner and M. Beller, *Chem. Eur. J.*, 2008, **14**, 7687-7698.
78. H. L. Yeung, K. C. Sham, C. S. Tsang, T. C. Lau and H. L. Kwong, *Chem. Commun.*, 2008, 3801-3803.
79. K. Matsumoto, Y. Sawada, B. Saito, K. Sakai and T. Katsuki, *Angew. Chem. Int. Ed.*, 2005, **44**, 4935-4939.
80. B. Saito and T. Katsuki, *Tetrahedron Lett.*, 2001, **42**, 3873-3876.
81. K. Matsumoto, Y. Sawada and T. Katsuki, *Synlett*, 2006, 3545-3547.
82. Y. Sawada, K. Matsumoto, S. Kondo, H. Watanabe, T. Ozawa, K. Suzuki, B. Saito and T. Katsuki, *Angew. Chem. Int. Ed.*, 2006, **45**, 3478-3480.
83. A. Berkessel, M. Brandenburg, E. Leitterstorf, J. Frey, J. Lex and M. Schafer, *Adv. Synth. Catal.*, 2007, **349**, 2385-2391.
84. Y. Shimada, S. Kondo, Y. Ohara, K. Matsumoto and T. Katsuki, *Synlett*, 2007, **15**, 2445-2447.
85. Y. Sawada, K. Matsumoto and T. Katsuki, *Angew. Chem. Int. Ed.*, 2007, **46**, 4559.
86. T. Satoh, *Chem. Rev.*, 1996, **96**, 3303-3325.
87. K. Matsumoto, T. Kubo and T. Katsuki, *Eur. J. Chem.,* 2009, **15**, 6573-6575.
88. K. Matsumoto, T. Oguma and T. Katsuki, *Angew. Chem. Int. Ed.*, 2009, **48**, 7432-7435.
89. D. Xiong, M. Wu, S. Wang, F. Li, C. Xia and W. Sun, *Tetrahedron: Asymmetry*, 2010, **21**, 374-378.
90. A. Berkessel, M. Brandenburg and M. Schafer, *Adv. Synth. Catal.*, 2008, **350**, 1287-1294.
91. S. Kondo, K. Saruhashi, K. Seki, K. Matsubara, K. Miyaji, T. Kubo, K. Matsumoto and T. Katsuki, *Angew. Chem. Int. Ed.*, 2008, **47**, 10195-10198.

92. D. Chatterjee, *Coord. Chem. Rev.*, 2007, **252**, 176-198.
93. H. Nishiyama, T. Shimada, T. Itoh, H. Sugiyama and Y. Motoyama, *Chemical Communications (Cambridge)*, 1997, 1863-1864.
94. M. K. Tse, C. Dobler, S. Bhor, M. Klawonn, W. Mαgerlein, H. Hugl and M. Beller, *Angew. Chem. Int. Ed.*, 2004, **43**, 5255-5260.
95. M. K. Tse, M. Klawonn, S. Bhor, C. Dobler, G. Anilkumar, H. Hugl, W. Magerlein and M. Beller, *Org. Lett.*, 2005, **7**, 987-990.
96. S. Bhor, G. Anilkumar, M. K. Tse, M. Klawonn, C. Dobler, B. Bitterlich, A. Grotevendt and M. Beller, *Org. Lett.*, 2005, **7**, 3393-3396.
97. G. Anilkumar, S. Bhor, M. K. Tse, M. Klawonn, B. Bitterlich and M. Beller, *Tetrahedron: Asymmetry*, 2005, **16**, 3536-3561.
98. M. K. Tse, H. Jiao, G. Anilkumar, B. Bitterlich, F. G. Gelalcha and M. Beller, *J. Organomet. Chem.*, 2006, **691**, 4419-4433.
99. E. Pizzo, P. Sgarbossa, A. Scarso, R. A. Michelin and G. Strukul, *Organometallics*, 2006, **25**, 3056-3062.
100. M. Colladon, A. Scarso, P. Sgarbossa, R. A. Michelin and G. Strukul, *J. Am. Chem. Soc.*, 2006, **128**, 14006-14007.
101. M. Colladon, A. Scarso, P. Sgarbossa, R. A. Michelin and G. Strukul, *J. Am. Chem. Soc.*, 2007, **129**, 7680-7689.
102. M. Colladon, A. Scarso, P. Sgarbossa, R. A. Michelin and G. Strukul, *J. Am. Chem. Soc.*, 2007, **129**, 7680.
103. H. Egami and T. Katsuki, *Angew. Chem.Int. Ed.*, 2008, **47**, 5171-5174.
104. W. A. Herrmann and F. E. Kuhn, *Acc. Chem. Res.*, 1997, **30**, 169-180.
105. C. C. Romão, F. E. Kühn and W. A. Herrmann, *Chem. Rev.*, 1997, **97**, 3197-3246.
106. W. A. Herrmann, F. E. Kühn, M. R. Mattner, G. R. J. Artus, M. R. Geisberger and J. D. G. Correia, *J. Organomet. Chem.*, 1997, **538**, 203-209.
107. H. Rudler, J. R. Gregorio, B. Denise, J. M. Bregeault and A. Deloffre, *J. Mol. Catal. A: Chem.*, 1998, **133**, 255-265.
108. S. W. Park, K. J. Kim and S. S. Yoon, *Bull. Korean. Chem. Soc.*, 2000, **21**, 446.
109. S. W. Park and S. S. Yoon, *J. Korean Chem. Soc.*, 2000, **44**, 81.
110. M. Sabater, M. E. Domine and A. Corma, *J. Catal.*, 2002, **210**, 192-197.
111. J. J. Haider, R. M. Kratzer, W. A. Herrmann, J. Zhao and F. E. Kuhn, *J. Organomet. Chem.*, 2004, **689**, 3735-3740.
112. W. A. Herrmann, R. M. Kratzer, H. Ding, W. R. Thiel and J. Glas, *J. Organomet. Chem.*, 1998, **555**, 293-295.

113. E. d. P. Carreiro, G. Yong-En and A. J. Burke, *J. Mol. Catal. A: Chem.*, 2005, **235**, 285-292.
114. W. Adam, C. R. Saha-Moller and P. A. Ganeshpure, *Chem. Rev.*, 2001, **101**, 3499-3548.
115. A. Berkessel and H. Gröger, *Asymmetric Organocatalysis*, VCH, Weinheim, Germany, 2004.
116. A. Berkessel and M. Frauenkron, *Tetrahedron: Asymmetry*, 1996, **7**, 671-672.
117. R. Kluge, H. Hocke and M. Schulz, *Tetrahedron: Asymmetry*, 1997, **8**, 2513-2516.
118. Y. Shi, *Acc. Chem. Res.*, 2004, **37**, 488-496.
119. D. Yang, *Acc. Chem. Res.*, 2004, **37**, 497-505.
120. O. A. Wong and Y. Shi, *Chem. Rev.*, 2008, **108**, 3958-3987.
121. L. Shu and Y. Shi, *Tetrahedron Lett.*, 1999, **40**, 8721-8724.
122. L. Shu and Y. Shi, *Tetrahedron*, 2001, **57**, 5213-5218.
123. L. Shu and Y. Shi, *J. Org. Chem.*, 2000, **65**, 8807-8810.
124. D. R. Kelly and S. M. Roberts, *Biopolymers*, 2006, **84**, 74-89.
125. A. Berkessel, B. Koch, C. Toniolo, M. Rainaldi, Q. B. Broxterman and B. Kaptein, *Biopolymers*, 2006, **84**, 90-96.
126. S. Julia, J. Masana and J. C. Vega, *Angew. Chem. Int. Ed.*, 1980, **19**, 929-931.
127. S. Julia, J. Guixer, J. Masana, J. Rocas, S. Colonna, R. Annuziata and H. Molinari, *J. Chem. Soc., Perkin Trans. 1*, 1982, 1317-1324.
128. A. Berkessel, N. Gasch, K. Glaubitz and C. Koch, *Org. Lett.*, 2001, **3**, 3839-3842.
129. S. Arai, H. Tsuge and T. Shioiri, *Tetrahedron Lett.*, 1998, **39**, 7563-7566.
130. S. Arai, H. Tsuge, M. Oku, M. Miura and T. Shiori, *Tetrahedron Lett.*, 2002, **58**, 1623-1630.
131. E. V. Dehmlow, D. Düttmann, B. Neumann and H.-G. Stammler, *Eur. J. Org. Chem.*, 2002, 2087-2093.
132. S.-S. Jew, J. H. Lee, B.-S. Jeong, M.-S. Yoo, M.-J. Kim, Y.-J. Lee, J. Lee, S.-H. Choi, K. Lee, M.-S. Lah and H.-G. Park, *Angew. Chem. Int. Ed.*, 2005, **44**, 1383-1385.
133. J. Lv, X. Wang, J. Liu, L. Zhang and Y. Wang, *Tetrahedron: Asymmetry*, 2006, **17**, 330-335.
134. K. Hori, M. Tamura, K. Tani, N. Nishiwaki, M. Ariga and Y. Tohda, *Tetrahedron Lett.*, 2006, **47**, 3115-3118.
135. C. P. Burke, L. Shu and Y. Shi, *J. Org. Chem.*, 2007, **72**, 6320-6323.
136. Z. Zhang, J. Tang, X. Wang and H. Shi, *J. Mol. Catal. A: Chem.*, 2008, **285**, 68-71.
137. P. C. B. Page, P. Parker, G. A. Rassias, B. R. Buckley and D. Bethell, *Adv. Synth. Catal.*, 2008, **350**, 1867-1874.

138. M. Marigio, J. Franzen, T. B. Poulsen, W. Zheng and K. A. Jørgensen, *J. Am. Chem. Soc.*, 2005, **127**, 6964-6965.
139. W. Zhuang, M. Marigo and K. A. Jorgensen, *Org. Biomol. Chem.*, 2005, **3**, 3883-3885.
140. H. Sunden, I. Ibrahem and A. Cordova, *Tetrahedron Lett.*, 2006, **47**, 99-103.
141. G.-L. Zhao, I. Ibrahem, H. Sunden and A. Cordova, *Adv. Synth. Catal.*, 2007, **349**, 1210-1224.
142. G. L. Zhao, P. Dziedzic, I. Ibrahem and A. Cordova, *Synlett*, 2006, 3521-3524.
143. X. Wang, C. M. Reisinger and B. List, *J. Am. Chem. Soc.*, 2008.
144. C. M. Reisinger, X. Wang and B. List, *Angew. Chem. Int. Ed.*, 2008, **47**, 8112-8115.
145. G. Peris, C. E. Jakobsche and S. J. Miller, *J. Am. Chem. Soc.*, 2007, **129**, 8710-8711.
146. A. Berkessel, *Angew. Chem.-Int. Edit.*, 2008, **47**, 3677-3679.
147. C. E. Jakobsche, G. Peris and S. J. Miller, *Angew. Chem. Int. Ed.*, 2008, **47**, 6707-6711.
148. S. Tanaka and K. Nasagawa, *Synlett*, 2009, 667-670 and references cited therein.
149. K. Sarma, N. Bhati, N. Borthakur and A. Goswami, *Tetrahedron*, 2007, **63**, 8735-8741.

Chapter 2 - Investigations on the effect of chiral binol-based additives on the stereoselectivity and activity of the TMTACN/manganese system in the epoxidation of olefins with hydrogen peroxide.

The use of additives to tune or modify the activity of a catalytic system is a well-established procedure. As mentioned in the previous chapter, many complexes were found to be more efficient when a co-catalyst was added to the reaction, either to influence the pH or the coordination sphere of the complex. The Mn/TMTACN system was no exception. De Vos firstly realised that the use of an oxalate buffer[1] in the reaction helped suppress the disproportionation of the oxidant; it was found that dicarboxylic acids and 1,3-diones could act as bridging ligands, altering the redox potential of the metal.[2] Other groups built on De Vos' discovery, trying to obtain asymmetric induction in the reaction by employing chiral additives such as ascorbic and aspartic acid, but failed to obtain any enantioselectivity. [3] Other co-catalysts have been screened over the past ten years; bicarbonate,[4] aromatic amino acids[5], salicylic acid,[6] biphenols[7] oxalate and other carboxylic acids.[6, 8] . Apart from ascorbic acid, none of the above additives contained a chiral centre, and in the case of the bisnaphthols, they were not used in their enantiopure form.

A specific class of biphenols, the bisnaphthols (or binols) have been extensively used as ligands in their enantiomerically pure forms in a variety of reactions[9] ranging from Diels-Alder, olefin metathesis, aldol reactions to asymmetric epoxidation. [10-12]

Quian and de Vries[13] used enantiopure 6,6'-disubstituted binol as a ligand in ytterbium based complexes for the epoxidation of unsaturated ketones. They showed how the simple use of (*S*)-Binol could give yields over 90 % and provide an *ee* of 44 %. When 6,6'-dibromo-binol was used, the *ee*. was raised to 60 % and when the substituents in these positions were phenyl groups, the *ee*. exceeded 90 %. In addition, the binol motif has previously been included in the structure of salen ligands used to catalyse several reactions, including highly enantioselective alkyne additions to aldehydes[14] and the asymmetric epoxidation with manganese as the metal. [15, 16]

It was the work on this class of additives by Lindsay-Smith[7] that inspired our research on the use of bisnaphthol derivatives as chiral co-ligands. While studying the effect of the TMTACN complex **122** (Scheme 2.1) in the oxidation of phenols with hydrogen peroxide, Lindsay-Smith noticed that these molecules underwent a one-electron oxidation which turned them into the corresponding radicals and that the ESI-MS trace of the reaction showed the presence of the $O=Mn^{V}$(TMTACN)(biphenol) complex (**123**). The phenol radicals clearly coupled forming

bisphenols which then coordinated to the metal centre. This suggested that complex **122** underwent reductive cleavage during the reaction and suggested that the active species was the mononuclear complex **123**.

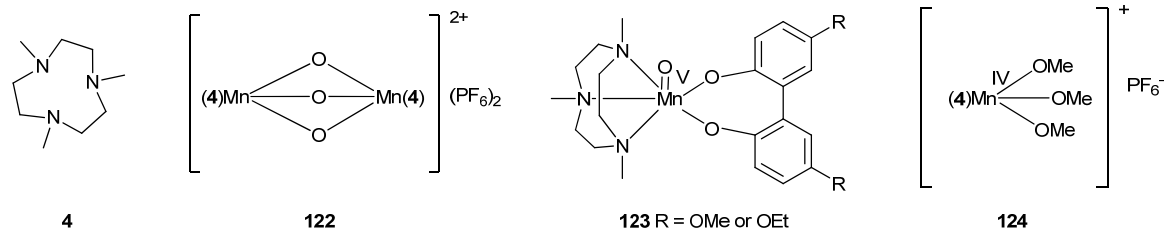

Scheme 2.1 TMTACN best known complex (122), a monomeric form (124) and the active species proposed by Lindsay-Smith the presence of bisphenols as a co-ligand (123).

The group then proceeded to study the effect of different additives on the activity of **122** in the epoxidation of cinnamic acid. A large number of structures were tested and the reactions analysed by mass spectrometry. The oxo-species was observed only when bisphenols and bisnaphthol were used as co-ligands, giving evidence of their stabilising effect. Interestingly, when other potentially coordinating additives were added, for other aromatic diols, the corresponding Mn(III)(**4**)(additive) species was observed by ES-MS but not the oxo-species. Analysis by ES-MS of other additives such as oxalic acid and ascorbic acid (which were found to enhance the catalytic activity of the Mn/TMTACN system) did not show any evidence for their coordination to the metal, suggesting that their role in the reaction might be that of redox co-catalysts, regenerating the catalyst from a potential inert form; a suggestion backed by the lack of enantioselectivity of the reaction when using ascorbic acid.

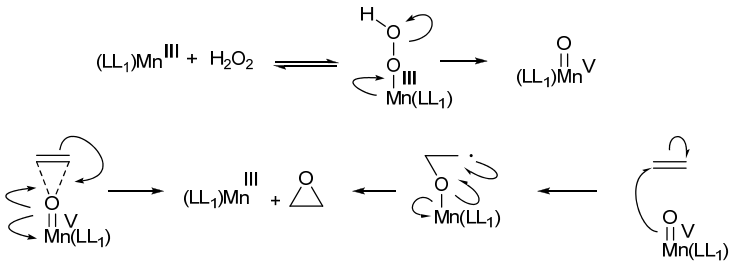

Scheme 2.2 Proposed mechanism for the formation of the active oxo species and mechanisms of oxygen transfer to olefins: concerted (left) stepwise (right). L = TMTACN, L_1 = bisphenol.

Lindsay-Smith proved that the additives coordinate to the metal and the formation of the proposed active species even when using the mononuclear complex **124** and when an *in situ* protocol was used, in which the metal salt, ligand and additive were added together, without the need to use a pre-formed complex. In these studies, though, Binol and the other additives were used as a racemic mixture and the enantioselectivity of the reaction was not considered. The

electronic and steric effects of substituents on the bisnaphthol backbone, as well, were not investigated.

It was therefore decided to explore the effect of optically pure binol and its derivatives on the enantioselectivity of the reaction including the effect of different ring substitutions on the reaction.

2.1 Synthesis of the TMTACN ligand

2.1.1 Retrosynthetic analysis

Our synthesis of TMTACN followed the well established Richman-Atkins cyclisation pathway[17] (Scheme 2.3) reported by Searle[18] with a few minor modifications to the experimental conditions.

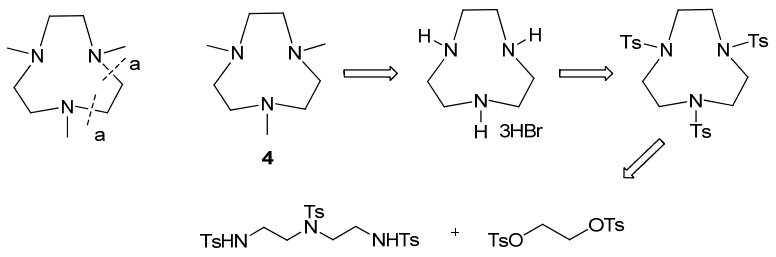

Scheme 2.3 Retrosynthetic analysis of the TMTACN backbone.

2.1.2 Preparation of tosylated triamine and glycol

The tosylation of the readily available diethylene triamine and ethylene glycol, necessary to obtain the cylisation partners **125** and **126** (Figure 2.1) were easily synthesised by reaction with tosyl chloride in DCM with an excess of TEA.

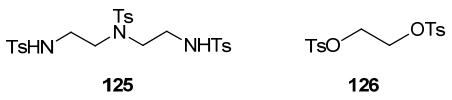

Figure 2.1 Cyclisation partners in the Richman-Atkins reaction.

The reaction mechanism generally requires the presence of a base to remove the HCl formed as a side product. When reacting with the triamine, the use of an additional base is not strictly required, as the amine can act as a base itself. Both reactions provide good yields and the presence of the tosyl group makes the products easy to purify by recrystallisation.

2.1.3 Synthesis of 1,4,7 tritosyl-1,4,7-triazacyclononane

The Richman-Atkins type cyclisation of **125** and **126** was a crucial step in the synthesis of the triprotected TMTACN (Scheme 2.4, **A**, **127**). This cyclisation required accurate control of the conditions to avoid the formation of side products (Scheme 2.4, **B** and **C**). The reaction consisted of two subsequent nucleophilic attacks of **125** on **126**, the first inter-molecular and the second intra-molecular. For the reaction to take place, **125** needed to be converted into its corresponding disodium salt in order to transform the sulfonamide into a stronger nucleophile.

The sodium salt can be generated in several different ways; using sodium hydroxide,[19] potassium carbonate, caesium carbonate,[20] or sodium ethoxide. Another way is to employ alkaline metal hydrides such as lithium hydride[21] or sodium hydride.[18] After the screening, it was found that sodium hydride in DMF afforded superior yields, especially when used in 95% purity.

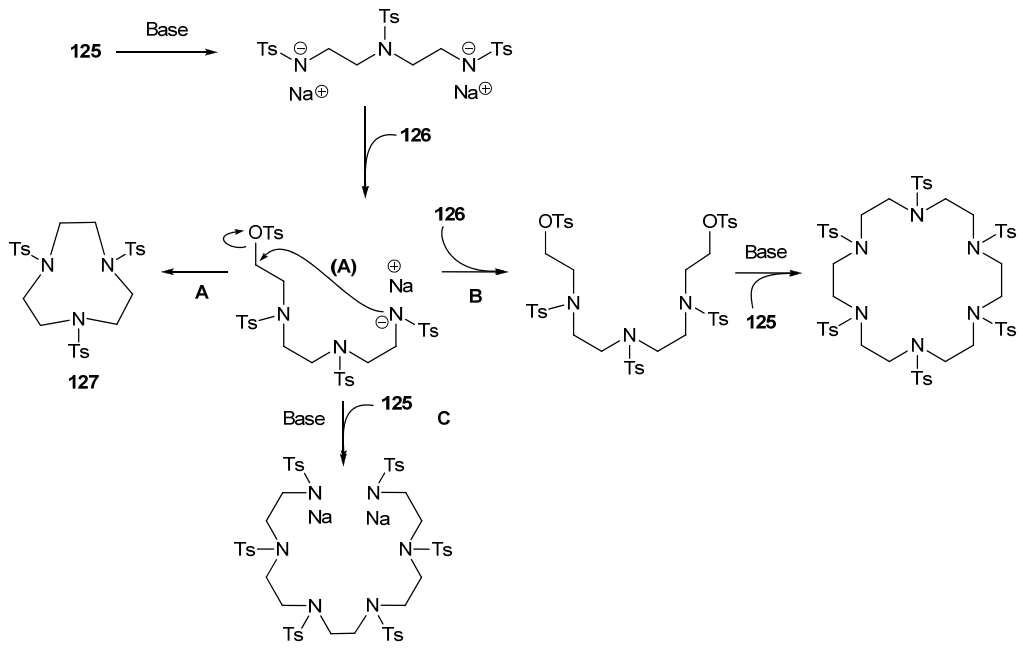

Scheme 2.4 Richmann-Atkins cyclisation and some possible side reactions.

As evident from Scheme 2.4, the cyclization is not straightforward; a number of other side reactions can take place,[22] leading to bigger macrocycles or products of partial addition.[23] To minimise these unwanted reaction pathways, the reaction needed to be performed in sequential steps. The disodium salt was generated first at RT, then the mixture was warmed to 75 °C and left stirring until the hydrogen evolution stopped. The reaction was then warmed to 105 °C and a solution of **126** added dropwise over a 2 hours period. The procedure was carried out under high dilution conditions, to promote the intramolecular reaction (**A**) leading to the desired product.

The slow addition of **126** at high temperature favours the smallest cycle, preventing path **B**; the high dilution prevents polymerization. Despite the accurate control of the conditions, side products were always recovered from the reaction, and a further recrystallisation step was always required.

2.1.4 Deprotection of 1,4,7 tritosyl-1,4,7-triazacyclononane

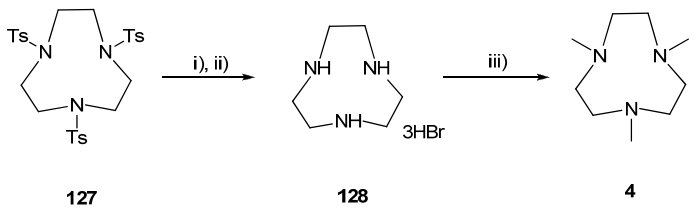

127 **128** **4**

Scheme 2.5 Deprotection and methylation of 127. i) H_2SO_4, Δ; ii) Et_2O, HBr; iii) HCHO, HCOOH, Δ.

Removal of the three protecting groups was achieved by heating **127** in concentrated sulfuric acid; this procedure yielded the hydrosulfate salt of the deprotected molecule (TACN H_2SO_4). The ideal temperature was found to be around 110 °C, which provided a good compromise between reaction time and product recovery. Higher temperatures, in fact, resulted in major loss of product *via* decomposition pathways, while keeping it too low prolonged the reaction for more than three days. Although other procedures were available[24] such as HBr/acetic acid,[25] ammonia and lithium[26] or sodium[27] in THF, the acid reflux was chosen for its simplicity. The product of the reaction is an extremely hygroscopic hydrosulfate salt. To recover the deprotected product, this salt needed to be converted into a more stable form, the hydrobromide **128**. The ion exchange was performed by addition of diethyl ether to the acidic mixture and treatment of the solid obtained with HBr. This procedure gave **128** as an air-stable solid.

2.1.5 Synthesis of 1,4,7-trimethyl-1,4,7-triazacyclononane (4)

The methylation of **128** was conducted using the Eschweiler-Clarke protocol,[28] using formaldehyde and formic acid under reflux. This procedure presents considerable advantages over the more common reaction which employs iodomethane, as amines tend to undergo multiple substitution when treated with an electrophile due to their reactivity. When in the presence of the alkylating agent, like iodomethane, a primary amine can react with up to three molecules of the electrophile giving a quaternary ammonium salt. The mechanism of the Eschweiler-Clarke methylation allows the reaction to stop after the second substitution, since the final product does not have the ability to form the two necessary extra bonds.

2.2 Synthesis of binol derivatives

Despite the absence of chiral carbon atoms, 1,1-bi-2-naphthol (binol) can exist in two different enantiomeric forms due to hindered rotation around the carbon-carbon bond that connects the two aromatic groups; [29] this class of axial isomerism is called atropisomerism. Atropisomerism arises when the free rotation around a single bond is impeded; when this happens the energetic barrier separating the two possible conformations allows for both the isomers to be isolated. Atropisomers can generally be converted into their racemate if sufficient energy is provided to the system usually in the form of thermal energy.

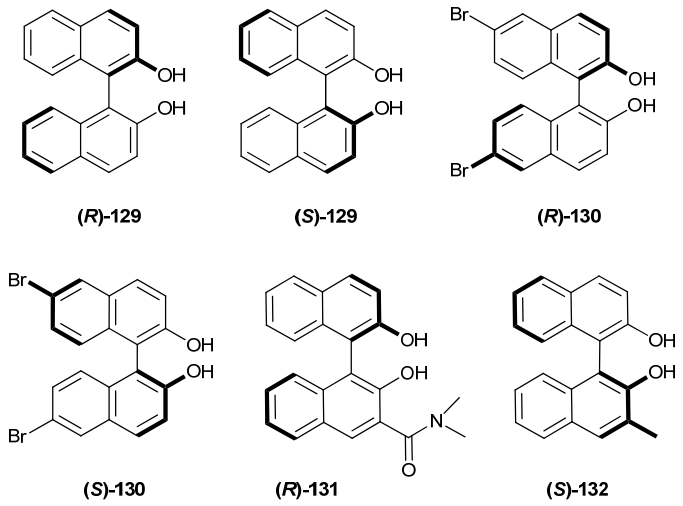

Figure 2.2 Variants of 1,1'-bi-2-naphthol (binol) and derivatives synthesised in this work.

We decided to synthesise and test a set of chiral binol derivatives with different characteristics (Figure 2.2) to explore different effects on the activity of the complex. Both (*R*) and (*S*)- Binol (**129**) were included in this study to assess how these chelating ligands can affect yields and enantioselectivity of the Mn/**4** epoxidation by introducing asymmetry in the complex and changing the electron density on the metal. Assuming that the active species of this complex is the monomeric highly valent oxo species suggested by several studies (Scheme 2.2 and Scheme 2.3),[7, 30-32] a co-ligand capable of donating electron density would stabilise this form and thus make it less reactive, as already suggested by Lindsay-Smith.[33] The latter effect was not considered a major drawback, since our main concern was inducing enantioselectivity in the reaction. Among the potential derivatives it was decided to test a structure bearing electron withdrawing groups in position 6,6' (**130**). Introducing a bromine atom at these positions can influence the electronic density at the oxygen atoms on the other end of the molecule, resulting in reduced donation to the metal centre and a less stabilised (and thus more reactive) oxo-species. 6,6'-dibromobinol has also been shown to catalyse some reactions with higher *ee*s

compared to its unsubstituted relative, possibly due to the steric hindrance of the additional groups. [13]

In order to increase asymmetry in the complex the 3-substituded binol **132** was also chosen. Monosubstituting the already chiral structure and bringing this modification closer to the reaction centre was expected to have a major impact on the enantioselectivity of the reaction. Derivative **132** along with other 3-substituted binols have successfully been employed in the asymmetric ethylation of benzaldehyde in combination with titanium isopropoxide providing high enantioselectivity (79 %).[34]

Along the same line, derivative **131** was synthesised following the methodology proposed by Woodward.[35] Introducing an extra coordinating arm not only increases the asymmetry near the reaction centre, but could also potentially coordinate to the metal via the amine, saturating the coordination sphere. In our view, the pendant arm might act as a labile switch, stabilising the complex under normal conditions, being displaced by hydrogen peroxide during the reaction to form the active species and binding back again after the oxygen transfer. Binols with nitrogen containing pendant arms in position 3 and 3' are known to be active ligands in the enantioselective dialkyl- and diphenylzinc addition to aldehydes and in the synthesis of cyanohydrins. [36-38]

2.2.1 Resolution of 1,1-bi-2-naphthol

Optically pure binol can be obtained by stereoselective coupling of biphenyls or by resolution of the racemic mixture of *S* and *R* isomers.[39] The latter procedure was chosen, being easier, cheaper, more reliable and less time-consuming.

Enantiopure binol was resolved using (*R*, *R*)-*trans*-diaminocyclohexane in toluene. [40] When heating the two reagents to reflux, an inclusion complex of **(*R*)-129**, with the chiral diamine and toluene formed, which crystallized out of the solution upon cooling. The optically pure binol was recovered by dissolving the inclusion complex in water/methanol and treatment with L-(+)-tartaric acid to form the corresponding diamine tartrate salt which is poorly soluble in methanol and was removed by filtration. The other enantiomer, **(*S*)-129**, was recovered from the mother liquor of the first resolution in a similar way, after removal of the remaining diamine by precipitating it as an ammonium tartrate salt.

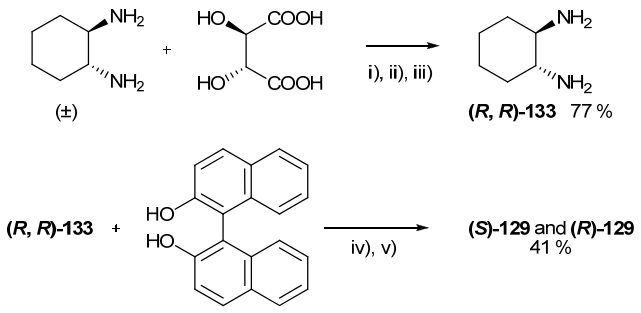

Scheme 2.6 Synthetic route to enantiopure Binol. i) H_2O, AcOH, reflux; ii) HCl/MeOH; iii) KOH; iv) toluene, reflux; v) L-(+)-tartaric acid, H_2O/MeOH, reflux.

The resolution of *trans*-1,2-diaminocyclohexane to isolate the (*R*, *R*) enantiomer was carried out using a known resolution procedure.[40]

2.2.2 Synthesis of 6,6'-di-brominated Binol

The brominated derivatives **130** were obtained by direct bromination of the binol isomers in dichloromethane at -78 °C exploiting the reactivity of the ring to direct the reaction in position 6 and 6'. The latter is in fact the most accessible reactive position while the others are disfavoured for steric reasons.

2.2.3 Synthesis of derivative 131

For the monosubstitution in position 3 on the ring we decided to make use of the intramolecular anionic Fries rearrangement. Intermediate **134** which is the substrate of the rearrangement was prepared by reaction with *N*, *N*-dimethyl carbamoyl chloride.[35] Binol and its reaction partner were reacted in a 1.1:1 ratio to avoid disubstitution.

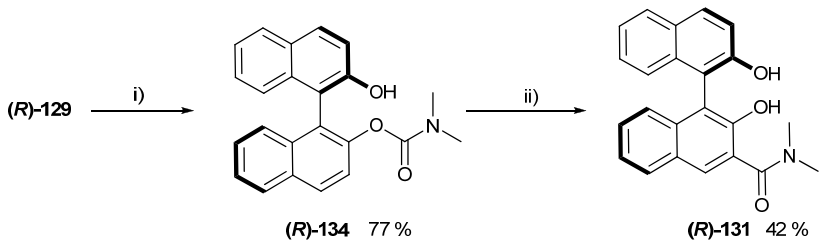

Scheme 2.7 Reaction scheme for structure 131. i) TEA, DMAP, *N*,*N*- dimethylcarbamyl chloride, DCM; ii) *sec*-BuLi, TMEDA, -100 °C to RT.

The intermediate was isolated and treated with *sec*-BuLi at -100 °C to lithiate the molecule in position 3 exploiting the directing properties of the carbamoyl group (*vide infra*). Allowing the reaction to slowly warm up to room temperature favored the Fries rearrangement that leads to the product. Unlike the usual Fries rearrangement, the anionic version does not require a Lewis acid

to promote it and thanks to the coordination to the lithium atom, the second fragment remains close to the molecule at all times, favoring the *ortho*-attack, especially at low temperatures. The standard and photo-induced versions of the Fries rearrangement favour the *para*-position (Scheme 2.8). For A and C (Scheme 2.8) the rearrangement can be both intra- and intermolecular. Generally, high temperatures yield the *ortho*-substituted product while lower temperatures favour the *para*-position.[41]

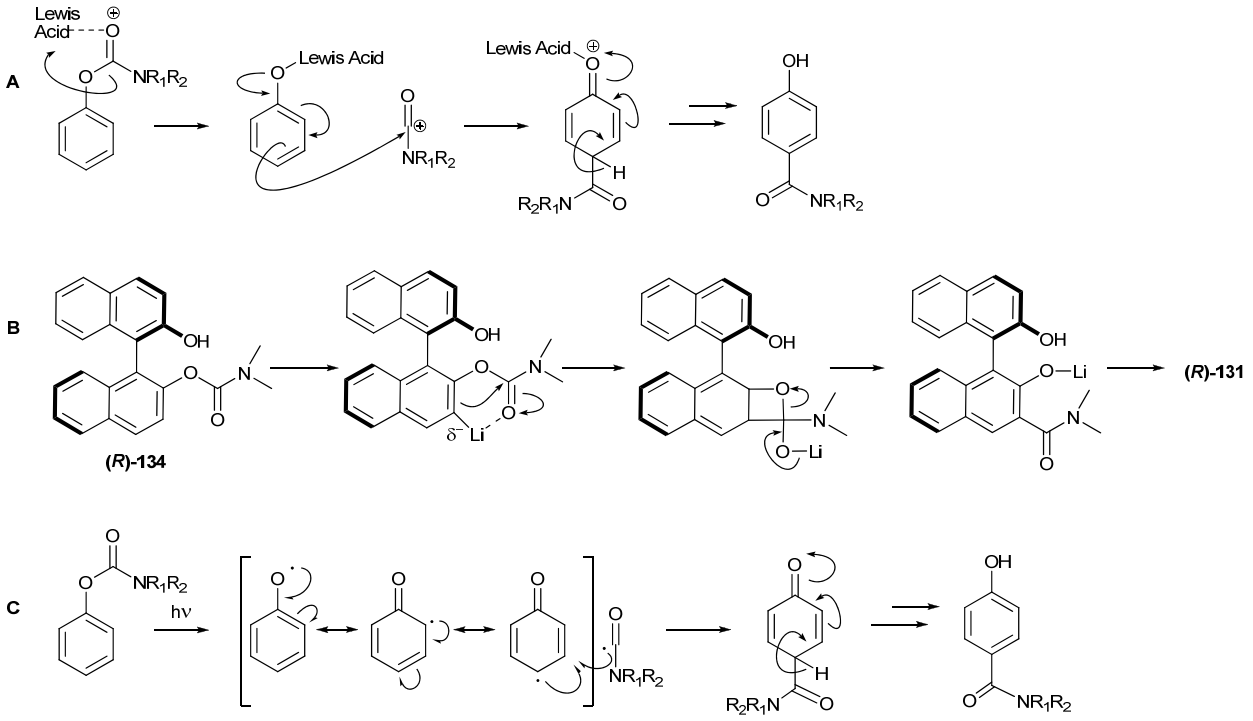

Scheme 2.8 Standard Fries rearrangement (A), anionic Fries rearrangement (B), photoinduced Fries rearrangement (C).

2.2.4 Synthesis of monosubstituted derivative 132

The monomethylation of **(*S*)-129** to give structure **(*S*)-132** was performed in three steps: protection of the alcoholic moiety, directed *ortho*-lithiation and methylation. The introduction of the methyl group in position 3 necessitated both protection of the alcoholic group to avoid unwanted reactions and at the same time a group that could direct the lithiation in the required position. To be successful, the directed metalation group (DMG) needs to be able to behave as a Lewis base (generally having an available lone pair of electrons), where lithium acts as the acid.[42, 43] The reaction is generally performed using alkyllithium reagents like *n*-, *sec*- or ^{t}-Bu-lithium. The mechanism involves coordination of the alkyllithium compound to the DMG followed by deprotonation in the nearest position (*ortho*); the formed aryllithium can then react with electrophiles in an aromatic electrophilic substitution.

The methoxyethyl ether (MEM) selected acts at the same time as protecting and directing group and is easily introduced by reaction of **129** with a base and subsequent reaction with methoxyethyl chloride.

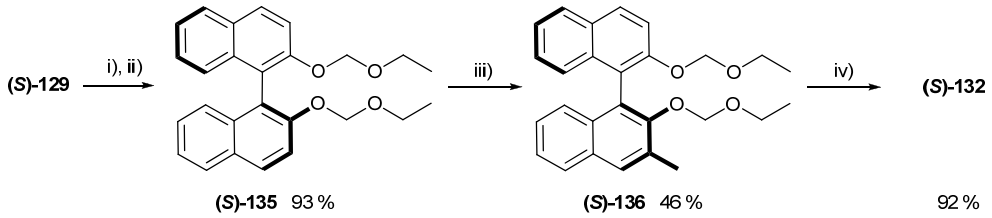

Scheme 2.9 Synthetic pathway to monomethylation of binol in position 3. i) NaH, THF, -78 °C; ii) methoxyethyl chloride, 0 °C; iii) ^{sec}-BuLi, THF, CH_3I, -78 °C; iv) conc. HCl, 60 °C.

The intermediate (**135**) was then treated with the strong base *sec*-BuLi to generate the *ortho*-lithiated species, which was then reacted with iodomethane to give **136**.[34] The MEM protecting group is then easily removed by warming **136** in the presence of hydrochloric acid.

2.3 Activity of additives in the asymmetric epoxidation of olefins.

Given their successful applications, the first explorations of the effect of the binol-based additives synthesized were performed following the conditions reported in the literature,[7, 44] generating the complex *in situ*[53] by addition of the selected components from stock solutions in ACN or water. The ratio of manganese/TMTACN/additive used was 1:3:2 as suggested by Lindsay-Smith.[7] In the study though, several variations to the published procedure were introduced. Lindsay-Smith employed a catalyst to substrate ratio of 1:1.6, but with the main aim being to perform a kinetic study of the reaction, and this high ratio was chosen to avoid errors due to catalyst degradation; in the presented tests, the catalyst loading stopped at 1 mol% since the interest focused on the use of the system as a catalyst. The other major modification regarded the solvent system; instead of a 1:1 mixture of water and ACN, ACN only was used, and the metal was added from a stock solution in water. The total volume of the test reactions was kept at 5.8 or 6 mL to avoid solubility issues, resulting from a different water to ACN ratio. Recognising styrene as one of the most used substrates in the epoxidation literature (as well as one of the most difficult), with a large number of systems active in its epoxidation to compare to, it was decided to make it the first test substrate.

2.3.1 Effect of the additives in the epoxidation of styrene

*2.3.1.1 Additives **129***

The first additives employed were **(*R*)**- and **(*S*)-129** (Table 2.1), and, as expected, the system was found to be active in the epoxidation of styrene with a catalyst loading of 1 % using 10 equivalents of hydrogen peroxide as the oxidant. In the presence of **(*S*)-129**, at RT, the consumption of styrene reached 94 % within 30 minutes with a 62 % yield of the epoxide; after this point, the epoxide started to decompose, probably to give diols or other over-oxidation products (Figure 2.3). Maximum values recorded after 30 minutes of the reaction are shown in Table 2.1. The reaction was carried out alongside blanks in which either the metal, the additive or TMTACN were absent and one where only the oxidant was present to monitor any existing background oxidation. No background oxidation was observed and the blanks did not result in any reaction apart from the one in which the additive was not added, which corresponds to the Mn/TMTACN system which proved extremely reactive with nearly quantitative conversions and very high epoxide yield after one hour (Table 2.1, Figure 2.3). Decomposition of the products was extremely low in this case, being barely noticeable over 3 hours.

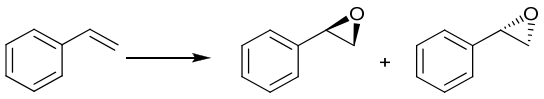

Additive	Max styrene consumption (%)	Max epoxide yield (%)
(*S*)-129	94	62
(*R*)-129	95	60
***rac*-129**	95	62
none[a]	99	96

Table 2.1 Activity of additives 129 in the epoxidation of styrene. Values obtained from chiral GC analysis. a) values after 1 h. $MnSO_4$ monohydrate 0.01 eq., TMTACN 0.03 eq., 129 0.02 eq., H_2O_2 10 eq. premixed with acetone (3:1 v/v), ACN, RT, substrate 1 mmol.

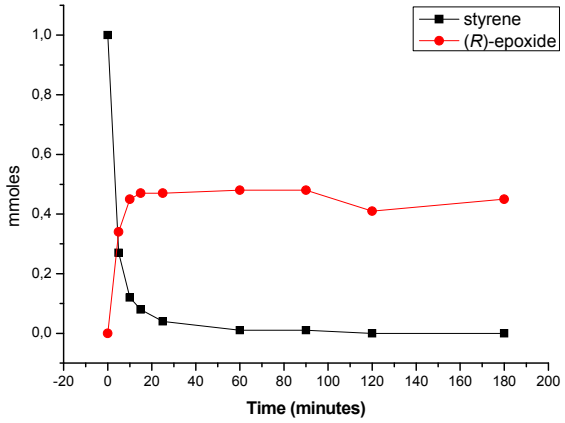

Figure 2.3 Reaction profile in the absence of additives.

Calculation of yields and conversion has then been made on the (*R)*-epoxide with the products assumed to be racemates.

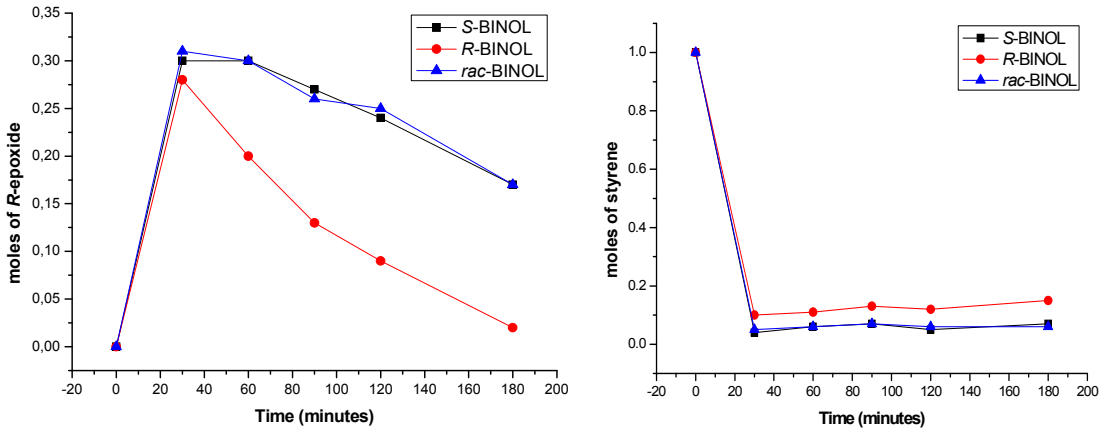

Figure 2.4 Epoxide formation (left) and styrene consumption (right) for additives 129.

Despite the activity of the system, no enantiomeric excess was observed and the oxidation produced a racemic mixture of epoxides. A slightly higher amount of the (S)-enantiomer was always detected via GC in both cases, but after a control test performed using racemic **129** and one without additives, the possibility of this being an actual *ee* was discarded. The difference was systematically present in all analyses, and the amounts of epoxides constantly differed by *ca*. 15 % of each other. The results with (*R*)-binol were slightly different; styrene consumption was lower and epoxide decomposition was faster, because the test procedure was still being refined. A repetition of the experiment gave values in line with the trend shown by **(*S*)-129**.

*2.3.1.2 Additives **130***

Trying to increase asymmetry in the complex, both of the enantiomers of 6,6'-dibromo-binol were synthesised and tested under the same conditions (Table 2.2); also *rac*-6,6'-dibromo-binol was employed in a control experiment. Again, styrene consumption was maximal after 30 minutes; epoxide decomposition was observed in this case too after the maximum conversion was reached (Figure 2.5). The difference between binol and its dibromo-derivative does not only lie in steric bulk; the Br-substituents, in fact, have an electronic effect on the π-system of the ring. Bromine exerts an inductive electron withdrawing effect that is transmitted through the aromatic system to the oxygen atom involved in the coordination with the metal. Less electronic density on the oxygen atom implies a reduced donation to the metal and this might affect the stability of the high valent oxo-species which is believed to be the active species in the transfer of oxygen to the alkene. The decreased stability can potentially make it more prone to react with the substrate.

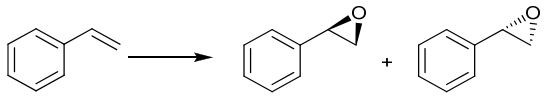

Additive	Max styrene consumption (%)	Max epoxide yield (%)
(*S*)-130	96	76
(*R*)-130	96	82
***rac*-130**	92	80

Table 2.2 Activity of additives 130 in the epoxidation of styrene. Values obtained from chiral GC analysis.

No enantioselectivity emerged from the test reactions, despite the newly introduced bulky substituents that proved effective in increasing the enantioselectivity of several other metal catalysed reactions.[13]

Once again we noticed a slight discrepancy between the epoxide yields, which can be probably attributed to the protocol employed for the preparation of the samples for GC analysis. A small aliquot of the reaction mixture is withdrawn and diluted in ACN and finally filtered through a silica plug before injection. Considering the rate of epoxide decomposition, a delay in the procedure may lead to a sample containing significantly less product; also, a withdrawal made few minutes after the 30 minutes mark will result in a slightly different amount of epoxide. The

results obtained, anyway, supported the first hypothesis since both conversions and yields proved superior to those obtained with structure **129**.

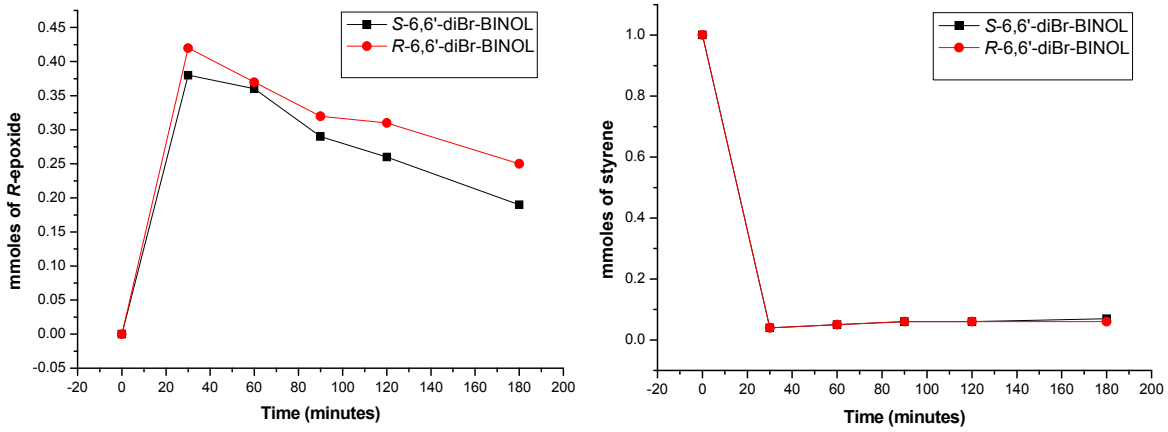

Figure 2.5 Epoxide formation (left) and styrene consumption (right) for additives 130.

The reactions were carried out alongside blanks in which either the metal, the additive or TMTACN were absent and one where only the oxidant was present to monitor any existing background oxidation. No background oxidation was observed and the blanks did not result in any reaction apart from the one in which the additive was removed, which corresponded the original Mn/TMTACN system (see Table 2.1).

*2.3.1.3 Additive **132***

The 3-methyl derivative of (*S*)-binol **(*S*)-132** was synthesized with the aim of making the structure of the catalyst more asymmetric. The 3,3'-methyl substituted binol was not considered because it was supposed to be unable to differentiate the space around the complex due to its symmetry.

Additive	Max styrene consumption (%)	Max epoxide yield (%)
(*S*)-132	97	76

Table 2.3 Epoxide formation and styrene consumption for additive 132.

Despite all our considerations, **(*S*)-132** gave no enantiomeric excess, although 97% of styrene consumption could be achieved in as little as 15 minutes. As with the other additives, after this peak the epoxide started decomposing again (Figure 2.6).

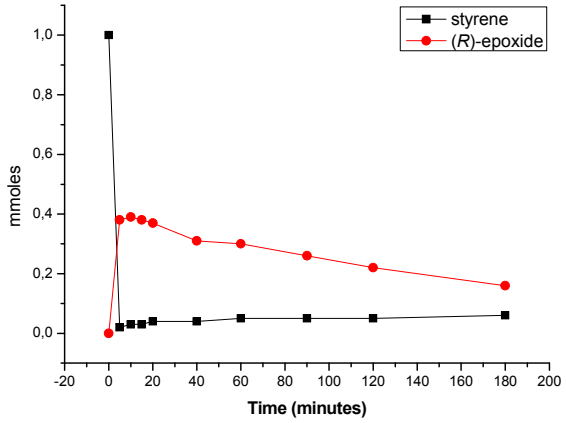

Figure 2.6 Reaction profile for additive (*S*)-132.

The reaction was conducted under the same conditions employed for derivative **129** and **130**; a test carried under the same conditions but without adding any additive resulted in 99 % consumption of the olefin in 60 minutes. The epoxides were obtained in a yield of over 96 %; once again with a profile compatible with the Mn/TMTACN system.

*2.3.1.4 Additive **131***

The last additive being tested was **(*R*)-131**, bearing a pendant arm which was thought to be able to coordinate to the metal centre. The test was performed using the standard reaction conditions (*vide supra*) with the addition of 1 mL of DMSO to solubilise the additive, which proved poorly soluble in water, acetonitrile and acetone. No activity was detected after a 3 hour reaction, with no substrate consumption occurring. Despite the lack of activity, it is reasonable to believe that coordination of the additive to the metal centre occurred; otherwise the results should match those of the Mn/TMTACN system. Additive **131** was chosen for the potential coordinating ability of its substituents, and the results suggested that coordination did occur, but that the binding to the metal was not reversible in the presence of hydrogen peroxide as we hoped. The extra coordination to the amine presumably saturates the coordination sphere of the complex (Figure 2.7) and in the absence of the postulated "ON/OFF" process in which the extra coordinating group is replaced by the oxo-species when in the presence of hydrogen peroxide, the active species cannot form. A further reason for the inactivity can also be found in the activity of the system in the oxidation of sulfoxides to sulfones[33] and is not possible to exclude *a priori* that the complex oxidised the DMSO and consumed all the oxidant without affecting the styrene.

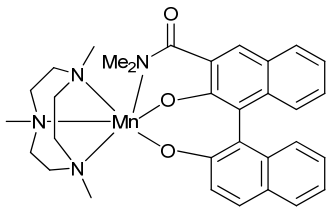

Figure 2.7 Proposed structure for the complex Mn/TMTACN/131.

2.3.1.5 Effect of additives on epoxide decomposition

Worried about the instability of the epoxides in this reaction conditions, a test was designed to determine if the acidic protons of binol could be catalyzing the decomposition of the products. In this test, an intermediate of the synthesis of **(*S*)-131**, (*S*)-2,2'-bis(methoxymethoxy)-1,1'-binaphthyl (**(*S*)-135**) was used as the additive. In this molecule the protons of the alcoholic moiety have been removed by transforming the groups into ethers. This structure should not be able to coordinate to the metal through its oxygen atoms and possesses no acidic proton that would be liberated or available to catalyse an epoxide ring-opening reaction. The standard conditions employed for the previous additives were used, and to our surprise the results proved to be nearly identical of those obtained when no additive was used (Figure 2.8).

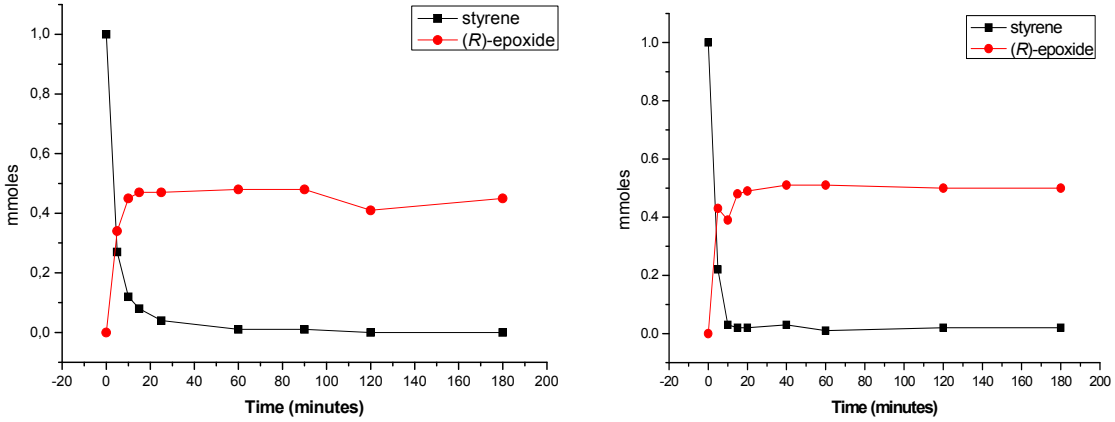

Figure 2.8 Reaction profile for Mn/TMTACN without additive (left), and Mn/135/TMTACN (right).

These results made us suspect that **(*S*)-135** was unable to coordinate to the manganese centre to produce the expected active species in our conditions. What can be noted, though, is that no epoxide decomposition is present, suggesting the phenolic additives play a role in the decomposition process.

To better understand this phenomenon, we explored the effect of the amount of additive on the decomposition process. In the original protocol, the binol additives were added in a two-fold excess, which left one equivalent free and unbound that could act as a proton donor and catalyse

the ring-opening of the epoxides. Reducing the amount of additive to one equivalent should ensure that all the binol is bound to manganese. Diminishing the amount of TMTACN in the reaction to observe the effect on the reaction rate and yield was also considered; the tridentate ligand is in fact added in a threefold excess.

A series of tests was then performed varying the ratio of the components, moving from the standard ratio of 1:2:3 for manganese/additive/TMTACN to 1:2:2 and 1:1:1 (Figure 2.9).

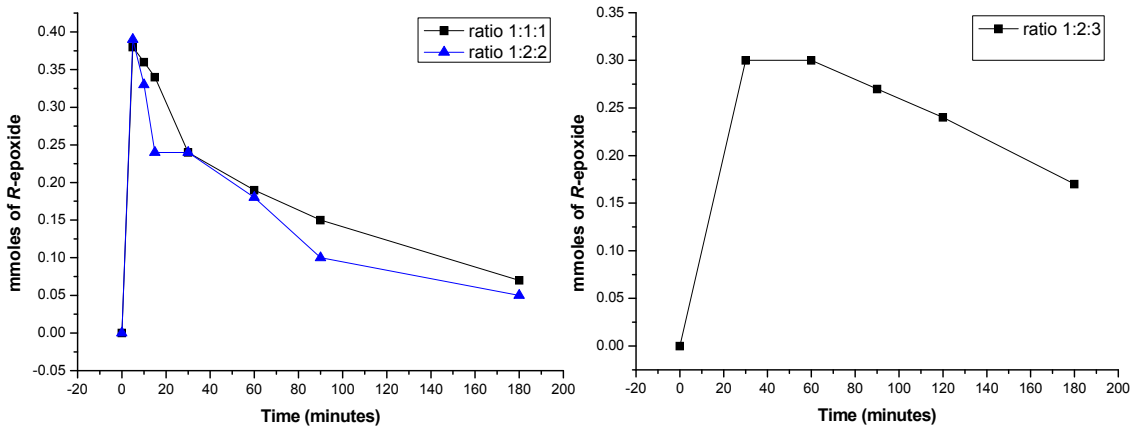

Figure 2.9 Reaction profiles for the epoxidation of styrene with Mn/(*S*)-129/TMTACN, ratios 1:1:1, and ratio 1:2:2 (left), ratio 1:2:3 (right).

The styrene consumption was comparable in both 1:2:2 and 1:1:1 systems, with around 90 % consumed after 15 minutes and the epoxide yield did not differ noticeably from the original conditions; the apparent difference is due to the timescale of the experiments. Unexpectedly, the 1:1:1 and the 1:2:2 system did not show any particular change in the reaction profile, leaving us without a clear explanation on the origin of the effect, and speculating that the acidic catalysis thought to be responsible for the degradation happens in the same way whether the additive is complexed to the metal or free.

2.4 Kinetic study of the epoxidation of styrene and selected derivatives

To deepen the understanding of the effect of binol-based additives on the activity of the Mn/TMTACN system, a simplified kinetic study of the epoxidation of styrene with hydrogen peroxide **122** was undertaken, the ultimate aim of which was to obtain a Hammett plot to cast light on the nature of the transition state of the epoxidation reaction.

In 1937, Hammett[45] empirically derived an equation to correlate the reaction rates of the hydrolysis of substituted benzoic acid esters and equilibrium constants for the ionisation of their

corresponding substituted benzoic acids, and showed them to have a linear free energy relationship. Only *meta*- and *para*-substituents were considered for their electronic effect, since *ortho*-substituents gave also a steric contribution to the outcome of the reaction. Hammett's equation (Equation 2.1) is one of the most used tools for the interpretation and prediction of mechanisms in organic reactions based on the electronic effect of substituents on the substrate; [46] the equation underwent several improvement and refinements over the years after its disclosure, but these still essentially correlate rates and equilibrium constants through a substituent specific constant (σ) and a reaction constant (ρ).

$$\log\left(\frac{k_s}{k_0}\right) = \rho \cdot \sigma$$

Equation 2.1 Hammett's equation expressed as a function of rate constants

Historically, the parameters were determined empirically from the comparison of the rate constant of the hydrolysis of the ethyl ester of benzoic acid (k_0) and the rate constant for the substituted ones (k_s); the slope of the plot of k_s/k_0 versus σ (ρ), described the sensitivity of the reaction to the electronic effect of the substituents, and provided information on the transition state of the reaction. The sign of ρ, in particular, indicates whether a reaction is accelerated or suppressed by electron-donating or electron-withdrawing groups, revealing if charge is built up in the transition state during the reaction, giving insight into the mechanism of the reaction. A negative value, for example, is correlated with a build-up of positive charge in the rate limiting step, which means that the reaction rate will be suppressed by electron-withdrawing substituents, while the size of the reaction constant tells how susceptible the reaction is to the effect of the substituents.

Hammett parameters have been measured for several families of reactions and for more than 500 substituents and several sets of them have appeared in the literature. It was noted that some substituents tended to deviate from linearity, an effect due to conjugation. The equation considers only an electronic effect of inductive nature, thus when plotting data for substituents with a strong electronic effect that can be transmitted through the ring by conjugation, they deviate from the linear trend; for this reason new sets of coefficients that consider this effect have been derived (σ^+ and σ^-). When the data fit better with the corrected values σ^+ and σ^-, it gives an indication that the transition state of the reaction is strongly influenced by conjugation effects. Hammett plots are also often used in the determination of structure-activity relationships in biological studies.[46, 47]

2.4.1 Kinetic studies on the epoxidation of styrene

In a study, Lindsay-Smith studied the electronic effect of substituents in the epoxidation of cinnamic acids with an *in situ* generated Mn/TMTACN complex in the presence of oxalic acid as the additive *via* a Hammett correlation.[33] Oxalic acid was found to increase the reaction rate three- to five-fold while bisnaphthols reduced it two- to three fold, suggesting a stabilization of the active species and a reduction of its reactivity. The reaction constant (ρ) obtained by the group indicated that the active oxidant is an electrophilic species since the negative ρ value calculated from their Hammett plot is consistent with a positive charge building up on the transition state.

To determine whether the reduction in reaction rate was due to the stabilizing effect of the electron-rich bisnaphthols ligands or to a different reaction pathway, it was decided to obtain a Hammett plot of the epoxidation of styrene with the system Mn/TMTACN/bisnaphthol for a limited number of substituted styrenes. For this study the *in situ* generation of the active system was substituted for the pre-formed TMTACN/Mn dimeric catalyst (**122**); in each reaction (*S*)-6, 6'-dibromo-binol (**(*S*)-130)** was included, the most active of the additives among those screened in this work. The dimer was employed after considering the work of Lindsay-Smith on the cleavage of **122** by additives such as **130** to form active monomeric species like **123**.[7, 31] These results confirmed that the structure arising from the cleavage would match the one prepared *in situ*. To rule out any contribution to the epoxidation given by the dimer alone, a series of kinetic experiments were performed with catalyst loading of 0.1, 0.5 and 1 mol% and resulted, not surprisingly, in a total lack of activity of the system in the epoxidation of styrene. The reaction with the lowest catalyst loading was monitored for three hours, the second (0.5 mol%) for two hours and the last for one hour, during which no consumption of substrate or epoxide formation was detected. To the best of our knowledge, no epoxidation of styrene catalysed by **122** alone has ever been reported, and even the early records of use of **122** in epoxidation catalysis involved the presence of additives. Although the first significant report of the activity of **122** in the epoxidation of alkenes by Hage *et al.*[48] did not use additives *per se*, a bicarbonate buffer was used, and a 100 fold excess of oxidant was required for activity. The first aim of using such buffer was obviously to control the pH of the reaction, but recent findings that bicarbonate is active in the epoxidation of alkenes with manganese(II) salts cannot preclude a secondary role as the oxidant, in addition to controlling the pH. [4, 49]

It has to be noted that the catalyst loading has been calculated as a function of the number of manganese centres and not on the dimer itself, since the active species is believed to be

monomeric and derived from cleavage of the dimer **122** by the additive. The derivation of a Hammett plot was undertaken to gather information on the nature of the transition state by the analysis of the value and sign of ρ. We included styrene (for reference) and two *para*-substituted styrenes (methyl- and chloro-) one electron donating and one electron withdrawing. At 1 mol% of catalyst loading, the epoxidation is generally complete within one hour therefore it was decided to study the behavior of the reaction in the first minutes to determine the initial reaction rates.

No kinetic study including **122** and a binol-based additive is present in the literature but it is reasonable to draw a parallel with the work of Shul'Pin[50] and Feringa.[51] Shul'Pin presented a detailed kinetic study of the epoxidation of cyclooctene with **122** in the presence of acetic acid and highlighted a series of different processes that involved the catalyst. The study postulates that the catalyst undergoes several transformations rather than converting simply into its active species (in epoxidation) and the existence of a number of competing processes at different stages of the reaction (Scheme 2.10).

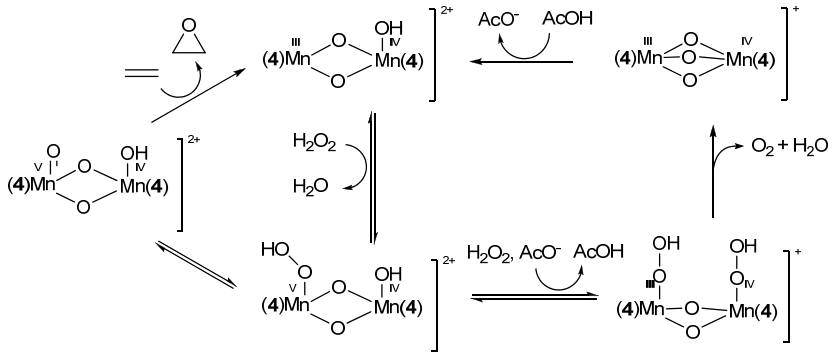

Scheme 2.10 Some of the species proposed by Shul'Pin to be present in the epoxidation of cyclooctene with 122, H_2O_2 and acetic acid.

Along the same lines, Feringa proposed an alternative mechanism involving the coordination of carboxylates to the metal centres, but that shared the hypothesis that multiple equilibria are at work in the generation of the active species in epoxidation (Scheme 2.11). Importantly, Feringa's study did not support the existence of dimmers in this system as proposed by Lindsay-Smith for the system under investigation herein.

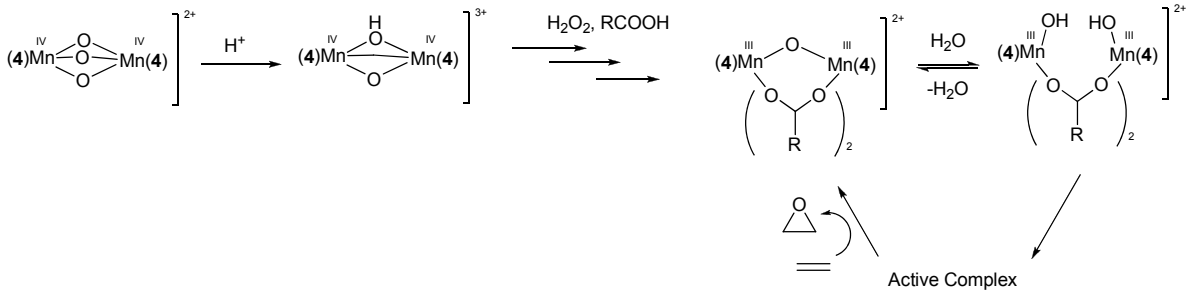

Scheme 2.11 Some of the intermediates proposed by Feringa in the epoxidation of alkenes with 122 and carboxylic acids

Although there are substantial differences between the systems discussed above and the one presented in this study given that no compelling mechanistic evidence is present in the literature regarding the cleavage of **122** by a bisnaphthol it must be assumed that related intermediates and equilibria are also present. The resulting reaction rates extracted from the kinetic data therefore do not represent the activity of a single species but rather a measure of the overall effect of all the ongoing processes in the first minutes of the reaction.

For the determination of the rate constants it was decided to consider only the initial phase of the reaction, where the concentration of substrate was considered constant and in large excess compared to the catalyst. The oxidant is added in large excess and is considered constant. Here the rate would only be dependent on the active catalytic species present in solution, assumed to be constant. In Equation 4.2, [Cat] represents the concentration of active catalytic species in the reaction, assumed to be equal or directly proportional to the concentration of catalyst employed.

$$v = -\frac{d[Olefin]}{dt} = k[Olefin][Cat]$$

Equation 4.2 Simplified rate equation for the epoxidation of olefins with the system presented.

In the first minutes, the reaction can be assumed to be first order in olefin, which leads to a simplification of the rate law (Equation 4.3). The rate constant can be determined as a function of the catalyst loading.

$$v = -\frac{d[Olefin]}{dt} = k_{obs}[Olefin] \text{ where } k_{obs} = k\,[Cat]$$

Equation 4.3

To obtain the value of k_{obs} from kinetic data, it is necessary to integrate and reorganise Equation 4.3 in the following way (Equations 4.4-4.6).

$$-\int \frac{d[Olefin]}{dt} = \int k_{obs}[Olefin]$$

$$\int \frac{1}{[Olefin]} d[Olefin] = -k_{obs} \int t\, dt$$

$$\ln[Olefin] = -k_{obs}\, t$$

Equation 4.4, 4.5 and 4.6 Integration of the rate law rate law

The rate constant (k_{obs}), can therefore be extrapolated as the slope of the curve of the logarithm of the concentration of substrate *versus* time. In this specific case, the constant k_{obs} is measured in the first stages of the reaction, and corresponds to the initial rate constant.

Experiments were performed with different catalyst loading to calculate the rate constant with respect to the concentration of active catalytic species. From a set of kinetic data with a constant substrate concentration it is then possible to graphically extrapolate *k* (Equations 4.2 and 4.7).

$$k_{obs} = k\,[Cat]$$

Equation 4.7

By plotting k_{obs} against the catalyst loading, it is in fact possible to determine the rate constant as the slope of the curve obtained.

2.4.1.1 Determination of the rate constant for styrene and derivatives and determination of the Hammet reaction constant

Styrene was used as the reference substrate for this kinetic study in order to determine the Hammett plot for the reaction. The formation of the epoxide was followed by HPLC for variable periods of time, with the emphasis on the earlier minutes where points were collected more often. Figure 2.10 shows the disappearance of substrate over time.

The epoxidation of styrene was then performed maintaining a constant concentration of styrene constant and varying the catalyst loading in order to determine its effect on the rate of the reaction. Reactions with a catalyst loading of 0.1, 0.25, 0.5, 1, 1.5 and 2 % were performed and monitored by HPLC. The reaction profiles and the calculated k_{obs} values are reported in Figure 2.10, 2.11 and Table 2.4.

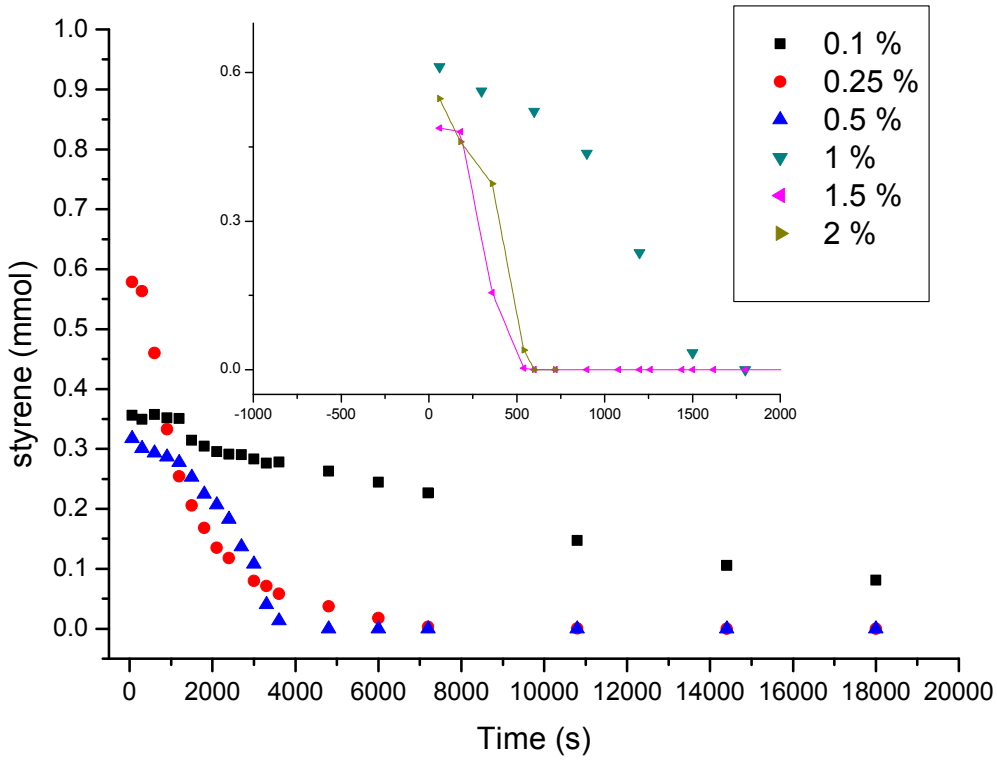

Figure 2.10 Reaction profiles of styrene epoxidation at different catalyst loadings (inset: 1 mol%, 1.5 mol% and 2 mol%); mmol = mmoles of styrene.

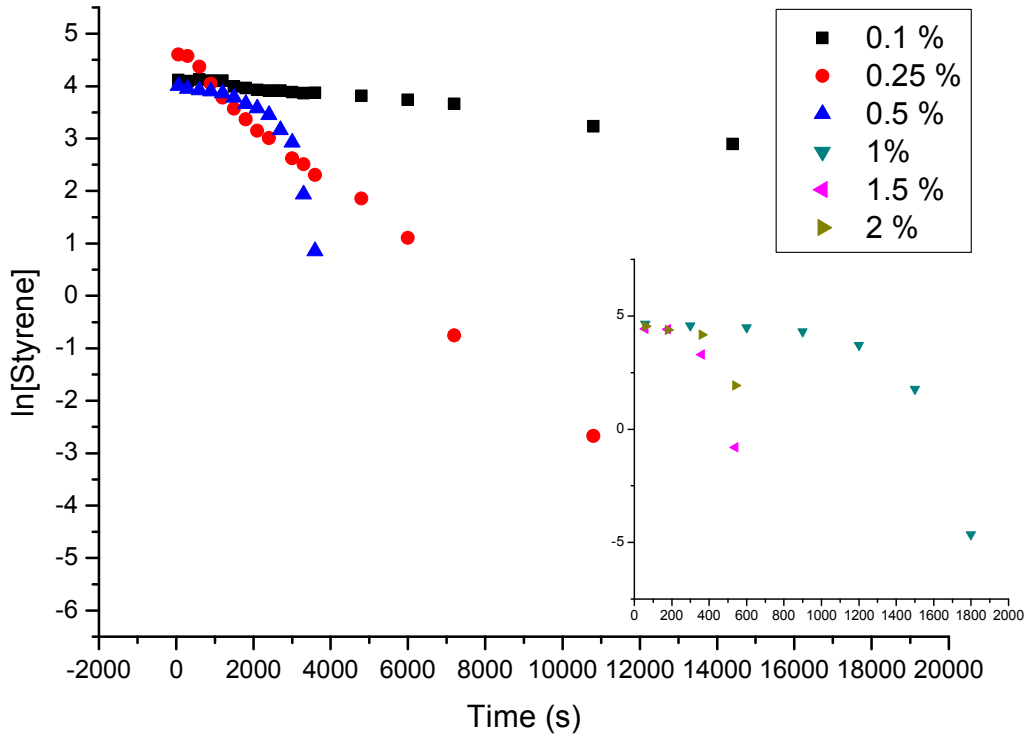

Figure 2.11 Plot of the logarithm of styrene concentration (mM) over time at different catalyst loadings (inset: 1.5 mol% and 2 mol%).

Entry	Catalyst loading (mol %)	k_{obs} (s^{-1})
1	0.1	8.34×10^{-5}
2	0.25	2.88×10^{-4}
3	0.5	6.70×10^{-4}
4	1	2.10×10^{-3}
5	1.5	4.00×10^{-3}
6	2	6.80×10^{-3}

Table 2.4 k_{obs} values calculated from the kinetic experiments.

Once the k_{obs} values had been obtained, it was possible to calculate the second order reaction rate (k) reported in Equation 4.2 (Figure 2.12). The value of [Cat] corresponds to the concentration of manganese-containing active catalytic species expressed in molarity.

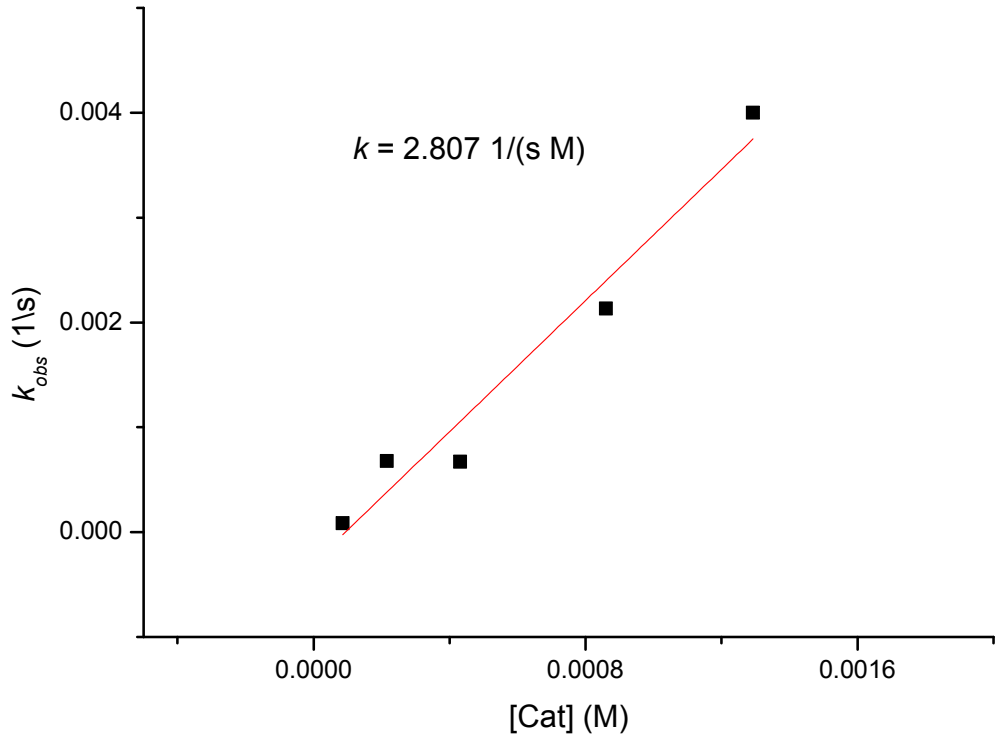

Figure 2.12 Graphical extrapolation of the rate constant from k_{obs}. The units for k are $s^{-1}M^{-1}$.

Plotting ln[k_{obs}] versus ln[Cat] gave a straight line, with a slope of approximately 1.3, giving an indication that the reaction could be first order with respect to the manganese containing active species. The k value obtained, given the approximations made earlier, represent only a preliminary and qualitative analysis of the kinetics of the reaction. A more detailed analysis would require that the mechanism of the cleavage of **122** and the process that generates the active species is known in detail.

To put the k value obtained from this study into context, it is worth comparing it with other epoxidations performed on styrene with different complexes and oxidants. A kinetic study of the epoxidation of styrene with **122** and (*S*)-6,6'-diBr-binol has never been presented. In many of these reports the kinetic constants presented are initial rates measured at a single concentration of catalyst rather than rate constants, which makes them difficult to compare. One of the closest comparisons to the system discussed in this section is the epoxidation of cinnamic acid performed by Lindsay-Smith mixing TMTACN, Mn(II)SO_4, and oxalic acid with hydrogen peroxide as the oxidant, for which the group measured an initial rate of 2.15×10^{-9} M^{-1} s^{-1} with the catalyst used in 60 mol%.[33] Another is the oxidation of styrene derivatives by ruthenium porphyrins with phenyliodine reported by Collman[52] which presented a rate constant of 2.19×10^{-3}

for styrene. Che[53] also determined a value for the rate constant of the ruthenium-porphyrin catalysed epoxidation of styrene. Here, their discussion was based upon the Michaelis-Menten approach to kinetics and resulted in a *k* value of 0.49 s^{-1} for the epoxidation of styrene. An example of epoxidation of dec-1-ene with **122**, hydrogen peroxide and several additives (carboxylic acids) was reported by Woitisky and Shul'pin.[50] In their work, the initial rates of reaction at 0.2 mol% catalyst loading ranged from $0.3x10^{-5}$ to $6.8x10^{-5}$ $M^{-1}s^{-1}$.

In order to draw the Hammett plot for the reaction, the remaining kinetic studies on the styrene derivatives only included the determination of k_{obs} (or observed rate constant) measured at 1 mol% catalyst loading for the purposes of brevity. All of the approximations and assumptions made in the previous section still apply.

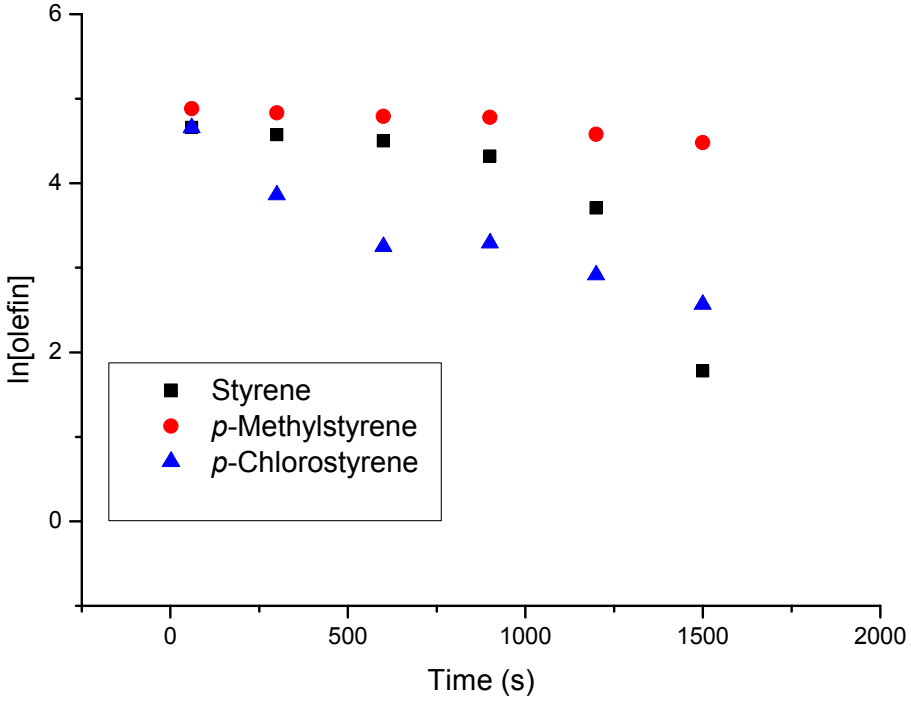

Figure 2.13 Pseudo-first order plots of the epoxidation of styrene and two derivatives for the determination of k_{obs}.

The construction of the Hammett plot was attempted using several sets of substituent constants (σ, σ^+ and σ^-) found in the literature[33, 46, 54] without obtaining a satisfactory linear relationship; success was achieved when the total substituent effect parameters[55] (TE) were used (Figure 4.14). This linear relationship has been used to suggest the presence of a carbon centered radical intermediate in the mechanism of the epoxidation of olefins with ruthenium porphyrins.[53, 56] Such a hypothesis could explain why the ^{1}H-NMR analysis of the epoxidation of *cis*-stilbene

with **122** and (*S*)-6, 6'-diBr-binol in the presence of hydrogen peroxide showed the formation of a mixture of *cis*- and *trans*-epoxide. To confirm this speculation, though, the epoxidation using **122** should be conducted in the presence of a radical trap which would inhibit the formation of epoxide from the intermediate, alongside with determination of k_{obs} for a larger number of *p*-substituted styrene derivatives to back-up the linear trend observed in Figure 2.14.

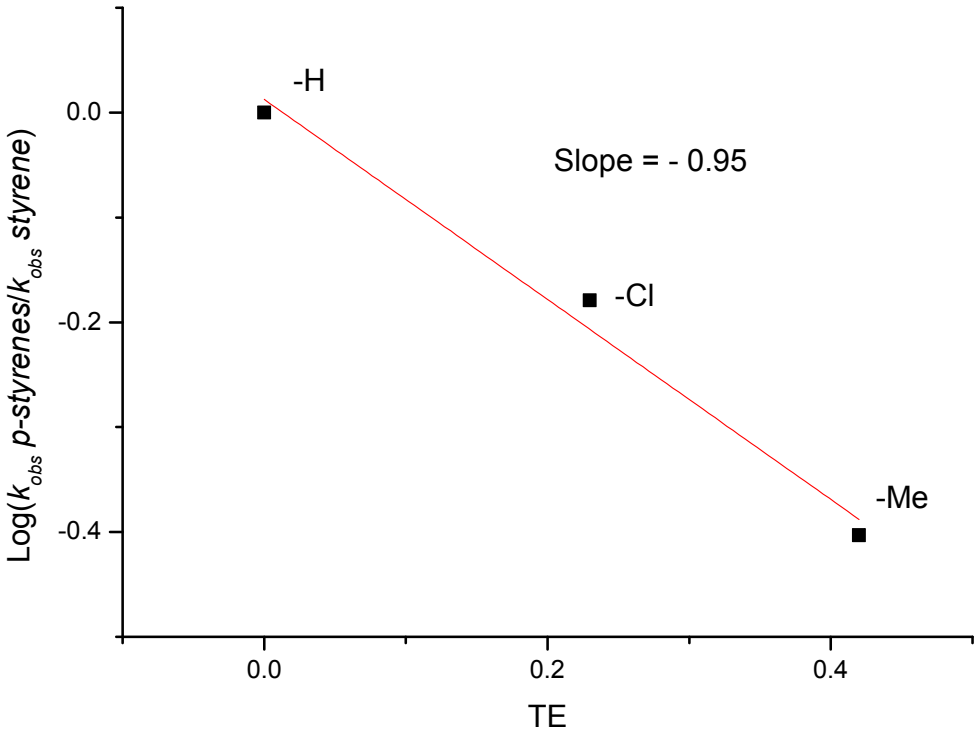

Figure 2.14 Hammett plot with total substituent effect parameters (TE)

2.5 Cyclic voltammetry studies

To obtain more information about the nature and the characteristics of the catalysts employed in this chapter (**122** plus additive and *in situ* formation of the catalyst) a brief electrochemical study was performed using cyclic voltammetry (CV). The instrumentation used a platinum working electrode, a silver reference electrode and a graphite counter electrode; the support electrolyte was tetrabutylammonium hexafluorophosphate. Ferrocene was used as internal standard. Voltammograms were recorded for **122**, **122** in the presence of **(*S*)-130**, the individual components of the *in situ* generated species such as TMTACN, **(*S*)-130** and manganese(II) salts. The significant parameters measured were the cathodic peaks (E_{pc}), the anodic peaks (E_{pa}) and if applicable, the redox potential for reversible processes (E_0). To support the hypothesis that the TMTACN/Mn dimer **122** is cleaved by bisphenols and bisnaphthols like **130**, voltammograms were recorded for the dimer alone and in the presence of bisnaphthol **130**; all measurements were conducted in ACN at room temperature after degassing the solution with nitrogen to remove traces of dissolved oxygen and 0.1 M support electrolyte (Figure 2.15).

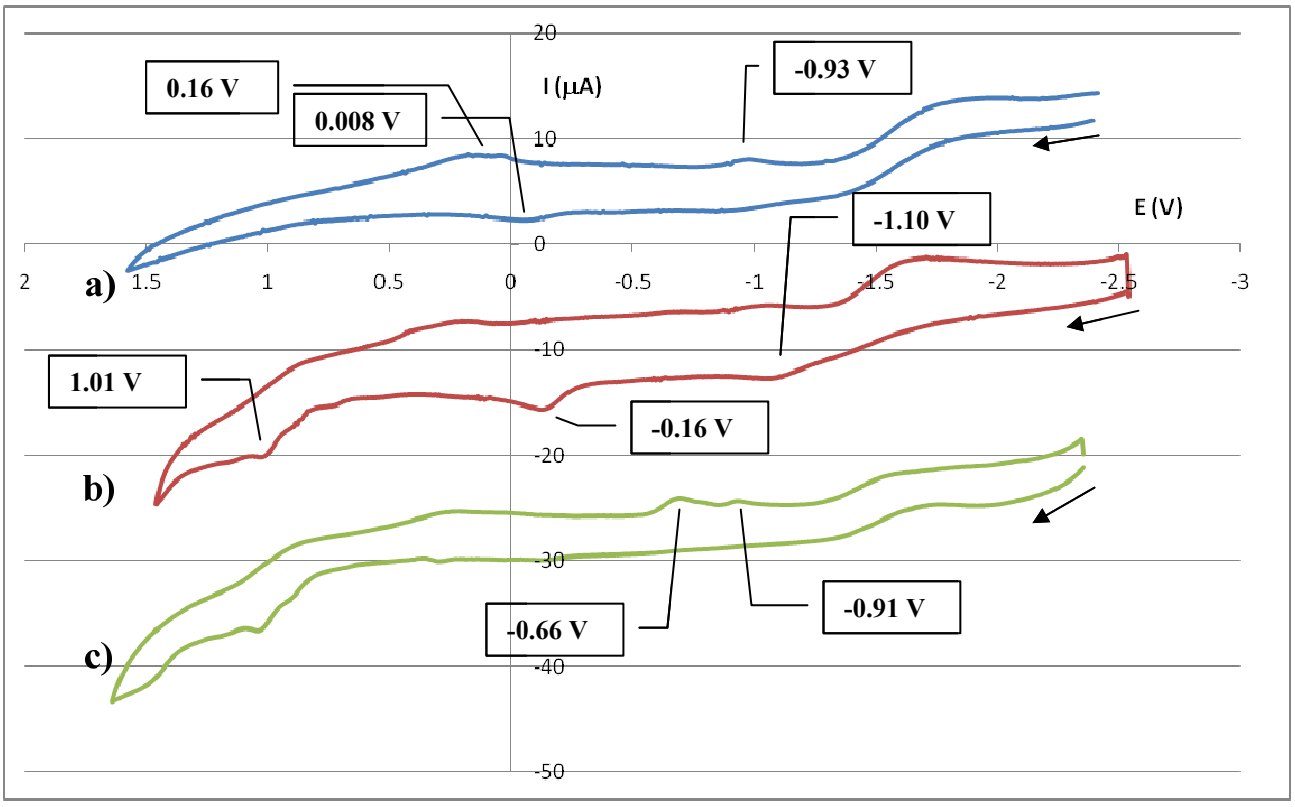

Figure 2.15 Cyclic voltammetry of (a) 122, (b) (*S*)-diBr-binol 130, and (c) 122 after addition of 130; all values were referenced to the couple ferrocene/ferrocenium (Fc/Fc^+).

The voltammogram of **122** (**a**) is in accordance with the values reported in the literature,[57] with an irreversible reduction at E_{pc} = -0.93 V (lit. 1.0 V) and an irreversible oxidation at E_{pa} = -0.008

V (lit. 0.0 V). A third irreversible reductive wave not reported in the literature appeared at E_{pc} = 0.16 V even when changing the scan rate. The voltammogram obtained after addition of **(*S*)-130** to the dimer (**c**) showed the loss of the oxidative wave at -0.008 V for **122** and at -0.16 V for **(*S*)-130**; the reductive wave previously appearing at -0.93 V in **122** is now shifted to -0.91 V. Significantly, a new reductive wave at -0.66 V appears, supporting the formation of a new species in solution.

Comparison with **(*S*)-130** was performed to unambiguously assign the cathodic processes to a new species formed following the cleavage of dimer **122** by **(*S*)-130**; the most significant processes identified for the additive were three anodic peaks at E_{pa} = -1.10 V, -0.16 V, 1.01 V corresponding to irreversible oxidations. The peak at E_{pa} = 1.01 V can still be seen in the dimer, potentially as a ligand-based oxidation of the new species formd, but no trace of the other oxidation processes are present; these results are fully compatible with the formation of a new species after reaction with binol, and confirm the presence of **(*S*)-130** in its structure.

The second set of experiments was designed to compare the species formed from the cleavage of the dimer with the species obtained preparing the monomeric complex *in situ*.

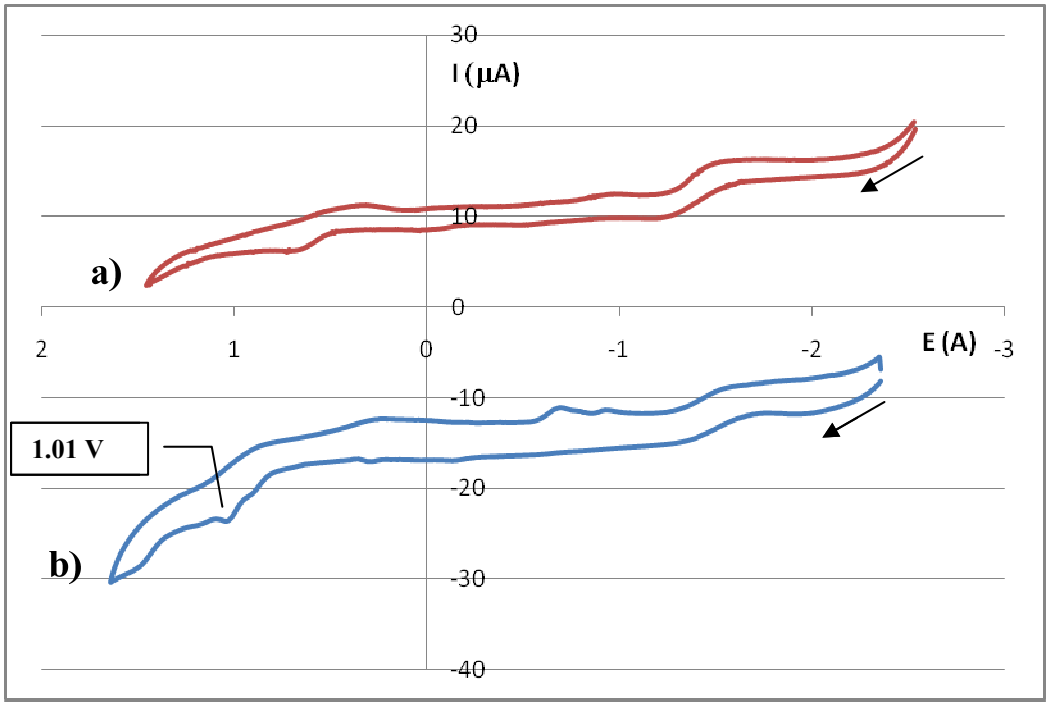

Figure 2.16 Cyclic voltammetry of: (a) *in situ* generated complex, (b) dimer in the presence of (*S*)-130.

It is evident from the comparison (Figure 2.16) that these voltammograms belong to different species. In the voltammograms of the *in situ* generated complex (**a**) it is not possible to see the cathodic peaks and the anodic, ligand-centred oxidation at E_{pa} = 1.01 V that characterise **b**.

Despite not matching the product of dimer-cleaving, **a** and **b** represent a new species that does not correspond to any of the reagents employed in its synthesis.

The different results obtained from the cleavage of the dimer and the *in situ* formation of the monomeric complex suggest that the species formed bear substantial structural differences. This result could be explained through a study of the cleavage mechanism. Both dimer-derived and *in situ* generated species, though, when in the presence of hydrogen peroxide, are effective in the epoxidation of styrene and present similar reactivity. This seems to suggest that the active species in the oxidative process is the same for both the structures.

2.6 Design and attempted syntheses of chiral TMTACN derivatives

Alongside with the use of chiral additives, in our efforts to induce asymmetry, we attempted the synthesis of a chiral derivative of TMTACN by modifying its backbone.

In recent years, several successful catalysts for enantioselective Michael additions, epoxidation, hydroxylation and C-H oxidation have incorporated the 2,2'-bipyrrolidine structure in optically active forms. [58-61]

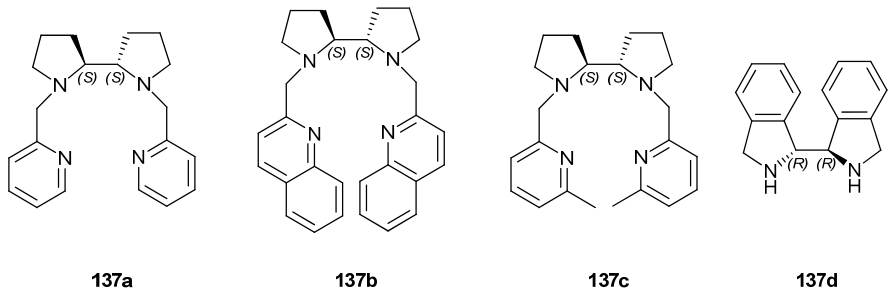

Figure 2.17 A selection of known ligands incorporating the 2,2'-bispyrrolidine group.

Chen and White[62] used an iron complex of **137a** with hydrogen peroxide to oxidise aliphatic tertiary carbons, inserting an OH group with a diastereomeric ratio up to 99:1, in the first example of highly diastereoselective C-H oxidation. Que *et al*, [61] one year later, presented their result on *cis*-dihydroxylation of olefins using iron complexes of **137d** and **137c**, once again with *ee*s generally over 70 % and a marked selectivity for diol over epoxide. Ligand **137d** has been employed in the Michael addition of malonates to nitroalkenes by Xia *et al.*[59] with *ee*s up to 80 %.

In our view, incorporating the same structure in the backbone of TMTACN could result in greater asymmetry in the complex and enantioselectivity in the reaction.

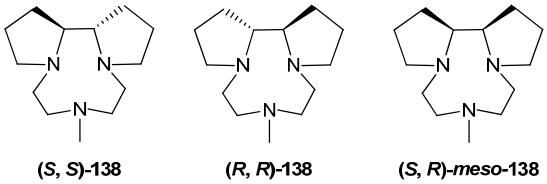

Figure 2.18 Possible isomers of a chiral TACN containing the 2,2'-bipyrrolidine motif.

2.6.1 Synthetic plan

To obtain the derivatives mentioned above, we decided to resort once again to the well established Richman-Atkins cyclisation we successfully applied to the synthesis of TMTACN (**4**). After the cyclisation, single detosylation and methylation would afford our desired ligand (Scheme 2.12).

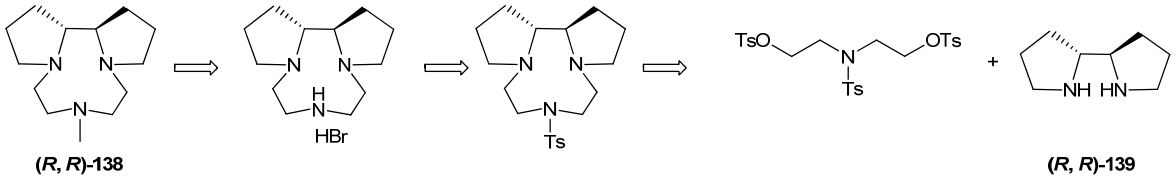

Scheme 2.12 Outline of the synthesis of chiral TACN derivative (*S*, *S*)-138.

The first step of the synthesis was the preparation of the optically pure bispyrrolidine core. Many syntheses were attempted, all of which involved in the synthesis of the product as a racemate, followed by resolution with tartaric acid to isolate the desired isomer. Our first attempt was the reaction between pyrrole and 2-pyrroldinone using phosphorous oxychloride in a Vilsmeier-Haak-type reaction (Scheme 2.13). [60, 63] The unsaturated reaction product (**140**) would then require exhaustive reduction to yield the racemate.

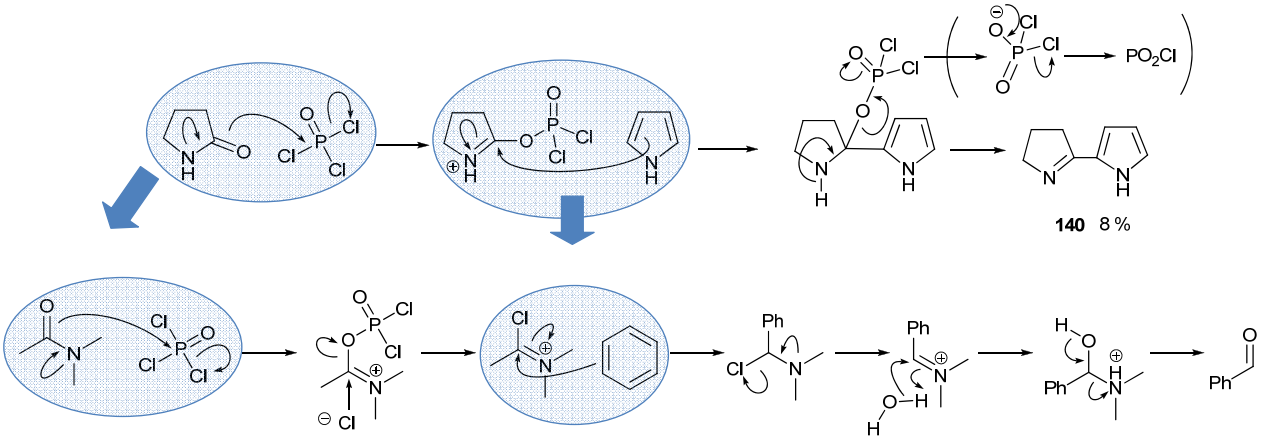

Scheme 2.13 Proposed mechanism for the pyrrole-pyrrolydinone coupling and mechanism of the Vilsmeier-Haak reaction with their similarities highlighted.

The reaction was performed several times making small adjustments to the conditions such as the speed of addition of the reagents and the reaction temperature, but always resulted in extremely low yields. Extraction and purfication of the desired product from the reaction mixture proved extremely challenging. Flash chromatography failed to separate the complex mixture of products that formed and the only effective way to isolate small amounts of the coupling product was found to be sublimation. This synthetic route proved unsuitable for our purposes, since in the following reduction step a large amount of mass would be lost even assuming smooth and high yielding reactions, let alone the resolution of the racemate.

After the failure of this synthesis, a thorough search through the literature for better yielding ways to produce a precursor of 2,2'-bipyrrolidine was undertaken. A promising route was thought to be the photochemical dimerisation of pyrrolidine (Scheme 2.14) proposed by Crabtree[64, 65] and later by Denmark *et al*. [60]

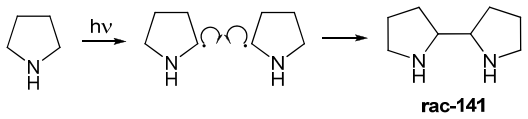

Scheme 2.14 Photodimerisation of pyrrolidine.

The reaction required pyrrolidine to be refluxed for about ten days in a photoreactor (14 eight watt low pressure Hg lamps) in the presence of mercury as the activator. The racemic product was then distilled from the mixture obtained. Not having access to a photoreactor, a different set-up was used, in an attempt to reproduce similar reaction conditions. A custom made glass reaction vessel with three necks, deep enough to contain an immersion Hg lamp with its own water cooling coat was used instead of the photoreactor. The other necks were fitted with condensers and nitrogen inlets. The reaction was repeated four times making slight changes in the set up and reaction time, but analysis by NMR spectroscopy of the resulting mixture revealed that none of them produced the desired product. Quite clearly the quality and intensity of the irradiation obtained and the working conditions with our set-up were too different from those reported, thus resulting in different products.

Another attempt to obtain the bipyrrolidine core was by pyrrole oxidative homocoupling. [66] The reaction is thought to proceed *via* a cation radical intermediate generated by the system PIFA-TMSBr by a one electron oxidation (Scheme 2.15); the generated species then reacts with another molecule of pyrrole with another one electron oxidation. The reaction is concluded with the loss of two protons to give pispyrrole **142**. TMSBr, a Lewis acid, activates PIFA by

coordinating to the trifluoroacetoxy ligands[67] but is a mild enough reagent to prevent the acid catalysed oligomerisation of the pyrrole.[68]

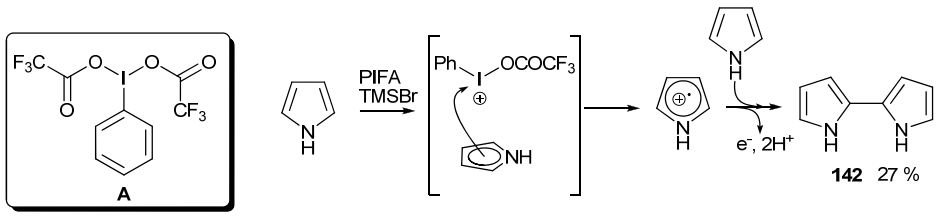

Scheme 2.15 Pyrrole homocoupling. A = phenyliodine bis(trifluoroacetate) (PIFA); TMSBr = bromotrimethylsilane.

The reaction was successful but since it required PIFA in a stoichometric amount, this procedure was only suitable for small scale synthesis, so this route was abandoned.

Our last attempt was the copper-catalysed coupling of Boc-protected pyrrolidines published by Dieter.[69] The reaction proceeds via formation of an organolithium compound (Scheme 2.16) that by reaction with iodide generates a copper(II) complex with two Boc-pyrrolidines. Reductive elimination from this species produces the desired Boc-bispyrrolidine which can be easily deprotected. The reaction begins with metalation of the pyrrolidine ring in position 2 by *sec*-buthyllitium, followed by reaction with copper iodide and lithium chloride to produce a dialkyl cuprate (**A**). Oxidation of this intermediate by iodine affords structure **B** (Scheme 2.16), lithium iodide and an iodine atom which goes back into the cycle to oxidise another molecule of **A**. Elimination of ***dl/meso*-143** involves a the two electrons reduction of the metal centre to generate Cu(0). The coordination of the carbonylic oxygen of the Boc groups to copper holds the two positions undergoing the coupling *cis*- to each other, an essential requirement for the elimination.

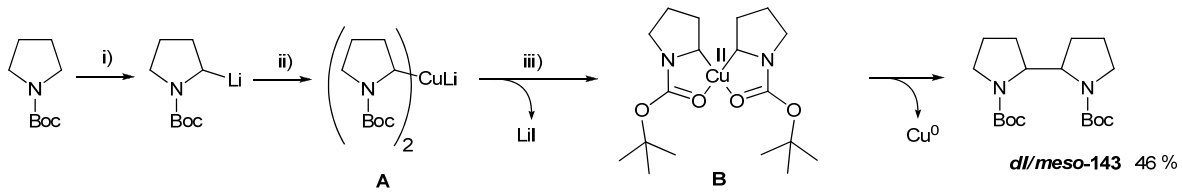

Scheme 2.16 Copper-catalysed homocoupling of Boc-pyrrolidine. i) *sec*-BuLi, -78 °C, THF, TMEDA; ii), LiCl CuI, -78 °C; iii) I_2, -78 °C.

The reaction proceeded smoothly and with reasonable yields. Analysis of the optical rotation of the product gave results compatible with a mixture of (*S, S*)- (*R,R*)- and (*S,R*)-meso-Boc-2,2'-bipyrrolidine.

Upon standing, part of the Boc-protected product crystallised as white crystals which were suitable for single crystal X-ray characterisation (Figure 2.19, Figure 2.20). The analysis of the structure reveals how the presence of the Boc-groups on the nitrogen forces the bonds around N(1) to be almost planar, distorting the geometry of the pyrrolidine ring which assumes a half chair-like conformation. The bond angles (101.6°(16), 103.4°(18), 104.0°(18) and 104.7°(18)) in the ring are slightly lower than expected for sp^3 carbons due to the strain of the 5-membered ring; while C(4)-N(1)-C(1) is higher (111.5°(16)) because of the near planarity of the bond with the Boc-group. The two bonds adjacent to the nitrogen, N(1)-C(1) and N(1)-C(4) (1.47 Å and 1.46(3) Å respectively) are shorter than their C-C counterparts (generally around 1.5 Å) because of the electronegativity of the heteroatom they are connected to.

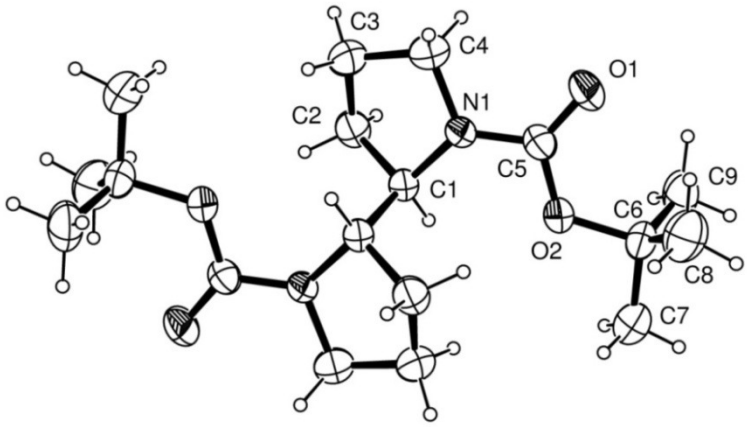

Figure 2.19 ORTEP [70]view of (*R*, *S*)-*meso*-Boc-protected 2,2'-bispyrroline (*meso*-143) with ellipsoids at 50 % probability.

	Bond Length (Å)		Bond Length (Å)
C(1)-N(1)	1.472(2)	**C(5)-O(2)**	1.344(3)
C(1)-C(2)	1.516(3)	**C(5)-N(1)**	1.355(3)
C(2)-C(3)	1.514(3)	**C(6)-O(2)**	1.475(2)
C(3)-C(4)	1.520(3)	**C(6)-C(9)**	1.508(3)
C(4)-N(1)	1.460(3)	**C(6)-C(7)**	1.510(3)

C(5)-O(1)	1.209(2)	**C(6)-C(8)**	1.513(3)

Table 2.5 Selected bond lengths for *meso*-143 with estimated standard deviations in brackets.

	Angle (°)		**Angle (°)**
N(1)-C(1)-C(2)	101.66(16)	**O(2)-C(6)-C(9)**	109.71(18)
N(1)-C(1)-C(1)#1	110.7(2)	**O(2)-C(6)-C(7)**	101.94(17)
C(2)-C(3)-C(4)	103.44(18)	**C(9)-C(6)-C(7)**	110.5(2)
C(3)-C(2)-C(1)	104.05(18)	**O(2)-C(6)-C(8)**	110.99(19)
N(1)-C(4)-C(3)	104.68(18)	**C(5)-N(1)-C(4)**	118.48(17)
O(1)-C(5)-O(2)	125.6(2)	**C(5)-N(1)-C(1)**	126.13(17)
O(1)-C(5)-N(1)	123.3(2)	**C(4)-N(1)-C(1)**	111.55(16)
O(2)-C(5)-N(1)	111.08(18)	**C(5)-O(2)-C(6)**	120.93(17)

Table 2.6 Selected bond angles for *meso*-143 with estimated standard deviations in brackets.

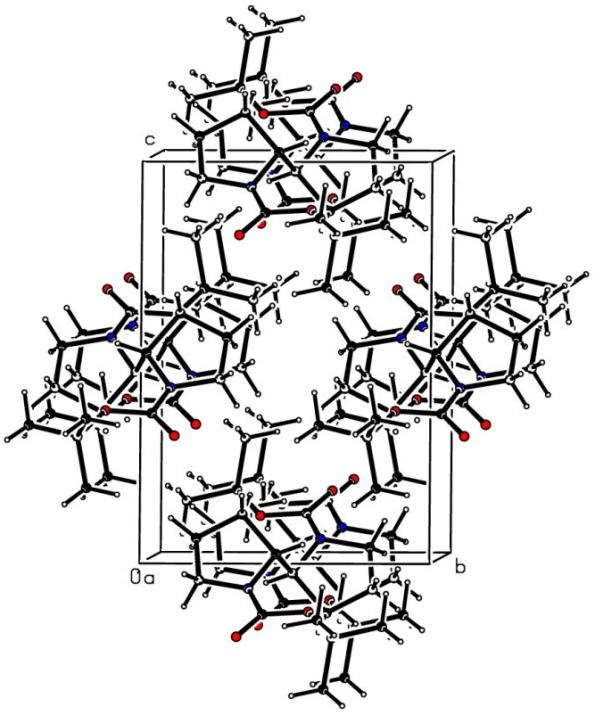

Figure 2.20 PLATON[71] view of the stacking of *meso*-143 in the crystalline cell.

The removal of the protecting group was firstly attempted with trifluoroacetic acid in DCM, yielding the corresponding trifluoroacetate salt which is generally converted into the amine with a basic aqueous work-up. The recovery of **144** from this procedure was disappointingly low, and lead us to consider a different acid.

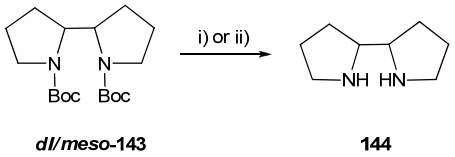

Scheme 2.17 Deprotection of 143. i) TFA, DCM, RT then $NaHCO_3$ (aq); ii) DCM, HCl, RT then NaOH (aq).

When concentrated HCl was used, the deprotection was more efficient and the work-up with NaOH afforded larger amounts of the desired product. **144** was obtained as a mixture of diastereoisomers.

We then decided to attempt a cyclisation to assess the feasibility of the reaction before embarking in the resolution process. Given the success of the conditions we used in the Richman-Atkins cyclisation, we tried to generate the disodium salt of 2,2'-bispyrrolidine by reaction with NaH in DMF and to react it with 2,2'-(tosylazanediyl)bis(ethane-2,1-diyl) bis(4-methylbenzenesulfonate) (**A**). To our disappointment, we recovered only unreacted diamine and compound **B** (Scheme 2.18) deriving from β-elimination from **A**.

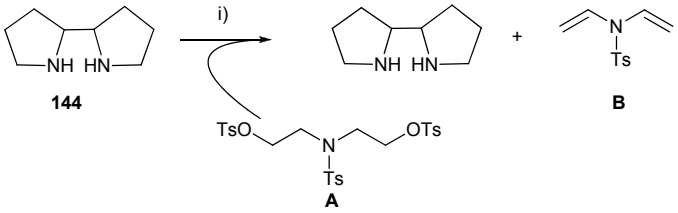

Scheme 2.18 Attempted Richman-Atkins cyclisation and undesired outcome. i) NaH, Δ, DMF.

Repeating the reaction at a lower temperature (40 °C and RT), working under higher dilution and slowing the addition of **A** resulted in the same product. One of the possible reasons for this unwanted process might reside in the base used, which might not have been strong enough to abstract the bispyrrolidine protons and remained in solution, reacting with the wrong molecule.

After the extremely time-consuming process of finding a viable way to the bispirrolidine core, the negative outcome of the cyclisation, together with the lack of enantioselectivity in our screening of additives persuaded us to revise our approach and move towards the synthesis of novel chiral ligands with potential for asymmetric epoxidation.

2.7 Conclusions and future work

The aim of the work presented in this section was to introduce chirality in the known TMTACN/manganese epoxidating system through the use of chiral additives with the ability to coordinate to the metal centre and create an asymmetric environment that could induce the preferential approach of the substrates to the active site of the catalyst. A number of additives have been screened for this purpose in the past, but all have failed to produce enantiomeric excess; the chiral binol derivatives used in this work were, unfortunately, no exception. The effect of chiral TMTACN derivatives could not be studied because of the lack of success in the attempted syntheses.

This study has highlighted that binol can coordinate to manganese together with ligand TMTACN and form complexes (as Lindsay-Smith first showed) and that different substituents on the binol backbone can affect the overall electronic properties of the catalyst and influence rate of reaction and yields. It was also proved that in the presence of (*S*)-6,6'-diBr-binol, the commercial TMTACN/manganese dimer **122** is cleaved and transformed into a different species, still active in the epoxidation of styrene but that species does not correspond to the one obtained when the constituents of the complex are mixed together. Comparison of the activity of these two species in the epoxidation of styrene, though, might suggest that the active species in the epoxidation is the same for both complexes. The lack of stereo- and enantioselectivity in the epoxidation with both of the procedures described might find an explaination in the oxygen-transfer mechanism. Although the Hammett correlation, is barely indicative at this stage, it is in accordance with the presence of a radical based species in the transition state of the epoxidation with **122** and **(*S*)-130**, in support of this, the epoxidation of *cis*-stilbene yielded a mixture of *cis*- and *trans*-epoxides, a result that is also compatible with a radical intermediate with free rotation around bonds in the transition state.

To support the assumption of the presence of a radical in the transition state, the Hammett correlation will need more experimental data on more *p*-substituted styrenes; the use of a radical trap in the epoxidation using the *in situ* generated complex or the cleaved dimer will also provide information on the nature of the oxygen transfer. A Hammett correlation will need to be determined for **122** and the *in situ* generated TMTACN/Mn system in the absence of binol, to determine if its presence significantly modifies the nature of the transition state of the epoxidation.

2.8 References

1. D. E. De Vos, B. F. Sels, M. Reynaers, Y. V. Subba Rao and P. A. Jacobs, *Tetrahedron Lett.*, 1998, **39**, 3221-3224.
2. J. R. Lindsay Smith and G. B. Shul'pin, *Tetrahedron Lett.*, 1998, **39**, 4909-4912.
3. A. Berkessel and C. A. Sklorz, *Tetrahedron Lett.*, 1999, **40**, 7965-7968.
4. B. S. Lane, M. Vogt, V. J. DeRose and K. Burgess, *J. Am. Chem. Soc.*, 2002, **124**, 11946-11954.
5. G. V. Nizova and G. B. Shul'pin, *Tetrahedron*, 2007, **63**, 7997-8001.
6. J. W. de Boer, P. L. Alsters, A. Meetsma, R. Hage, W. R. Browne and B. L. Feringa, *Dalton Trans.*, 2008, 6283-6295.
7. J. R. Lindsay Smith, B. C. Gilbert, A. Mairata i Payeras, J. Murray, T. R. Lowdon, J. Oakes, R. Pons i Prats and P. H. Walton, *J. Mol. Catal. A: Chem.*, 2006, **251**, 114-122.
8. J. W. deBoer, J. Brinksma, W. R. Browne, A. Meetsma, P. L. Alsters, R. Hage and B. L. Feringa, *J. Am. Chem. Soc.*, 2005, **127**, 7990-7991.
9. Y. Chen, S. Yekta and A. K. Yudin, *Chem. Rev.*, 2003, **103**, 3155-3212.
10. M. Bougauchi, S. Watanabe, T. Arai, H. Sasai and M. Shibasaki, *J. Am. Chem. Soc.*, 1997, **119**, 2329-2330.
11. S. Watanabe, Y. Kobayashi, T. Arai, H. Sasai, M. Bougauchi and M. Shibasaki, *Tetrahedron Lett.*, 1998, **39**, 7353-7356.
12. R. Chen, C. Qian and J. G. de Vries, *Tetrahedron*, 2001, **57**, 9837-9842.
13. R. Chen, C. Qian and J. G. de Vries, *Tetrahedron Lett.*, 2001, **42**, 6919-6921.
14. Z. B. Li and L. Pu, *Org. Lett.*, 2004, **6**, 1065-1068.
15. B. Meunier, *Chemical Reviews,* 1992, **92**, 1411-1456.
16. T. Hamada, T. Fukuda, H. Imanishi and T. Katsuki, *Tetrahedron*, 1996, **52**, 515-530.
17. P. G. Graham and D. C. Weatherburn, *Aust. J. Chem.*, 1983, **36**, 2349-2354.
18. G. H. Searle and R. J. Geue, *Aust. J. Chem.*, 1984, **37**, 959-970.
19. N. J. Schoenfeldt, A. W. Korinda and J. M. Notestein, *Chem. Commun.*, **46**, 1640-1642.
20. F. R. J. Erik W. Scheuermann, Majid Motevalli, D. Vaughan Griffiths and and M. Watkinson, *New J. Chem.*, 2002, **26**, 1054–1059.
21. G. Stones, R. Tripoli, C. L. McDavid, K. Roux-Duplatre, A. R. Kennedy, D. C. Sherrington and C. L. Gibson, *Org. Biomol. Chem.*, 2008, **6**, 374-384.
22. B. M. S. Kim, M. S., *Tetrahedron Lett.*, 1999, **40**, 7687-7690.
23. S. Pulacchini and M. Watkinson, *Eur. J. Org. Chem.*, 2001, 4233-4238.

24. A. J. Blake, J. P. Danks, A. Harrison, S. Parsons, P. Schooler, G. Whittaker and M. Schroder, *J. Chem. Soc. Dalton Trans.*, 1998, 2335-2340.
25. L. G. a. U. R. Barth´el´emy Nyasse, *Chem. Commun.*, 1997, 1017-1018.
26. T. Nishimura, Y. Yasuhara and T. Hayashi, *Org. Lett.*, 2006, **8**, 979-981.
27. W. Ye, D. Leow, S. L. M. Goh, C.-T. Tan, C.-H. Chian and C.-H. Tan, *Tetrahedron Lett.*, 2006, **47**, 1007-1010.
28. H. T. Clarke, H. B. Gillespie and S. Z. Weisshaus, *J. Am. Chem. Soc.*, 1933, **55**, 4571-4587.
29. P. Lloyd-Williams and E. Giralt, *Chem. Soc. Rev.*, 2001, **30**, 145-157.
30. B. C. Gilbert, N. W. J. Kamp, J. R. L. Smith and J. Oakes, *J. Chem. Soc., Perkin Trans. 2*, 1997, 2161-2165.
31. B. C. Gilbert, N. W. J. Kamp, J. R. L. Smith and J. Oakes, *J. Chem. Soc., Perkin Trans. 2*, 1998, 1841-1843.
32. B. C. Gilbert, J. R. L. Smith, A. Mairata i Payeras and J. Oakes, *Org. Biomol. Chem.*, 2004, **2**, 1176-1180.
33. B. C. Gilbert, J. R. Lindsay Smith, A. Mairata i Payeras, J. Oakes and R. Pons i Prats, *J. Mol. Catal. A: Chem.*, 2004, **219**, 265-272.
34. T. Harada and K. Kanda, *Org. Lett.*, 2006, **8**, 3817-3819.
35. M. R. Dennis and S. Woodward, *J. Chem. Soc., Perkin Trans. 1*, 1998, 1081-1085.
36. J. Casas, C. Najera, J. M. Sansano and J. M. Saa, *Org. Lett.*, 2002, **4**, 2589-2592.
37. C. Najera, J. M. Sansano and J. M. Saa, *Eur. J. Org. Chem.*, 2009, 2385-2400.
38. K. Ito, Y. Tomita and T. Katsuki, *Tetrahedron Lett.*, 2005, **46**, 6083-6086.
39. J. M. Brunel, *Chem. Rev.*, 2005, 857-897.
40. H. Shanz, J. *et al*, *Tetrahedron: Asymmetry*, 2003, **14**, 2763-2769.
41. Laszlo Kurti and B. Czako, *Strategic applications of named reactions in organic synthesis - Background and Detailed Mechanisms*, Elsevier Academic Press, 2005.
42. V. Snieckus, *Pure Appl. Chem.*, 1990, **62**, 2047-2056.
43. T. K. Pradhan, S. C. Ghosh and A. De, *Arkivoc*, 2003, 158-173.
44. D. E. De Vos and T. Bein, *J. Organomet. Chem.*, 1996, **520**, 195-200.
45. L. P. Hammett, *J. Am. Chem. Soc.*, 1937, **59**, 96-103.
46. C. Hansch, A. Leo and R. W. Taft, *Chem. Rev.*, 1991, **91**, 165-195.
47. S. L. Keenan, K. P. Peterson, K. Peterson and K. Jacobson, *J. Chem. Educ.*, 2008, **85**, 558-560.

48. R. Hage, J. E. Iburg, J. Kerschner, J. H. Koek, E. L. M. Lempers, R. J. Martens, U. S. Racherla, S. W. Russell, T. Swarthoff, M. R. P. Vanvliet, J. B. Warnaar, L. Vanderwolf and B. Krijnen, *Nature*, 1994, **369**, 637-639.
49. B. S. Lane and K. Burgess, *J. Am. Chem. Soc.*, 2001, **123**, 2933-2934.
50. C. B. Woitiski, Y. N. Kozlov, D. Mandelli, G. V. Nizova, U. Schuchardt and G. B. Shul'pin, *J. Mol. Catal. A: Chem.*, 2004, **222**, 103-119.
51. J. W. d. Boer, W. R. Browne, S. R. Harutyunyan, L. Bini, T. D. Tiemersma-Wegman, P. L. Alsters, R. Hage and B. L. Feringa, *Chem. Commun.*, 2008, 3747-3749.
52. J. P. Collman, L. Zeng, H. J. H. Wang, A. Lei and J. I. Brauman, *Eur. J. Org. Chem.*, 2006, 2707-2714.
53. T. S. Lai, H. L. Kwong, R. Zhang and C. M. Che, *J. Chem. Soc. Dalton Trans.*, 1998, 3559-3564.
54. Y. Takahata and D. P. Chong, *Int. J. Quantum Chem*, 2005, **103**, 509-515.
55. Y. D. Wu, C. L. Wong, K. W. K. Chan, G. Z. Ji and X. K. Jiang, *J. Org. Chem.*, 1996, **61**, 746-750.
56. D. Chatterjee, *Inorg. Chim. Acta*, 2008, **361**, 2177-2182.
57. R. Hage, B. Krijnen, J. B. Warnaar, F. Hartl, D. J. Stufkens and T. L. Snoeck, *Inorg. Chem.*, 1995, **34**, 4973-4978.
58. O. Andrey, A. Alexakis, A. Tomassini and G. Bernardinelli, *Adv. Synth. Catal.*, 2004, **346**, 1147-1168.
59. Q. M. Zhu, H. M. Huang, D. J. Shi *et al.*, *Org. Lett.*, 2009, **11**, 4536-4539.
60. S. E. Denmark, J. Fu and M. J. Lawler, *J. Org. Chem.*, 2006, **71**, 1523-1536.
61. K. Suzuki, P. D. Oldenburg and L. Que, *Angew. Chem. Int. Edit.*, 2008, **47**, 1887-1889.
62. M. S. Chen and M. C. White, *Science*, 2007, **318**, 783-787.
63. H. Rapoport and N. Castagnoli, *J. Am. Chem. Soc.*, 1962, **84**, 2178-2181.
64. R. R. Ferguson, C. G. Boojamra, S. H. Brown and R. H. Crabtree, *Heterocycles*, 1989, **28**, 121-124.
65. P. Krajnik, R. R. Ferguson and R. H. Crabtree, *New J. Chem.*, 1993, **17**, 559-566.
66. T. Dohi, K. Morimoto, A. Maruyama and Y. Kita, *Org. Lett.*, 2006, **8**, 2007-2010.
67. G. Pohnert, *Journal Fur Praktische Chemie-Practical Applications and Applied Chemistry*, 2000, **342**, 731-734.
68. A. Matsumoto, T. Kitajima and K. Tsutsumi, *Langmuir*, 1999, **15**, 7626-7631.
69. R. K. Dieter, S. J. Li and N. Y. Chen, *J. Org. Chem.*, 2004, **69**, 2867-2870.
70. L. Farrugia, *J. Appl. Crystallogr.*, 1997, **30**, 565.
71. A. L. Spek, *J. Appl. Crystallogr.*, 2003, **36**, 7-13.

Chapter 3 - Synthesis and activity of novel chiral tridentate ligands based on an L-proline backbone in the epoxidation of alkenes

Following the lack of success in our investigations into the asymmetric epoxidation of alkenes with a chiral derivative of TMTACN and the use of chiral binol additives, we decided to revise our approach. We moved our focus from TMTACN and considered the synthesis of a linear chiral tridentate ligand with the same donor atoms as other non-cyclic chiral tridentate ligands that have proven to be active in oxidation reactions,[1, 2] including the epoxidation of alkenes.[3, 4]

In the design of this new structure we considered several factors. Our structure had to include at least one stereogenic centre close to the reaction centre to increase asymmetry; it had to be based on a general structure that had already proved active in epoxidation; finally, it had to be easily synthesised and have potential for facile modifications to tune its activity.

3.1 Design and synthetic plan

Searching for a structural motif to include in this ligand, we noted the activity of L-proline and its derivatives in a number of catalysts in a wide range of reactions. Proline has not only found applications as an organocatalyst in many reactions, by generally generating enamine or iminium intermediates, e.g. in the aldol reaction and Mannich-type reactions,[5, 6] but also in metal-catalysed epoxidations both alone or when included in a more complex structure. [7-9]

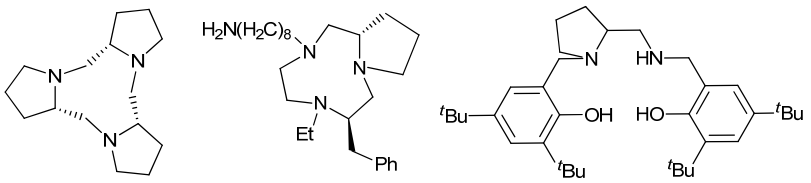

6 14a 145

Figure 3.1 Ligands used in the epoxidation of alkenes incorporating the proline group.

Given the good enantioselectivities obtained when the proline moiety was included in a metal complex, it was decided to include it in the design. Proline alone, though, could not provide the desired coordination environment. Even when converted into prolinamide and eventually reduced it would provide a maximum of two coordinating sites; the next step was then to introduce the missing coordinating group. The potential effect of a larger number of stereocentres on the enantioselectivity that the ligand might provide was the reason behind the introduction of one extra stereogenic centre in the structure.

The presence of a tosyl group and a benzyl group on the terminal nitrogen atoms was inspired by the recent work of Beller.[8, 10] Beller`s ligands (Figure 3.2) proved extremely active in the iron-catalysed epoxidation of olefins with hydrogen peroxide, providing enantiomeric excesses up to 97 % and generally not lower than 80 %. In these studies, Beller found that the ligands containing a group capable of intramolecular hydrogen bonding, like a fluorine atom, a carbonyl or a sulfonyl group, and a hydrogen donor (alcohols, amines) were the most active in the epoxidation of alkenes and gave the highest yields and *ee*s. Beller`s choice fell on the sulfonamidic group (**48**), which provided the best results. To match his most active ligand, we decided to include a sulphonamide group and a mono-benzylated amine in our structure (**146**).

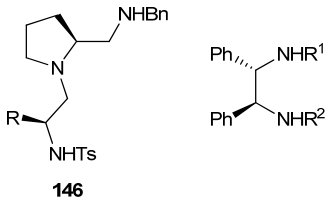

(*S, S*)-48a $R^1 = SO_2Ph$, $R^2 = H$
(*S, S*)-48b $R^1 = SO_2(p\text{-MePh})$, $R^2 = H$
(*S, S*)-48c $R^1 = SO_2Ph$, $R^2 = Bn$
(*R, R*)-48d $R^1 = SO_2(p\text{-MePh})$, $R^2 = Bn$
(*S, S*)-48d $R^1 = SO_2(p\text{-MePh})$, $R^2 = Bn$
(*S, S*)-50a $R^1 = 4\text{-}PhC_6H_4$, $R^2 = H$
(*S, S*)-50b $R^1 = 4\text{-}^tBuC_6H_4$, $R^2 = H$
(*S, S*)-50c $R^1 = 4\text{-}PhC_6H_4$, $R^2 = Bn$
(*S, S*)-50d $R^1 = 4\text{-}^tBuC_6H_4$, $R^2 = Bn$
(*S, S*)-50e $R^1 = 4\text{-}MeC_6H_4$, $R^2 = 4\text{-}MeBn$

Figure 3.2 General structure of the novel tridentate ligand developed in our work (146) and structure of Beller`s ligands (right).

3.2 Reaction with aziridines and sulfamidates: towards a library of ligands

3.2.1 Reaction with chiral aziridines

The partner for the synthesis of the L-proline-based ligand was found in chiral aziridines derived from amino acids. Aziridines, like epoxides, have a specific and predictable reactivity; activated aziridine rings undergo nucleophilic ring-opening at the less hindered carbon following a S_N2 mechanism, aziridines with electron withdrawing groups on the ring undergo electrophilic ring opening (Scheme 3.1). [11]

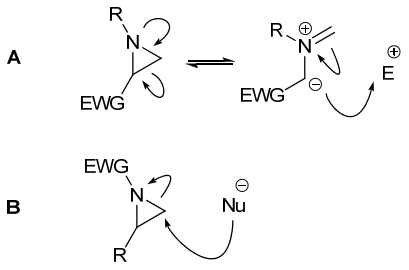

Scheme 3.1 A) Electrophilic ring-opening; B) nucleophilic ring-opening of activated aziridines.

The overall reaction scheme started with esterification of the carboxylic acid on the proline ring, followed by reaction with a tosyl protected aziridine, conversion of the ester into an amide, reduction of the amide to amine and benzylation of the free amine (Scheme 3.2).

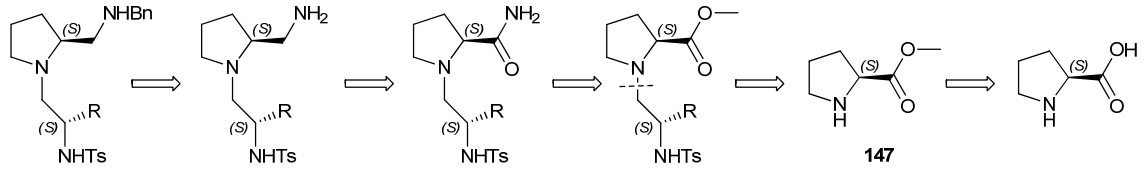

Scheme 3.2 Overall retrosynthetic plan for the synthesis of a novel proline-based chiral ligand; aziridine route.

The aziridines were synthesised in a two step procedure starting from the corresponding amino alcohols using a combination of two known syntheses;[12, 13] aminoacids were reduced to amino alcohols using an excess of lithium aluminium hydride (LAH). The ring-closing process resembles the synthesis of chiral epoxides via ring closing of halohydrins and proceeds with inversion of configuration when a stereocentre is subject to nucleophilic attack. The reaction has a large henthalpy because of the ring strain but this is compensated by a low entropic term, due to the special closeness of the atoms involved in the reaction and to the fact that the transition state can assume only a few conformations and most of them can react.[14]

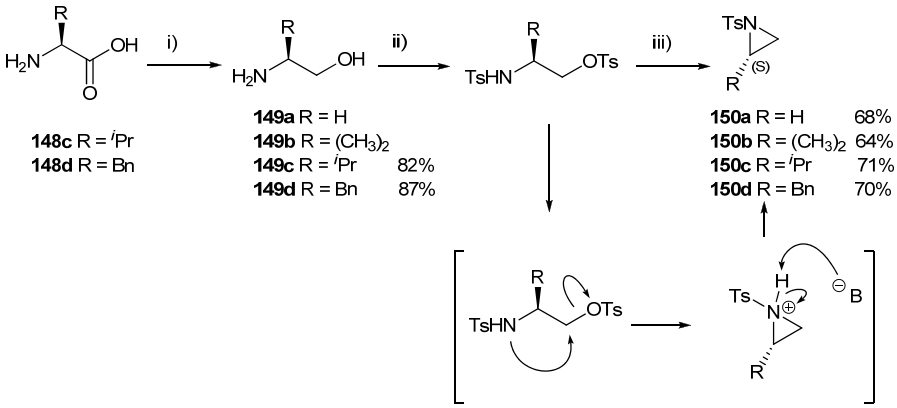

Scheme 3.3 Synthesis of chiral aziridines via reduction of amino acids and subsequent cyclisation. i) LAH, THF, reflux, 24 h; ii) pyridine, TsCl; iii) benzene, KOH (20 %), overnight. Simplified mechanism of ring closing between brackets.

The choice of aziridines as the reaction partner allowed to immediately introduce a variety of substituents on the ligand backbone, depending on the starting amino acid. It was decided to start the synthesis using two achiral aziridines and two chiral analogues (Scheme 3.3) with different bulkiness; this to to study the effect of the second chiral centre and of the steric hindrance on the side chain simultaneously. The introduction of the tosyl-group proceeded smoothly and afforded each derivative in good yield, with the only drawback represented by the sometimes difficult

removal of the excess pyridine employed. The di-tosylated derivatives could be precipitated from the reaction mixture by the addition of water and collected by filtration, but the constant presence of residual pyridine in the NMR spectra required a further purification step, dissolving the materials in a suitable organic solvent and performing several washings with dilute acid and water, which reduced the overall yield. The cyclization, a combination of Moberg's[13] and Gibson's[12] procedures, afforded the aziridines in high purity and acceptable yields.

Once the aziridines and the methyl ester of L-proline were obtained in sufficient amounts it was possible to move onto the next synthetic step, the nucleophilic ring opening. This reaction proved to be more complicated than expected, due to the unforeseen lack of reactivity of the secondary amine of proline. The reaction was first attempted in the presence of potassium carbonate, but to great disappointment no reaction was observed even after 16 hours. The lack of reactivity was attributed to the weakness of the base. The next step consisted in testing a series of different bases with increasing strength: triethylamine, *n*-BuLi, sodium hydride and *in situ* generated LDA.

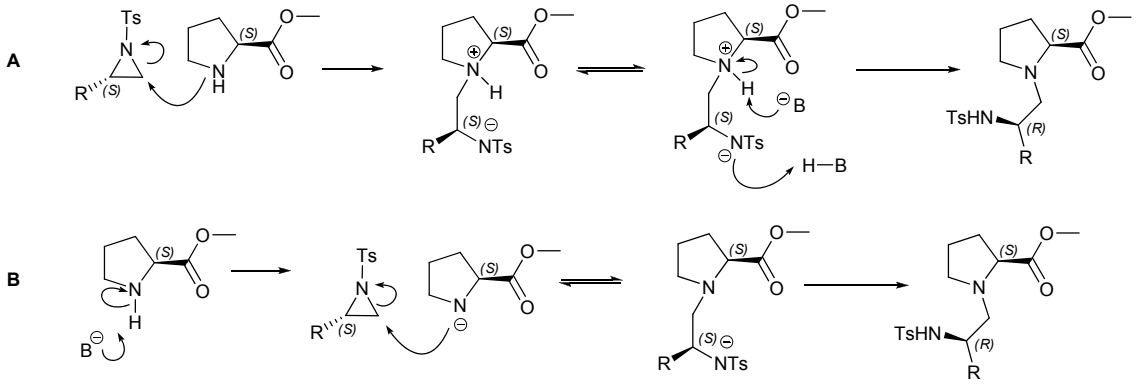

Scheme 3.4 Proposed mechanisms for aziridine ring opening by proline with weak base (A) and strong bases (B).

All of the bases screened gave roughly the same yields, which only went over 40% in the case of **149b** and **149c**. Such variability in one of the very first steps of the synthesis threatened the plan of establishing a procedure which could be used to quickly generate a library of ligands. As a result, the decision to shift the attention to an aziridine analogue with higher reactivity in this reaction, namely cyclic sulfamidates.

3.2.2 Reaction with chiral cyclic sulfamidates

Cyclic sulfamidates are cyclic structures generally consisting of five or six members that undergo ring-opening by nucleophiles following an S_N2 mechanism with inversion of configuration at the electrophilic carbon. The regioselectivity of the attack occurs preferentially

at the oxygen bearing carbon and it is unaffected by the substituents on the ring or on the nitrogen atom; in this regard, their reactivity closely resembles that of aziridines with an electron withdrawing group on the nitrogen.[15-17] The nucleophilic ring opening reaction produces a sulfamic acid intermediate that is then hydrolysed under acidic conditions (Scheme 3.5). [18]

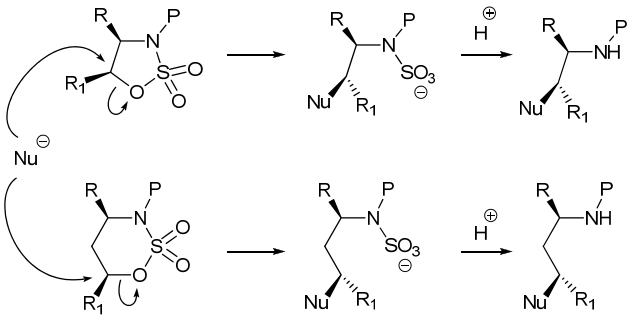

Scheme 3.5 General ring opening mechanism for 5- and 6-membered sulfamidate rings.

Five-membered sulfamidates can be synthesised from 1,2 diols[19] and β-aminoalcohols[20] in a variety of ways. More rigid amino alcohols like prolinol or aromatic amino alcohols can be reacted with sulfuryl chloride (SO_2Cl_2) and triethylamine and form the sulfamidate ring in a single reaction step,[21, 22] while more flexible substrates are generally converted in multi-step reactions in which a sulfamidite is generated and then oxidised to the sulfamidate. The most common route to sulfamidites is by reaction of amino alcohols with thionyl chloride and triethylamine in the presence of imidazole.[16, 20] The oxidation to the sulfamidate is achieved by reaction with an excess of sodium periodate in the presence of catalytic $RuCl_3$.

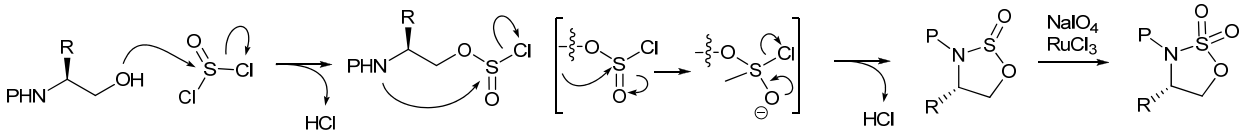

Scheme 3.6 Simplified mechanism of formation of sulfamidite rings from *N*-protected β-aminoalcohol. Imidazole is used to neutralise the hydrochloric acid formed.

A series of Boc and benzyl protected sulfamidates were prepared starting from their respective amino alcohols. The new protecting groups were introduced to expand the library of ligands further. The reaction with benzyl protected sulfamidates could open the way to *N*, *N*-dibenzyl derivatives and derivatives with the benzyl group and the tosyl group swapped, while the Boc-protected sulfamidates would allow easy deprotection of the nitrogen and further substitutions (Scheme 3.7).

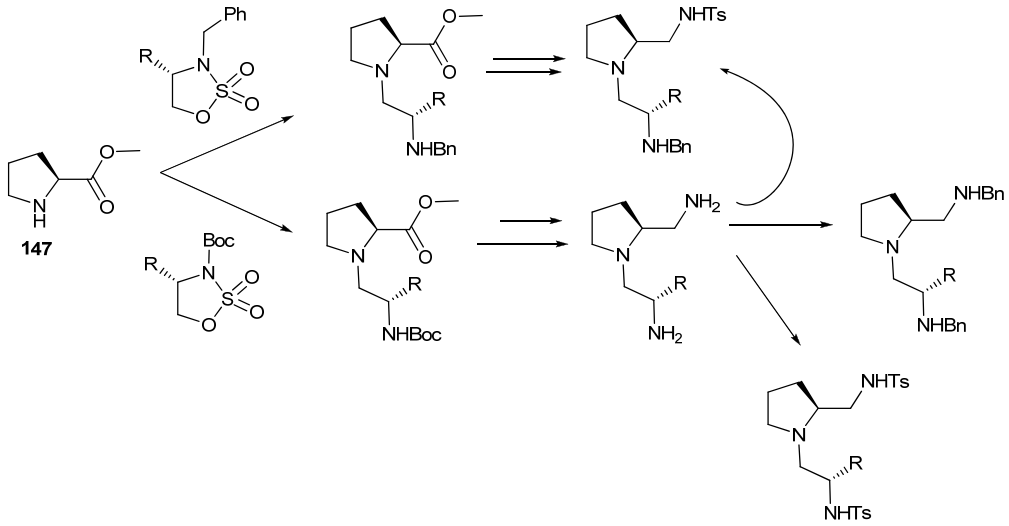

Scheme 3.7 Possible development of the library of ligands through the use of sulfamidates. R = alkyl group.

For the synthesis of these sulfamidates the starting were the β-amino alcohols employed in the synthesis of tosylaziridines with the addition of L-prolinol. Benzyl protection of the sulfamidate was obtained at the amino alcohol stage by reaction with benzoyl chloride in the presence of a base and subsequent reduction of the product. The formation of the sulfamidate followed the procedure outlined in Scheme 3.8. Boc protection was achieved reacting the amino alcohol with di-^{t}Bu-dicarbonate. Both the sulfamidites and sulfamidates were obtained in acceptable to good yields.

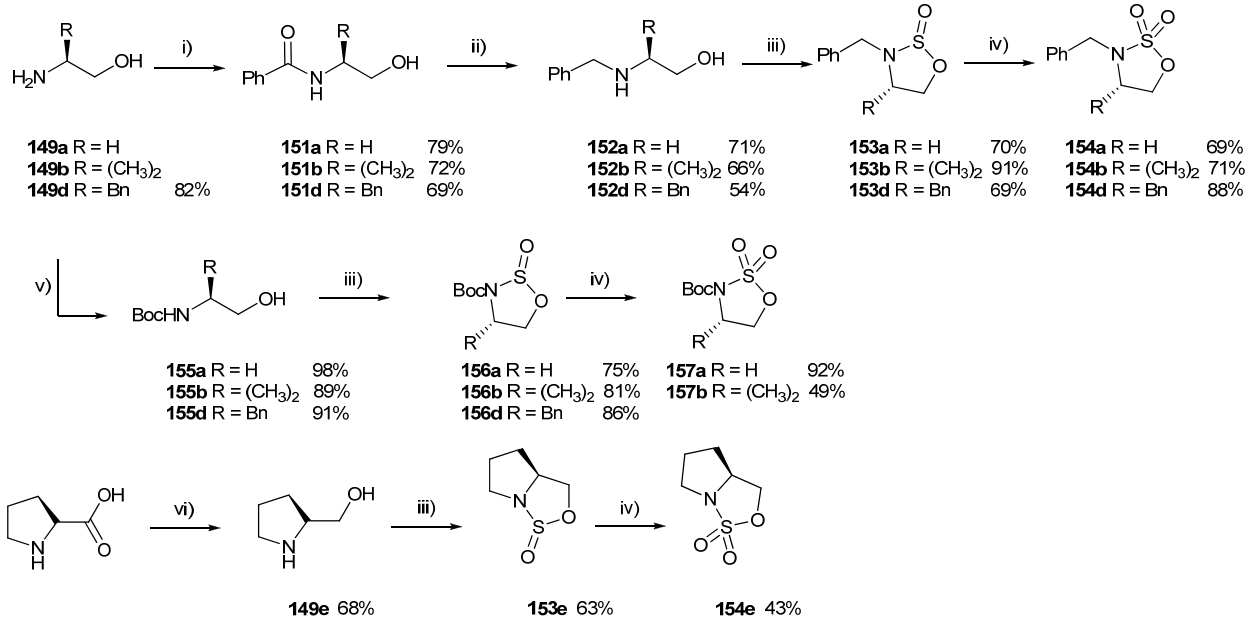

Scheme 3.8 Reaction scheme for benzyl- and Boc-protected sulfamidates. i) Benzoyl chloride, K_2CO_3, MeOH; ii) LAH, THF, reflux; iii) $SOCl_2$, TEA, imidazole, DCM; iv) $NaIO_4$, $RuCl_3$, H_2O/EtOAc; v) Boc_2O, DCM; vi) LAH, THF, reflux.

After completing the synthesis of the sulfamidates, the synthesis of the library of ligands was once again attempted. L-Proline methylester (**147**) was reacted with the newly synthesised electrophiles in the presence of triethylamine as the base. Analysis of the reactions *via* TLC showed complete consumption of the sulfamidates, but after working up, no sign of the expected product was present and the proline was recovered unreacted. We then proceeded to screen a variety of different bases (NaH, ^{t}BuLi, LDA) but to no avail. Consumption of the sulfamidate was always observed but without formation of the addition product.

In the synthesis of TMTACN and other cyclisations,[23] as well as in other reactions,[24] the inorganic base Cs_2CO_3 has been shown to improve yields and allowing for mild reaction conditions. The improvements to the yields were so impressive that scientists coined the expression the "caesium effect".[25, 26] This effect is still empirically measured; no clear and accurate explanation of its origin has been reported. Caesium ions have low charge density and a low degree of solvation compared to other alkali metal salts. In aprotic solvents, caesium will be "naked" (paired with very few solvent molecules), and thus be more reactive. This makes its salts very well balanced bases, strong enough but tolerated by many functional groups.

Hoping that the "caesium effect" would solve the problem, Cs_2CO_3 was used as the base in a last attempt in coupling sulfamidates and proline using DMF as the solvent but once again, no reaction was observed and this time both the starting materials were recovered from the reaction even after 24 hours at reflux. Very disappointingly, every effort made to react the sulfamidates with their partner failed, leaving no other choice than to go back to the use of aziridines.

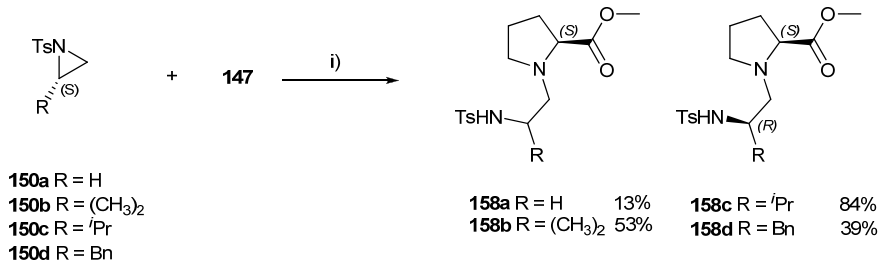

150a R = H
150b R = $(CH_3)_2$
150c R = ^{i}Pr
150d R = Bn

158a R = H 13%
158b R = $(CH_3)_2$ 53%
158c R = ^{i}Pr 84%
158d R = Bn 39%

Scheme 3.9 Reaction of tosyl protected aziridines with proline methylester. i) TEA, ACN, 1 to 3 days.

The ^{1}H-NMR analysis of the compounds we obtained revealed an interesting effect. Moving from the starting material (L-proline methyl ester-HCl, **147**) to structures **158**, the chemical shift of the α-hydrogen (CHN) and of the protons of the methylene group (CH_2N) next to the nitrogen atom of the proline backbone showed a marked change. All of the protons moved upfield, compared to the starting material, an expected effect since the nitrogen lost its positive charge and was now neutral.

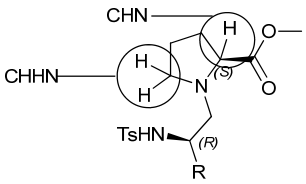

158a R = H
158b R = $(CH_3)_2$
158c R = ^{i}Pr
158d R = Bn

Figure 3.3 General structure of 158 with highlighted proton groups.

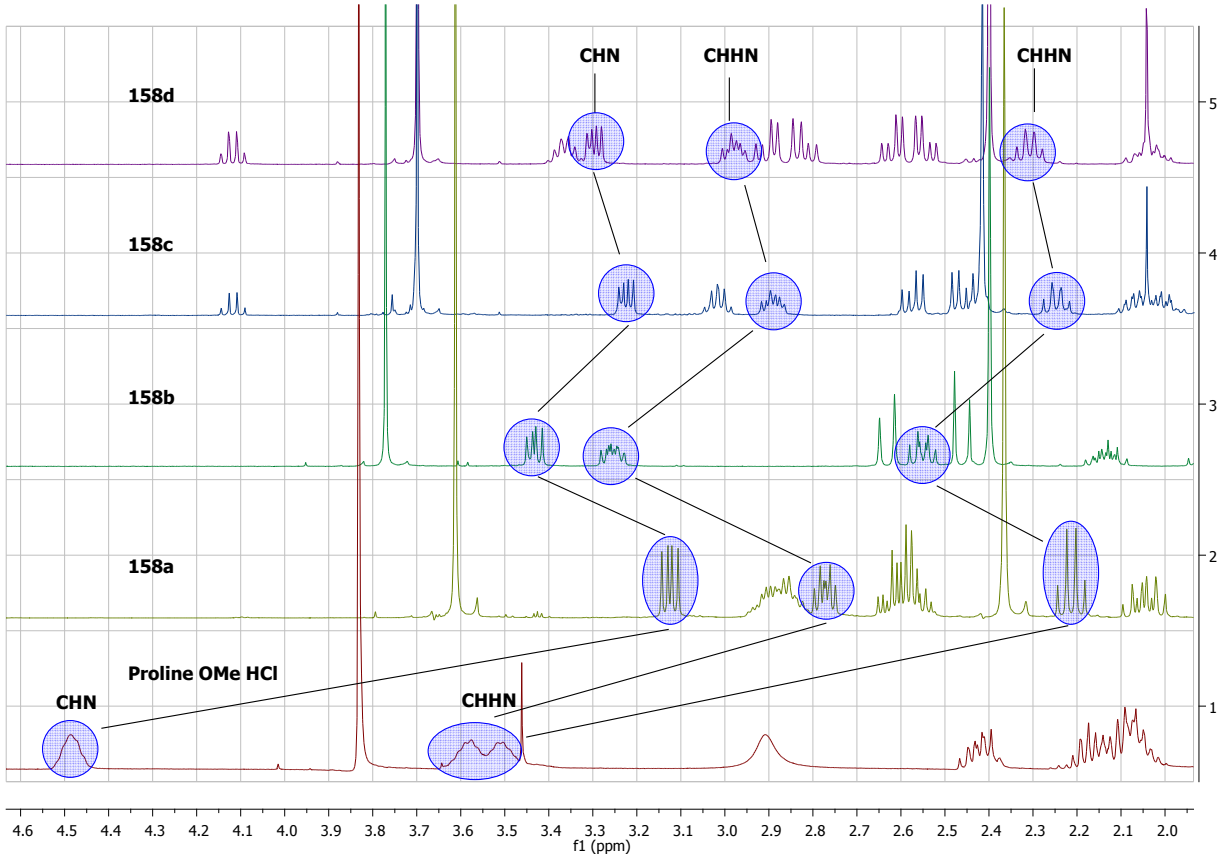

Figure 3.4 Comparison of the ^{1}H-NMR spectra of derivatves 158 and starting material.

The unexpected change observed was the very large change in the signals for the CH_2N protons, which not only moved upfield, but now appeared as two distinct signals (one per proton) separated on average by 0.6 ppm. The trend was the same for all of the derivatives with the exception of **158b**, where the value was 0.69 ppm. Even the distance between the CHN and CH_2N remained constant in a range of 0.30-0.35 ppm for the more downfield and 0.95-0.98 ppm for the other. In the case of **158b**, the separation was slightly smaller, with 0.18 ppm and 0.87 respectively.

A differentiation in the chemical shift of these two protons (CH_2N) was expected due to their diastereotopic nature, but it appeared that the introduction of substituents on the proline nitrogen

enhanced their separation, a phenomenon that is not observed for the other protons on the ring. Possible explanations lie in the increased rigidity of the system due to intramolecular hydrogen bonding that render the proline ring inversion process energetically disfavoured and potentially lock the molecule into one conformation or in very different conformations induced by the substituents. In an effort to understand this, an attempt to obtain X-Ray structures of all of the derivatives was undertaken, but only structure **158b** was recovered as a crystalline solid and provided crystals suitable for single crystal X-ray analysis (Figure 3.5).

The single crystal X-Ray analysis confirmed the formation of the expected product with the predicted regiochemistry. The nucleophilic attack occurred at the less hindered carbon atom as picted in Scheme 3.1 (**B**). The N-S bond length in the sulfonamide group is 1.60(15) Å and falls in the expected range (1.60-1.63 Å).[27] This value stands in between the length of a double N-S bond (1.54 Å)[28] and a single N-S bond (1.69 Å),[29] suggesting partial double bond character. The sum of the angles around N(2) amounts to 354°, almost planar and very close to the typical value for an sp^2-hybridised centre. The sum of the angles around the second nitrogen atom N(1), with a total value of 331°, appears very close to the *ca*. 327° required by ideal sp^3 hybridisation. As expected, the distances C(2)-O(1) (1.20(2) Å) and C(2)-(O2) (1.34(2) Å) are compatible with the bond lengths in carbonyl compounds, with the first bond noticeably shorter because of its double bond character, the near planarity of the angles around C(2), with a sum of 359.8° further supports the sp^2 hybridisation.

Observation of the structure also revealed a network of intramolecular hydrogen bonds between the carbonylic oxygen, the proline nitrogen and the sulfonamidic proton (Figure 3.5), suggesting that this kind of structures can generate the kind of intramolecular hydrogen bonding that Beller believed to be crucial for the activity of his catalysts[8, 10] despite the presence of the proline ring separating the terminal groups. The stacking in the unit cell (Figure 3.6) also shows that no other inter-molecular hydrogen bonding is present to influence the geometry at least in the solid state. The length of the intramolecular hydrogen bonds N(2)-H...O(1) and N(2)-H...N(1) are reported in Table 3.1. An estimate of the strength of the interaction is given by the D...A distances. These distances should amount to less than the sum of the van der Waals radii of donor and acceptor, in this case oxygen (1.52 Å) and nitrogen (1.55 Å). [30] Both N(2)...O(1) and N(2)...N(1) are significantly smaller than this sum, indicating strong hydrogen bonds.

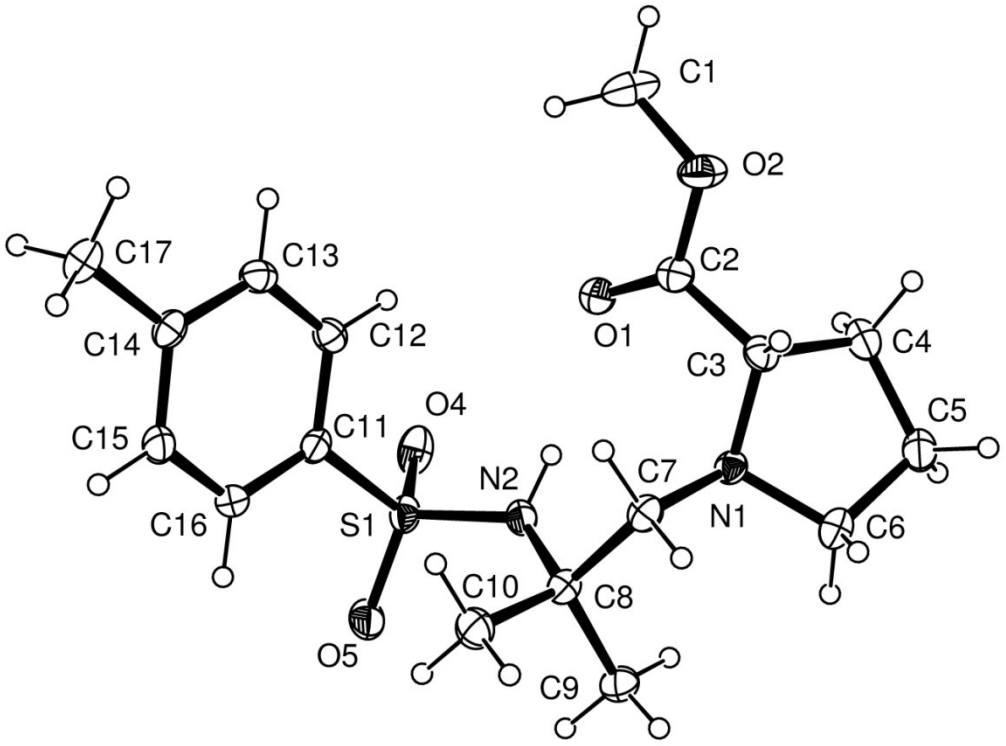

Figure 3.5 ORTEP[31] view of compound 158b with 50% probability displacement ellipsoids.

	Bond Length (Å)
C(2)-O(1)	1.203(2)
C(2)-O(2)	1.343(2)
C(2)-C(3)	1.508(2)
C(3)-N(1)	1.457(2)
C(7)-N(1)	1.469(2)
C(7)-C(8)	1.535(2)
C(8)-N(2)	1.485(2)
N(2)-S(1)	1.6087(15)
O(4)-S(1)	1.4391(14)
O(5)-S(1)	1.4373(14)

Table 3.1 Selected bond lengths (Å) for 158b with estimated standard deviations.

D-H...A	d(D-H) (Å)	d(H...A) (Å)	d(D...A) (Å)	(DHA) (°)
N(2)-H...O(1)	0.84	2.13	2.94	163 (2)
N(2)-H...N(1)	0.84	2.46	2.85	108 (18)

Table 3.2 Hydrogen bonds for 158b with estimated standard deviations.

	Angle (°)		Angle (°)
O(1)-C(2)-O(2)	123.32(16)	**C(7)-N(1)-C(6)**	113.77(13)
O(1)-C(2)-C(3)	126.85(15)	**C(8)-N(2)-S(1)**	128.69(12)
O(2)-C(2)-C(3)	109.77(15)	**C(8)-N(2)-H(2)**	114.0(16)
N(1)-C(3)-C(2)	113.24(14)	**S(1)-N(2)-H(2)**	111.6(16)
C(2)-C(3)-C(4)	109.58(14)	**C(2)-O(2)-C(1)**	115.39(15)
N(1)-C(7)-C(8)	113.71(13)	**O(5)-S(1)-O(4)**	119.65(8)
N(2)-C(8)-C(10)	113.68(14)	**O(5)-S(1)-N(2)**	108.72(8)
N(2)-C(8)-C(9)	108.18(14)	**O(4)-S(1)-N(2)**	105.40(8)
N(2)-C(8)-C(7)	105.49(13)	**O(5)-S(1)-C(11)**	107.04(8)
C(3)-N(1)-C(7)	114.85(13)	**O(4)-S(1)-C(11)**	106.82(8)
C(3)-N(1)-C(6)	104.86(13)	**N(2)-S(1)-C(11)**	108.87(8)

Table 3.3 Selected bond angles (°) for 158b with estimated standard deviations.

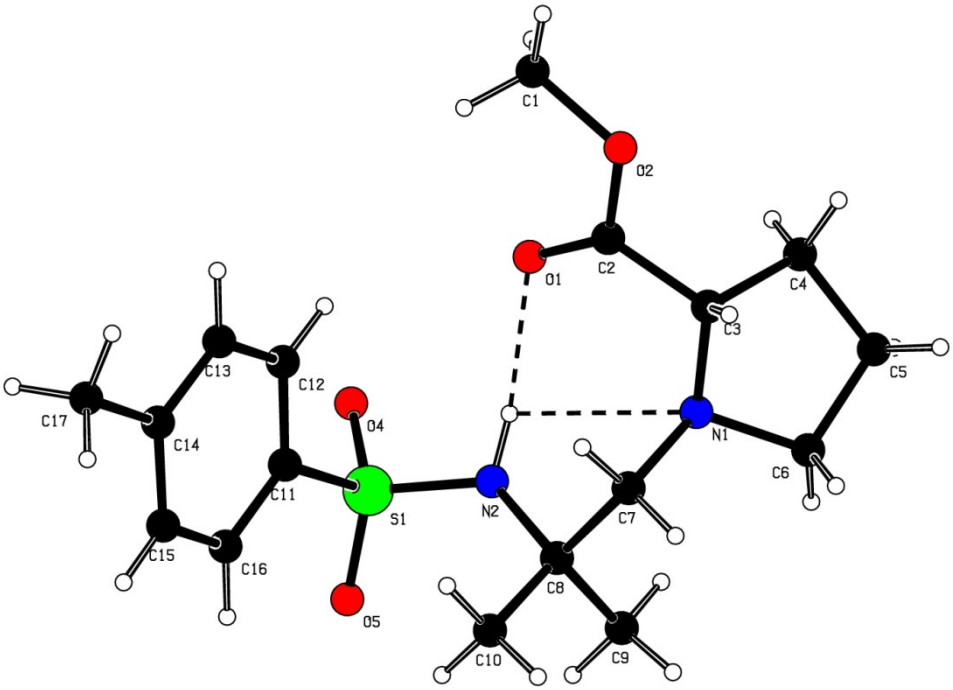

Figure 3.6 PLATON plot. [32] Intramolecular hydrogen bonding in structure 158b.

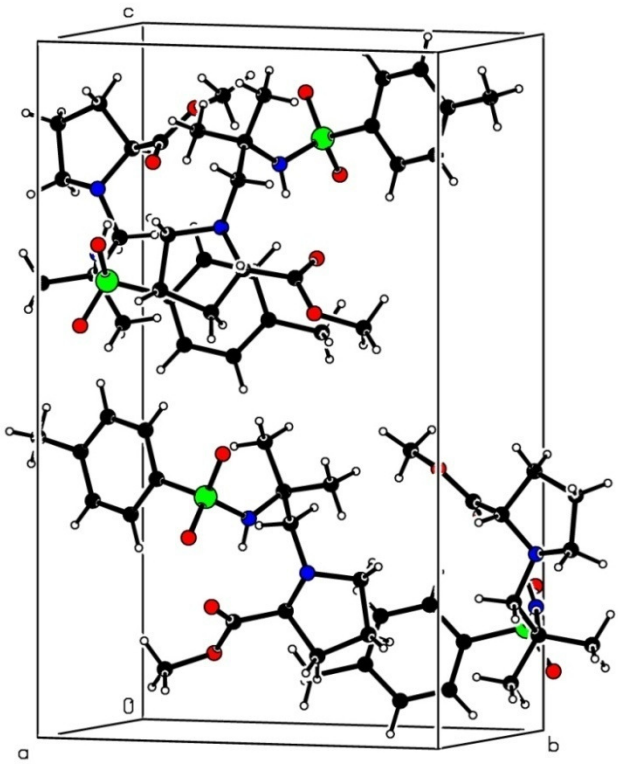

Figure 3.7 PLATON[32] view of the unit cell for structure 158b.

Despite the useful information it provided, the crystal structure obtained gave no clear explanation of the origin of the effect observed in the NMR spectra and unfortunately it was impossible to make a comparison with the structures of **158a**, **158c** and **158d** which might have given a better understanding of this phenomenon.

3.2.3 Amide formation and reduction to amine

The most common way to convert an ester into a terminal amide is by treatment of the substrate with ammonia in polar solvents. [33-35] Conversion of the methyl ester into the corresponding amide was achieved by stirring the compound overnight in MeOH in the presence of an excess of ammonium hydroxide. The disappearance of the substrate was monitored by TLC and the work-up solely consisted in the total evaporation of the solvents, which left behind **159b** as a solid and **159c** as an oil. Subsequent reduction of the amide with LAH afforded the desired amine.

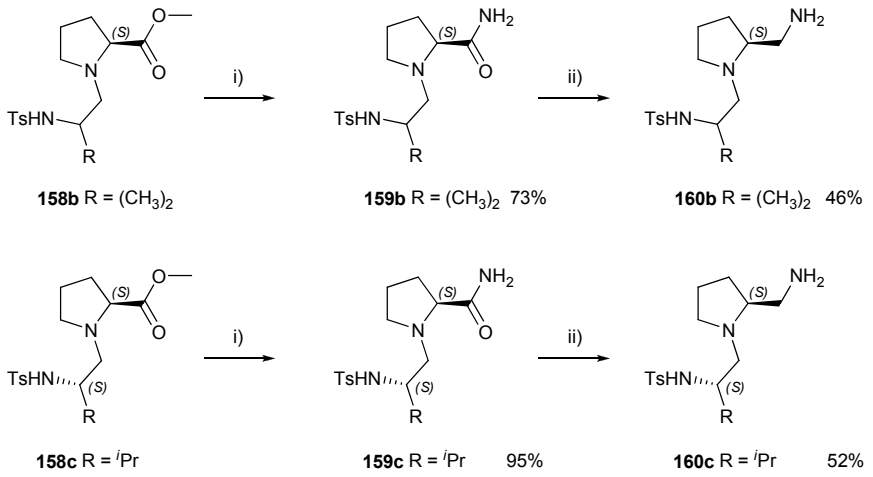

Scheme 3.10 Reagents: i) NH_3 (aq.), MeOH; ii) LAH, THF.

The crystallisation of **159c** was attempted but unsuccessful, while **159b** was obtained in a crystalline form suitable for single crystal X-Ray diffraction (Figure 3.8). From the PLATON view of the molecule (Figure 3.9) it appears that, in the solid state, a network of hydrogen bonds causes **159b** to aggregate with a second molecule forming a dimer, very different from structure **158b**, where all the hydrogen bonds are intramolecular. Observing the stacking in the unit cell (Figure 3.10) it is possible to see how the unit is constituted by the aforementioned dimer and that there is no further hydrogen bonding between different dimers. The hydrogen bond lengths are all compatible with strong bonds, since the D...A distance is smaller than the sum of the van der Waal radii of donor and acceptor. Among them, N(1A)-H(1A)...N(2A) and N(1B)-

H(1C)...N(2B) are potentially the strongest bonds, with a difference between the sum of the radii and bond length of 0.48 Å and 0.46 Å respectively.

The N-S bonds lengths in the sulfonamide groups are 1.60(2) Å (N3a-S1a) and 1.61(2) Å (N3b-S1b) again falling in the expected range (1.60-1.63 Å).[27] The value being in between double (1.54 Å)[28] and single N-S bond (1.69 Å),[29] suggests partial double bond character. The sum of the angles around N(2) amounts to 349°, in the middle of to the typical values for sp^3 and sp^2 hybridisation. The proline nitrogen, N(2), presents a slightly distorted sp^3 hybridised centre, with the sum of bond angles equal to 336°, where 327° would represent perfect tetrahedral geometry. The amide group centered on C(1) is perfectly planar, and the bond lengths observed for C(1)-O(1) (1.239(3) Å) and C(1)-N(1) (1.325(4) Å) correspond to those expected for primary amides.[36]

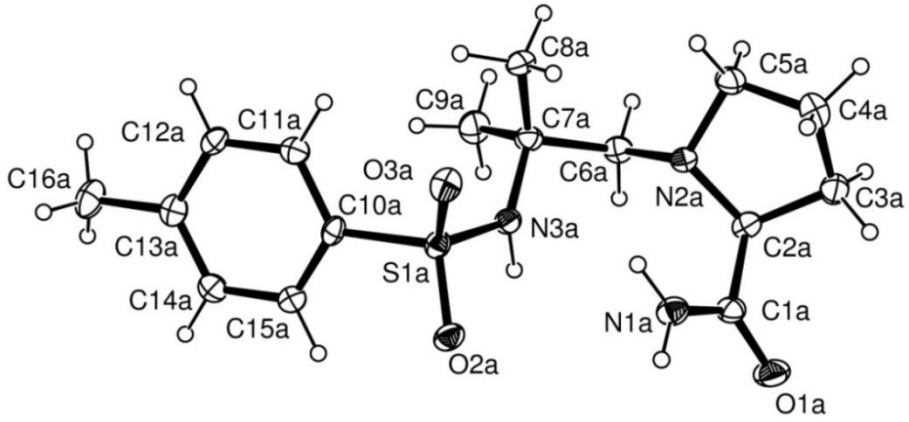

Figure 3.8 ORTEP[31] view of structure 159b with 50% probability displacement ellipsoids.

	Bond Length (Å)		Bond Length (Å)
C(1A)-O(1A)	1.239(3)	**C(1B)-O(1B)**	1.248(3)
C(1A)-N(1A)	1.325(4)	**C(1B)-N(1B)**	1.311(3)
C(1A)-C(2A)	1.523(4)	**C(1B)-C(2B)**	1.525(4)
C(2A)-N(2A)	1.476(3)	**C(2B)-N(2B)**	1.482(3)
C(6A)-N(2A)	1.469(3)	**C(6B)-N(2B)**	1.467(4)
C(6A)-C(7A)	1.540(4)	**C(6B)-C(7B)**	1.541(4)
C(7A)-N(3A)	1.494(3)	**C(7B)-N(3B)**	1.499(3)
N(3A)-S(1A)	1.614(2)	**N(3B)-S(1B)**	1.606(2)
O(2A)-S(1A)	1.4458(19)	**O(2B)-S(1B)**	1.4481(19)
O(3A)-S(1A)	1.4333(19)	**O(3B)-S(1B)**	1.4301(19)

Table 3.4 Selected bond lengths for structure 159b with estimated standard deviations.

	Angle (°)		Angle (°)		Angle (°)
O(1A)-C(1A)-N(1A)	123.7(3)	**O(1B)-C(1B)-N(1B)**	124.1(2)	**O(3A)-S(1A)-O(2A)**	118.90(11)
O(1A)-C(1A)-C(2A)	119.5(2)	**O(1B)-C(1B)-C(2B)**	118.7(2)	**O(3A)-S(1A)-N(3A)**	109.43(11)
N(1A)-C(1A)-C(2A)	116.8(2)	**N(1B)-C(1B)-C(2B)**	117.2(2)	**O(2A)-S(1A)-N(3A)**	104.27(11)
N(2A)-C(2A)-C(1A)	113.1(2)	**N(2B)-C(2B)-C(1B)**	113.7(2)	**O(3A)-S(1A)-C(10A)**	106.81(11)
N(2A)-C(2A)-C(3A)	106.2(2)	**N(2B)-C(2B)-C(3B)**	105.6(2)	**O(2A)-S(1A)-C(10A)**	106.74(12)
C(1A)-C(2A)-C(3A)	110.3(2)	**C(1B)-C(2B)-C(3B)**	110.3(3)	**N(3A)-S(1A)-C(10A)**	110.60(11)
N(2A)-C(6A)-C(7A)	115.4(2)	**N(2B)-C(6B)-C(7B)**	115.4(2)	**O(3B)-S(1B)-O(2B)**	118.75(12)
N(3A)-C(7A)-C(8A)	113.1(2)	**N(3B)-C(7B)-C(8B)**	111.5(2)	**O(3B)-S(1B)-N(3B)**	110.14(12)
N(3A)-C(7A)-C(9A)	109.1(2)	**N(3B)-C(7B)-C(8B)**	111.5(2)	**O(2B)-S(1B)-N(3B)**	103.94(11)
N(3A)-C(7A)-C(6A)	104.3(2)	**N(3B)-C(7B)-C(6B)**	104.0(2)	**O(3B)-S(1B)-C(10B)**	107.74(11)
C(6A)-N(2A)-C(2A)	115.6(2)	**C(6B)-N(2B)-C(2B)**	115.4(2)	**O(2B)-S(1B)-C(10B)**	106.42(12)
C(2A)-N(2A)-C(5A)	107.73(19)	**C(6B)-N(2B)-C(5B)**	115.3(2)	**N(3B)-S(1B)-C(10B)**	109.57(12)
C(7A)-N(3A)-S(1A)	129.67(17)	**C(7B)-N(3B)-S(1B)**	129.50(19)		

Table 3.5 Selected bond Angles (°) for structure 159b with estimated standard deviations.

D-H...A	d(D-H) (Å)	d(H...A) (Å)	d(D...A) (Å)	(DHA) (°)
N(1A)-H(1A)...N(3A)	0.91(3)	2.55(3)	3.164(3)	125(2)
N(1A)-H(1A)...N(2A)	0.91(3)	2.35(3)	2.718(3)	104(2)
N(1B)-H(1C)...N(2B)	0.84(3)	2.29(3)	2.735(3)	113(3)
N(1B)-H(1C)...N(3B)	0.84(3)	2.37(3)	3.070(3)	141(3)
N(1A)-H(1B)...O(2B)#1	0.83(3)	2.20(4)	3.028(3)	170(3)
N(3A)-H(3C)...O(1B)#1	1.01(3)	1.84(4)	2.836(3)	169(3)
N(1B)-H(1D)...O(2A)#2	0.96(3)	2.05(3)	2.999(3)	170(3)
N(3B)-H(3F)...O(1A)#2	0.85(4)	1.98(4)	2.830(3)	177(3)

Table 3.6 Hydrogen bonds for 159b with estimated standard deviations.

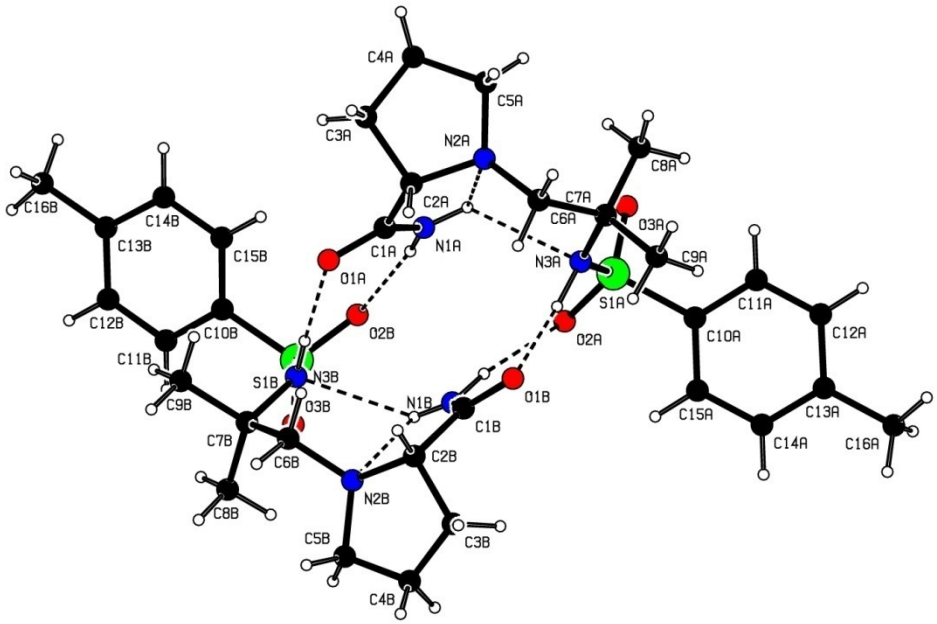

Figure 3.9 PLATON[32] view of the dimeric nature of structure 159b in the solid state with highlighted hydrogen bonds.

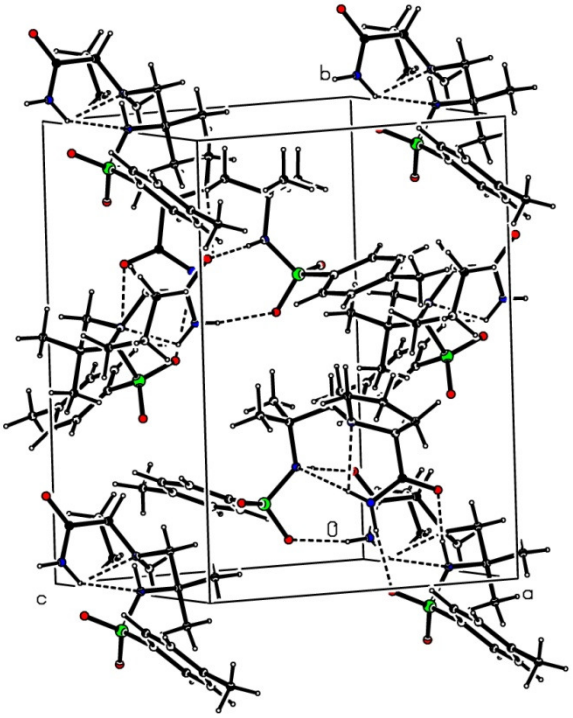

Figure 3.10 PLATON[32] view of the unit cell for 159b.

The next step was to assess if the combinations of intra- and intermolecular hydrogen bonds had an effect on the ^{1}H-NMR spectra of **158b**, **159b** and **160b**.

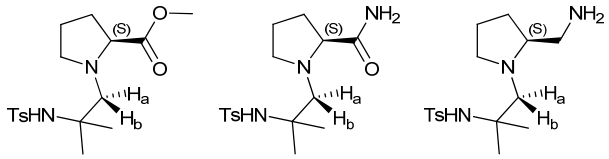

158b **159b** **160b**

Figure 3.11

The most interesting effect involved a series of shifts in the position of the methylenic protons marked in Figure 3.11. Moving from the ester to the amide, a slight shift downfield (*ca.* 0.09 ppm) can be observed for both hydrogens; when the carbonyl is removed by reduction, the shifts become more consistent (Figure 3.12) with a very small shift downfield for A (*ca.* 0.03 ppm) but with a great difference in the position of B, which moved *ca.* 0.23 ppm upfield. The NMR spectra seem not to resent significantly from the big structural changes observed in the solid state for **158b** and **159b**, and unfortunately, no crystals suitable for X-Ray analysis were obtained for **160b**, whose refined structure could help clarify the large change in the chemical shifts we observed. The most likely explanation lies in a different arrangement of the hydrogen bonds due

to the disappearance of an H-bond acceptor (e.g. the carbonyl oxygen) which in turns influences the spatial arrangement of the molecules.

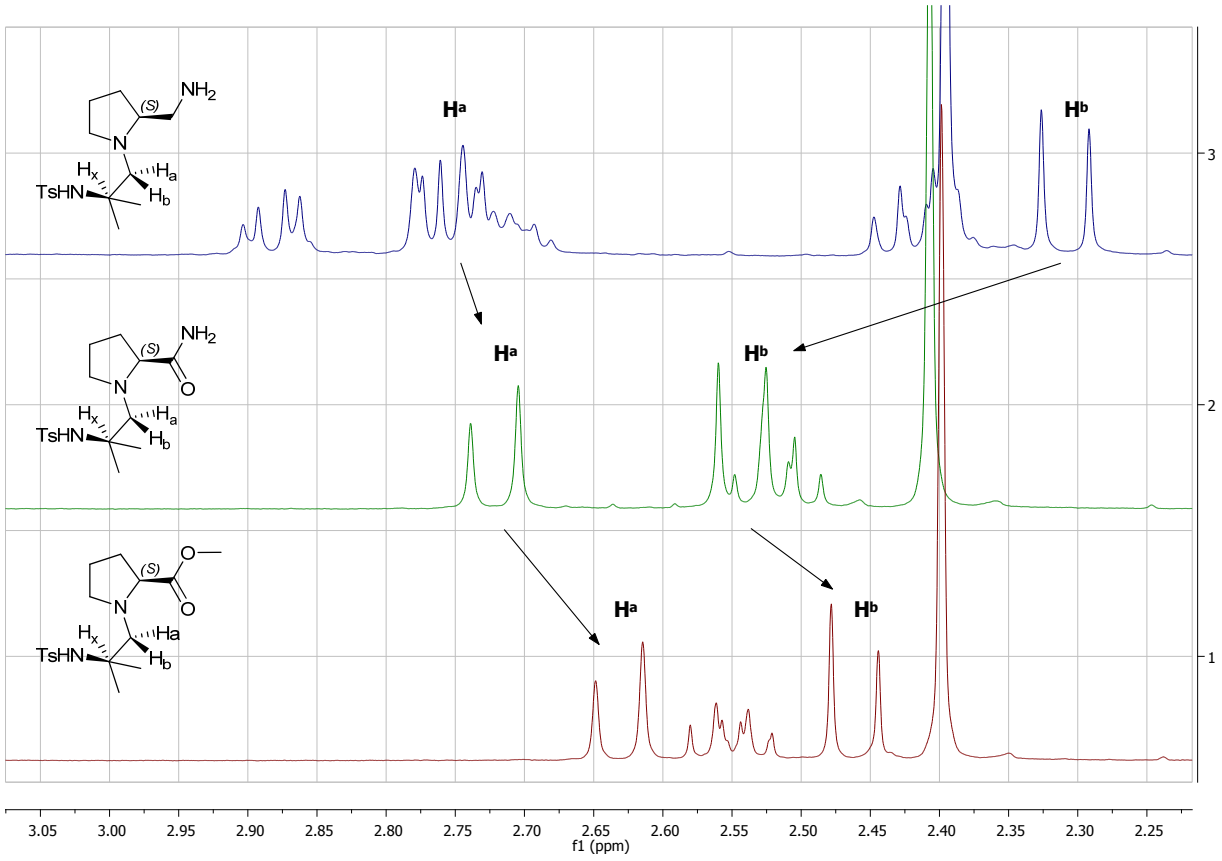

Figure 3.12 Comparison between ^{1}H-NMR spectra of 158b, 159b and 160b.

A similar analysis was undertaken for the proton NMR of compounds **158c** and **159c**. Considering their structure, an ABX system was expected for the part of the molecule highlighted in Figure 3.13.

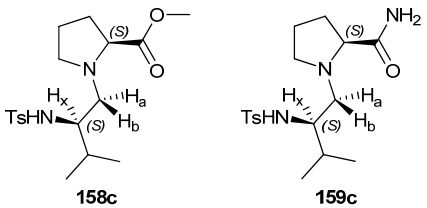

Figure 3.13

The separation between the nuclei H_a and H_b (0.11 ppm) was found to be much larger than their coupling constant (*ca.* 12 Hz) which made the system simpler to analyse since there was no merging of the signals into a more complex pattern, giving a simplified ABX system. A similar spectrum was expected for **159c**, but the separation of the three signals due to the ABX system

grew larger with no apparent reason, making it resemble to an AMX system instead (Figure 3.14).

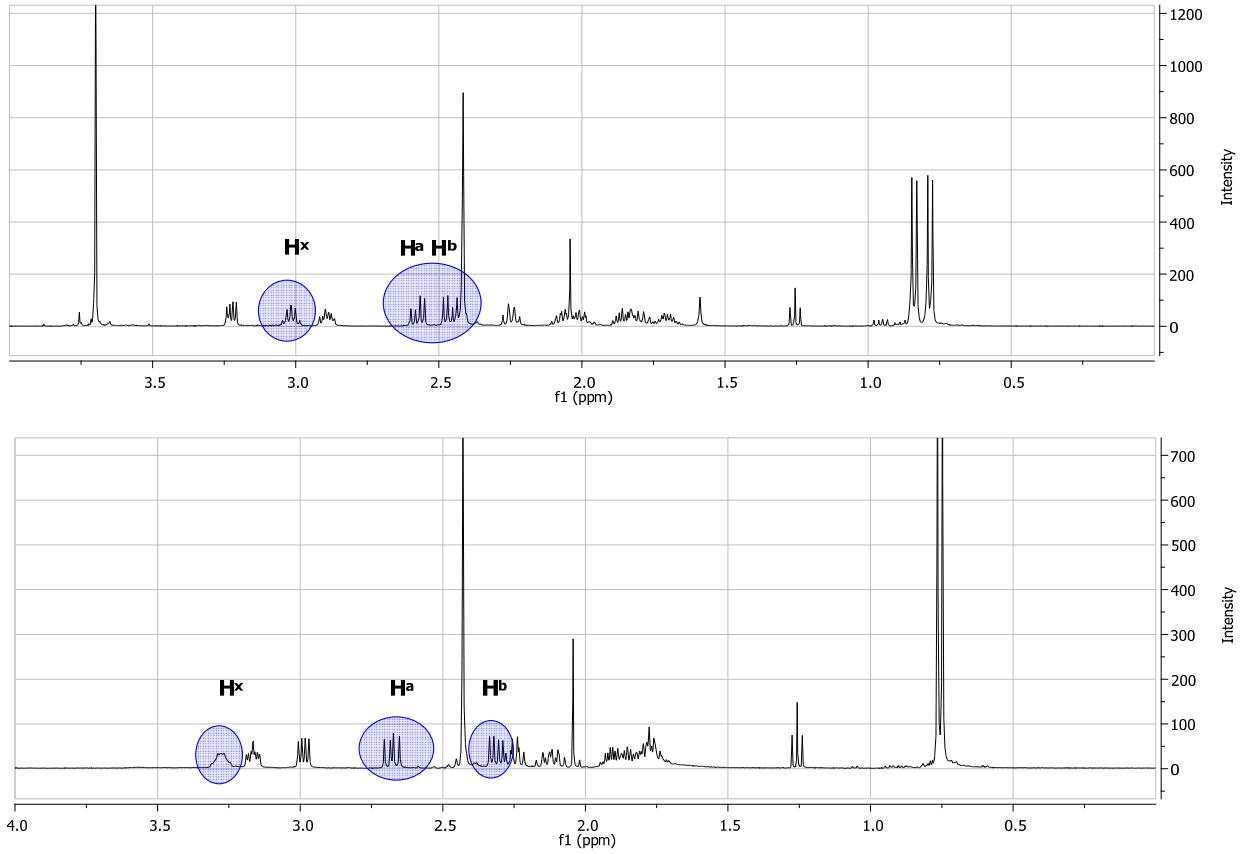

Figure 3.14 ^{1}H-NMR (in $CDCl_3$) of compound 158c (top) and 159c (bottom).

In the ^{1}H-NMR of **159c** the signals corresponding to H_a and H_b shifted (Figure 3.15, *ca.* 0.11 ppm downfield for H_a and *ca.* 0.16 ppm upfield for H_b from their previous position), and the separation between H_a and H_b became 0.36 pm. The X term of the system shifted downfield too (0.25 ppm from its previous chemical shift). The changes in the molecular structure from ester to amide are spatially very far from the protons examined, sufficient to suggest that a conformational change or a new intramolecular or intermolecular phenomenon is responsible for these protons being in a dissimilar chemical environment where the shielding (or de-shielding) effects are different.

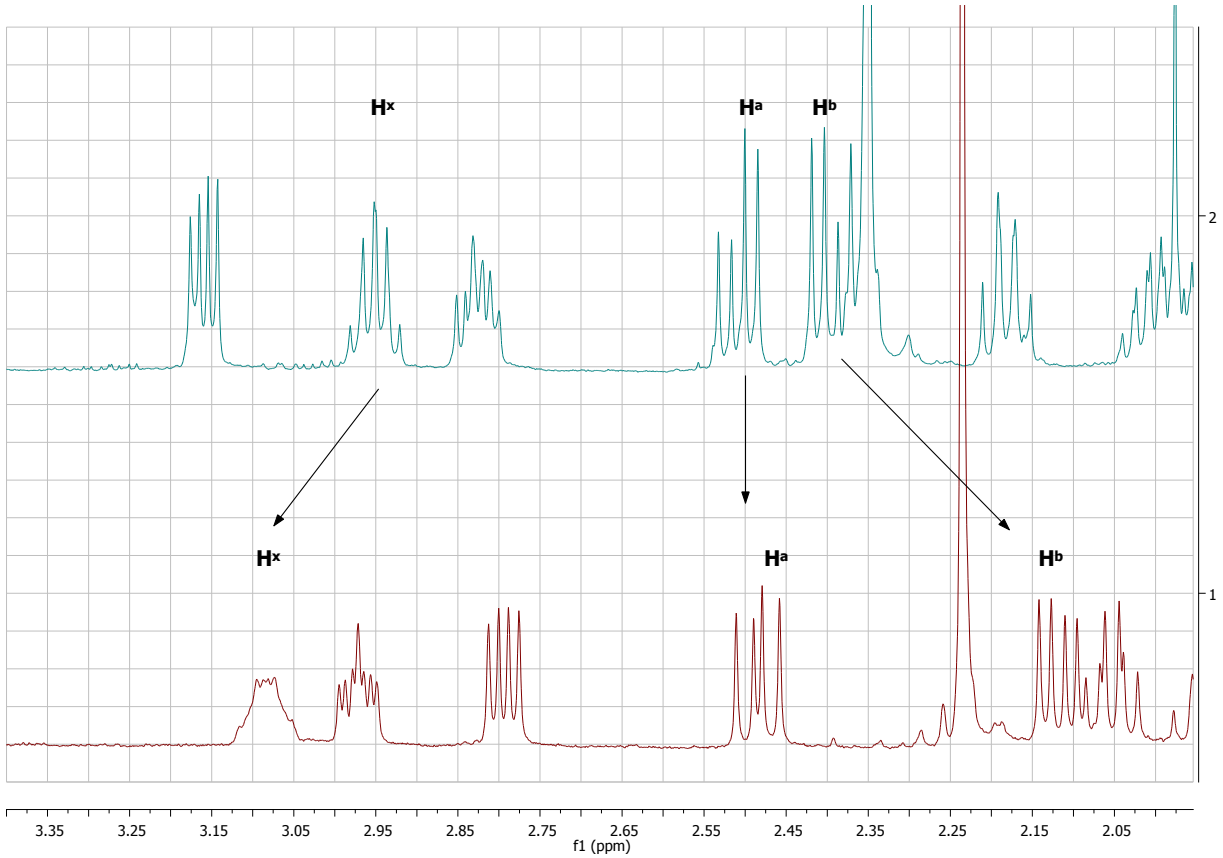

Figure 3.15 Comparison of the chemical shifts of the ABX system in structure 158c (top) and 159c (bottom).

The ^{1}H-NMR analysis of **160c** showed little difference in the chemical shift for H_a and H_b, amounting to 0.04 ppm upfield for the first and 0.04 ppm downfield for the second. The biggest change was observed for H_x which moved ca. 0.2 ppm upfield getting close to the position it held in structure **158c** (Figure 3.16). The single structural difference between **159c** and **160c** is the disappearance of the carbonyl group, which is an H-bond acceptor.

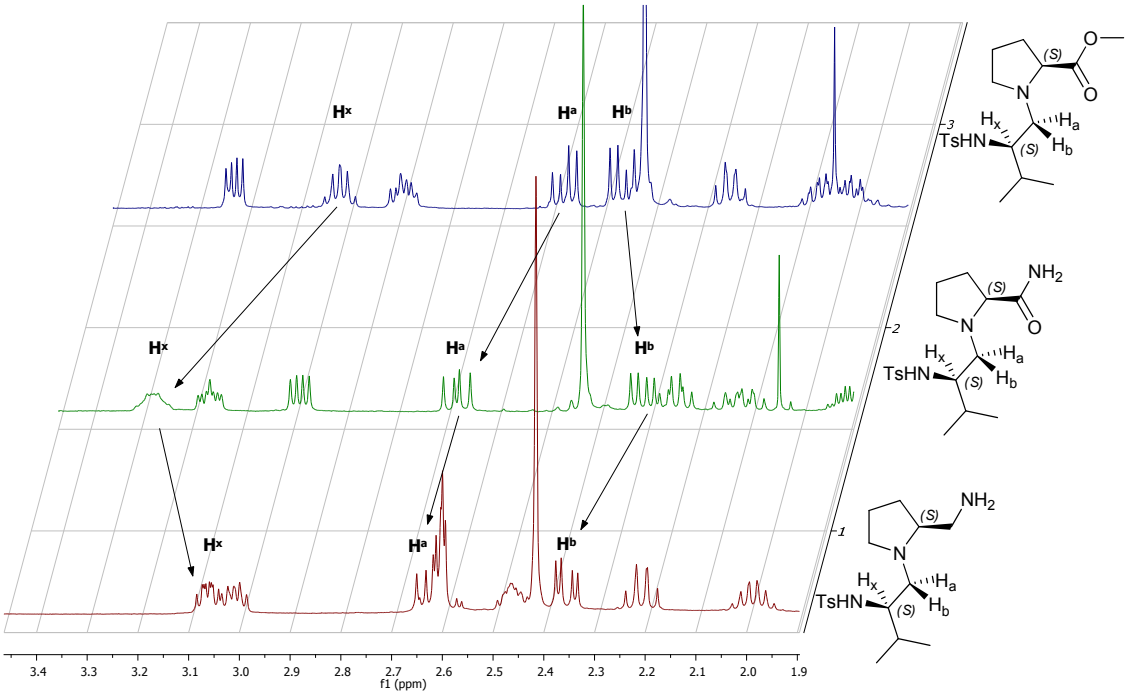

Figure 3.16 Comparison of ^{1}H-NMR spectra of 158c, 159c and 160c.

As for **158b** and **159b**, it was proposed that the presence of the amide in structure **159c** allowed the formation of an inter- and intramolecular network of hydrogen bonds, like those observed for **159b** (Figure 3.9). This network of hydrogen bonds forces the molecule to assume a particular conformation, not excluding the formation of dimers like in **159b**. The disruption of part of this network after the reduction to the primary amine is potentially inducing another conformational change that affects the chemical surrounding of H_x in **160c**. A single crystal X-Ray study of these three species might cast more light on the nature of this effect but despite repeated attempts to prepare crystals, it was impossible to obtain them even in a solid form. This attempt to find the origin of the unexpected changes in chemical shift and couplings by comparing NMR spectra and crystal structures, despite the efforts put into it, proved unsuccessful to draw a definitive conclusion.

3.2.4 Benzylation of 160c

The last step consisted of the benzylation of the primary amine of **160c**. This could be achieved either by reaction with benzoyl chloride and subsequent reduction (steps ii and iii, Scheme 3.11) or by direct reaction with benzyl bromide (step i, Scheme 3.11). The latter option was selected to reduce the loss of mass which would inevitably occur in a two-step reaction, which was particularly important given the difficulties experienced earlier in the synthesis.

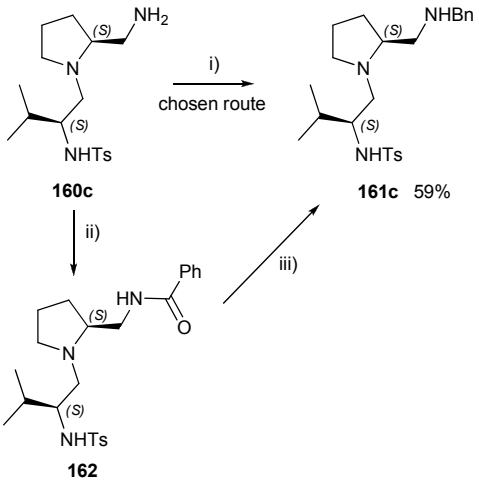

Scheme 3.11 Final synthetic step in the synthesis. i) BnBr, K_2CO_3, DCM; ii) benzoyl chloride, TEA; iii) $LiAlH_4$, THF, reflux.

A stoichiometric amount of the alkylating agent was used to reduce the chance of dibenzylation, due to the intrinsic reactivity of amines. The reaction with benzoyl chloride would prevent this over substitution, since the amide formed is much less reactive than a secondary amine due to the delocalisation of the lone pair on the structure. Unfortunately as feared, a mixture of mono- and dialkylated products was obtained but it was still possible to obtain **161d** in 59% yield after purification. The ^{1}H-NMR of **161c** did not show any significant change in the chemical shift for the ABX system compared to starting material **160c**, as this transformation is unlikely to modify the network of hydrogen bonds no change in the interaction was expected.

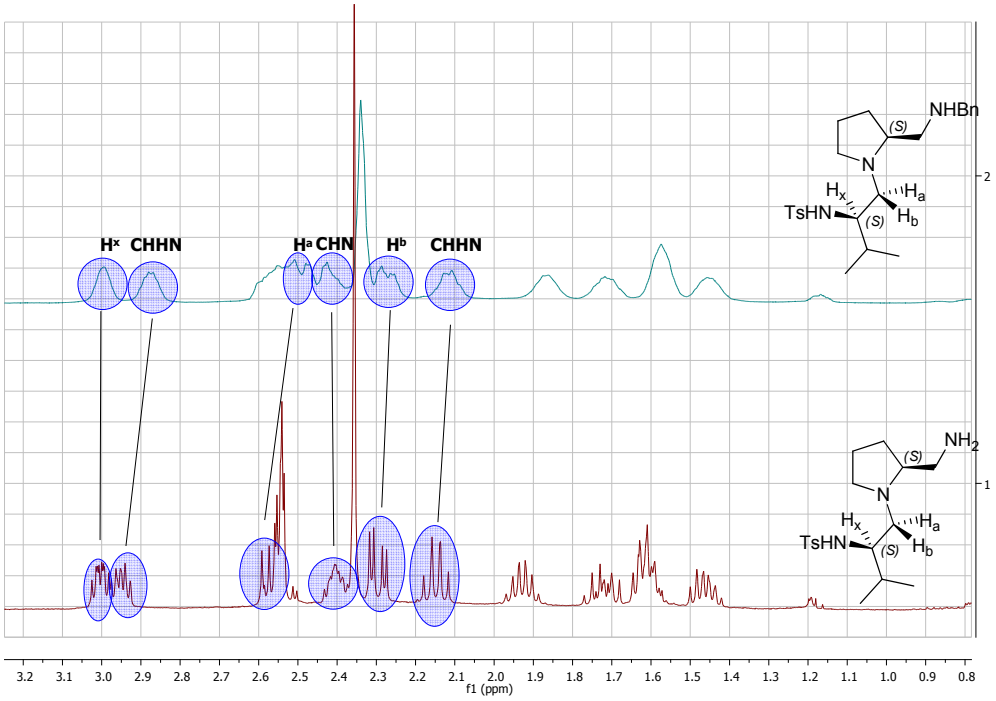

Figure 3.17 Comparison of selected regions of the ^{1}H-NMR spectra of 160c (bottom) and 161c (top).

The plan of building a large library of ligands based on the general structures **A**, **B**, **C**, **D** and **E** illustrated in Figure 3.18 has encountered many synthetic obstacles. The unexpected lack of reactivity of the Boc-protected sulfamidates precluded the use of this methodology for derivatives **B**, **C** and **E**. The reaction with benzyl-protected sulfamidates was not successful either. Luckily, the reaction with tosyl-protected aziridines was partially successful and allowed to start working on derivative **A** and potentially **D**. This way of introducing the R into the molecule allows for a variety of electron donating groups and other potentially coordinating groups; and together with the possibility of combinging different groups on the terminal nitrogens makes this structures potentially very versatile ligands.

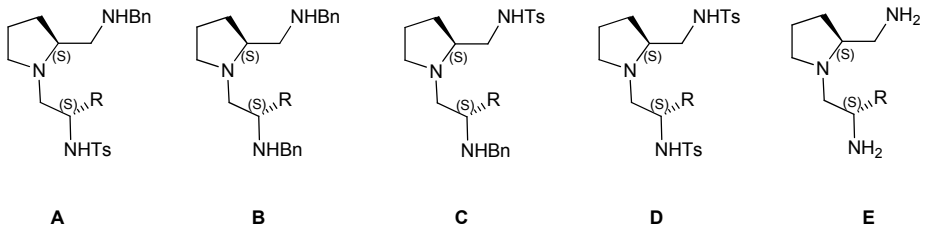

Figure 3.18 Potential structures that could be obtained through the presented synthetic plans.

3.3 Screening for activity in the epoxidation of alkenes

After obtaining the first ligand (**161c**) its activity in the asymmetric epoxidation of alkenes was tested before moving on with the synthesis of other derivatives. The substrate we chose for our preliminary activity tests was styrene. To expand the scope of the screening, intermediate **160c** was also included for comparison.

For the first tests, conditions similar to those reported by Beller using chiral tridentate nitrogen-containing ligands were chosen.[8, 37-39] Since the ligand design here presented was closely based on results presented by his group, it was thought that, given the similiarities in the structures, these ligands would have a similar reactivity. Iron(III) chloride hexahydrate was chosen as the source of metal. Tests in the presence and absence of pyridine dicarboxylic acid (H_2Pydic) as a co-catalyst were also performed. Tests were performed on styrene, generating the complex *in situ*, with a catalyst loading of 1%, introducing 1 mol% of H_2Pydic and with hydrogen peroxide (10 eq.) as the oxidant. As in Beller's work, the solvent was *tert*-amyl alcohol; this alcohol is an environmentally friendly media which has been used with success in several epoxidations with hydrogen peroxide. [38, 40, 41] The tertiary alcohol provides good solubility for the reaction partners

and is not oxidised by hydrogen peroxide under these conditions, so no competing reaction was expected.

The tests on **160c** and **161c** were performed alongside blank reactions in which the ligand and the metal were absent to confirm that any reactivity observed originated from the formation of a metal-ligand species in solution. Ligand, metal, substrate and standard were added from freshly prepared stock solutions in acetonitrile or water. Unfortunately under these conditions, this system did not prove active in the epoxidation of styrene.

In the search for activity, it has been considered worthwhile changing the metal centre. Since manganese is generally the metal of choice for most of the metal catalysed epoxidations with hydrogen peroxide, we switched our source of metal to manganese(II) sulfate. The reactions were carried out under the same conditions as for iron(III) chloride, once again with and without co-catalyst. Even in this case, no product of epoxidation was observed. A summary of the conditions is reported in Table 3.7.

Entry	Ligand (eq.)	Metal salt (eq.)	Additive (eq.)
1	**161c** (0.01)	$FeCl_3$ (0.01)	no
2	**161c** (0.01)	$FeCl_3$ (0.01)	H_2Pydic (0.01)
3	**161c** (0.01)	$MnSO_4$ (0.01)	no
4	**161c** (0.01)	$MnSO_4$ (0.01)	H_2Pydic (0.01)
5	**160c** (0.01)	$FeCl_3$ (0.01)	no
6	**160c** (0.01)	$FeCl_3$ (0.01)	H_2Pydic (0.01)
7	**160c** (0.01)	$MnSO_4$ (0.01)	no
8	**160c** (0.01)	$MnSO_4$ (0.01)	H_2Pydic (0.01)

Table 3.7 Attempted epoxidation using Beller`s conditions. Oxidant added over 5 minutes, oxidant was hydrogen peroxide (10 eq.), solvent was *tert*-amyl alcohol.

After the disappointing results obtained in *tert*-amyl alcohol, we applied a slight modification to the previous procedure, and replaced the alcohol with ACN, a similarly polar but aprotic solvent. ACN has a record of successful use in epoxidation reactions (see Chapter 1) and has good solvating properties; the rest of the procedure was left untouched. Hydrogen peroxide was again employed as the oxidant and we screened the same metal salts. To further disappointment, no

reaction was observed; the substrate was not consumed and no new species formed in any of the test runs performed in the new solvent.

An obvious reason for the inactivity of this system was that the lack of oxidation products was due to the known catalase-like activity of these two metals. Catalases are manganese- or iron containing ubiquitous enzymes,[42, 43] which role is to decompose hydrogen peroxide into water and oxygen and are known to have some of the highest turnover numbers among enzymes; many manganese(II) complexes are known to catalyse the disproportionation of hydrogen peroxide.[44] This suspicion was also backed up by the vigorous bubbling observed in the reaction upon addition of hydrogen peroxide, a clear sign of oxygen evolution. The current literature on epoxidation presents several different procedures for the addition of the oxidant to the reaction; most of them differ by the timescale of the addition and by the physical means (syringe pump, dropwise, addition in one portion) through this is achieved.[45] It was therefore decided to change the rate of addition, from 5 to 20 minutes and to dilute the oxidant with acetonitrile to assess if this different methodology would have an impact on the reaction. But the reactivity did not change and the disproportionation could still be observed with manganese. This is likely to be because the rate of the catalase activity is much greater than the epoxidation and dilution simply slows down the process. See Table 3.8 for a list of the conditions used.

Entry	Ligand (eq.)	Metal salt (eq.)	Additive (eq.)	Other conditions
1	**161c** (0.01)	$FeCl_3$ (0.01)	no	A
2	**161c** (0.01)	$FeCl_3$ (0.01)	H_2Pydic (0.01)	A
3	**161c** (0.01)	$FeCl_3$ (0.01)	no	B
4	**161c** (0.01)	$FeCl_3$ (0.01)	H_2Pydic (0.01)	B
5	**161c** (0.01)	$MnSO_4$ (0.01)	no	A
6	**161c** (0.01)	$MnSO_4$ (0.01)	H_2Pydic (0.01)	A
7	**161c** (0.01)	$MnSO_4$ (0.01)	no	B
8	**161c** (0.01)	$MnSO_4$ (0.01)	H_2Pydic (0.01)	B
9	**160c** (0.01)	$FeCl_3$ (0.01)	no	A
10	**160c** (0.01)	$FeCl_3$ (0.01)	H_2Pydic (0.01)	A
11	**160c** (0.01)	$FeCl_3$ (0.01)	no	B
12	**160c** (0.01)	$FeCl_3$ (0.01)	H_2Pydic (0.01)	B

13	**160c** (0.01)	$MnSO_4$ (0.01)	no	A
14	**160c** (0.01)	$MnSO_4$ (0.01)	H_2Pydic (0.01)	A
15	**160c** (0.01)	$MnSO_4$ (0.01)	no	B
16	**160c** (0.01)	$MnSO_4$ (0.01)	H_2Pydic (0.01)	B

Table 3.8 Solvent was acetonitrile, hydrogen peroxide (10 eq.) diluted in acetonitrile. A: Oxidant over 5 minutes; B: Oxidant over 20 minutes; a) H_2O_2:ACN 1:1 v/v.

In another attempt to suppress the catalase effect we employed the same strategy described in Chapter 2 for the manganese/TMTACN system and which has been widely used, mixing hydrogen peroxide with acetone prior to the addition. The role of acetone in preventing disproportionation is thought to result from the formation of a perhemiketal (Scheme 3.12) in the presence of hydrogen peroxide[46] which does not undergo the same process as the original oxidant in the presence of manganese. The perhemiketal then acts as a reservoir of hydrogen peroxide and slowly releases it into the reaction. In our tests we also attempted to add acetone to the mixture prior to the addition of oxidant.

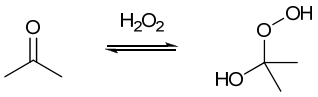

Scheme 3.12 Equilibrium between acetone and its perhemiketal formed in the presence of hydrogen peroxide.

When the catalytic reaction was repeated mixing the oxidant with acetone instead of acetonitrile, no vigorous evolution of oxygen occurred, a sign that disproportionation had been avoided, but once again even after 24 hours the substrate remained unreacted. Table 3.9 shows the conditions used.

Entry	Ligand (eq.)	Metal salt (eq.)	Oxidant (eq.)	Additive (eq.)	Other conditions
1	**161c** (0.01)	$FeCl_3$ (0.01)	H_2O_2 (10) in acetone [a]	no	A
2	**161c** (0.01)	$FeCl_3$ (0.01)	H_2O_2 (10) in acetone [a]	H_2Pydic (0.01)	A
3	**161c** (0.01)	$MnSO_4$ (0.01)	H_2O_2 (10) in acetone [a]	no	A
4	**161c** (0.01)	$MnSO_4$ (0.01)	H_2O_2 (10) in acetone [a]	H_2Pydic (0.01)	A
5	**161c** (0.01)	$FeCl_3$ (0.01)	H_2O_2 (10)	no	B[a]
6	**161c** (0.01)	$FeCl_3$ (0.01)	H_2O_2 (10)	H_2Pydic (0.01)	B[a]

7	**161c** (0.01)	$MnSO_4$ (0.01)	H_2O_2 (10)	no	B[a]
8	**161c** (0.01)	$MnSO_4$ (0.01)	H_2O_2 (10)	H_2Pydic (0.01)	B[a]
9	**160c** (0.01)	$FeCl_3$ (0.01)	H_2O_2 (10) in acetone [a]	no	A
10	**160c** (0.01)	$FeCl_3$ (0.01)	H_2O_2 (10) in acetone [a]	H_2Pydic (0.01)	A
11	**160c** (0.01)	$MnSO_4$ (0.01)	H_2O_2 (10) in acetone [a]	no	A
12	**160c** (0.01)	$MnSO_4$ (0.01)	H_2O_2 (10) in acetone [a]	H_2Pydic (0.01)	A
13	**160c** (0.01)	$FeCl_3$ (0.01)	H_2O_2 (10)	no	B[a]
14	**160c** (0.01)	$FeCl_3$ (0.01)	H_2O_2 (10)	H_2Pydic (0.01)	B[a]
15	**160c** (0.01)	$MnSO_4$ (0.01)	H_2O_2 (10)	no	B[a]
16	**160c** (0.01)	$MnSO_4$ (0.01)	H_2O_2 (10)	H_2Pydic (0.01)	B[a]

Table 3.9 Solvent was acetonitrile. A: Oxidant over 5 minutes; B: Oxidant over 5 minutes, acetone in the mixture; a) H_2O_2:acetone 1:3 v/v.

After these disappointing results, it was decided to switch to a different oxidant. Costas and coworkers[47] have reported the epoxidation of alkenes by *in situ* generated peracetic acid with hydrogen peroxide. Two different strategies were adopted this time, the first involving the *in situ* generation of the oxidant by adding acetic acid to the reaction mixture before the oxidant; the second using commercial peracetic acid. In this set of catalytic runs, no co-catalyst was employed. Again, the tests were conducted using both **160c** and **161c** and again no sign of epoxidation or substrate consumption was observed. The conditions are reported in Table 3.10.

Entry	Ligand (eq.)	Metal salt (eq.)	Oxidant (eq.)	Other conditions
1	**161c** (0.01)	$FeCl_3$ (0.01)	H_2O_2 (10) in ACN [a]	A
2	**161c** (0.01)	$FeCl_3$ (0.01)	Peracetic acid (10)	
3	**161c** (0.01)	$MnSO_4$ (0.01)	H_2O_2 (10) in ACN [a]	A
4	**161c** (0.01)	$MnSO_4$ (0.01)	Peracetic acid (10)	
5	**160c** (0.01)	$FeCl_3$ (0.01)	H_2O_2 (10) in ACN [a]	A
6	**160c** (0.01)	$FeCl_3$ (0.01)	Peracetic acid (10)	

7	**160c** (0.01)	$MnSO_4$ (0.01)	H_2O_2 (10) in ACN [a]	A
8	**160c** (0.01)	$MnSO_4$ (0.01)	Peracetic acid (10)	

Table 3.10 Attempted epoxidation using Costas' conditions. Solvent was acetonitrile. A: Acetic acid (14 eq.) in the reaction, oxidant over 5 mins; a) H_2O_2:ACN 1:1 v/v.

3.4 Conclusions

After the failure of **160c** and **161c** to produce any epoxidation, the synthesis of the other derivatives planned to be included in this study was abandoned, since the modifications on the structure were not considered significant enough to cause a complete change in the reactivity but were designed to finely tune any reactivity if present.

Although inactive in the epoxidation of alkenes in the conditions tested, a synthetic route to a potential library of ligands bearing one or more chiral centres has been established. This synthesis does not present any risk of racemisation. The low yield obtained when aziridines were employed in the synthesis of **158** and the total lack of activity of the sulfamidates remains confusing. If the optimal conditions were found this could have opened the way to the synthesis of a wider library of ligands (Figure 3.18, **A**, **B**, **C**, **D**, **E**). In addition to the different bases that we screened when trying to optimise the reaction with sulfamidates, different solvents could also be tested. The lack of catalytic activity of the ligand tested might be due to the inability to coordinate to the metal centres in solution since the synthesis of an authentic complex to prove the coordinating ability of our structures was never attempted.

3.5 References

1. G. de Ruiter, J. S. Costa, K. Lappalainen, O. Roubeau, P. Gamez and J. Reedijk, *Inorg. Chem. Commun.*, 2008, **11**, 787-790.
2. M. Bagherzadeh, L. Tahsini, R. Latifi, V. Amani, A. Ellern and L. K. Woo, *Inorg. Chem. Commun.*, 2009, **12**, 476-480.
3. G. Ilyashenko, D. Sale, M. Motevalli and M. Watkinson, *J. Mol. Catal. A: Chem.*, 2008, **296**, 1-8.
4. D. Chatterjee, S. Basak, A. Riahi and J. Muzart, *Catal. Commun.*, 2007, **8**, 1345-1348.
5. P. I. Dalko and L. Moisan, *Angew. Chem. Int. Ed.*, 2004, **43**, 5138-5175.
6. A. Dondoni and A. Massi, *Angew. Chem. Int. Ed.*, 2008, **47**, 4638-4660.
7. C. Bolm, N. Meyer, G. Raabe, T. Weyhermuller and E. Bothe, *Chem. Commun.*, 2000, 2435-2436.
8. F. G. Gelalcha, B. Bitterlich, G. Anilkumar, M. K. Tse and M. Beller, *Angew. Chem. Int. Ed.*, 2007, **46**, 7293-7296.
9. K. Matsumoto, T. Oguma and T. Katsuki, *Angew. Chem. Int. Ed.*, 2009, **48**, 7432-7435.
10. F. G. Gelalcha, G. Anilkumar, M. K. Tse, A. Brueckner and M. Beller, *Chem. Eur. J.*, 2008, **14**, 7687-7698.
11. X. E. Hu, *Tetrahedron*, 2004, **60**, 2701-2743.
12. G. Stones, R. Tripoli, C. L. McDavid, K. Roux-Duplatre, A. R. Kennedy, D. C. Sherrington and C. L. Gibson, *Org. Biomol. Chem.*, 2008, **6**, 374-384.
13. M. Cernerud, H. Adolfsson and C. Moberg, *Tetrahedron: Asymmetry*, 1997, **8**, 2655-2662.
14. J. Clayden, S. Warren, N. Greeves and P. Wothers, *Organic Chemistry*, 4 edn., Oxford University Press, 2005.
15. J. F. Bower, PhD Thesis, University of Bristol, 2007.
16. J. F. Bower, J. Svenda, A. J. Williams, J. P. H. Charmant, R. M. Lawrence, P. Szeto and T. Gallagher, *Org. Lett.*, 2004, **6**, 4727-4730.
17. R. E. Meléndez and W. D. Lubell, *Tetrahedron*, 2003, **59**, 2581-2616.
18. B. M. Kim and S. M. So, *Tetrahedron Lett.*, 1998, **39**, 5381-5384.
19. K. C. Nicolaou, X. H. Huang, S. A. Snyder, P. B. Rao, M. Bella and M. V. Reddy, *Angew. Chem. Int. Ed.*, 2002, **41**, 834.
20. A. J. Williams, S. Chakthong, D. Gray, R. M. Lawrence and T. Gallagher, *Org. Lett.*, 2003, **5**, 811-814.

21. D. Alker, K. J. Doyle, L. M. Harwood and A. Mcgregor, *Tetrahedron: Asymmetry*, 1990, **1**, 877-880.
22. K. K. Andersen, D. D. Bray, S. Chumpradit, M. E. Clark, G. J. Habgood, C. D. Hubbard and K. M. Young, *J. Org. Chem.*, 1991, **56**, 6508-6516.
23. B. U. W. Maes, K. T. J. Loones, T. H. M. Jonckers, G. L. F. Lemiere, R. A. Dommisse and A. Haemers, *Synlett*, 2002, 1995-1998.
24. J. P. Wolfe and S. L. Buchwald, *J. Org. Chem.*, 2000, **65**, 1144-1157.
25. G. Dijkstra, W. H. Kruizinga and R. M. Kellogg, *J. Org. Chem.*, 1987, **52**, 4230-4234.
26. T. Flessner and S. Doye, *Journal Fur Praktische Chemie-Chemiker-Zeitung*, 1999, **341**, 186-190.
27. F. H. Allen, *Acta Crystallogr. B*, 2002, **58**.
28. R. Hoppenheit, E. Lork, J. Petersen and R. Mews, *Chem. Commun.*, 1997, 1659-1660.
29. D. W. J. Cruickshank, *J. Chem. Soc.*, 1961, 5486-5504.
30. J. Graton, M. Berthelot and C. Laurence, *J. Chem. Soc., Perkin Trans. 2*, 2001, 2130-2135.
31. L. Farrugia, *J. Appl. Crystallogr.*, 1997, **30**, 565.
32. A. L. Spek, *J. Appl. Crystallogr.*, 2003, **36**, 7-13.
33. J. Zhou, R. He, K. M. Johnson, Y. Ye and A. P. Kozikowski, *J. Med. Chem.*, 2004, **47**, 5821-5824.
34. J. H. Cho, D. L. Bernard, R. W. Sidwell, E. R. Kern and C. K. Chu, *J. Med. Chem.*, 2006, **49**, 1140-1148.
35. S. K. Srivastava, A. Agarwal, P. M. S. Chauhan, S. K. Agarwal, A. P. Bhaduri, S. N. Singh, N. Fatima and R. K. Chatterjee, *Biorg. Med. Chem.*, 1999, **7**, 1223-1236.
36. F. H. Allen and I. J. Bruno, *Acta Crystallogr., Sect. B: Struct. Sci*, 2010, **66**, 380-386.
37. F. G. Gelalcha, G. Anilkumar, M. K. Tse, A. Brückner and M. Beller, *Chem. Eur. J.*, 2008, **14**, 7687-7698.
38. M. K. Tse, M. Klawonn, S. Bhor, C. Dobler, G. Anilkumar, H. Hugl, W. Magerlein and M. Beller, *Org. Lett.*, 2005, **7**, 987-990.
39. S. Bhor, G. Anilkumar, M. K. Tse, M. Klawonn, C. Dobler, B. Bitterlich, A. Grotevendt and M. Beller, *Org. Lett.*, 2005, **7**, 3393-3396.
40. M. Klawonn, M. K. Tse, S. Bhor, C. Dobler and M. Beller, *J. Mol. Catal. A: Chem.*, 2004, **218**, 13-19.
41. M. K. Tse, S. Bhor, M. Klawonn, G. Anilkumar, H. J. Jiao, A. Spannenberg, C. Dobler, W. Magerlein, H. Hugl and M. Beller, *Chem. Eur. J.*, 2006, **12**, 1875-1888.

42. N. N. Gerasimchuk, A. Gerges, T. Clifford, A. Danby and K. Bowman-James, *Inorg. Chem.*, 1999, **38**, 5633.

43. A. Horn, G. L. Parrilha, K. V. Melo, C. Fernandes, M. Horner, L. d. C. Visentin, J. A. S. Santos, M. S. Santos, E. C. A. Eleutherio and M. D. Pereira, *Inorg. Chem.*, **49**, 1274-1276.

44. L. Dubois, D. F. Xiang, X. S. Tan, J. Pecaut, P. Jones, S. Baudron, L. Le Pape, J. M. Latour, C. Baffert, S. Chardon-Noblat, M. N. Collomb and A. Deronzier, *Inorg. Chem.*, 2003, **42**, 750-760.

45. B. S. Lane and K. Burgess, *Chem. Rev.*, 2003, **103**, 2457-2474.

46. D. E. De Vos and T. Bein, *J. Organomet. Chem.*, 1996, **520**, 195-200.

47. I. Garcia-Bosch, A. Company, X. Fontrodona, X. Ribas and M. Costas, *Org. Lett.*, 2008, **10**, 2095-2098.

Chapter 4 - Synthesis and activity of a series of chiral tri- tetra- and pentadentate ligands based on the cyclohexanediamine backbone.

In the continuing effort to develop a system for the asymmetric epoxidation of unfunctionalised alkenes, the activity of ligands based on the chiral backbone of *trans*-cyclohexanediamine was explored. The diaminocyclohexane motif is considered a privileged scaffold for ligand design, due to the activity of the large number of ligands for inorganic- and organocatalysis[1] that incorporate its structure.

Enantiopure diaminocyclohexane has been successfully introduced in many active epoxidation catalysts, [2-9] in the catalysis of 1,2-nucleophilic additions,[10] asymmetric alkylations, [11-13], asymmetric aziridination[14, 15] and it is also commercially available as a mixture of *cis*- and *trans*-isomers. In addition, many well established procedures for the resolution of the racemate can be found in the literature to access the single enantiomers. [9, 16-18]

Having identified *trans*-diaminocyclohexane as a possible backbone for the ligands, the next step was identifying the additional coordinating groups to insert into the structure. The choice fell on pyridyl substituents, known for their coordinating ability; their nitrogen is in fact a good σ–donor and they can accept π–backdonation from the metal, forming stable complexes with a wide range of metal ions. [19] Pyridine (Py) is possibly the best known and one of the most widely used coordinating groups in the synthesis of metal complexes and their application in catalysis. Py-containing ligands have found applications in cyclopropanation, aldol reactions and epoxidations.[20-23] Ligands derived from a combination of cyclohexanediamine backbone and pyridine substituents have proved active not only in epoxidation, but also in the ring opening of epoxides[24] and allylic alkylations[25] as well as in many other reactions.[26]

4.1 Design and synthetic plans

Inspired by the work of Stack, [3, 4] two 1,2-diaminocyclohexane based chiral ligands containing respectively one and three pyridyl groups attached to the structure were synthesised (Figure 4.1).

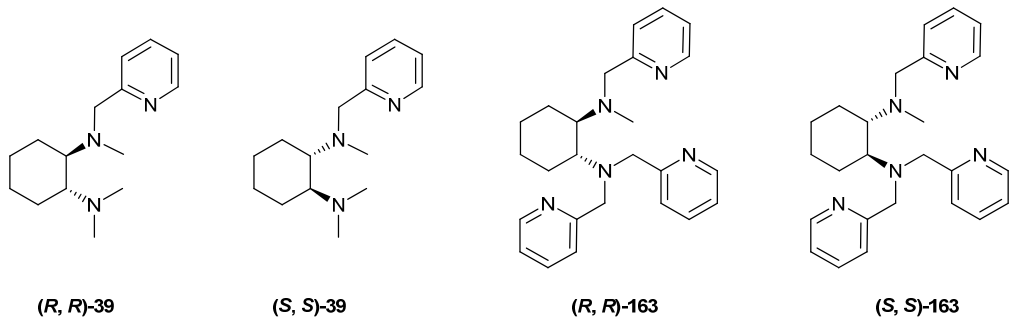

Figure 4.1 Cyclohexane diamine derived ligands bearing pyridyl groups synthesised in this study.

The tridentate ligands (**39**) have been synthesised and tested by Stack in the epoxidation of terminal alkenes with peracetic acid and manganese as the metal. Their encouraging results (up to 95% conversion and 92% epoxide yield) inspired the investigation of the stereoselectivity of this system, which was not previously studied. In addition to this, the substrate investigated by Stack was limited to 1,2-octene, leaving space for further development.

The pentadentate ligands (**163**) were thought of as a hybrid between Stack`s structures and the very active salens developed by Berkessel, Katsuki and Shitama[27-29] in an attempt to combine the best features of both systems and give increased levels of asymmetric induction.

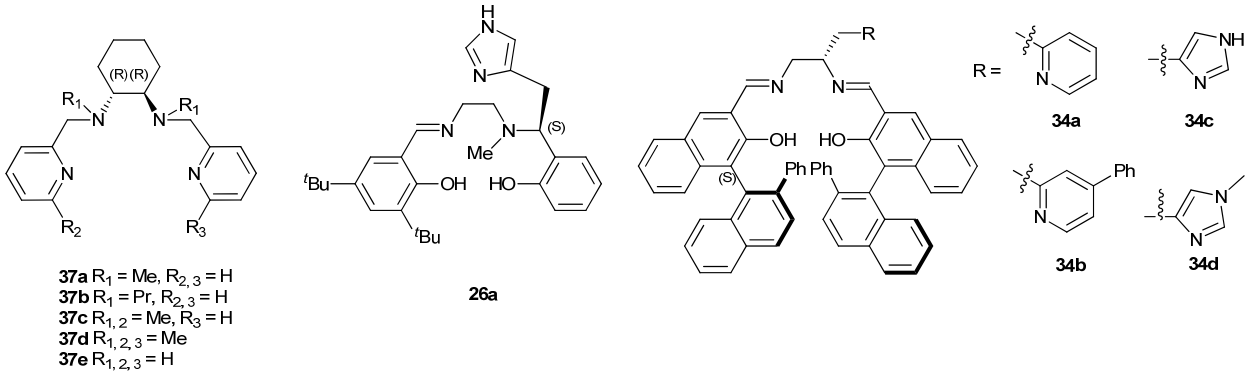

Figure 4.2 Selection of Stack's ligands (37) and some of the pentadentate salens from Berkesell (26) and Katsuki (34).

The last structure designed was a tetradentate ligand that slightly differentiates itself from the others, not containing any pyridyl group. Its structure was still based on enantiomerically pure diaminocyclohexane, but the other two coordinating groups chosen were triazole rings obtained by a 1,3 dipolar cycloaddition (known as the copper(I) catalysed Huisgen 1,3-dipolar cycloaddition[30]) between an alkyne and an azide. The coordinating activity of the triazole ring has been previously proved in work conducted in this group on scorpionate complexes[31-33] and by several other groups worldwide. [34-36] A closely related structure to the one developed, although achiral, has recently been employed in the epoxidation of alkenes.[37]

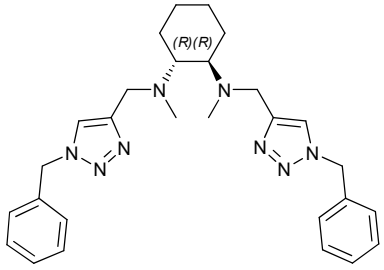

(*R*, *R*)-164

Figure 4.3 The cyclohexanediamine-based "click" tetradentate ligand synthesised in this work.

The synthetic strategy adopted for the synthesis of the "click" ligand can also allow for a wide number of modifications just by changing the cycloaddition partners therefore allowing subsequent optimisation of any active systems.

4.2 Tridentate ligand 39

The synthesis of the tridentate derivative from diaminocyclohexane requires de-symmetrisation of the molecule in the early stages of the synthetic path via a selective double protection of one of the amines leaving the second untouched (Scheme 4.1, **A**).

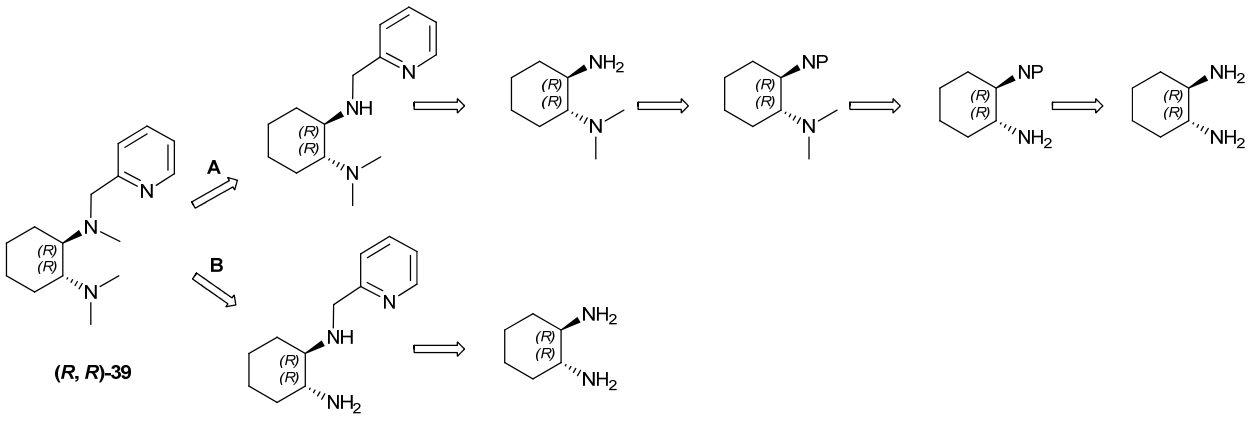

Scheme 4.1 The proposed retrosynthetic approach to the synthesis of the tridentate ligand; P = protecting group.

An alternative procedure (**B**), involving fewer steps, was also considered but the lack of selectivity in the first step convinced us to discard it and proceed with the more laborious but reliable one.

4.2.1 Synthesis

The synthesis was performed starting from enantiopure (*R*, *R*) and (*S*, *S*)-cyclohexanediamine, which were obtained by resolution of the racemic mixture of *cis*- and *trans*-isomers as described in Chapter 2 (Scheme 4.2).

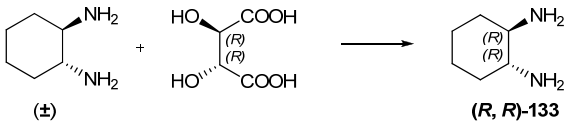

Scheme 4.2 Resolution of diaminocyclohexane.

A single resolution allows one of the enantiomers to be obtained in the form of a tartrate salt while the second has to be recovered from the mother liquor following a longer procedure. To speed up the production of starting material, parallel resolutions were performed using both (+)- and (-)-tartaric acid, which immediately yields the (*R*, *R*)- and the (*S*, *S*)-tartrate salts respectively.

4.2.1.1 Monoprotection of cyclohexanediamine

Next, to desymmetrise the molecule, one of the primary amines present in the starting material **133** required to be selectively protected. The amine also needed to be exhaustively protected to prevent it from reacting during the following steps. Among the many protecting groups available, the phthalimide group was selected as it is easy to introduce and remove and stable under the reaction conditions to be used for the following steps.

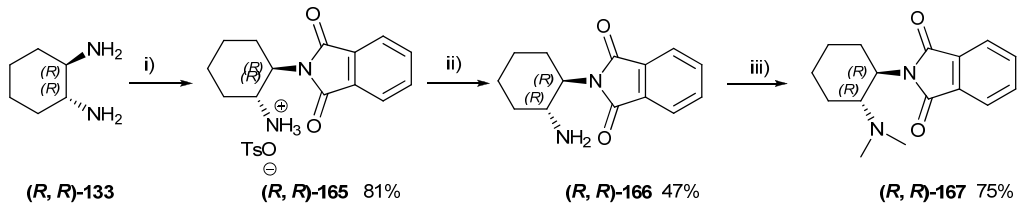

Scheme 4.3 Selective monoprotection of cyclohexanediamine with phthalic anhydride and Eschweiler-Clarke methylation. i) phthalic anhydride, tosic acid, dry toluene, reflux; ii) $NaHCO_3$ (sat.), DCM; iii) HCOOH, HCHO, H_2O/MeOH, reflux.

Looking for the ideal conditions for this protection, a very effective procedure was discovered[38] involving the use of phthalic anhydride and tosic acid in toluene, which upon refluxing the mixture using a Dean-Stark apparatus gives **(*R*, *R*)-165**. The efficacy of this procedure has been ascribed to a combination of the steric effect of the protecting group, which disfavour a second attack, and the tosic acid which protonates the product as it forms and precipitates out preventing further reaction.

The salt can be removed from the reaction mixture by filtration and further purified by recrystallisation in 1,4-dioxane. When the intermediate salt (**165**) is stirred in a mixture of DCM and saturated sodium bicarbonate, the free amine (**166**) migrates into the organic phase and can be easily recovered by evaporating the solvent.

4.2.1.2 Eschweiler-Clarke methylation

Once the monoprotected **(*R, R*)-167** was obtained, the next transformation was the complete methylation of the free amine using the reliable Eschweiler-Clarke method reported in Chapter 2 in the synthesis of TMTACN. Once more, the procedure resulted successful and **(*R*, *R*)-167** was obtained in an encouraging 75% yield after recrystallisation from ethyl acetate and diethyl ether.

4.2.1.3 Removal of the phthalimide protecting group

The protecting group we introduced is selectively removed by reaction with hydrazine, a procedure that leaves the other functionalities in the molecule untouched and allows for easy recovery of the product.

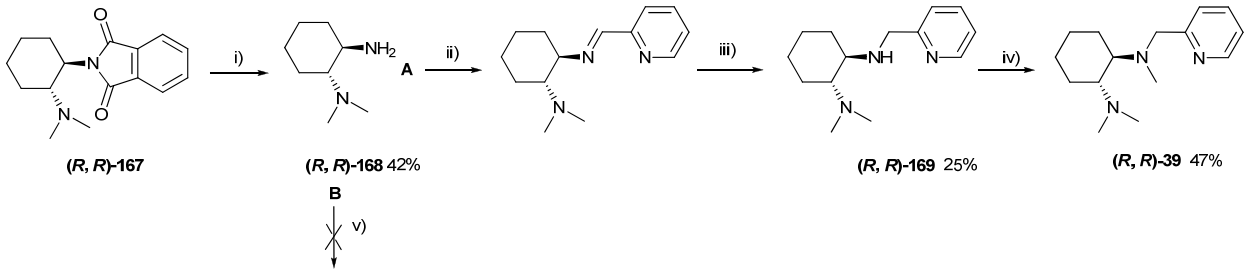

Scheme 4.4 Deprotection with hydrazine and correspondent mechanism and synthesis of 169 (via reductive amination (A), via nucleophilic substitution (B)) and methylation. i) hydrazine hydrate, EtOH; ii) pyridine 2-carboxyaldehyde, under N_2, toluene, molecular sieves; iii) $NaBH_4$, MeOH, reflux, iv) HCOOH, HCHO, H_2O/MeOH, reflux; v) 2-chloromethylpyridine, K_2CO_3, DCM.

The side product of the reaction, phthaloyl hydrazide, is poorly soluble in the solvent used and precipitates out through the reaction; further addition of diethyl ether causes the remaining contaminant to precipitate. After filtration, **(*R*, *R*)-168** was recovered by evaporation of the solvents.

4.2.1.4 Reductive amination with pyridine 2-carboxyaldehyde

Our first approach to the insertion of the pyridyl group on **168** was employing 2-chloromethyl pyridine in an S_N2 reaction, in the presence of K_2CO_3 as the base to neutralise the acid formed in the process. Unfortunately, although the alkylating agent was used in a stoichometric amount, a

complex mixture, possibly containing mono- and disubstituted amines, alongside with quaternarisation products was formed.

To circumvent the issue of multiple substitution, it was chosen to use a reductive amination, in which the primary amine reacts with an aldehyde to produce an imine, which is then reduced to the desired amine. Similar procedures have been reported before with different conditions, [39, 40] generally with regard to the solvent. The reaction was undertaken in a range of solvents, in EtOH in the presence of anhydrous $MgSO_4$, in dry DCM, diethyl ether, and toluene. For the success of the reaction it is crucial to avoid water in the mixture, since the condensation itself generates water and the presence of excess water will push the equilibrium towards the starting materials. For this reaction, toluene proved to be the ideal solvent in conjunction with activated 4Å molecular sieves.

After the condensation was complete, the solvent was removed and the residue redissolved in MeOH. Treatment with an excess of sodium borohydride under reflux afforded amine **(*R*, *R*)-169**.

4.2.1.5 Final methylation

The final methylation leading to the desired product **39** was again performed using the Eschweiler-Clarke protocol already employed in one of the previous synthetic steps.

4.2.1.6 Complexation attempts

Due to the possible coordination modes of the ligand, which in principle can act both as a bidentate and tridentate ligand, the synthesis of its complexes was attempted with an excess of ligand with respect to the trifluoromethanesulfonate (TfO^-) salt of the desired metal since depending on the type of coordination, up to three ligand could be bound to the metal centre. The procedure consisted of adding a solution of ligand in ACN to the metal salt suspended or dissolved in ACN in a Schlenk tube under nitrogen and the mixture was then stirred at RT for two hours. All the products were recovered as microcrystalline powders after removal of the solvents and trituration in petroleum spirit.

Complexes were first prepared using manganese(II), iron(II) and then using cobalt(II) and copper(II) trifluoromethanesulfonate salts. Although it was impossible to obtain crystals suitable for single crystal X-Ray studies, each compound was analysed by mass spectrometry.

Each complex gave an ion at *m/z* 248 (Figure 4.4) which corresponds to $[$**(*R, R*)-39**$+H]^+$, a peak at *m/z* 203 attributable to $[$**(*R, R*)-39-**$N(CH_3)_2]^+$ and another major signal at *m/z* 262 which was

believed to derive from the ligand (as it appeared in all samples) but was not assigned. The mass spectrum of the cobalt and copper containing powder revealed the presence of fragments corresponding to [M((***R, R***)-**39**)(OTf)]$^+$ where the ligand might act as tridentate donor and another species where the OTf anion is replaced by ACN. The iron containing compound showed only one significant peak at *m/z* 248, and no fragment compatible with an ((***R, R***)-**39**)-Fe species. Even in the case of manganese, the only metal for which a complex of **39** is known,[3, 4, 41] no ions indicating complexation were observed. It has to be noted though, that no structure was ever published for (**39**)-Mn(OTf); the complex was generated *in situ* and employed in the epoxidation of terminal alkenes.

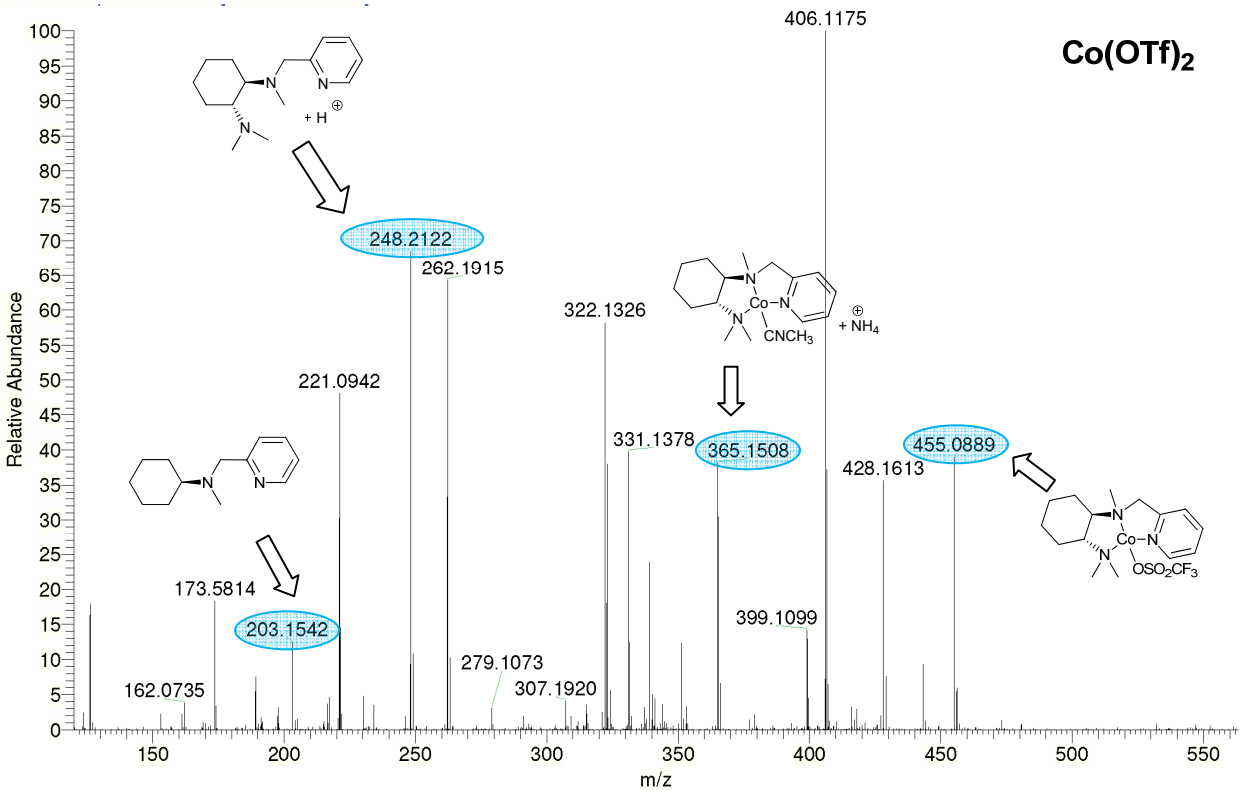

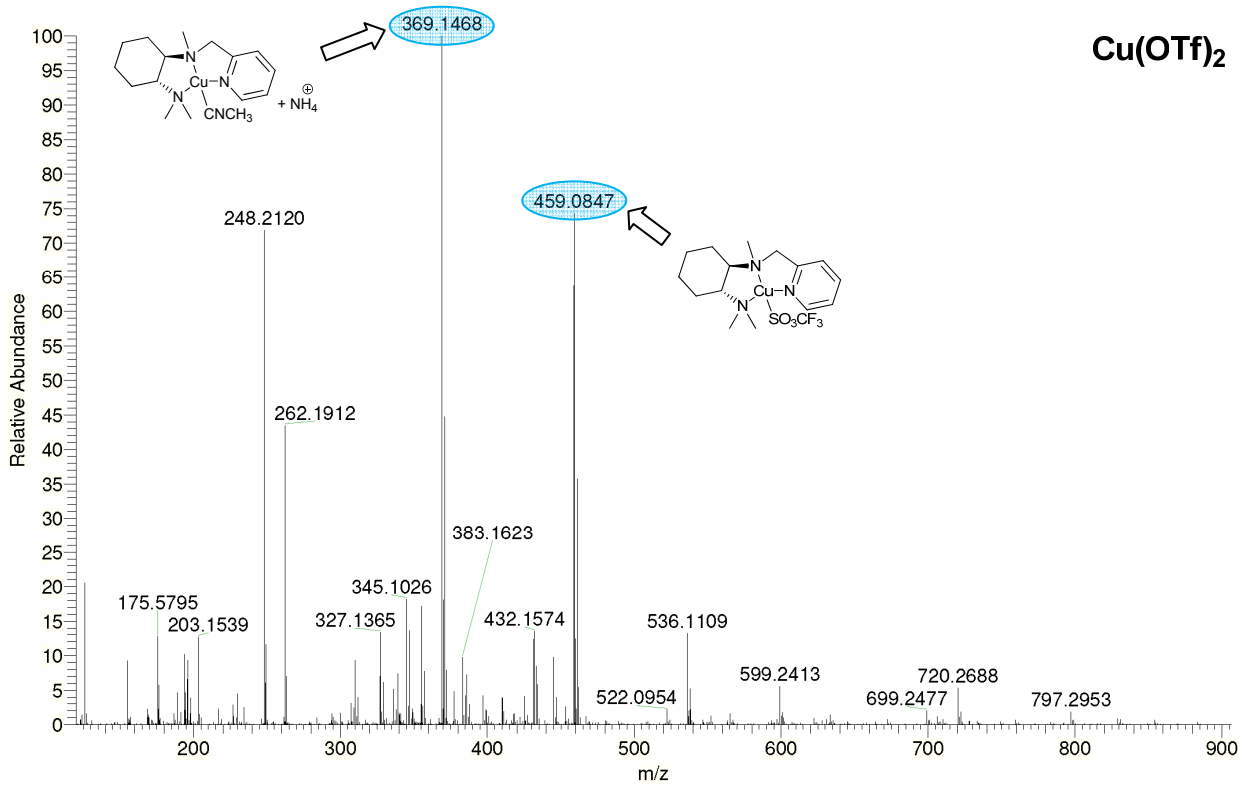

Figure 4.4 Mass spectrometry analysis of the microcrystalline powders obtained by reaction of $Co(OTf)_2$ and $Cu(OTf)_2$ with (*R, R*)-39, with significative fragments highlighted.

4.2.2 Tests for activity in the epoxidation of alkenes

Although lacking confirmation of the formation of the manganese and iron-(**39**) species, it was decided to assess their potential activity in the epoxidation of alkenes as previously reported. Not having an authentic complex available, the putative catalyst was prepared *in situ* by addition of equimolar amounts of **(*R, R*)-39** and of the desired metal trifluorometanesulfonate (OTf) from stock solutions directly in the reaction mixture before the addition of substrate and oxidant. Following the results reported by Stack *et al.*[3, 4, 41] in the epoxidation of terminal alkenes with peracetic acid, the screening was based on iron and manganese trifluoromethanesulfonates and commercial peracetic acid as the oxidant. The reactions were carried out in acetonitrile with a catalyst loading of 1 mol% and with 2 equivalents of oxidant with respect to the substrate.

The first metal tested was iron(II) in the form of iron(II)$(OTf)_2$, alongside with blanks to attribute unambiguously any reactivity to the complex. To exclude the intervention of other species in the epoxidation, experiments were performed, in which either the metal, the ligand or both were not present; the tests were performed on styrene, 1,2-dihydronaphthalene, *trans*-stilbene and cinnamyl alcohol as the substrates. Disappointingly, no reaction was observed for any of the

substrates after 4 hours, apart from a negligible amount of background oxidation due to the peracetic acid alone that was observed with 1,2-dihydronaphthalene after a 2 h reaction and for styrene, which showed traces of epoxide after *c.a.* 48 hours; even in this case this was due to the activity of peracetic acid alone. One last set of tests was performed by generating peracetic acid *in situ* by adding 5 equivalents of glacial acetic acid in the reaction followed by 5 equivalents of hydrogen peroxide, but no noticeable styrene consumption took place.

The same tests were performed replacing iron with manganese as the metal, with a catalyst loading of 1 mol% and 2 equivalents of peracetic acid as well as with the *in situ* generation of the oxidant with the same substrate scope. Unfortunately the same lack of activity was again observed. These results were not completely unexpected. Considering that the complexation attempts did not produce any identifiable coordination complex for these two metals, it is very likely that in even more dilute conditions and in the presence of an oxidant, their reaction would be even less effective and would fail to produce an active catalytic species.

It was in part due to the failure of these tests that the cobalt(II) and copper(II) complexes of this ligand were prepared to demonstrate that complexes could be formed, but the screening of these complexes was not performed.

4.3 Pentadentate ligand 163

For our pentadentate ligand, we used a modification of the protocol described by Kodanko[42, 43] (Figure 4.5) for the synthesis of a similar structure. Kodanko`s study focused only on the synthesis and characterisation cobalt(II) and iron(II) complexes of his ligand, which were prepared as a racemate. The related ligands presented in this work have been prepared starting from both enantiomers of 1,2-*trans*-diaminocyclohexane and bear a methyl substituent at the nitrogen where a benzyl group is present in Kodanko`s structure.

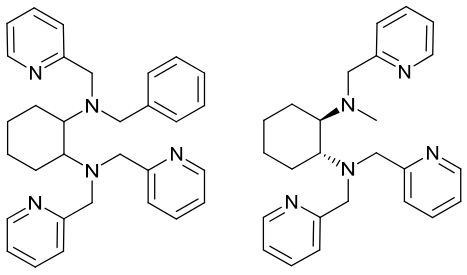

170 (*R*, *R*)-163

Figure 4.5 Kodanko`s structure (170) and our pentadentate ligand 163.

Pentadentate ligands can occupy up to five coordination sites in an octahedral complex, leaving at least one coordinative vacancy that can react with a different compound, such as an oxidant, to form a different species and become active as a catalyst.

4.3.1 Synthesis of 163

The synthetic plan for **(*R*, *R*)** and **(*S*, *S*)-163** closely matches a series of known procedures,[39, 42] with a few minor adjustments which proved to be more effective (Scheme 4.5).

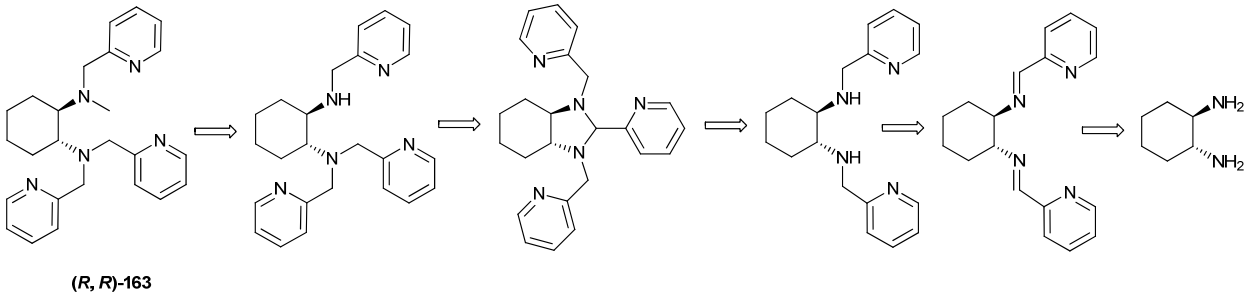

Scheme 4.5 Retrosynthetic plan to our pentadentate ligand; the same route was followed for the (*S*, *S*)-enantiomer but starting from (*S*, *S*)-diaminocyclohexane.

4.3.1.1 Reductive amination

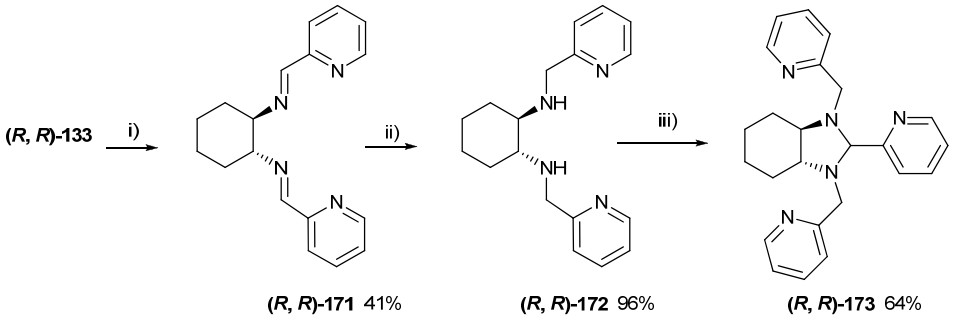

Scheme 4.6 Reductive amination leading to intermediate (*R*, *R*)-172 and formation of the aminal. i) pyridine 2-carboxyaldehyde, MeOH, 4 Å molecular sieves, RT; ii) $NaBH_4$, MeOH, reflux; iii) pyridine 2-carboxyaldehyde, Et_2O, 4Å molecular sieves, N_2, RT.

Generally, the steps of a reductive amination are carried out in a rapid sequence, without isolating the imine intermediate. In this case, after reaction of diaminocyclohexane with pyridine 2-carboxyaldehyde in methanol, the imine was recovered as a white solid, and fully characterised. The amine was obtained by reduction with $LiAlH_4$ in refluxing THF under a nitrogen atmosphere.

4.3.1.2 Synthesis of the aminal

The formation of the aminal intermediate is very similar to the first step of a reductive amination, where the reduction step is replaced by the reaction with the lone pair of the second amine that attacks the imine formed in the first step. Loss of water and the formation of a five membered ring drive the reaction to completion.

4.3.1.3 Reduction of the aminal intermediate and final methylation

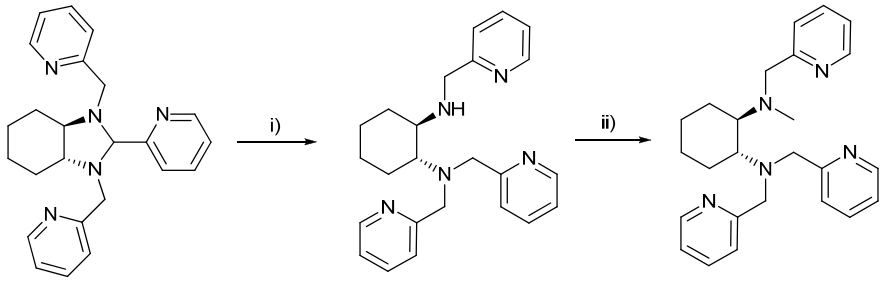

Scheme 4.7 Reduction of the aminal and Eschweiler-Clark methylation. i) $NaCNBH_3$, MeOH, TFA, N_2, RT; ii) HCOOC, HCHO, H_2O/MeOH, reflux.

The next step consisted in the reduction of the aminal in order to obtain a free secondary amine that can be methylated to obtain the final compound. Sodium cyanoborohydride easily reduces imines when in the form of iminium ions. [44, 45] The acid is needed to protonate one of the aminal nitrogens promoting its opening to form an iminium ion which is then rapidly reduced by the cyanoborohydride and to maintain the low pH required by the reaction.

The reaction proceeded in a clean and efficient way, and the product did not require any further purification after a basic aqueous workup. The final structure was obtained once again using the solid Eschweiler-Clarke procedure.

4.3.2 Synthesis and characterisation of metal complexes of (*R, R*)-163

The synthesis of a series of complexes with various metal trifluoromethanesulfonates was undertaken; $Cu(OTf)_2$, $Co(OTf)_2$, $Mn(OTf)_2$, $Fe(OTf)_2$ were used as the sources of metal. The complexes were prepared by mixing equimolar amounts of ligand and metal salt in ACN in a Schlenk tube under a nitrogen atmosphere. The complexes were recovered as microcrystalline powders after removal of the solvents and trituration in petroleum spirit. Attempts to obtain crystals suitable for a determination of the structure X-Ray diffraction were successful only for the copper(II) complex. The lack of success in obtaining crystals was attributed to the extreme

hygroscopicity of the powders obtained. Samples of all the powders obtained were analysed by mass spectrometry to prove the effective coordination to the metal. Most of the samples showed an ion corresponding to the [M((***R, R*)-163**)(OSO_2CF_3)] species; the formation of the complex was further confirmed by high resolution mass measurements on the more significant fragments.

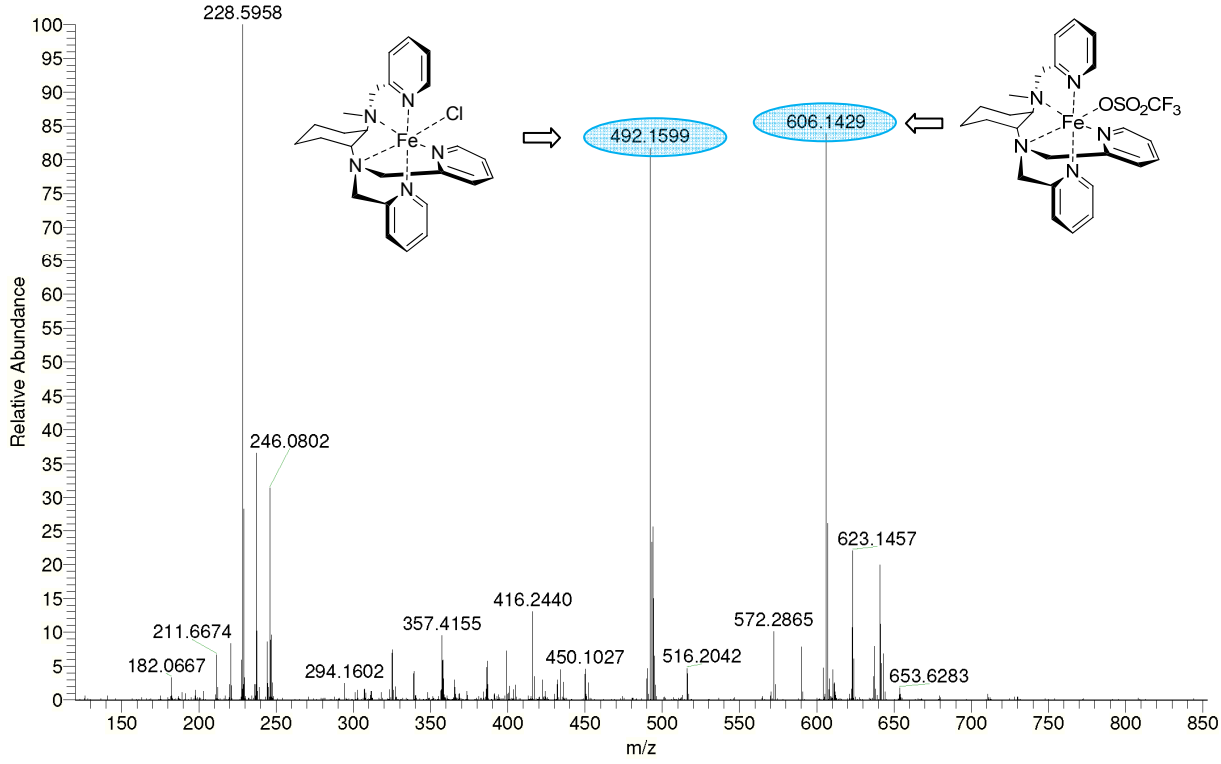

Figure 4.6 Mass analysis of [Fe((*R, R*)-163)(OSO_2CF_3)].

For [Fe(**(*R, R*)-163**)(OSO_2CF_3)], the mass analysis showed the presence of a peak compatible with a hexacoordinate iron(II), complexed with one molecule of ligand and one OTf ion in the coordination sphere.

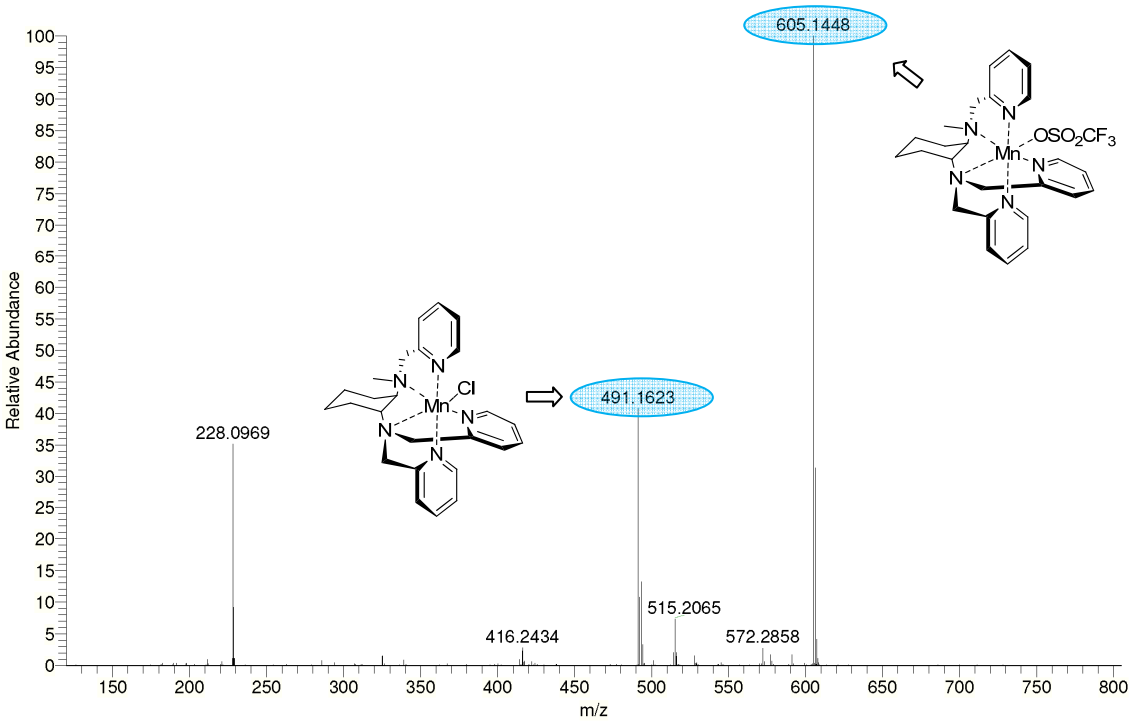

Figure 4.7 Mass analysis of [Mn((*R, R*)-163)(OSO_2CF_3)].

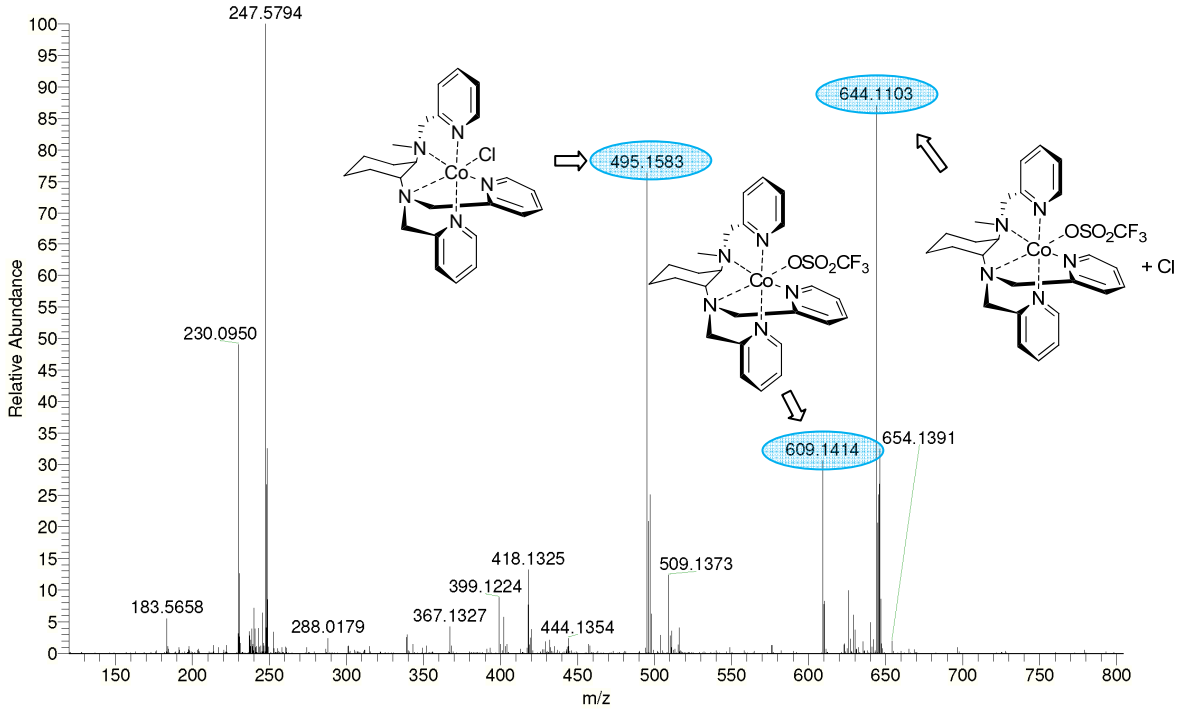

Figure 4.8 Mass analysis of [Co((*R, R*)-163)(OSO_2CF_3)].

Similarly for [Mn(**(*R, R*)-163**)(OSO_2CF_3)] and [Co(**(*R, R*)-163**)(OSO_2CF_3)], the mass traces contain peaks corresponding to hexacoordinate species, proving the formation of the complexes; the same signal can be observed for the copper complex. The mass spectrum of the cobalt complex shows a very intense peak at *m/z* 644.1 which is consistent with the species [Co(***R, R*)-163**)(OTf)+Cl]$^+$, presumably formed during the ionisation process.

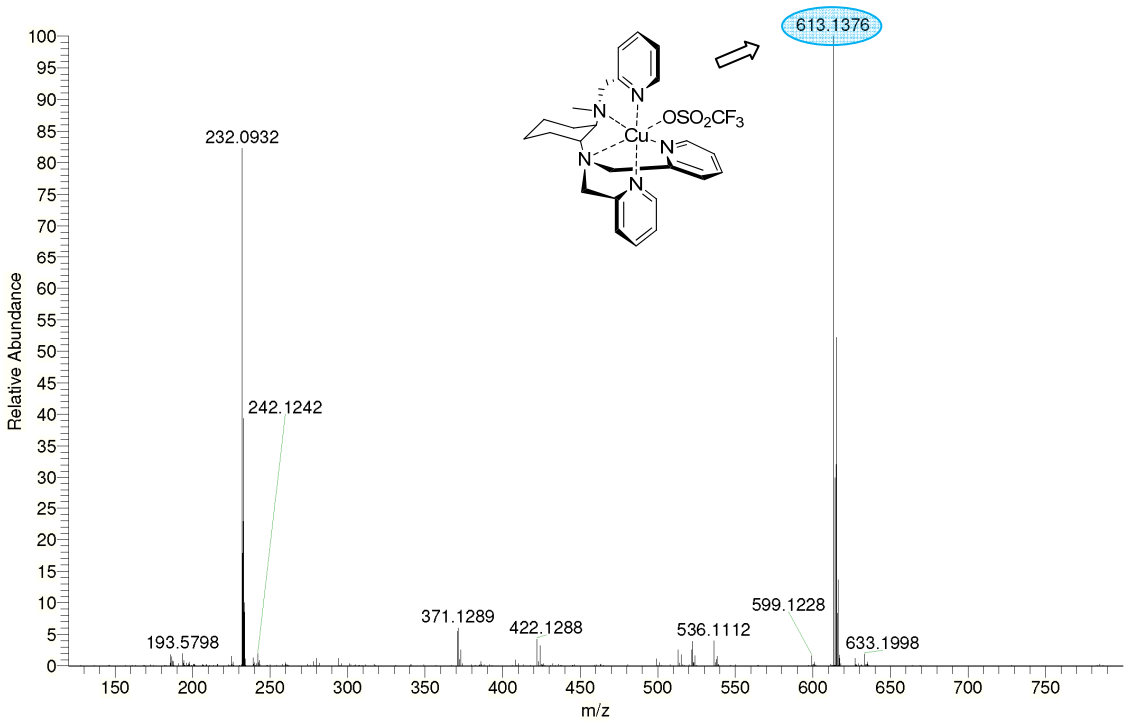

Figure 4.9 Mass analysis of [Cu((*R, R*)-163)(OSO_2CF_3)].

Structural characterisation of the complexes by single crystal X-Ray diffraction would be needed to determine the actual geometry of the complexes and coordination sphere. Unfortunately, suitable crystals were only obtained for the copper(II) complex, whose structure is described and discussed below.

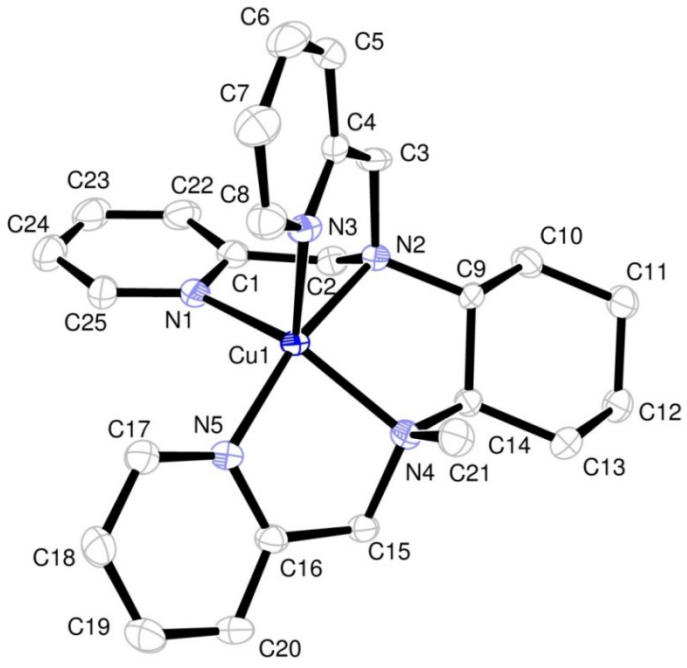

Figure 4.10 ORTEP[46] structure of complex [Cu(*R, R*)-163](OTf)$_2$ with 50% probability displacement ellipsoids with OTf$^-$ omitted for clarity.

Despite the presence of a molecular ion at *m/z* 613 for this complex which is consistent with a six-coordinate copper(II) centre, the crystal structure clearly revealed it to be a five-coordinate in the solid state with two non-coordinating OTf^- anions balancing the cationic charge (Figure 4.10).

	Bond Length (Å)
Cu(1)-N(1)	2.039(2)
Cu(1)-N(2)	2.0197(17)
Cu(1)-N(3)	2.110(2)
Cu(1)-N(4)	2.019(2)
Cu(1)-N(5)	1.9885(17)

Table 4.1 Selected bond lengths (Å) for [Cu(*R, R*)-163](OTf)$_2$ with estimated standard deviations.

	Bond Angle (°)
N(1)-Cu(1)-N(2)	82.84(8)
N(1)-Cu(1)-N(3)	100.67(9)
N(1)-Cu(1)-N(4)	142.14(8)
N(1)-Cu(1)-N(5)	100.75(8)
N(2)-Cu(1)-N(3)	82.68(8)
N(2)-Cu(1)-N(4)	87.36(8)
N(2)-Cu(1)-N(5)	166.99(8)
N(3)-Cu(1)-N(4)	114.25(8)
N(3)-Cu(1)-N(5)	108.66(8)
N(4)-Cu(1)-N(5)	82.17(8)

Table 4.2 Selected bond angles (°) for complex [Cu(*R, R*)-163](OTf)$_2$ with estimated standard deviations.

Some penta-coordinate copper(II) complexes of a similar ligand (*N, N, N', N'*-tetrakis-(2-pyridylmehyl)ethylenediamine = TPEN, Figure 4.11), have been synthesised and characterised by Marsich *et al.*[47] and Blindauer *et al.*; [48] the complexes differed from each other by the counter-ion employed, PF_6^-, and ClO_4^-.

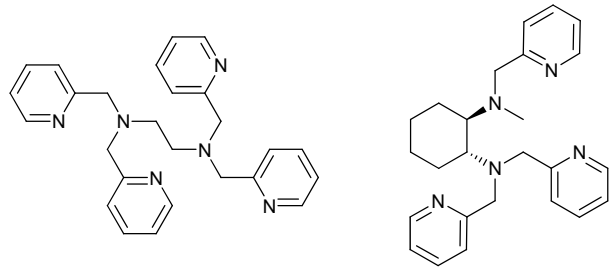

175 (*R*, *R*)-163

Figure 4.11 TPEN ligand used by Marsich and Blindauer (175) and ligand (*R, R*)-163 synthesised in this work.

Although the TPEN ligand is potentially hexadentate, both of their complexes were pentacoordinate, with two counter-ions in the outer coordination sphere as in [Cu(***R, R***)-**163**](OTf)$_2$. Pentacoordinate copper(II) complex can exist in trigonal bipyramidal or square pyramidal geometry or distorted versions of the two.[49, 50] Blindauer and Marsich found a dependency of the geometry on the counter-ion; with perchlorate pushing the complex towards a distorted trigonal bipyramidal and hexafluorophosphate favouring a slightly distorted square pyramidal. Using these structures as a reference, it was possible to assign a distorted square pyramidal geometry to [Cu(***R, R***)-**163**](OSO$_2$CF$_3$)$_2$, with N(3) as the axial ligand. Two pyridine and the aliphatic nitrogen donors lie in the basal plane while the third pyridine occupies the apical position N(3).

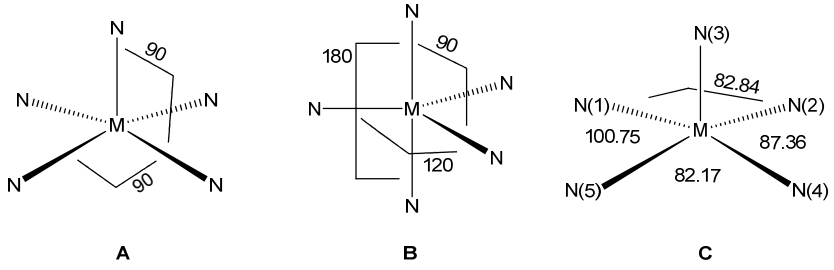

Figure 4.12 Comparison between perfect square-based pyramidal geometry (A), trigonal bipyramidal (B) and [Cu(*R, R*)-163](OSO$_2$CF$_3$)$_2$ (C).

In [Cu(***R, R***)-**163**](OSO$_2$CF$_3$)$_2$, the angles between the copper atom and the N(1), N(2), N(4) and N(5) are compatible with the 90 ° required by the square pyramidal geometry (Figure 4.12, **C**), and the angles between N(3) and the nitrogens of the base are between 100.67 °(9) and 114.25 °(8), with the exception of N(3)-Cu-N(2) which is slightly smaller (82.68 °(8)). The Cu-N(3) bond is also longer (2.110 Å (2)) compared to the other copper-nitrogen distances (1.9885(17), 2.019(2), 2.0197(17), and 2.039(2) Å), further confirming its axial position. The distorted square pyramidal geometry is also backed by the value of the Addison parameter[51, 52]

(τ) calculated for the complex which has a value of 0.41, where 1 correspond to a regular trigonal bipyramidal and 0 for a perfect square-based pyramid.

The Cu-N distances for the pyridyl groups are all consistent with those generally observed for similar complexes containing substituted pyridines (1.98-2.16 Å).[53] The distance between the metal centre and the aliphatic nitrogens is almost identical for both N(4) and N(2) 2.0190(2) and 2.0197(17) Å; and is slightly shorter than those found in other cyclohexanediamine based copper-amine complexes (2.06-2.16 Å).[54-56] This bond length is still compatible with a Cu(II)-N species, being consistently longer than the length observed for Cu(III)-N (~1.94 Å).[56]

4.3.3 Activity tests of ((*R, R*)-163)-metal complexes

The pentadentate ligand **(*R, R*)-163** was tested in the epoxidation of various alkenes both generating the active species *in situ*, by addition of all the constituents directly in the reaction mixture from stock solutions. The first epoxidation tests were conducted on *trans*-stilbene, employing a catalyst loading of 1 mol% for both methods and 2 equivalents of peracetic acid. The reactions were carried out in acetonitrile at room temperature alongside several blanks to identify any activity as being due to the complexes and exclude any side reaction catalysed by the metal, the ligand or the oxidant alone.

The copper(II) and cobalt(II) preformed complexes as well as the *in situ* generated complexes proved ineffective and left the substrate untouched even after 2 hours, with no sign of background oxidation; the manganese(II) complexes too, were unable to oxidise *trans*-stilbene over 2 hours. When the iron(II) complex was tested, though, activity was observed just after 30 minutes of reaction. The substrate was readily being consumed and during the HPLC analysis of the reaction mixture it was possible to see a number of other peaks appearing and growing in intensity with time, until after two hours all of the substrate had been consumed. A very intense signal was present at a retention time compatible with that of one of the enantiomers of *trans*-stilbene epoxide, which appeared extremely promising. The sample was then spiked with racemic *trans*-stilbene epoxide and re-analysed to confirm the presence of the enantiomer, but the results proved that this peak belonged to a different chemical species.

Analysis of the reaction mixture by ^{1}H-NMR spectroscopy proved complex and not useful to the identification of the products, given the large amount of species in solution. The sample was also analysed *via* HPLC-MS but the chemical ionisation used to generate the charged species proved unsuitable for the analysis; the mass trace corresponding to the peaks observed in the UV-chromatogram could not be distinguished from the background noise even when higher or lower

concentrations were used in the analysis. A last attempt with GC-MS allowed to identify at least one of the species as benzoic acid, suggesting that the other products might result from overoxidation of the substrate and successive degradation.

The next test substrate chosen was cinnamyl alcohol. In this case, copper(II) and cobalt(II) proved inactive, but when iron(II) and manganese(II) species were used, the substrate was consumed within 2 hours. The disappearance of the substrate was accompanied by the formation of several other peaks in the HPLC chromatogram; unfortunately, none of these corresponded to cinnamyl alcohol epoxide. After this, the copper(II) and cobalt(II) complexes were abandoned and the screening was continued with only manganese(II) and iron(II) on 1,2-dihydronaphthalene and styrene.

The iron(II) complex proved extremely active with 1,2-dihydronaphthalene, consuming all of the substrate in less than one hour, but once again, did not produce the corresponding epoxide but a mixture of presumably oxidised products. Similar behaviour was shown by the manganese complex. In both chromatograms, small traces of epoxide were observed, but a comparison with the background oxidation given by peracetic acid alone excluded the involvement of the catalytic species.

Styrene was tested only with the iron(II) complex, which afforded 73% of styrene consumption in 4 hours, with complete consumption in 6 hours. In this case, the reaction did not produce epoxides and the other species formed in the reaction were not identified. Styrene was the only substrate that was not completely consumed within 2 hours, making it the less reactive substrate in the series tested. To assess where the lack of reactivity generated, if electronic factors were determining the reactivity, the reaction was repeated on *p*-methyl-, *p*-methoxy, and *p*-chlorostyrene. The two electron rich styrenes were consumed within an hour, while the styrene bearing the electron withdrawing group was left untouched after 4 hours, suggesting that the active species in the reaction is electrophilic in nature.

4.4 “Click”-generated tetradentate ligand 164

The triazole moiety appears in large number of ligands, due to the ease of its synthesis and its good coordinating properties,[57-60] as well as the fact that its steric- and electronic properties can be readily modified by introducing different substituents. Very recently, a tetradentate ligand containing two triazole rings proved to be active in the epoxidation of alkenes with manganese$(OTf)_2$ and peracetic acid (Figure 4.13).[37]

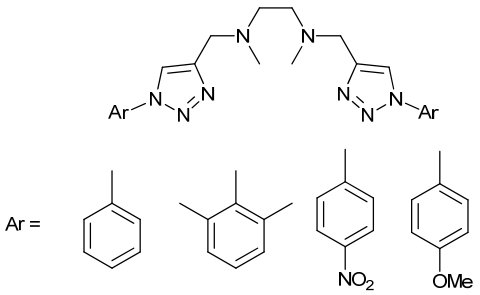

Figure 4.13 Hao and Wang "click"- tetradentate ligands.

Triazole moieties have also appeared in scorpionate complexes active as metal-specific sensors.[61-63] With the aim of creating a chiral ligand with a simple synthesis and whose electronic properties could be easily tuned, we decided to replace the pyridyl group we employed so far with the triazole group, introduced with a Huisgen dipolar cycloaddition (**(*R*, *R*)-164**, Figure 4.3, Scheme 4.8.)

4.4.1 Synthesis

The retro-synthetic analysis goes back once more to the cyclohexanediamine backbone; after resolving the starting material into its enantiomers, only four synthetic steps lead to the desired ligand.

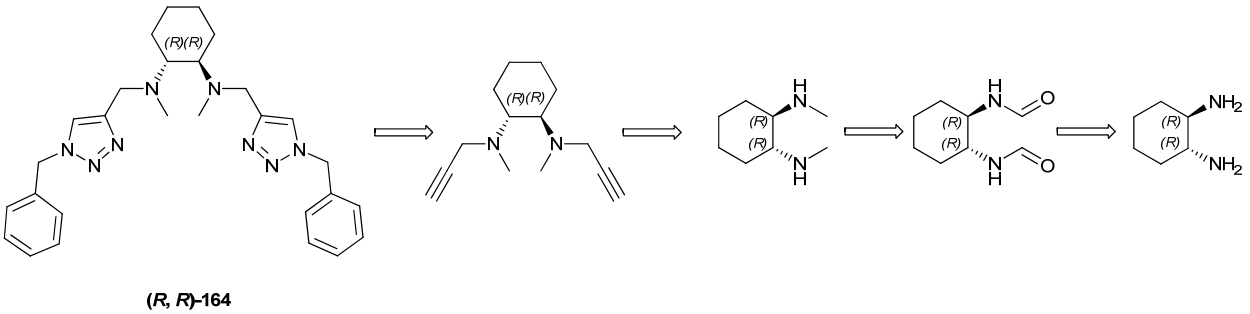

Scheme 4.8 Retrosynthetic analysis of the proposed "click"tetradentate ligand.

4.4.1.1 Methylation of (R, R)-trans-1,2-cyclohexanediamine

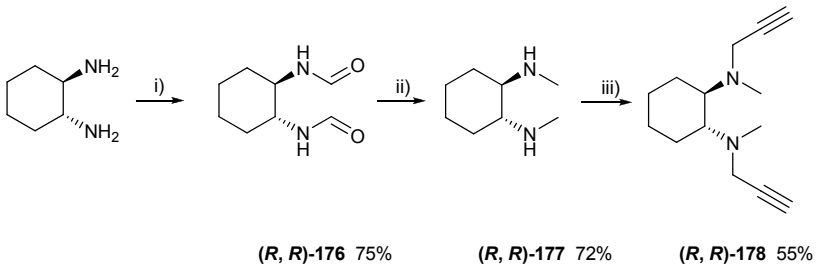

Scheme 4.9 Methylation of cyclohexanediamine and reaction with propargyl bromide. i) Ethyl formate, 50 °C, 3 h; ii) $LiAlH_4$, THF, N_2, reflux, 24 h; iii) Sodium hydride, propargyl bromide, THF, N_2, RT.

To avoid a multiple methylation of the amine that can occur with reagents such as methyl iodide or with the Eschweiler-Clarke procedure, formylation and subsequent reduction was chosen as the preferred reaction. The reaction between the primary amine and ethyl formate stops at the formate and provides **(*R*, *R*)-176** in good yields, as the formate, in fact, is less reactive than a secondary amine because of the delocalisation of the lone pair.

The final product was obtained by exhaustive reduction of the formate with $LiAlH_4$ in THF.

4.4.1.2 Introduction of the alkinyl-pendant arms

The reaction with propargyl bromide was initially carried out following the procedure of Hao *et al.*[37] using DMF and potassium carbonate as the base to capture the proton being liberated in the nucleophilic substitution, but these conditions did not allow to obtain the desired product. A second and successful attempt was performed in THF with NaH as the base under a nitrogen atmosphere. Rather than remove the proton from the equilibrium, sodium hydride is more likely to abstract a proton from the amine group transforming it in a better nucleophile.

4.4.1.3 Synthesis of azide and 1,3-Huisgen cycloaddition

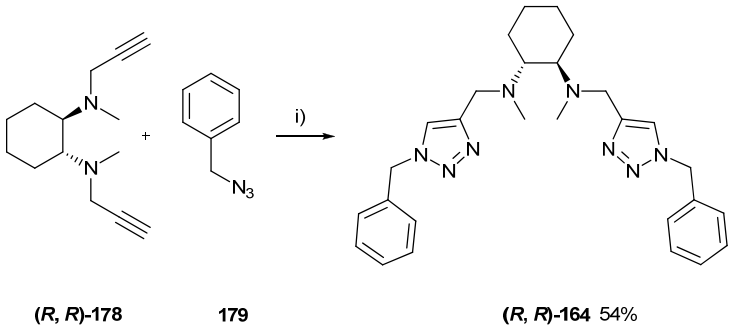

(*R*, *R*)-178 **179** **(*R*, *R*)-164** 54%

Scheme 4.10 Huisgen cycloaddiction. i) CuI, TEA, THF, N_2.

The final step of the ligand synthesis consisted of the copper(I) catalysed Huisgen cycloaddition of alkyne **(*R*, *R*)-178** and benzyl azide (**179**). The azide was synthesised from benzyl bromide by reaction with azide-activated IRA-900 resin in acetonitrile at RT; this procedure greatly simplified the purification of the azide, as it only requires a simple filtration to remove the resin.

The copper(I) catalysed Huisgen cycloaddition is a known "click" reaction between a 1,3-dipole like nitrile oxides, azides, diazoalkanes and a dipolarophile such as an alkyne, cyanide or alkene (Figure 4.14).[30, 64]

Figure 4.14

The presence of copper(I) directs the reaction towards the 1,4 addition product rather than a mixture of 1,4 and 1,5 products. The exact mechanism of the copper-catalysed cycloaddition is still the subject of debate, although recently disclosed results propose the synergic participation of two copper atoms in the catalytic cycle (Scheme 4.11).[65]

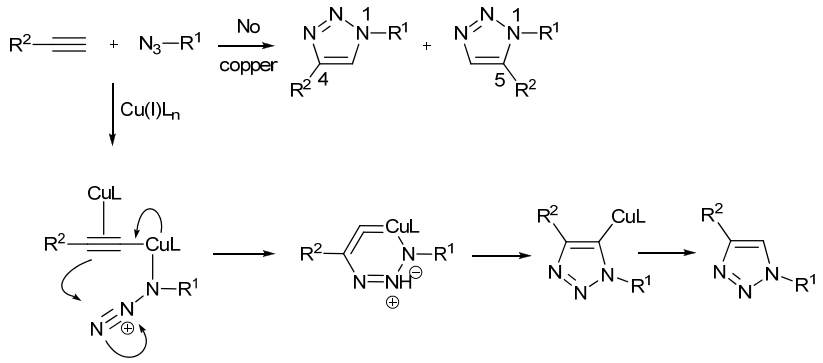

Scheme 4.11 Proposed mechanism for the Cu(I)-catalysed Huisgens 1,3-dipolar cycloaddition.

The reaction generally proceeds quickly with a copper(I) loading of 5 to 10 mol% which is achieved either by directly using a source of copper(I) such as copper(I) iodide or by *in situ* reduction of a copper(II) salt with sodium ascorbate.[30, 66] In this case copper(I) iodide was used in 10 mol% but no reaction was observed even after 24 hours. Increasing the amount of copper(I) iodide to 30 mol% and lastly to 50 mol% did not improve the situation; no formation of the product was observed. After the aqueous work-up, though, only the azide was recovered in significant quantities, with only traces of the alkyne recovered. This phenomenon was initially attributed to the affinity of the molecule with the aqueous phase, but it was soon realised that **(*R*, *R*)-178** can also be a good chelating ligand for copper(I). A brief bibliographic research confirmed this supposition; diamines like cyclohexanediamine proved to be extremely good ligands for copper(I) and have been employed in several reactions. [66-68] It was suspected that the copper(I) added immediately bound to the alkyne and was no longer able to catalyse the cycloaddition. When the reaction was repeated using 1.1 equivalents of copper(I) iodide with respect to the alkyne, it was found to reach completion within twelve hours, providing the final product **(*R*, *R*)-164**.

4.4.2 Synthesis of (*R*, *R*)-164 metal complexes

Complexes of the newly synthesised ligand were prepared with $Mn(OTf)_2$, $Fe(OTf)_2$, $Cu(OTf)_2$ and $Cu(SO_4)$ in acetonitrile under an inert atmosphere in a Schlenk tube. A solution of the ligand in ACN was added to a suspension of the metal salt in ACN and stirred for an hour, after which time, the solvent was removed and the residue triturated with petroleum ether (60-80 °) to obtain a microcrystalline powder. Both the powders obtained proved to be extremely hygroscopic and become deliquescent on exposure to air in less than 30 minutes, which made their handling problematic.

This highly hygroscopic character is believed to be the main reason why every crystallisation attempt proved unsuccessful, leaving mass spectrometry as the primary characterisation tool for the complexes.

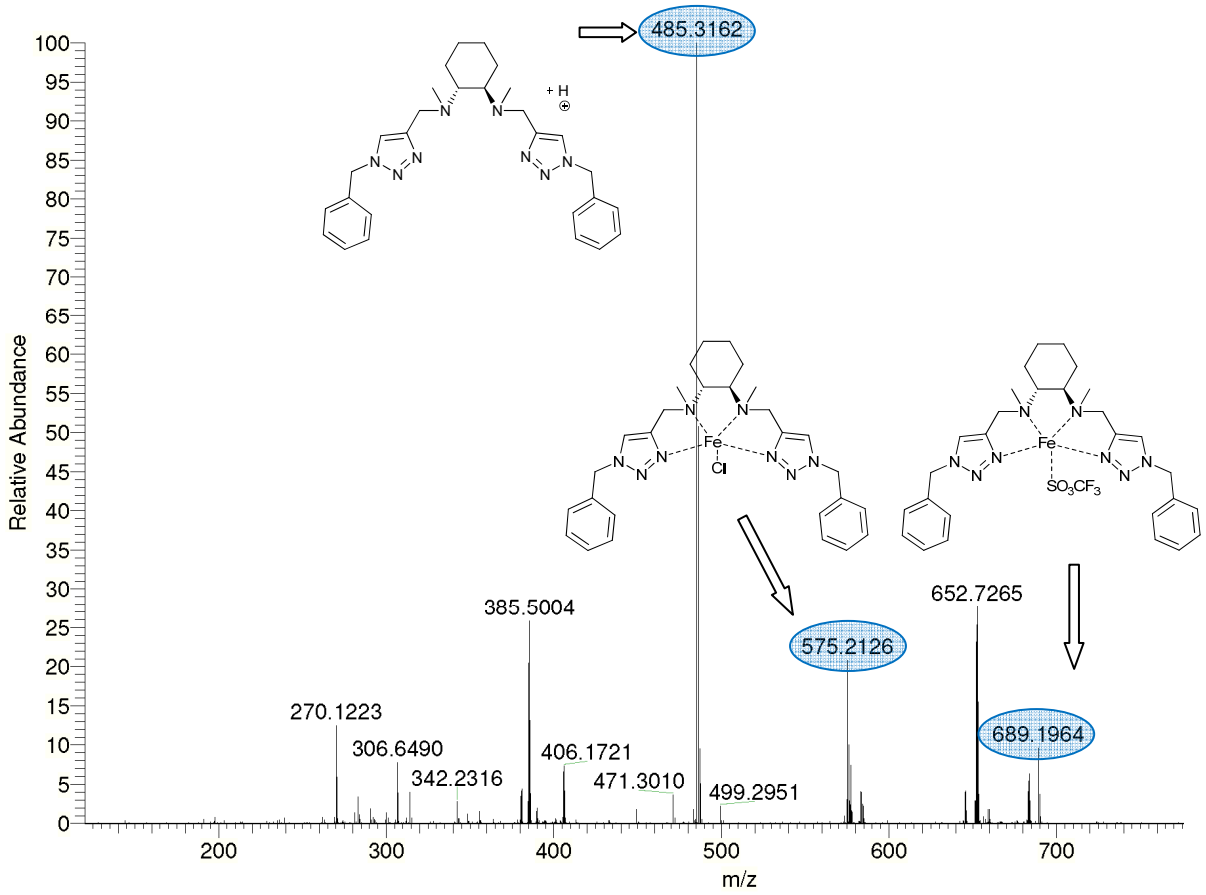

Figure 4.15 Powder obtained by reaction of 164 and $Fe(OTf)_2$, mass analysis.

The the mass analysis of the product of the reaction between **164** and $Fe(OTf)_2$ showed two peaks which could easily be assigned to [Fe(**164**)] complexes. The complex was expected to be hexacoordinate, with four coordination sites occupied by the ligand and the remaining two complexed with OTf⁻ groups or solvent molecules; the peak with *m/z* 689 corresponds to a

possible fragmentation of this species, where one OTf⁻ group has been removed. The second most significant peak is to be found at *m/z* 575, and it might correspond to [Fe(**164**)] after loss of both the OTf⁻ groups and the addition of a chloride ion. The most intense peak at *m/z* 485 corresponds to the protonated free ligand, which might be derived from fragmentation of the initial complex or as a residue from the complexation.

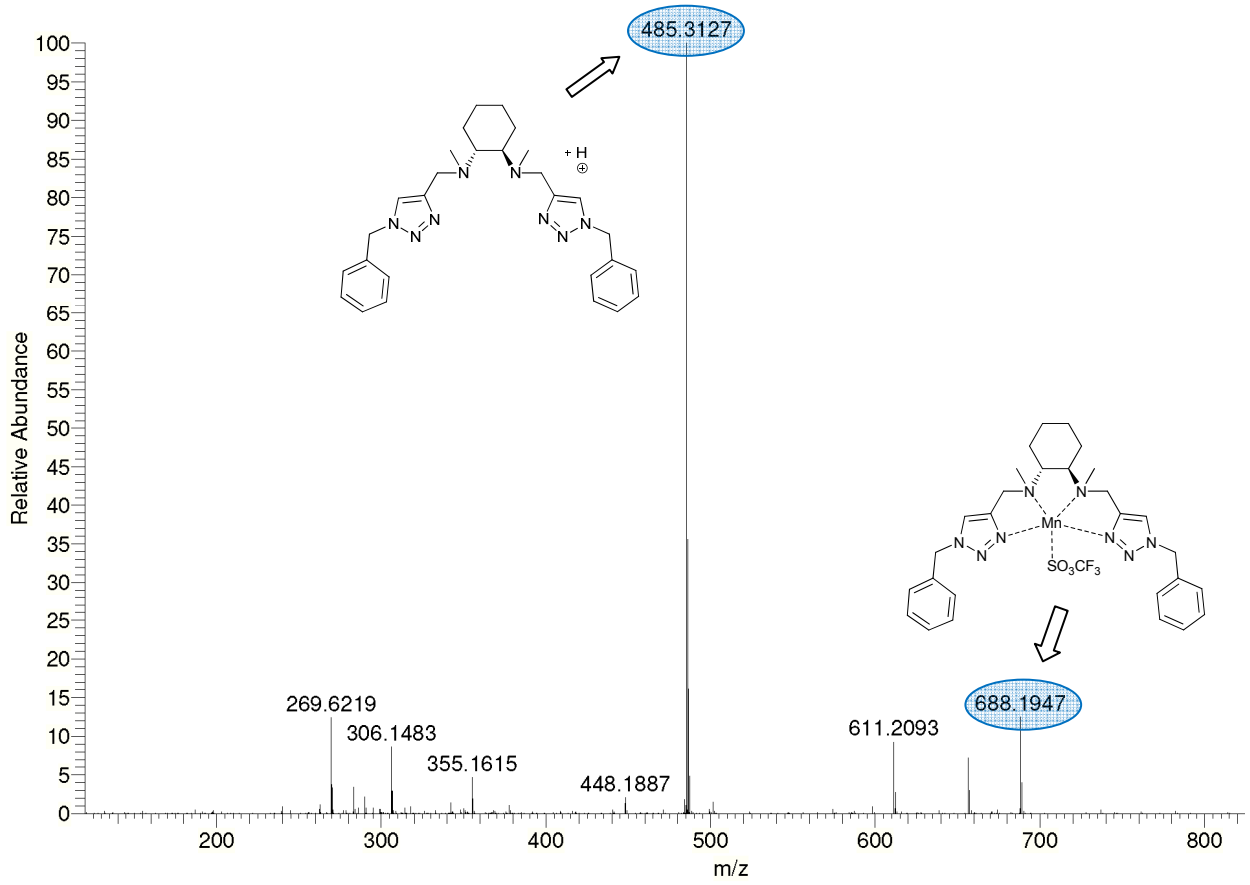

Figure 4.16 Mass analysis of the powder obtained by reaction of 164 and $Mn(OTf)_2$.

As for the iron, the reaction between **164** and $Mn(OTf)_2$ produced a metal-**164** complex as it can be noted by the fragment at *m/z* 688, corresponding to the expected octahedral complex minus one OTf⁻ anion. Even in this case the analysis was characterised by the presence of the peak of the free ligand protonated.

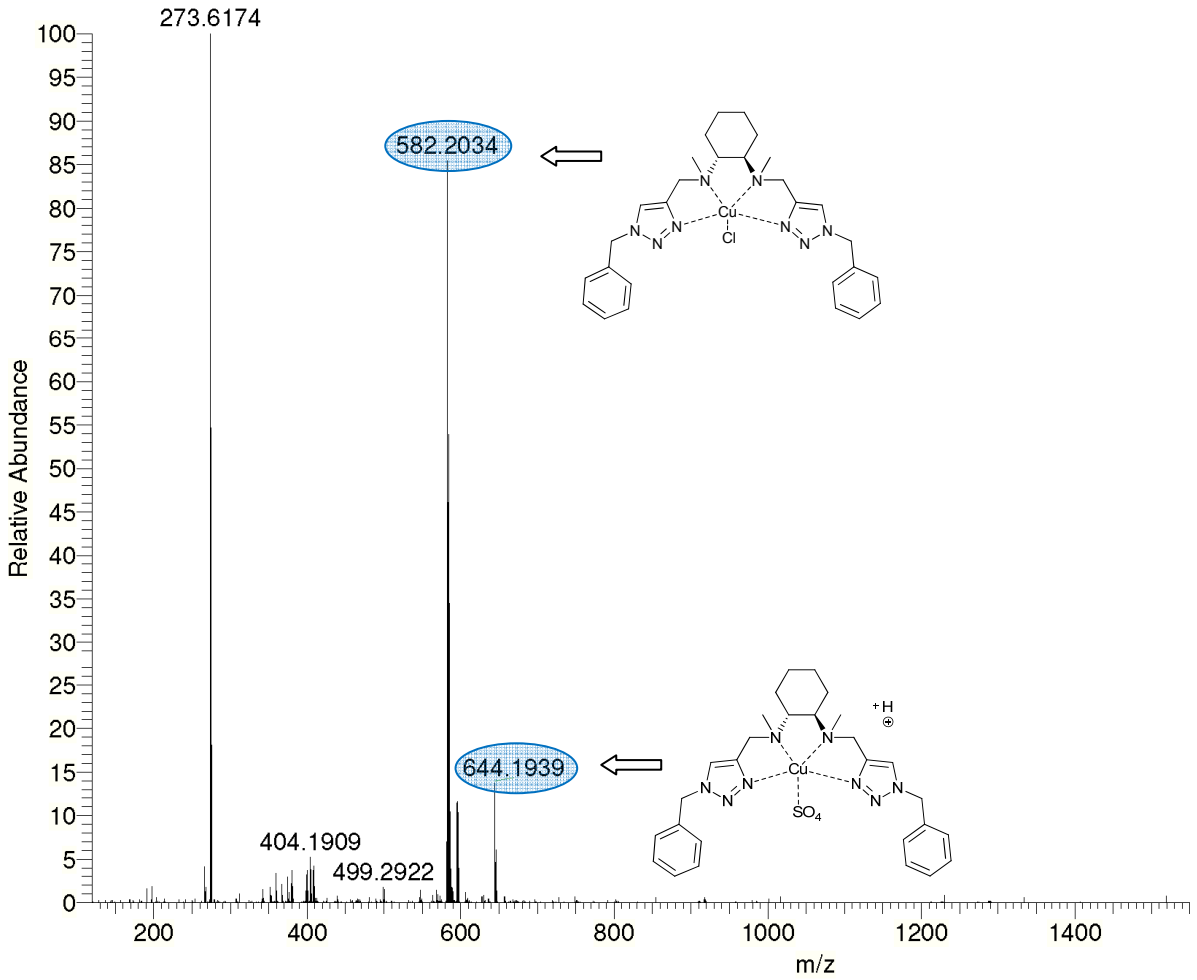

Figure 4.17 Mass analysis of the solid obtained by reaction of 164 and Cu(SO_4).

The mass analysis of the reaction of **164** and Cu(SO_4) revealed the presence of a fragment with the compatible with [[Cu(**164**)(SO_4)]+H]$^+$. The actual geometry of the complex could be tetra- or pentacoordinate depending on the placement of the sulfate ion in the inner or outer coordination sphere of the metal; at *m/z* 582 a peak compatible with the species [Cu(**164**)(Cl)] was found, the most intense signal at *m/z* 273 was left unassigned. The presence of these fragments confirms the success of the reaction but left unknown the real structure of the complex.

4.4.2.1 Epoxidation attempts

The newly obtained ligand **(*R, R*)-164** was then tested for activity. The active species were generated *in situ* mixing equimolar amounts of ligand and metal from stock solutions. The chosen substrates were 1,2 dihydronaphthalene and cinnamyl alcohol, and the oxidation was attempted both with copper, manganese and iron salts and with both peracetic acid and hydrogen peroxide as the oxidant, plus an attempt with *in situ* generated peracetic acid. Further activity tests on the microcrystalline powders obtained were also conducted in collaboration with Prof. Miquel Costas (Universitat de Girona, Catalunya, Spain), but the result of these tests,

disappointingly, were negative, with the only observed reactivity due to background oxidation when peracetic acid was employed but no conversion.

4.5 Conclusions and future work

Despite the lack of activity of some ligands and the unclear reactivity of others, this study produced two novel structures with proven coordinating capabilities (**163** and **164**). It also expanded the screening of ligand **39** to a larger number of alkenes which are structurally and electronically different from the only substrate presented in Stack's study, revealing its scarce reactivity towards electron rich substrates. Ligand **164**, thanks to its modular synthesis, opens the way to the synthesis of large number of derivatives with various electronic effects through the use of different azides; the choice of an alternative azide precursor might allow isolable complexes to be prepared and characterised rather than the highly hygroscopic complexes prepared herein. Moreover, these might also have superior reactivity towards alkenes. Ligand **163** proved to be active in the oxidation of alkenes, although not specifically in epoxidation. Further screening of different solvents and oxidants might help in tuning its reactivity to match the required target.

4.6 References

1. A. Berkessel, M. C. Ong, M. Nachi and J. M. Neudörfl, *ChemCatChem*, **2**, 1215-1218.
2. L. Gomez, I. Garcia-Bosch, A. Company, X. Sala, X. Fontrodona, X. Ribas and M. Costas, *Dalton Trans.*, 2007, 5539-5545.
3. A. Murphy, G. Dubois and T. D. P. Stack, *J. Am. Chem. Soc.*, 2003, **125**, 5250-5251.
4. A. Murphy, A. Pace and T. D. P. Stack, *Org. Lett.*, 2004, **6**, 3119-3122.
5. M. Wu, B. Wang, S. F. Wang, C. G. Xia and W. Sun, *Org. Lett.*, 2009, **11**, 3622-3625.
6. R. Irie, N. Hosoya and T. Katsuki, *Synlett*, 1994, 255-256.
7. M. A. Garcia, A. Meou and P. Brun, *Synlett*, 1996, 1049-&.
8. R. I. Kureshy, N.-u. H. Khan, S. H. R. Abdi, S. T. Patel and R. V. Jasra, *Tetrahedron: Asymmetry*, 2001, **12**, 433-437.
9. Y. L. Bennani and S. Hanessian, *Chem. Rev.*, 1997, **97**, 3161-3195.
10. H. Takahashi, T. Kawakita, M. Ohno, M. Yoshioka and S. Kobayashi, *Tetrahedron*, 1992, **48**, 5691-5700.
11. S. G. Davies, G. B. Evans and A. A. Mortlock, *Tetrahedron: Asymmetry*, 1994, **5**, 585-606.
12. S. G. Davies and A. A. Mortlock, *Tetrahedron Lett.*, 1992, **33**, 1117-1120.
13. S. G. Davies and A. A. Mortlock, *Tetrahedron*, 1993, **49**, 4419-4438.
14. Z. Li, K. R. Conser and E. N. Jacobsen, *J. Am. Chem. Soc.*, 1993, **115**, 5326-5327.
15. Z. Li, R. W. Quan and E. N. Jacobsen, *J. Am. Chem. Soc.*, 1995, **117**, 5889-5890.
16. G. Y. Zhang, Y. Q. Liao, Z. H. Wang, H. Nohira and T. Hirose, *Tetrahedron: Asymmetry*, 2003, **14**, 3297-3300.
17. C. Guo, J. Qiu, X. M. Zhang, D. Verdugo, M. L. Larter, R. Christie, P. Kenney and P. J. Walsh, *Tetrahedron*, 1997, **53**, 4145-4158.
18. T. A. Whitney, *J. Org. Chem.*, 1980, **45**, 4214-4216.
19. J. A. McCleverty and T. J. Meyer, *Comprehensive Coordination Chemistry II* Elsevier, 2003.
20. H. Nishiyama, Y. Itoh, H. Matsumoto, S. B. Park and K. Itoh, *J. Am. Chem. Soc.*, 1994, **116**, 2223-2224.
21. H. Nishiyama, S. B. Park, M. Haga, K. Aoki and K. Itoh, *Chem. Lett.*, 1994, 1111-1114.
22. D. L. Christenson, C. J. Tokar, C. Havlin, B. Chamberlain and W. B. Tolman, *Abstr. Papers Am. Chem. Soc.*, 1995, **209**, 111-INOR.
23. D. L. Christenson, C. J. Tokar and W. B. Tolman, *Organometallics*, 1995, **14**, 2148-2150.

24. H. Adolfsson and C. Moberg, *Tetrahedron: Asymmetry*, 1995, **6**, 2023-2031.
25. B. M. Trost, K. Dogra, I. Hachiya, T. Emura, D. L. Hughes, S. Krska, R. A. Reamer, M. Palucki, N. Yasuda and P. J. Reider, *Angew. Chem. Int. Ed.*, 2002, **41**, 1929-+.
26. H.-L. Kwong, H.-L. Yeung, C.-T. Yeung, W.-S. Lee, C.-S. Lee and W.-L. Wong, *Coord. Chem. Rev.*, 2007, **251**, 2188-2222.
27. A. Berkessel, M. Frauenkron, T. Schwenkreis and A. Steinmetz, *J. Mol. Catal. A: Chem.*, 1997, **117**, 339-346.
28. A. Berkessel, M. Frauenkron, T. Schwenkreis, A. Steinmetz, G. Baum and D. Fenske, *J. Mol. Catal. A: Chem.*, 1996, **113**, 321-342.
29. H. Shitama and T. Katsuki, *Tetrahedron Lett.*, 2006, **47**, 3203-3207.
30. V. V. Rostovtsev, L. G. Green, V. V. Fokin and K. B. Sharpless, *Angew. Chem. Int. Ed.*, 2002, **41**, 2596-2599.
31. E. Tamanini, K. Flavin, M. Motevalli, S. Piperno, L. A. Gheber, M. H. Todd and M. Watkinson, *Inorg. Chem.*, 2010, **49**, 3789-3800.
32. E. Tamanini, S. E. J. Rigby, M. Motevalli, M. H. Todd and M. Watkinson, *Eur. Chem J.*, 2009, **15**, 3720-3728.
33. E. Tamanini, A. Katewa, L. M. Sedger, M. H. Todd and M. Watkinson, *Inorg. Chem.*, 2009, **48**, 319-324.
34. A. Nadler, C. Hain and U. Diederichsen, *Eur. J. Org. Chem.*, 2009, 4593-4599.
35. H. Struthers, B. Spingler, T. L. Mindt and R. Schibli, *Chem. Eur. J.*, 2008, **14**, 6173-6183.
36. A. Maisonial, P. Serafin, M. Traikia, E. Debiton, V. Thery, D. J. Aitken, P. Lemoine, B. Viossat and A. Gautier, *Eur. J. Inorg. Chem.*, 2008, 298-305.
37. E. R. Hao, Z. Y. Wang, L. J. Jiao and S. W. Wang, *Dalton Trans.*, 2010, **39**, 2660-2666.
38. M. Kaik and J. Gawronski, *Tetrahedron: Asymmetry*, 2003, **14**, 1559-1563.
39. H.-J. Cristau, P. P. Cellier, S. Hamada, J.-F. Spindler and M. Taillefer, *Org. Lett.*, 2004, **6**, 913-916.
40. Z. Guoqi, Y. Eiji and D. W. Wolf, *Adv. Synth. Catal.*, 2009, **351**, 1255-1262.
41. A. Murphy and T. D. P. Stack, *J. Mol. Catal. A: Chem.*, 2006, **251**, 78-88.
42. M. M. Hammoud, J. J. McKamie, M. J. Heeg and J. J. Kodanko, *Dalton Trans.*, 2008, 4843-4845.
43. A. I. Abouelatta, J. A. Sonk, M. M. Hammoud, D. M. Zurcher, J. J. McKamie, H. B. Schlegel and J. J. Kodanko, *Inorg. Chem.*, 2010, **49**, 5202-5211.
44. C. F. Lane, *Synthesis-Stuttgart*, 1975, 135-146.
45. R. F. Borch, Bernstei.Md and H. D. Durst, *J. Am. Chem. Soc.*, 1971, **93**, 2897-&.

46. L. Farrugia, *J. Appl. Crystallogr.*, 1997, **30**, 565.
47. N. Marsich, G. Nardin, L. Randaccio and A. Camus, *Inorg. Chim. Acta*, 1998, **278**, 237-240.
48. C. A. Blindauer, M. T. Razi, S. Parsons and P. J. Sadler, *Polyhedron*, 2006, **25**, 513-520.
49. H. Keypour, S. Salehzadeh, R. G. Pritchard and R. V. Parish, *Transition Met. Chem.*, 2002, **27**, 720-723.
50. S. J. Brudenell, L. Spiccia and E. R. T. Tiekink, *Inorg. Chem.*, 1996, **35**, 1974-1979.
51. A. W. Addison, T. N. Rao, J. Reedijk, J. van Rijn and G. C. Verschoor, *J. Chem. Soc., Dalton Trans.*, 1984, 1349-1356.
52. S. Youngme, P. Phuengphai, C. Pakawatchai, P. Kongsaeree and N. Chaichit, *Acta Crystallogr., Sect. B: Struct. Sci*, 2008, **64**, 318-329.
53. V. C. Copeland, P. P. Singh, W. E. Hatfield and D. J. Hodgson, *Inorg. Chem.*, 1972, **11**, 1826.
54. A. P. Cole, V. Mahadevan, L. M. Mirica, X. Ottenwaelder and T. D. P. Stack, *Inorg. Chem.*, 2005, **44**, 7345-7364.
55. J. T. York, L. Bar-Nahum and W. B. Tolman, *Inorg. Chem.*, 2007, **46**, 8105-8107.
56. J. T. York, E. C. Brown and W. B. Tolman, *Angew. Chem. Int. Ed.*, 2005, **44**, 7745-7748.
57. J. A. Kitchen, N. G. White, M. Boyd, B. Moubaraki, K. S. Murray, P. D. W. Boyd and S. Brooker, *Inorg. Chem.*, 2009, **48**, 6670-6679.
58. B. Beyer, C. Ulbricht, D. Escudero, C. Friebe, A. Winter, L. Gonzalez and U. S. Schubert, *Organometallics*, 2009, **28**, 5478-5488.
59. D. Schweinfurth, R. Pattacini, S. Strobel and B. Sarkar, *Dalton Trans.*, 2009, 9291-9297.
60. D. Urankar, B. Pinter, A. Pevec, F. De Proft, I. Turel and J. Kosmrlj, *Inorg. Chem.*, 2010, **49**, 4820-4829.
61. E. Tamanini, K. Flavin, M. Motevalli, S. Piperno, L. A. Gheber, M. H. Todd and M. Watkinson, *Inorg. Chem.*, 2010, **49**, 3789-3800.
62. E. Tamanini, A. Katewa, L. M. Sedger, M. H. Todd and M. Watkinson, *Inorg. Chem.*, 2009, **48**, 319-324.
63. E. Tamanini, S. E. J. Rigby, M. Motevalli, M. H. Todd and M. Watkinson, *Chem. Eur. J.*, 2009, **15**, 3720-3728.
64. H. C. Kolb, M. G. Finn and K. B. Sharpless, *Angew. Chem. Int. Ed.*, 2001, **40**, 2004-2021.
65. V. Aucagne, J. Berna, J. D. Crowley, S. M. Goldup, K. D. Haenni, D. A. Leigh, P. J. Lusby, V. E. Ronaldson, A. M. Z. Slawin, A. Viterisi and D. B. Walker, *J. Am. Chem. Soc.*, 2007, **129**, 11950-11963.

66. J. E. Hein, J. C. Tripp, L. B. Krasnova, K. B. Sharpless and V. V. Fokin, *Angew. Chem. Int. Ed.*, 2009, **48**, 8018-8021.

67. D. S. Surry and S. L. Buchwald, *Chemical Science*, 2010, **1**, 13-31.

68. I. H. Chen, M. Kanai and M. Shibasaki, *Org. Lett.*, **12**, 4098-4101.

Chapter 5 - Experimental

5.1 General remarks

All reagents were purchased from Aldrich, Acros, Merk, Fluka, Solchemar LDA or Avocado and were used without further purification unless otherwise stated. The hydrogen peroxide used in the epoxidation procedures was bought from Sigma Aldrich as a 30 % solution in water. Solvents that were required to be anhydrous were dried according to reported procedures[1] as follows. Acetonitrile was refluxed overnight with calcium hydride under a nitrogen atmosphere and collected over 4Å molecular sieves. THF was refluxed over metallic sodium and benzophenone under a nitrogen atmosphere and freshl used. DMF, DCM, diethyl ether and toluene were obtained anhydrous from a MBraun MB SPS-800 solvent purification rig. Nitrogen used for inert athmosphere was oxygen-free grade. Thin layer chromatography was performed on either silica gel 60 F_{254} plates (Merk) or neutral aluminium oxide 60 F_{254} plates (Merk). Flash chromatography was performed on silica gel (VWR, 40-63 μm) or on aluminium oxide (BDH, 90 active neutral, 0.063-0.2 mm). Cyclic voltammetry was performed on an EG&G instruments Versastat II workstation, using tetrabutylammonium hexaphosphate as the support electrolyte, a platinum working electrode, a graphite counter electrode and a silver reference electrode. Melting points were measured on a Stuart SMP3 melting point apparatus and are uncorrected. Optical rotation were determined using a Jasco P-1010 polarimeter, $[\alpha]^{25}_{D}$ values are given in 10^{-1} deg cm^3 g^{-1}. ^{1}H-NMR and ^{13}C-NMR were recorded using a Jeol JNM-EX spectrometer at 270 MHz and 67.5 MHz or at 400 MHz and at 100.2 MHz on a Bruker AV400 or a Bruker AMX400 and normalized on the signal of tetramethylsilane (TMS); multiplicity is expressed as follows: s = singlet, d = doublet, t = triplet, q = quartet, m = multiplet and combinations of the above for more complex patterns. IR spectra were recorded on a Perkin Elmer Spectrum 65 IR spectrometer equipped with ATR accessory unless otherwise stated (e.g. KBr or nujol®). Uv/Vis spectra were obtained on a HP 8453 spectrophotometer, absorption maxima (λ_{max}) are expressed in nm, the molar extinction coefficients (ε) are expressed in $Lmol^{-1}cm^{-1}$. Electrospray ionisation mass spectroscopy was obtained from the EPSRC national mass spectrometry service centre, University of Wales on a Thermofisher LTQ Orbitrap XL. Water is always intended as distilled water and was obtained from an Elga Purelab Option distillation system. High Performance Liquid Chromatography was performed on a Perkin Elmer Series 200 instrument equipped with UV-Vis detector using a Chiralpak IA, Chiralcel AS-RH, Chiralcel

OJ, Chirlacel OD or Lichrosphere RP select B analytical column. Gas chromatography was performed on a HP 5890 equipped with a Chrompack capillary column CP Chirasil-dex CB, 0.25μm. X-Ray cristallography analysis was performed by Majid Motevalli, QMUL; the intensity data were collected on a CAD-4 diffractometer and Mo Kα radiation(λ 0.71069 Å) using ω-2θ scan at 160 K. The unit cell parameters were determined by least-squares refinement on 25 automatically centred reflections[2] ($9.25 \leq \theta \leq 13.70°$). All data were corrected for absorption by empirical methods (ψ scan)[2]and for Lorentz-polarization effects by XCAD4.[3] The structure was solved by Direct method using SHELXS-97[4] program, refined anisotropically (non-hydrogen atoms) by full-matrix least-squares on F^2 using SHELXL-97[4] program. The H atoms were calculated geometrically and refined with a riding model. The programs ORTEP-3[5]and PLATON[6] were used for drawing the molecules. WINGX[7] was used to prepare material for publication.

5.2 Synthetic procedures

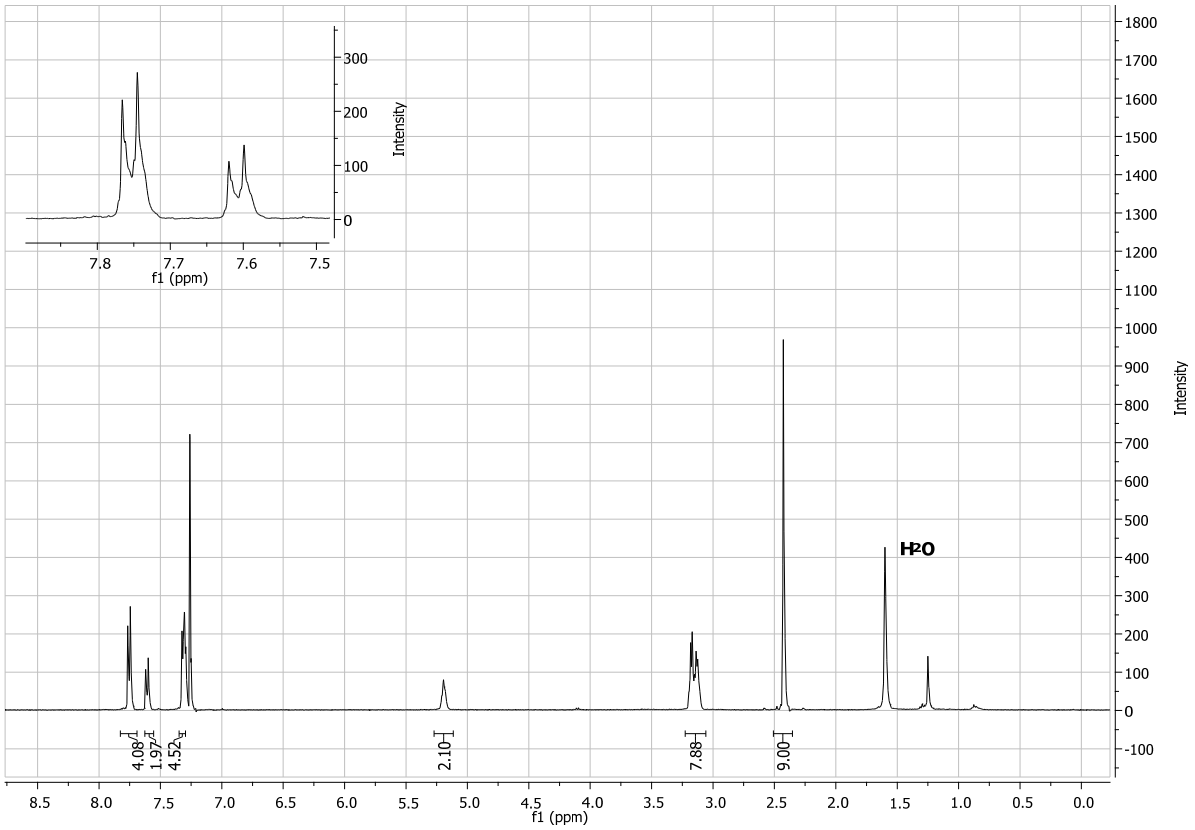
H2O
4.08
1.97
4.52
2.10
7.88
9.00
f1 (ppm)
Intensity

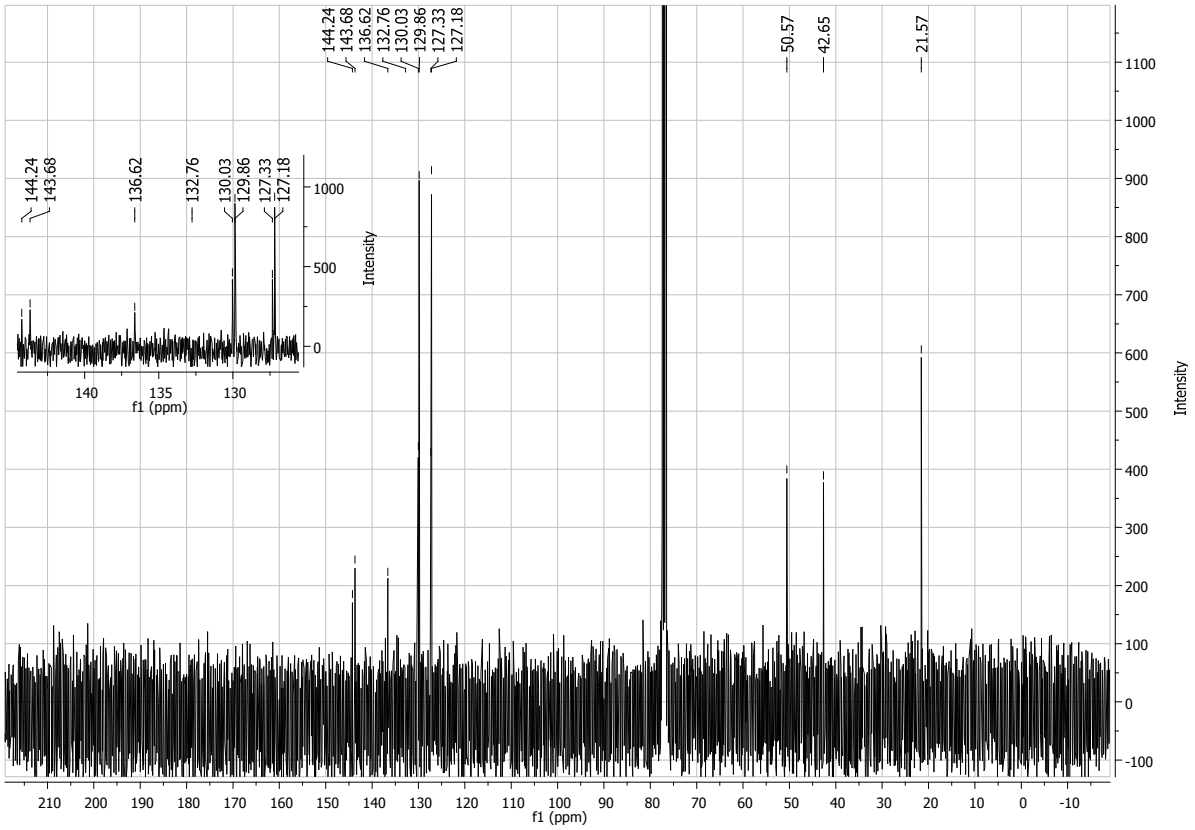
144.24
143.68
136.62
132.76
130.03
129.86
127.33
127.18
50.57
42.65
21.57
f1 (ppm)
Intensity

N,N',N''-Tri-(p-toluenesulfonyl)-diethylenetriamine (125)[8]

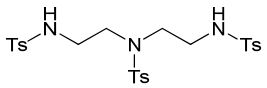

To a stirred solution of diethylenetriamine (8.6 mL, 80 mmol) in distilled water, solid K_2CO_3 (22.1 g, 0.160 mol) was added at room temperature. The solution was then warmed to 60 °C and added with solid *p*-toluenesulfonyl chloride (50.3 g, 260 mmol) in small portions over a period of an hour and then left stirring for 3 more hours during which the formation of a white solid was observed. The mixture was then left cooling down and filtered. The solid was washed with water and ethanol, dried *in vacuo*, and then refluxed overnight in ethanol. Compound **125** (23.7 g, 84 %) was recovered from the solution as colourless crystals.

IR (neat, ν_{max}/cm^{-1}): 3282, 2997, 2850, 1596, 1458, 1323, 1153; ^{1}H-NMR (400 MHz, δ-$CDCl_3$): 2.44 (9H, s, ArC*H*$_3$), 3.10-3.22 (8H, m, C*H*$_2$), 4.98-5.08 (2H, m, N*H*Ts), 7.28-7.35 (6H, m, Ar*H*), 7.61 (2H, d, J_1 = 7.9 Hz), 7.76 (4H, d, J_1 = 7.6 Hz); ^{13}C-NMR (100.2 MHz, δ-$CDCl_3$): 21.5, 42.6, 50.5,127.18, 127.3, 129.8, 130.0, 132.7, 136.6, 138.8, 143.6, 144.2.

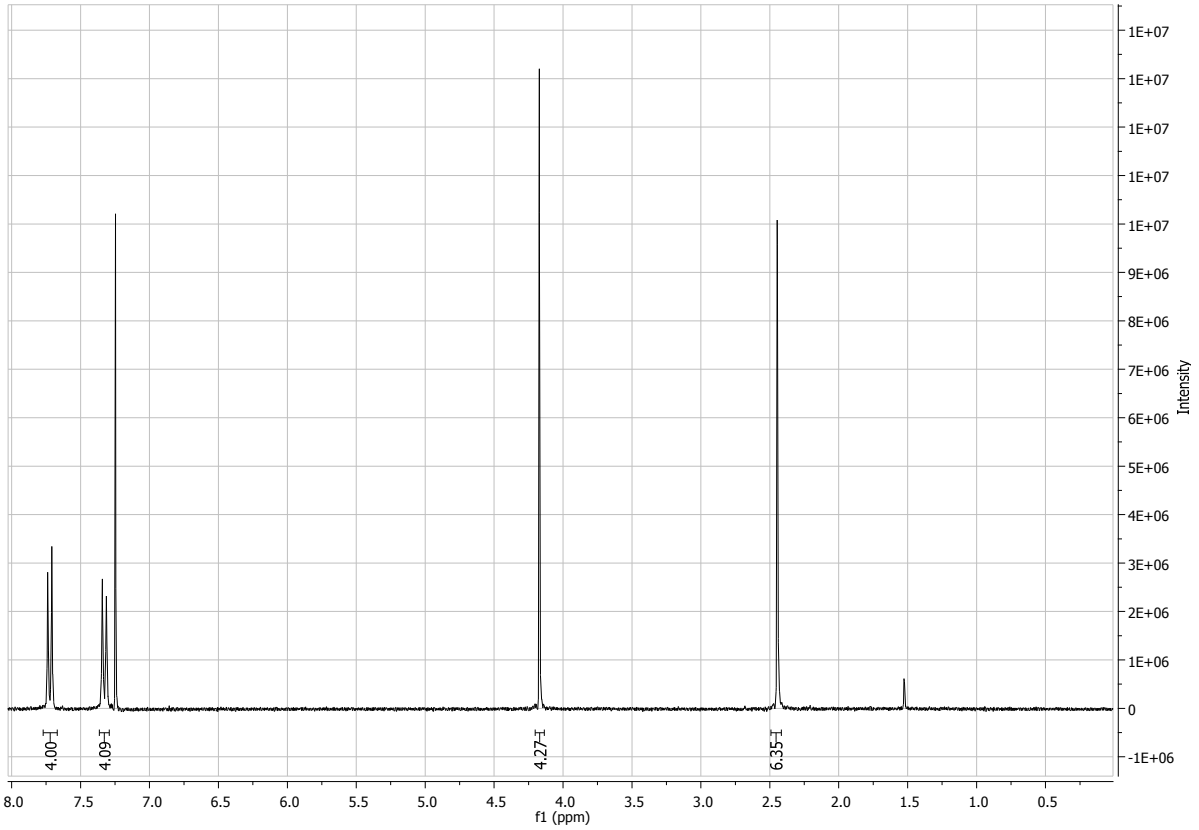
4.00
4.09
4.27
6.35
f1 (ppm)
Intensity

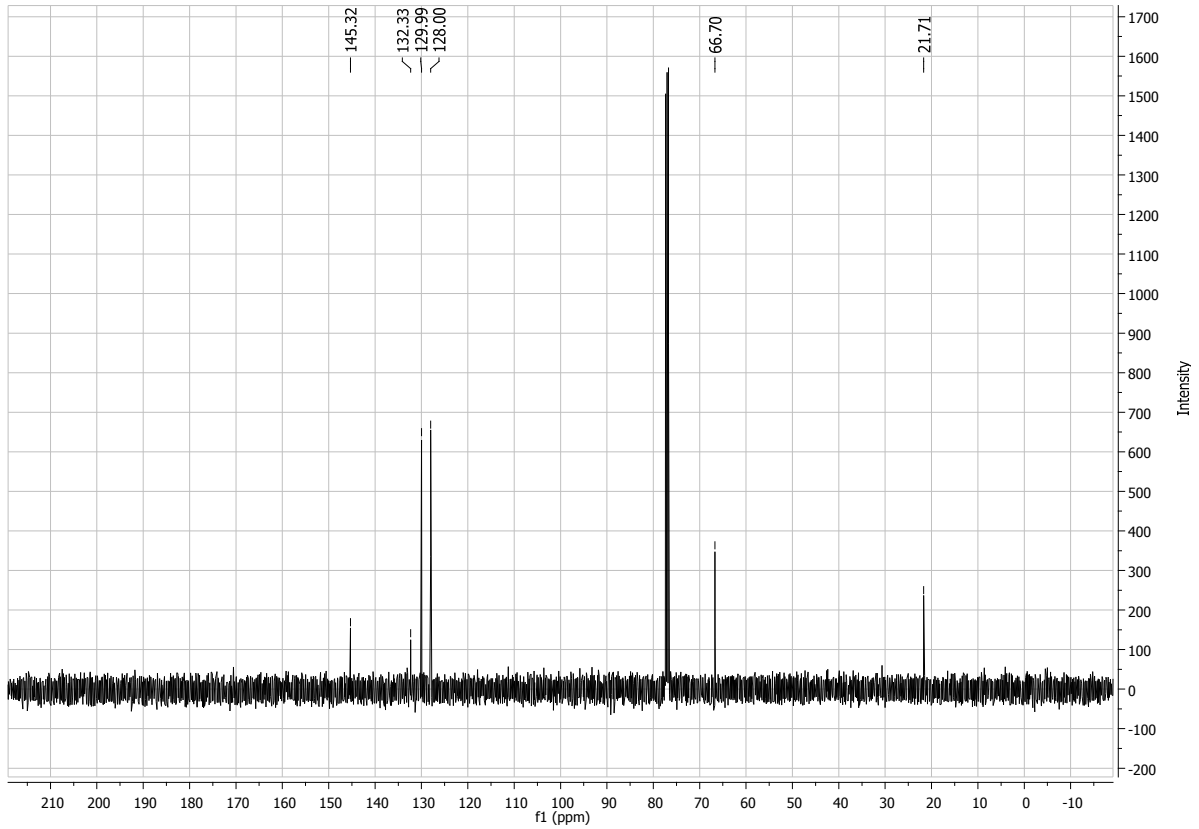
145.32
132.33
129.99
128.00
66.70
21.71
f1 (ppm)
Intensity

1,2-di-(*p*-toluenesulfonyloxy)-ethane (126)[9]

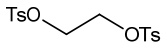

To a mixture of ethylene glycol (2.79 mL, 50.0 mmol) and *p*-toluenesulfonychloride (22.7 g, 125 mmol) in DCM kept around 0 °C with an ice bath, triethylamine (56 mL, 0.40 mol) was added dropwise over a 2 hour period. The solution was then stirred at RT for 2 more hours, during which the formation of a white solid was observed. Water was added to the mixture and stirring maintained for further 5-10 minutes. The solid was then filtered and washed with an aqueous 1M solution of H_2SO_4 and successively with water. Recrystallization from diethyl ether and acetone gave bistosylate **126** (15.1 g, 82 %) as colourless crystals.

IR (neat, ν_{max}/cm^{-1}): 2923, 2854, 1454, 1377, 1296, 1176; ^{1}H-NMR (270 MHz, δ-$CDCl_3$): 2.44 (6H, s, ArCH_3), 4.17 (4H, s, CH_2), 7.32 (4H, d, J_1 = 8.4 Hz, Ar*H*), 7.72 (4H, d, J_1 = 8.2 Hz, Ar*H*); ^{13}C-NMR (100.2 MHz, δ-$CDCl_3$): 21.70, 66.7, 128.0, 129.9, 132.3, 145.3.

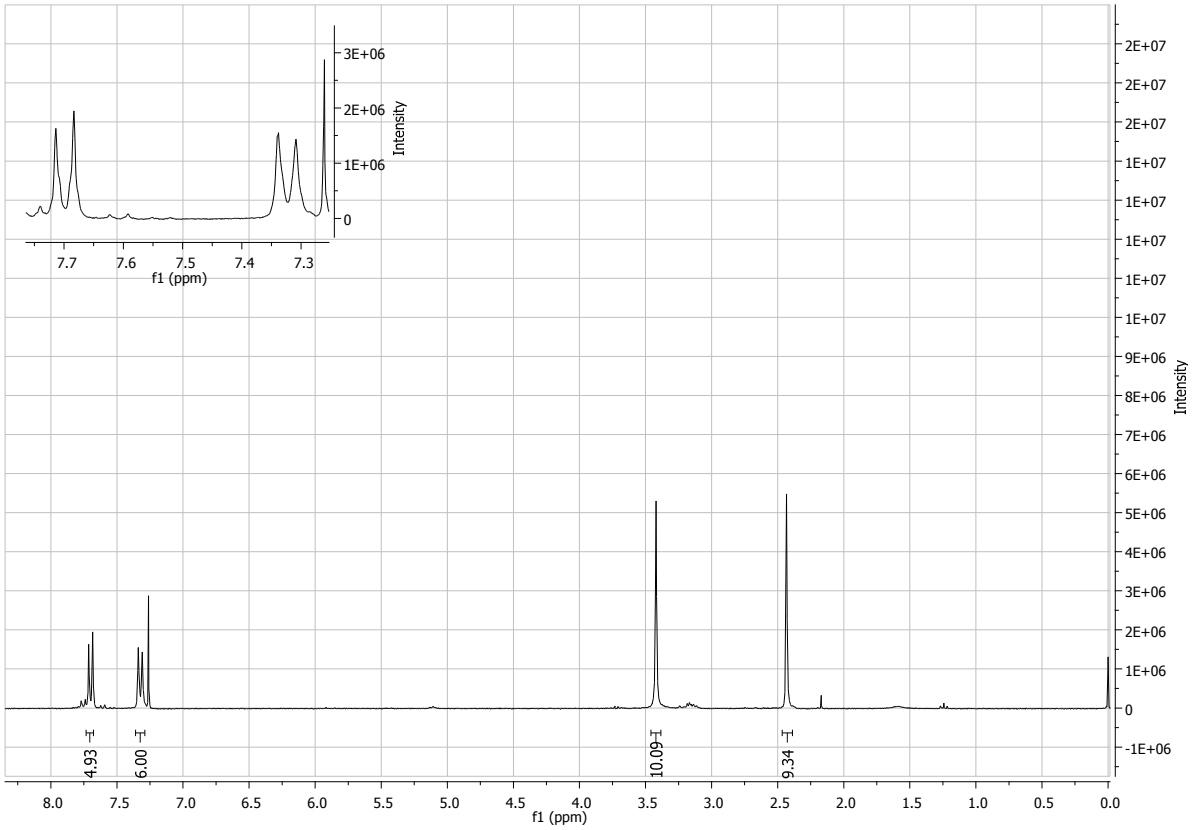
3E+06
2E+06
1E+06
0
Intensity
7.7
7.6
7.5
7.4
7.3
f1 (ppm)
4.93
6.00
10.09
9.34
8.0
7.5
7.0
6.5
6.0
5.5
5.0
4.5
4.0
3.5
3.0
2.5
2.0
1.5
1.0
0.5
0.0
f1 (ppm)
Intensity

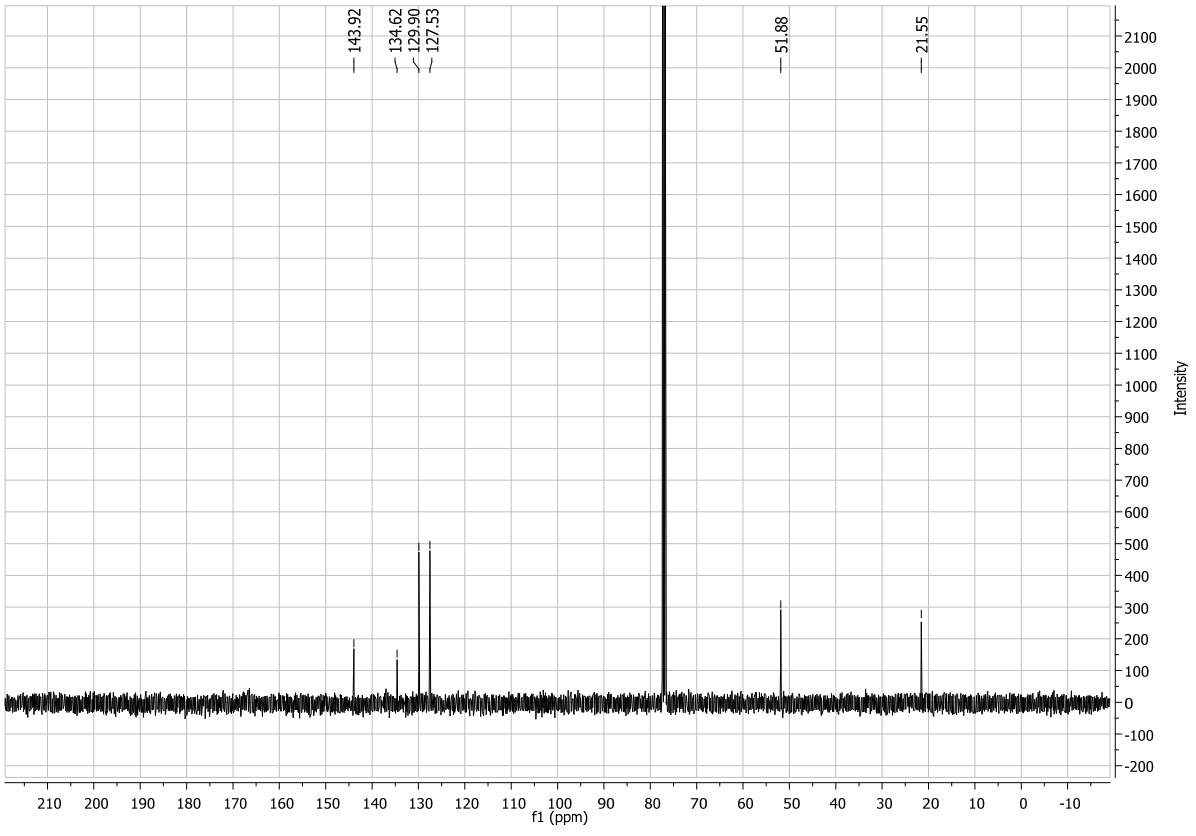
143.92
134.62
129.90
127.53
51.88
21.55
210
200
190
180
170
160
150
140
130
120
110
100
90
80
70
60
50
40
30
20
10
0
-10
f1 (ppm)
Intensity

1,4,7-tri-(p-toluenesulfonyl)-1,4,7-triazacyclononane (127)[10, 11]

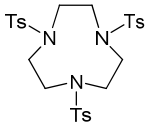

To a solution of **125** (15.0 g, 26.5 mmol) in dry DMF (150 mL) kept at RT, NaH (1.50 g, 63.6 mmol) was added in small aliquots. When the efferscence ceased, the mixture was brought to 100 °C and a solution of **126** dissolved in dry DMF (150 mL) was added dropwise over a period of 2 hours. The solution was left stirring at 100 °C for two more hours after the addition and finally water (500 mL) was added dropwise, until a colourless precipitate formed. Tritosylate **127** (15 g, 96 %) was filtered, washed with water, EtOH, Et_2O and then dried *in vacuo*.

IR (neat, ν_{max}/cm^{-1}): 2920, 2850, 1458, 1377, 1334, 1319, 1149; ^{1}H-NMR (270 MHz, δ-$CDCl_3$): 2.41 (9H, s, C*H*$_3$), 3.40 (12H, s, C*H*$_2$), 7.12 (6H, d, J_1 = 8.2 Hz, Ar*H*), 7.68 (6H, d, J_1 = 8.2 Hz, Ar*H*); ^{13}C-NMR (100.2 MHz, δ-$CDCl_3$): 21.5, 51.8, 127.5, 129.9, 134.6, 143.9; *m/z* (ESI): 609.2 (90 %), 592.2 (100); HRMS (ESI): $[C_{27}H_{33}N_3O_6S_3+NH_4]^+$ requires 609.1870 found 609.1880.

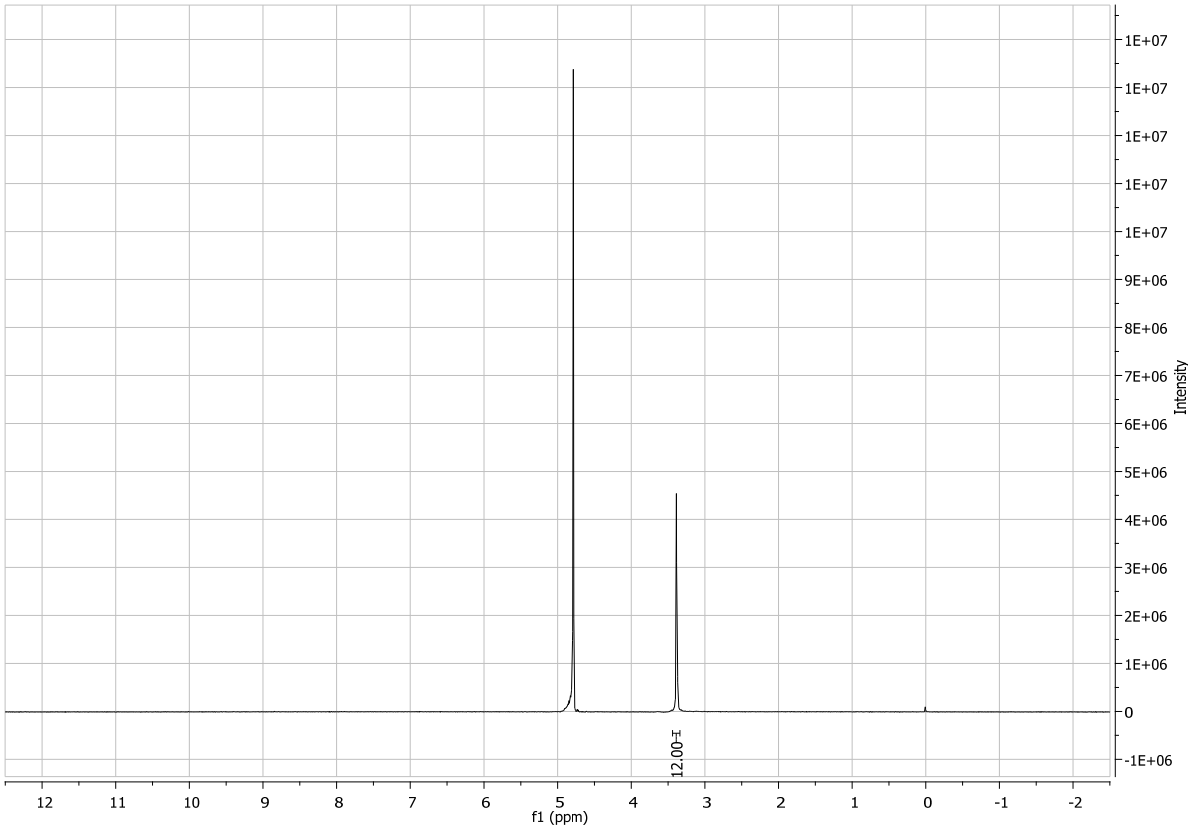
1E+07
1E+07
1E+07
1E+07
1E+07
9E+06
8E+06
7E+06
6E+06
5E+06
4E+06
3E+06
2E+06
1E+06
0
-1E+06
Intensity
12.00
12 11 10 9 8 7 6 5 4 3 2 1 0 -1 -2
f1 (ppm)

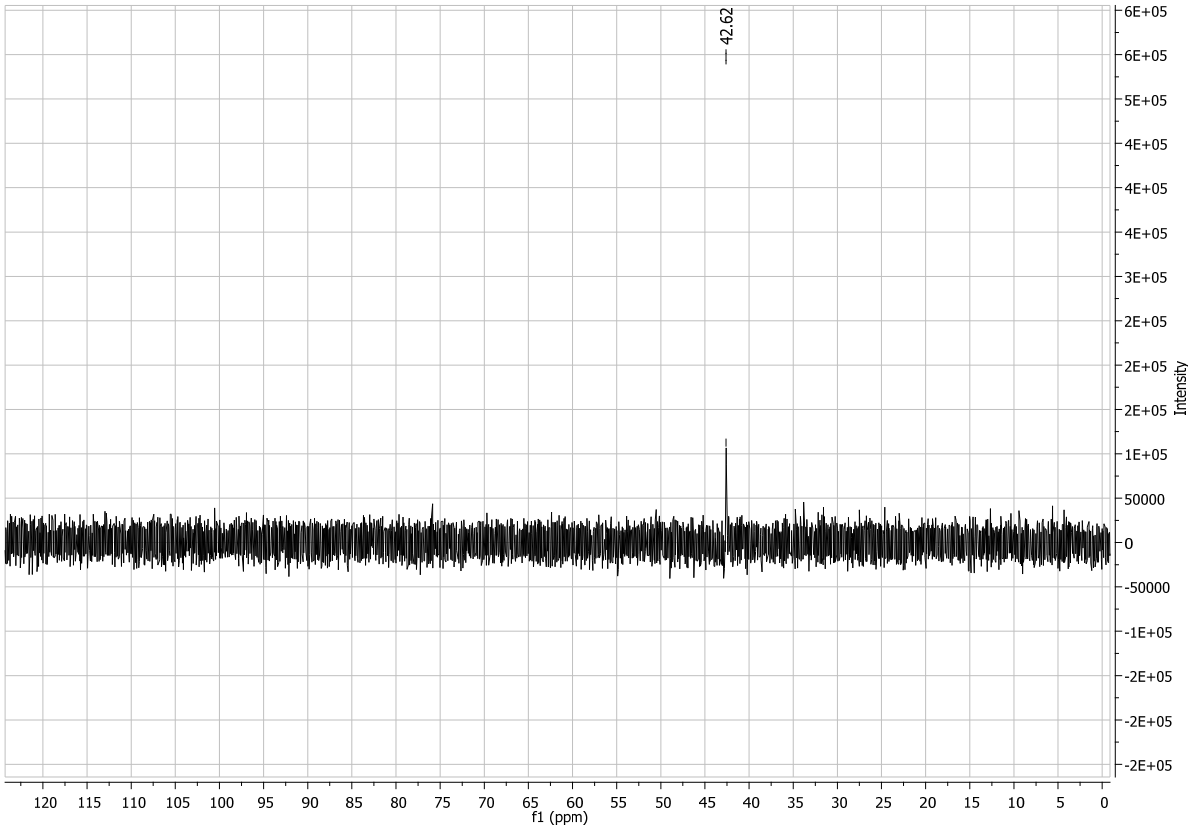
42.62
6E+05
6E+05
5E+05
4E+05
4E+05
4E+05
3E+05
2E+05
2E+05
2E+05
1E+05
50000
0
-50000
-1E+05
-2E+05
-2E+05
-2E+05
Intensity
120 115 110 105 100 95 90 85 80 75 70 65 60 55 50 45 40 35 30 25 20 15 10 5 0
f1 (ppm)

TACN tri-hydrobromide salt (128)[10, 11]

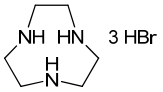

Following a modification of the reported procedures, removal of the tosyl protecting groups was achieved adding concentrated H_2SO_4 (45 mL) to **127** (9.00 g, 15.2 mmol), and leaving the mixture refluxing at 105 °C for 72 hours. The solution turned dark brown at around 80 °C. The mixture was then cooled to RT and added dropwise (over 30 minutes) into a flask containing diethyl ether (100 mL) in an ice bath with vigorous stirring. A brown solid precipitated. The solution was carefully decanted before HBr 48 % (aq, 50 mL) was added to the remaining suspension of solid under stirring. The mixture was left stirring for 2 hours and the precipitate collected by filtration. Compound **128** (2.2 g, 39 %) was recovered as a pale pink solid.

IR (neat, ν_{max}/cm^{-1}): 3390, 2997, 2850, 1458, 1377; ^{1}H-NMR (270 MHz, δ-D_2O): 3.38 (12H, s, CH_2); ^{13}C-NMR (67.6 MHz, δ-D_2O): 42.2; *m/z* (ESI): 341.2 (90 %), 339.2 (100), 279.1 (50); HRMS (ESI): $[C_6H_{17}Br_3N_3]^-$ requires 367.8978 found 367.8978.

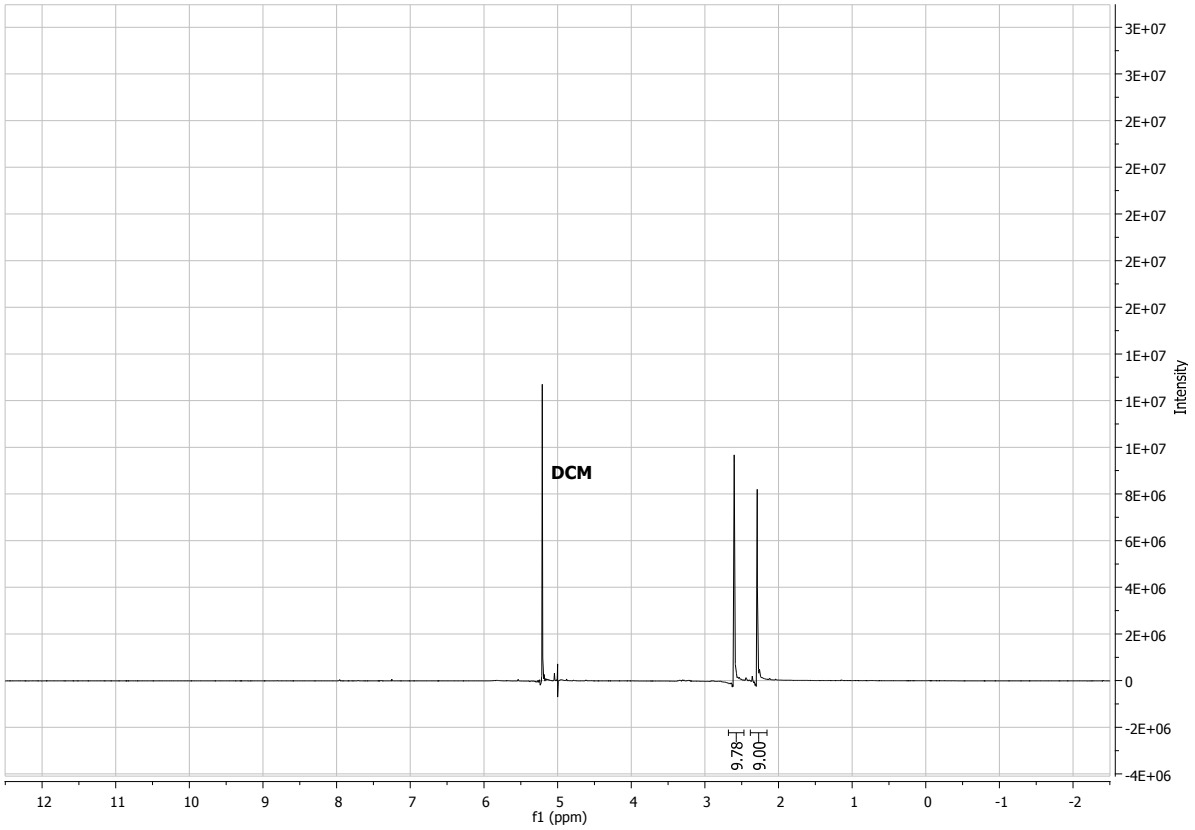
DCM
9.78
9.00
f1 (ppm)
Intensity

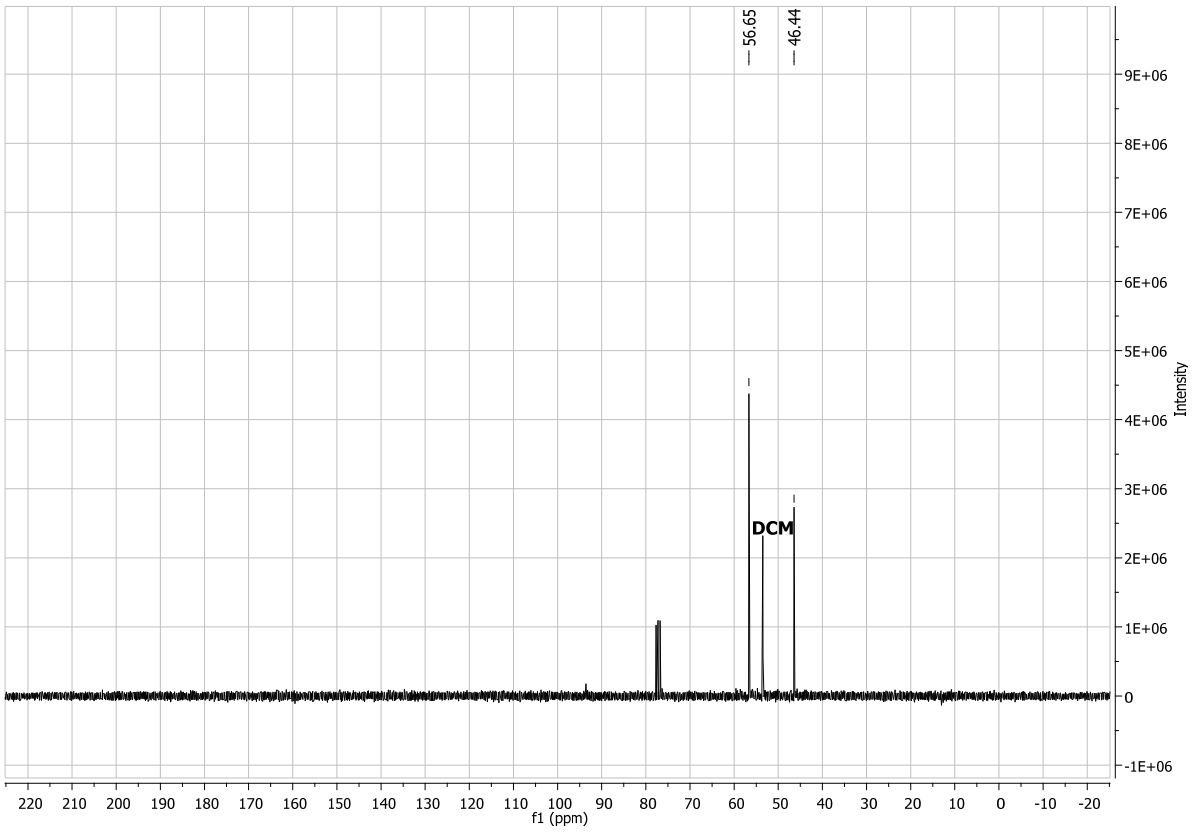
56.65
46.44
DCM
f1 (ppm)
Intensity

1,4,7-trimethyl-1,4,7-triazacyclononane (4)[12]

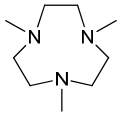

Following a modification of the reported procedure, to a solution of **128** (2.0 g, 5.4 mmol) in MeOH, formic acid (11.4 mL) and formaldehyde (10.6 mL) were added. After addition of water (1.3 mL) the solution was refluxed at 80 °C for 24 hours. The mixture was then transferred in a flask containing ice cold water (30 mL) and the pH was raised to 12 by addition of an aqueous solution of NaOH (50 % w/w) keeping the temperature below 20 °C. After the solution was basified, it was transferred into a separating funnel, washed eith saturated NaCl and extracted 4 times with DCM. The solvents were evaporated under reduced pressure, keeping the bath temperature around 25-30° C. The fully methylated product (700 mg, 75 %) was obtained as a yellow oil.

IR (neat, ν_{max}/cm^{-1}): 2940, 2799, 1448, 1370; ^{1}H-NMR (270 MHz, δ-$CDCl_3$): 2.64 (12H, s, CH_2), 2.37 (9H, s, CH_3); ^{13}C-NMR (67.6 MHz, δ-$CDCl_3$): 46.5, 56.9; *m/z* (ESI): 220.1 (20 %), 172.2 (100); HRMS (ESI): $[C_9H_{22}N_3]^+$ requires 172.1808 found 172.1808.

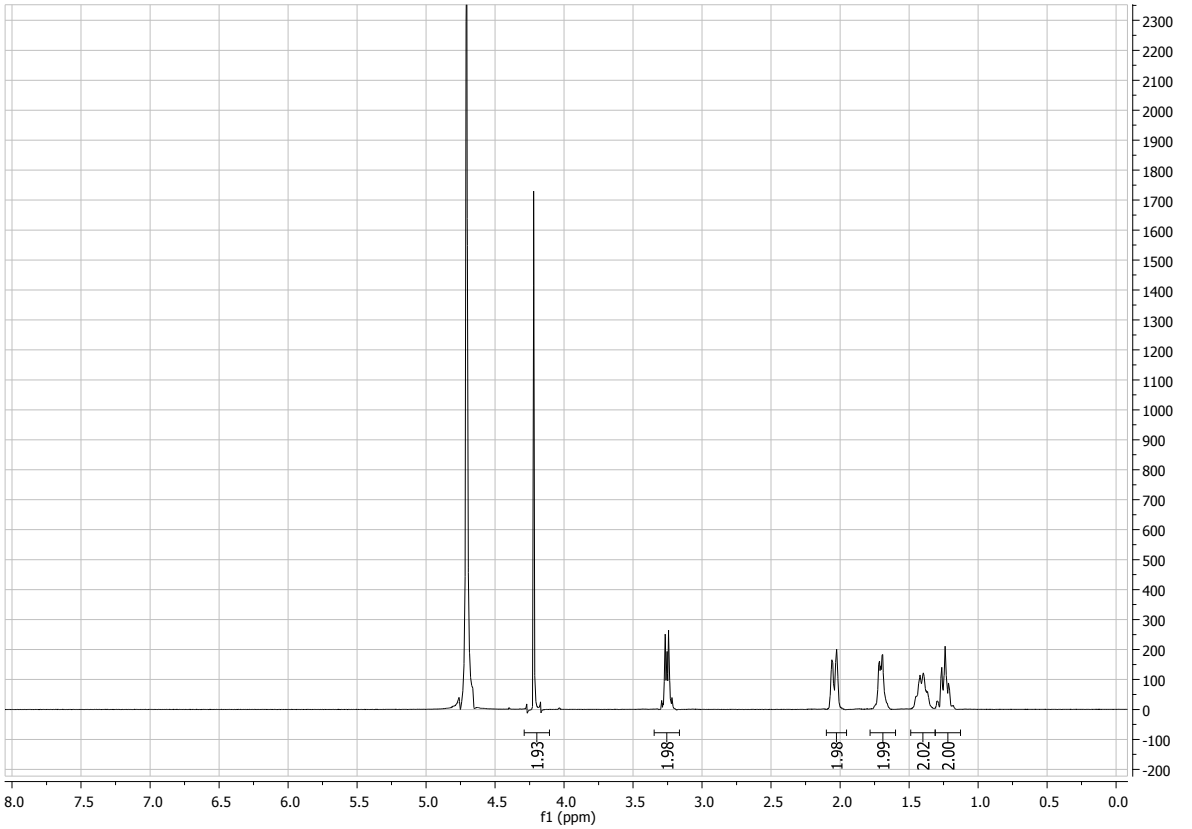
1.93
1.98
1.98
1.99
2.02
2.00
f1 (ppm)

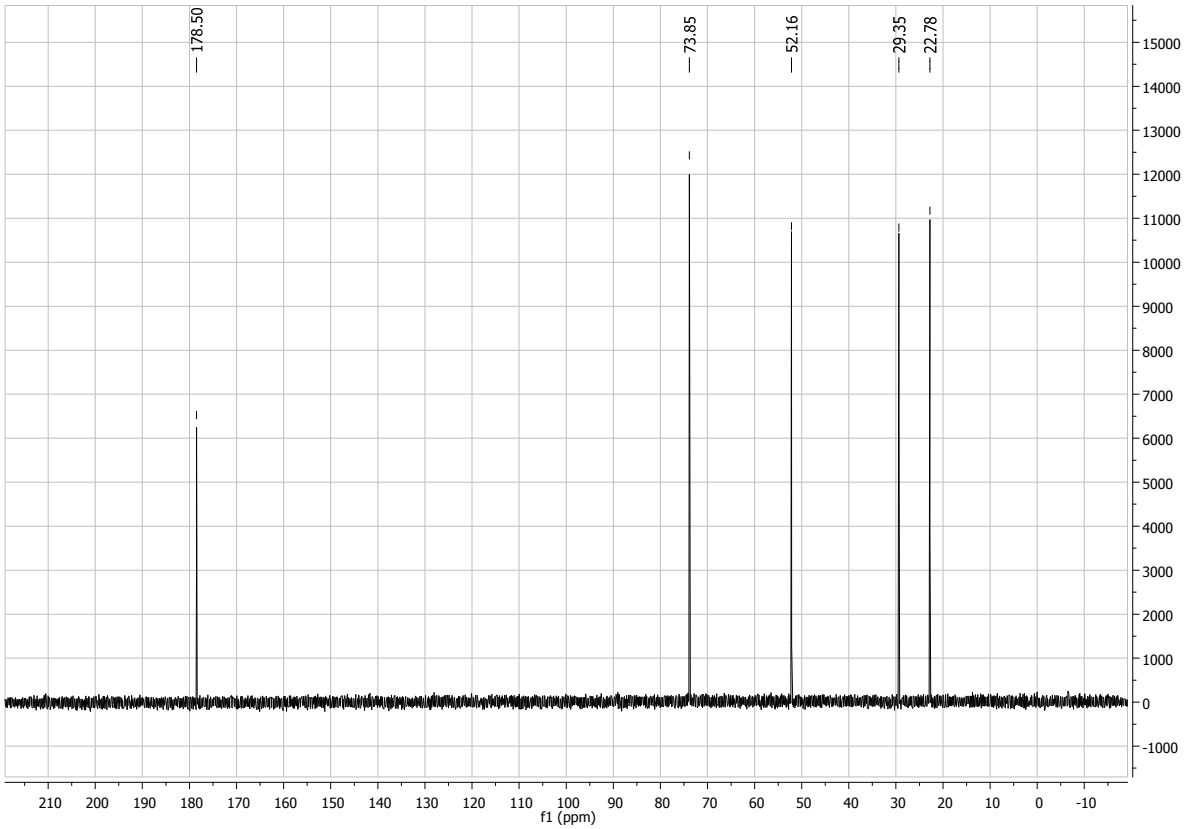
178.50
73.85
52.16
29.35
22.78
f1 (ppm)

Resolution of cyclohexanediamine, formation of L-tartaric acid-(133) salt[13]

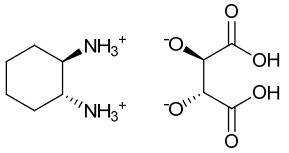

To a solution of racemic *trans*-diaminocyclohexane (12 mL, 0.10 mol) in water (20 mL) at RT, L-(+)-tartaric acid (7.5 g, 50 mmol) was added in small portions over a period of 30 minutes. The solution was then brought to 90 °C and glacial acetic acid (10 mL) was slowly added dropwise. The mixture was then heated at 90 °C for a further hour, until a white precipitate appeared. The mixture was then cooled to RT and filtered. The solid was collected and washed with ice-cold water (20 mL) and MeOH (20 mL) to yield (*R, R*)- *trans*-cyclohexanediamine tartrate salt (10.5 g, 39 %) as a colourless, crystalline solid. The (*S*, *S*) isomer was obtained replacing L-(+)-tartaric acid with D-(-)-tartaric acid in the procedure.

mp 200 °C (dec.); $[\alpha]^{25}_{D}$ = - 50.8 (c = 1, 10 % aq KOH), (1*S*, 2*S* isomer), $[\alpha]^{25}_{D}$ = 49.7 (c = 1, 10 % aq KOH), (1*R*, 2*R* isomer); IR (neat, ν_{max}/cm^{-1}): 3000, 2900, 1651, 1596, 1531; ^{1}H-NMR (400 MHz, δ-D_2O): 1.14-1.31 (2H, m, C*H*$_2$CH$_2$CH), 1.32-1.47 (2H, m, C*H*$_2$CH$_2$CH), 1.61-1.77 (2H, m, CH$_2$C*H*$_2$CHN), 1.97-2.08 (2H, m, CH$_2$C*H*$_2$CHN), 3.18-3.23 (2H, m, CH$_2$CH$_2$C*H*N), 4.32 (2H, m, C*H*COOH); ^{13}C-NMR (100.2 MHz, δ-D_2O): 22.7, 29.3, 52.1, 73.8, 178.5.

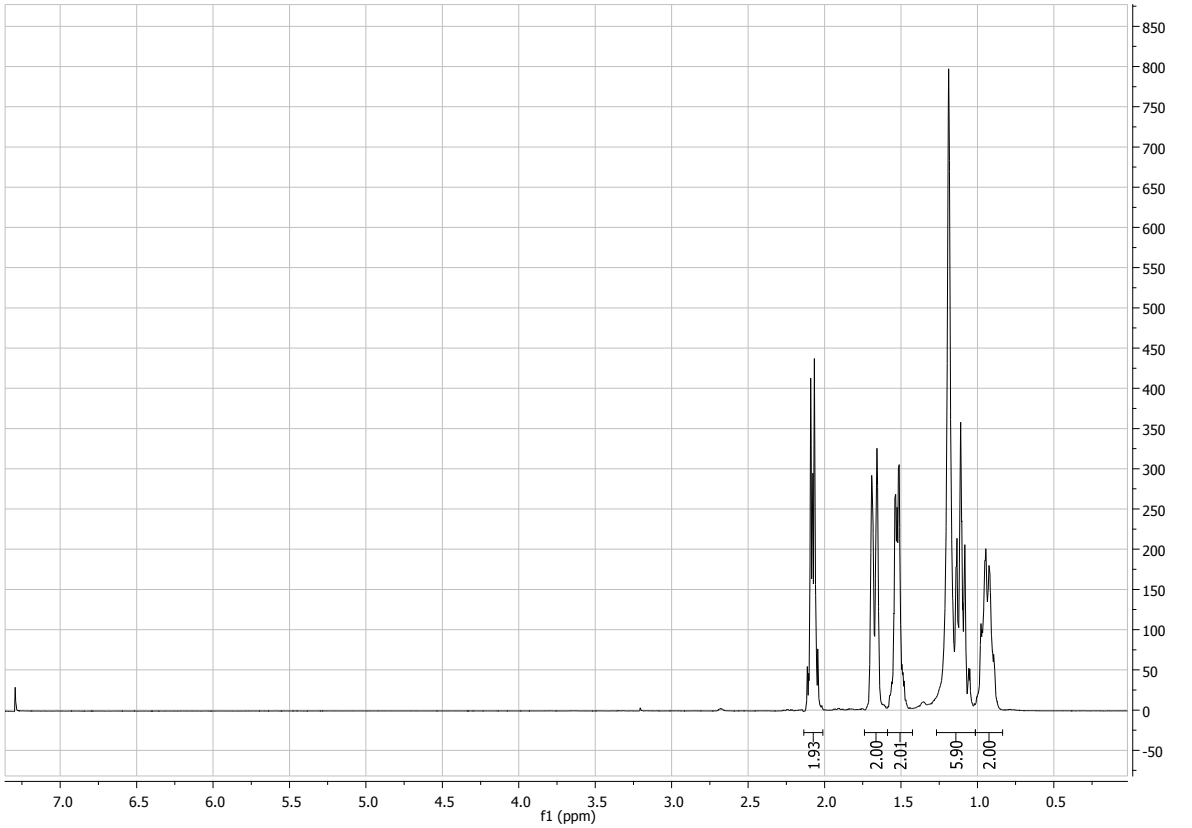
1.93
2.00
2.01
5.90
2.00
f1 (ppm)

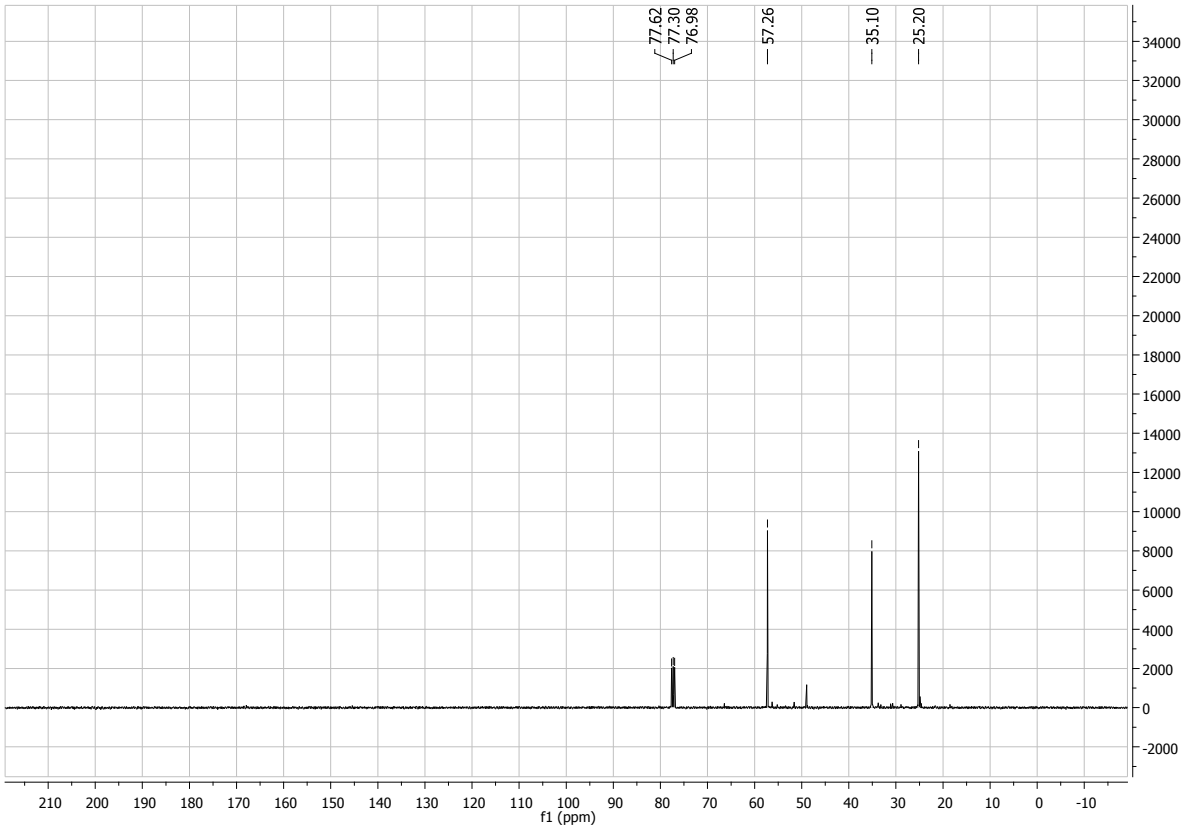
77.62
77.30
76.98
57.26
35.10
25.20
f1 (ppm)

Resolution of cyclohexanediamine, liberation of (*R, R*)-*trans*-diaminocyclohexane (133)[13]

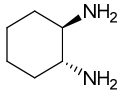

The tartrate salt of (*R, R*)-*trans*-diaminocyclohexane (6.0 g, 22 mmol) was dissolved in the minimum amount of a saturated solution of KOH. (*R,R*)-*trans*-diaminocyclohexane·separates as a yellow oil forming a layer on top of the aqueous phase and was recovered by decantation. The layer recovered was dissolved in DCM and dried on anhydrous $MgSO_4$. Evaporation of the solvent gave **133** (2 g, 77 %) as a pale yellow liquid.

$[\alpha]^{25}_D$ = -38.1 (c = 5, Benzene), (1*S*, 2*S* isomer), lit.[14] -41.6 (c = 5, Benzene), $[\alpha]^{25}_D$ = 36.6 (c = 5, Benzene), (1*R*, 2*R* isomer); IR (neat, ν_{max}/cm^{-1}): 3360, 3281, 2978, 1588, 1432; ^{1}H-NMR (400 MHz, δ-$CDCl_3$): 0.86-1.01 (2H, m, C*H*$_2$CH$_2$CH), 1.03-1.28 (6H, m, C*H*$_2$CH$_2$CH, N*H*$_2$), 1.46-1.58 (2H, m, CH$_2$C*H*$_2$CHN), 1.61-1.74 (2H, m, CH$_2$C*H*$_2$CHN), 2.01-2.12 (2H, m, CH$_2$CH$_2$C*H*N); ^{13}C-NMR (100.2 MHz, δ-$CDCl_3$): 25.2, 35.1, 57.2; *m/z* (ESI): (2HCl salt): 115.12 (M-2Cl).

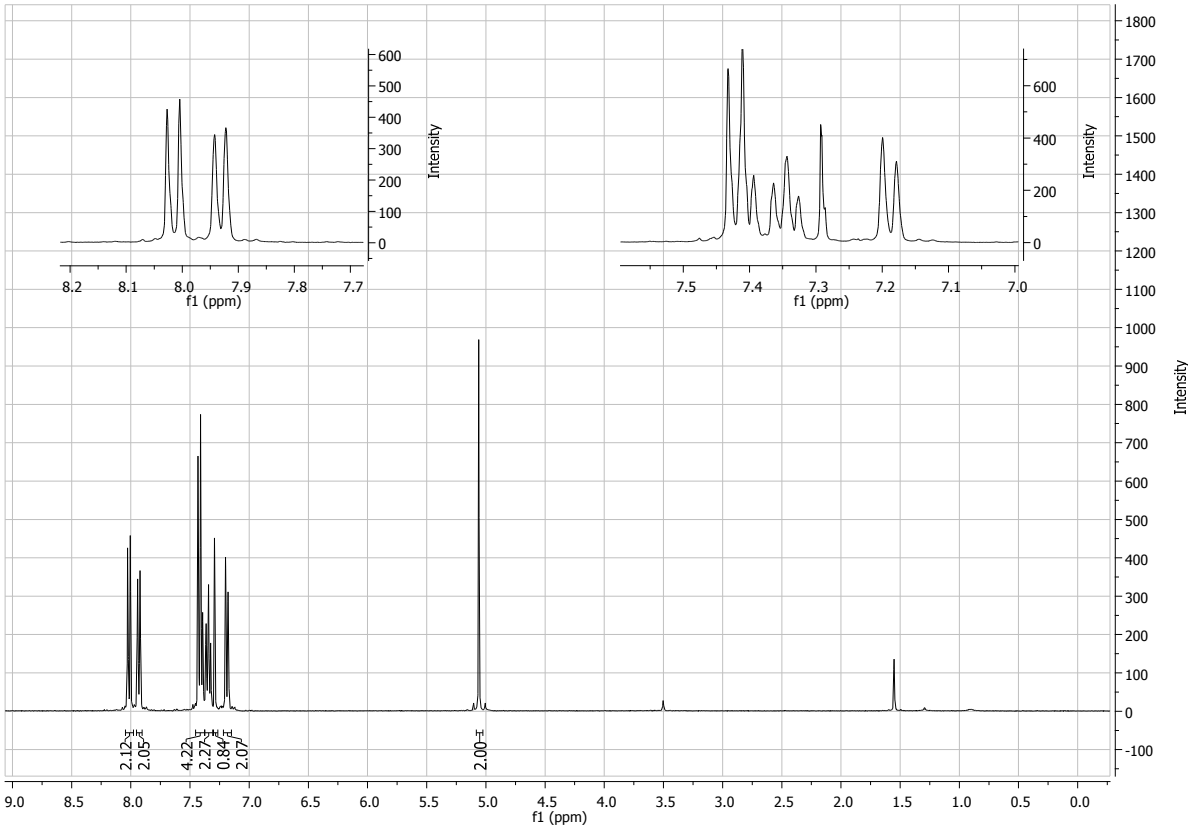
f1 (ppm)
Intensity
2.12
2.05
4.22
2.27
0.84
2.07
2.00

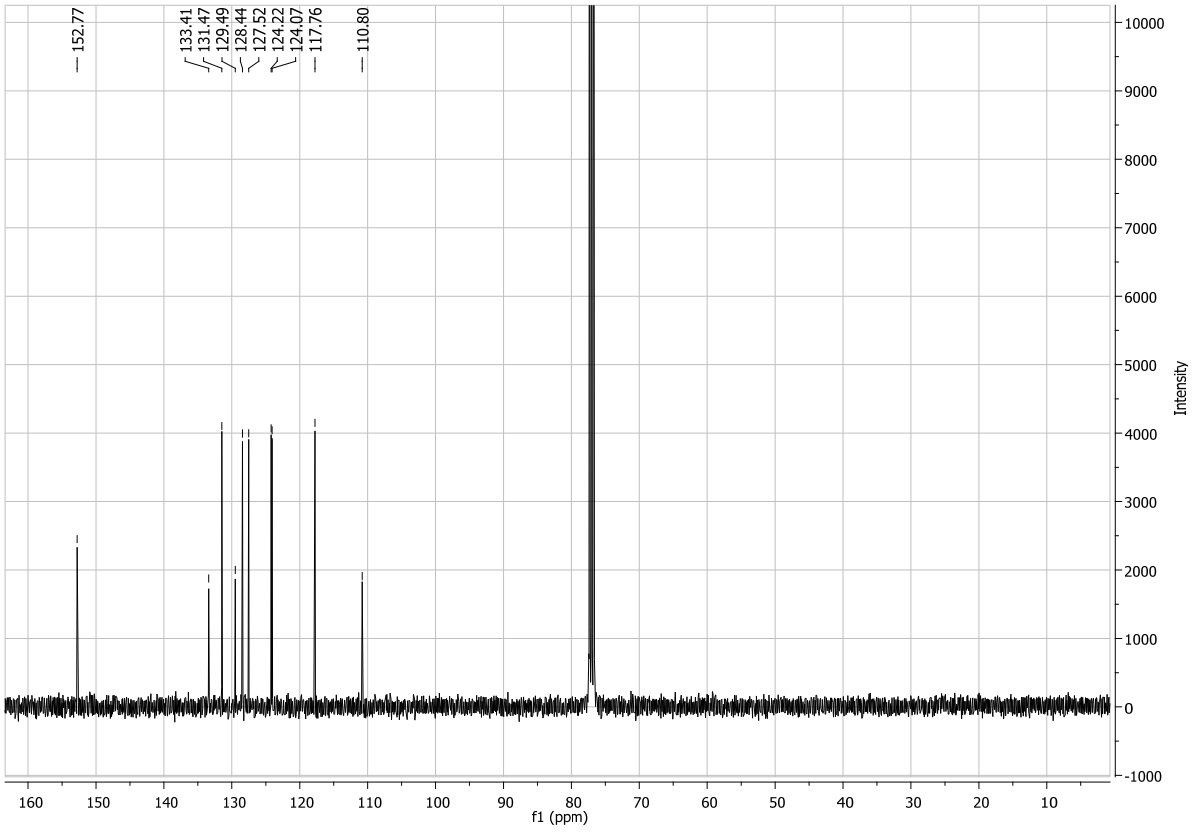
152.77
133.41
131.47
129.49
128.44
127.52
124.22
124.07
117.76
110.80
f1 (ppm)
Intensity

(*R*, *R*) and (*S*, *S*) - 2,2'-dihidroxy-1,1'-bi-naphthol (129)[13]

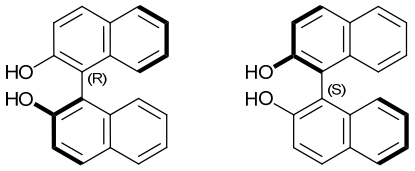

To a solution of **133** (2.51 g, 22.0 mmol) in toluene (60 mL) kept at RT, was added racemic binol (5.73 g, 20.0 mmol). The resulting slurry was stirred at RT for 30 minutes, then warmed to 100 °C for 10-15 minutes before cooling it to RT over a two hour period. During this period, a solid precipitates out as white needles. The precipitate was collected by filtration, washed with toluene (20 mL) and dried *in vacuo* to yield a (*R*, *R*)-binol-(*R, R*)-*trans*-diaminocyclohexane toluene inclusion complex (4.7 g, 95 %). The filtrate contained the (*S*)-enantiomer of binol.

The (*R,R*)-binol-(*R,R*)-*trans*-diaminocyclohexane toluene inclusion complex (4.10 g, 8.30 mmol) was dissolved in a water/MeOH mixture (9 mL/80 mL) and L-(+)-tartaric acid (1.38 g, 9.20 mmol) was added; the mixture was then refluxed overnight. After cooling to RT, a precipitate formed, which was collected by filtration, washed with MeOH (20 mL) and oven dried at 100 °C. Water (30 mL) was added to the mother liquor and MeOH was then evaporated under reduced pressure. Once most of the MeOH was evaporated, (*R, R*)-**129** (1.5 g, 26 %) precipitated out as a colurless crystalline solid and was collected by filtration.

The mother liquor recovered after filtering the (*R,R*)-binol-(*R,R*)-*trans*-diaminocyclohexane·toluene inclusion complex was evaporated under reduced pressure, giving a yellow resin. This was then dissolved in a water/MeOH mixture (1 mL/9 mL), to which L-(+)-tartaric acid was added (1.1 eq. with respect to the amount of diamine) and heated at reflux for 16 hours. Upon cooling, the (*R, R*)- cyclohexane diamine-tartrate salt precipitated and was collected by filtration, washed with MeOH (2 x 10 mL) and oven dried at 100 °C. The mother liquors were poured into water (30 mL) and the MeOH evaporated under reduced pressure until precipitation of a yellow solid occurred. The solid was filtered, washed with water and dried *in vacuo* to yield (*S, S*)-**129** (2.4 g, 41 %) as a yellow crystalline material.

mp 204-212 °C, lit.[15] 211-212° C; $[\alpha]^{25}_{D}$ = 34.5 (c = 1, THF), (*R*, *R* isomer), lit.[16] 35.5 (c = 1, THF), $[\alpha]^{25}_{D}$ = 34.5 (c = 1, THF), lit.[16] 35.0 (c = 1, THF), (*S*,*S* isomer); IR (neat, ν_{max}/cm^{-1}): 3500, 1616, 1593, 1510, 1350 ; ^{1}H-NMR (400 MHz, δ-$CDCl_3$): 5.06 (2H, s, O*H*), 7.19 (2H, d, J_1 = 8.4 Hz, Ar*H*), 7.28-7.30 (1H, m Ar*H*), 7.34 (2H, t, J_1 = 7.5 Hz, Ar*H*), 7.38-7.44 (4H, m, Ar*H*), 7.93 (2H, d, J_1 = 8.3 Hz, Ar*H*), 8.02 (2H, d, J_1 = 8.9 Hz, ArH); ^{13}C-NMR (100.2 MHz, δ-$CDCl_3$): 110.8, 117.7, 124.0, 124.2, 127.5, 128.4, 129.4, 131.4, 133.4, 152.7; *m/ z* (ESI): 285.7.

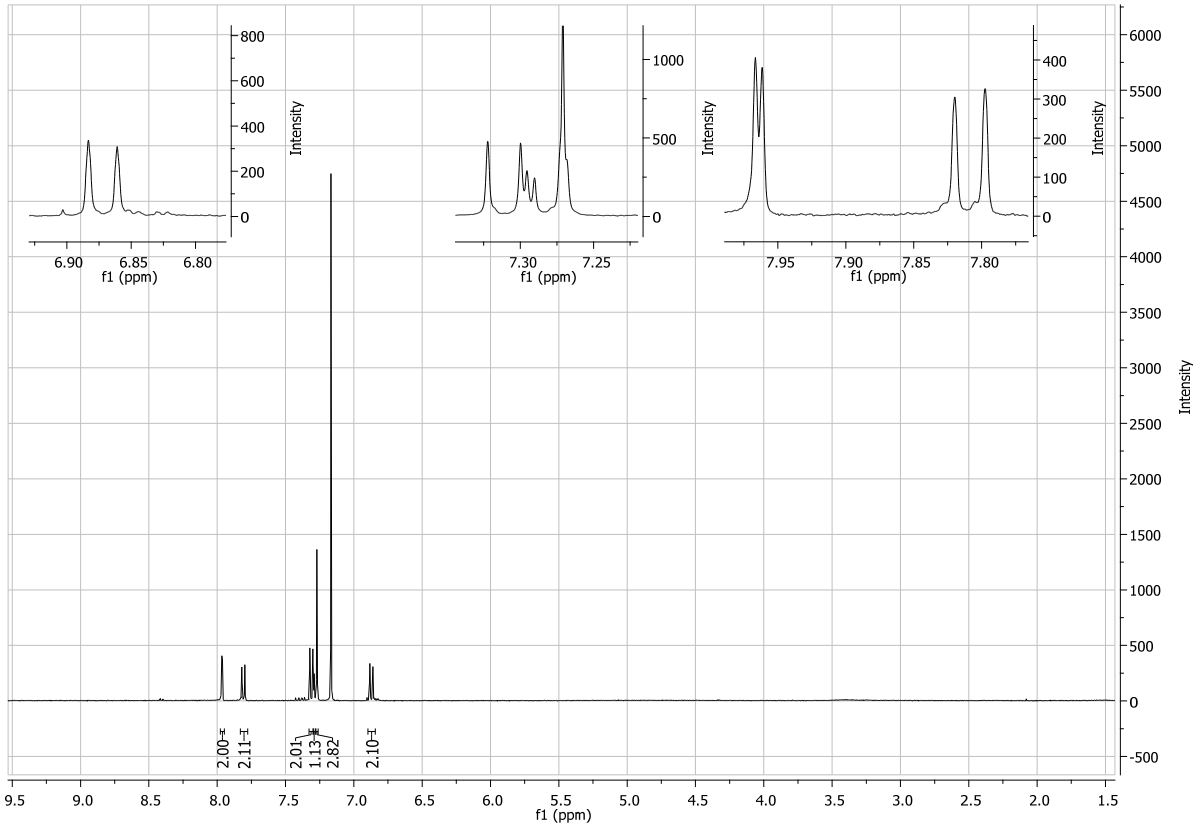
f1 (ppm)
Intensity
2.00
2.11
2.01
1.13
2.82
2.10

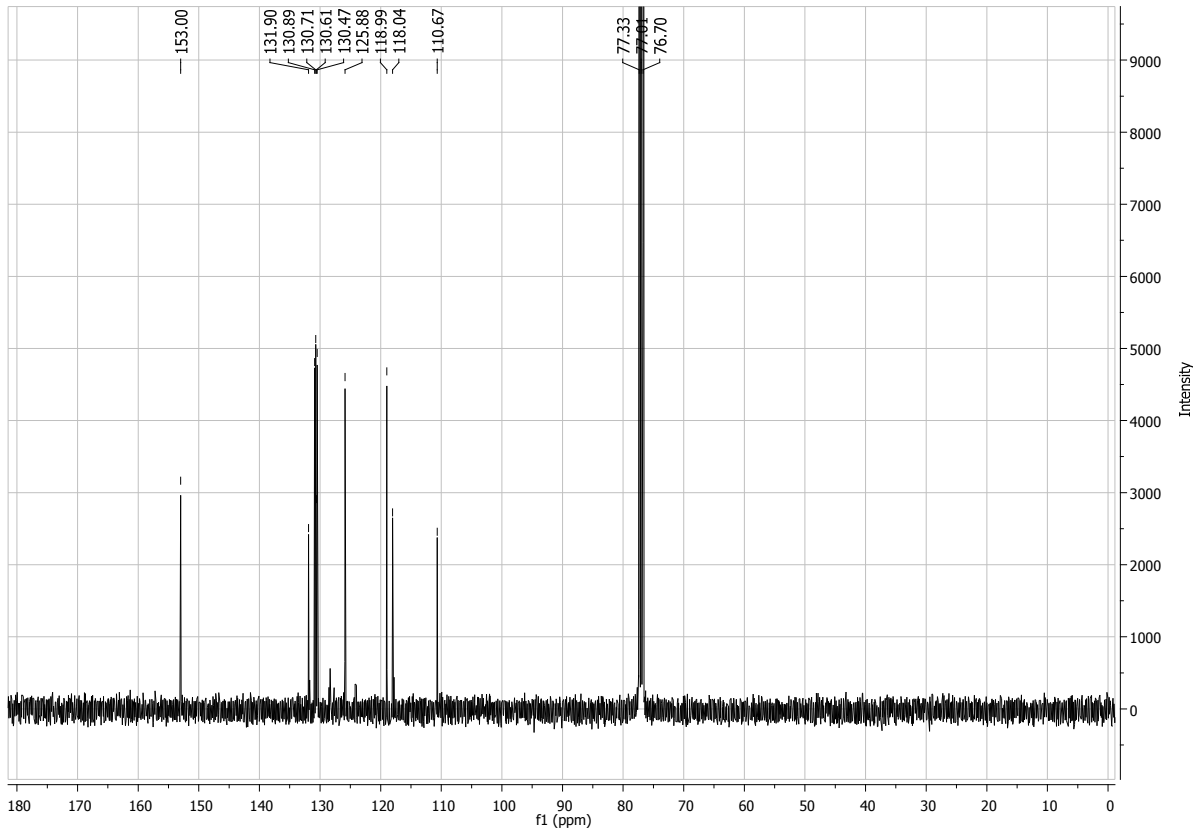
153.00
131.90
130.89
130.71
130.61
130.47
125.88
118.99
118.04
110.67
77.33
77.01
76.70
f1 (ppm)
Intensity

6,6'-dibromo-2,2'-dihidroxy-1,1'-bi-naphthol (130)[17]

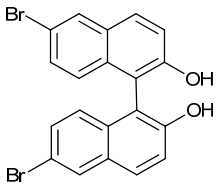

To a stirred solution of *rac*-binol (3.00 g, 10.4 mmol) in DCM, at -78 °C under a nitrogen atmosphere, was added bromine (1.50 mL, 27.9 mol) dropwise over a period of 30 minutes. The mixture was then allowed to stir for a further three hours at -78 °C. The reaction was monitored by TLC (DCM/MeOH 9:1) until the reaction was considered complete. The excess of bromine was neutralized by addition of a 50% solution of sodium bisulfate. The organic phase was then separated and washed with saturated aqueous NaCl and dried over $MgSO_4$. After removal of the solvent under reduced pressure, **130** (1.5 g, 36 %) was recrystallised from benzene/cyclohexane. The same procedure was used to obtain the **(*R*)-130** and **(*S*)-130** starting from the respective enantiopure **129**.

mp 200-206 °C, lit.[17] 208 °C; $[\alpha]^{25}_{D}$ = -116.9 (c = 1, DCM, (*R*)-isomer), 101.3 ((*S*)-isomer) (lit.[18]-129, c = 1, DCM, (*R*)-isomer); IR (neat, ν_{max}/cm^{-1}): 3490, 1612, 1589, 1496, 1350; ^{1}H-NMR (400 MHz, δ-$CDCl_3$): 6.87 (2H, dd, J_1 = 8.9 Hz, Ar*H*), 7.26-7.27 (3H, m, Ar*H*), 7.29 (1H, d, J_1 = 2.1 Hz, Ar*H*), 7.31 (2H, d, J_1 = 8.9 Hz, Ar*H*), 7.81 (2H, d, J_1 = 8.9 Hz, Ar*H*), 7.96 (2H, d, J_1 = 2.0 Hz, Ar*H*); ^{13}C-NMR (100.2 MHz, δ-$CDCl_3$): 110.6, 118.0, 118.9, 125.8, 130.4, 130.6, 130.7, 130.8, 131.9, 153.0; *m/z* (ESI-^{79}Br): 444.9 $(M+H)^+$; HRMS (ESI-^{79}Br): [$C_{20}H_{12}Br_2O_2$] requires 441.9199 found 441.9192.

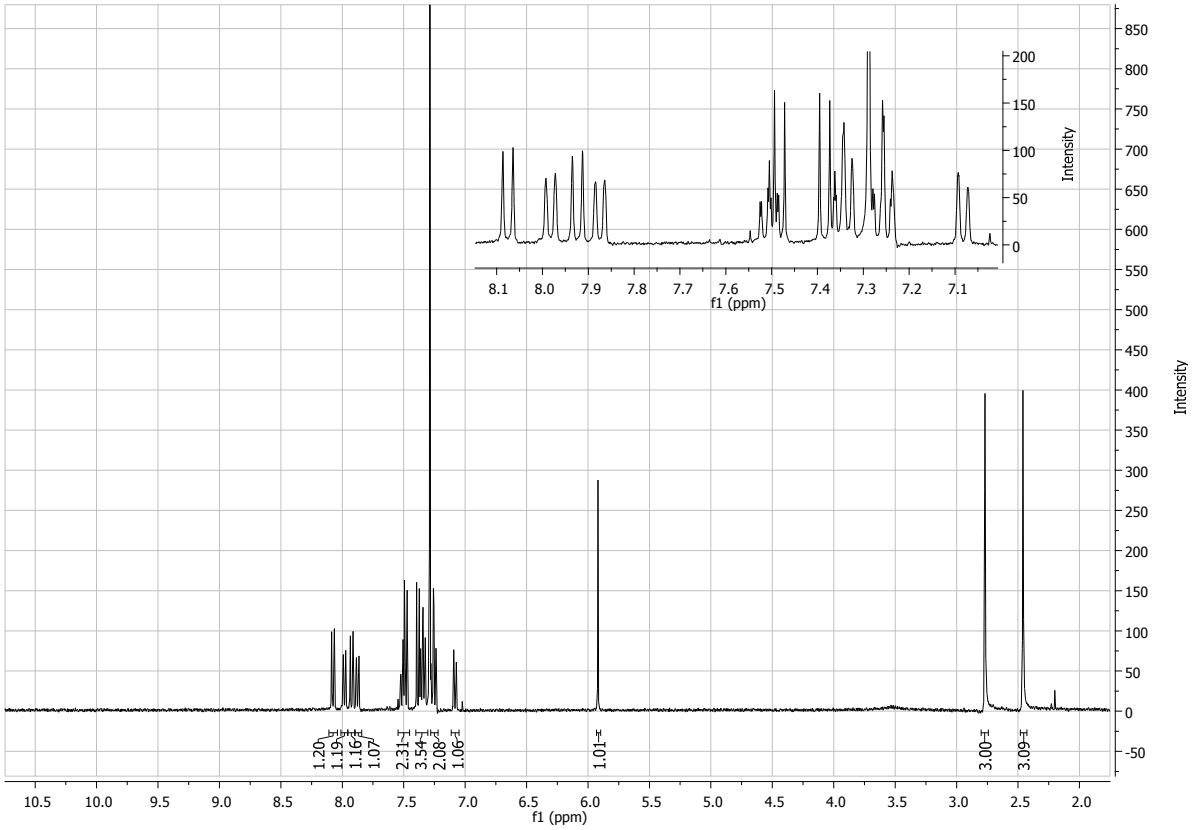
1.20
1.19
1.16
1.07
2.31
3.54
2.08
1.06
1.01
3.00
3.09
f1 (ppm)
Intensity

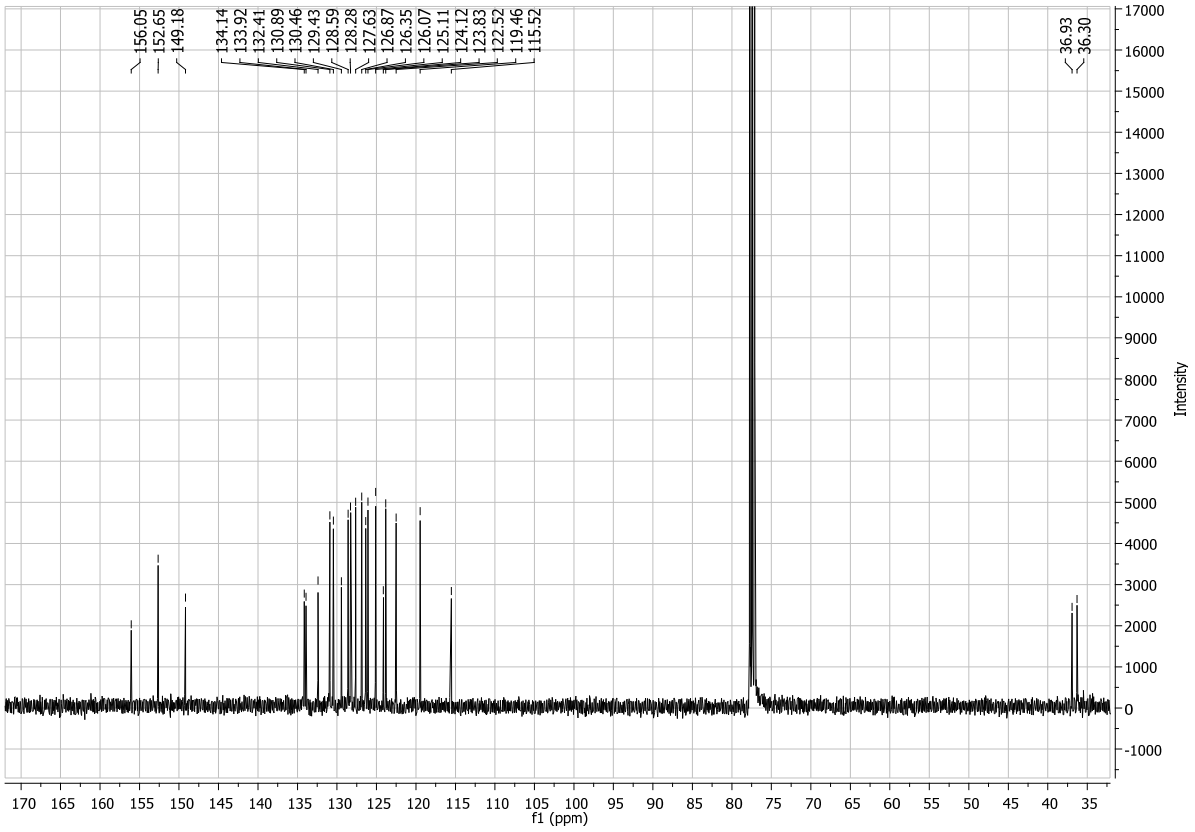
156.05
152.65
149.18
134.14
133.92
132.41
130.89
130.46
129.43
128.59
128.28
127.63
126.87
126.35
126.07
125.11
124.12
123.83
122.52
119.46
115.52
36.93
36.30
f1 (ppm)
Intensity

(*R*)-2'-Hydroxy-1,1'-binaphthyl-2-yl dimethylcarbamate ((*R*)-134)[19]

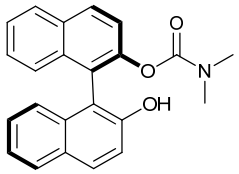

A stirred solution of **(*R*)-129** (1.0 g, 3.5 mmol) in DCM (50 mL) kept under a nitrogen athmosphere, was added with triethylamine (0.56 mL, 4.0 mmol) and *N,N'*-dimethylamino pyridine (DMAP, 42.8 mg, 0.350 mmol). After stirring for five minutes, *N,N'*-dimethylcarbamyl chloride (0.39 mL, 4.2 mmol) was added in a single portion and the reaction left stirring at RT overnight. The endpoint of the reaction was determined *via* TLC (Et_2O/petroleum spirit 40°/60° 1:1) after 18 hours. Saturated NH_4Cl (50 mL) was then added to the mixture and left stirring for a further 20 minutes, after which the organic layer was separated and washed with dilute ammonia (20 mL) to remove the excess of *N,N'*-dimethylcarbamyl chloride; an acidic wash (2 x 20 mL HCl 2N) followed. The organic phase was finally washed with water and brine and dried over $MgSO_4$. Evaporation of the solvent under reduced pressure gave **(*R*)-134** (980 mg, 77 %) as yellow powder. Further purification was performed *via* flash chromatography on silica gel (Et_2O/ petroleum spirit 1:1).

mp 206 °C, lit.[19] 204 °C; $[\alpha]^{25}_D$ = 175 (c = 5, $CHCl_3$) (lit.[19] 154, c = 5, $CHCl_3$); IR (neat, ν_{max}/cm^{-1}): 3500, 2923, 2852, 1701, 1460, 1377; ^{1}H-NMR (400MHz, δ-$CDCl_3$): 2.46 (3H, s, C*H*$_3$), 2.77 (3H, s, C*H*$_3$), 5.92 (1H, s, O*H*), 7.08 (1H, d, J_1 = 8.4 Hz, Ar*H*), 7.20-7.27 (2H, m, Ar*H*), 7.30-7.40 (3H, m, Ar*H*), 7.41-7.53 (2H, m, Ar*H*), 7.87 (1H, d, J_1 = 8.0 Hz, Ar*H*), 7.92 (1H, d, J_1 = 8.8 Hz, Ar*H*), 7.98 (1H, d, J_1 = 8.2 Hz, Ar*H*), 8.07 (1H, d, J_1 = 8.8 Hz, Ar*H*); ^{13}C-NMR (100.2 MHz, δ-$CDCl_3$): 36.3, 36.9, 115.5, 119.4, 122.5, 123.8, 124.1, 125.1, 126.0, 126.3, 126.8, 127.6, 128.2, 128.5, 129.4, 130.4, 130.8, 132.4, 133.9, 134.1, 149.1, 152.6, 156.0; *m/z* (ESI): 358.1 $(M+H)^+$; HRMS (ESI): $[C_{23}H_{19}NO_3+H]^+$ requires 358.1438 found 358.1440.

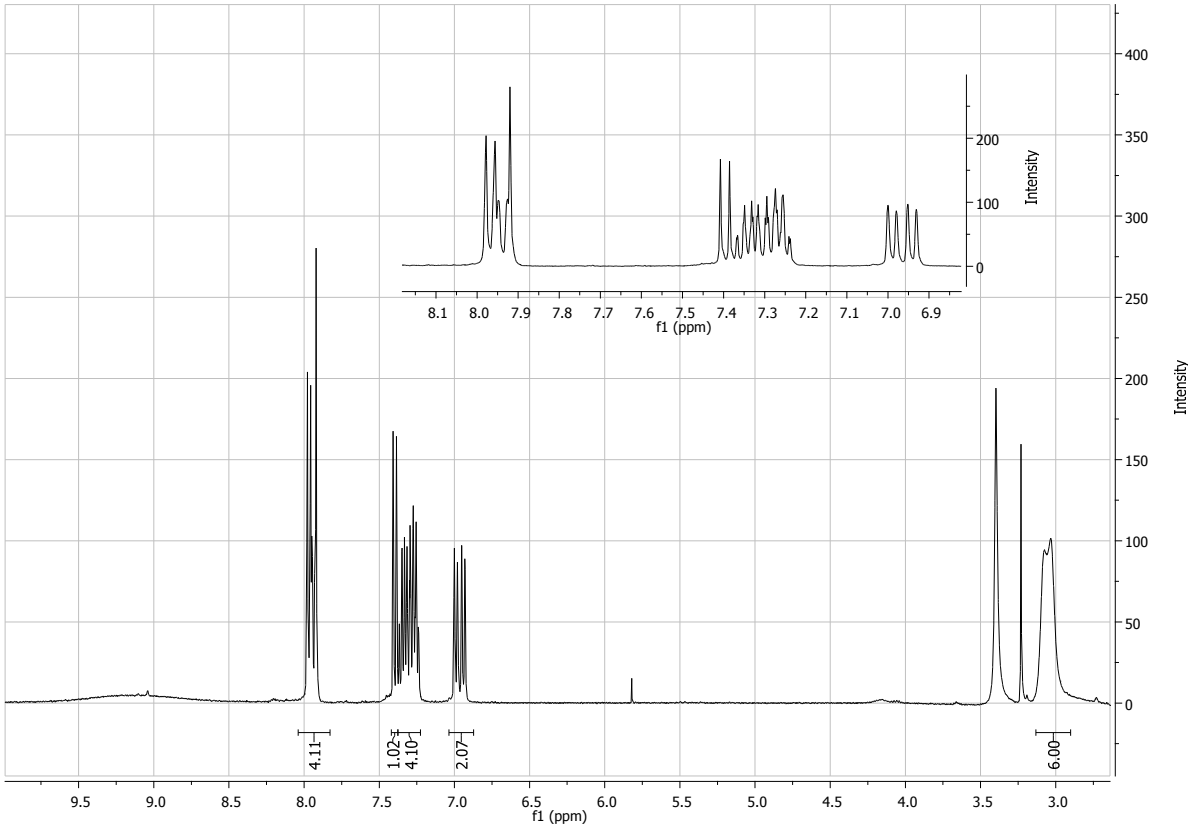
4.11
1.02
4.10
2.07
6.00
f1 (ppm)
Intensity

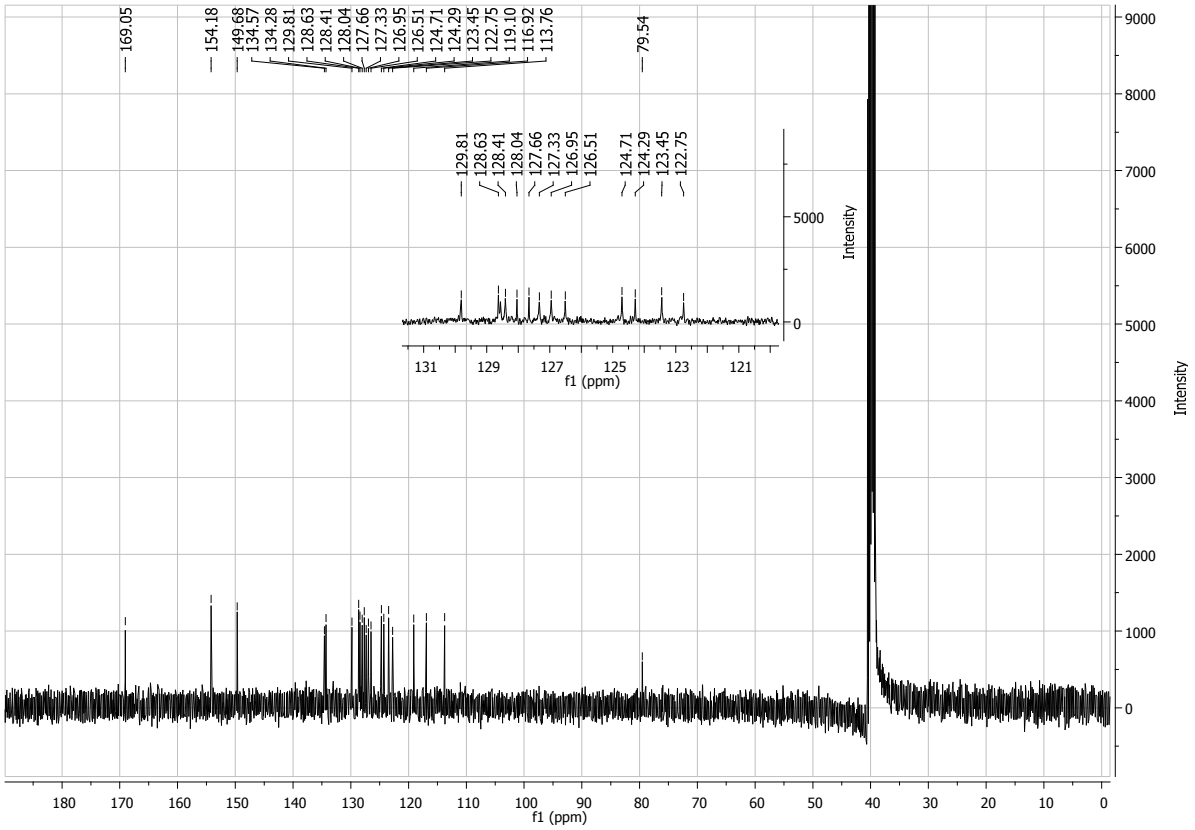
169.05
154.18
149.68
134.57
134.28
129.81
128.63
128.41
128.04
127.66
127.33
126.95
126.51
124.71
124.29
123.45
122.75
119.10
116.92
113.76
79.54
f1 (ppm)
Intensity

(*R*)-2,2'-Dihydroxy-N,N-dimethyl-1,1'-binaphthyl-3-carboxamide ((*R*)-131)[19]

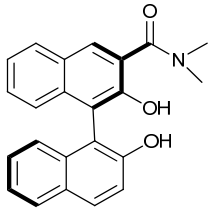

A solution of **(*R*)-134** (590 mg, 1.65 mmol) and TMEDA (383 mg, 3.30 mmol, dried over 4 Å molecular sieves) in dry THF (40 mL) was cooled down to -100 °C under a nitrogen atmosphere, then ^{sec}-BuLi (2.60 mL, 3.60 mmol, from 1.4 M solution) was added dropwise, carefully keeping the temperature below -100 °C and stirred for further 30 minutes after the addition was completed. The solution was then allowed to slowly warm to RT overnight. Once the reaction was complete (TLC petroleum ether/Et_2O), the mixture was treated with saturated NH_4Cl (50 mL) and extracted into DCM (4 x 25 mL). Evaporation of the solvent gave **(*R*)-131** (250 mg, 42 %) as a yellow solid. Further purification was obtained by recrystallisation from MeOH/H_2O.

mp 264.7-265.2 °C, lit.[19] 262-264 °C; $[\alpha]^{25}_D$ = 139 (c = 2, DMSO-d_6), (lit.[19] 137); IR (neat, ν_{max}/cm^{-1}): 3514, 3190, 2923, 2953, 2853, 1612, 1456; ^{1}H-NMR (400 MHz, δ-DMSO-d): 2.85 (6H, s, N(C*H*$_3$)$_2$), 6.97 (2H, dd, J_1 = 19.4 Hz, J_2 = 8.3 Hz, Ar*H*), 7.22-7.37 (4H, m, Ar*H*), 7.40 (1H, dd, J_1 = 8.9 Hz, Ar*H*), 7.90-7.99 (4H, m, Ar*H*); ^{13}C-NMR (100.2 MHz, δ-DMSO-d_6): 79.5, 113.7, 116.9, 119.1, 122.7, 123.4, 124.2, 124.7, 126.5, 126.9, 127.3, 127.6 (2 x *C*H), 128.0, 128.4, 128.6, 129.8, 134.2, 134.5, 149.6, 154.1, 169.0; *m/z* (ESI): 358.4 $(M+H)^+$; HRMS (ESI): $[C_{23}H_{19}NO_3+H]^+$ requires 358.1438 found 358.1438.

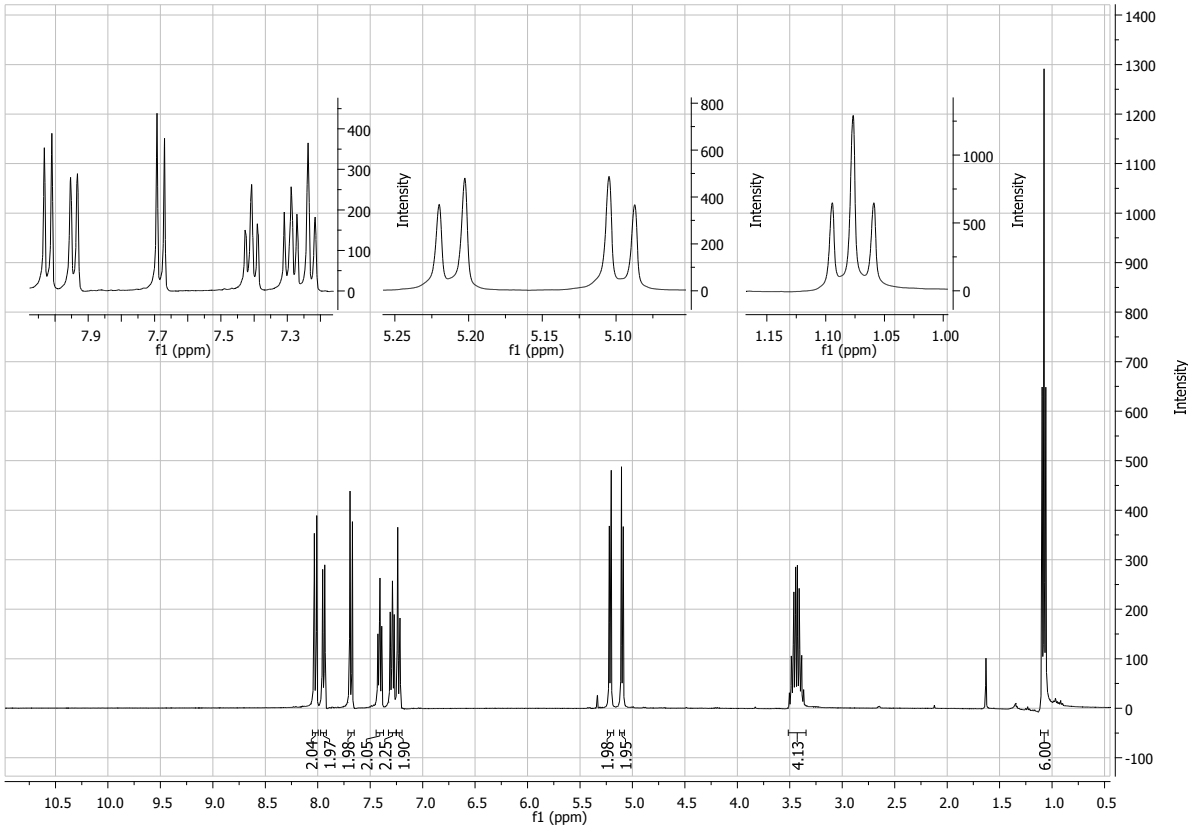
f1 (ppm)
Intensity
2.04
1.97
1.98
2.05
2.25
1.90
1.98
1.95
4.13
6.00

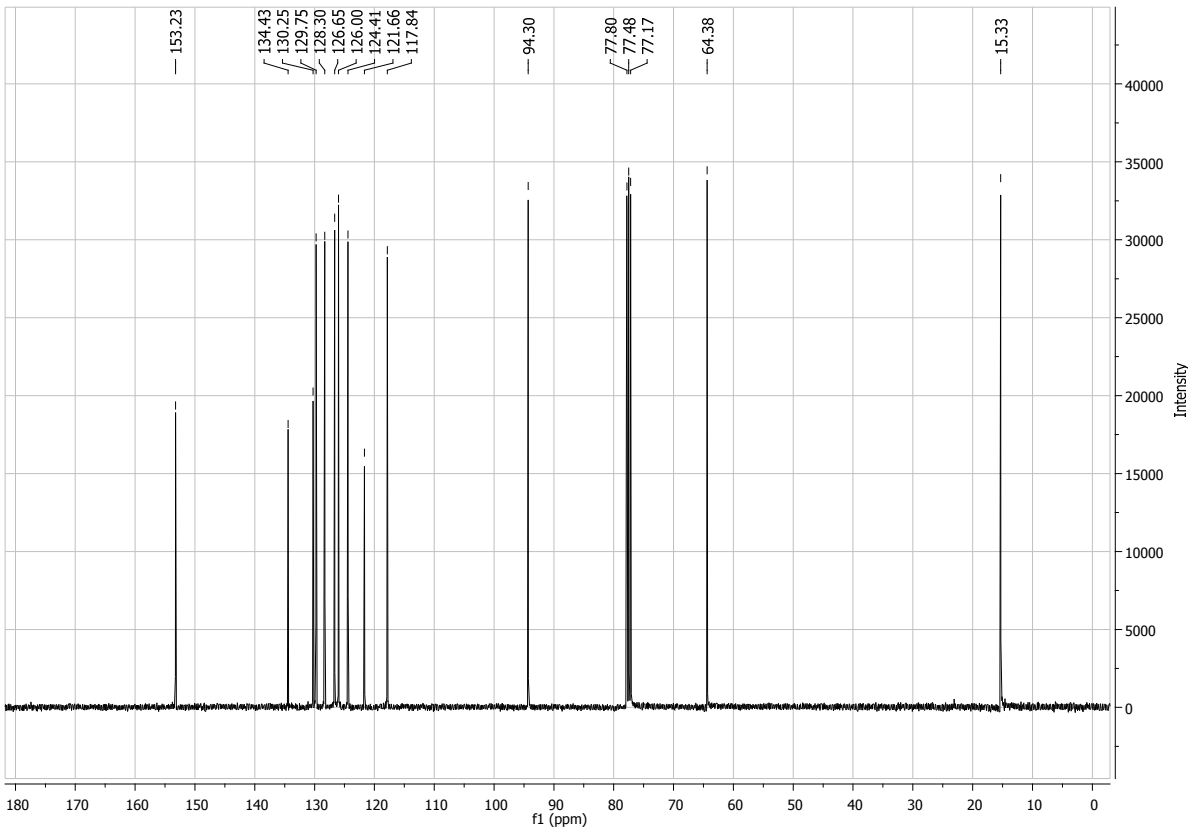
153.23
134.43
130.25
129.75
128.30
126.65
126.00
124.41
121.66
117.84
94.30
77.80
77.48
77.17
64.38
15.33
f1 (ppm)
Intensity

(*S*)-2,2'-Bis(ethoxymethoxy)-1,1'-binaphthyl ((*S*)-135)[20]

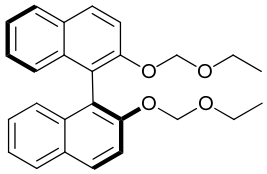

Following a modification of a reported procedure, to a suspension of NaH (410 mg, 17.5 mmol) in dry THF (40 mL) kept at 0 °C with an ice bath and under a nitrogen atmosphere, **(*S*)-129** (1.0 g, 3.5 mmol) was added. The resulting mixture was stirred at 0 °C for 10 minutes then metoxyethyl chloride (650 µL, 7.00 mmol) was added in portions. The reaction mixture was then allowed to warm to RT and left stirring overnight. Quenching was performed by addition of distilled water (20 mL). The organic layer was separated and the mother liquor was extracted with EtOAc (3 x 20 mL). The reunited organic phases were then washed with brine, dried on $MgSO_4$. Evaporation of the solvent under reduced pressure yielded **(*S*)-135** (1.3 g, 93 %) as a yellow resin that was used in the next step without further purification.

$[\alpha]^{25}_D$ = -89.3 (c = 1, THF); IR (neat, ν_{max}/cm^{-1}): 3058, 2976, 2900, 2252, 1504, 1231, 1012; ^{1}H-NMR (400 MHz, δ-$CDCl_3$): 1.08 (6H, t, J_1 = 7.1 Hz, , CH_3), 3.34-3.51 (4H, m, CH_2CH$_3$), 5.10 (2H, d, J_1 = 7.0 Hz, OCH_2O), 5.21 (2H, d, J_1 = 7.0 Hz, OCH_2O), 7.23 (2H, d, J_1 = 8.5 Hz, Ar*H*), 7.25-7.32 (2H, m, Ar*H*), 7.37-7.44 (2H, m, Ar*H*), 7.67 (2H, d, J_1 = 9.0 Hz, Ar*H*), 7.94 (2H, d, J_1 = 8.1 Hz, Ar*H*), 8.02 (2H, d, J_1 = 9.0 Hz, Ar*H*); ^{13}C-NMR (100.2 MHz, δ-$CDCl_3$): 15.3, 64.3, 94.3, 117.8, 121.6, 124.4, 126.0, 126.6, 128.3, 129.7, 130.2, 134.4, 153.2; *m/z* (ESI): 420.2 $(M+NH_4)^+$; HRMS (ESI): $[C_{26}H_{26}O_4+NH_4]^+$ requires 420.2169 found 420.2165.

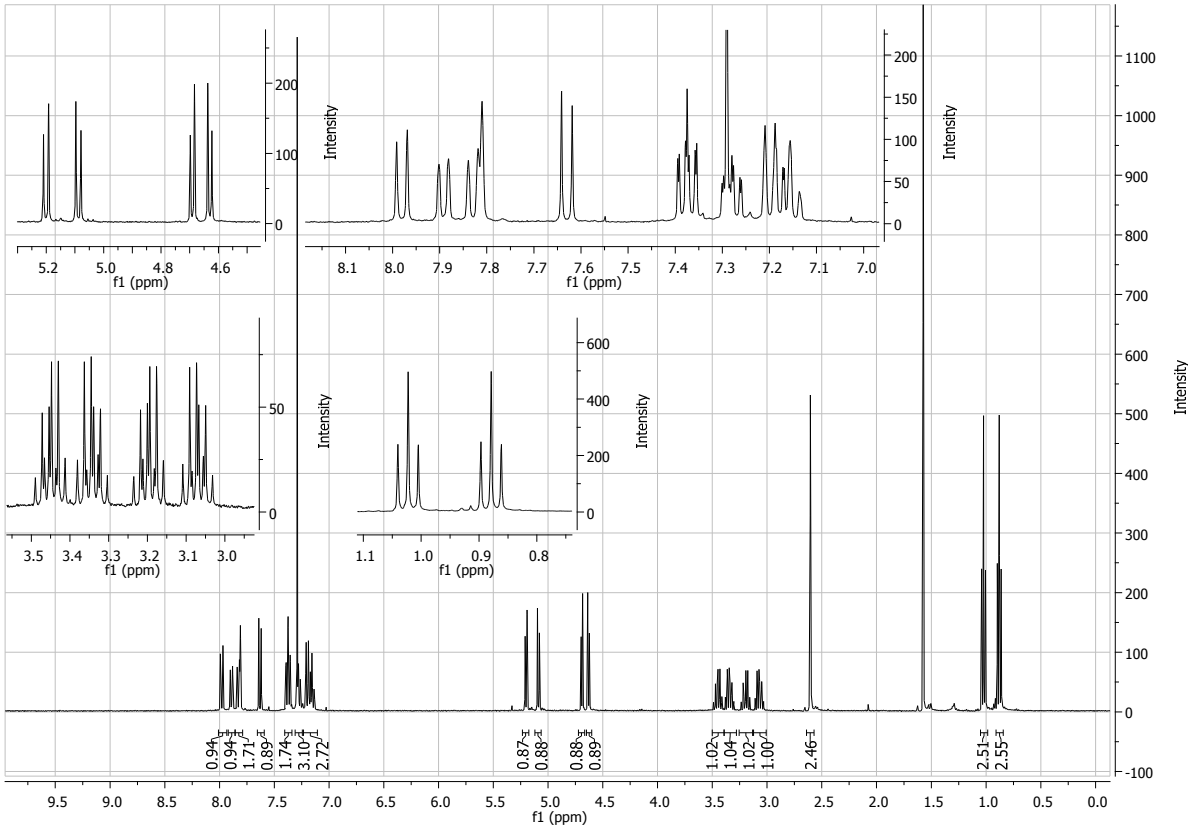
f1 (ppm)
Intensity
0.94
0.94
1.71
0.89
1.74
3.10
2.72
0.87
0.88
0.88
0.89
1.02
1.04
1.02
1.00
2.46
2.51
2.55

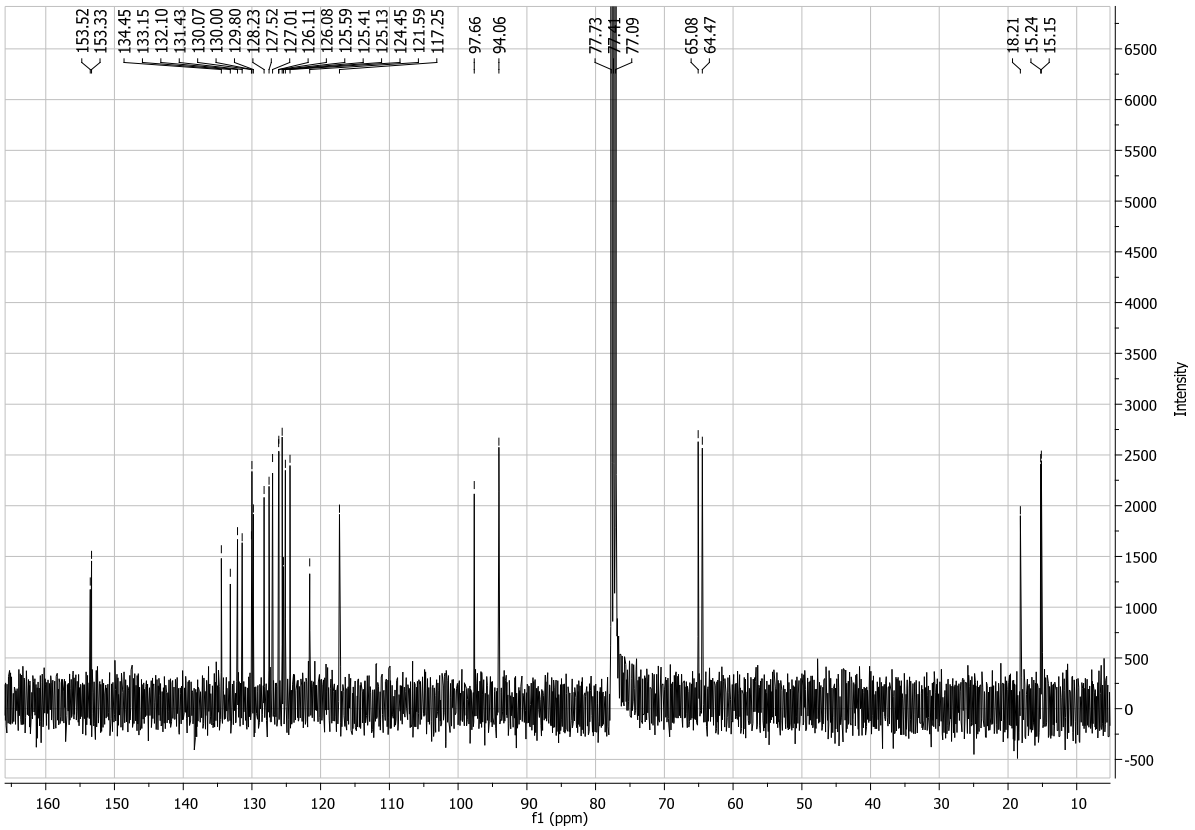
153.52
153.33
134.45
133.15
132.10
131.43
130.07
130.00
129.80
128.23
127.52
127.01
126.11
126.08
125.59
125.41
125.13
124.45
121.59
117.25
97.66
94.06
77.73
77.41
77.09
65.08
64.47
18.21
15.24
15.15
f1 (ppm)
Intensity

(*S*)-2,2'-Bis(ethoxymethoxy)-3-methyl-1,1'-binaphthyl ((S)-136)[21]

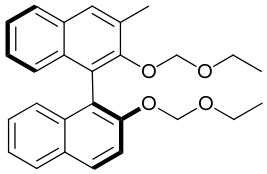

Using the procedure reported by Harada,[21] a stirred solution of **(*S*)-135** (950 mg, 2.36 mmol) in dry THF (50 mL) kept under a nitrogen atmosphere and cooled at -78 °C, *sec*-BuLi (3.00 mL, 4.25 mmol) was added dropwise. After stirring at – 78 °C for further 1.5 hours, iodomethane (265 μL, 4.25 mmol) was carefully added. After the addition, the mixture was allowed to warm up to room temperature and let stirring for one more hour. The endpoint of the reaction was determined via TLC (Hexane/EtOAc). The mixture was then added with saturated aqueous NH_4Cl (30 mL) and the aqueous phase extracted with EtOAc (4 X 25mL). The combined organic phases were washed with brine, dried over $MgSO_4$ and the solvents evaporated under reduced pressure to give **(*S*)-136** (500 mg, 46 %) as a yellow oil. Further purification was obtained *via* flash chromatography on silica gel (Hexane/AcOEt from 99:1 to 90:10).

mp 109 °C; $[\alpha]^{25}_D$ = -82.2 (c = 1, THF); IR (nujol, ν_{max}/cm^{-1}): 2922, 1463, 1377, 1234, 721; ^{1}H-NMR (400 MHz, δ-$CDCl_3$): 0.87 (3H, t, J_1 = 7.1 Hz, CH_2CH_3), 1.02 (3H, t, J_1 = 7.1 Hz, CH_2CH_3), 2.60 (3H, s, CH_3), 3.07 (1H, dq, J_1 = 9.5 Hz, J_2 = 7.1 Hz, CH_2), 3.20 (1H, dq, J_1 = 9.4 Hz, J_2 = 7.1 Hz, CH_2), 3.34 (1H, dq, J_1 = 9.6 Hz, J_2 = 7.1 Hz, CH_2), 3.45 (1H, dq, J_1 = 9.4 Hz, J_2 = 7.1 Hz, CH_2), 4.63 (1H, d, J_1 = 5.7 Hz, OCH_2O), 4.69 (1H, d, J_1 = 5.7 Hz, OCH_2O), 5.09 (1H, d, J_1 = 7.1 Hz, OCH_2O), 5.20 (1H, d, J_1 = 7.1 Hz, OCH_2O), 7.11-7.22 (3H, m, Ar*H*), 7.24-7.30 (3H, m, Ar*H*), 7.37 (2H, ddd, J_1 = 8.1 Hz, J_2 = 6.6 Hz, J_3 = 1.4 Hz, Ar*H*), 7.63 (1H, d, J_1 = 9.1 Hz, Ar*H*), 7.79-7.84 (2H, m, Ar*H*), 7.89 (1H, d, J_1 = 9.1 Hz, Ar*H*), 7.98 (1H, d, J_1 = 9.1 Hz, Ar*H*); ^{13}C-NMR (100.2 MHz, δ-$CDCl_3$): 15.1, 15.2, 18.2, 64.4, 65.0, 94.0, 97.6, 117.2, 121.5, 124.4, 125.1, 125.4, 125.5, 126.0, 126.1, 127.0, 127.5, 128.2, 129.8, 130.0, 130.07, 131.4, 132.1, 133.1, 134.4, 153.3, 153.5; *m/z* (ESI): 417.2 $(M+H)^+$; HRMS (ESI): $[C_{27}H_{28}O_4]$ requires 416.1982 found 416.1981.

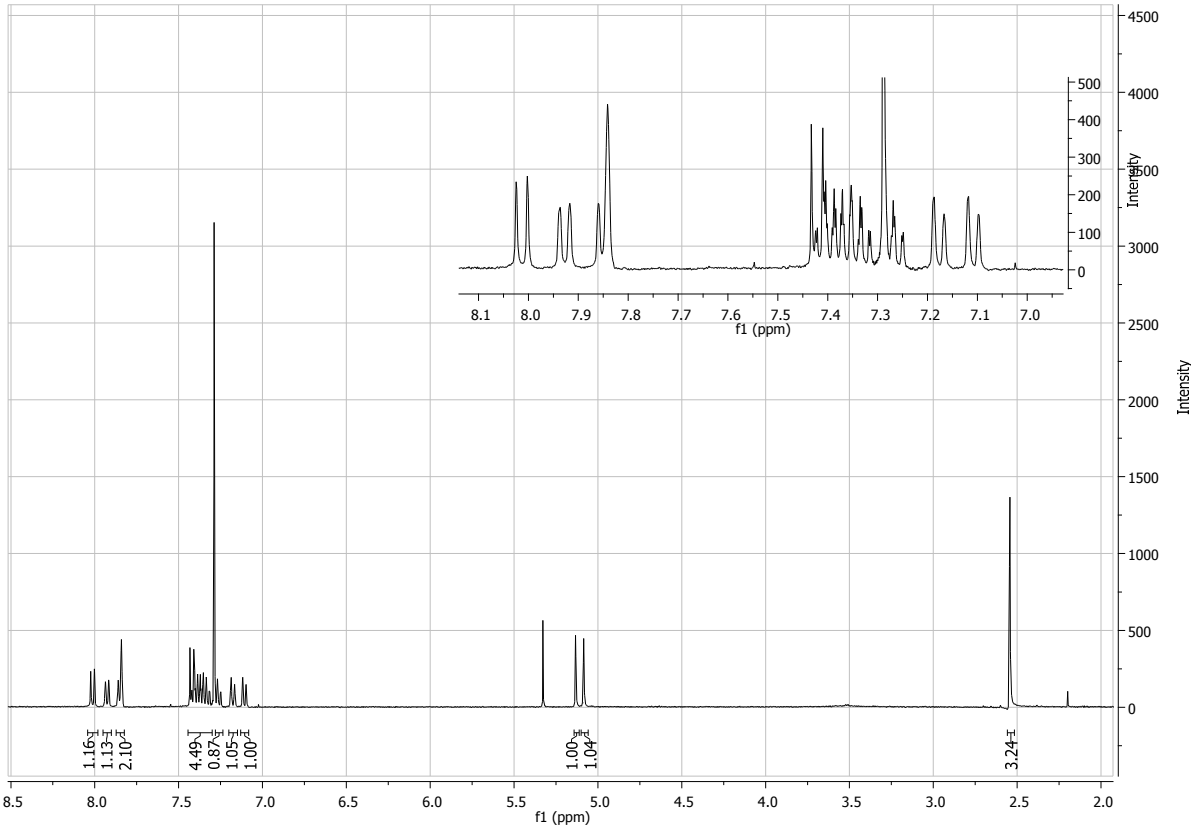
1.16
1.13
2.10
4.49
0.87
1.05
1.00
1.00
1.04
3.24
f1 (ppm)
Intensity

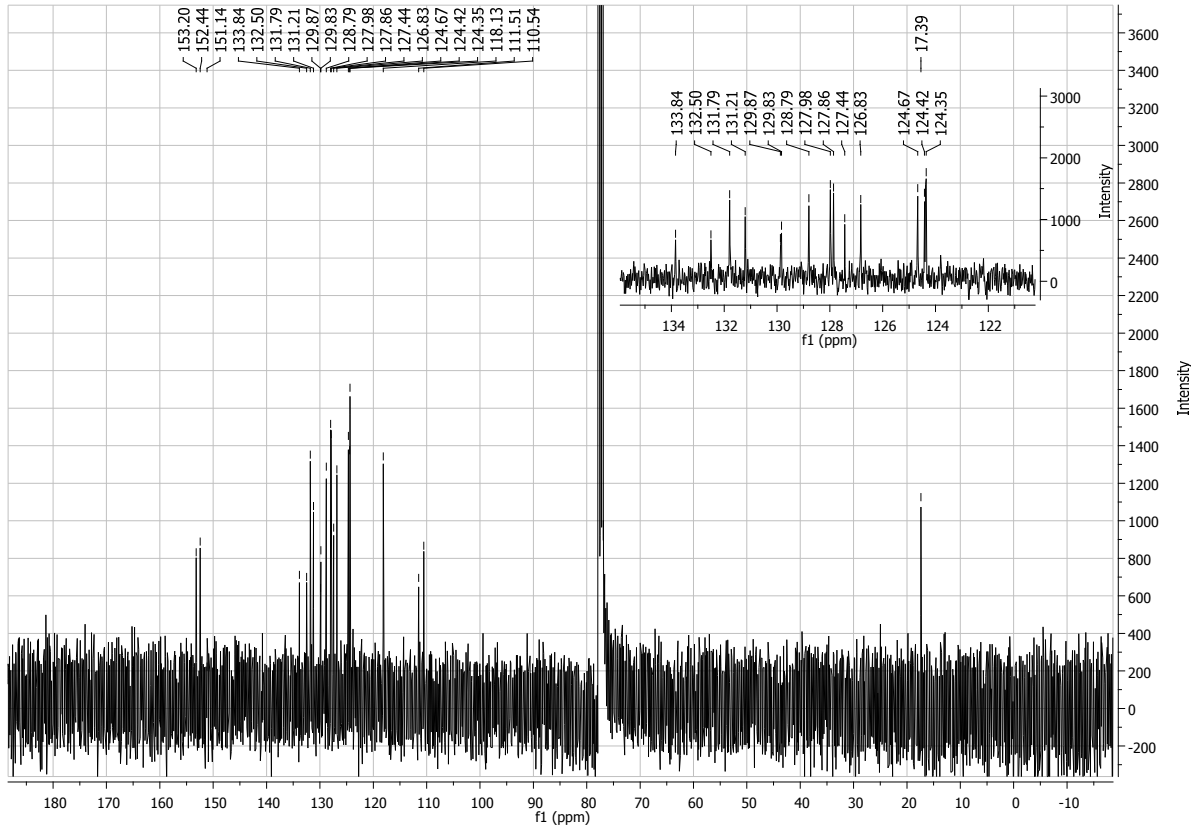
153.20
152.44
151.14
133.84
132.50
131.79
131.21
129.87
129.83
128.79
127.98
127.86
127.44
126.83
124.67
124.42
124.35
118.13
111.51
110.54
17.39
f1 (ppm)
Intensity

(*S*)-3-Methyl-1,1'-binaphthyl-2,2'-diol ((*S*)-132)[19]

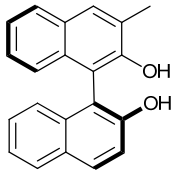

A solution of **(S)-136** (150 mg, 0.360 mmol) in methanol (10 mL) was heated to 60 °C and added with concentrated HCl (5 mL). Heating and stirring were maintained for one hour while the reaction was monitored via TLC (DCM/MeOH 99:1). After complete removal of the protecting group, the solvent was removed under reduced pressure to give **(*S*)-132** (100 mg, 92 %) as a pale yellow powder. The crude material was further purified by flash chromatography on silica gel (DCM/MeOH 99:1).

mp 132 °C, lit.[19] 137 °C; $[\alpha]^{25}_{D}$ = -18.0 (c = 1.5, $CHCl_3$), ((*S*)-isomer) lit.[19] 25.0 ((*R*)-isomer); IR (neat, ν_{max}/cm^{-1}): 3501, 2954, 2853, 1463, 1377, 821; ^{1}H-NMR (400MHz, δ-$CDCl_3$): 2.54 (3H, s, C*H*$_3$), 5.08 (1H,s, O*H*), 5.13 (1H, s, O*H*), 7.11 (1H, d, J_1 = 8.0 Hz, Ar*H*), 7.17 (1H, d, J_1 = 7.9 Hz, Ar*H*), 7.24-7.27 (1H, m, Ar*H*), 7.31-7.44 (4H, m, Ar*H*), 7.82-7.87 (2H, m, Ar*H*), 7.93 (1H, d, J_1 = 7.6 Hz, Ar*H*), 8.01 (1H, d, J_1 = 8.9 Hz, Ar*H*); ^{13}C-NMR (100.2 MHz, δ-$CDCl_3$):17.3, 110.5, 111.5, 118.1, 124.35, 124.42, 124.67, 126.8, 127.4, 127.8, 127.9, 128.7, 129.83, 129. 87, 131.2, 131.7, 132.5, 133.8, 152.4, 153.2; *m/z* (ESI): 300.1 (100 %); HRMS (ESI): $[C_{21}H_{16}O_2]^+$ requires 300.1145 found 300.1147.

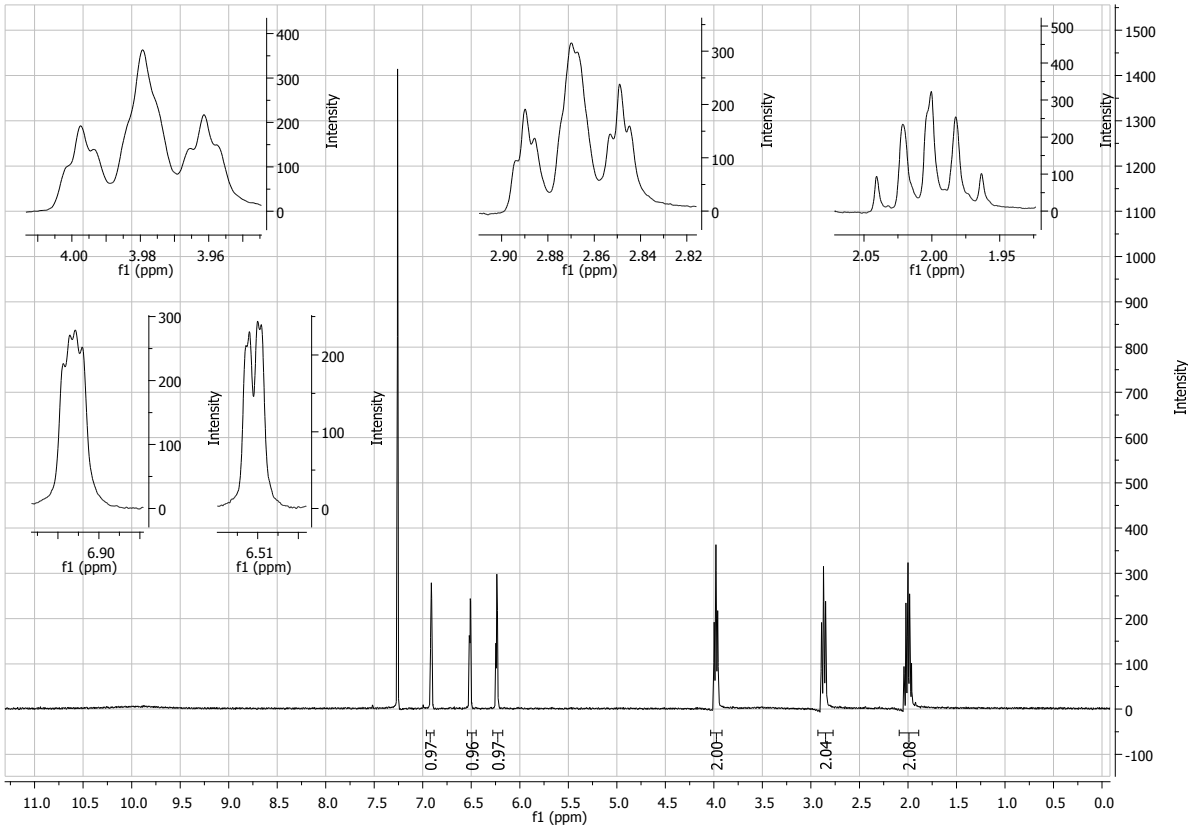
f1 (ppm)
Intensity
0.97
0.96
0.97
2.00
2.04
2.08

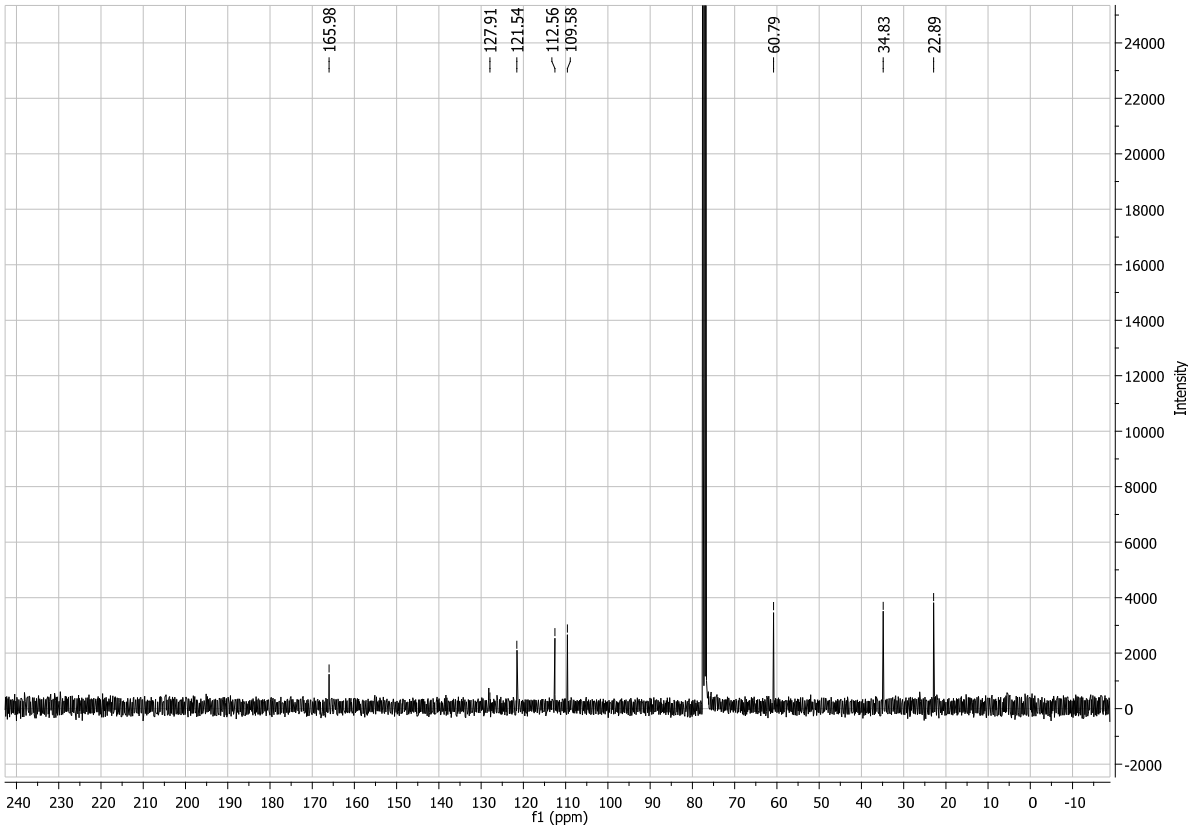
165.98
127.91
121.54
112.56
109.58
60.79
34.83
22.89
f1 (ppm)
Intensity

2-(3,4-dihydro-2H-pyrrol-5-yl)-1H-pyrrole (140)[22, 23]

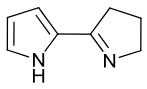

A three necked round bottom flask containing pyrrole (31.2 mL, 450 mmol), was cooled at -10 °C. $POCl_3$ was then added dropwise over a period of an hour. Using the same dropping funnel, pirrolidinone (7.8 mL, 92 mmol) was added dropwise with extreme caution over three hours, keeping the temperature always below 0 °C. After the addition finished, the mixture was allowed to warm up to room temperature and diluted with $CHCl_3$ (50 mL).

The mixture was then transferred into a bigger flask, added with water (200 mL) and sodium acetate (80 g). The pH of the solution was adjusted to 10 by addition of KOH (10 M) and the phases separated.

The aqueous phase was extracted with $CHCl_3$ (3 x 20 mL). The combined organic phases were washed with HCl (0.5 M, 5 x 20 mL). The combined aqueous washing were basified to pH 10 with KOH (10 M) and extracted again with $CHCl_3$ (3 x 20 mL). All the organic phases were then reunited, dried over $MgSO_4$ and the solvents removed under reduced pressure to yield a thik dark brown oil. Purification of the crude was performed using sublimation, which gave **140** (1 g, 8 %) as colourless crystals

IR (neat, ν_{max}/cm^{-1}): 3113, 2961, 2865, 1590, 1434; ^{1}H-NMR (400 MHz, δ-$CDCl_3$): 1.93-2.07 (2H, m, C*H*$_2$), 2.90 (2H, ddd, J_1 = 9.0 Hz, J_2 = 3.3 Hz, J_3 = 1.6 Hz, C*H*$_2$), 3.97-4.03 (2H, m, C*H*$_2$), 6.17-6.32 (1H, m, Ar*H*), 6.54 (1H, dd, J_1 = 3.5 Hz, J_2 = 1.0 Hz, Ar*H*), 6.94 (1H, dd, J_1 = 2.4 Hz, J_2 = 1.3 Hz, Ar*H*); ^{13}C-NMR (100.2 MHz, δ-$CDCl_3$): 22.8, 34.8, 60.7, 109.5, 112.5, 121.5, 127.9, 165.9; *m/z* (ESI): 65.2 (30 %), 93.1 (30), 117.0 (15), 135.0 (100); HRMS (ESI): $[C_8H_{10}N_2+H]^+$ requires 135.0917 found 135.0917.

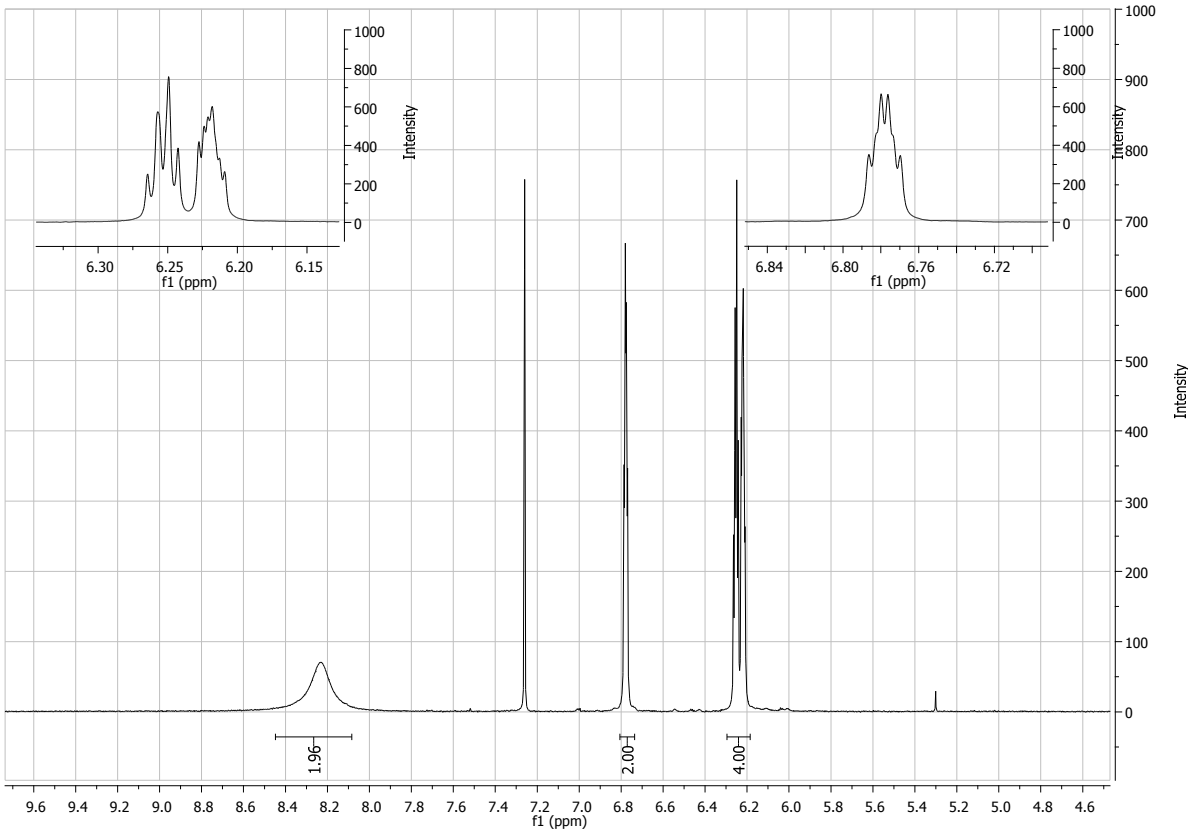
1.96
2.00
4.00
f1 (ppm)
Intensity

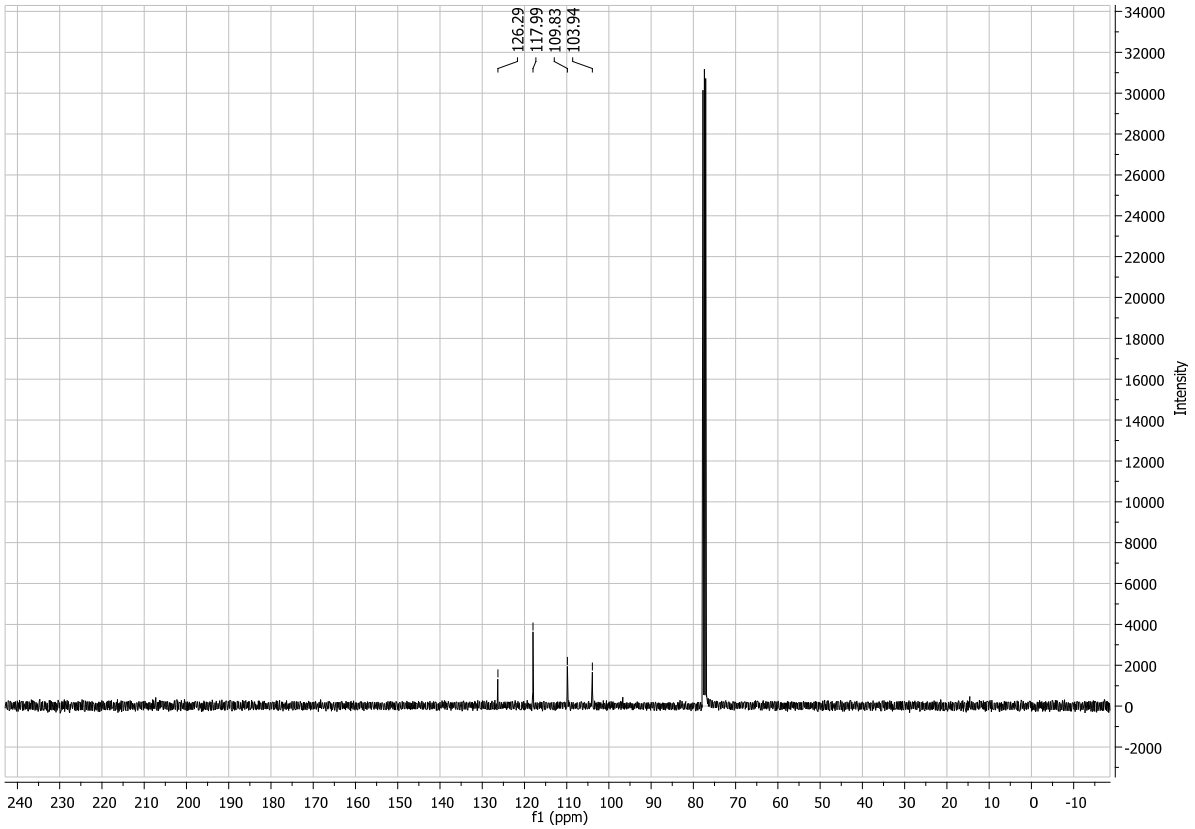
126.29
117.99
109.83
103.94
f1 (ppm)
Intensity

1H,1'H-2,2'-bipyrrole (142)[24]

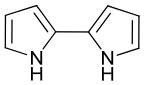

Pyrrole (0.62 mL, 8.9 mmol) was dissolved in dry DCM and the resulting solution cooled to -70 °C under an inert atmosphere. After five minutes stirring at -70 °C, trimethylbromosilane (0.76 mL, 5.8 mmol) and bis(trifluoroacetoxy)iodo]benzene (PIFA, 1.25 g, 2.9 mmol) were added and the reaction was left stirring keeping the temperature below -40 °C. When the temperature stopped increasing, the mixture was allowed to warm up to room temperature, saturated $NaHCO_3$ was added and the reaction was left stirring until no more effervescence was observed. The phases were separated and the organic layer extracted with DCM (3 x 20 mL). All the organic layers were finally reunited, washed with brine and dried over $MgSO_4$. After removal of the solvent under reduced pressure, **142** (259 mg, 66 %) was initially recovered as a yellow solid. Flash chromatography on silica gel (hexane/EtOAc 8:2) gave pure **142** (100 mg, 27 %) as a colourless powder.

IR (neat, ν_{max}/cm^{-1}): 3362, 2952, 2922, 2853, 1575, 1455; ^{1}H-NMR (400 MHz, δ-$CDCl_3$): 6.19-6.28 (4H, m, Ar*H*), 6.76-6.79 (2H, m, Ar*H*), 8.23 (2H, broad s, N*H*); ^{13}C-NMR (100.2 MHz, δ-$CDCl_3$): 103.9, 109.8, 117.9, 126.2.

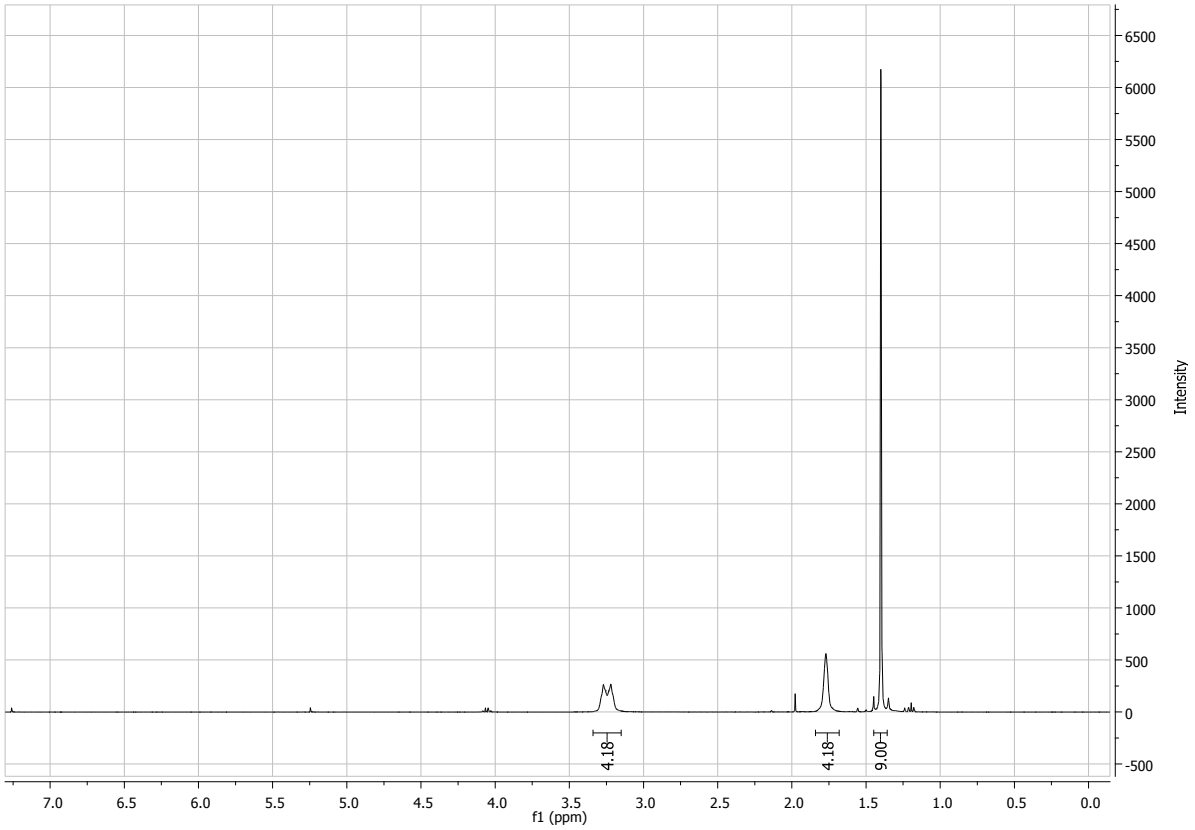
4.18
4.18
9.00
f1 (ppm)
Intensity

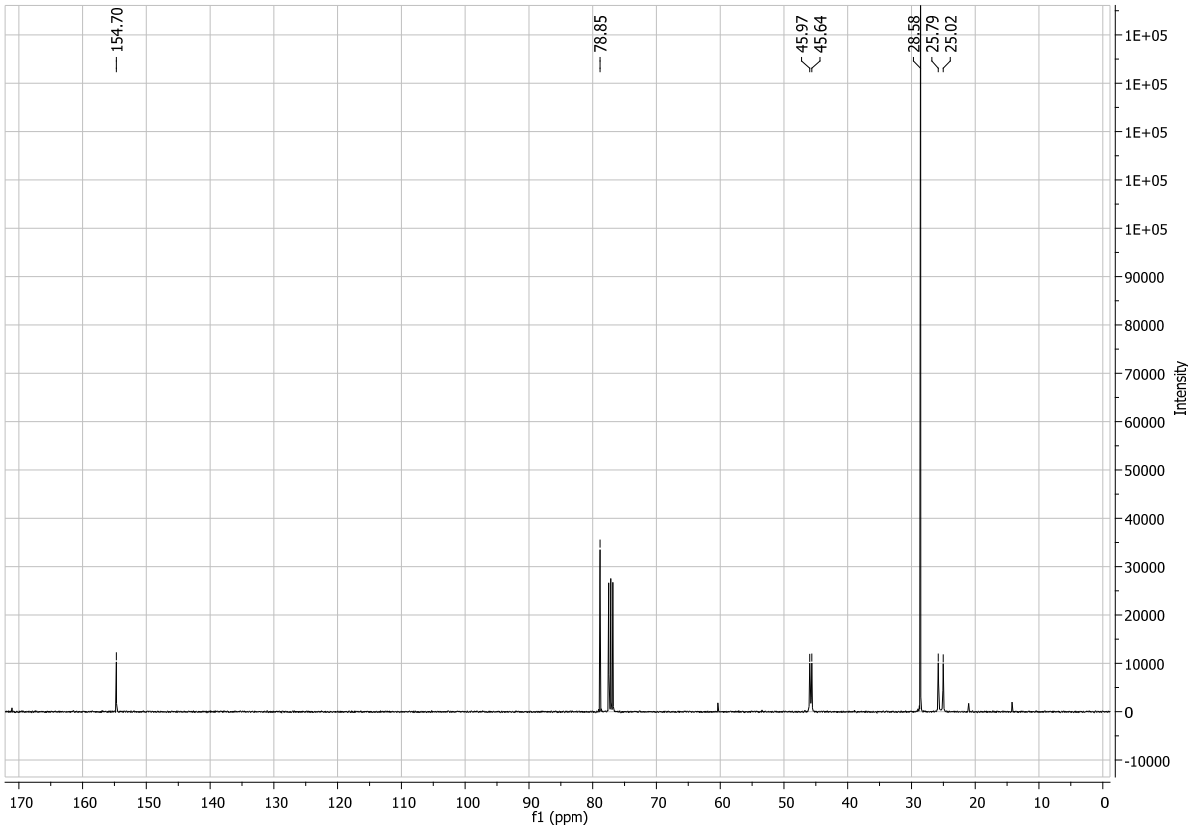
154.70
78.85
45.97
45.64
28.58
25.79
25.02
f1 (ppm)
Intensity

tert-butyl pyrrolidine-1-carboxylate[25]

A solution of di-*tert*-butyl-dicarbonate (23.5 g, 108 mmol) in DCM (50 mL) was added dropwise to a stirred solution of pyrrolidine (10 mL, 0.19 mol) in DCM (60 mL) cooled in an ice bath. After the addition, the mixture was stirred at RT for two hours and monitored *via* TLC (DCM/MeOH 9:1). After the limiting reagent disappeared from the mixture, the organic phase was washed with saturated NH_4Cl and the solvents evaporated at reduced pressure to give pure *N*-Boc-pyrrolidine (17 g, 92 %) as a thick oil.

IR (neat, ν_{max}/cm^{-1}): 2974, 2874, 1697, 1542, 1401, 1168; ^{1}H-NMR (400 MHz, δ-$CDCl_3$): 1.43 (9H, s, (CH_3)$_3$), 1.76-1.86 (4H, m, CH_2CH_2N), 3.21-3.33 (4H, m, CH_2CH_2N); ^{13}C-NMR (100.2 MHz, δ-$CDCl_3$): 25.0, 25.7, 28.5, 45.6, 45.9, 78.8, 154.7.

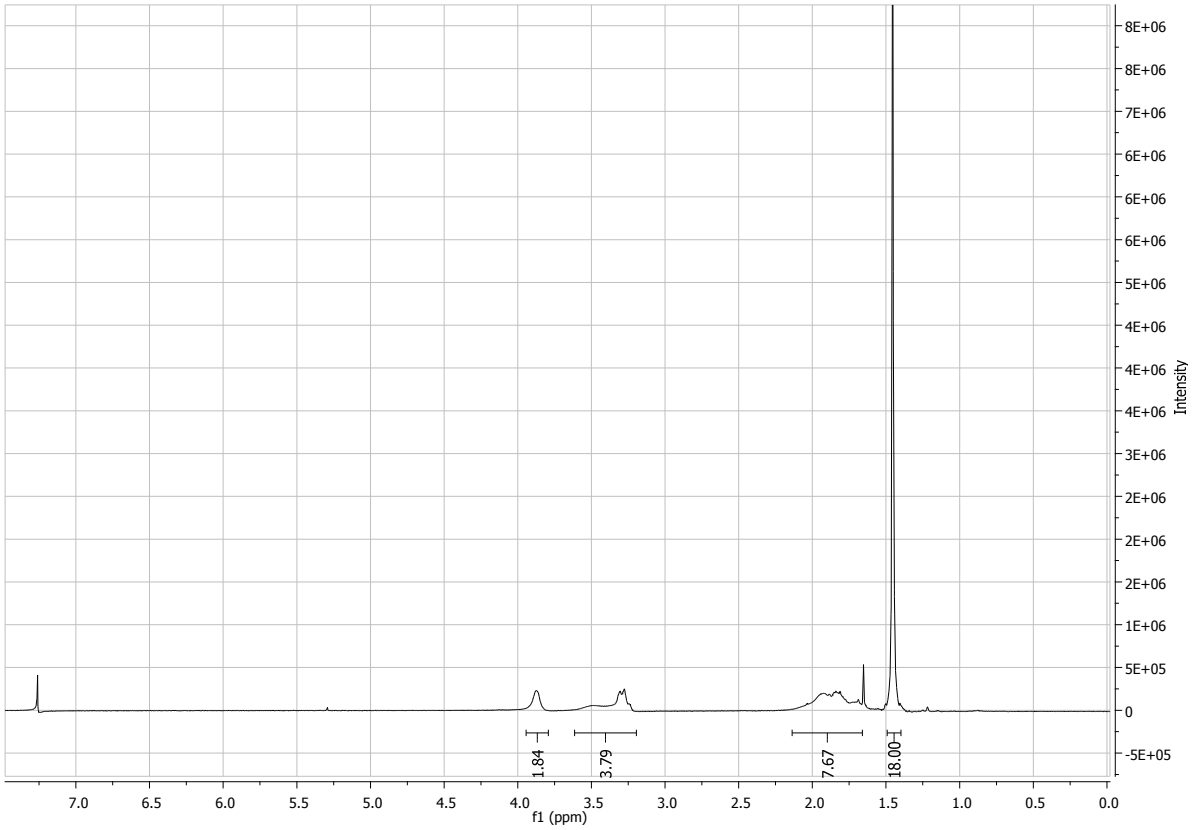
8E+06
8E+06
7E+06
6E+06
6E+06
6E+06
5E+06
4E+06
4E+06
4E+06
3E+06
2E+06
2E+06
2E+06
1E+06
5E+05
0
-5E+05
Intensity
1.84
3.79
7.67
18.00
7.0
6.5
6.0
5.5
5.0
4.5
4.0
3.5
3.0
2.5
2.0
1.5
1.0
0.5
0.0
f1 (ppm)

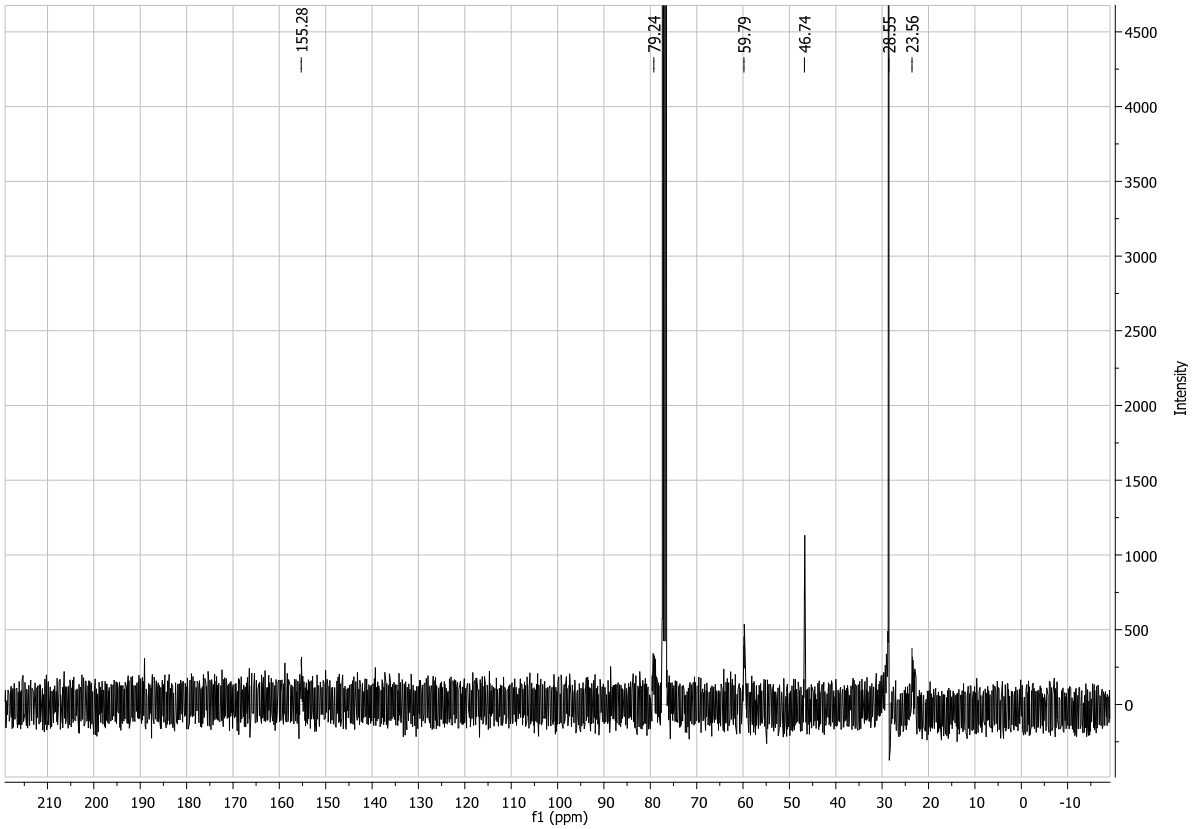
155.28
79.24
59.79
46.74
28.55
23.56
4500
4000
3500
3000
2500
2000
1500
1000
500
0
Intensity
210
200
190
180
170
160
150
140
130
120
110
100
90
80
70
60
50
40
30
20
10
0
-10
f1 (ppm)

di-*tert*-butyl 2,2'-bipyrrolidine-1,1'-dicarboxylate (*dl/meso*-143)[26]

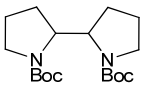

A solution of *N*-Boc-pyrrolidine (7.00 g, 40.9 mmol) and TMEDA (12.3 mL, 81.8 mmol) in dry THF (50 mL) was cooled to -78 °C. Once the temperature was reached, ^{sec}-BuLi was added dropwise never allowing the temperature to exceed -60 °C. In the meantime, solid CuI (3.90 g, 20.4 mmol) and LiCl (1.70 g, 40.9 mmol) were dried *in vacuo* and then dissolved in dry THF (30 mL). The mixture of the two salts was stirred at room temperature until coloured blue and subsequently cooled to -78 °C and added through a cannula to the cooled Boc-pyrrolidine solution. The resulting mixture was then allowed to warm up to -30 °C for 30 minutes and cooled again to -78 °C. A solution of iodine (5.20 g, 20.4 mmol) in dry THF pre-cooled to -78 °C was then added through a cannula again, and the mixture allowed to warm up to -30° C for two hours before it was allowed to return to room temperature. The resulting black mixture was then diluted with diethyl ether (50 mL) and washed with saturated NH_4Cl. The organic phase was separated and the aqueous layer extracted with Et_2O (3 x 20 mL). The crude product was purified *via* flash chromatography on silica gel (hexane/EtOAc 9:1 to 7:3) to yield ***dl/meso*-143** (4.00 g, 46 %) as a yellow oil.

IR (neat, ν_{max}/cm^{-1}): 2980, 2868, 1678, 1511, 1399; ^{1}H-NMR (400 MHz, δ-$CDCl_3$): 1.45 (18H, s, (C*H*$_3$)$_3$), 1.66-2.11 (8H, m, CH$_2$C*H*$_2$CH$_2$CHN, CH$_2$CH$_2$C*H*$_2$CHN), 3.16-3.62 (4H, m, C*H*$_2$N), 3.73-4.02 (2H, m, C*H*N); ^{13}C-NMR (100.2 MHz, δ-$CDCl_3$): 23.5, 28.5, 46.9, 59.7, 79.3, 155.1; *m/z* (ESI): 141.1 (15 %), 185.1 (100), 241.1 (70), 341.2 (90); HRMS (ESI): $[C_{18}H_{32}N_2O_4+H]^+$ requires 341.2435 found 341.2441.

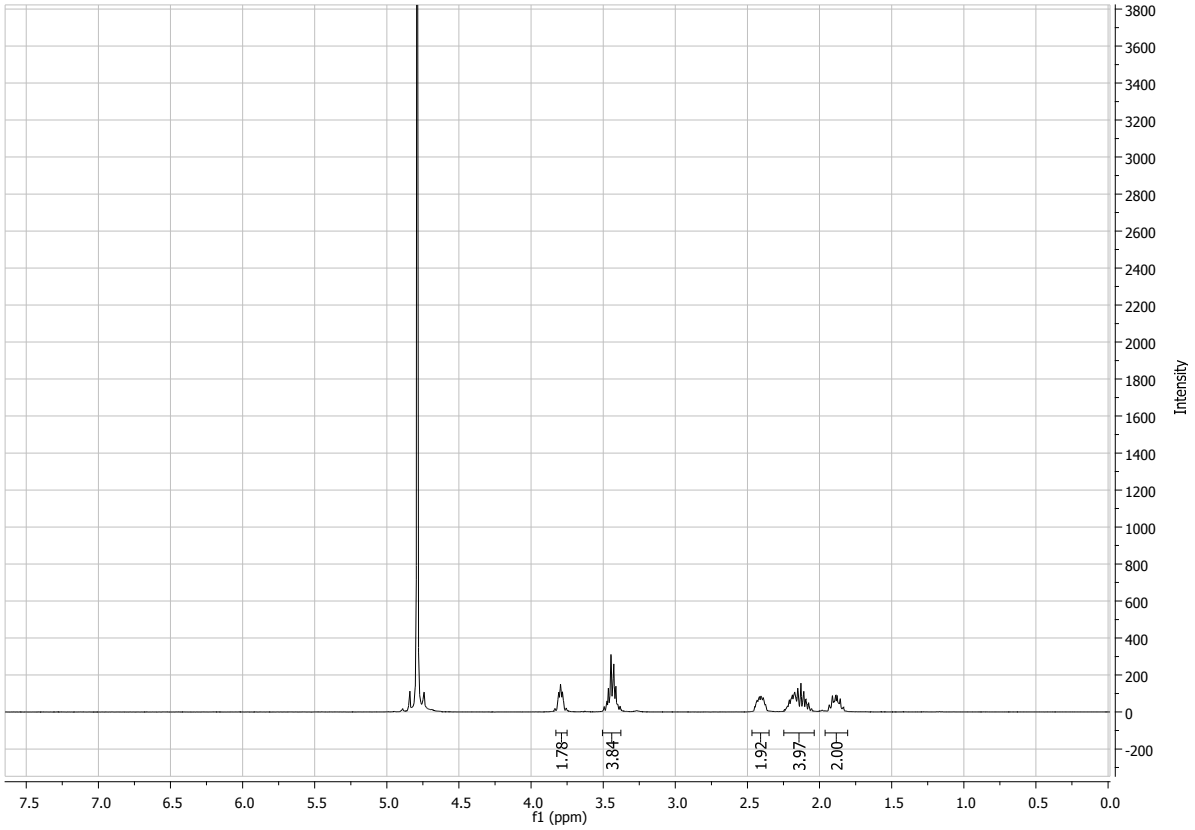
1.78
3.84
1.92
3.97
2.00
f1 (ppm)
Intensity

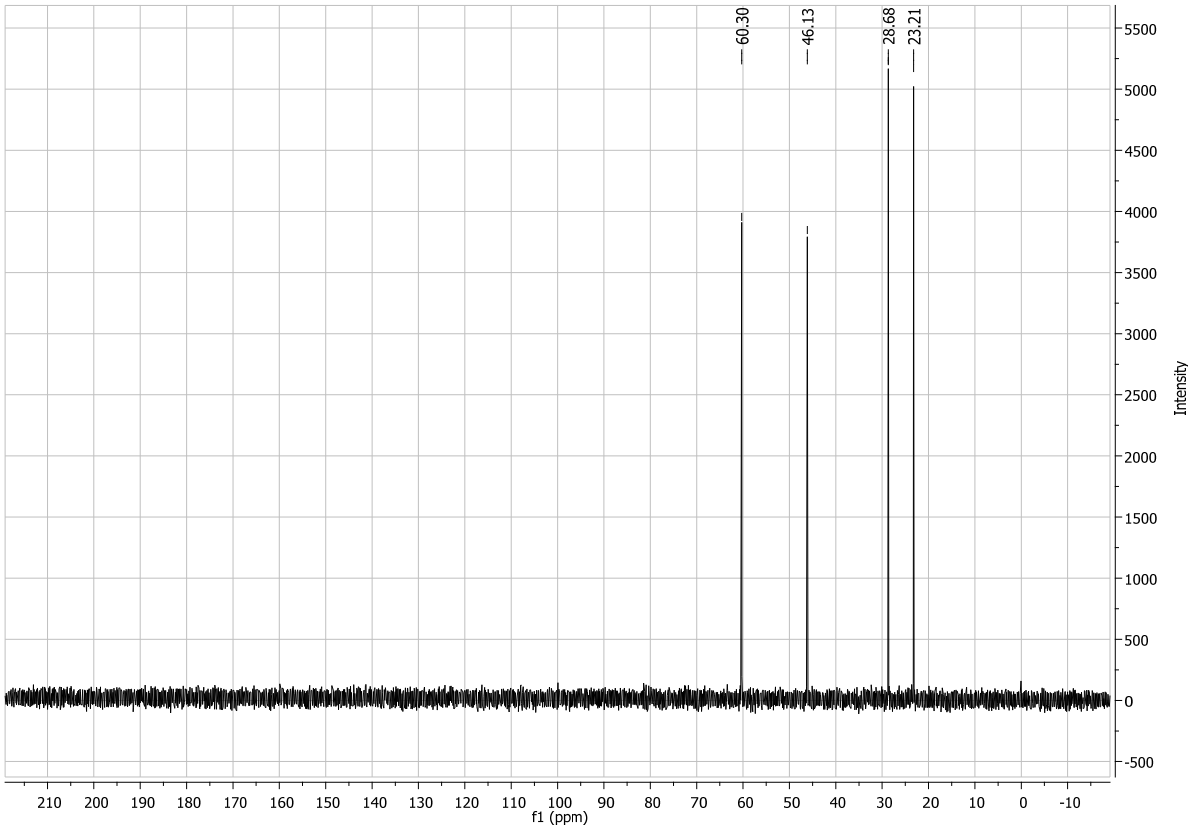
60.30
46.13
28.68
23.21
f1 (ppm)
Intensity

2,2'-bipyrrolidine (144)[27]

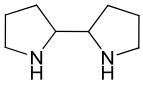

Following a modification of the reported procedure. A solution of ***dl/meso*-143** (3.0 g, 8.8 mmol) in MeOH (40 mL) was added with conc. HCl (6 mL) and stirred at room temperature. The reaction was monitored *via* TLC (DCM/EtOAc 1:1). Once all the starting material was consumed, the solvents were removed under reduced pressure and the hydrochloride of the product was recovered as a white solid. The solid was redissolved in water (3 mL) and basified to pH 10 with an aqueous solution of NaOH (20 % w/w). The resulting mixture was extracted with diethyl ether (3 x 20 mL), the organic phases reunited and the solvents removed under reduced pressure to yield **144** (1 g, 81 %) as a colourless oil.

^{1}H-NMR (400 MHz, δ-D_2O): 1.82-1.95 (2H, m, $CH_2CH_2CH_2CHN$), 2.06-2.24 (4H, m, $CH_2CH_2CH_2CHN$), 2.35-2.45 (2H, m, $CH_2CH_2CH_2CHN$), 3.37-3.49 (4H, m, CH_2N), 3.75-3.82 (2H, m, CHN); ^{13}C-NMR (100.2 MHz, δ-D_2O): 23.2, 28.6, 46.1, 60.3; *m/z* (ESI): 141.1 (100 %), 281.2 (30), 317.2 (55); HRMS (ESI): $[C_8H_{17}N_2\text{-}2HCl+H]^+$ requires 141.1286 found 141.1384.

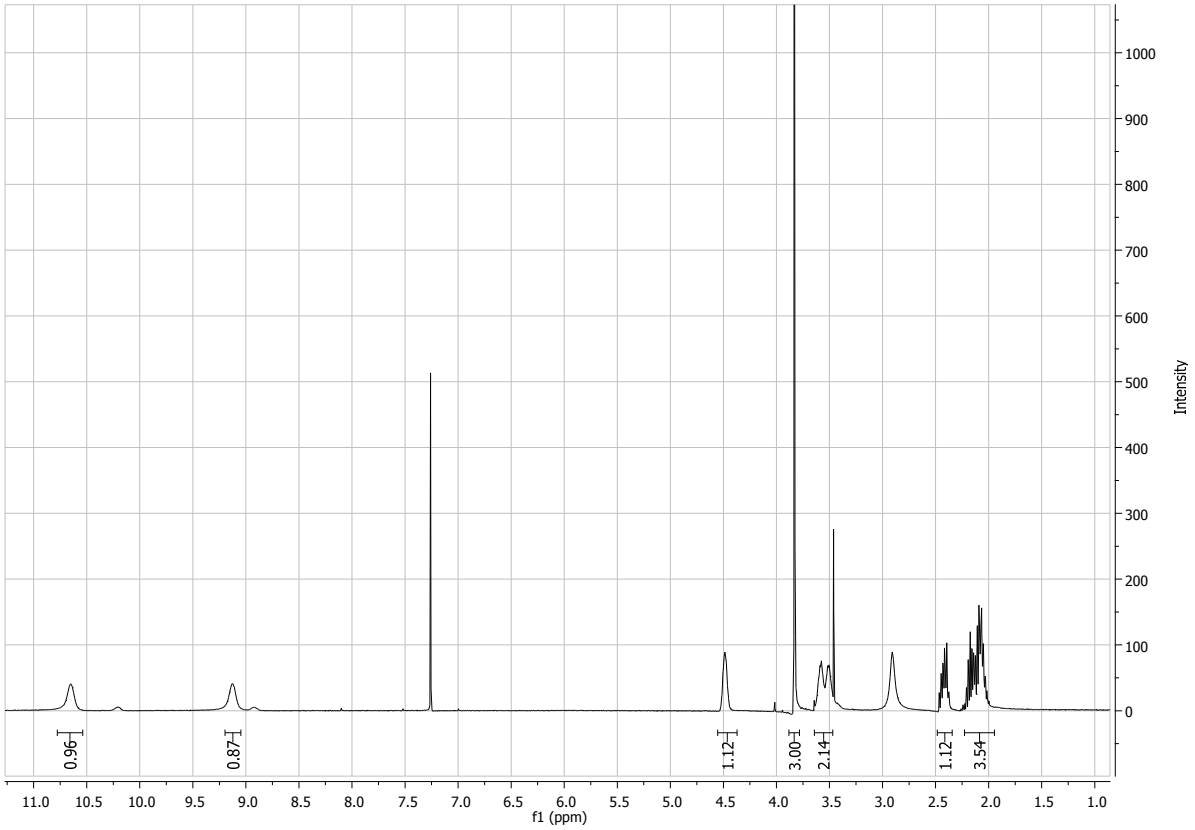
0.96
0.87
1.12
3.00
2.14
1.12
3.54
f1 (ppm)
Intensity

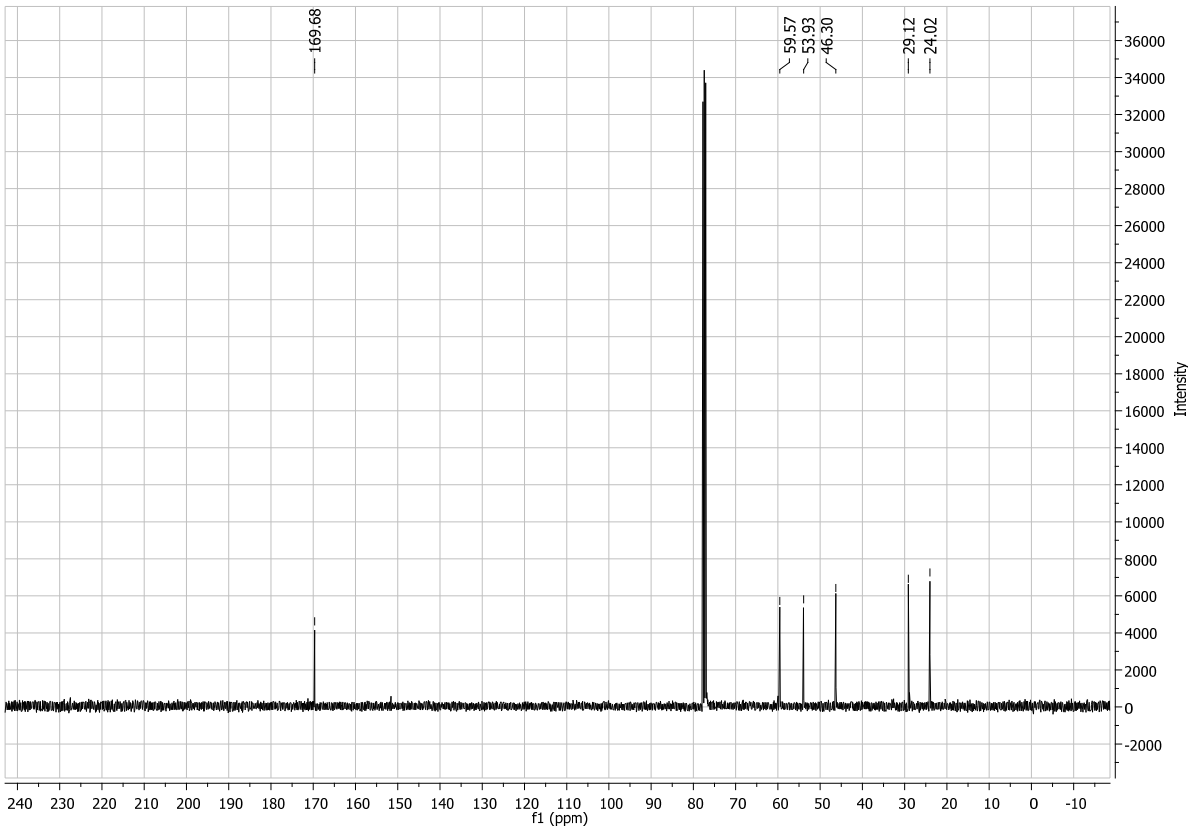
169.68
59.57
53.93
46.30
29.12
24.02
f1 (ppm)
Intensity

(*S*)-Methyl pyrrolidine-2-carboxylate hydrochloride (147)[28]

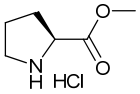

To a stirred suspension of L-proline (12.0 g, 100 mmol) in methanol (50 mL) kept at -0 °C in an ice bath, was added $SOCl_2$ (9.50 mL, 130 mmol) dropwise over a period of 20 minutes. After the addition was complete, the mixture was stirred for 30 minutes at 0° C allowed to warm to room temperature and refluxed overnight. The solvents where then removed under reduced pressure to give L-proline methyl ester hydrochloride **147** (15.6 g, 94 %) as a viscous colourless oil.

$[\alpha]^{25}_{D}$ =-33 (c = 1, H_2O), lit.[28] -31; IR (neat, ν_{max}/cm^{-1}): 3382, 2922, 2852, 1747, 1456, 1242; ^{1}H-NMR (400 MHz, δ-$CDCl_3$): 1.94-2.24 (3H, m, $CH_2CH_2CH_2CHN$, $CH_2CH_2CH_2CHN$), 2.30-2.51 (1H, m, $CH_2CH_2CH_2CHN$), 3.48-3.66 (2H, m, $CH_2CH_2CH_2CHN$) 3.84 (3H, s, OCH_3), 4.37-4.55 (1H, m, $CH_2CH_2CH_2CHN$), 9.10 (1H, s, NH_2^+), 10.60 (1H, s, NH_2^+); ^{13}C-NMR (100.2 MHz, δ-$CDCl_3$): 24.0, 29.1, 46.3, 53.9, 59.5, 169.6; *m/z* (ESI): 295.1 (5 %), 259.2 (5), 129.9 (100), 116.0 (20), 70.1 (18); HRMS (ESI): $[C_6H_{11}NO_2+H]^+$ requires 130.0863 found 130.0863.

General procedure for the preparation of aminoalcohols from aminoacids[29]

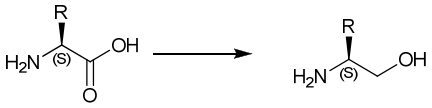

To a stirred suspension of $LiAlH_4$ (3 eq.) in dry THF kept under a nitrogen atmosphere and cooled in an ice bath, the desired amminoacid (1 eq.) was added in small portions. After the effervescence ended, the mixture was refluxed overnight and the reaction monitored *via* TLC (DCM/MeOH 9:1). After complete consumption of the starting material, heating was stopped and the mixture cooled to room temperature and subsequently in an ice bath. Water (1 mL per gram of $LiAlH_4$ used) was carefully added, followed by aqueous KOH (20 %, 2 mL per gram of $LiAlH_4$ used) and more water (3 mL per gram of $LiAlH_4$ used). The mixture was left stirring until all the salts were coloured white. The solid was then filtered over a pad a celite, recovered, and refluxed for further 30 minutes in dry THF to maximise the recovery. After a second filtration, both the filtrates were reunited and dried over $MgSO_4$. Evaporation of the solvents under reduced pressure gave the desired aminoalcohol in variable yields as yellow oils which did not need further purification.

(*S*)-valinol (149c)[29]

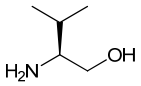

As described in the general procedure (87 % yield). ^{1}H-NMR (400 MHz, δ-$CDCl_3$): 0.92 (3H, d, (C*H*$_3$)$_2$, J_1 = 5.0 Hz), 0.94 (3H, d, (C*H*$_3$)$_2$, J_1 = 4.9 Hz), 1.52-1.63 (1H, m, C*H*(CH$_3$)$_2$), 2.35 (2H, broad s, N*H*$_2$), 2.55-2.61 (1H,m, C*H*NH$_2$), 3.29 (1H, dd, J_1 = 10.5 Hz, J_2 = 8.1 Hz, C*H*$_2$OH), 3.64 (1H, dd, J_1 = 10.6 Hz, J_2 = 4.1 Hz, C*H*$_2$OH); ^{13}C-NMR (100.2 MHz, δ-$CDCl_3$): 17.7, 19.8, 30.1, 58.0, 64.5.

(*S*)-phenylalaninol (149d)[29]

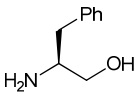

As described in the general procedure (82 % yield). ^{1}H-NMR (400 MHz, δ-$CDCl_3$): 2.30 (2H, broad s, N*H*$_2$), 2.58 (1H, dd, J_1 = 13.1 Hz, J_2 = 8.6 Hz, C*H*$_2$OH), 2.82 (1H, dd, J_1 = 13.5 Hz, J_2 = 5.1 Hz, C*H*$_2$OH), 3.10-3.22 (1H, m, C*H*), 3.43 (1H, dd, J_1 = 10.3 Hz, J_2 = 7.4 Hz, C*H*$_2$Ph), 3.67 (1H, dd, J_1 = 10.5 Hz, J_2 = 3.3 Hz, C*H*$_2$Ph); ^{13}C-NMR (100.2 MHz, δ-$CDCl_3$): 40.3, 50.6, 54.2, 65.7, 126.5, 128.6, 129.2, 138.2.

(*S*)-prolinol (149e)[30]

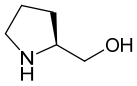

As described in the general procedure (68 % yield). ^{1}H-NMR (400 MHz, δ-$CDCl_3$): 1.36-1.49 (1H, m, $CH_2CH_2CH_2CHN$), 1.66-1.91 (3H, m, $CH_2CH_2CH_2CHN$, $CH_2CH_2CH_2CHN$), 2.88-2.98 (2H, m, $CH_2CH_2CH_2CHN$), 3.26-3.41 (2H, m, $CH_2CH_2CH_2CHN$, C*H*$_2$OH), 3.47-3.62 (3H, m, C*H*$_2$Ph, N*H*, O*H*); ^{13}C-NMR (100.2 MHz, δ-$CDCl_3$): 25.6, 27.4, 46.1, 59.9, 64.2.

General procedure for the synthesis of tosyl protected aziridines[31, 32]

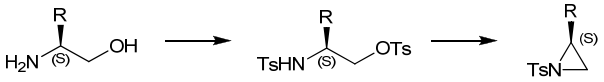

A solution of tosyl chloride (2.4 eq.) in pyridine was cooled with an ice bath. The desired aminoalcohol (1 eq.) was dissolved in pyridine and added dropwise to the cooled mixture. Stirring was continued while the reaction was allowed to return to RT. After completion was determined *via* TLC analysis (DCM/MeOH 9:1), water was added to the mixture until a solid appeared. The solid was filtered, dissolved in chloroform and washed with water in a separating funnel. The organic layer was recovered and dried over $MgSO_4$. Evaporation of the solvent under reduced pressure gave the di-tosylated intermediate with sufficient purity for the cyclisation step. The di-tosylated derivative of the chosen aminoalcohol (1 eq.) was dissolved in benzene and mixed with a solution of KOH (20 % w/w, 10 eq.).The mixture was vigorously stirred overnight at room temperature. The formation of a precipitate was observed.

After completion, the solid was filtered off and the organic phase separated, dried over $MgSO_4$ and the solvent evaporated under reduced pressure to yield the desired tosyl protected aziridine as solids in variable yields.

_N_-tosyl aziridine (150a)[33]

As described in the general procedure (68 % yield). ^{1}H-NMR (400 MHz, δ-$CDCl_3$): 2.39 (4H, s, CH_2), 2.50 (3H, s, ArCH_3), 7.38 (2H, d, J_1 = 8.0 Hz, Ar*H*), 7.86 (2H, d, J_1 = 8.0 Hz, Ar*H*); ^{13}C-NMR (100.2 MHz, δ-$CDCl_3$): 22.0, 27.8, 128.4, 130.1, 145.0.

2,2-dimethyl-1-tosylaziridine (150b)

As described in the general procedure (64 % yield). ^{1}H-NMR (400 MHz, δ-$CDCl_3$): 1.53 (6H, s, (CH_3)$_2$), 2.42 (3H, s, ArCH_3), 7.30 (2H, d, J_1 = 8.6 Hz, Ar*H*), 7.82 (2H, d, J_1 = 8.6 Hz, Ar*H*); ^{13}C-NMR (100.2 MHz, δ-$CDCl_3$): 23.1, 42.3, 48.2, 127.8, 129.7, 138.4, 144.1.

(*S*)-2-isopropyl-1-tosylaziridine (150c)[34]

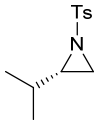

As described in the general procedure (71 % yield). ^{1}H-NMR (400 MHz, δ-$CDCl_3$): 0.83 (3H, d, J_1 = 6.7 Hz, (CH_3)$_2$), 0.93 (3H, d, J_1 = 6.7 Hz, (CH_3)$_2$), 1.44 (1H, dq, J_1 = 13.8 Hz, J_2 = 6.8 Hz, C*H*(CH$_3$)$_2$), 2.13 (1H, d, J_1 = 4.6 Hz, CH_2N), 2.47 (3H, s, ArCH_3), 2.51-2.57 (1H, m, C*H*N), 2.64 (1H, d, J_1 = 4.6 Hz, CH_2N), 7.36 (2H, d, J_1 = 8.0 Hz, Ar*H*), 7.86 (2H, d, J_1 = 8.0 Hz, Ar*H*); ^{13}C-NMR (100.2 MHz, δ-$CDCl_3$): 19.0, 19.5, 21.6, 30.1, 32.7, 46.2, 128.1, 129.5, 135.2, 144.4.

(S)-2-benzyl-1-tosylaziridine (150d)[35]

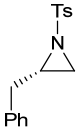

As described in the general procedure (71 % yield). ^{1}H-NMR (400 MHz, δ-$CDCl_3$): 2.16 (1H, m, C*H*CH_2N), 2.40 (3H, s, TsC*H*$_3$), 2.65 (1H, dd, J_1 = 14.4 Hz, J_2 = 7.2 Hz, C*H*$_2$N), 2.72 (1H, d, J_1 = 6.8 Hz, C*H*$_2$N), 2.84 (1H, dd, J_1 = 14.5 Hz, J_2 = 5.2 Hz, C*H*$_2$Bn), 2.98 (1H, m, C*H*$_2$Bn), 7.21-7.48 (7H, m, Ar*H*), 7.85 (2H,d, J_1 = 8.0 Hz, Ar*H*); ^{13}C-NMR (100.2 MHz, δ-$CDCl_3$): 21.8, 36.2, 42.3, 126.6, 128.2, 128.4, 128.5, 128.8, 130.1, 135.4, 144.8, 156.0.

General procedure for the preparation of benzyl protected aminoalcohols

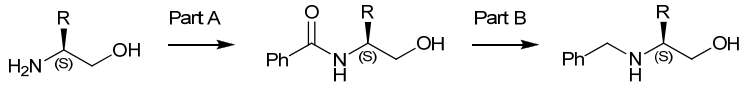

Part A[36]

The desired aminoalcohol (1 eq.) was dissolved in MeOH and the solution cooled in an ice bath before solid K_2CO_3 (1.1 eq.) was added in one portion. To the cooled stirred mixture, benzoyl chloride (1.1 eq.) was added dropwise over 10 minutes and the resulting mixture allowed to return to room temperature. Disappearance of the substrate was determined *via* TLC (DCM/MeOH 9:1). The reaction was then diluted with water and the MeOH evaporated. The remaining aqueous phase was extracted with EtOAc (4 x 20 mL), and the reunited organic phases dried on $MgSO_4$. Evaporation of the solvent under reduced pressure gave the pure desired intermediate.

***N*-(2-hydroxyethyl)benzamide (151a)[37]**

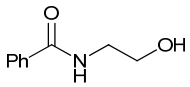

As described in the general procedure (79 % yield). IR (neat, ν_{max}/cm^{-1}): 3297, 2937, 2876, 1633, 1536, 1291, 1291; ^{1}H-NMR (400 MHz, δ-$CDCl_3$): 3.59-3.74 (2H, m, C*H*$_2$NH), 3.81-3.92 (2H, m, C*H*$_2$O), 7.39-7.58 (3H, m, Ar*H*), 7.81 (2H, d, J_1 = 8.0 Hz, Ar*H*); ^{13}C-NMR

(100.2 MHz, δ-$CDCl_3$): 42.8, 62.5, 126.9, 128.6, 131.6, 134.1, 134.2, 168.5; *m/z* (ESI): 188.0 (70 %), 270.0 (10), 353.1 (100) ; HRMS (ESI): $[C_9H_{11}NO_2+H]^+$ requires 166.0863 found 166.0860.

_N_-(1-hydroxy-2-methylpropan-2-yl)benzamide (151b)[38]

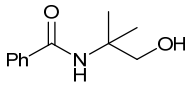

As described in the general procedure (72 % yield). IR (neat, ν_{max}/cm^{-1}): 3175, 2982, 2851, 1721, 1627, 1577; ^{1}H-NMR (400 MHz, δ-$CDCl_3$): 1.46 (6H, s, $(CH_3)_2$), 3.71 (2H, s, CH_2O), 6.26 (1H, s, O*H*), 7.40-7.54 (3H, m, Ar*H*), 7.73-7.78 (2H, m, Ar*H*), 8.06 (1H, d, J_1 = 8.2 Hz, Ar*H*); ^{13}C-NMR (100.2 MHz, δ-$CDCl_3$): 24.7, 56.5, 70.7, 126.9, 128.3, 128.6, 129.5, 131.6, 132.9, 134.8, 168.4; *m/z* (ESI): 194.1 (100 %), 216.0 (10); HRMS (ESI): $[C_{11}H_{15}NO_2+H]^+$ requires 194.1176 found 194.1174.

(*S*)-*N*-(1-hydroxy-3-phenylpropan-2-yl)benzamide (151d)[39]

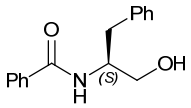

As described in the general procedure (69 % yield). $[\alpha]^{25}_D$ = -75.5 (c = 0.9, MeOH), lit.[40] -76.5 (c = 0.9, MeOH); IR (neat, ν_{max}/cm^{-1}): 3305, 3028, 1635, 1530, 1284; ^{1}H-NMR (400 MHz, δ-DMSO-d_6): 2.75-2.85 (1H, m, CH_2Ph), 2.91-3.01 (1H, m, CH_2Ph), 3.46-3.56 (1H, m, CH_2OH), 4.10-4.22 (1H, m, C*H*NH), 4.83-4.89 (1H, m, C*H*OH), 7.12-7.20 (1H, m, Ar*H*), 7.22-7.30 (4H, m, Ar*H*), 7.40-7.54 (3H, m, Ar*H*), 7.74-7.82 (2H, m, Ar*H*), 8.18 (1H, d, J_1 = 8.1 Hz, N*H*) ;^{13}C-NMR (100.2 MHz, δ-DMSO-d_6): 36.4, 53.2, 62.8, 72.8, 125.8, 127.1, 128.0, 128.1, 129.0, 130.9, 134.7, 139.4, 165.9; *m/z* (ESI): 256.1 (100 %), 278.1 (40); HRMS (ESI): $[C_{16}H_{17}NO_2+H]^+$ requires 256.1332 found 256.1335.

Part B[29]

To a suspension of $LiAlH_4$ (2 eq.) in dry THF kept under a nitrogen atmosphere and cooled in an ice bath, the desired substrate was added in portions over a period of 10 minutes. After the effervescence subsided, the suspension was refluxed overnight and monitored via TLC (DCM/MeOH 9:1). After all the starting material was consumed, the reaction was allowed to

warm to room temperature and was then cooled again in an ice bath. The mixture was then carefully added with water (1 mL per gram of $LiAlH_4$ used), followed by aqueous KOH (20%, 2 mL per gram of $LiAlH_4$ used) and water (3 mL per gram of $LiAlH_4$ used). The mixture was left stirring until the salts were coloured white. The solid was then filtered over a pad of celite, recovered, and refluxed for further 30 minutes in dry THF. After a second filtration, both the filtrates were reunited and dried over $MgSO_4$. Evaporation of the solvents under reduced pressure gave the desired aminoalcohol in variable yields as yellow oils which could be used in the next step without purification.

2-(benzylamino)ethanol (152a)[41]

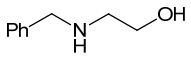

As described in the general procedure (71 % yield). IR (neat, ν_{max}/cm^{-1}): 3295, 2835, 1494, 1452,1047; ^{1}H-NMR (400 MHz, δ-$CDCl_3$): 2.78 (2H, s, NC*H*$_2$), 3.62-3.69 (2H, m, C*H*$_2$OH), 3.80 (2H, s, PhC*H*$_2$NH), 7.12-7.43 (5H, m, Ar*H*); ^{13}C-NMR (100.2 MHz, δ-$CDCl_3$): 50.7, 53.6, 60.8, 126.9, 127.1, 128.2, 128.5, 139.8.

2-(benzylamino)-2-methylpropan-1-ol (152b)[42]

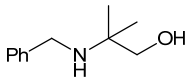

As described in the general procedure, purified by flash cromatography on silica gel (DCM/EtOAc 5:5) (66 % yield). IR (neat, ν_{max}/cm^{-1}): 3294, 3030, 2862, 1476, 1328, 1072; ^{1}H-NMR (400 MHz, δ-$CDCl_3$): 1.10 (6H, s, (C*H*$_3$)$_2$), 3.28 (2H, s, C*H*$_2$Ph), 3.62 (2H, s, C*H*$_2$O), 7.14-7.31 (5H, m, ArC*H*); ^{13}C-NMR (100.2 MHz, δ-$CDCl_3$): 24.1, 46.4, 54.1, 68.3, 127.1, 128.2, 128.5, 140.5.

(S)-2-(benzylamino)-3-phenylpropan-1-ol (152d)[43]

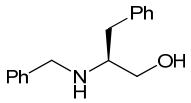

As described in the general procedure (54 % yield). $[\alpha]^{25}_D$ = -11.5 (c = 1.2, MeOH), lit.[44] -11.1 (c = 1.2, MeOH); IR (neat, ν_{max}/cm^{-1}): 3026, 2919, 2854, 1494, 1451, 1344; ^{1}H-NMR

(400 MHz, δ-$CDCl_3$): 2.74-2.91 (2H, m, CHCH_2Ph), 2.95-3.05 (1H, m, CH_2OH), 3.33-3.42 (1H, m, CH_2OH), 3.64-3.72 (1H, m, C*H*NH), 3.81 (2H, s, PhCH_2N), 7.15-7.39 (10H, m, ArC*H*); ^{13}C-NMR (100.2 MHz, δ-$CDCl_3$): 38.1, 51.0, 59.3, 62.4, 126.4, 127.1, 128.0, 128.5, 128.6, 129.2, 138.4, 139.8.

General procedure for the Boc protection of aminoalcohols[45]

To a stirred solution of the chosen aminoalcohol (1 eq.) in DCM was added triethylamine (1 eq.). After five minutes, a solution of di-*tert*-butyl-dicarbonate (1 eq.) in DCM was added dropwise and the reaction monitored via TLC (EtOAc/DCM 1:1). Once the substrate was completely consumed, the mixture was transferred into a separating funnel and washed with saturated NH_4Cl. The organic phase was recovered, washed with brine and dried over $MgSO_4$. Evaporation of the solvent under reduced pressure gave the Boc-protected product in variable yields. The materials were sufficiently pure to be used in the following steps.

tert-butyl 2-hydroxyethylcarbamate (155a)[46]

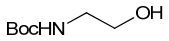

As described in the general procedure (98 % yield). IR (neat, ν_{max}/cm^{-1}): 3339, 2978, 1684, 1520, 1167; ^{1}H-NMR (400 MHz, δ-$CDCl_3$): 1.43 (9H, s, (CH_3)$_3$), 3.28 (2H, dd, J_1 = 10.0 Hz, J_2 = 5.0 Hz, CH_2NH), 3.68 (2H, t, J_1 = 5.0 Hz, CH_2O), 5.12 (1H, broad s, N*H*) ; ^{13}C-NMR (100.2 MHz, δ-$CDCl_3$): 28.3 , 43.1, 62.3, 79.6, 156.8.

***tert*-butyl 1-hydroxy-2-methylpropan-2-ylcarbamate (155b)[47]**

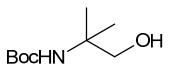

As described in the general procedure (89 % yield). IR (neat, ν_{max}/cm^{-1}): 3480, 3300, 2990, 2897, 1687, 1532; ^{1}H-NMR (400 MHz, δ-$CDCl_3$): 1.27 (6H, s, (CH_3)$_2$), 1.46 (9H, s, (CH_3)$_3$), 3.61 (2H, d, J_1 = 5.6 Hz, CH_2OH), 4.07 (1H, broad s, N*H*), 4.68 (1H, broad s, O*H*); ^{13}C-NMR (100.2 MHz, δ-$CDCl_3$): 24.7, 28.3, 31.2, 54.3, 70.9, 79.8, 156.1.

(S)-tert-butyl 1-hydroxy-3-phenylpropan-2-ylcarbamate (155d)[46]

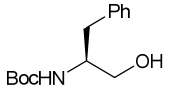

As described in the general procedure (91 % yield). IR (neat, ν_{max}/cm^{-1}): 3351, 2983, 2936, 2873, 1685, 1525, 1166; ^{1}H-NMR (400 MHz, δ-$CDCl_3$): 1.35 (9H, s, (CH_3)$_3$), 2.77 (2H, d, J_1 = 6.6 Hz, CH_2Ph), 3.44-3.54 (1H, m, CH_2OH), 3.57-3.64 (1H, m, CH_2OH), 3.80 (1H, broad s, C*H*), 4.65 (1H, broad s, N*H*), 7.04-7.32 (5H, m, Ar*H*); ^{13}C-NMR (100.2 MHz, δ-$CDCl_3$): 28.3, 30.9, 37.5, 53.7, 64.4, 79.7, 126.5, 128.5, 129.3, 137.8, 156.2.

General procedure for the synthesis of cyclic sulfamidites and sulfamidates[48]

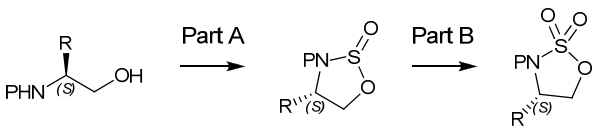

Part A

A solution of the N-protected aminoalcohol of choice (1eq.) and imidazole (4.5 eq.) in dry DCM was cooled in an ice bath under a nitrogen atmosphere. Triethylamine (2.5 eq.) was then added and the solution stirred for 10 minutes followed by slow dropwise addition of a solution of $SOCl_2$ (1.2 eq.) in dry DCM (total volume about 15 mL). The mixture was then stirred in the ice bath for four hours or until TLC analysis (EtOAc/DCM 1:1) showed disappeareance of the aminoalcohol. The reaction was then added with water (50 mL) and stirred for 20 minutes, after which the phases were separated and the aqueous phase extracted with DCM (3 x 20 mL). The combined organic phases were washed with brine, dried over $MgSO_4$ and the solvent evaporated under reduced pressure. Different yields were obtained depending on the substrate. Generally further purification by flash chromatography on silica gel was necessary before moving to the next step.

_N_-Boc-sulfamidite (1536a)[49]

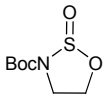

As described in the general procedure, after flash cromatography (DCM/EtOAc 6:4) (75 % yield). IR (neat, ν_{max}/cm^{-1}): 2997, 2899, 1720, 1396, 1320, 1256; ^{1}H-NMR (400 MHz, δ-$CDCl_3$): 1.76 (9H, s, CH_3), 3.78 (1H, ddd, J_1 = 10.9 Hz, J_2 = 9.7 Hz, J_3 = 7.4 Hz, CH_2O), 4.06-4.14 (1H, m, CH_2N), 4.93 (1H, ddd, J_1 = 9.2 Hz, J_2 = 7.4 Hz, J_3 = 2.1 Hz, CH_2N), 5.20 (1H, ddd, J_1 = 10.8 Hz, J_2 = 9.2 Hz, J_3 = 6.5 Hz, CH_2O); ^{13}C-NMR (100.2 MHz, δ-$CDCl_3$): 28.5, 44.3, 70.8, 84.2, 151.6; *m/z* (ESI): 152.0 (100 %), 169.0 (60), 208.0 (40), 225.1 (50).

3-(tert-butyloxycarbonyl)-4,4-dimethyl-[1,2,3]-oxathiazolidine-2-oxide (156b)[42]

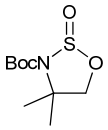

As described in the general procedure (81 % yield). IR (neat, ν_{max}/cm^{-1}): 2980, 2939, 1722, 1698, 1313, 1157; ^{1}H-NMR (400 MHz, δ-$CDCl_3$): 1.43 (3H, s, CH_3), 1.54 (9H, s, (CH_3)$_3$), 1.62 (3H, s, CH_3), 4.35 (1H, d, J_1 = 8.6 Hz, CH_2O), 4.84 (1H, d, J_1 = 8.4 Hz, CH_2O); ^{13}C-NMR (100.2 MHz, δ-$CDCl_3$): 23.5, 28.4, 52.1, 66.3, 81.7, 152.8; *m/z* (ESI): 253.1 (100 %), 425.2 (30).

(*S*)-*tert*-butyl 4-benzyl-1,2,3-oxathiazolidine-3-carboxylate 2-oxide (156d)

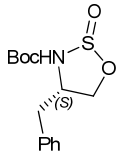

As described in the general procedure (86 % yield). $[\alpha]^{25}_{D}$ = -23.1 (c = 1, MeOH); IR (neat, ν_{max}/cm^{-1}): 2980, 2928, 1717, 1692, 1324, 1076; ^{1}H-NMR (400 MHz, δ-$CDCl_3$): 1.47 (9H. S, (CH_3)$_3$), 1.49 (9H. S, (CH_3)$_3$), 2.54 (1H, dd, J_1 = 13.2 Hz. J_2 = 10.2 Hz, CH_2Ph), 2.75 (1H, dd, J_1 = 13.2 Hz. J_2 = 10.1 Hz, CH_2Ph), 2.99-3.18 (1H, m, CH_2Ph), 3.52 (1H, dd, J_1 = 13.3 Hz. J_2 = 4.0 Hz, CH_2Ph), 4.09-4.19 (2H, m, CHCH$_2$Ph), 4.42 (2H, dd, J_1 = 9.2 Hz, J_2 = 6.9 Hz, CH_2O), 4.71 (2H, dd, J_1 = 9.1 Hz. J_2 = 8.3 Hz, CH_2O), 7.01-7.31 (10H, m, ArH); ^{13}C-

NMR (100.2 MHz, δ-$CDCl_3$, most signals doubled): 28.6, 38.2 (39.9), 57.9 (58.1), 72.5, 84.2 (84.3), 127.5, 129.2, 129.4, 129.8, 136.9 (137.1), 151.6.

_N_-benzylsulfamidite 2-oxo-3-phenylmethyl-1,2,3-oxathiazolidine (153a)[50]

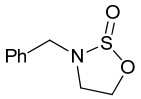

As described in the general procedure after flash chromatography on silica gel (DCM/EtOAc 6:4) (70 % yield). IR (neat, ν_{max}/cm^{-1}): 3030, 2904, 2858, 1496, 1147, 895.4; ^{1}H-NMR (400 MHz, δ-$CDCl_3$): 3.25–3.35 (1H, m, NC$H_2$$CH_2$O), 3.40–3.50 (1H, m, NC$H_2$$CH_2$O), 4.96–4.06 (1H, m, PhCH_2N), 4.30–4.40 (2H, m, NCH_2CH_2O, PhCH_2N), 4.77-4.86 (1H, m, NCH_2CH_2O), 7.32-7.45 (5H, m, Ar*H*);^{13}C-NMR (100.2 MHz, δ-$CDCl_3$): 46.8, 50.2, 71.7, 126.9, 128.0, 128.2, 128.6, 128.7, 136.1; *m/z* (ESI): 152.1 (10 %), 198.0 (100).

3-benzyl-4,4-dimethyl-1,2,3-oxathiazole-2-oxide (153b)[42]

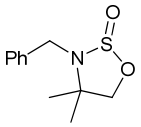

As described in the general procedure (91% yield). IR (neat, ν_{max}/cm^{-1}): 2974, 1496, 1368, 1140, 949; ^{1}H-NMR (400 MHz, δ-$CDCl_3$): 1.17 (3H, s, CH_3), 1.38 (3H, s, CH_3), 4.04-4.24 (2H, m, CH_2O), 4.57 (2H, d, J_1 = 8.0 Hz, CH_2Ph), 7.16-7.30 (3H, m, Ar*H*), 7.31-7.37 (2H, m, Ar*H*); ^{13}C-NMR (100.2 MHz, δ-$CDCl_3$): 24.5, 25.4, 44.3, 61.9, 82.3, 127.8, 128.69, 128.66, 137.2; *m/z* (ESI): 226.0 (100 %), 248.0 (10), 451.1 (10).

(*S*)-3-benzyl-4-benzyl-1,2,3-oxathiazole-2-oxide (153d)[51]

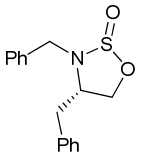

As described in the general procedure, after flash chromatography (DCM/EtOAc 6:4) (69 % yield). $[\alpha]^{25}_D$ = 3.96 (c = 1, $CHCl_3$); IR (neat, ν_{max}/cm^{-1}): 3062, 3029, 2927, 2862, 1497, 1150, 1029; ^{1}H-NMR (400 MHz, δ-$CDCl_3$): 2.52 (1H, dd, J_1 = 13.5 Hz, J_2 = 9.1 Hz, PhCH_2),

2.73-2.96 (2H, m, PhCH_2), 3.10 (1H, dd, J_1 = 13.4 Hz, J_2 = 4.0 Hz, PhCH_2), 3.45-3.55 (1H, m, C*H*), 3.71-3.83 (1H, m, C*H*), 4.04-4.18 (4H, m, PhCH_2N), 4.18-4.34 (2H, m, CH_2O), 4.52-4.63 (2H, m, CH_2O), 6.89-7.43 (20H, m, ArC*H*);^{13}C-NMR (100.2 MHz, δ-DCl_3): 38.8 (38.9), 48.9 (49.1), 60.1 (62.3), 74.5 (75.4), 126.9, 127.0, 128.0. 128.1, 128.5, 128.7, 128.84, 128.89, 129.0, 129.1, 136.0, 136.3, 136.8, 137.3.

2-(*R*, *S*)-5-(*S*)-<3.3.0>-1-aza-2-thia-3-oxabicyclooctane-2-oxide (153e)[52]

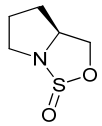

As described in the general procedure, purified by flash cromatography on silica gel (DCM/EtOAc 6:4) (63 % yield). ^{1}H-NMR (400 MHz, δ-$CDCl_3$): 1.11-1.21 (1H, m , $CH_2CH_2CH_2CHN$) 1.22-1.31 (1H, m, $CH_2CH_2CH_2CHN$), 1.65-1.80 (1H, m, $CH_2CH_2CH_2CHN$), 1.86-2.05 (2H, m, $CH_2CH_2CH_2CHN$, $CH_2CH_2CH_2CHN$), 3.16-3.34 (1H, m, $CH_2CH_2CH_2CHN$), 3.59-3.70 (1H, m, CH_2O), 3.72-3.83 (1H, m, CH_2O), 3.91-4.08 (1H, m, C*H*N); ^{13}C-NMR (100. 2 MHz, δ-$CDCl_3$): 25.1, 28.4, 28.5, 31.1, 44.6, 48.0, 64.7, 65.2, 71.3, 74.2.

Part B

To a suspension of sodium periodate (3.5 eq.) and $RuCl_3$ (0.005 eq.) in water, cooled in an ice bath, was added a solution of the chosen sulfamidite in EtOAc (1eq.) dropwise over 30 minutes. The mixture was stirred in the ice bath until TLC (DCM/EtOAc 1:1) showed total consumption of the sulfamidite. The phases were then separated and the aquous layer extracted with EtOAc (4 x 20 mL). The combined organic phases were washed with brine, dried over $MgSO_4$ and the solvent was evaporated under reduced pressure to give the desired product.

2,2-dioxo[1,2,3]oxathiazolidine-3-carboxylic acid tert-butyl ester (157a)[49]

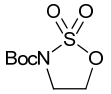

As described in the general procedure (92 % yield). ^{1}H-NMR (400 MHz, δ-$CDCl_3$):1.57 (9H, s, (CH_3)$_3$), 4.03 (2H, t, J_1 = 6.6 Hz, CH_2O), 4.63 (2H, t, J_1 = 6.8 Hz, CH_2N) ^{13}C-NMR (100.2 MHz, δ-$CDCl_3$): 28.4, 42.5, 61.4, 81.4, 161.9.

3-(tert-butyloxycarbonyl)-4,4-dimethyl-[1,2,3]-oxathiazolidine-2,2-dioxide (157b)[42]

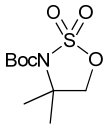

As described in the general procedure, purified by flash chromatography on silica gel (DCM/EtOAc 6:4) (49 % yield). ^{1}H-NMR (400 MHz, δ-$CDCl_3$): 1.38 (9H, s, (CH_3)$_3$), 1.41 (6H, s, (CH_3)$_2$), 4.06 (2H, s, CH_2O); ^{13}C-NMR (100.2 MHz, δ-$CDCl_3$): 23.8, 28.0, 62.5, 75.8, 85.2, 164.0.

***N*-benzylsulfamidate (154a)[49]**

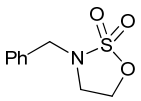

As described in the general procedure, after purification by flash chromatography on silica gel (DCM/EtOAc 6:4) (69 % yield). ^{1}H-NMR (400 MHz, δ-$CDCl_3$): 3.29-3.39 (2H, ddd, J_1 = 6.5 Hz, J_2 = 3.9 Hz, J_3 = 2.2 Hz, CH_2CH_2O), 4.16 (2H, d, J_1 = 3.2 Hz, NCH_2Ph), 4.45 (2H, ddd, J_1 = 9.2 Hz, J_2 = 5.2 Hz, J_3 = 2.4 Hz, CH$_2$CH_2O), 7.22-7.34 (5H, m, Ar*H*); ^{13}C-NMR (100.2 MHz, δ-$CDCl_3$): 47.1, 51.5, 66.7, 128.5, 128.7, 128.9, 129.0, 130.2, 134.3.

3-benzyl-4,4-dimethyl-[1,2,3]-oxathiazolidine-2,2-dioxide (154b)[42]

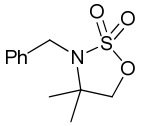

As described in the general procedure (71 % yield). ^{1}H-NMR (400 MHz, δ-$CDCl_3$): 1.23 (6H, s, (CH_3)$_2$), 4.16-4.23 (4H, m, CH_2O, NCH_2Ph), 7.14-7.44 (5H, m, Ar*H*); ^{13}C-NMR (100.2 MHz, δ-$CDCl_3$): 23.5, 45.4, 62.0, 77.8, 128.0, 128.3, 128.6, 135.8.

(4*S*) 3,4-dibenzyl[1,2,3]oxathiazolidine-2,2-dioxide (154d)[51]

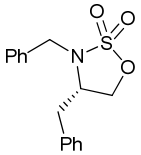

As described in the general procedure (88 % yield). m.p. 62.5-63 °C, lit.[51] 64 °C; $[\alpha]^{25}_{D}$ = -32 (c = 1 $CHCl_3$), lit.[51] – 34 (c = 1 $CHCl_3$); ^{1}H-NMR (400 MHz, δ-$CDCl_3$): 2.75 (1H, dd, J_1 = 13.5 Hz, J_2 = 9.5 Hz, CHCH_2Ph), 3.03 (1H, dd, J_1 = 13.5 Hz, J_2 = 5.5 Hz, CHCH_2Ph), 3.77 (1H, dtd, J_1 = 9.5 Hz, J_2 = 6.3 Hz, J_3 = 5.4 Hz, C*H*CH_2Ph), 4.23-4.28 (1H, m, CH_2O), 4.32-4.36 (3H, m, CH_2O, PhCH_2N), 7.02-7.07 (2H, m, Ar*H*), 7.25-7.43 (8H, m, Ar*H*); ^{13}C-NMR (100.6 MHz, δ-$CDCl_3$): 38.4, 50.7, 60.0, 70.4, 127.3, 128.5, 128.7, 128.8, 128.9, 129.01, 129.08, 134.5, 135.2.

5-(*S*)-<3.3.0>-1-aza-2-thia-3-oxabicyclooctane-2,2-dioxide (154e)[52]

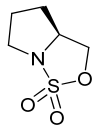

As described in the general procedure, purified by flash cromatography on silica gel (DCM/EtOAc 6:4) (43 % yield) $[\alpha]^{25}_{D}$ = -47.4 (c = 1 $CHCl_3$), lit.[53] -43.2 (c = 1.02, $CHCl_3$); ^{1}H-NMR (400 MHz, δ-$CDCl_3$): 1.76 (1H, ddd, J_1 = 16.7 Hz, J_2 = 9.7 Hz, J_3 = 5.3 Hz, $CH_2CH_2CH_2$CHN), 1.85-1.96 (2H, m, $CH_2CH_2CH_2$CHN), 2.14 (1H, dq, J_1 = 12.7 Hz, J_2 = 7.4 Hz, $CH_2CH_2CH_2$CHN), 3.21 (1H, dt, J_1 = 11.2 Hz, J_2 = 7.2 Hz, C$H_2$$CH_2CH_2$CHN), 3.59-3.68 (1H, m, C$H_2$$CH_2CH_2$CHN), 3.98 (1H, dd, J_1 = 8.7 Hz, J_2 = 6.0 Hz, CH_2O), 4.22 (1H, ddd, J_1 = 13.1 Hz, J_2 = 6.8 Hz, J_3 = 4.2 Hz, $CH_2CH_2CH_2$C*H*N), 4.49 (1H, dd, CH_2O, J_1 = 8.7 Hz, J_2 = 6.9 Hz); ^{13}C-NMR (100. 2 MHz, δ-$CDCl_3$): 25.1, 31.3, 51.0, 62.4, 71.7.

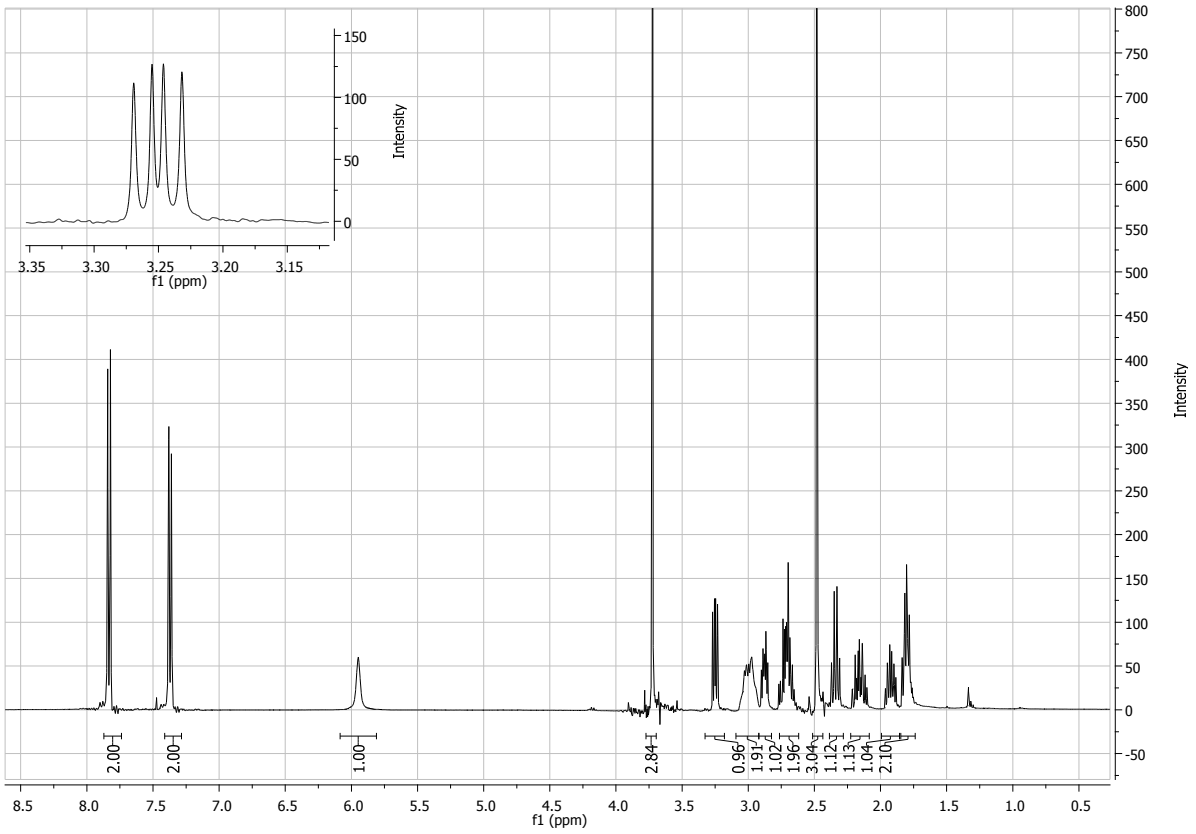
Intensity
f1 (ppm)
2.00
2.00
1.00
2.84
0.96
1.91
1.02
1.96
3.04
1.12
1.13
1.04
2.10

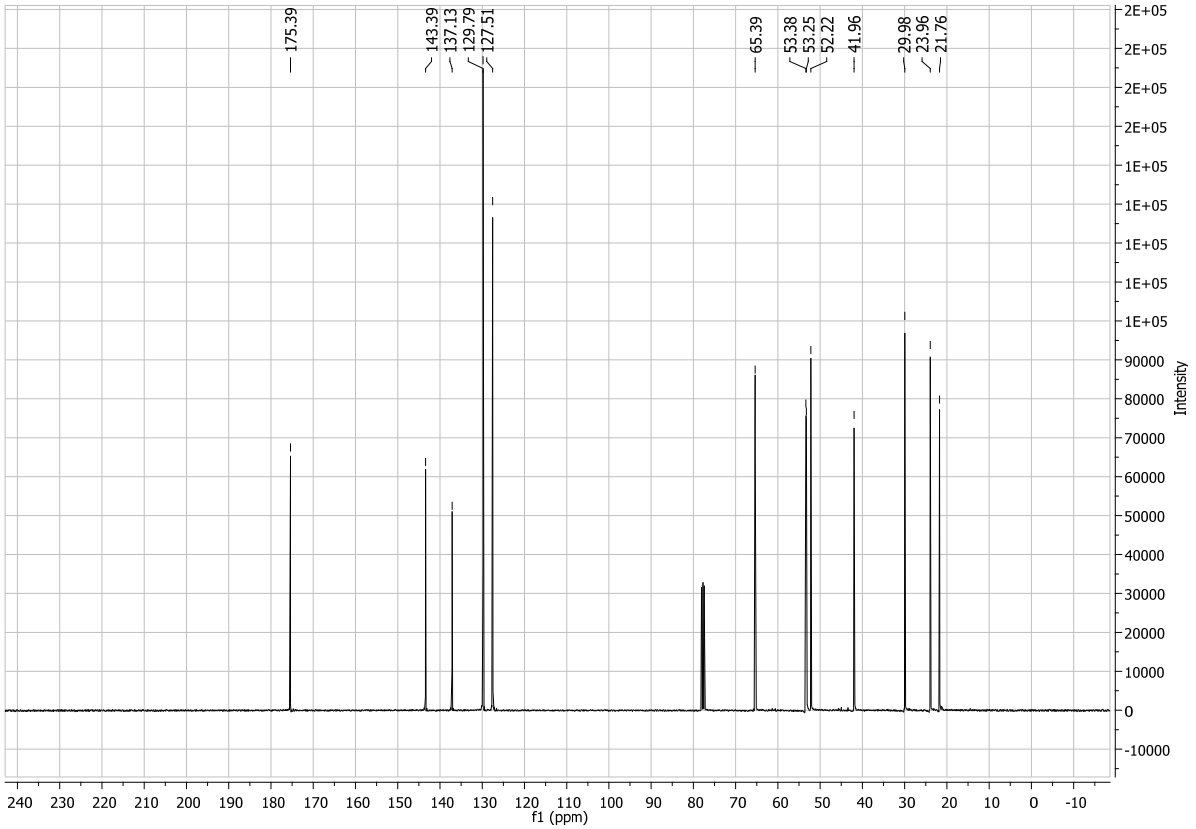
175.39
143.39
137.13
129.79
127.51
65.39
53.38
53.25
52.22
41.96
29.98
23.96
21.76
Intensity
f1 (ppm)

(*S*)-methyl 1-(2-(4-methylphenylsulfonamido)ethyl)pyrrolidine-2-carboxylate (158a)

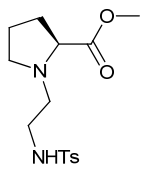

To a stirred solution of proline methyl ester hydrochloride (**147**) (2.30 g, 13.9 mmol) in acetonitrile (80 mL) was added TEA (1 eq.). A white precipitate of triethylamine hydrochloride was observed. After stirring at RT for ten minutes, **150a** (2.32 g, 13.9 mmol) dissolved in acetonitrile (20 mL). After addition of a further equivalent of triethylamine, the reaction was heated to reflux until disappearance of the aziridine spot on TLC (DCM/AcOEt 6:4). On this scale, the reaction needed 2 days to reach apparent completion. The solvent was then evaporated and the crude product purified by flash chromatography (DCM/EtOAc 6:4) to yield **158a** (500 mg, 13 %) as a yellow oil.

$[\alpha]^{25}_{D}$ = -28.0 (c = 1, DCM); IR: 3325, 2978, 1744, 1698, 1517, 1165; ^{1}H-NMR (400 MHz, δ-$CDCl_3$): 1.74-1.84 (2H, m, $CH_2CH_2CH_2CH$), 1.86-1.97 (1H, m, $CH_2CH_2CH_2CH$), 2.09-2.22 (1H, m, $CH_2CH_2CH_2CH$), 2.34 (1H, dd, J_1 = 16.4 Hz, J_2 = 8.2 Hz, $CH_2CH_2CH_2CH$), 2.48 (3H, s, Ar-CH_3), 2.66-2.77 (2H, m, NCH_2CH_2NHTs), 2.83-2.91 (1H, m, $CH_2CH_2CH_2CH$), 2.91-3.05 (2H, m, NCH_2CH_2NHTs), 3.25 (1H, dd, J_1 = 9.3 Hz, J_2 = 5.7 Hz, $CH_2CH_2CH_2CH$), 3.72 (3H, s, OCH_3), 5.95 (1H, broad s, N*H*), 7.36 (2H, d, J_1 = 8.2 Hz, Ar*H*), 7.83 (2H, d, J_1 = 8.4 Hz, Ar*H*); ^{13}C-NMR (100.2 MHz, δ-$CDCl_3$): 21.7, 23.9, 29.9, 41.9, 52.2, 53.2, 53.3, 65.3, 127.5, 129.7, 137.1, 143.3, 175.3; *m/z* (ESI): 327.1 (100 %), 653.2 (70); HRMS (ESI): $[C_{15}H_{22}N_2O_4S+H]^+$ requires 327.1373 found 327.1375.

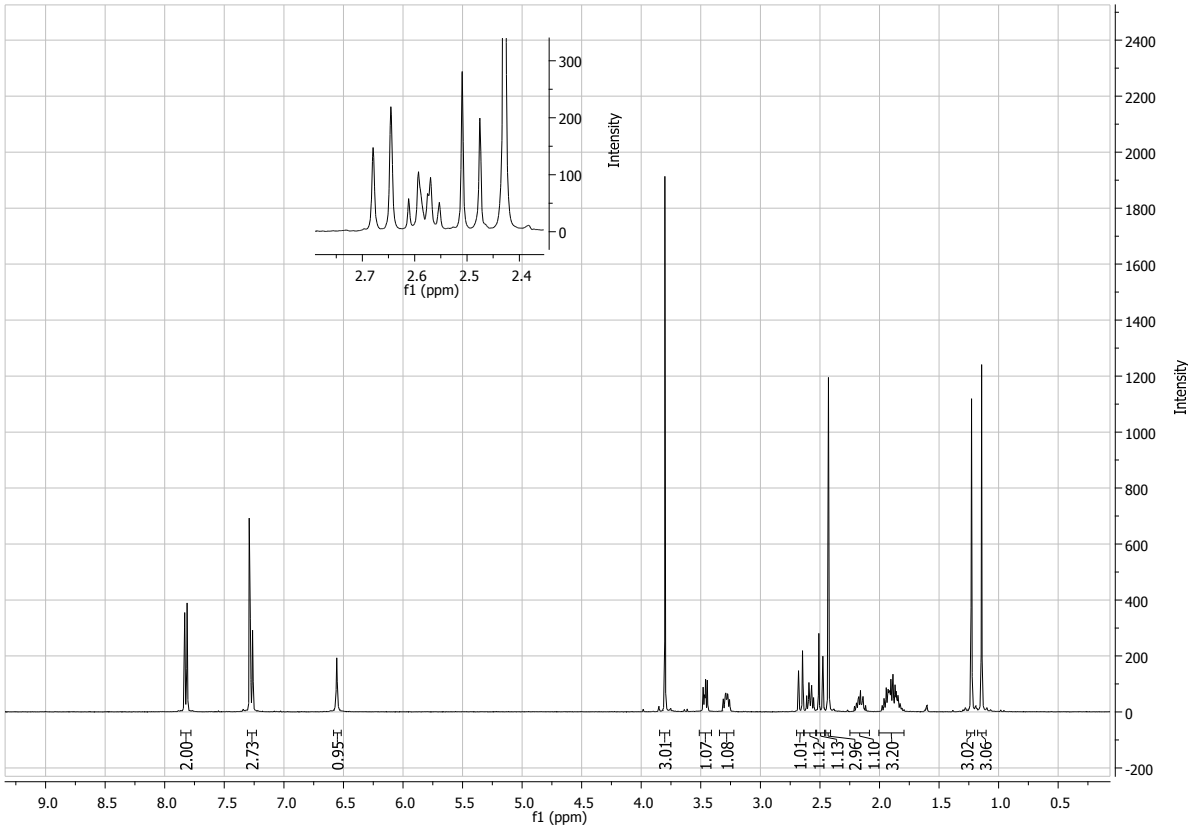
Intensity
f1 (ppm)
2.00
2.73
0.95
3.01
1.07
1.08
1.01
1.12
1.13
2.96
1.10
3.20
3.02
3.06

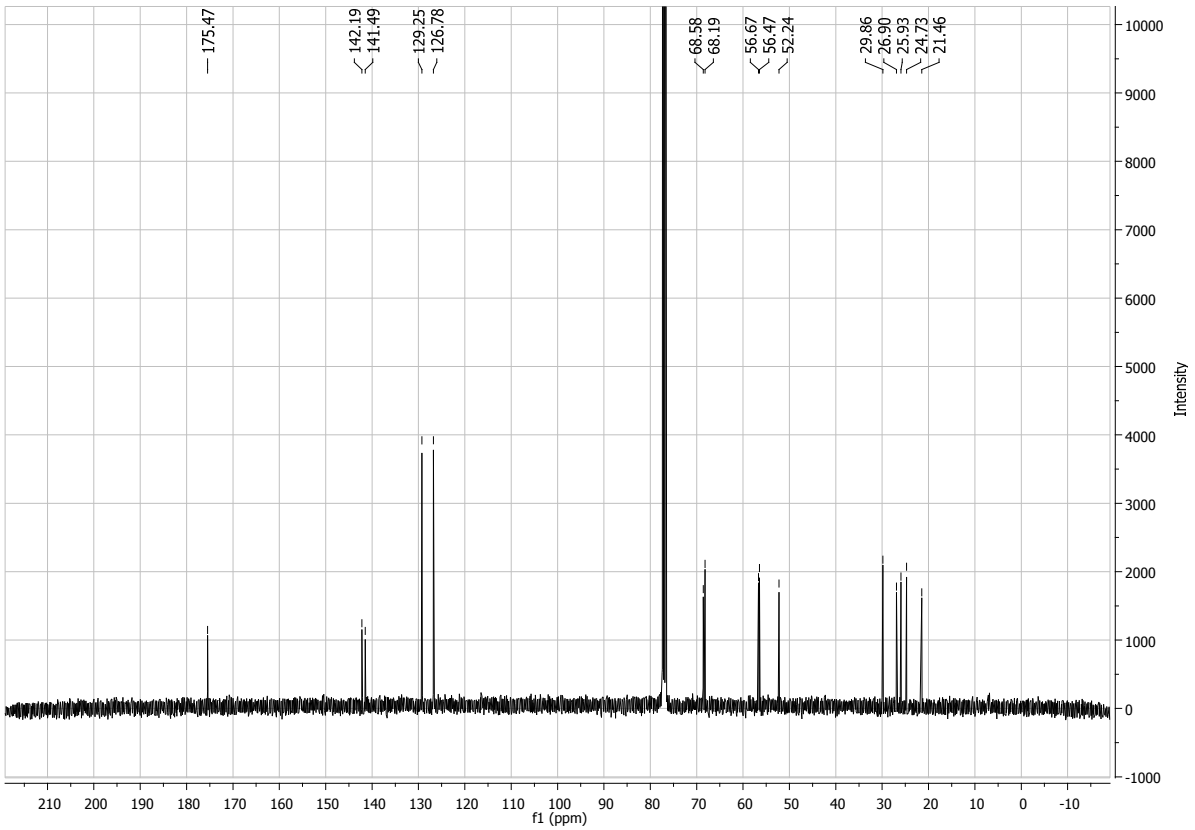
175.47
142.19
141.49
129.25
126.78
68.58
68.19
56.67
56.47
52.24
29.86
26.90
25.93
24.73
21.46
Intensity
f1 (ppm)

(*S*)-methyl 1-(2-methyl-2-(4-methylphenylsulfonamido)propyl)pyrrolidine-2-carboxylate (158b)

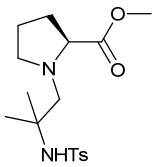

To a solution of **147** (700 mg, 4.23 mmol) and **150b** (1.00g, 4.23 mmol) in acetonitrile (40 mL), TEA (1.00 mL, 8.88 mmol) was added. The solution was warmed to 50 °C for 3 days and monitored *via* TLC (DCM/AcOEt 7:3). Once complete, the solvents were evaporated under reduced pressure to yield an orange solid. Flash chromatography on silica gel (DCM/AcOEt 7:3) gave **158b** (800 mg, 53 %) as a colourless solid.

$[\alpha]^{25}_{D}$ = -34.0 (c = 1, DCM); IR (neat, ν_{max}/cm^{-1}): 3246, 2976, 2877, 1732, 1437, 1322, 1150; ^{1}H-NMR (400 MHz, δ-$CDCl_3$): 1.14 (3H, s, C*H*$_3$), 1.22 (3H, s, C*H*$_3$), 1.79-1.99 (3H, m, $CH_2CH_2CH_2CH$, $CH_2CH_2CH_2CH$), 2.10-2.22 (1H, m, $CH_2CH_2CH_2CH$), 2.42 (3H, s, Ts-C*H*$_3$), 2.49 (1H, d, J_1 = 13.6 Hz, $CH_2C(CH_3)_2NH$), 2.53-2.62 (1H, m, C*H*$_2$N), 2.69 (1H, d, J_1 = 13.6 Hz, $CH_2C(CH_3)_2NH$), 3.23-3.34 (1H, m, C*H*$_2$N), 3.43-3.49 (1H, m, C*H*N), 3.56 (3H, s, OC*H*$_3$), 6.56 (1H, s, N*H*), 7.27 (2H, d, J_1 = 8.6 Hz, Ar*H*), 7.82 (2H, d, J_1 = 8.6 Hz Ar*H*); ^{13}C-NMR (100.2 MHz, δ-$CDCl_3$): 21.4, 24.7, 25.9, 26.9, 29.8, 52.2, 56.4. 56.6, 68.1, 68.5, 126.7, 129.2, 141.4, 142.1, 175.4; *m/z* (ESI): 709.3 (20 %), 355.2 (100); HRMS (ESI): $[C_{17}H_{26}N_2O_4S+H]^+$ requires 355.1679 found 355.1681.

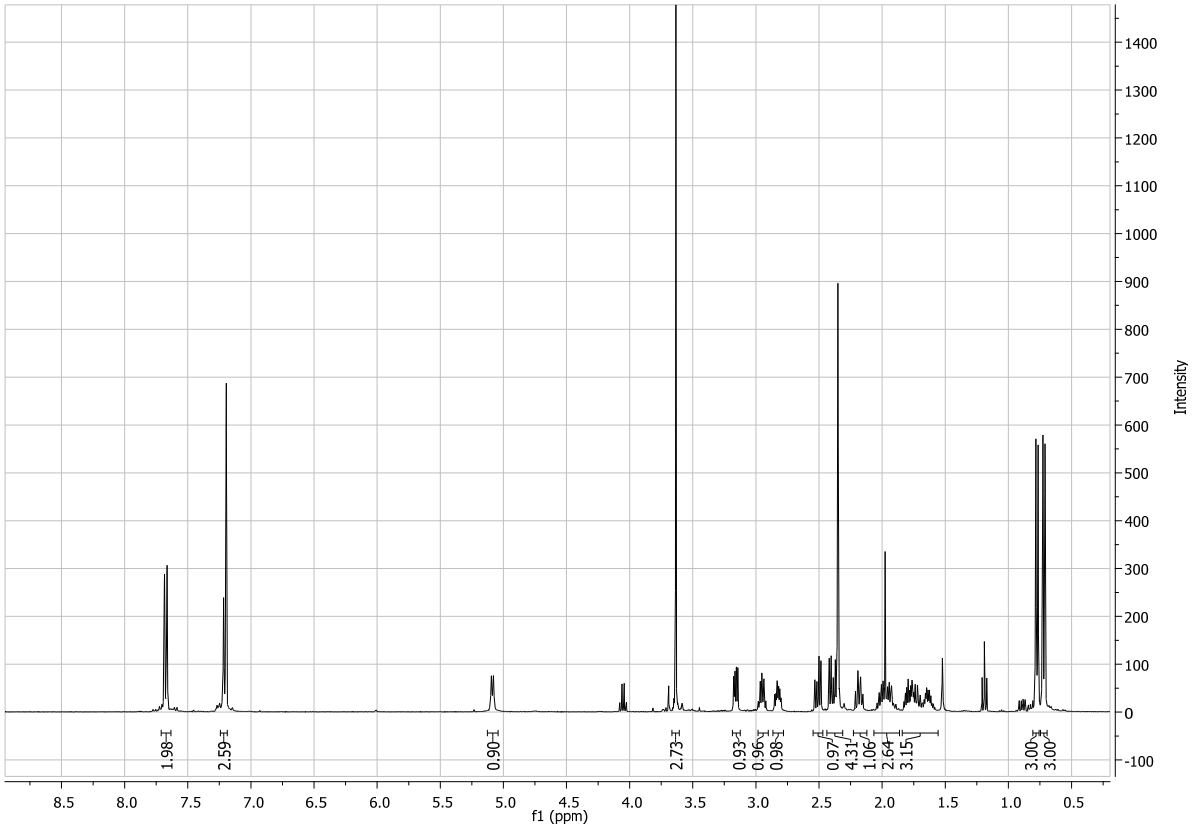
1.98
2.59
0.90
2.73
0.93
0.96
0.98
0.97
4.31
1.06
2.64
3.15
3.00
3.00
f1 (ppm)
Intensity

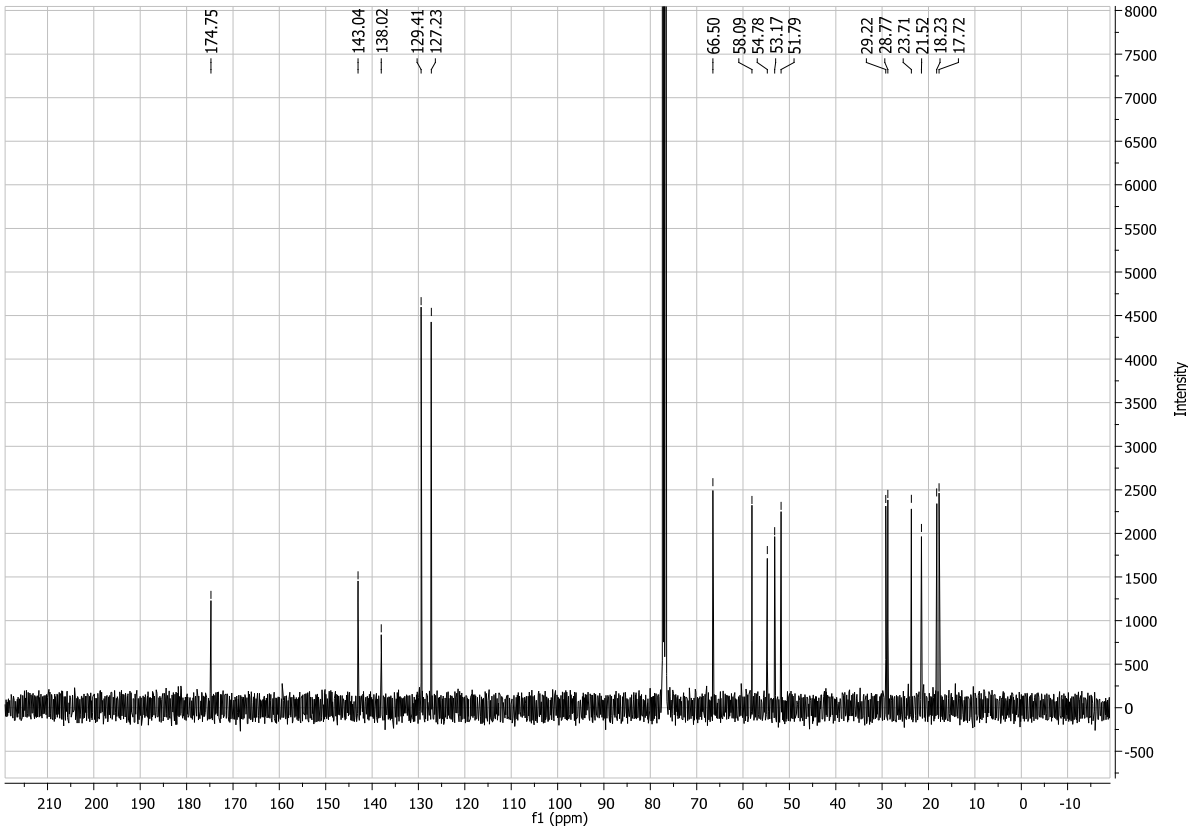
174.75
143.04
138.02
129.41
127.23
66.50
58.09
54.78
53.17
51.79
29.22
28.77
23.71
21.52
18.23
17.72
f1 (ppm)
Intensity

(*S*)-Methy1-((*S*)-3-methyl-2-(4-methylphenylsulfonamido)butyl)pyrrolidine-2-carboxylate (158c)

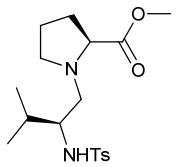

To a solution of **147** (700 mg, 4.18 mmol) and **150c** (1.00 g, 4.23 mmol) in acetonitrile (40 mL) was added TEA (1.00 mL, 8.88 mmol). The solution was warmed to 50 °C for 3 days and monitored *via* TLC (DCM/AcOEt 7:3). Once complete, the solvents were evaporated under reduced pressure to yield an orange solid. Flash chromatography on silica gel (DCM/AcOEt 7:3) gave **158c** (1.3 g, 84 %) as a yellow oil.

$[\alpha]^{25}_{D}$ = -36.5 (c = 1.25, DCM); IR (neat, ν_{max}/cm^{-1}): 3286, 2960, 1733, 1495, 1329; ^{1}H-NMR (400 MHz, δ-$CDCl_3$): 0.72 (3H, d, J_1 = 6.8 Hz, $CH(CH_3)_2$), 0.77 (3H, d, J_1 = 6.7 Hz, $CH(CH_3)_2$), 1.57-1.68 (2H, m, $CH_2CH_2CH_2CHN$), 1.69-1.86 (1H, m, $CH_2CH_2CH_2CHN$), 1.88-2.06 (2H, m, $CH_2CH_2CH_2CHN$, $CH(CH_3)_2$), 2.13-2.23 (1H, m, $CH_2CH_2CH_2CHN$), 2.35 (3H, s, Ts-CH_3), 2.39 (1H, dd, J_1 = 13.0 Hz, J_2 = 6.3 Hz, $CH_2CHNHTs$), 2.51 (1H, dd, J_1 = 12.9 Hz, J_2 = 6.3 Hz, $CH_2CHNHTs$), 2.79-2.86 (1H, m, $CH_2CH_2CH_2CHN$), 2.90-2.94 (1H, m, $CHCH(CH_3)_2$), 3.16 (1H, dd, J_1 = 8.8 Hz, J_2 = 4.5 Hz, $CH_2CH_2CH_2CHN$), 3.63 (3H, s, OCH_3), 5.09 (1H, d, J_1 = 6.4 Hz, N*H*Ts), 7.20 (2H, d, J_1 = 8.3 Hz, Ar*H*), 7.67 (2H, d, J_1 = 8.3 Hz, Ar*H*); ^{13}C-NMR (100.2 MHz, δ-$CDCl_3$): 17.7, 18.2, 21.5, 23.7, 28.7, 29.2, 51.7, 53.1, 54.7, 58.0, 66.5, 127.2, 129.4, 138.0, 143.0, 174.7; *m/z* (ESI): 737.3 (15 %) 369.2 (M+H, 100); HRMS (ESI): $[C_{18}H_{28}N_2O_4S+H]^+$ requires 369.1843 found 369.1841.

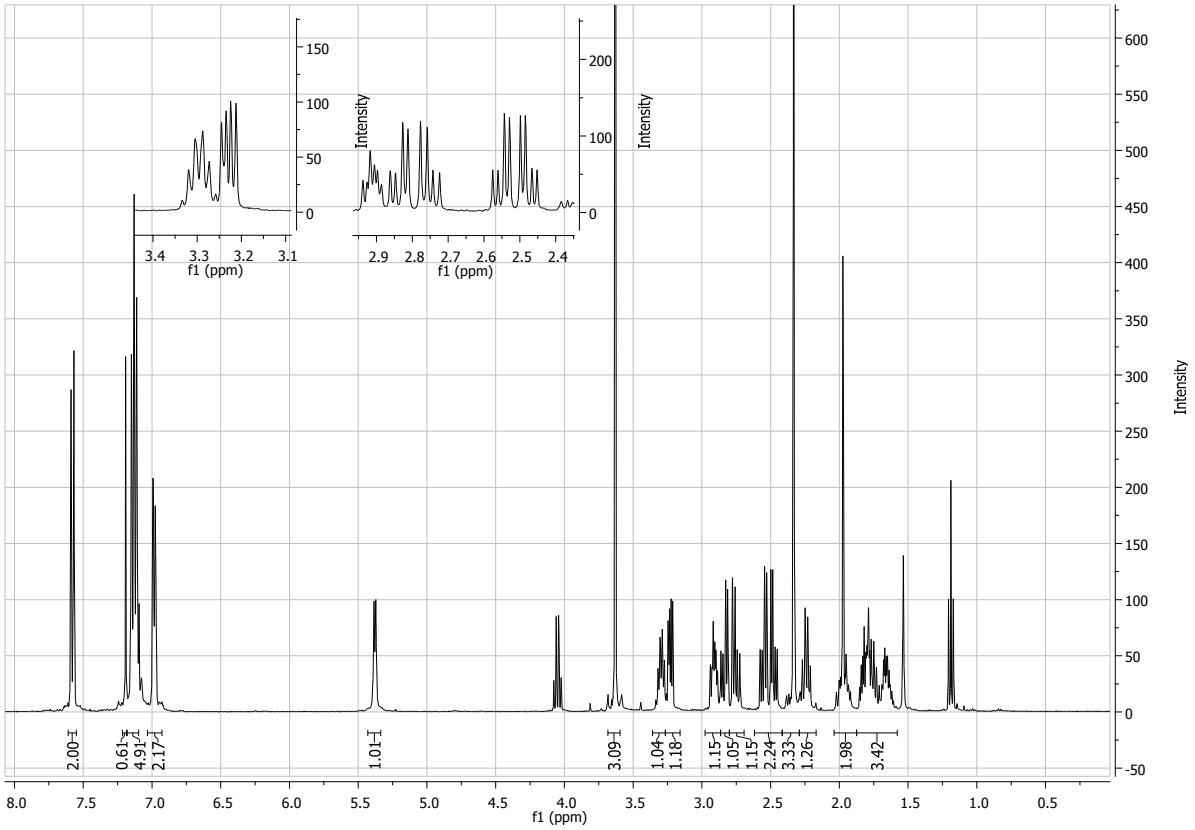
f1 (ppm)
Intensity
2.00
0.61
4.91
2.17
1.01
3.09
1.04
1.18
1.15
1.05
1.15
2.24
3.33
1.26
1.98
3.42

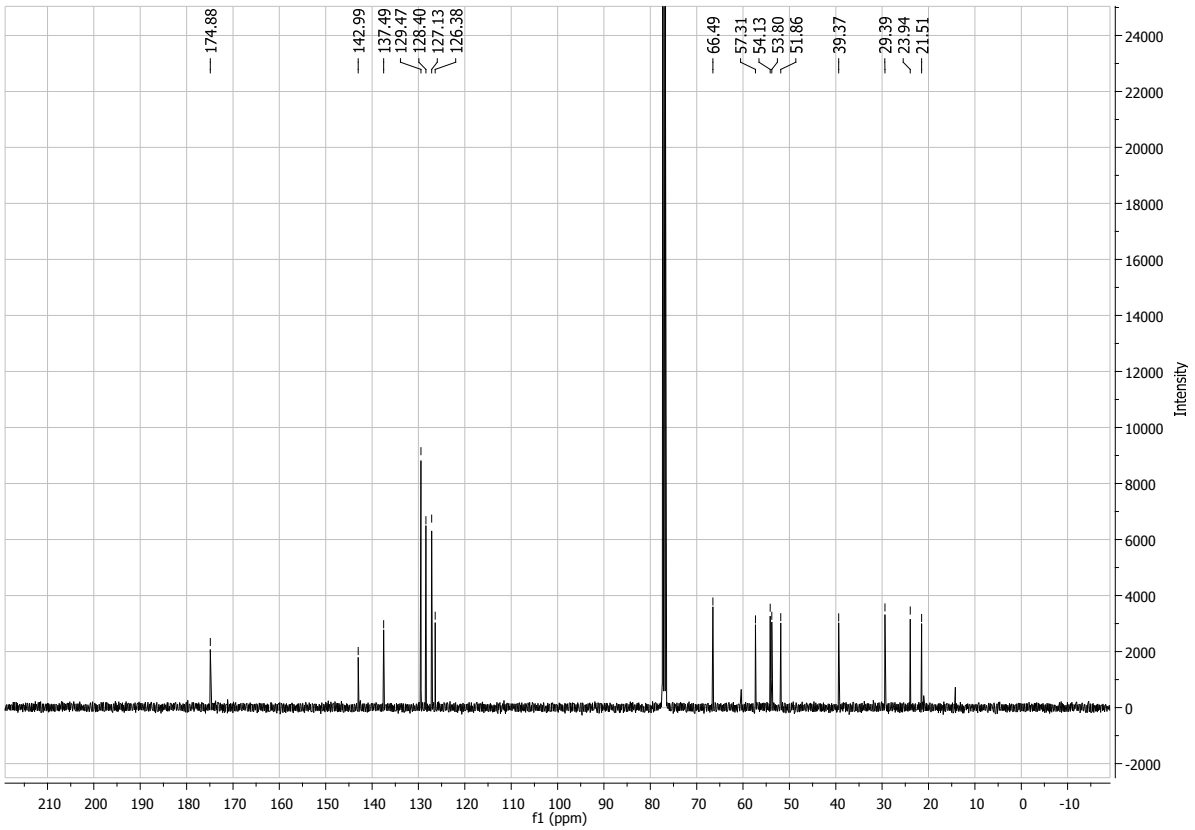
f1 (ppm)
Intensity
174.88
142.99
137.49
129.47
128.40
127.13
126.38
66.49
57.31
54.13
53.80
51.86
39.37
29.39
23.94
21.51

(*S*)-methyl 1-((*S*)-2-(4-methylphenylsulfonamido)-3-phenylpropyl)pyrrolidine-2-carboxylate (158d)

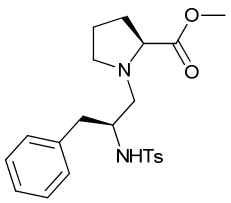

To a stirred solution of **147** (600 mg, 3.62 mmol) in acetonitrile (80 mL) was added TEA (1 eq.). A white precipitate of triethylamine hydrochloride was observed. After stirring at RT for ten minutes, **150d** (1.00 g, 3.62 mmol) dissolved in acetonitrile (20 mL). After addition of a further equivalent of TEA, the reaction was heated to reflux until disappearance of the aziridine spot on TLC (DCM/AcOEt 6:4). The solvent was then evaporated and the crude product purified by flash chromatography (DCM/EtOAc 6:4) to yield **158d** (600 mg, 39 %) as a pale yellow oil.

$[\alpha]^{25}_{D}$ = -40.1 (c = 1, DCM); IR (neat, ν_{max}/cm^{-1}): 3283, 2950, 1730, 1598, 1289, 1328, 1153; ^{1}H-NMR (400 MHz, δ-$CDCl_3$): 1.59-1.71 (1H, m, $CH_2CH_2CH_2CH$), 1.71-1.76 (2H, m, $CH_2CH_2CH_2CH$), 1.89-2.03 (1H, m, $CH_2CH_2CH_2CH$), 2.17-2.29 (1H, m, $CH_2CH_2CH_2CH$), 2.32 (3H, s, Ts-CH_3), 2.48 (1H, dd, J_1 = 12.9 Hz, J_2 = 5.7 Hz, $CHCH_2Ph$). 2.55 (1H, dd, J_1 = 13.0 Hz, J_2 = 5.8 Hz, $CHCH_2Ph$), 2.75 (1H, dd, J_1 = 13.9 Hz, J_2 = 7.5 Hz, $NCH_2CHNHTs$), 2.84 (1H, dd, J_1 = 13.9 Hz, J_2 = 5.8 Hz, $NCH_2CHNHTs$), 2.87-2.94 (1H, m, $CH_2CH_2CH_2CH$), 3.19-3.25 (1H, m, $CH_2CH_2CH_2CH$), 3.26-3.33 (1H, m, $NCH_2CHNHTs$), 3.63 (3H, s, OCH_3), 5.38 (1H, d, J_1 = 5.3 Hz, NH), 6.95-7.01 (2H, m, ArH), 7.07-7.16 (5H, m, ArH), 7.58 (2H, d, J_1 = 8.1 Hz, ArH); ^{13}C-NMR (100.2 MHz, δ-$CDCl_3$): 21.5, 23.9, 29.3, 39.3, 51.8, 53.8, 54.1, 57.3, 66.4, 126.3, 127.1, 128.4, 129.4, 137.4, 142.9, 174.8.

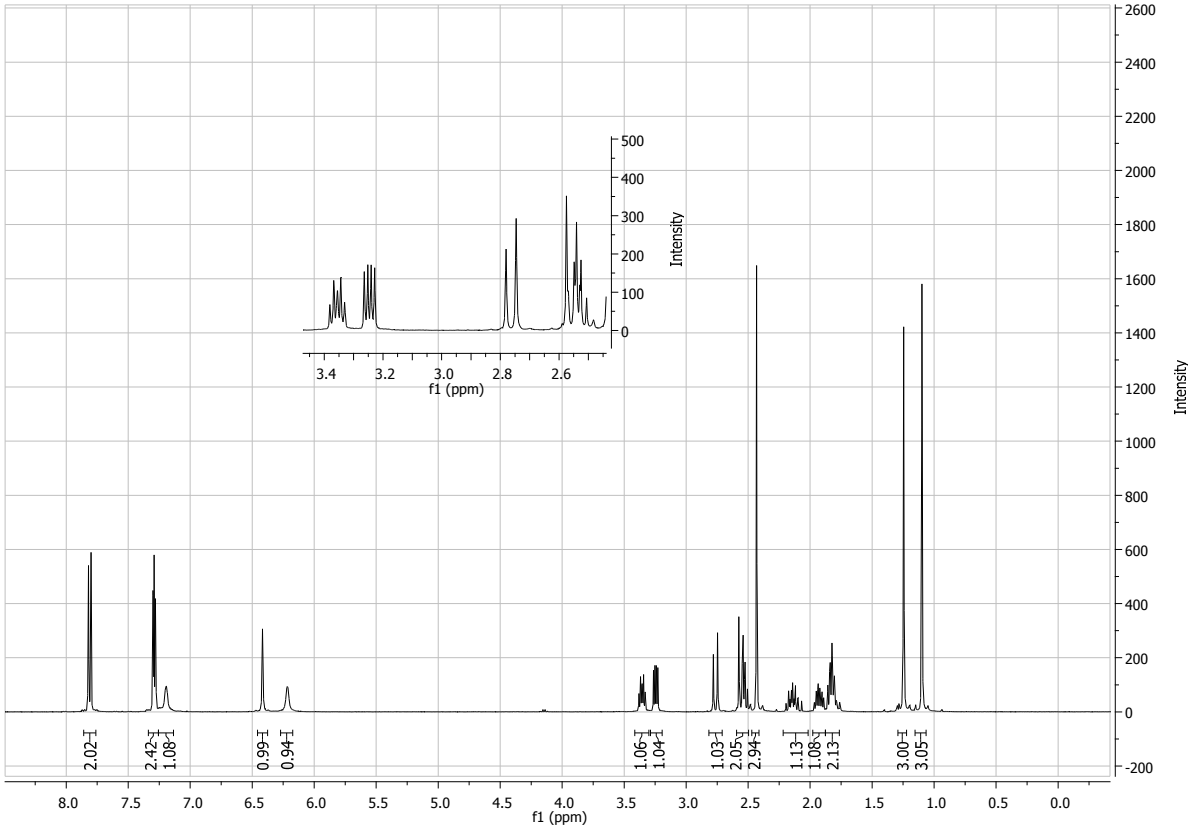
2.02
2.42
1.08
0.99
0.94
1.06
1.04
1.03
2.05
2.94
1.13
1.08
2.13
3.00
3.05
f1 (ppm)
Intensity

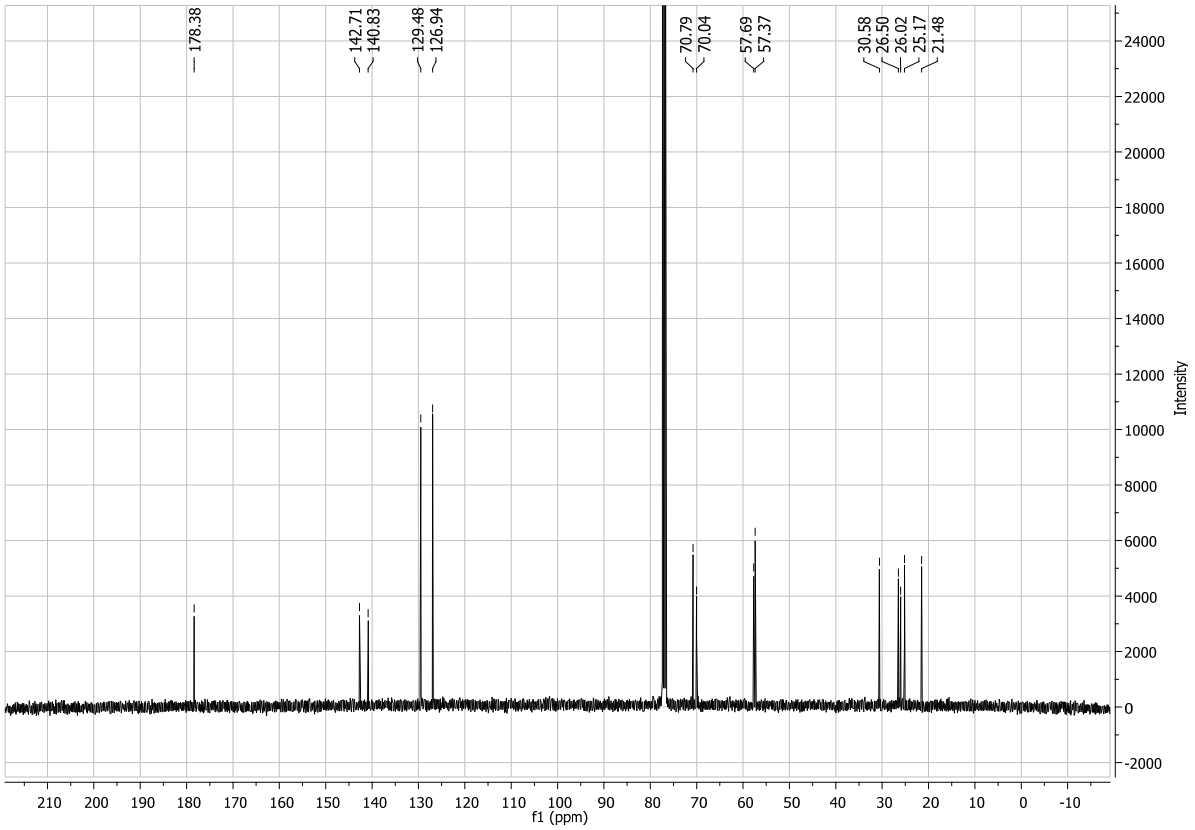
178.38
142.71
140.83
129.48
126.94
70.79
70.04
57.69
57.37
30.58
26.50
26.02
25.17
21.48
f1 (ppm)
Intensity

(*S*)-1-(2-methyl-2-(4-methylphenylsulfonamido)propyl)pyrrolidine-2-carboxamide (159b)

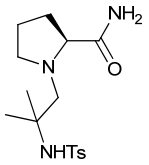

To a solution of **158b** (1.5 g, 4.4 mmol) in MeOH (15 mL) was added aqueous ammonia (relative density 0.88, 40 mL); on adding the latter, the formation of a white precipitate could be immediately observed. The mixture was allowed to stir at room temperature for 2 hours and refluxed overnight. Evaporation of all the solvents gave **159b** (1.3 g, 87 %) as a colourless solid. Recrystallisation from chloroform/petroleum spirit gave **159b** (1.1 g, 73 %) in higher purity.

$[\alpha]^{25}_{D}$ = -58.5 (c = 1, DCM); IR (neat, ν_{max}/cm^{-1}): 3429, 3380, 3173, 2974, 2876, 1665, 1367, 1316; ^{1}H-NMR (400 MHz, δ-$CDCl_3$): 1.11 (3H, s, C*H*$_3$), 1.24 (3H, s, C*H*$_3$), 1.75-1.86 (2H, m, $CH_2CH_2CH_2CH$), 1.87-1.99 (1H, m, $CH_2CH_2CH_2CH$), 2.05-2.21 (1H, m, $CH_2CH_2CH_2CH$), 2.43 (3H, s, Ts-C*H*$_3$), 2.49-2.60 (2H, m, C*H*$_2$N, C*H*$_2$C(CH$_3$)), 2.73 (1H, d, J_1 = 13.8 Hz, C*H*$_2$C(CH$_3$)), 3.25 (1H, dd, J_1 = 9.3 Hz, J_2 = 4.8 Hz, C*H*N), 3.30-3.41 (1H, m, C*H*$_2$N), 6.22 (1H, s, N*H*$_2$), 6.42 (1H, s, N*H*), 7.23 (1H, s, N*H*$_2$), 7.29 (2H, d, J_1 = 8.5 Hz, Ar*H*), 7.80 (2H, d, J_1= 8.5 Hz, Ar*H*); ^{13}C-NMR (100.2 MHz, δ-$CDCl_3$): 21.4, 25.1, 26.0, 26.5, 30.5, 57.3, 57.6, 70.0, 70.7, 126.9, 129.4, 140.8, 142.7, 178.3; *m/z* (ESI): 340.2 (100 %), 679.3 (10); HRMS (ESI): $[C_{16}H_{25}N_3O_3S+H]^+$ requires 340.1696 found 340.1694.

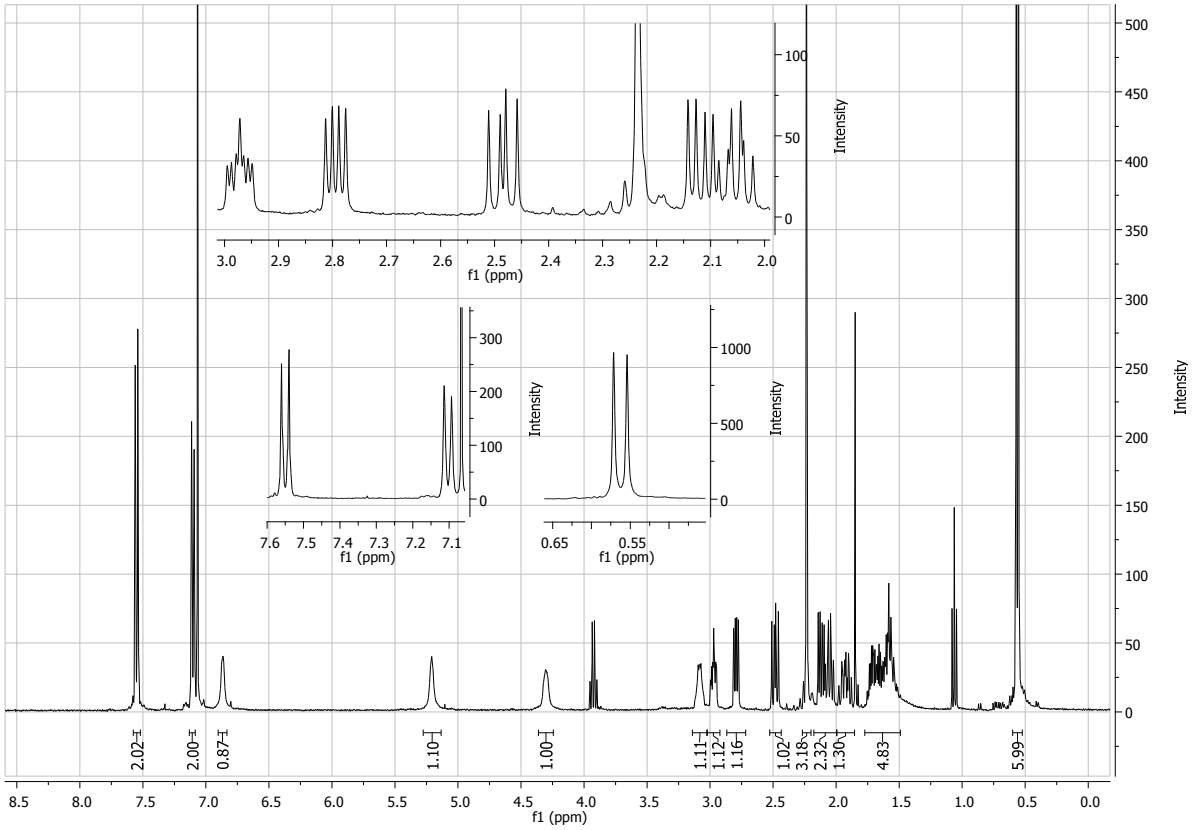
f1 (ppm)
Intensity
2.02
2.00
0.87
1.10
1.00
1.11
1.12
1.16
1.02
3.18
2.32
1.30
4.83
5.99

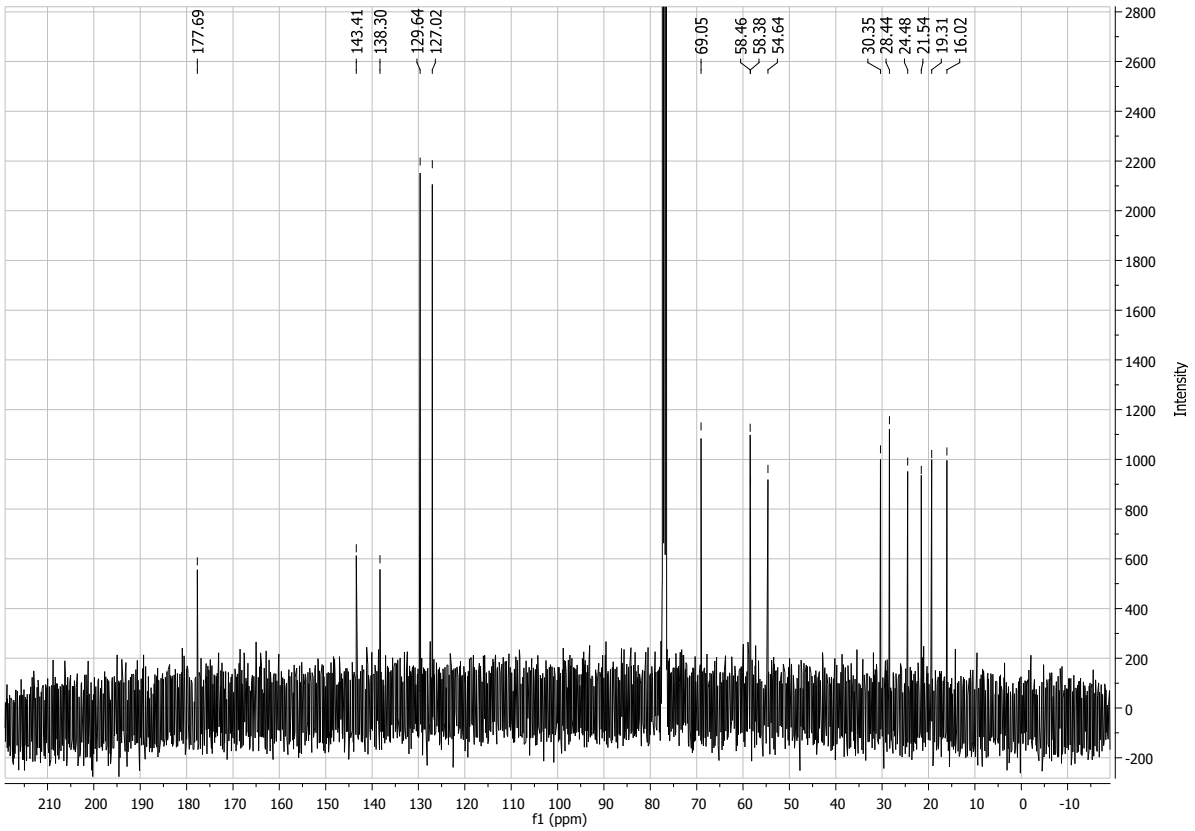
f1 (ppm)
Intensity
177.69
143.41
138.30
129.64
127.02
69.05
58.46
58.38
54.64
30.35
28.44
24.48
21.54
19.31
16.02

(*S*)-1-((*S*)-3-Methyl-2-(4-methylphenylsulfonamido)butyl)pyrrolidine-2-carboxamide (159c)

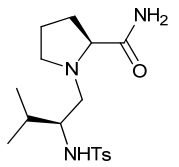

To a solution of **158c** in MeOH (15 mL) was added dilute ammonia (40 mL) and the resulting mixture allowed to stir at room temperature overnight. Evaporation of the solvents under reduced pressure gave **159c** as a thick yellow oil, that was purified by flash chromatography on silica gel (DCM/ethyl acetate 1:1) to give **159c** (1.0 g, 95 %) as a pale yellow solid.

m.p. 62.7–63.3 °C; $[\alpha]^{25}_{D}$ = -55.0 (c = 1, DCM); IR (KBr, ν_{max}/cm^{-1}): 3442, 3291, 3190, 2959, 1672,1460, 1326; ^{1}H-NMR (400 MHz, δ-$CDCl_3$): 0.56 (6H, d, J_1 = 6.9 Hz, C*H*$_3$), 1.49-1.76 (4H, m, $CH_2CH_2CH_2CHN$, $CH_2CH_2CH_2CHN$, $CH(CH_3)_2$), 1.86-1.99 (1H, m, $CH_2CH_2CH_2CHN$), 2.01-2.07 (1H, m, $CH_2CH_2CH_2CHN$,), 2.12 (1H, dd, J_1 = 12.6 Hz, J_2 = 5.9 Hz, $CH_2CHNHTs$), 2.24 (3H, s, Ts-C*H*$_3$), 2.48 (1H, dd, J_1 =12.6 Hz, J_2 = 8.5 Hz, $CH_2CHNHTs$), 2.79 (1H, dd, J_1 = 9.8 Hz, J_2 = 5.0 Hz, $CH_2CH_2CH_2CHN$), 2.97 (1H, ddd, J_1 = 9.1 Hz, J_2 = 6.5 Hz, J_3 = 3.0 Hz, $CH_2CH_2CH_2CHN$), 3.03-3.12 (1H, m, $CHCH(CH_3)_2$), 4.30 (1H, s, N*H*$_2$), 5.21 (1H, s, N*H*), 6.86 (1H, s, N*H*$_2$), 7.10 (2H, d, J_1 = 8.6 Hz, Ar*H*), 7.55 (2H, d, J_1 = 8.6 Hz, Ar*H*); ^{13}C-NMR (100.2 MHz, δ-$CDCl_3$): 16.0, 19.3, 21.5, 24.4, 28.4, 30.3, 54.6, 58.3, 58.4, 69.0, 127.0, 129.6, 138.3, 143.4, 177.6; *m/z* (ESI): 849.4 (5 %), 707.3 (50), 496.2 (2), 354.1 (100); HRMS (ESI): $[C_{17}H_{27}N_3O_3S+H]^+$ requires 354.1846 found 354.1847.

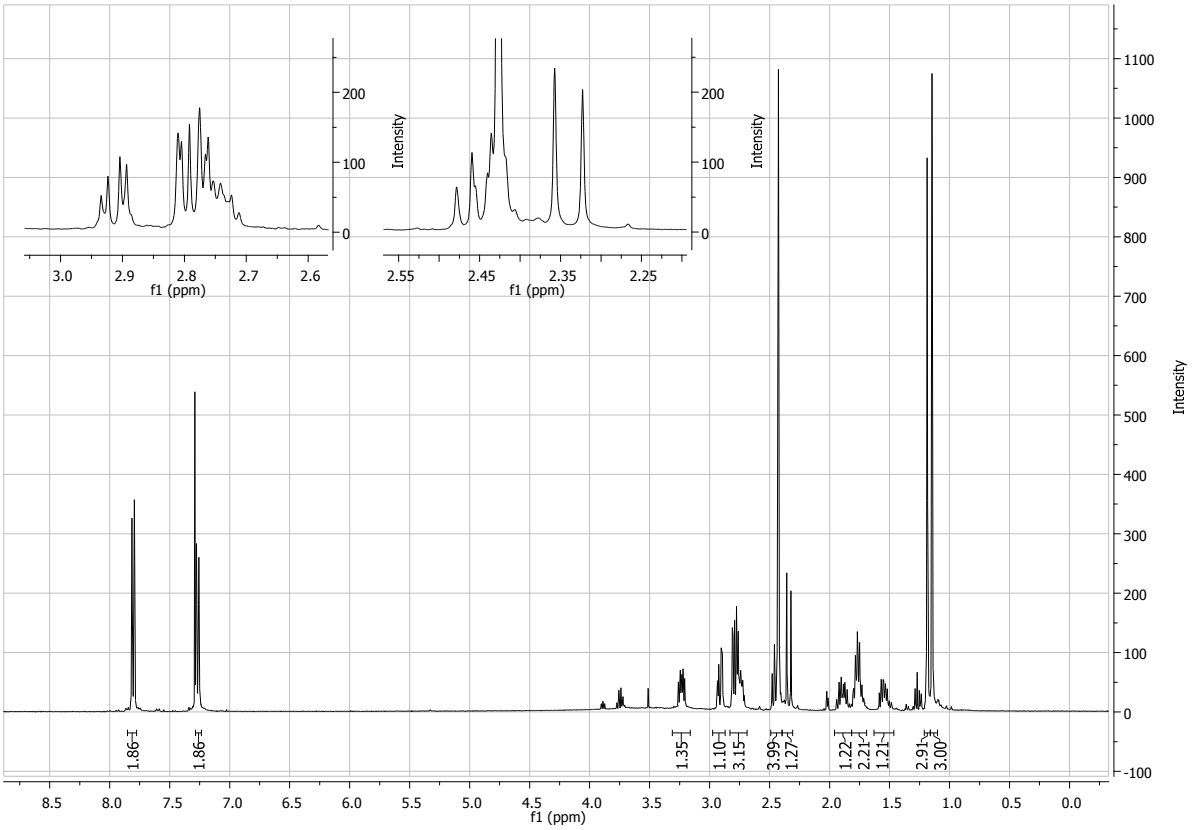
f1 (ppm)
Intensity
1.86
1.86
1.35
1.10
3.15
3.99
1.27
1.22
2.21
1.21
2.91
3.00

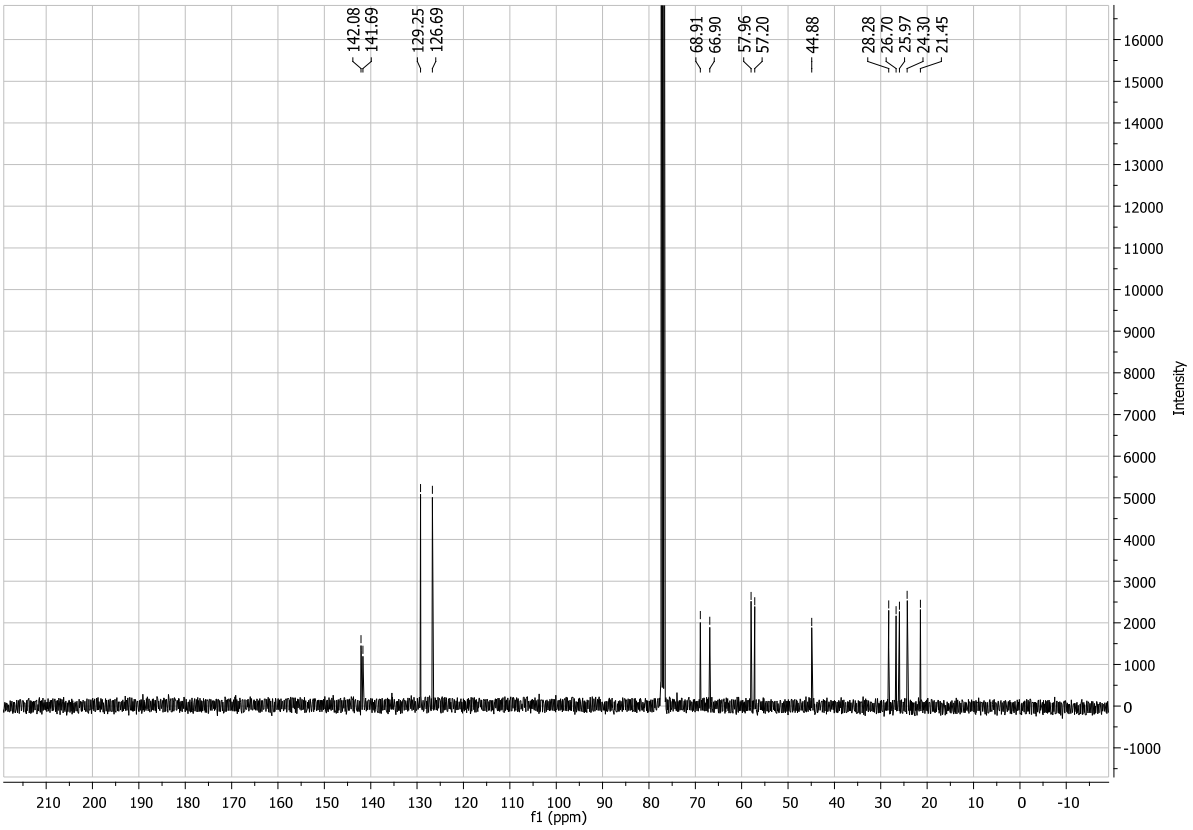
142.08
141.69
129.25
126.69
68.91
66.90
57.96
57.20
44.88
28.28
26.70
25.97
24.30
21.45
f1 (ppm)
Intensity

(*S*)-N-(1-(2-(aminomethyl)pyrrolidin-1-yl)-2-methylpropan-2-yl)-4-methylbenzene sulfonamide (160b)

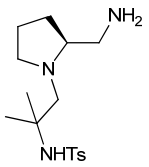

To a stirred suspension of $LiAlH_4$ (1.50 g, 40.5 mmol) in dry THF (50 mL) kept under a nitrogen atmosphere, **159b** (2.50 g, 7.36 mmol) was added in portions over 5 minutes. The mixture was then refluxed overnight and quenched by careful addition of a 10 % aqueous solution of KOH (w/w, 6 mL). Refluxing was continued until the aluminium salts were coloured white. The precipitate was filtrated and the organic layer recovered. Further recovery of the product was obtained by refluxing the salts in THF for 1 hour and combining the organic phases together. Once the solvents were evaporated, flash chromatography (petroleum spirit/diethyl ether then chloroform/MeOH) on the thick orange oil obtained yielded **160b** (1.1 g, 46 %) as a pale yellow oil.

$[\alpha]^{25}_D$ = -23.7 (c = 1, DCM); IR (neat, ν_{max}/cm^{-1}): 3440 (br), 3061, 2969, 2873, 1315, 1302,1145; ^{1}H-NMR (400 MHz, δ-$CDCl_3$): 1.14 (3H, s, C*H*$_3$), 1.18 (3H, s, C*H*$_3$), 1.47-1.60 (1H, m, $CH_2CH_2CH_2CH$), 1.72-1.81 (2H, m, $CH_2CH_2CH_2CH$), 1.83-1.95 (1H, m, $CH_2CH_2CH_2CH$), 2.34 (1H, d, J_1 = 13.8 Hz, $CH_2C(CH_3)_2$), 2.42 (3H, s, Ts-C*H*$_3$), 2.43-2.48 (1H, m, C*H*$_2$N), 2.70-2.82 (3H, m, C*H*N, $CH_2C(CH_3)_2$, C*H*$_2$NH), 2.88 (1H, dd, J_1 = 11.6 Hz, J_2 = 4.4 Hz, C*H*$_2$NH), 3.19-3.27 (1H, m, C*H*$_2$N), 7.26 (2H, d, J_1 = 8.3 Hz, Ar*H*), 7.80 (2H, d, J_1 = 8.3 Hz, Ar*H*); ^{13}C-NMR (100.2 MHz, δ-$CDCl_3$): 21.4, 24.3, 25.9, 26.7, 28.2, 44.8, 57.2, 57.9, 66.9, 68.9, 126.6, 129.2, 141.6, 142.0; *m/z* (ESI): 326.1 (100 %), 651.3 (40), HRMS (ESI): $[C_{16}H_{27}N_3O_2S+H]^+$ requires 326.1897 found 326.1894.

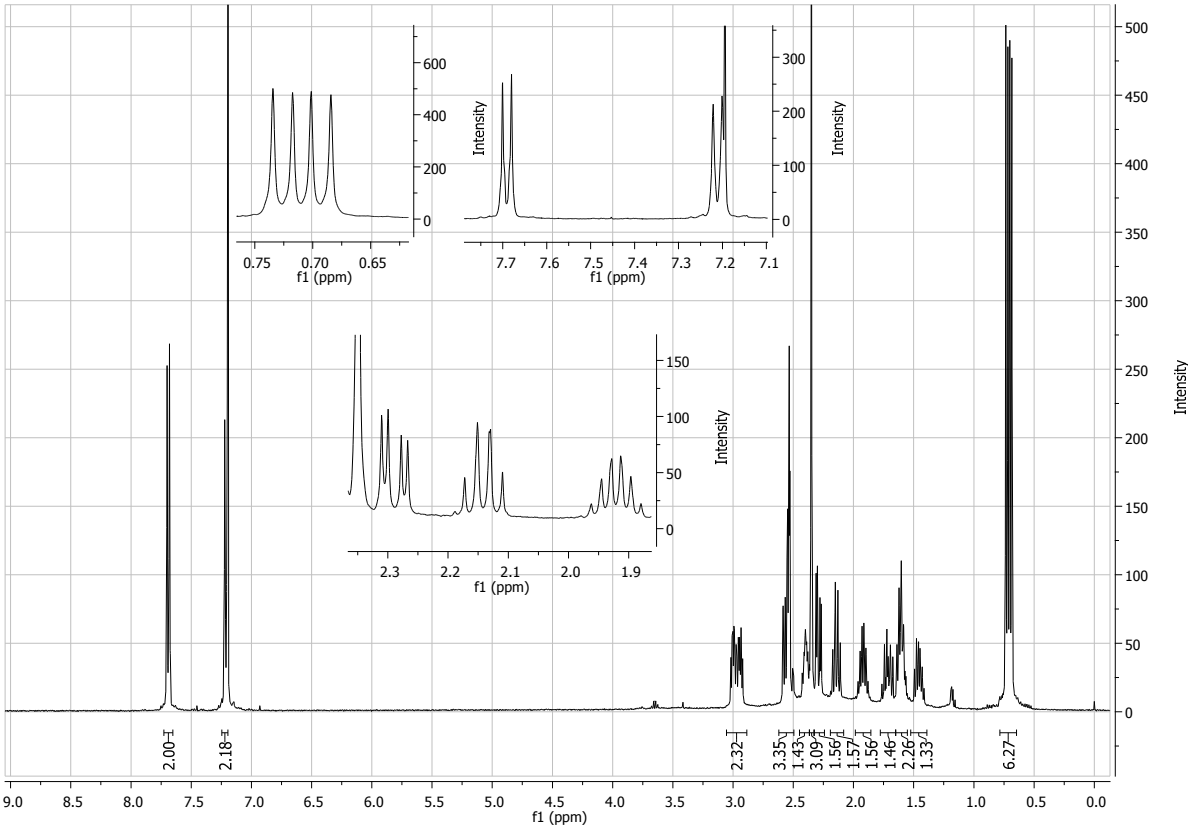
f1 (ppm)
Intensity
2.00
2.18
2.32
3.35
1.43
3.09
1.56
1.57
1.56
1.46
2.26
1.33
6.27

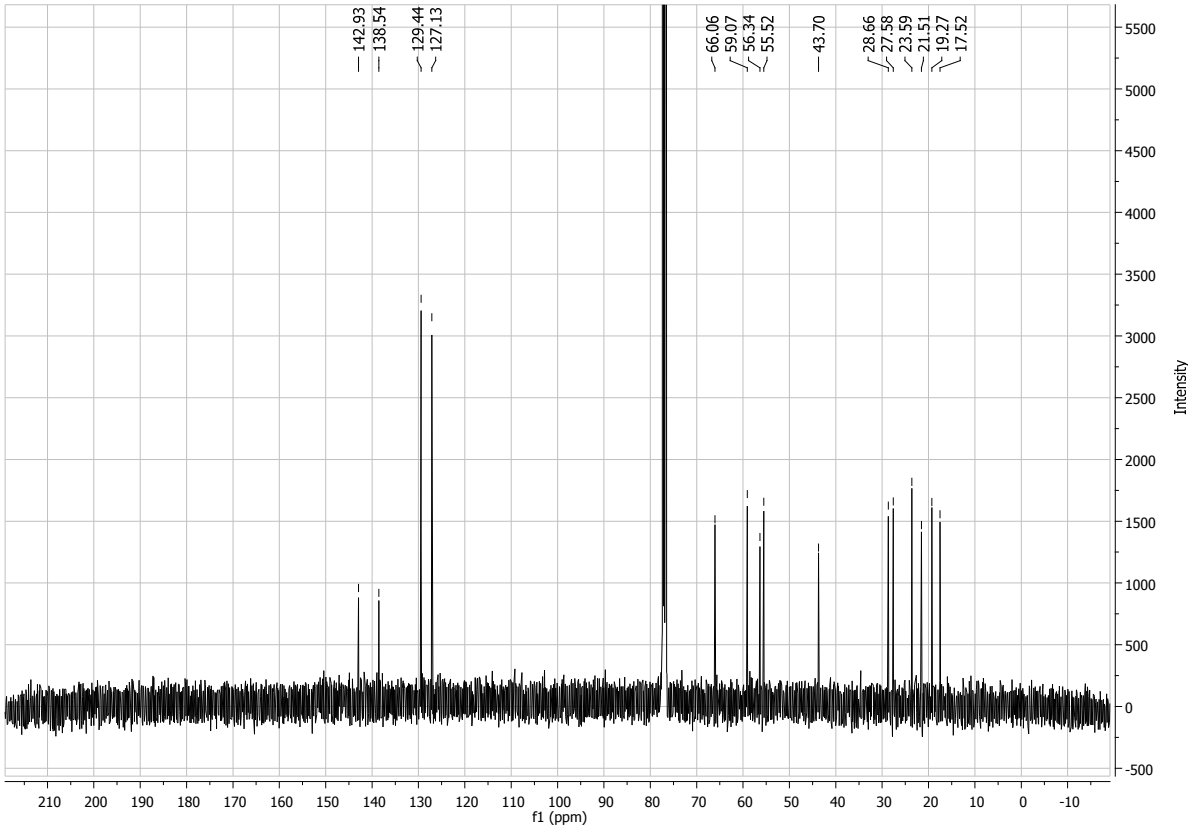
142.93
138.54
129.44
127.13
66.06
59.07
56.34
55.52
43.70
28.66
27.58
23.59
21.51
19.27
17.52
f1 (ppm)
Intensity

_N_-((_S_)-1-((_S_)-2-(Aminomethyl)pyrrolidin-1-yl)-3-methylbutan-2-yl)-4-methylbenzene sulfonamide (160b)

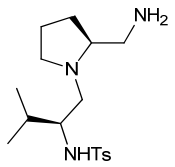

To a stirred suspension of $LiAlH_4$ (430 mg, 11.3 mmol) in dry THF (50 mL) kept under a nitrogen atmosphere, **159b** (1.0 g, 2.8 mmol) was added in portions over 5 minutes. The mixture was then refluxed overnight and quenched by careful addition of a 10% aqueous solution of KOH (w/w, 10 mL). Refluxing was continued until the aluminium salts were coloured white. The mixture was filtrated and the organic layer recovered. Further recovery of the product was obtained by refluxing the precipitated salts in THF for one hour and combining the organic phases together. Once the solvents were evaporated, the product was recovered as a pale yellow oil (900 mg). The product was purified by flash chromatography on silica gel (DCM/MeOH 9:1 then chloroform/MeOH 9:1). After purification, **160b** (0.5 g, 52 %) was obtained as a yellow solid.

m.p. 139-140 °C; $[\alpha]^{25}_D$ = -23.4 (c = 0.5, MeOH); IR (KBr, ν_{max}/cm^{-1}): 3355, 3302, 3061, 2959, 2798, 1598, 1321; ^{1}H-NMR (400 MHz, δ-$CDCl_3$): 0.69 (3H, d, J_1 = 6.8 Hz, CH_3), 0.71 (3H, d, J_1 = 6.9 Hz, CH_3), 1.40-1.51 (1H, m, $CH_2CH_2CH_2CHN$), 1.55-1.65 (2H, m, $CH_2CH_2CH_2CHN$), 1.65-1.77 (1H, m, $CH_2CH_2CH_2CHN$), 1.92 (1H, td, J_1 = 13.5 Hz, J_2 = 6.8 Hz, CH(CH_3)$_2$), 2.10-2.20 (1H, m, CH_2CH_2CH_2CHN), 2.27 (1H, dd, J_1 = 13.0 Hz, J_2 = 4.3 Hz, CH_2CHNHTs), 2.34 (3H, s, Ts-CH_3), 2.36-2.43 (1H, m, $CH_2CH_2CH_2CHN$), 2.48-2.60 (3H, m, CH_2NH_2, CH_2CHNHTs), 2.90-2.96 (1H, m, CH_2CH_2CH_2CHN), 2.97-3.02 (1H, m, $CH_2CHNHTs$), 7.21 (2H, d, J_1 = 8.3 Hz, ArH), 7.70 (2H, d, J_1 = 8.3 Hz, ArH); ^{13}C-NMR (100.2 MHz, δ-$CDCl_3$): 17.5, 19.2, 21.5, 23.5, 27.5, 28.6, 43.7, 55.5, 56.3, 59.0, 66.0, 127.1, 129.4, 138.5, 142.9; *m/z* (ESI): 362.1 (10 %), 340.2 (M+H); HRMS (ESI): $[C_{17}H_{29}N_3O_2S+H]^+$ requires 340.2053 found 340.2060.

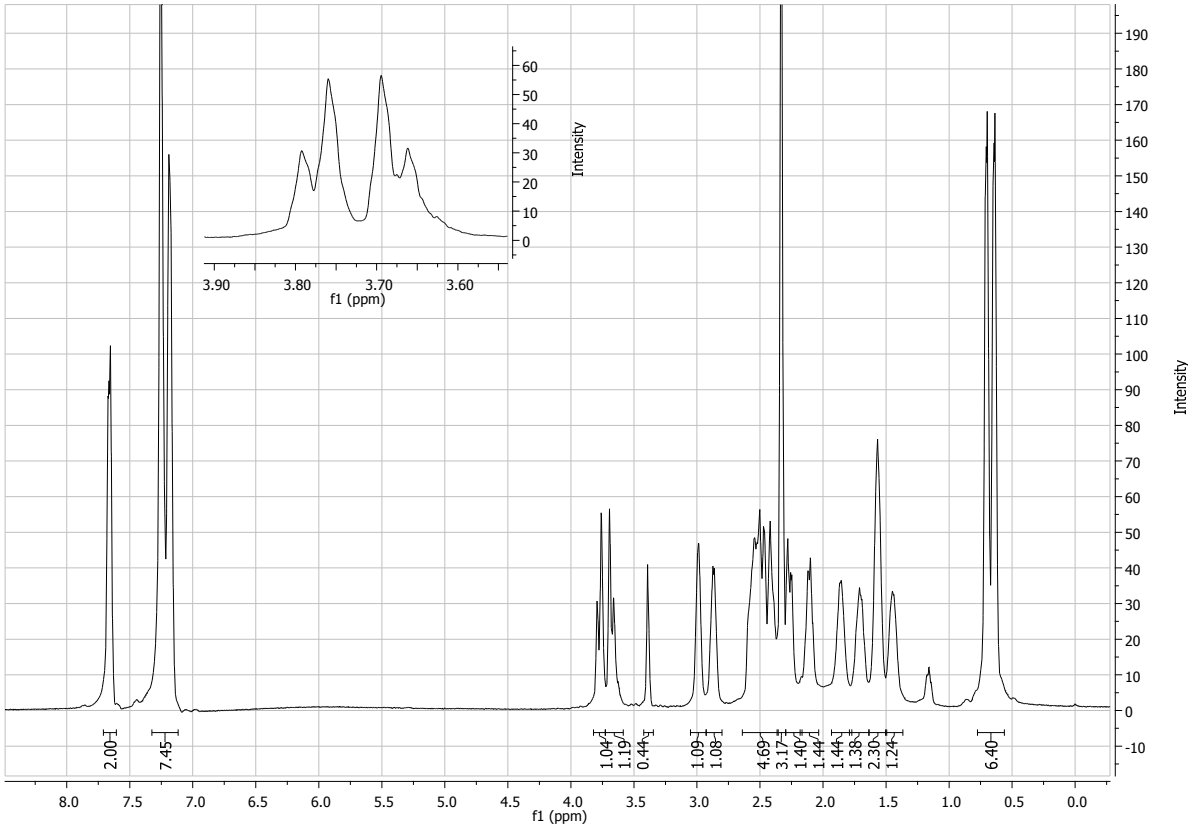
Intensity
f1 (ppm)
2.00
7.45
1.04
1.19
0.44
1.09
1.08
4.69
3.17
1.40
1.44
1.44
1.38
2.30
1.24
6.40

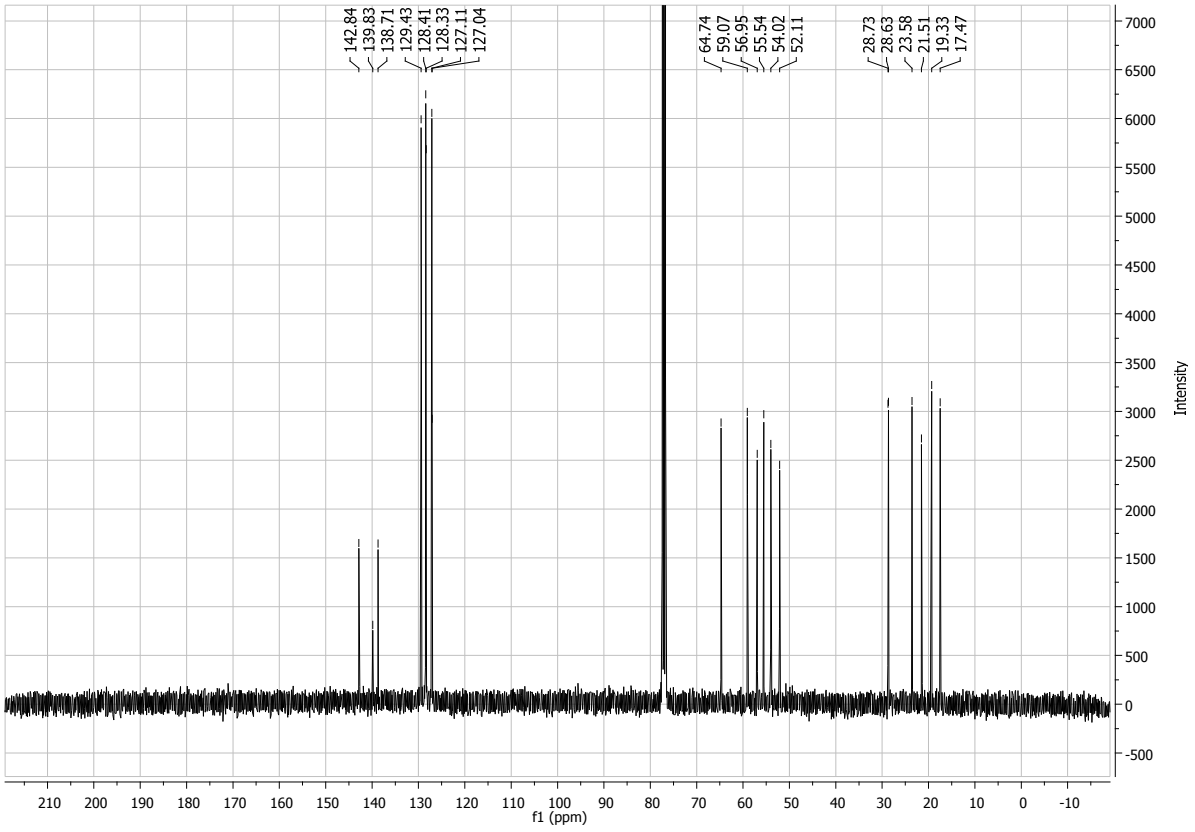
142.84
139.83
138.71
129.43
128.41
128.33
127.11
127.04
64.74
59.07
56.95
55.54
54.02
52.11
28.73
28.63
23.58
21.51
19.33
17.47
Intensity
f1 (ppm)

_N_-((_S_)-1-((_S_)-2-((Benzylamino)methyl)pyrrolidin-1-yl)-3-methylbutan-2-yl)-4-methylbenzenesulfonamide (161c)

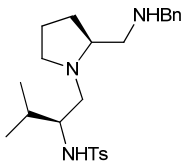

To a solution of **160c** (200 mg, 0.590 mmol) in DCM kept at room temperature was added K_2CO_3 (85 mg, 0.65 mmol). After stirring for 10 minutes, benzyl bromide was added (70 µl, 0.59 mmol) and the stirring continued. TLC (DCM/MeOH 9:1) showed completion after 16 hours. Evaporation of the solvents under reduced pressure gave the product as a dark resin. The crude was then purified by flash chromatography on silica gel (DCM/ethyl acetate 1:1) to yield the desiderd product as a thick pale yellow resin (0.15 g, 59 %).

$[\alpha]^{25}_D$ = -15.9 (c = 1, DCM); IR (neat, ν_{max}/cm^{-1}): 3583, 3284, 3062, 3027, 2960, 2807, 1453, 1327; ^{1}H-NMR (400 MHz, δ-$CDCl_3$): 0.54-0.77 (6H, m, (C*H*$_3$)$_2$), 1.36-1.48 (1H, m, $CH_2CH_2CH_2CHN$), 1.49-1.64 (2H, m, $CH_2CH_2CH_2CHN$) 1.63-1.77 (1H, m, $CH_2CH_2CH_2CHN$), 1.77-1.93 (1H, m, C*H*(CH$_3$)$_2$), 2.03-2.17 (1H, m, C*H*$_2$CH$_2$CH$_2$CHN), 2.20-2.30 (1H, m, C*H*$_2$CHNHTs), 2.33 (3H, s, Ts-C*H*$_3$) 2.36-2.62 (4H, m, C*H*$_2$NHBn, $CH_2CH_2CH_2CHN$, C*H*$_2$CHNHTs), 2.79-2.92 (1H, m, C*H*$_2$CH$_2$CH$_2$CHN), 2.94-3.04 (1H, m, (CH$_3$)$_2$CHC*H*), 3.39 (1H, s, N*H*), 3.67 (1H, d, J_1 = 13.1 Hz, C*H*$_2$Bn), 3.77 (1H, d, J_1 = 13.1 Hz, C*H*$_2$Bn), 7.14-7.29 (7H, m, Ar*H*), 7.62-7.70 (2H, m, Ar*H*); ^{13}C-NMR (100.2 MHz, δ-$CDCl_3$): 17.4, 19.3, 21.5, 23.5, 28.6, 28.7, 52.1, 54.0, 55.5, 56.9, 59.0, 64.7, 127.0, 127.1, 128.3, 128.4, 129.4, 138.7, 139.8, 142.8; *m/z* (ESI): 859.4 (5 %), 520.2 (5), 430.2 (100), 323.1 (5); HRMS (ESI): $[C_{24}H_{35}N_3O_2S+H]^+$ requires 430.2523 found 430.2527.

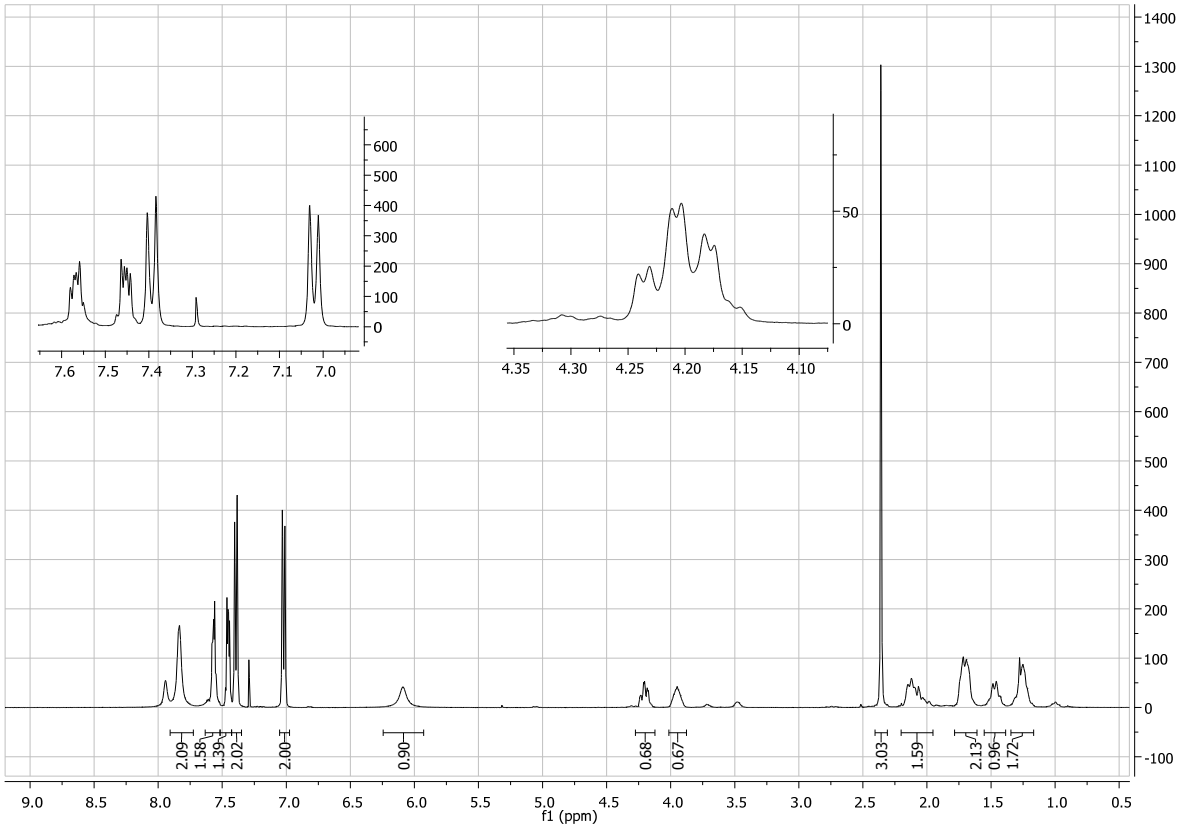
2.09
1.58
1.39
2.02
2.00
0.90
0.68
0.67
3.03
1.59
2.13
0.96
1.72
f1 (ppm)

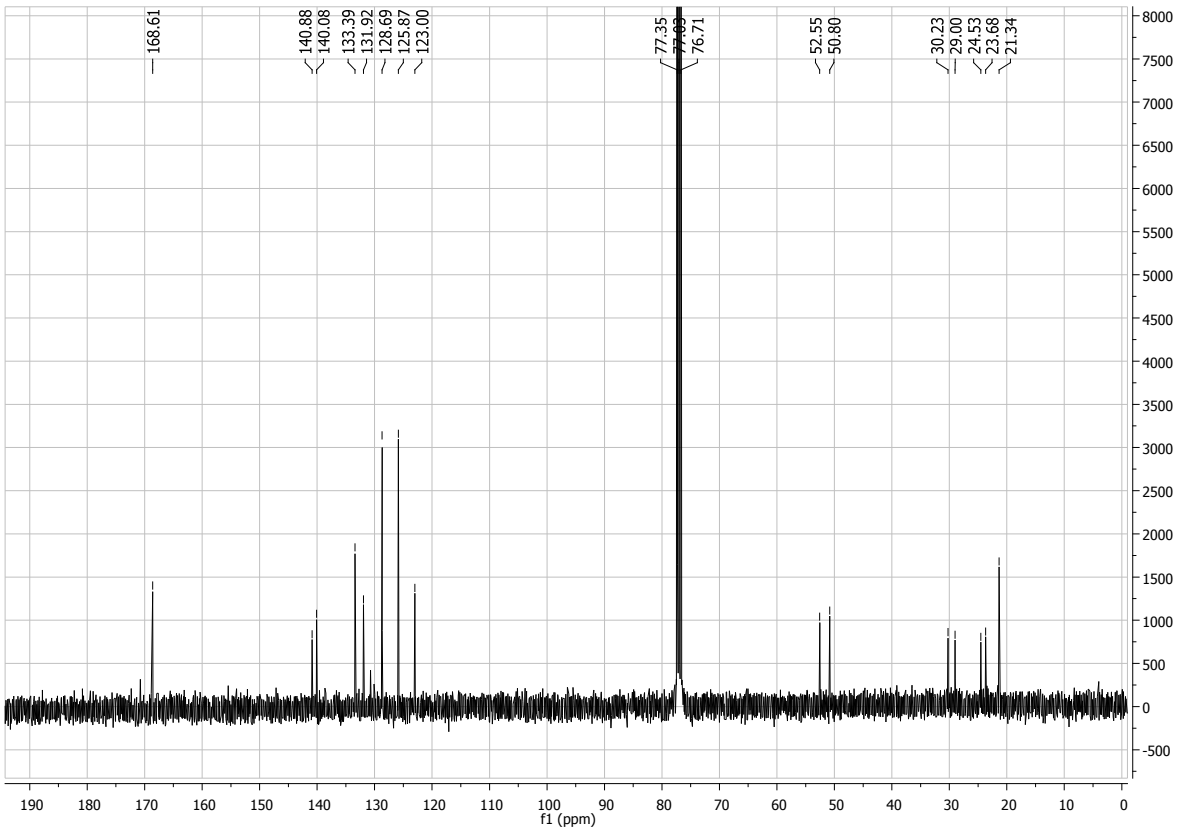
168.61
140.88
140.08
133.39
131.92
128.69
125.87
123.00
77.35
77.03
76.71
52.55
50.80
30.23
29.00
24.53
23.68
21.34
f1 (ppm)

(1*R*, 2*R*)-2-(1,3-dioxoisoindolin-2-yl)cyclohexanaminium 4-methylbenzenesulfonate ((*R*, *R*)-165)[54]

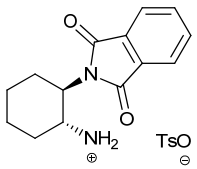

A solution of *p*-toluenesulfonic acid monohydrate (13.3 g, 70.0 mmol) in xylene or toluene, **(*R*, *R*)-133** (8.0 g, 70 mmol) and phthalic anhydride (10.3 g, 70.0 mmol) was heated using a Dean-Stark trap and the water-organic solvent azeotrope distilled off as it formed. The distillation was continued overnight and the system was then allowed to cool down to room temperature. Shortly afterwards, the product began precipitating. The solid was filtered and washed with cold 1,4-dioxane and hexane to yield **(*R*, *R*)-165** (20.0 g, 81 %) as a grey solid that was purified by recrystallisation from dioxane/ toluene.

The same procedure was used to obtain the (1*S*, 2*S*) isomer.

m.p. 238.7-243.2 °C, lit.[54] 249-252 °C; $[\alpha]^{25}_{D}$ = -14.7 (c = 1, $CHCl_3$), lit[54] – 15.8 (c = 1 $CHCl_3$); IR (neat, ν_{max}/cm^{-1}): 3512, 1703, 1386, 1370, 1126, 1037, 1013; ^{1}H-NMR (400 MHz, δ-$CDCl_3$): 1.20-1.34 (2H, m, C*H*$_2$CH$_2$CHN), 1.40-1.54 (1H, m, CH$_2$C*H*$_2$CHN), 1.64-1.80 (3H, m, C*H*$_2$CH$_2$CHN, CH$_2$C*H*$_2$CHN), 1.96-2.23 (2H, m, CH$_2$C*H*$_2$CHN), 2.37 (3H, s, Ts-C*H*$_3$), 3.89-4.02 (1H, m, CH$_2$CH$_2$C*H*N), 4.22 (1H, dt, J_1 = 11.0 Hz, J_2 = 3.0 Hz, CH$_2$CH$_2$C*H*N), 6.09 (1H, broad s, N*H*), 7.02 (2H, d, J_1 = 8.6 Hz, Ar*H*), 7.39 (2H, d, J_1 = 8.6 Hz, Ar*H*), 7.41-7.48 (2H, m, Ar*H*), 7.54-7.60 (2H, m, Ar*H*), 8.05-8.08 (2H, broad s, N*H*); ^{13}C-NMR (100.2 MHz, δ-$CDCl_3$): 21.3, 23.6, 24.5, 29.0, 30.2, 50.8, 52.5, 123.0, 125.8, 128.6, 131.9, 133.3, 140.0, 140.8, 168.6; *m/z* (ESI, cation): 245.1 (100 %), 277.1 (25); (ESI, anion) 171.0; HRMS (ESI): $[C_{14}H_{17}O_2N_2]^+$ requires 245.1285 found 245.1284.

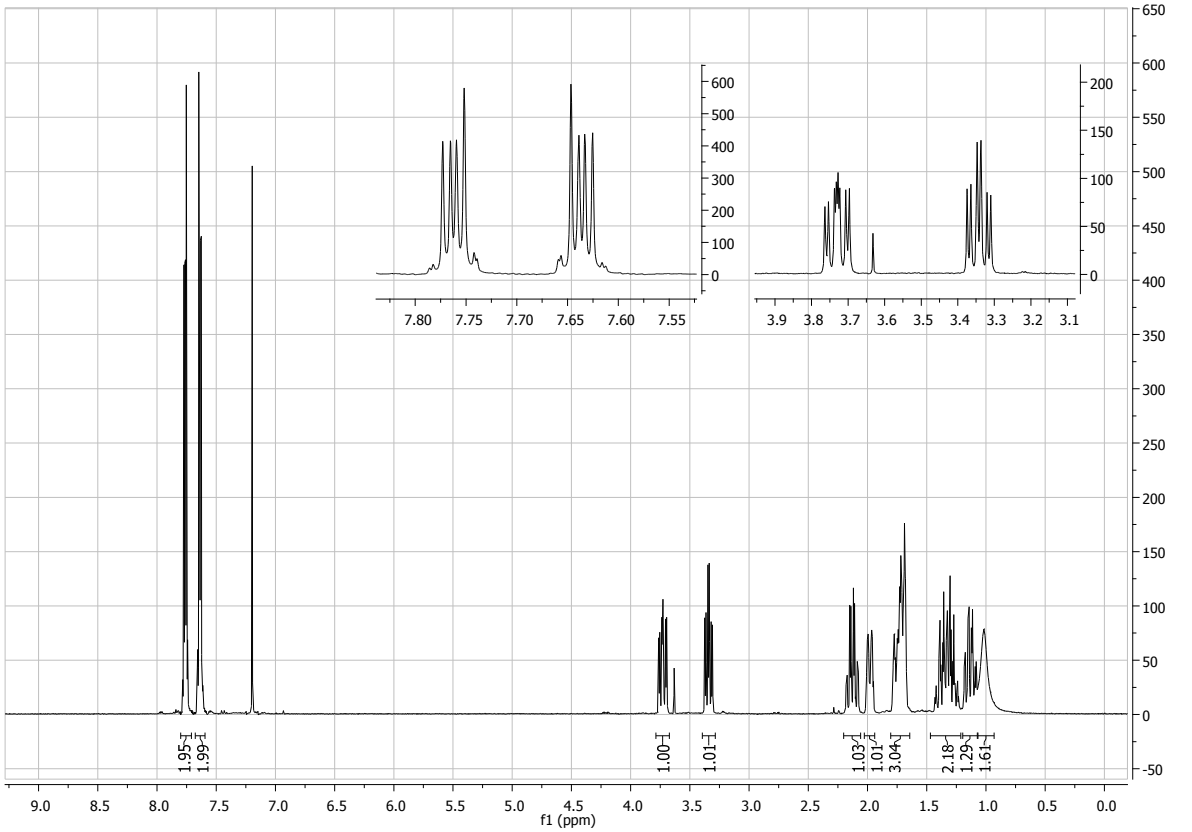
1.95
1.99
1.00
1.01
1.03
1.01
3.04
2.18
1.29
1.61
f1 (ppm)

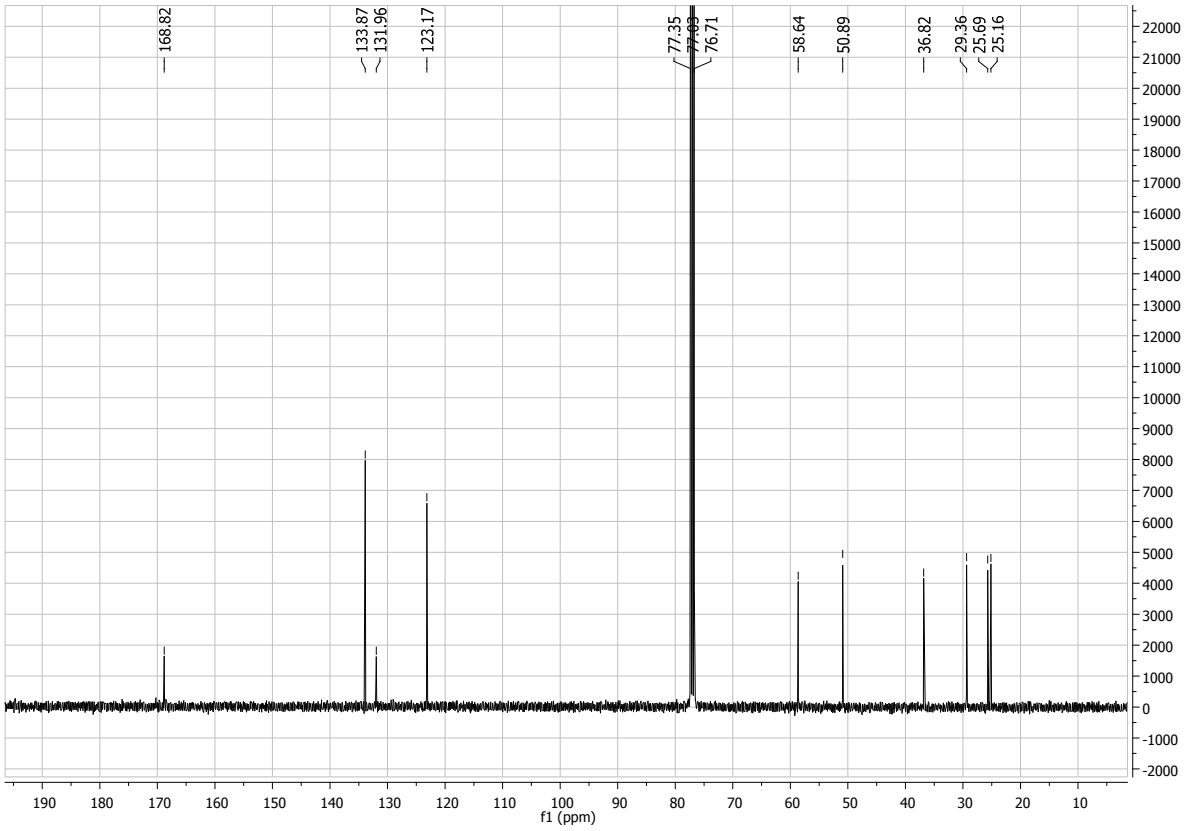
168.82
133.87
131.96
123.17
77.35
77.03
76.71
58.64
50.89
36.82
29.36
25.69
25.16
f1 (ppm)

2-((1*R*, 2*R*)-2-aminocyclohexyl)isoindoline-1,3-dione ((*R*, *R*)-166)[54]

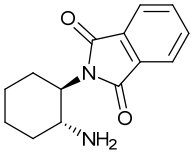

The monoprotected diamine **((*R*, *R*)-165)** (8.00 g, 56.9 mmol) was dissolved in DCM (100 mL) and stirred overnight with saturated sodium bicarbonate solution (20 mL). The layers were separated and the aqueous phase extracted with DCM (3 x 20 mL) and ethyl acetate (2 x 20 mL). The combined organic phases were dried over $MgSO_4$ and the solvent evaporated *in vacuo* to yield **(*R*, *R*)-166** (8.0 g, 47 %) as a light yellow powder.

The same procedure was used to obtain the (1*S*, 2*S*) isomer.

m.p. 120.7-125.2 °C, lit.[54] 123-125 °C; $[\alpha]^{25}_{D}$ = -20 (c = 1, $CHCl_3$), lit[54] -79.3 (c = 1, $CHCl_3$), (*S*, *S*) isomer; $[\alpha]^{25}_{D}$= 17.5 (c = 1 $CHCl_3$); IR (neat, ν_{max}/cm^{-1}): 3364, 2963, 2863, 1695, 1368; ^{1}H-NMR (400 MHz, δ-$CDCl_3$): 1.02 (2H, broad s, N*H*$_2$), 1.06-1.21 (1H, m, CH_2CH_2CHN), 1.24-1.44 (2H, m, CH_2CH_2CHN), 1.65-1.80 (3H, m, CH_2CH_2CHN, CH_2CH_2CHN), 1.93-2.02 (1H, m, CH_2CH_2CHN), 2.06-2.18 (1H, m, CH_2CH_2CHN), 3.36 (1H, dt, J_1 = 10.6 Hz, J_2 = 3.9 Hz, CH_2CH_2CHN), 3.70-3.78 (1H, m, CH_2CH_2CHN), 7.60-7.65 (2H, m, Ar*H*), 7.22-7.78 (2H, m, Ar*H*); ^{13}C-NMR (100.2 MHz, δ-$CDCl_3$): 25.2, 25.6, 29.3, 36.5, 50.8, 58.6, 123.1, 131.9, 133.87, 168.8; *m/z* (ESI): 199.1 (5 %), 228.1 (5), 245.1 (100), 267.1 (10); HRMS (ESI): $[C_{14}H_{16}N_2O_2+H]^+$ requires 245.1285 found 245.1286.

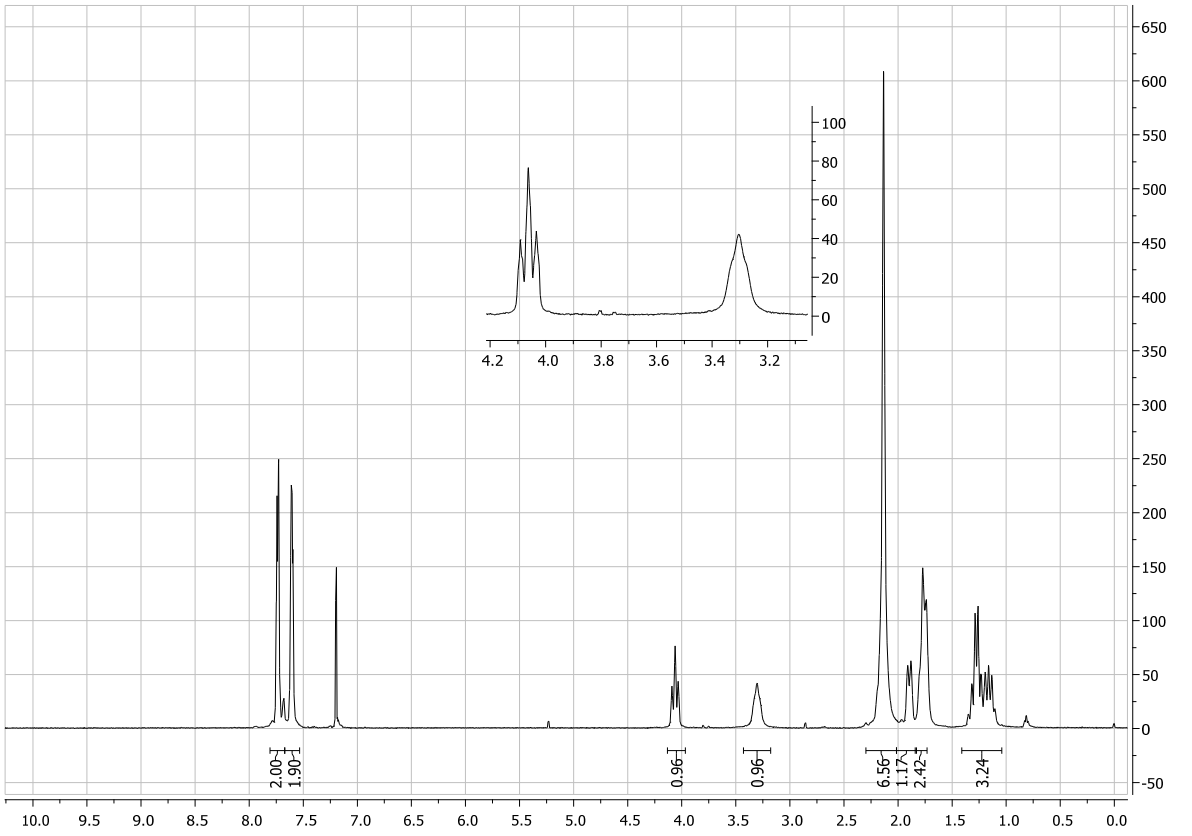
2.00
1.90
0.96
0.96
6.56
1.17
2.42
3.24

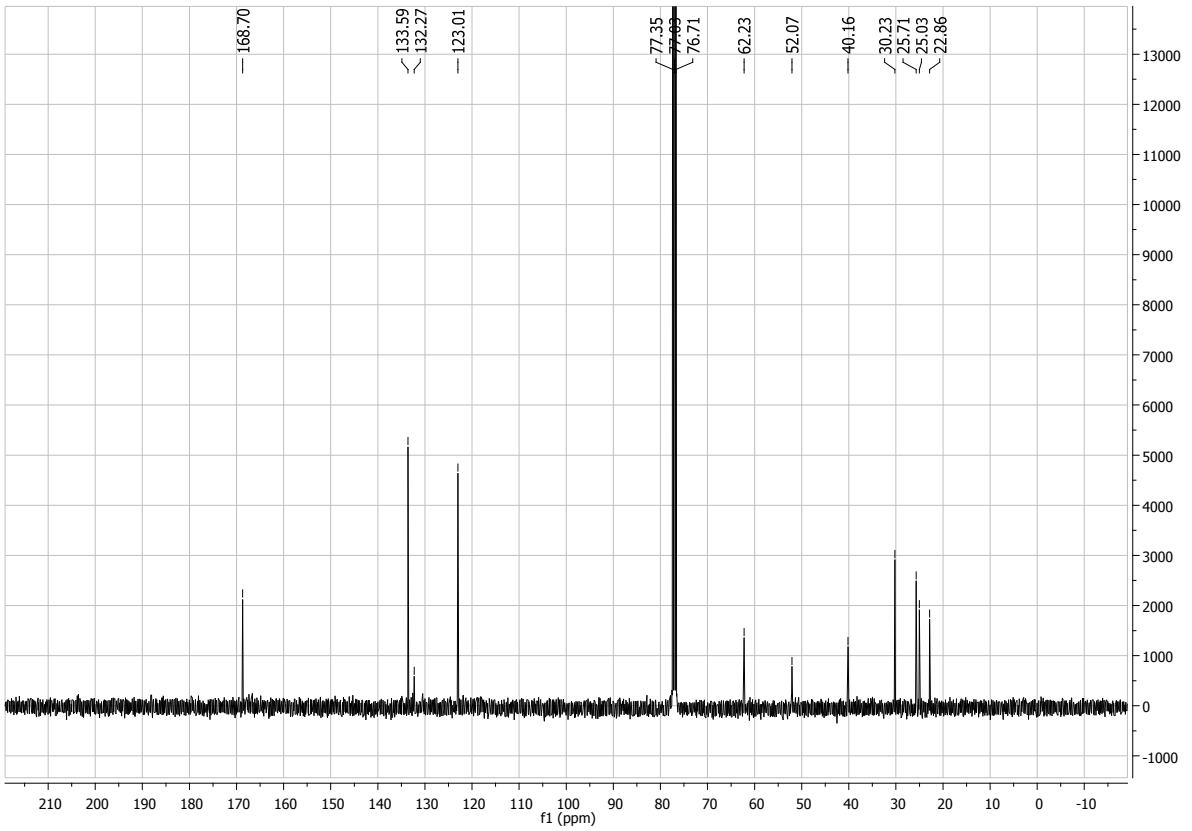
168.70
133.59
132.27
123.01
77.35
77.03
76.71
62.23
52.07
40.16
30.23
25.71
25.03
22.86
f1 (ppm)

2-((1*R*,2*R*)-2-(dimethylamino)cyclohexyl)isoindoline-1,3-dione ((*R*, *R*)-167)[54]

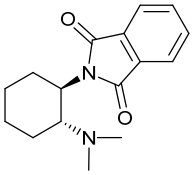

The free amine **(*R*, *R*)-166** (3.0 g, 12.3 mmol) was added with formaldehyde (2.9 g, 37 %, 27.0 mmol) and formic acid (4.60 mL, 123 mmol) and refluxed overnight at about 105 °C. Disappearing of the starting material was monitored via TLC (DCM/MeOH 9:1, Al_2O_3). Once the reaction reached completion, the mixture was evaporated and the residue dissolved in DCM (30 mL), washed twice with saturated sodium bicarbonate solution. The organic phase was then dried and evaporated *in vacuo* to yield a dark orange oil. **(*R*, *R*)-167** (2.5 g, 75 %) was obtained after recrystallisation from ethyl acetate-diethyl ether as a white solid.

mp 128.2-129 °C, lit.[54] 117-120 °C, $[\alpha]^{25}_{D}$ = -27.5 (c = 1, $CHCl_3$), lit.[54] -32.5 (c = 1, $CHCl_3$); IR (neat, ν_{max}/cm^{-1}): 2929, 2859, 1760, 1330; ^{1}H-NMR (400 MHz, δ-$CDCl_3$): 1.07-1.37 (3H, m, C*H*$_2$CH$_2$CHN(CH$_3$)$_2$, C*H*$_2$CH$_2$CHN, CH$_2$C*H*$_2$CHN), 1.67-1.83 (3H, m, C*H*$_2$CH$_2$CHN(CH$_3$)$_2$, CH$_2$C*H*$_2$CHN, CH$_2$C*H*$_2$CHN(CH$_3$)$_2$), 1.85-1.94 (1H, m, C*H*$_2$CH$_2$CHN), 2.05-2.21 (7H, m, 2 x C*H*$_3$, CH$_2$C*H*$_2$CHN(CH$_3$)$_2$), 3.22-3.37 (1H, m, CH$_2$CH$_2$C*H*N), 4.01-4.11 (1H, m, CH$_2$CH$_2$C*H*N(CH$_3$)$_2$), 7.57-7.63 (2H, m, Ar*H*), 7.70-7.77 (2H, m, Ar*H*); ^{13}C-NMR (100.2 MHz, δ-$CDCl_3$): 22.8, 25.0, 25.7, 30,2, 40.1, 52.0, 62.2, 123.0 132.2 , 133.5, 168.7; *m/z* (ESI): 260.1 (5 %), 273.1 (100), 291.1 (90), 305.1 (70), 313.1 (10); HRMS (ESI): $[C_{16}H_{20}N_2O_2, M+H]^+$ requires 273.1598 found 273.1600.

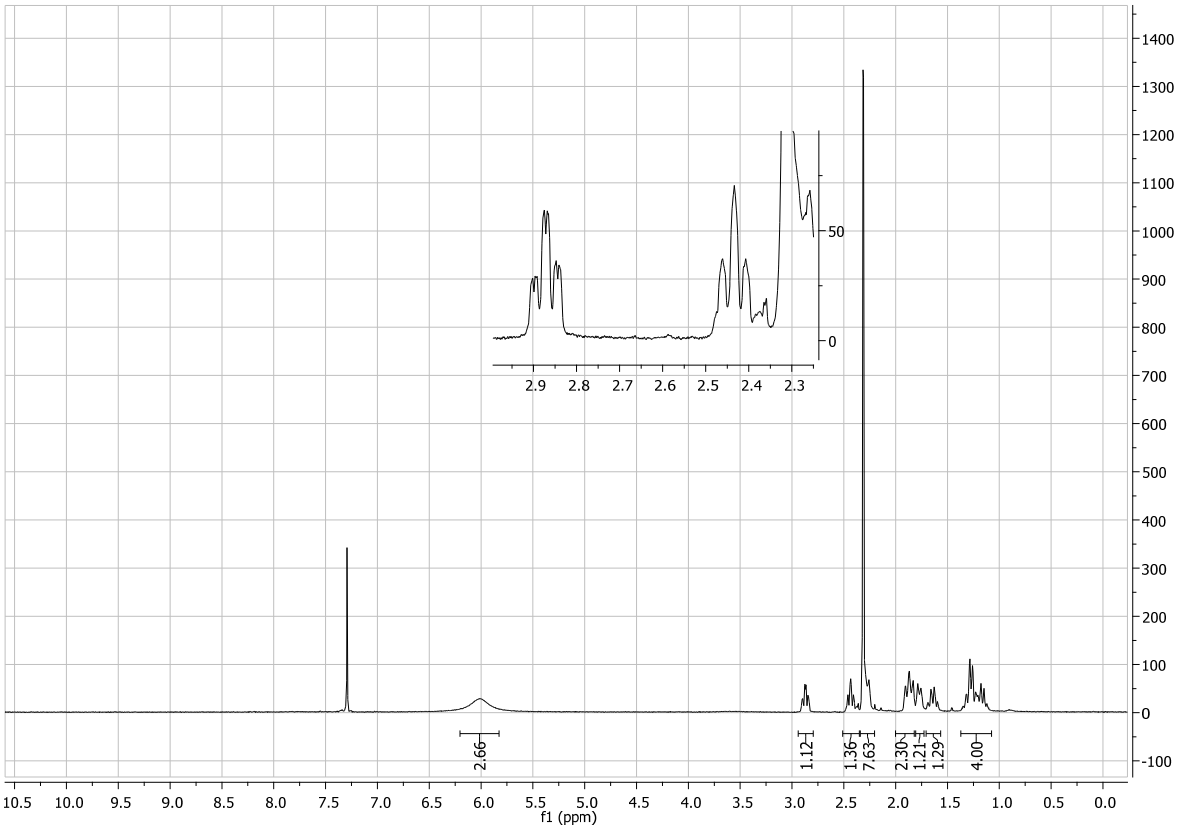
2.66
1.12
1.36
7.63
2.30
1.21
1.29
4.00
f1 (ppm)

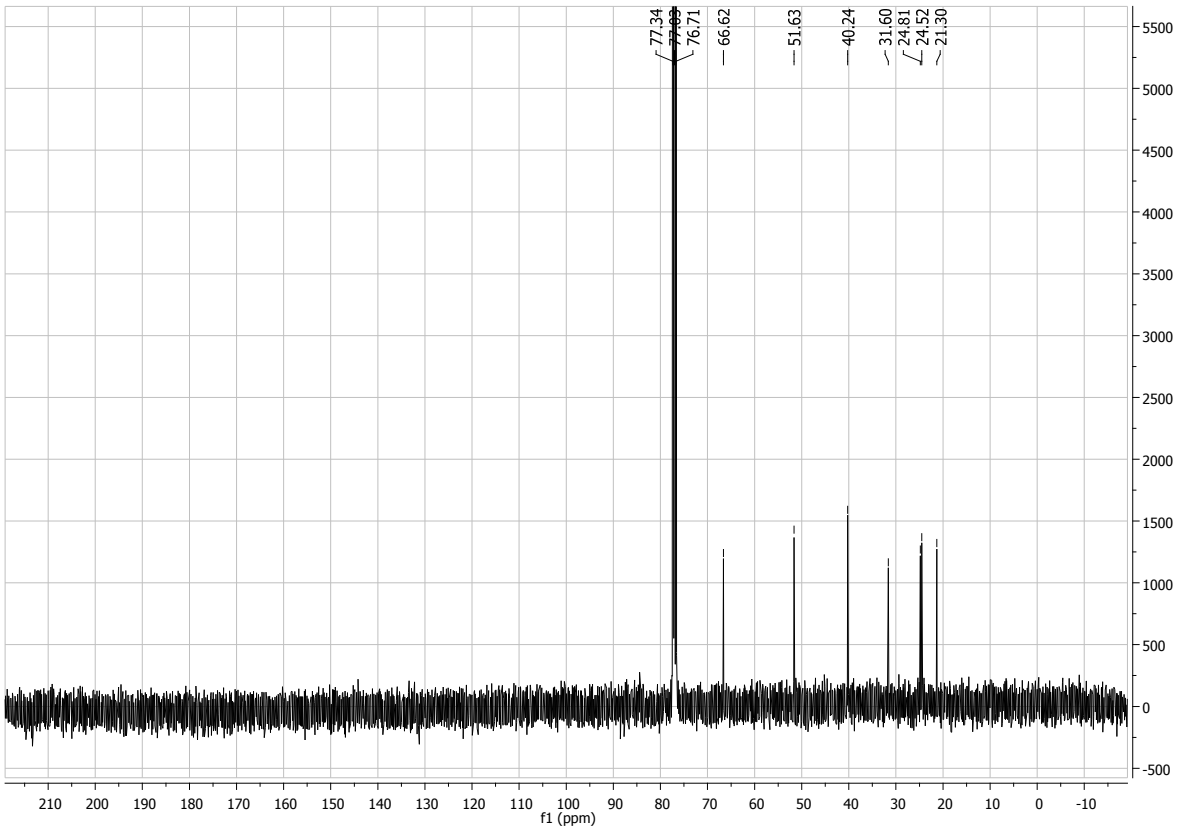
77.34
76.71
66.62
51.63
40.24
31.60
24.81
24.52
21.30
f1 (ppm)

(1*R*, 2*R*)-*N*1, *N*1-dimethylcyclohexane-1,2-diamine ((*R*, *R*)-168)[55]

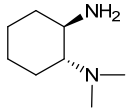

Phthalimide protected amine **(*R*, *R*)-167)** (2.50 g, 9.10 mmol) was dissolved in ethanol (20 mL) and added with hydrazine hydrate (1.07 mL, 34.6 mmol). The mixture was refluxed until TLC (Al_2O_3, DCM/MeOH 9:1 or DCM/EtOAc 1:1) showed disappearing of the starting material. Et_2O was then added to precipitate phthaloyl hydrazide and the resulting solid filtered. The solvents were evaporated *in vacuo* to leave a thick orange oil that was purified by flash chromatography on neutral alumina (DCM/MeOH from 100 % to 90 %). After the purification, **(*R*, *R*)-168** (0.50 g, 42 %) was obtained as a yellow oil.

$[\alpha]^{25}_D$ = -51.6 (c = 0.45, EtOH), lit.[55] -51 (c = 0.45, EtOH); IR (neat, ν_{max}/cm^{-1}): 3336, 3288, 2990, 2936, 2880, 2720, 1670, 1550, 1432, 1034; ^{1}H-NMR (400 MHz, δ-$CDCl_3$): 1.03-1.36 (4H, m, C*H*$_2$CH$_2$CHN, CH$_2$C*H*$_2$CHN), 1.55-1.70 (1H, m, C*H*$_2$CH$_2$CHN), 1.72-1.95 (3H, m, CH$_2$C*H*$_2$CHN, C*H*$_2$CH$_2$CHN), 2.32 (6H, s, 2 x C*H*$_3$), 2.43 (1H, td, J_1 = 10.4 Hz J_2 = 3.9 Hz, CH$_2$CH$_2$C*H*N), 2.88 (1H, td, J_1 = 10.5 Hz J_2 = 4.01Hz, CH$_2$CH$_2$C*H*NH$_2$), 6.00 (2H, bs, N*H*$_2$); ^{13}C-NMR (100.2 MHz, δ-$CDCl_3$): 21.3, 24.5, 24.8, 31.6, 40.2, 51.6, 66.6; *m/z* (ESI): 60.2 (10 %), 98.0 (5), 126.0 (10), 143.0 (100), 144.0 (10); HRMS (ESI): [$C_8H_{18}N_2$, M+H]$^+$ requires 143.1543 found 143.1539.

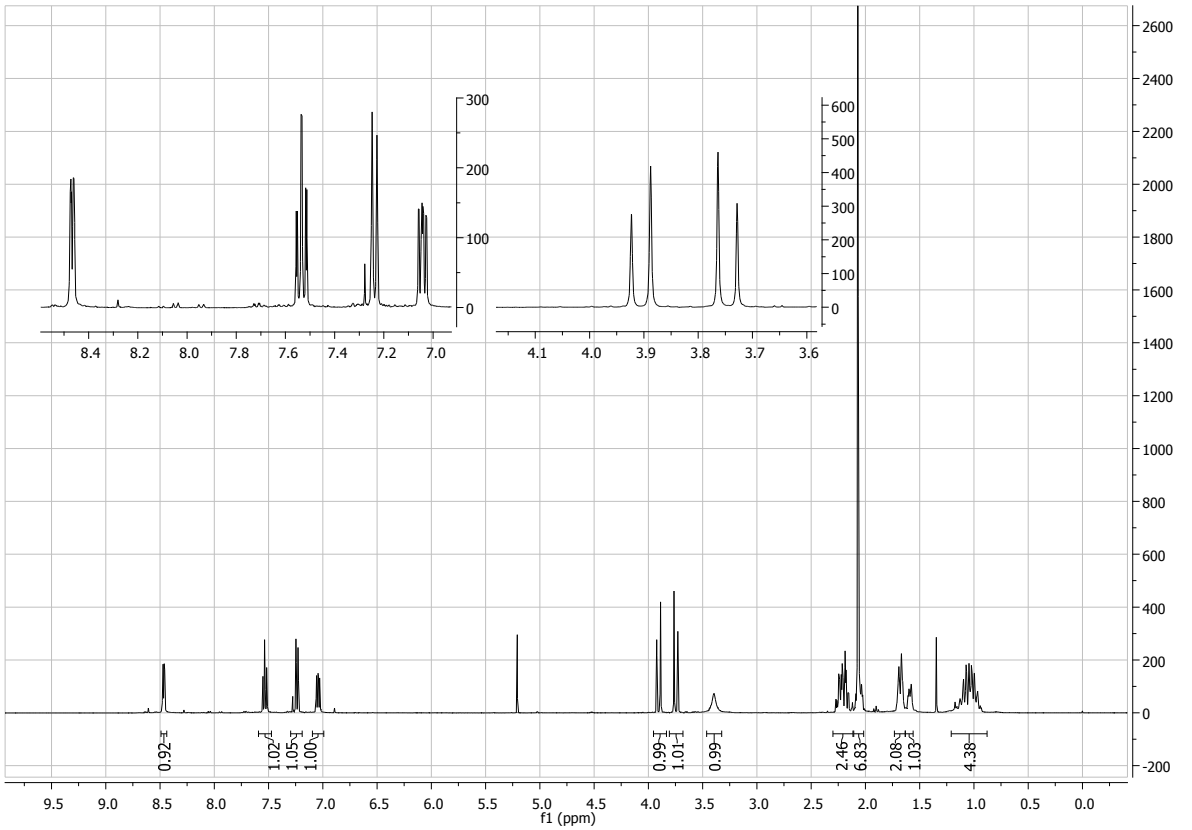
0.92
1.02
1.05
1.00
0.99
1.01
0.99
2.46
6.83
2.08
1.03
4.38
f1 (ppm)

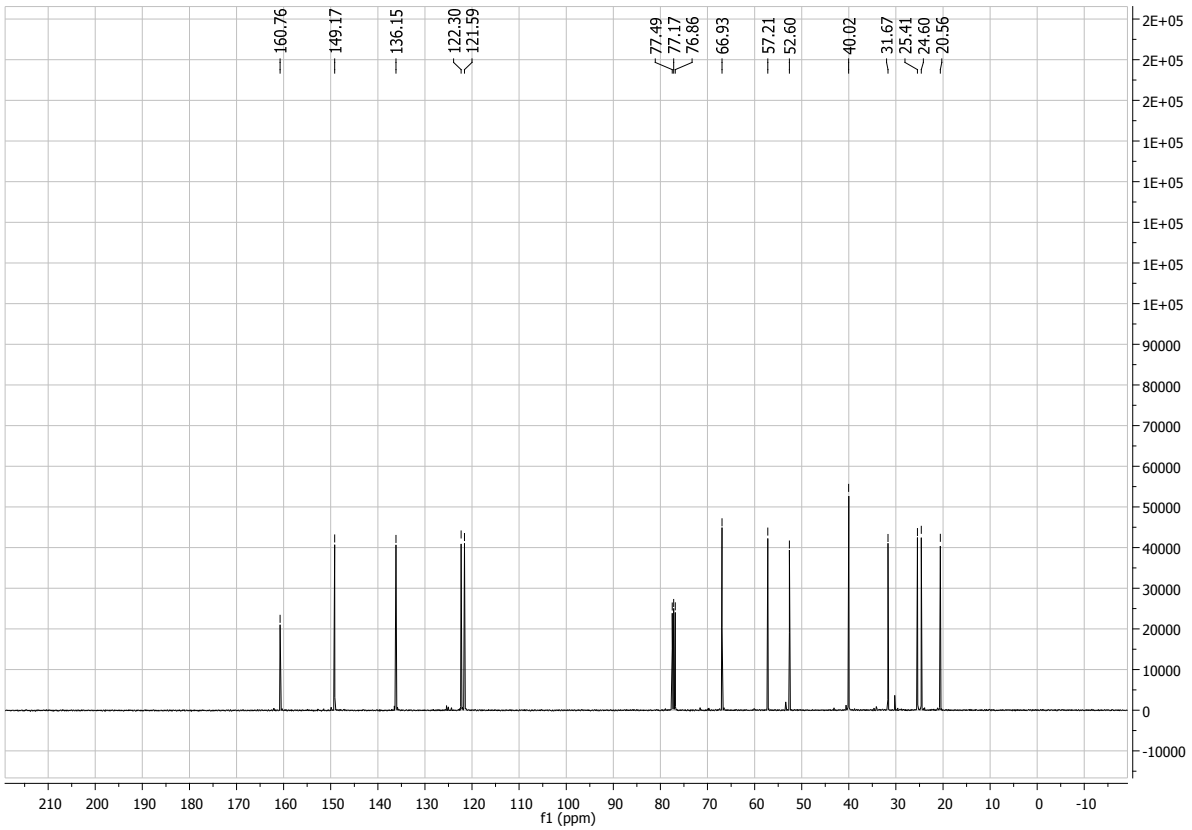
160.76
149.17
136.15
122.30
121.59
77.49
77.17
76.86
66.93
57.21
52.60
40.02
31.67
25.41
24.60
20.56
f1 (ppm)

(1*R*, 2*R*)-*N*1, *N*1-dimethyl-*N*2-(pyridin-2-ylmethyl)cyclohexane-1,2-diamine ((*R*, *R*)-169)[56]

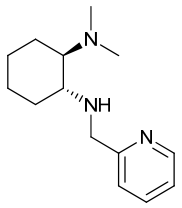

Following a modification of the cited procedure. A solution of **(*R*, *R*)-168** (1.0 g, 7.0 mmol) in toluene was transferred into a flask containing activated molecular sieves and kept under a nitrogen atmosphere. After stirring for five minutes at RT, pyridine 2-carboxyaldehyde (667 μL, 7.00 mmol) was added *via* a syringe and the stirring continued until all the starting material disappeared (TLC DCM/MeOH 9:1, Al_2O_3). After completion, the solvents were evaporated and the residue dissolved in MeOH. An excess of sodium borohydride (530 mg, 14.0 mmol) was then added in portions and the mixture left refluxing overnight. The solvent was then removed and the residue dissolved in DCM, washed with water (15 mL). The organic phase was recovered, dried over $MgSO_4$ and the solvent removed under reduced pressure to yield **(*R*, *R*)-169** (400 mg, 25 %) as a yellow oil.

$[\alpha]^{25}_D$ = -46.6 (c = 0.1, $CHCl_3$); IR (neat, ν_{max}/cm^{-1}): 3288, 2926, 2856, 2823, 2779, 1590, 1569, 1454, 1432, 1114, 1045, 754; ^{1}H-NMR (400 MHz, δ-$CDCl_3$): 0.91-1.22 (4H, m, C*H*$_2$CH$_2$CHN, CH$_2$C*H*$_2$CHN), 1.54-1.63 (1H, m, C*H*$_2$CH$_2$CHN), 1.63-1.74 (2H, m, C*H*$_2$CH$_2$CHN CH$_2$C*H*$_2$CHN), 1.99-2.10 (7H, m, CH$_2$C*H*$_2$CHN, 2 x C*H*$_3$), 2.11-2.29 (2H, m, CH$_2$CH$_2$C*H*N), 3.40 (1H, bs, N*H*), 3.75 (1H, d, J_1 = 14.1 Hz, NC*H*$_2$Py), 3.91 (1H, d, J_1 = 14.1 Hz, NC*H*$_2$Py), 7.01-7.07 (1H, m, C*H*Py), 7.21-7.26 (1H, m, C*H*Py), 7.53 (1H, td, J_1 = 7.6 Hz, J_2 = 1.8 Hz, C*H*Py), 8.47 (1H, ddd, J_1 = 4.9 Hz, J_2 = 1.8 Hz, J_3 = 0.9 Hz, C*H*Py); ^{13}C-NMR (100.2 MHz, δ-$CDCl_3$): 20.5, 24.6, 25.4, 31.6, 40.0, 52.6, 57.2, 66.9, 121.5, 122.3, 136.1, 149.1, 160.6; *m/z* (ESI): 189.1 (40 %), 234.1 (100), 246.1 (20), 246.1 (15); HRMS (ESI): $[C_{14}H_{23}N_3+H]^+$ requires 234.1965 found 234.1966.

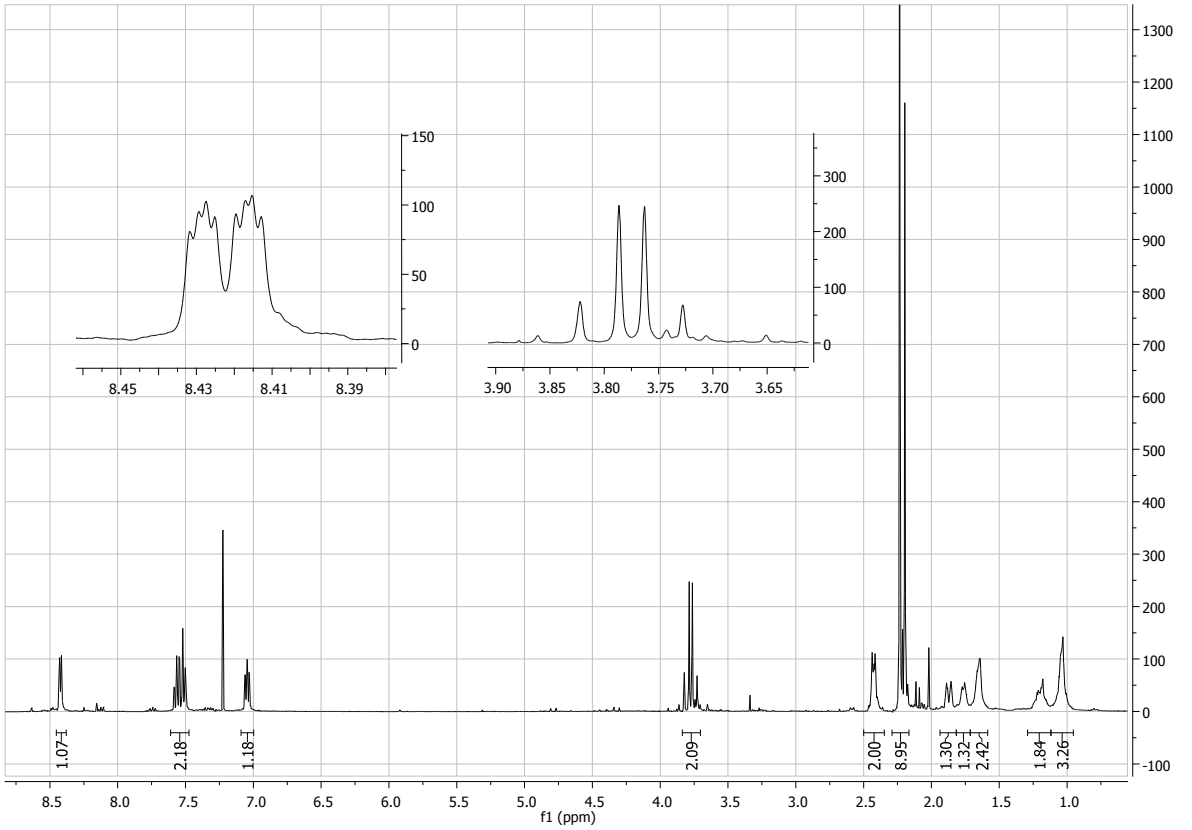
1.07
2.18
1.18
2.09
2.00
8.95
1.30
1.32
2.42
1.84
3.26
f1 (ppm)

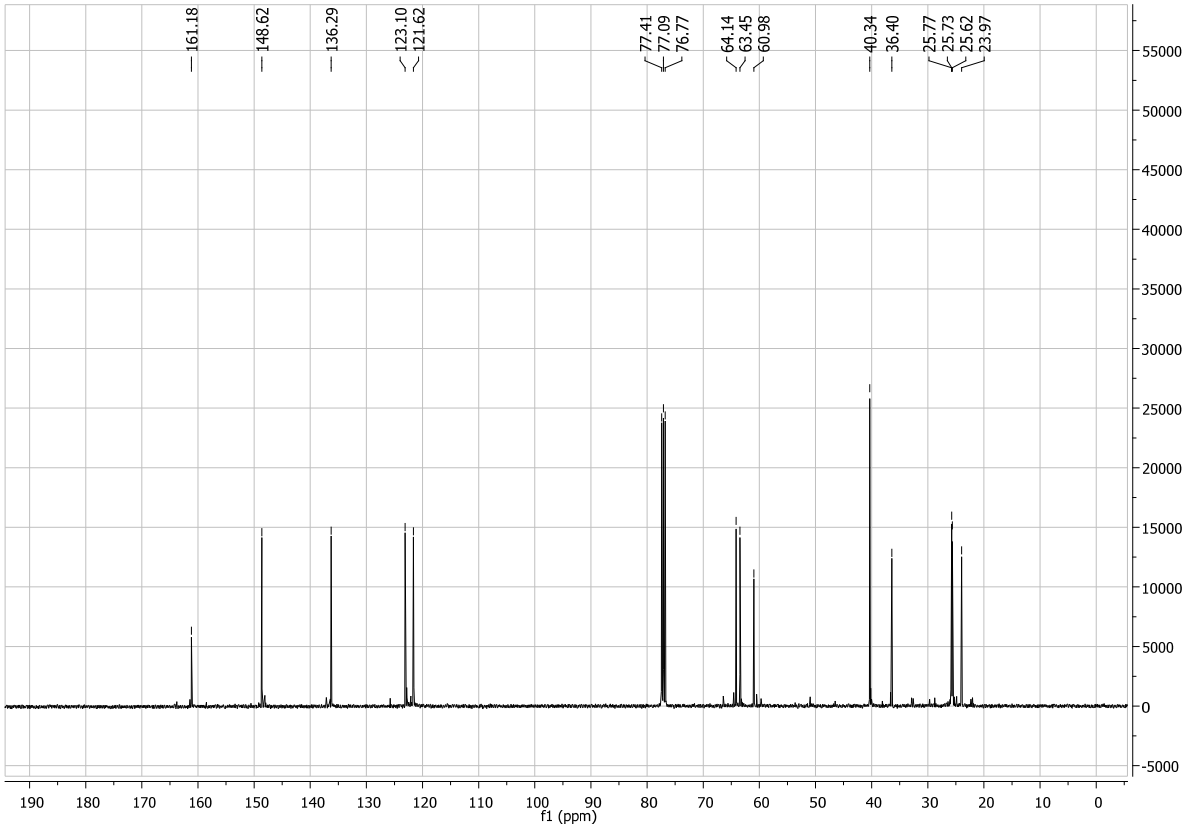
161.18
148.62
136.29
123.10
121.62
77.41
77.09
76.77
64.14
63.45
60.98
40.34
36.40
25.77
25.73
25.62
23.97
f1 (ppm)

(1*R*, 2*R*)-*N*1, *N*1, *N*2-trimethyl-*N*2-(pyridin-2-ylmethyl)cyclohexane-1,2-diamine ((*R*, *R*)-39)[56]

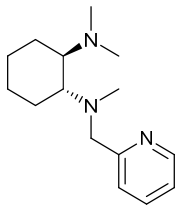

(*R*, *R*)-169 (1.0 g, 4.3 mmol) was dissolved in MeOH (5 mL). To this solution were added formaldehyde (2.00 g, 36 %, 22.0 mmol) and formic acid (1.6 mL, 43 mmol) and the resulting mixture refluxed to completion. The disappearing of the substrate was monitored *via* TLC (DCM/MeOH 9:1, Al_2O_3). When the substrate is consumed, the solvents were evaporated, the residue was dissolved in DCM and washed with saturated $NaHCO_3$. The organic phase was dried over anhydrous $MgSO_4$ and distilled off at reduced pressure to give **(*R*, *R*)-39** (500 mg, 47 %) as a dark brown oil

$[\alpha]^{25}_D$ = -10.0 (c = 0.1, $CHCl_3$); IR (neat, ν_{max}/cm^{-1}): 756, 1045, 1432, 1568, 2774, 2855, 2927; ^{1}H-NMR (400 MHz, δ-$CDCl_3$): 0.94-1.09 (3H, m, C*H*$_2$CH$_2$CHN, CH$_2$C*H*$_2$CHN), 1.11-1.27 (1H, m, CH$_2$C*H*$_2$CHN), 1.57-1.68 (2H, m, C*H*$_2$CH$_2$CHN, CH$_2$C*H*$_2$CHN), 1.69-1.78 (1H, m, C*H*$_2$CH$_2$CHN), 1.81-1.90 (1H, m, CH$_2$C*H*$_2$CHN), 2.18 (3H, s, C*H*$_3$), 2.22 (6H, s, 2 x C*H*$_3$), 2.35-2.45 (2H, m,CH$_2$CH$_2$C*H*N), 3.73 (1H, d, J_1 = 14.3 Hz, C*H*$_2$), 3.79 (1H, d, J_1 = 14.3 Hz, C*H*$_2$), 6.99-7.05 (1H, m, C*H*Py), 7.46-7.58 (2H, m, C*H*Py), 8.42 (1H, ddd, J_1 = 4.9 Hz, J_2 = 1.7 Hz, J_3 = 1.0 Hz, C*H*Py); ^{13}C-NMR (100.2 MHz, δ-$CDCl_3$): 23.9, 25.6, 25.73, 25.77, 36.4, 40.3, 60.9, 63.4, 64.1, 121.6, 123.1, 136.2, 148.6, 161.1; *m/z* (ESI): 203.1 (25 %), 248.2 (100), 262.1 (30); HRMS (ESI): $[C_{15}H_{25}N_3+H]^+$ requires 248.2121 found 248.2124.

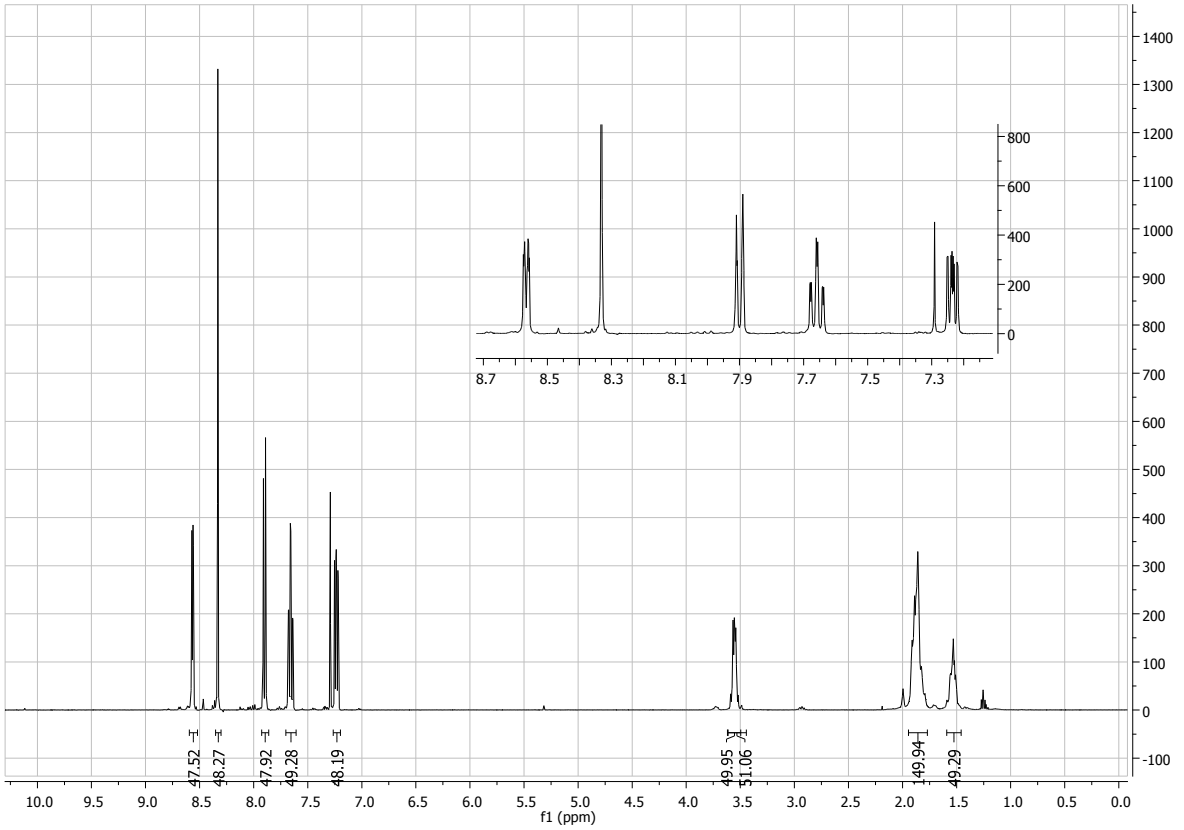
47.52
48.27
47.92
49.28
48.19
49.95
31.06
149.94
49.29
f1 (ppm)

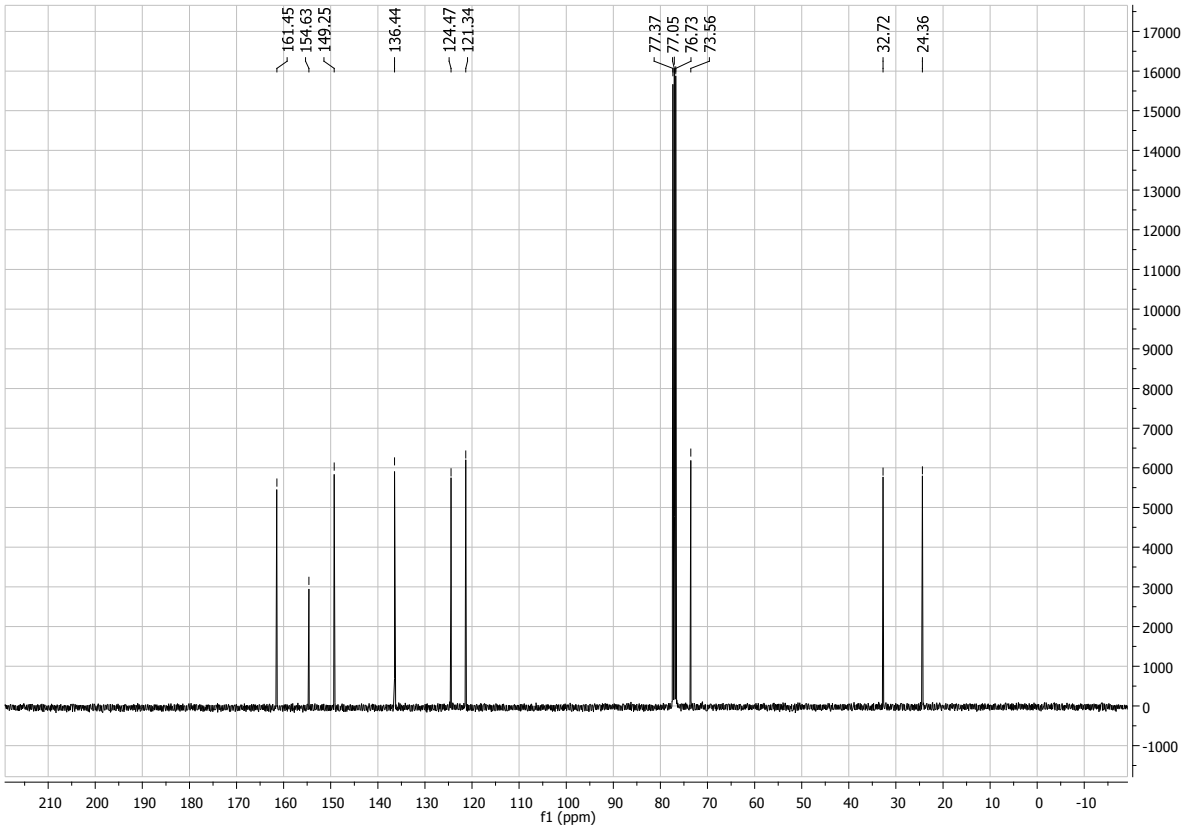
161.45
154.63
149.25
136.44
124.47
121.34
77.37
77.05
76.73
73.56
32.72
24.36
f1 (ppm)

(1*R*, 2*R*)-*N*1, *N*2-bis(pyridin-2-ylmethylene)cyclohexane-1,2-diamine ((*R*, *R*)-171)[57]

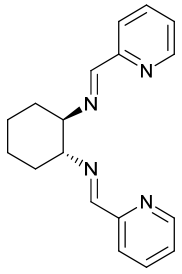

(*R, R*)-133 (2.74 mL, 22.7 mmol) and pyridine - 2 - carboxyaldehyde (6.64 mL, 45.4 mmol) were mixed in MeOH at RT in the presence of 4Å molecular sieves and left stirring overnight. The reaction was monitored by TLC (DCM/MeOH 9:1 on Al_2O_3). After completion, the solvent was evaporated *in vacuo* to yield **(*R*, *R*)-171** (2.70 g, 41 %) as a white solid which was pure enough to be employed in the following step.

mp. 139 °C, lit.[57] 140-141 °C (EtOH); $[\alpha]^{25}_D$ = -181.8 (c = 1, $CHCl_3$), (1*S*, 2*S*) isomer, $[\alpha]^{25}_D$ = 172.0 (c = 1, $CHCl_3$), (1*R*, 2*R*) isomer; IR (neat, ν_{max}/cm^{-1}): 2927, 2862, 1644, 1586, 1567, 1468, 775; ^{1}H-NMR (400 MHz, δ-$CDCl_3$): 1.45-1.62 (2H, m, C*H*$_2$CH$_2$CHN), 1.77-1.98 (6H, m, C*H*$_2$CH$_2$CHN, CH$_2$C*H*$_2$CHN), 3.51-3.61 (2H, m, CH$_2$CH$_2$C*H*N), 7.24 (2H, ddd, J_1 = 7.5 Hz , J_2 = 4.5 Hz , J_3 = 1.2 Hz, C*H*Py), 7.63-7.69 (2H, m, C*H*Py), 7.91 (2H, dt, J_1 = 7.9 Hz, J_2 = 1.0 Hz, C*H*Py), 8.34 (2H, s, NC*H*Py), 8.57 (2H, ddd, J_1 = 4.9 Hz, J_2 = 1.7 Hz, J_3 = 0.9 Hz, C*H*Py); ^{13}C-NMR (100.2 MHz, δ-$CDCl_3$): 24.3, 32.7, 73.5, 121.3, 124.4, 136.4, 149.2, 154.6, 161.4; *m/z* (ESI): 204.1 (100 %), 226.1 (15), 293.1 (15); HRMS (ESI): $[C_{18}H_{20}N_4, M+H]^+$ requires 293.1761 found 293.1762.

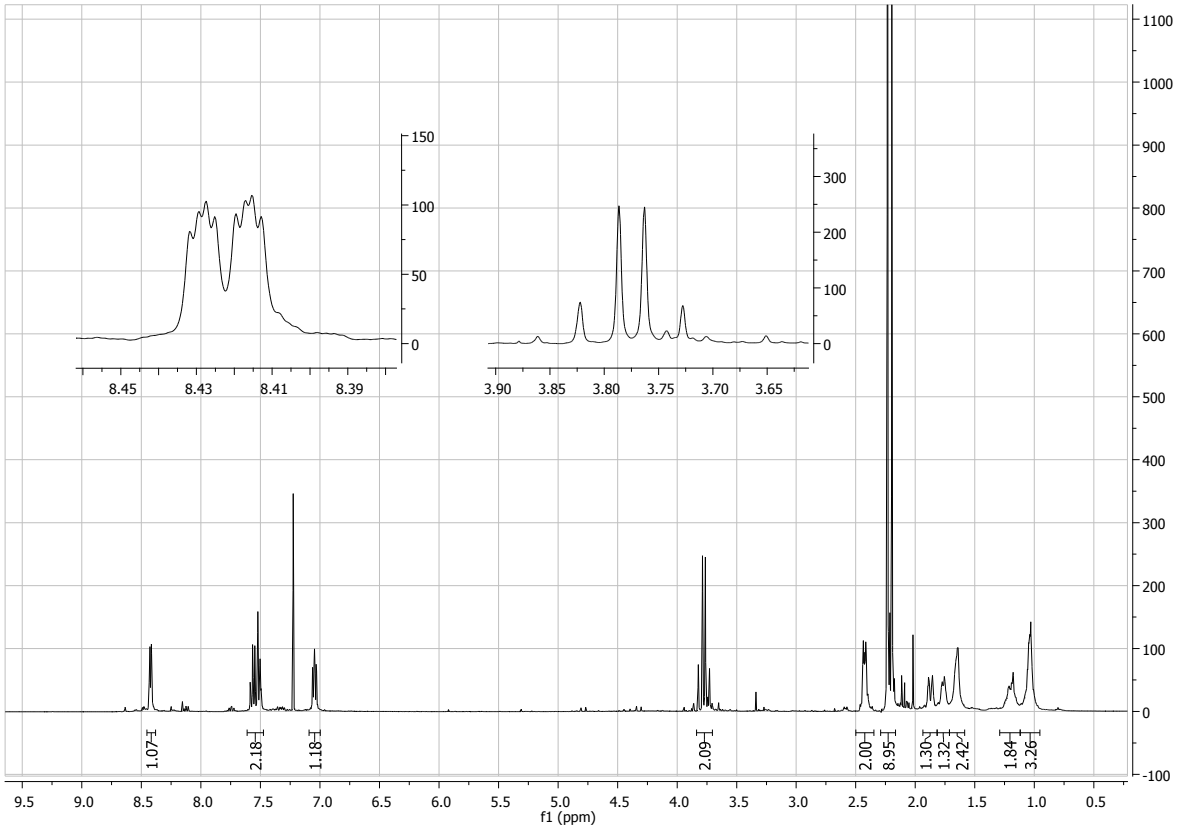
8.45
8.43
8.41
8.39
3.90
3.85
3.80
3.75
3.70
3.65
1.07
2.18
1.18
2.09
2.00
8.95
1.30
1.32
2.42
1.84
3.26
f1 (ppm)

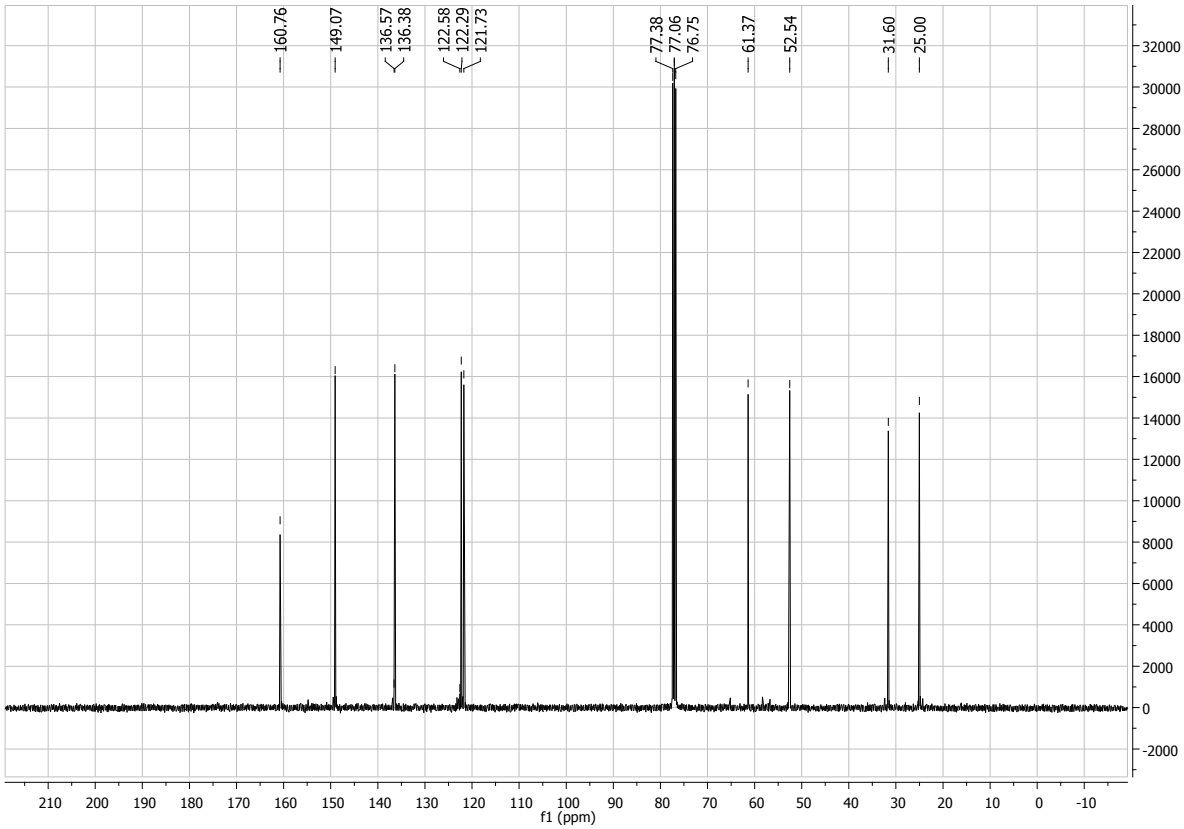
160.76
149.07
136.57
136.38
122.58
122.29
121.73
77.38
77.06
76.75
61.37
52.54
31.60
25.00
f1 (ppm)

(1*R* ,2*R*)-*N*1, *N*2-bis(pyridin-2-ylmethyl)cyclohexane-1,2-diamine ((*R*, *R*)-172)[58]

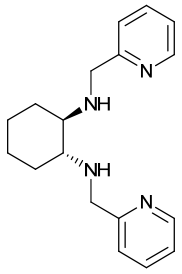

To a solution of **(*R*, *R*)-171** (2.60 g, 8.90 mmol) in MeOH (20 mL) was added $NaBH_4$ (0.841 g, 0.222 mol) and the resulting mixture was stirred at RT overnight and monitored *via* TLC (DCM/MeOH 9:1). When all the starting material disappeared, the solvent was evaporated and the residue dissolved in DCM (20 mL) and water (10 mL). After 5 minutes stirring, the layers were separated and the organic phase dried over $MgSO_4$ and evaporated *in vacuo* to yield **(*R*, *R*)-172** (2.5 g, 96 %) as a thick yellow oil.

$[\alpha]^{25}_D$ = -66.4 (c = 1, $CHCl_3$), (1*S*,2*S*) isomer, $[\alpha]^{25}_D$ = 66.3 (c = 1 $CHCl_3$), (1*R*, 2*R*) isomer; IR (neat, ν_{max}/cm^{-1}): 3294, 3007, 2924, 2853, 1590, 1568, 1432, 1119, 752; ^{1}H-NMR (400 MHz, δ-$CDCl_3$): 1.01-1.16 (2H, m, CH_2CH_2CHNH, CH_2CH_2CHNH), 1.17-1.33 (2H, m, CH_2CH_2CHNH, CH_2CH_2CHNH), 1.64-1.79 (2H, m, CH_2CH_2CHNH), 2.08-2.20 (2H, m, CH_2CH_2CHNH), 2.21-2.51 (4H, m, CH_2CH_2CHNH, NH_2), 3.83 (2H, d, J_1 = 14.2 Hz, NCH_2Py), 4.01 (2H, d, J_1 = 14.2 Hz, NCH_2Py), 7.04-7.16 (2H, m, C*H*Py), 7.41 (2H, d, J_1 = 7.8 Hz, C*H*Py), 7.63 (2H, tt, J_1 = 5.1 Hz, J_2 = 2.5 Hz, C*H*Py), 8.51-8.56 (2H, m, C*H*Py); ^{13}C-NMR (100.6 MHz, δ-$CDCl_3$): 25.0, 31.6, 52.5, 61,3 121.7, 122.2, 136.3, 149.0, 160.7, ; *m/z* (ESI) :189.1 (45 %), 297.2 (100), 319.1 (10); HRMS (ESI): $[C_{18}H_{24}N_4, M+H]^+$ requires 297.2074 found 297.2073.

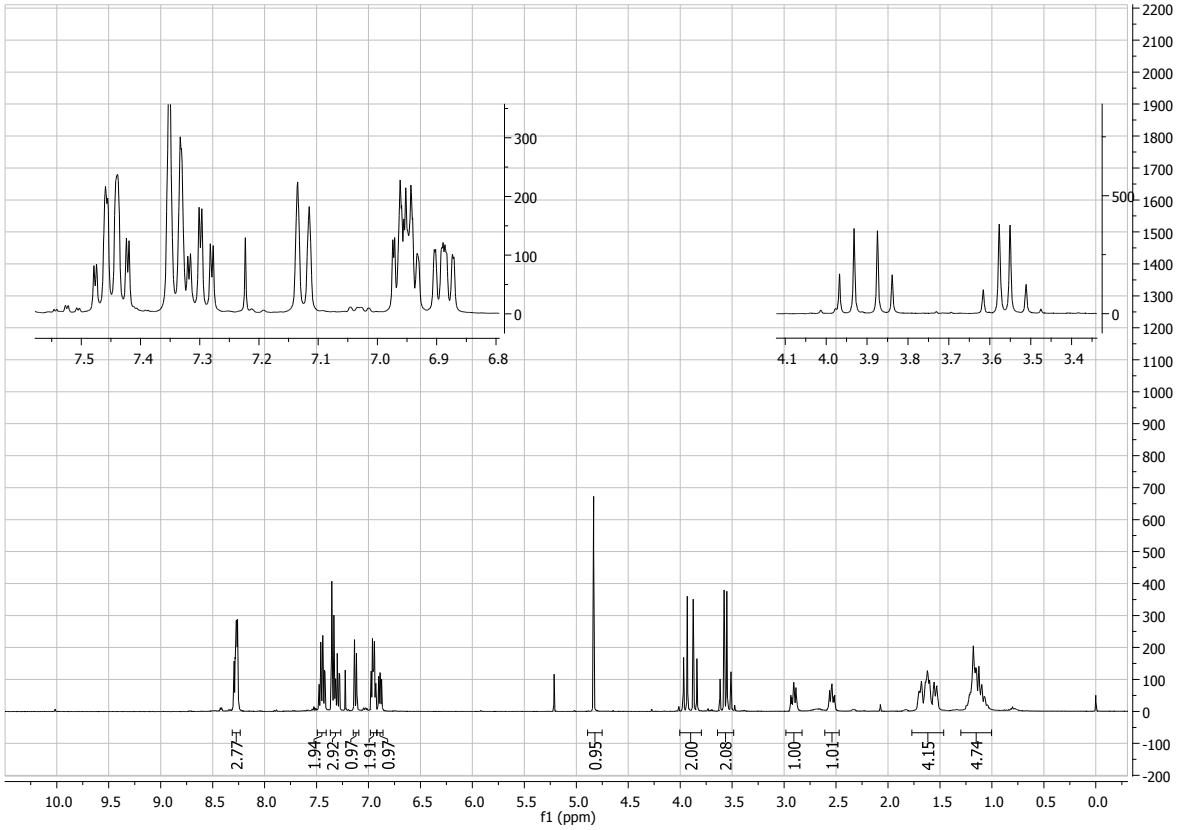
2.77
1.94
2.92
0.97
1.91
0.97
0.95
2.00
2.08
1.00
1.01
4.15
4.74
f1 (ppm)

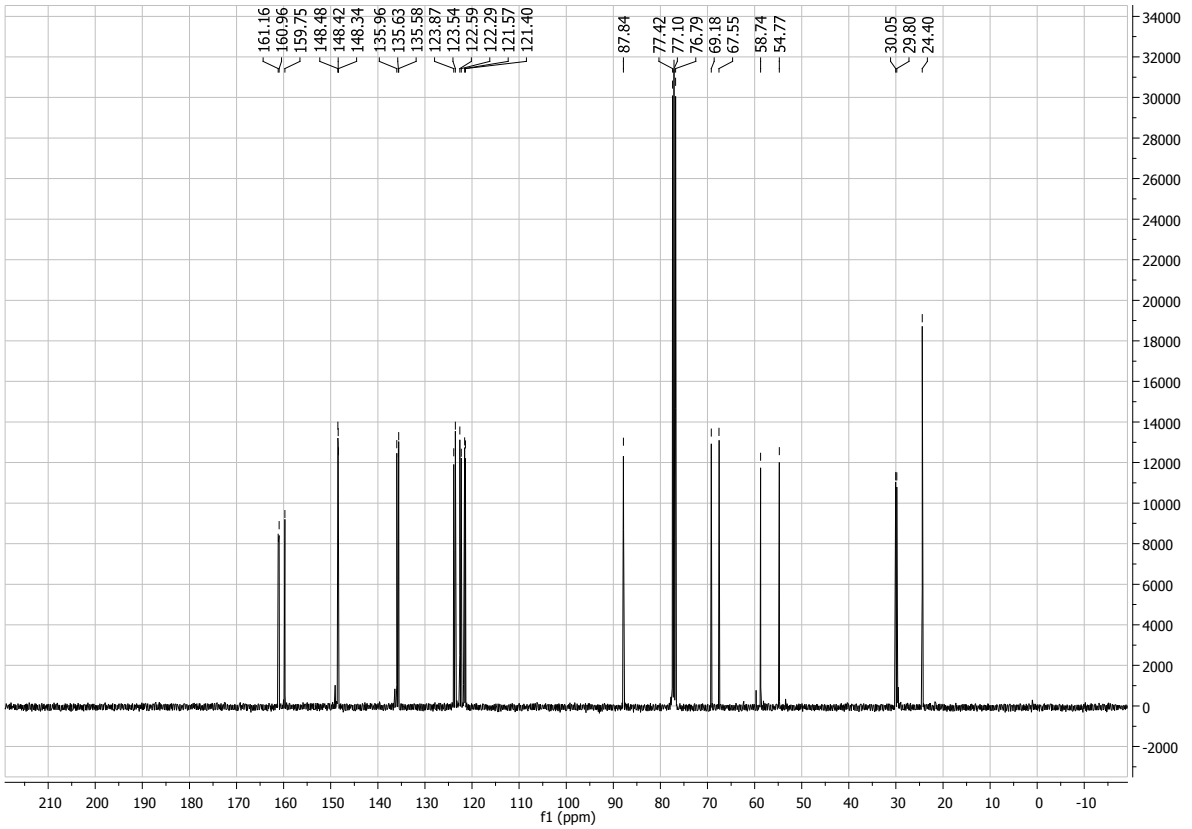
161.16
160.96
159.75
148.48
148.42
148.34
135.96
135.63
135.58
123.87
123.54
122.59
122.29
121.57
121.40
87.84
77.42
77.10
76.79
69.18
67.55
58.74
54.77
30.05
29.80
24.40
f1 (ppm)

(1*R*, 2*R*)-2-(pyridin-2-yl)-1,3-bis(pyridin-2-ylmethyl)octahydro-1H-benzo[d]imidazole ((*R*, *R*)-173)[59]

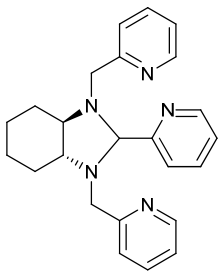

4Å molecular sieves were added to a solution of **(*R*, *R*)-172** (0.60 g, 2.0 mmol) in dry Et_2O and the flask sealed with a septum. Subsequently, pyridine-2- carboxaldehyde (0.19 mL, 2.0 mmoles) was added with a syringe and the reaction mixture was left stirring at RT overnight. TLC vas used to determine completion (DCM/MeOH 9:1 on Al_2O_3). After completion, the mixture was filtered and washed with a 10 % solution of sodium bisulfite in water. The organic phase was separated, dried on $MgSO_4$ and evaporated under reduced pressure to give product **(*R*, *R*)-173** (500 mg, 64 %) as a brown oil.

$[\alpha]^{25}_D$ = -56.2 (c = 1, $CHCl_3$), (1*S*, 2*S*) isomer, $[\alpha]^{25}_D$ = 59.2 (c = 1, $CHCl_3$), (1*R*, 2*R*) isomer; IR (neat, ν_{max}/cm^{-1}): 3050, 3010, 2980, 2880, 1580, 1460; ^{1}H-NMR (400 MHz, δ-$CDCl_3$): 1.00-1.28 (4H, m, C*H*$_2$CH$_2$CHN, CH$_2$C*H*$_2$CHN), 1.46-1.76 (4H, m, C*H*$_2$CH$_2$CHN, CH$_2$C*H*$_2$CHN), 2.48-2.59 (1H, m, CH$_2$CH$_2$C*H*N), 2.85-2.98 (1H, m, CH$_2$CH$_2$C*H*N), 3.53 (1H, d, J_1 = 15.6 Hz, NC*H*$_2$Py), 3.60 (1H, d, J_1 = 15.6 Hz, NC*H*$_2$Py), 3.85 (1H, d, J_1= 14.3 Hz, NC*H*$_2$Py), 3.95 (1H, d, J_1 = 14.3 Hz, NC*H*$_2$Py), 4.83 (1H, s, NC*H*(Py)), 6.85-6.91 (1H, m, C*H*Py), 6.92-6.98 (2H, m, C*H*Py), 7.13 (1H, d, J_1 = 7.8 Hz, C*H*Py) 7.30 (1H, td, J_1 = 7.7 Hz, J_2 = 1.8 Hz, C*H*Py), 7.34 (2H, dd, J_1 = 7.8 Hz, J_2 = 0.8 Hz, C*H*Py), 7.45 (2H, ddd, J_1 = 8.3 Hz, J_2 = 7.7 Hz, J_3 = 1.8 Hz, C*H*Py), 8.24-8.31 (3H, m, C*H*Py); ^{13}C-NMR (100.2 MHz, δ-$CDCl_3$): 24.4, 29.8, 30.0, 54.7, 58.7, 67.5, 69.1, 87.8, 121.4, 121.5, 122.2, 122.5, 123.5, 123.8, 135.5, 135.6, 135.9, 148.3, 148.43, 148. 48, 159.75, 160.9, 161.1; *m/z* (ESI): 189.1 (10 %), 307.1 (20), 386.2 (100), 402.2 (15); HRMS (ESI): $[C_{24}H_{27}N_5+H]^+$ requires 386.2326 found 386.2329.

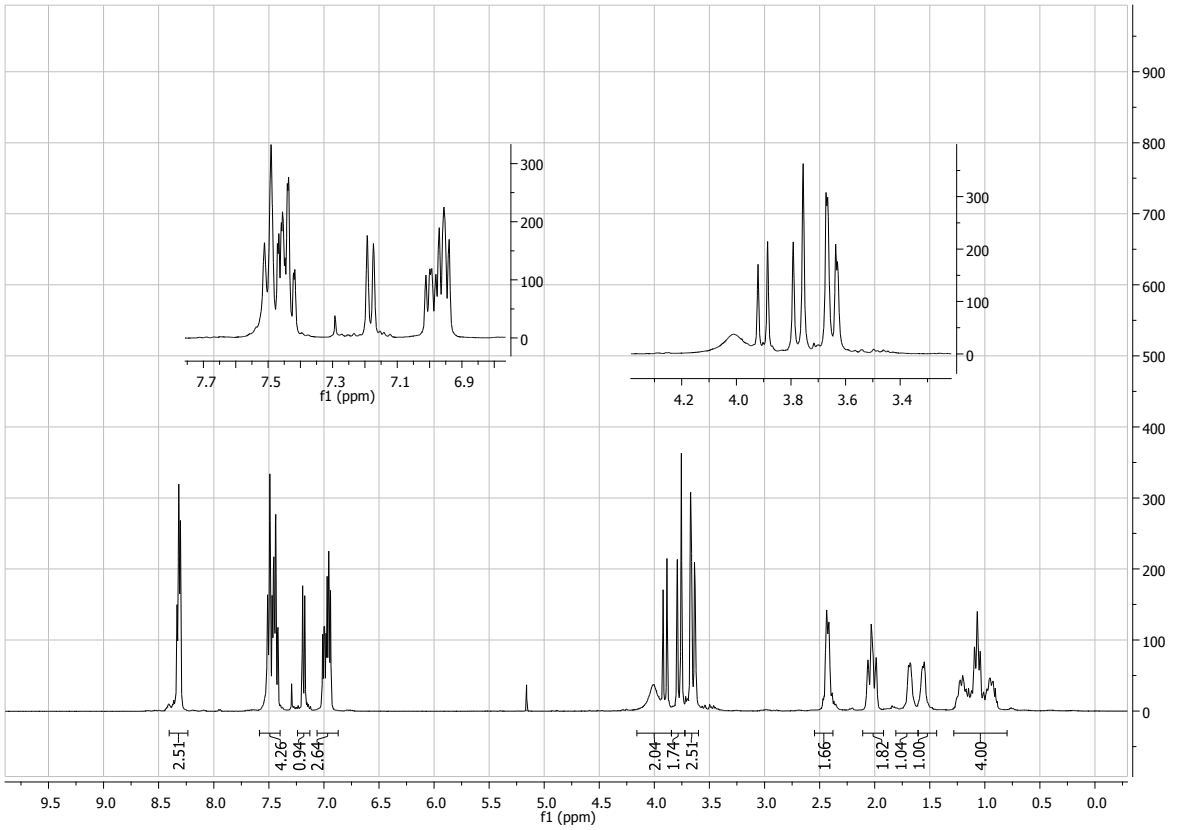
f1 (ppm)
2.51
4.26
0.94
2.64
2.04
1.74
2.51
1.66
1.82
1.04
1.00
4.00

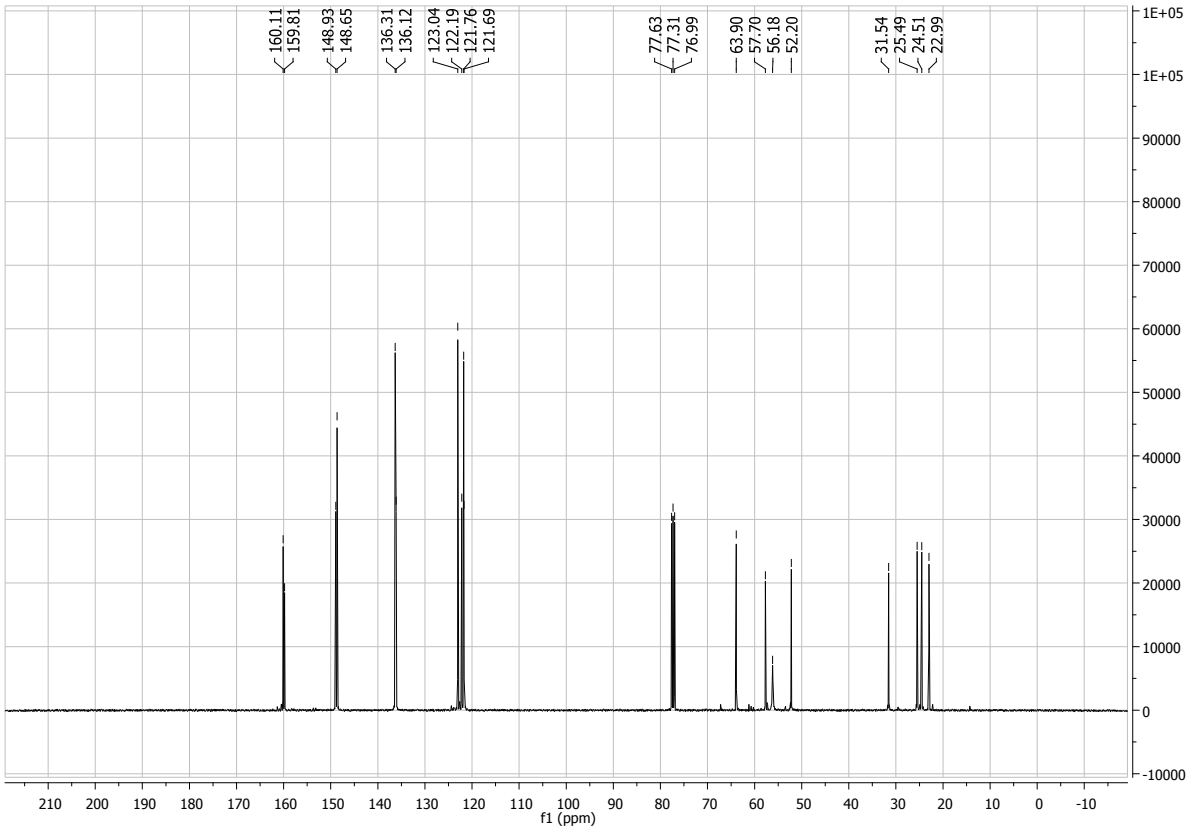
160.11
159.81
148.93
148.65
136.31
136.12
123.04
122.19
121.76
121.69
77.63
77.31
76.99
63.90
57.70
56.18
52.20
31.54
25.49
24.51
22.99
f1 (ppm)

(1*R*, 2*R*)-*N*1, *N*1, *N*2-tris(pyridin-2-ylmethyl)cyclohexane-1,2-diamine ((*R*, *R*)-174)[59]

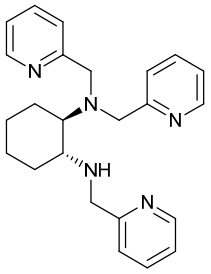

To a solution of **(*R*, *R*)-173** (0.80 g, 2.1 mmol) and $NaCNBH_3$ (0.16 g, 2.5 mmol) in dry MeOH and under nitrogen, trifluoroacetic acid (0.31 mL, 4.2 mmol) was added dropwise and the mixture left stirred at RT under a nitrogen atmosphere. TLC (DCM/MeOH 9:1) after one day showed the presence of substrate and several other compounds. A second equivalent of reducing agent was added and stirring continued for another day, after which the reaction was complete (TLC). The mixture was then poured in 10 mL of a 20 % solution of sodium hydroxide and stirred for 2 hours, after which it was extracted with DCM (3 x 20 mL). The combined organic phases were dried over $MgSO_4$ and the solvents evaporated under reduced pressure. After evaporation, **(*R*, *R*)-174** (0.6 g, 74 %) was obtained as a thick pale yellow oil.

$[\alpha]^{25}_D$ = -29.8 (c = 0.66, $CHCl_3$), (1*S*, 2*S*) isomer $[\alpha]^{25}_D$ = 29.2 (c = 1, $CHCl_3$), (1*R*, 2*R*) isomer; IR (neat, ν_{max}/cm^{-1}): 3049, 3006, 2927, 2855, 1590, 1568, 1473, 1432, 755; ^{1}H-NMR (400 MHz, δ-$CDCl_3$): 0.84-1.31 (4H,m, C*H*$_2$CH$_2$CHN, CH$_2$C*H*$_2$CHN), 1.46-1.59 (1H, m, C*H*$_2$CH$_2$CHN), 1.61-1.75 (1H, m, CH$_2$C*H*$_2$CHN), 1.95-2.11 (2H, m, C*H*$_2$CH$_2$CHN, CH$_2$C*H*$_2$CHN), 2.34-2.52 (2H, m, CH$_2$CH$_2$C*H*N), 3.67 (3H, d, J_1 = 13.9 Hz, NC*H*$_2$Py), 3.77 (2H, d, J_1 = 14.2 Hz, NC*H*$_2$Py), 3.89 (1H, d, J_1 = 13.9 Hz, NC*H*$_2$Py), 4.00 (1H, broad s, N*H*) 6.92-7-03 (3H, m, C*H*Py), 7.17 (1H, d, J_1 = 7.6 Hz, C*H*Py), 7.41-7.52 (5H, m, C*H*Py), 8.30-8.35 (3H, m, C*H*Py); ^{13}C-NMR (100.2 MHz, δ-$CDCl_3$): 22.9, 24.5, 25.4, 31.5, 52.2. 56.1, 57.7, 63.9, 121.6, 121.7, 122.1, 123.0, 136.1, 136.3, 148.6, 148.9, 159.8, 160.1; *m/z* (ESI): 197.8 (5 %), 311.7 (5), 388.2 (10), 410.2 (100); HRMS (ESI): $[C_{24}H_{29}N_5+Na]^+$ requires 410.2302 found 410.2306.

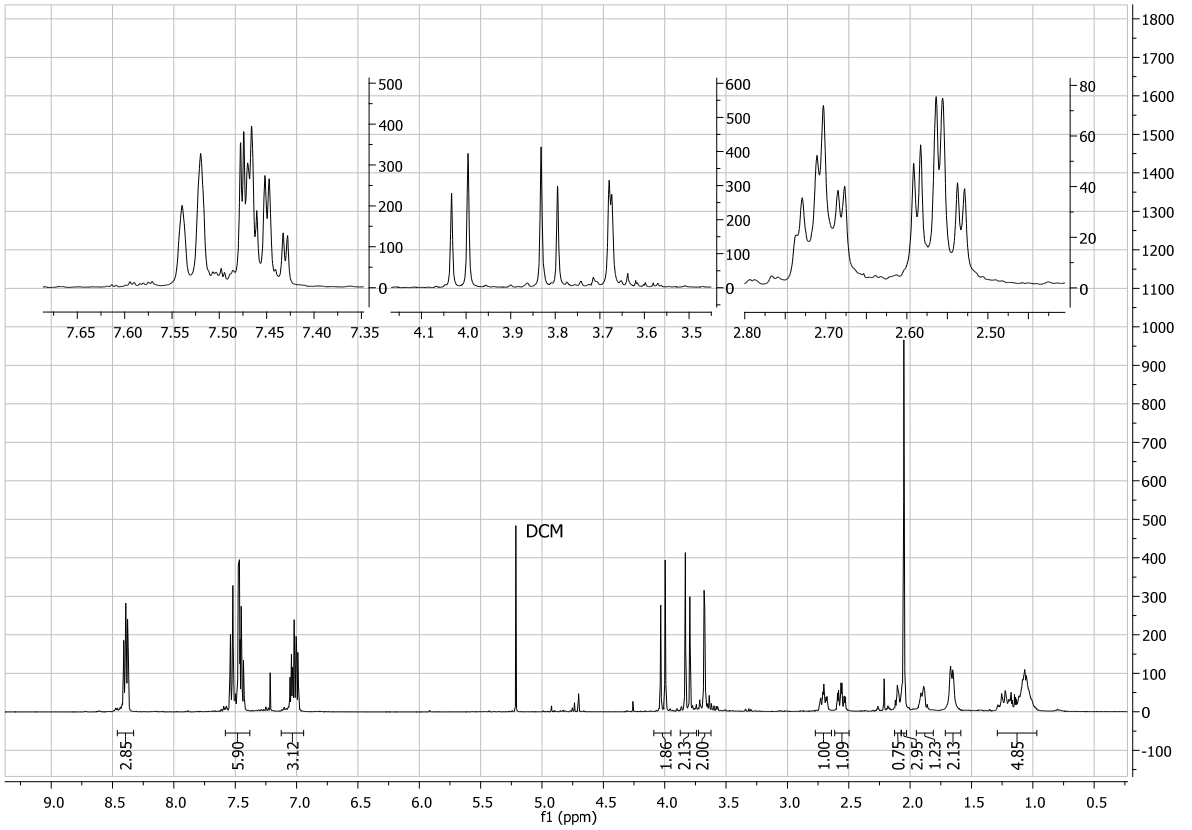
DCM
2.85
5.90
3.12
1.86
2.13
2.00
1.00
1.09
0.75
2.95
1.23
2.13
4.85
f1 (ppm)

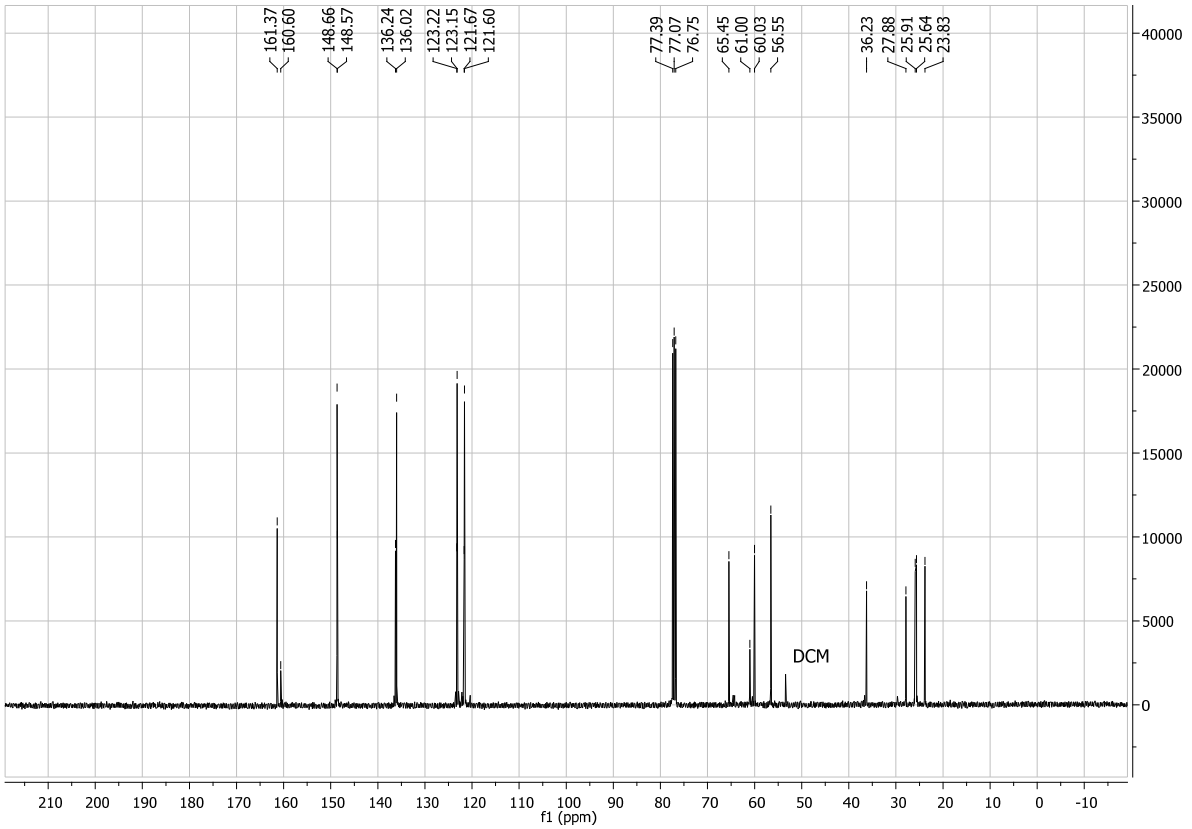
161.37
160.60
148.66
148.57
136.24
136.02
123.22
123.15
121.67
121.60
77.39
77.07
76.75
65.45
61.00
60.03
56.55
36.23
27.88
25.91
25.64
23.83
DCM
f1 (ppm)

(1*R*, 2*R*)-*N*1-methyl-*N*1, *N*2, *N*2-tris(pyridin-2-ylmethyl)cyclohexane-1,2-diamine ((*R*, *R*)-163)

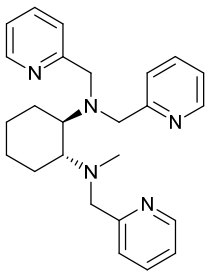

(*R*, *R*)-174 (300 mg, 0.770 mmoles) was dissolved in formaldehyde (30 % solution in water, 85.5 mg, 0.850 mmol) and formic acid (145 µL, 3.85 mmol). The mixture was refluxed for one night until the starting material disappearance is observed by TLC (DCM/MeOH 9:1 on Al_2O_3). Once the starting amine was completely consumed, the solvents were removed by rotary evaporation, the residue dissolved in DCM (20 mL) and washed with saturated $NaHCO_3$ (10 mL). The aqueous layer was extracted with DCM (2 x 20 mL) and the combined organic phases were dried over $MgSO_4$ end evaporated *in vacuo* to yield **(*R*, *R*)-163** (200 mg, 65 %) as a yellow oil

$[\alpha]^{25}_D$ = -6.6 (c= 0.5, $CHCl_3$), (1*S*, 2*S*) isomer , $[\alpha]^{25}_D$ = 7.2 (c= 0.5, $CHCl_3$), (1*R*, 2*R*) isomer; IR (neat, ν_{max}/cm^{-1}): 2927, 2852, 1589, 1567, 1472, 1432, 1355, 756; ^{1}H-NMR (400 MHz, δ-$CDCl_3$): 0.94-1.33 (4H, m, C*H*$_2$CH$_2$CHN, CH$_2$C*H*$_2$CHN), 1.60-1.70 (2H, m, C*H*$_2$CH$_2$CHN, CH$_2$C*H*$_2$CHN), 1.86-1.94 (1H, m, C*H*$_2$CH$_2$CHN), 2.04 (3H, s, C*H*$_3$), 2.08-2.13 (1H, m, CH$_2$C*H*$_2$CHN), 2.56 (1H, dt, J_1 = 11.0 Hz, J_2 = 3.5 Hz, CH$_2$CH$_2$C*H*N), 2.71 (1H, dt, J_1 = 10.5 Hz, J_2 = 3.2 Hz, CH$_2$CH$_2$C*H*N), 3.68 (2H, d, J_1= 2.2 Hz, NC*H*$_2$Py), 3.81 (2H, d, J_1= 14.7 Hz, NC*H*$_2$Py), 4.01 (2H, d, J_1= 14.7 Hz, NC*H*$_2$Py), 6.96-7.09 (3H, m, C*H*Py), 7.41-7.50 (4H, m, C*H*Py), 7.53 (2H, d, J_1= 7.8 Hz, C*H*Py), 8.35-8.44 (3H, m, C*H*Py); ^{13}C-NMR (100.2 MHz, δ-$CDCl_3$): 23.8, 25.6, 25.9, 27.8, 36.2, 56.5, 60.0, 61.0, 65.4, 121.60, 121.67, 123.1, 123.2, 136.0, 136.2, 148.5, 148.6, 160.6, 161.3; *m/z* (ESI): 203.1 (15 %), 280.1 (5), 402.2 (100);HRMS (ESI): $[C_{25}H_{31}N_5+H]^+$ requires 402.2657 found 402.2655.

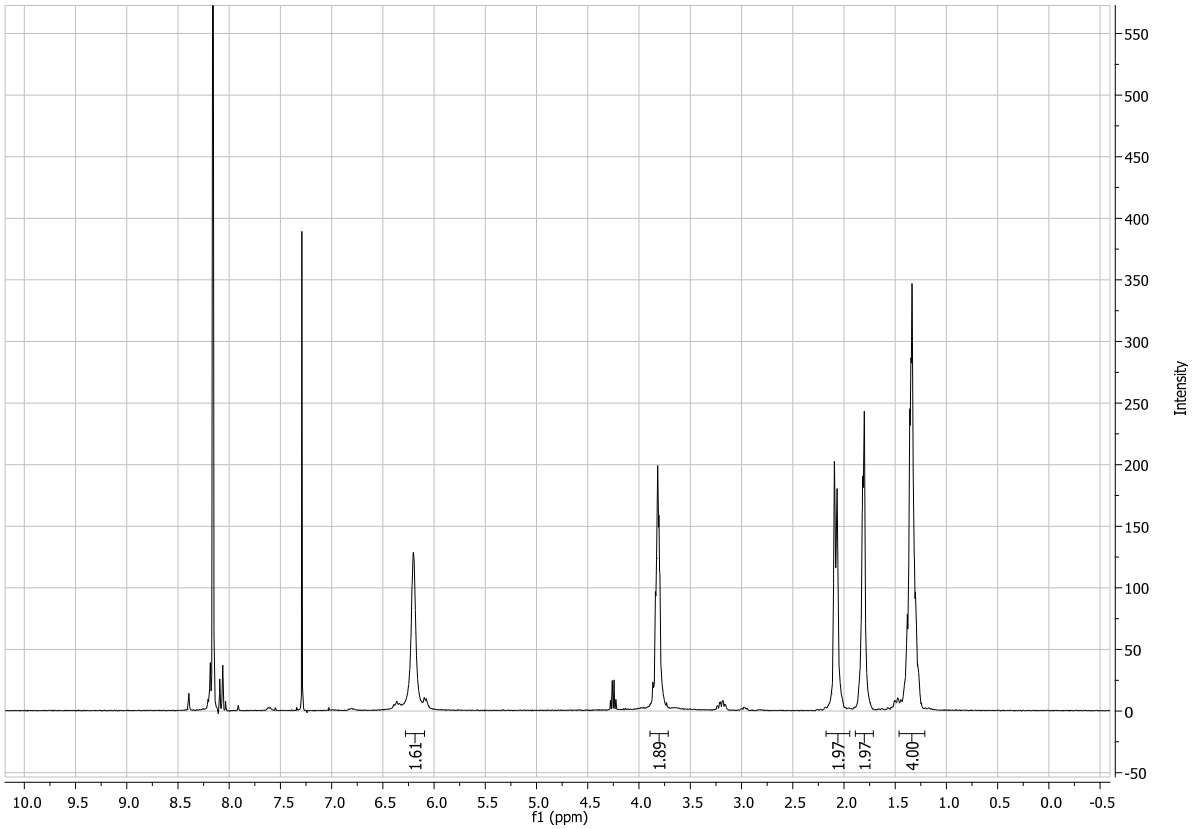
1.61
1.89
1.97
1.97
4.00
f1 (ppm)
Intensity

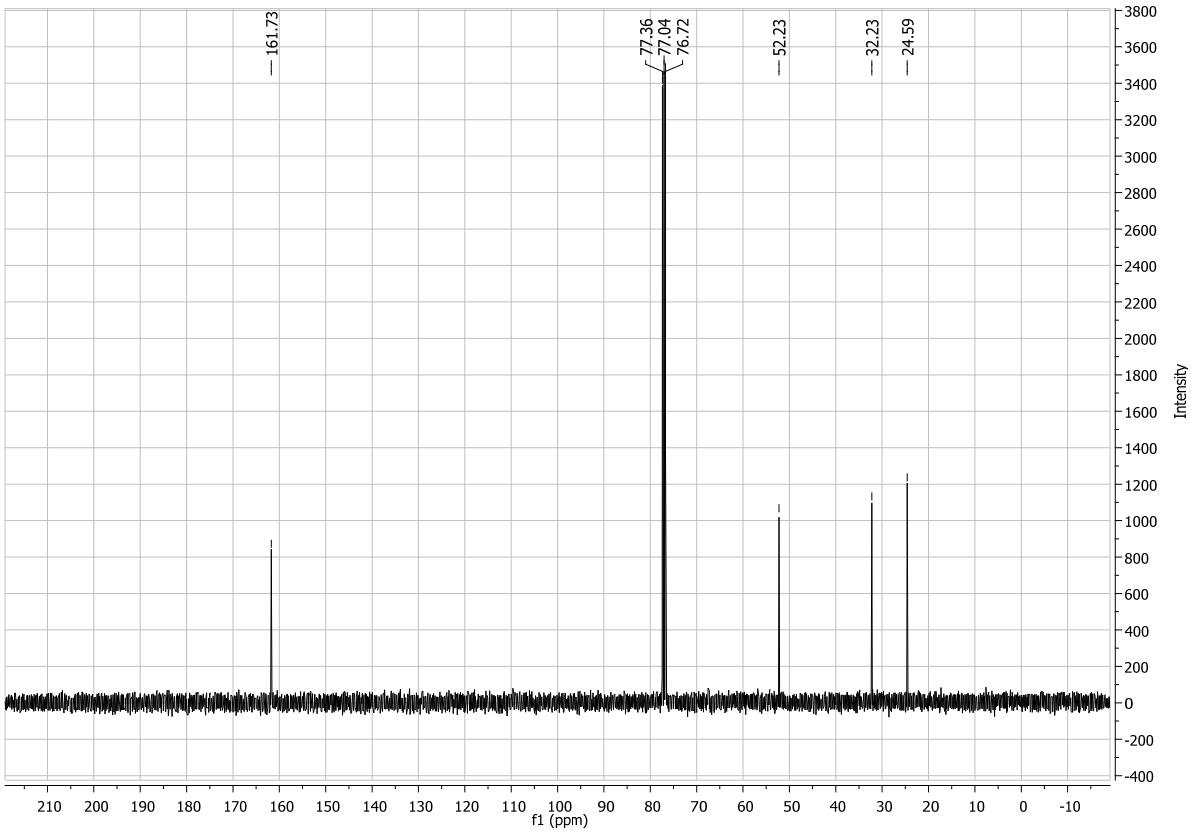
161.73
77.36
77.04
76.72
52.23
32.23
24.59
f1 (ppm)
Intensity

***N*, *N*'-((1*R*, 2*R*)-cyclohexane-1,2-diyl)diformamide ((*R*, *R*)-176)[60]**

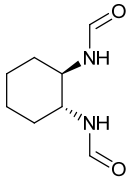

Ethyl formate (20.0 mL, 293 mmol) and **(*R*, *R*)-133** (5.00 mL, 41.6 mmol) were added together in a round bottom flask open to air and stirred at 50 °C. After two hours a white solid formed in the flask and EtOAc (10 mL) was added to maintain the efficiency of the stirring; the reaction was then warmed for further two hours. After a total of four hours, the mixture was allowed to cool to RT and the solid filtered and washed with EtOAc (2 x 20 mL). Product **(*R*, *R*)-176** (5.3 g, 75 %) was recovered as a colourless solid.

mp 140-142 °C, lit.[60] 143-145 °C; $[\alpha]^{25}_{D}$ = -119.3 (c = 0.63, DMSO), lit.[60] -121.0 (c = 0.63, DMSO); IR (neat, ν_{max}/cm^{-1}): 3264, 3068, 2933, 2894, 2856, 1642, 1550, 1388, 1300, 1252, 1231; ^{1}H-NMR (400 MHz, δ-$CDCl_3$): 1.22-1.43 (4H, m, C*H*$_2$CH$_2$CH, CH$_2$C*H*$_2$CH), 1.74-1.86 (2H, m, C*H*$_2$CH$_2$CH), 2.01-2.13 (2H, m, CH$_2$C*H*$_2$CH), 3.74-3.88 (2H, m, CH$_2$CH$_2$C*H*), 6.19 (2H, broad s, N*H*$_2$); ^{13}C-NMR (100.2 MHz, δ-$CDCl_3$): 24.5, 32.2, 52.2, 161.7; *m/z* (ESI): 143.1 (20 %), 193.0 (100), 363.1 (60); HRMS (ESI): $[C_8H_{14}N_2O_2+Na]^+$ requires 193.0945 found 193.0944.

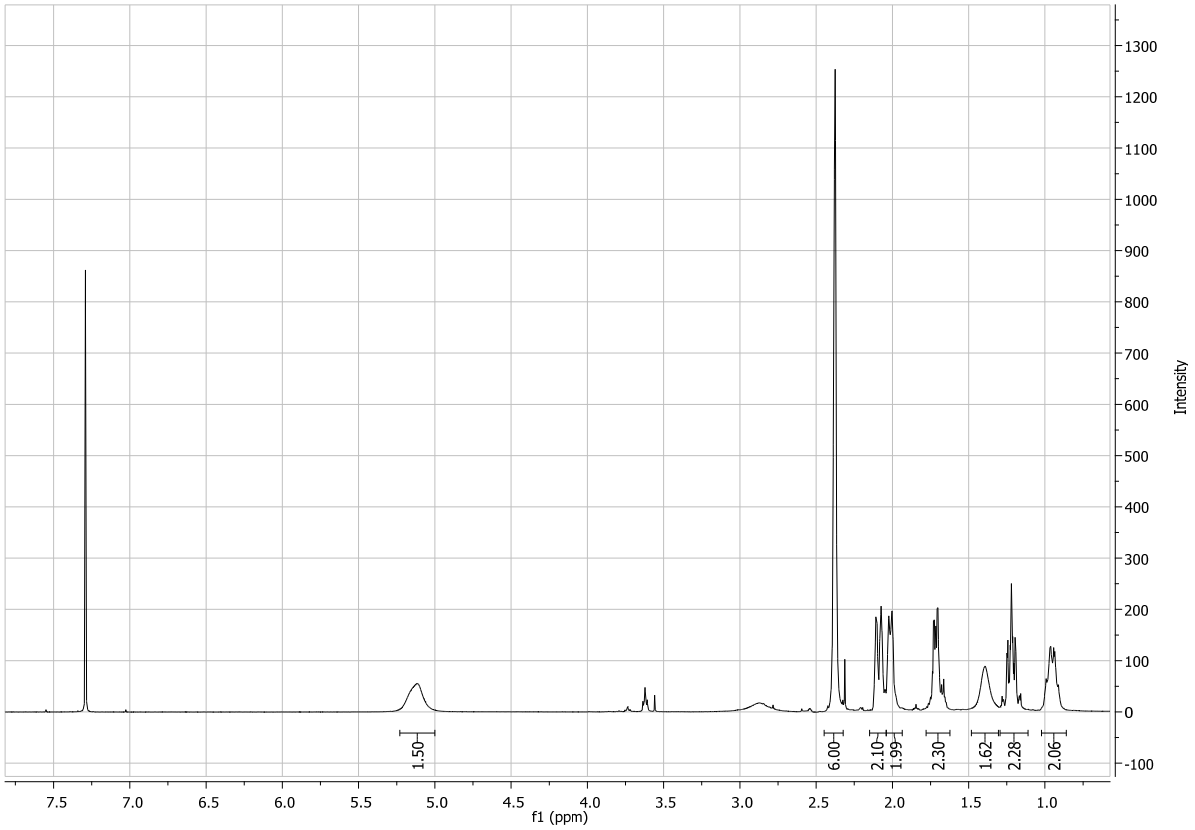
1.50
6.00
2.10
1.99
2.30
1.62
2.28
2.06
f1 (ppm)
Intensity

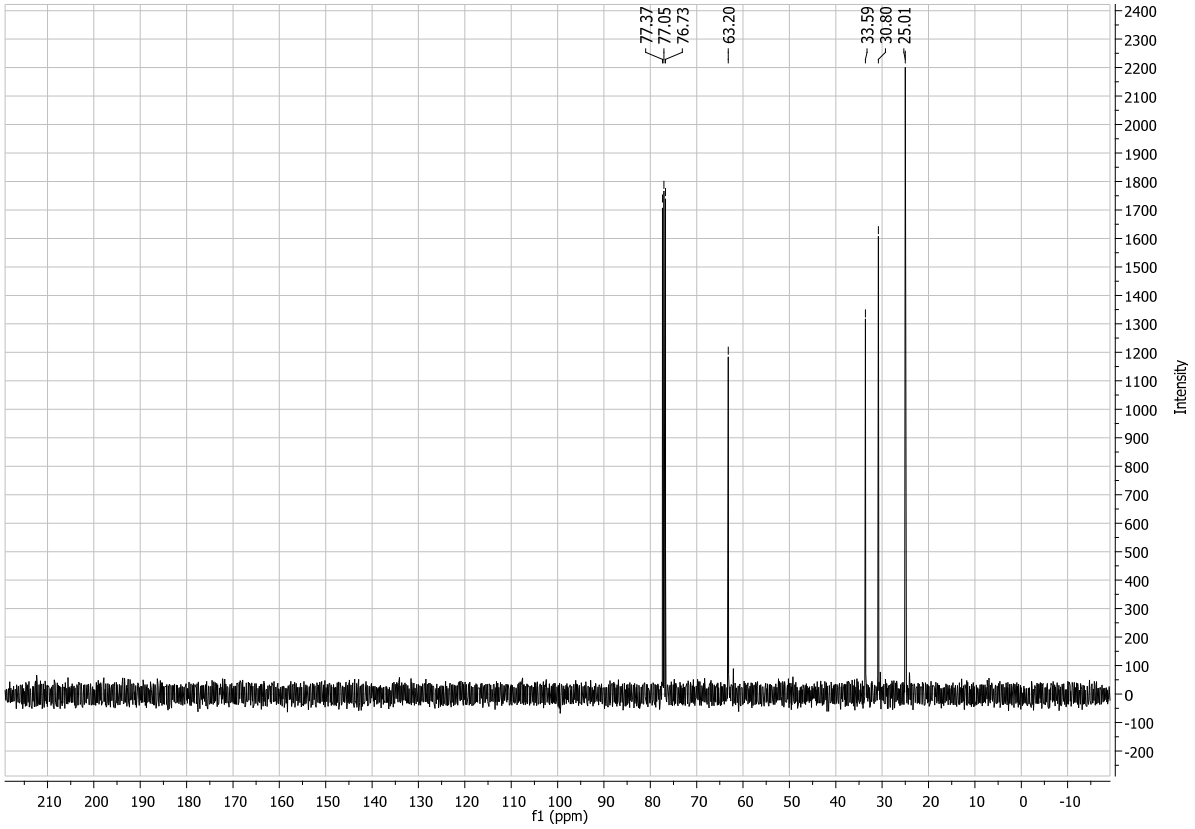
77.37
77.05
76.73
63.20
33.59
30.80
25.01
f1 (ppm)
Intensity

(1*R*, 2*R*)-*N*1, *N*2-dimethylcyclohexane-1,2-diamine ((*R*, *R*)-177)[61]

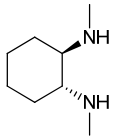

To a suspension of $LiAlH_4$ (3.00 g, 79.0 mmol) in dry THF, kept under a nitrogen atmosphere, **(*R*, *R*)-176** (3.00 g, 17.6 mmol) was added in portions over 10 minutes. After the effervescence stopped, the mixture was refluxed for 48 hours and followed by TLC (Al_2O_3, DCM/MeOH 9:1). Once complete, the reaction was quenched by sequential addition of water (1 mL per gram of $LiAlH_4$ used), KOH (w/w, 20 %, 2 mL per gram of $LiAlH_4$ used) and more water (3 mL per gram of $LiAlH_4$ used) under stirring. When the salts turned white, the mixture was filtered on a pad of Celite. Recovery was improved by stirring the filtered salts in boiling THF for 30 minutes and filtering them again. The reunited organic phases were washed with brine and dried on $MgSO_4$. After removal of the solvents, product **(*R*, *R*)-177** (1.8 g, 72 %) was recovered as a pale yellow oil.

$[\alpha]^{25}_D$ = -136.4 (c = 1.15, $CHCl_3$), lit.[62] -144.2 (c = 1.15, $CHCl_3$), (1*R*, 2*R*) isomer; IR (neat, ν_{max}/cm^{-1}): 3282, 2931, 2855, 2788, 1449, 1144; ^{1}H-NMR (400 MHz, δ-$CDCl_3$): 0.86-1.02 (2H, m, CH_2CH_2CH), 1.14-1.29 (2H, m, CH_2CH_2CH), 1.36 (1H, br, N*H*), 1.62-1.79 (2H, m, CH_2CH_2CH), 1.94-2.04 (2H, m, CH_2CH_2CH), 2.04-2.14 (2H, m, CH_2CH_2CH), 2.37 (6H, s, 2 x CH_3), 5.12 (1H, broad s, N*H*); ^{13}C-NMR (100.2 MHz, δ-$CDCl_3$): 25.0, 30.8, 33.5, 63.2; *m/z* (ESI): 129.1 (5 %), 143.2 (100), 155.2 (20); HRMS (ESI): $[C_8H_{16}N_2+H]^+$ requires 141.1386 found 141.1386.

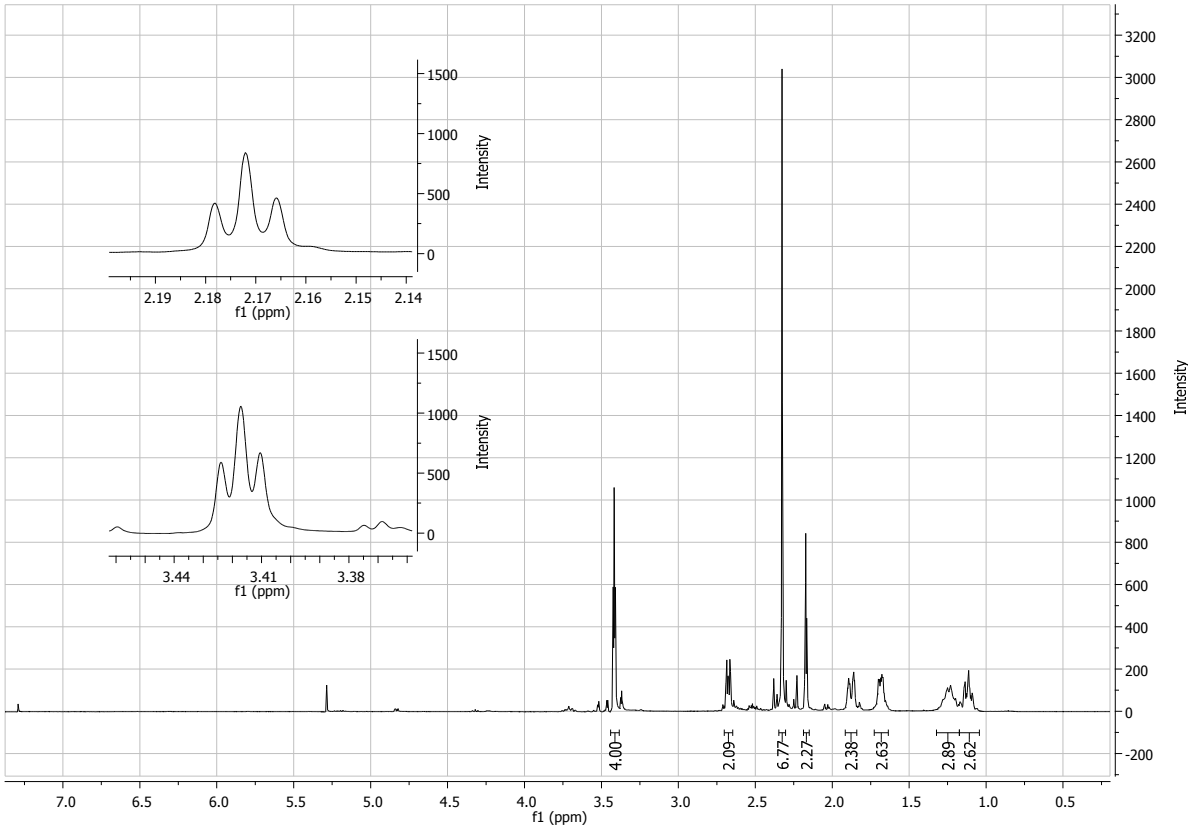
Intensity
f1 (ppm)
4.00
2.09
6.77
2.27
2.38
2.63
2.89
2.62

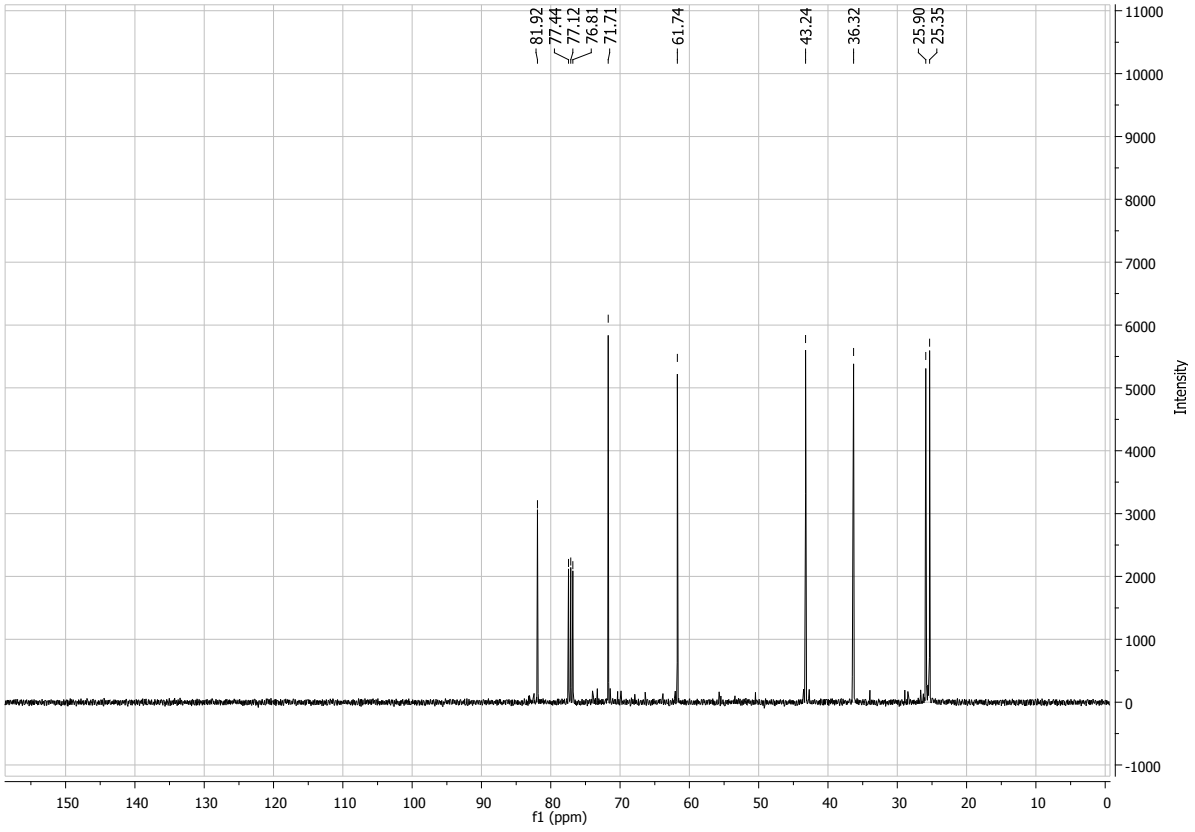
81.92
77.44
77.12
76.81
71.71
61.74
43.24
36.32
25.90
25.35
Intensity
f1 (ppm)

(1*R*, 2*R*)-*N*1, *N*2-dimethyl-*N*1, *N*2-di(prop-2-ynyl)cyclohexane-1,2-diamine ((*R*, *R*)-178)

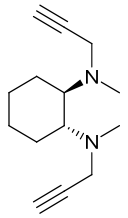

To a solution of **(*R*, *R*)-177** (600 mg, 4.20 mmol) in dry THF and under a nitrogen atmosphere, sodium hydride (305 mg, 12.7 mmol) was added in portions over a period of 10 minutes. The suspension was cooled in an ice bath and allowed to stir for further 10 minutes before propargyl bromide (1.05 g, 8.80 mmol) was added dropwise through a septum. The temperature was kept below 10 °C during the entire process. The reaction was allowed to warm up overnight with constant stirring and monitored via TLC (DCM/MeOH 9:1). After the reaction reached completion, the solid was filtered off and washed with THF (2 x 10 mL). The organic phase was dried on $MgSO_4$ and the solvent removed under reduced pressure to give **(*R*, *R*)-178** (800 mg, 87 %) as a dark brown oil. Further purification of the product was achieved via flash chromatography on silica (DCM/MeOH 95:5 to 9:1, 500 mg recovered, 55 %).

$[\alpha]^{25}_D$ = -256.5 (c = 0.6, DCM); IR (neat, ν_{max}/cm^{-1}): 3302, 2930, 2856, 2788, 2361,1669, 1448, 1358, 1030; ^{1}H-NMR (400 MHz, δ-$CDCl_3$): 1.06-1.16 (2H, m, CH_2CH_2CH), 1.17-1.31 (2H, m, CH_2CH_2CH), 1.63-1.73 (2H, m, CH_2CH_2CH), 1.82-1.92 (2H, m, CH_2CH_2CH), 2.17 (2H, t, J_1 = 2.5 Hz, CC*H*), 2.32 (6H, s,2 x CH_3), 2.63-2.71 (2H, m, CH_2CH_2CH), 3.40-3.43 (4H, t, J_1 = 2.6 Hz, NCH_2CCH); ^{13}C-NMR (100.2 MHz, δ-$CDCl_3$): 25.3, 25.9, 36.3, 43.2, 61.7, 71.7, 81.9; *m/z* (ESI): 166.1 (75 %), 219.18 (100), 273.1 (40); HRMS (ESI): $[C_{14}H_{22}N_2+H]^+$ requires 219.1856 found 219.1853.

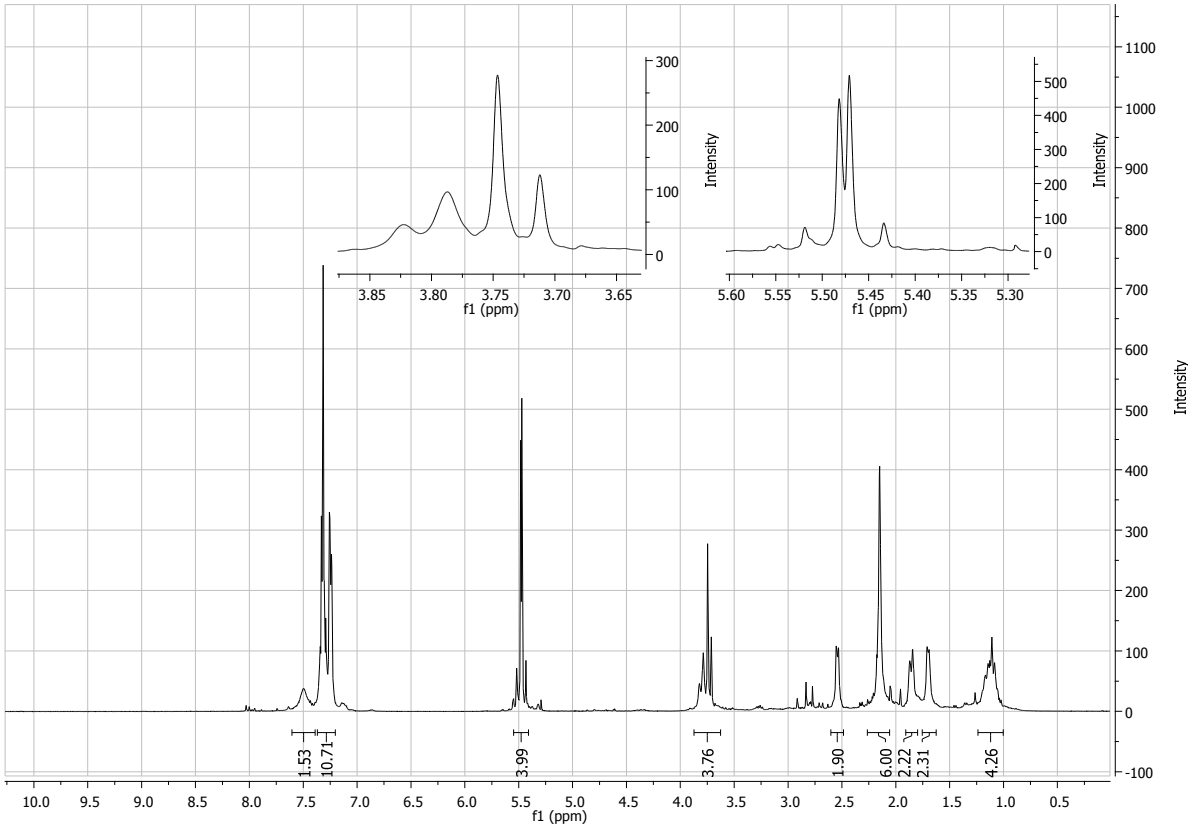
f1 (ppm)
Intensity
1.53
10.71
3.99
3.76
1.90
6.00
2.22
2.31
4.26

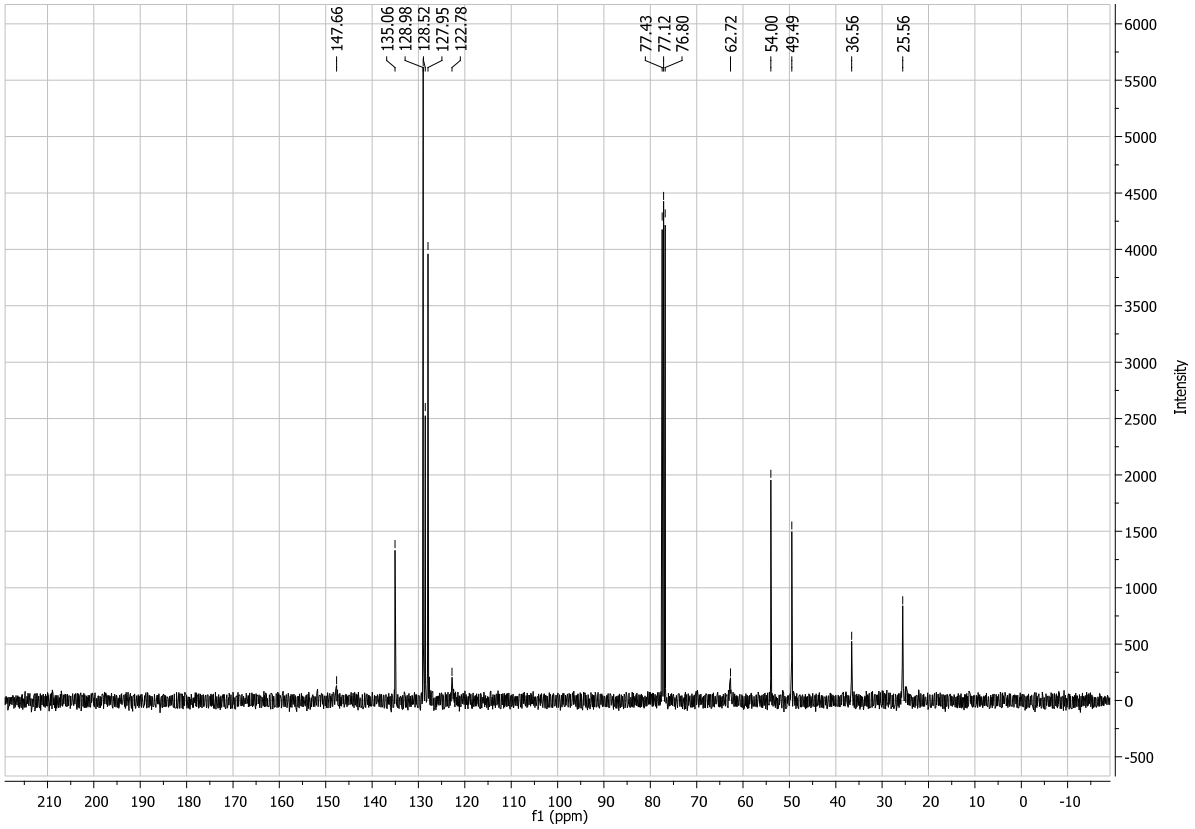
147.66
135.06
128.98
128.52
127.95
122.78
77.43
77.12
76.80
62.72
54.00
49.49
36.56
25.56
f1 (ppm)
Intensity

(1*R*, 2*R*)-*N*1,*N*2-bis((1-benzyl-1H-1,2,3-triazol-4-yl)methyl)-*N*1, *N*2-dimethylcyclohexane -1,2-diamine ((*R*, *R*)-164)

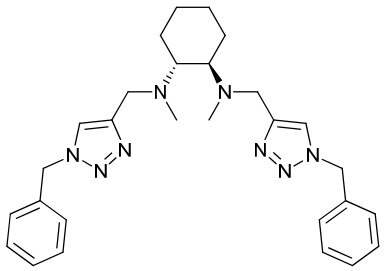

Benzyl azide (**179**) (0.46 g, 2.3 mmol) and **(R, R)-178** (0.50 g, 3.4 mmol) were mixed together in dry THF and kept under a nitrogen atmosphere. Copper iodide (0.48 g, 2.5 mmol) and TEA (2 mL) were then added to the mixture, and the flask covered in aluminium foil to screen it from light. The reaction was stirred at room temperature, and the disappearance of benzyl azide monitored via TLC (Petroleum spirit/EtoAC 1:1). Once all the benzyl azide has been consumed, one more equivalent of it was added and the reaction stirred for an equal amount of time. After completion, the mixture was diluted with ammonia solution (20 mL) and transferred into a separating funnel. The aqueous layer was separated and extracted with DCM (3 x 50 mL), and the reunited organic phases washed several times with ammonia solution until the aqueous layer was colourless. The organic phase was then dried over $MgSO_4$ and the solvents removed under reduced pressure to yield **(*R*, *R*)-164** (1.0 g, 90 %) as a dark brown oil. The pure compound was obtained by flash chromatography on silica (petroleum spirit/EtOAc 9:1 to 100 % EtoAc) followed by chromatography on Al_2O_3 on the cleaner fraction (Chloroform/IPA from 100 % DCM to 90:10, 0.6 g recovered, 54 %).

$[\alpha]^{25}_D$= -6.8 (c = 1, $CHCl_3$); IR (neat, ν_{max}/cm^{-1}): 3398, 2932, 2857, 1649, 1497, 1454, 1048; ^{1}H-NMR (400 MHz, δ-$CDCl_3$): 0.99-1.22 (4H, m, CH_2CH_2CH, CH_2CH_2CH), 1.61-1.75 (2H, m, CH_2CH_2CH), 1.78-1.91 (2H, m, CH_2CH_2CH), 2.15 (6H, s, 2 x CH_3), 2.47-2.59 (2H, m, CH_2CH_2CH), 3.73 (2H, d, J_1 = 13.7 Hz, NCH_2CCHN), 3.80 (2H, d, J_1 = 14.0 Hz, NCH_2CCHN), 5.45 (2H, d, J_1 = 14.9 Hz, CH_2Ph), 5.50 (2H, d, J_1 = 14.9 Hz, CH_2Ph), 7.19-7.39 (10H, m, Ar*H*), 7.49 (2H, broad s, NCH_2CCHN); ^{13}C-NMR (100.6 MHz, δ-$CDCL_3$): 25.5, 36.5, 49.4, 53.9, 62.7, 122.7, 127.9, 128.5, 128.9, 135.0, 147.6; *m/z* (ESI): 283.1 (10%), 485.3 (100), 611.2 (10) HRMS (ESI): $[C_{28}H_{36}N_8H+H]^+$ requires 485.3149 found 485.3148.

5.3 General complexation procedures

Complexation of ligand (*R*, *R*)-163 to metal trifluorosulfonates.

The selected metal(II)-trifluorosulfonate was dissolved in 2 mL ACN in a flame dried Shlenck tube and kept under a nitrogen athmosphere. An equimolar solution of ligand **(*R*, *R*)-163** in ACN was added through a septum in one portion and the mixture left stirring for three hours at RT. The solvent was then removed and the residue triturated in petroleoum ether (60°/80°) until a microcrystalline powder was obtained. The filtration was performed under nitrogen and the product immediately stored under nitrogen.

$Fe(OTf)_2$ (88.2 mg, 0.250 mmol) according to the general procedure, was reacted with **(*R*, *R*)-163** (100 mg, 0.250 mmol). A colour change from pale yellow to red was observed in the first minutes of stirring. A bright red powder was obtained (100 mg, 81 %).

λ_{max} (H_2O): 252 (ε 6700), 350 (ε 1117), 486 (ε 72.3), 572 (ε 101); *m/z* (ESI): 228.5 (10 %), 246.0 (30), 492.1 (80), 606.1 (85), 623.1 (25); HRMS (ESI): [$C_{25}H_{31}N_5FeCl$, M-CF_3SO_3-CH_3+Cl]$^+$ requires 492.1612 found 492.1599, [$C_{26}H_{31}N_5FeF_3SO_3$, M-CH_3]$^+$ requires 606.1444 found 606.1429.

$Mn(OTf)_2$ (17.6 mg, 50.0x10^{-3} mmol) according to the general procedure, was reacted with **(*R*, *R*)-163** (20 mg, 50.0x10^{-3} mmol). A colour change from pale yellow to brown was observed in the first minutes of stirring. A brown powder was obtained (20 mg, 65 %).

λ_{max} (H_2O): 257 (ε 3656); *m/z* (ESI): 228.0 (35 %), 491.1 (40), 606.1 (85), 605.1 (100, [M-CH_3]$^+$); HRMS (ESI): [$C_{25}H_{31}N_5Mn$, M-CF_3SO_3-CH_3]$^{2+}$ requires 228.0974 found 228.0969.

$Cu(OTf)_2$ (18.1 mg, 50.0x10^{-3} mmol) was reacted with **(*R*, *R*)-163** (20 mg, 50.0x10^{-3} mmol) according to the general procedure.in ACN was then added via a siringe and the mixture stirred for three hours at RT. A colour change from pale yellow to brown and finally blue was observed over the first minutes after the addition. A bright blue powder was recovered (24 mg, 76 %).

λ_{max} (H_2O): 209 (ε 10332), 258 (ε 8427), 291 (ε 2820), 658 (ε 165); *m/z* (ESI): 232.0 (85 %), 613.1 (100); HRMS (ESI): $[C_{26}H_{31}N_5CuF_3SO_3, M\text{-}CH_3]^+$ requires 613.1390 found 613.1376.

$Co(OTf)_2$ (18.2 mg, $50.0x10^{-3}$ mmol) was dissolved in ACN and reacted with ligand **(*R*, *R*)-163** (20 mg, $50.0x10^{-3}$ mmol). The colour of the mixture changed from pale yellow to bright red in the first minutes of stirring. A bright red powder was recovered (22 mg, 77 %).

λ_{max} (H_2O): 254 (ε 12825), 517 (ε 67); *m/z* (ESI): 230.0 (50 %), 247.5 (100), 495.1 (75), 609.1 (35), 644.1 (85); HRMS (ESI): $[C_{25}H_{31}N_5CoCl, M\text{-}CF_3SO_3\text{-}CH_3\text{+}Cl]^+$ requires 495.1595 found 495.1583, $[C_{26}H_{31}N_5CoF_3SO_3, M\text{-}CH_3]^+$ requires 609.1426 found 609.1414.

Complexation of ligand (*R*, *R*)-164 to metal salts

The selected metal salt was dissolved in 2 mL ACN in a flame dried Shlenck tube and kept under a nitrogen athmosphere. An equimolar solution of ligand **(*R*, *R*)-164** in ACN was added through a septum in one portion and the mixture left stirring for three hours at RT. The solvent was then removed and the residue triturated in petroleoum ether (60°/80°) until a microcrystalline powder was obtained. The filtration was performed under nitrogen and the product immediately stored under nitrogen.

$Mn(OTf)_2$ (17.6 mg, $50.0x10^{-3}$ mmol) was reacted with ligand **(*R*, *R*)-164** (24.2 mg, $50.0x10^{-3}$ mmol) A dark brown powder was obtained (30 mg, 71 %).

m/z (ESI): 269.6 (15 %), 485.3 (100), 611.2 (10), 688.1 (10); HRMS (ESI): $[C_{29}H_{36}N_8F_3SO_3Mn, M\text{-}CF_3SO_3]^+$ requires 688.1958 found 688.1947.

$Fe(OTf)_2$ (17.7 mg, $50.0x10^{-3}$ mmol) was reacted with **(*R*, *R*)-164** (24.2 mg, $50.0x10^{-3}$ mmol). A brick red powder was obtained (20 mg, 48 %).

m/z (ESI): 270.1 (10 %), 385.5 (25), 485.3 (100), 575.2 (25), 652.7 (30); HRMS (ESI): $[C_{29}H_{36}N_8F_3SO_3Fe, M\text{-}CF_3SO_3]^+$ requires 689.1928 found 689.1930.

$Cu(SO_4)$ (25.3 mg, 0.159 mmol) was suspended in ACN and mixed with a solution of ligand **(*R*, *R*)-164** (76.8 mg, 0.159 mmol) A brown powder was obtained (50 mg, 49 %).

m/z (ESI): 273.6 (100 %), 582.2 (85), 644.1 (15); HRMS (ESI): $[C_{28}H_{37}CuN_8O_4S]^+$ requires 644.1938 found 644.1939.

Complexation of ligand (*R*, *R*)-39 to metal salts

The selected metal salt was dissolved in 2 mL ACN in a flame dried Shlenck tube and kept under a nitrogen athmosphere. An solution containing 2 eq.of ligand **(*R*, *R*)-164** with respect to the metal in ACN was added through a septum in one portion and the mixture left stirring for three hours at RT. The solvent was then removed and the residue triturated in petroleoum ether (60°/80°) until a microcrystalline powder was obtained. The filtration was performed under nitrogen and the product immediately stored under nitrogen.

5.4 General epoxidation procedures

General procedure for the epoxidation of alkenes with *in situ* formation of the Mn/TMTACN/additive system with hydrogen peroxide

In a vial, the reagents were mixed in this order: 0.5 or 1 mmol of the desired alkene from a stock solution in ACN, 1 mol% $Mn(SO_4)$ from a stock solution in water, 3 mol% TMTACN from a stock solution in ACN, 2 mol% binol-based additive from a stock solution in ACN and 0.1 mmol of decane (GC analysis) or naphthalene (HPLC analysis) from a stock solution in ACN (internal standard). The reagents were allowed to stir for 5 minutes before hydrogen peroxide (17 eq.) premixed with acetone in a 1:3 ratio (v/v) was added over 5 minutes. The total volume of the reaction was kept at 5.8 mL

At selected intervals of time, 100 µL of the reaction mixture were withdrawn, diluted to 2 mL with IPA and filtered through a plug of silica gel. The analysis was carried out either by GC or HPLC.

For the GC analysis, 5 µL of the resulting solution were injected into column. The relevant GC parameters used were: injector T = 200 °C, initial T = 120 °C, final T = 200 °C, detector T = 200 °C, T increase rate = 1.5 °C/s
For the HPLC analysis, 1 µL of the resulting mixture was injected into the selected column *via* an autosampler. The columns used in this study were: Daicel Chiralpak IA, Daicel Chiralcel OD, Daicel Chiralcel OJ, Daicel Chiralcel AS-RH or Merck LiChrospher RP Select-B depending on the substrate.

General procedure for the epoxidation of styrene and derivatives with dimer 122 in the presence of additive (*S*)-130 with hydrogen peroxide

In a vial, the reagents were mixed in this order: 0.5 mmol of the desired alkene from a stock solution in ACN, 0.5 mol% **122** from a stock solution in ACN, 1 mol% **(*S*)-130** from a stock solution in ACN and 0.1 mmol of dichlorobenzene from a stock solution in ACN (internal standard). The reagents were allowed to stir for 5 minutes before hydrogen peroxide (17 eq.) premixed with acetone in a 1:3 ratio (v/v) was added over 5 minutes. The total volume of the reaction was kept at 5.8 mL
At selected intervals of time, 100 µL of the reaction mixture were withdrawn, diluted to 2 mL with IPA and filtered through a plug of silica gel. The analysis was carried out by HPLC. For the HPLC analysis, 1 µL of the resulting mixture was injected into the selected column *via* an autosampler. The column used for styrene and all the derivatives was a Merck LiChrospher RP Select-B with the solvent pair H_2O/ACN.

General procedure for the epoxidation of styrene with ligands 160c and 161c with hydrogen peroxide in *tert*-amyl-alcohol.

In a vial, the reagents were mixed in this order: 0.5 mmol of the styrene from a stock solution in ACN, 1 mol% metal salt from a stock solution in water ($MnSO_4$ or $FeCl_3$), 1 mol% selected ligand (**160c** or **161c**) from a stock solution in ACN and 0.1 mmol of naphtalene from a stock solution in ACN (internal standard). The reagents were allowed to stir for 5 minutes before hydrogen peroxide (10 eq.) was added over 5 minutes.
At selected intervals of time, 100 µL of the reaction mixture were withdrawn, diluted to 2 mL with IPA and filtered through a plug of silica gel. The analysis was carried out by HPLC. For

the HPLC analysis, 1 μL of the resulting mixture was injected into the selected column *via* an autosampler. The column used for styrene was a Daicel Chirapak IA.

General procedure for the epoxidation of styrene with ligands 160c and 161c with hydrogen peroxide in *tert*-amyl-alcohol in the presence of H_2pydic.

In a vial, the reagents were mixed in this order: 0.5 mmol of styrene from a stock solution in ACN, 1 mol% metal salt from a stock solution in water ($MnSO_4$ or $FeCl_3$), 1 mol% selected ligand (**160c** or **161c**) from a stock solution in ACN, 1 mol% additive (H_2pydic) from a stock solution in ACN and 0.1 mmol of naphtalene from a stock solution in ACN (internal standard). The reagents were allowed to stir for 5 minutes before hydrogen peroxide (10 eq.) was added over 5 minutes.
At selected intervals of time, 100 μL of the reaction mixture were withdrawn, diluted to 2 mL with IPA and filtered through a plug of silica gel. The analysis was carried out by HPLC. For the HPLC analysis, 1 μL of the resulting mixture was injected into the selected column *via* an autosampler. The column used for styrene was a Daicel Chirapak IA.

General procedure for the epoxidation of styrene with ligands 160c and 161c with diluted hydrogen peroxide in acetonitrile.

In a vial, the reagents were mixed in this order: 0.5 mmol of styrene from a stock solution in ACN, 1 mol% metal salt from a stock solution in water ($MnSO_4$ or $FeCl_3$), 1 mol% selected ligand (**160c** or **161c**) from a stock solution in ACN and 0.1 mmol of naphtalene from a stock solution in ACN (internal standard). The reagents were allowed to stir for 5 minutes before hydrogen peroxide (10 eq.) diluted in ACN (1:1 v/v) was added over 5 or 20 minutes.
At selected intervals of time, 100 μL of the reaction mixture were withdrawn, diluted to 2 mL with IPA and filtered through a plug of silica gel. The analysis was carried out by HPLC. For the HPLC analysis, 1 μL of the resulting mixture was injected into the selected column *via* an autosampler. The column used for styrene was a Daicel Chirapak IA.

General procedure for the epoxidation of styrene with ligands 160c and 161c with diluted hydrogen peroxide in acetonitrile in the presence of H_2pydic.

In a vial, the reagents were mixed in this order: 0.5 mmol of styrene from a stock solution in ACN, 1 mol% metal salt from a stock solution in water ($MnSO_4$ or $FeCl_3$), 1 mol% selected ligand (**160c** or **161c**) from a stock solution in ACN, 1 mol% additive (H_2pydic) from a stock solution in ACN and 0.1 mmol of naphtalene from a stock solution in ACN (internal standard). The reagents were allowed to stir for 5 minutes before hydrogen peroxide (10 eq.) diluted in ACN (1:1 v/v) was added over 5 or 20 minutes.
At selected intervals of time, 100 µL of the reaction mixture were withdrawn, diluted to 2 mL with IPA and filtered through a plug of silica gel. The analysis was carried out by HPLC. For the HPLC analysis, 1 µL of the resulting mixture was injected into the selected column *via* an autosampler. The column used for styrene was a Daicel Chirapak IA.

General procedure for the epoxidation of styrene in acetonitrile with ligands 160c and 161c with hydrogen peroxide premixed with acetone.

In a vial, the reagents were mixed in this order: 0.5 mmol of styrene from a stock solution in ACN, 1 mol% metal salt from a stock solution in water ($MnSO_4$ or $FeCl_3$), 1 mol% selected ligand (**160c** or **161c**) from from a stock solution in ACN and 0.1 mmol of naphtalene from a stock solution in ACN (internal standard). The reagents were allowed to stir for 5 minutes before hydrogen peroxide (10 eq.) premixed in acetone in a 1:3 ratio (v/v) was added over 5 minutes.
At selected intervals of time, 100 µL of the reaction mixture were withdrawn, diluted to 2 mL with IPA and filtered through a plug of silica gel. The analysis was carried out by HPLC. For the HPLC analysis, 1 µL of the resulting mixture was injected into the selected column *via* an autosampler. The column used for styrene was a Daicel Chirapak IA.

General procedure for the epoxidation of styrene in acetonitrile with ligands 160c and 161c with hydrogen peroxide premixed with acetone in the presence of H_2pydic.

In a vial, the reagents were mixed in this order: 0.5 mmol of styrene from a stock solution in ACN, 1 mol% metal salt from a stock solution in water ($MnSO_4$ or $FeCl_3$), 1 mol% selected ligand (**160c** or **161c**) from a stock solution in ACN, 1 mol% additive (H_2pydic) from a stock

solution in ACN and 0.1 mmol of naphtalene from a stock solution in ACN (internal standard). The reagents were allowed to stir for 5 minutes before hydrogen peroxide (10 eq.) premixed in acetone in a 1:3 ratio (v/v) was added over 5 minutes.
At selected intervals of time, 100 μL of the reaction mixture were withdrawn, diluted to 2 mL with IPA and filtered through a plug of silica gel. The analysis was carried out by HPLC. For the HPLC analysis, 1 μL of the resulting mixture was injected into the selected column *via* an autosampler. The column used for styrene was a Daicel Chirapak IA.

General procedure for the epoxidation of styrene in acetonitrile with ligands 160c and 161c with hydrogen peroxide with acetone in the mixture.

In a vial, the reagents were mixed in this order: 0.5 mmol of styrene from a stock solution in ACN, 1 mol% metal salt from a stock solution in water ($MnSO_4$ or $FeCl_3$), 1 mol% selected ligand (**160c** or **161c**) from a stock solution in ACN and 0.1 mmol of naphtalene from a stock solution in ACN (internal standard); finally, 2 mL of acetone were added to the mixture and the reagents were allowed to stir for 5 minutes before hydrogen peroxide (10 eq.) was added over 5 minutes.
At selected intervals of time, 100 μL of the reaction mixture were withdrawn, diluted to 2 mL with IPA and filtered through a plug of silica gel. The analysis was carried out by HPLC. For the HPLC analysis, 1 μL of the resulting mixture was injected into the selected column *via* an autosampler. The column used for styrene was a Daicel Chirapak IA.

General procedure for the epoxidation of styrene in acetonitrile with ligands 160c and 161c with hydrogen peroxide with acetone in the mixture in the presence of H_2pydic.

In a vial, the reagents were mixed in this order: 0.5 mmol of styrene from a stock solution in ACN, 1 mol% metal salt from a stock solution in water ($MnSO_4$ or $FeCl_3$), 1 mol% selected ligand (**160c** or **161c**) from a stock solution in ACN, 1 mol% additive (H_2pydic) from a stock solution in ACN and 0.1 mmol of naphtalene from a stock solution in ACN (internal standard; finally, 2 mL of acetone were added to the mixture and the reagents were allowed to stir for 5 minutes before hydrogen peroxide (10 eq.) was added over 5 minutes.
At selected intervals of time, 100 μL of the reaction mixture were withdrawn, diluted to 2 mL with IPA and filtered through a plug of silica gel. The analysis was carried out by HPLC. For

the HPLC analysis, 1 μL of the resulting mixture was injected into the selected column *via* an autosampler. The column used for styrene was a Daicel Chirapak IA.

General procedure for the epoxidation of styrene in acetonitrile with ligands 160c and 161c with peracetic acid.

In a vial, the reagents were mixed in this order: 0.5 mmol of styrene from a stock solution in ACN, 1 mol% metal salt from a stock solution in water ($MnSO_4$ or $FeCl_3$), 1 mol% selected ligand (**160c** or **161c**) from a stock solution in ACN and 0.1 mmol of naphtalene from a stock solution in ACN (internal standard). The reagents were allowed to stir for 5 minutes before commercial peracetic acid (2 eq.) was added to the mixture over 5 minutes.
At selected intervals of time, 100 μL of the reaction mixture were withdrawn, diluted to 2 mL with IPA and filtered through a plug of silica gel. The analysis was carried out by HPLC. For the HPLC analysis, 1 μL of the resulting mixture was injected into the selected column *via* an autosampler. The column used for styrene was a Daicel Chirapak IA.

General procedure for the epoxidation of styrene in acetonitrile with ligands 160c and 161c with *in situ* generated peracetic acid.

In a vial, the reagents were mixed in this order: 0.5 mmol of styrene from a stock solution in ACN, 1 mol% metal salt from a stock solution in water ($MnSO_4$ or $FeCl_3$), 1 mol% selected ligand (**160c** or **161c**) from a stock solution in ACN and 0.1 mmol of naphtalene from a stock solution in ACN (internal standard). Acetic acid (14 eq.) was added to the mixture and the mixture stirred for 5 minutes before hydrogen peroxide (10 eq.) diluted in ACN (1:1 v/v) was added over 5 minutes.
At selected intervals of time, 100 μL of the reaction mixture were withdrawn, diluted to 2 mL with IPA and filtered through a plug of silica gel. The analysis was carried out by HPLC. For the HPLC analysis, 1 μL of the resulting mixture was injected into the selected column *via* an autosampler. The column used for styrene was a Daicel Chirapak IA.

General procedure for the epoxidation of alkenes with ligands 39, 163 and 164 with peracetic acid.

In a vial, the reagents were mixed in this order: 0.5 mmol of the selected alkene from a stock solution in ACN, 1 mol% of the desired metal salt ($Mn(OTf)_2$, $Fe(OTf)_2$, $Cu(OTf)_2$ or $Co(OTf)_2$) from a stock solution in water, 1 mol% selected ligand (**39, 163** or **164**) from a stock solution in ACN and 0.1 mmol of naphtalene from a stock solution in ACN (internal standard). The mixture was allowed to stir for 5 minutes before peracetic acid (2 eq.) was added in a single portion.
At selected intervals of time, 100 μL of the reaction mixture were withdrawn, diluted to 2 mL with IPA and filtered through a plug of silica gel. The analysis was carried out by HPLC. For the HPLC analysis, 1 μL of the resulting mixture was injected into the selected column *via* an autosampler. The columns used in this analyses were: Daicel Chiralpak IA, Daicel Chiralcel OD, Daicel Chiralcel OJ, Daicel Chiralcel AS-RH or Merck LiChrospher RP Select-B depending on the substrate.

General procedure for the epoxidation of alkenes with ligand 164 with hydrogen peroxide.

In a vial, the reagents were mixed in this order: 0.5 mmol of the selected alkene from a stock solution in ACN, 1 mol% of the desired metal salt ($Mn(OTf)_2$, $Fe(OTf)_2$) from a stock solution in water, 1 mol% ligand **164** from a stock solution in ACN and 0.1 mmol of naphtalene from a stock solution in ACN (internal standard). The mixture was allowed to stir for 5 minutes before hydrogen peroxide (10 eq.) premixed with acetone in a 1:3 ratio (v/v) was added over 5 minutes.
At selected intervals of time, 100 μL of the reaction mixture were withdrawn, diluted to 2 mL with IPA and filtered through a plug of silica gel. The analysis was carried out by HPLC. For the HPLC analysis, 1 μL of the resulting mixture was injected into the selected column *via* an autosampler. The columns used in this analyses were: Daicel Chiralpak IA, Daicel Chiralcel OD, Daicel Chiralcel OJ, Daicel Chiralcel AS-RH or Merck LiChrospher RP Select-B depending on the substrate.

5.5 References

1. J. Leonard, B. Lygo and G. Procter, *Advanced practical organic chemistry*, Second edition edn., Stanley Thornes LTD, 1995.
2. Enraf-Nonius, *CAD-4/PC Software, Version 1.5c. **1994**, Delft, The Netherlands*, (1994).
3. K. Harms, *Harms, K. XCAD4. Program for data reduction. **1996** Philipps-Universität, Marburg, Germany.*
4. G. M. Sheldrick, *Acta Crystallographica Section A*, 2008, **64**, 112-122.
5. L. Farrugia, *J. Appl. Crystallogr.*, 1997, **30**, 565.
6. A. L. Spek, *J. Appl. Crystallogr.*, 2003, **36**, 7-13.
7. L. Farrugia, *J. Appl. Crystallogr.*, 1999, **32**, 837-838.
8. J. Gao, H. He, X. Zhang, X. Lu and J. Kang, *Indian J. Chem., Sect B*, 2002, **41**, 372.
9. E. M. D. Keegstra, J. W. Zwikker, M. R. Roest and L. W. Jenneskens, *J. Org. Chem.*, 1992, **57**, 6678-6680.
10. G. H. Searle and R. J. Geue, *Aust. J. Chem.*, 1984, **37**, 959-970.
11. D. W. White, B. A. Karcher, R. A. Jacobson and J. G. Verkade, *J. Am. Chem. Soc.*, 1979, **101**, 4921-4925.
12. G. H. Searle and R. J. Geue, *Aust. J. Chem.*, 1984, **37**, 959-970.
13. H.-J. Schanz, M. A. Linseis and D. G. Gilheany, *Tetrahedron: Asymmetry*, 2003, **14**, 2763-2769.
14. K. Onuma, T. Ito and A. Nakamura, *Bull. Chem. Soc. Jpn.*, 1980, **53**, 2016-2019.
15. K. Yoshizawa, S. Toyota and F. Toda, *Tetrahedron*, 2004, **60**, 7767-7774.
16. P. Wipf and J. K. Jung, *J. Org. Chem.*, 2000, **65**, 6319-6337.
17. T. Sakamoto, H. Yonehara and C. Pac, *J. Org. Chem.*, 1994, **59**, 6859-6861.
18. G. D. Y. Sogah and D. J. Cram, *J. Am. Chem. Soc.*, 1979, **101**, 3035-3042.
19. M. R. Dennis and S. Woodward, *J. Chem. Soc., Perkin Trans. 1*, 1998, 1081-1085.
20. T. R. Wu, L. Shen and J. M. Chong, *Org. Lett.*, 2004, **6**, 2701-2704.
21. T. Harada and K. Kanda, *Org. Lett.*, 2006, **8**, 3817-3819.
22. T. Oishi, M. Hirama, L. R. Sita and S. Masamune, *Synthesis-Stuttgart*, 1991, 789-792.
23. H. Rapoport and N. Castagnoli, *J. Am. Chem. Soc.*, 1962, **84**, 2178-2181.
24. T. Dohi, K. Morimoto, A. Maruyama and Y. Kita, *Org. Lett.*, 2006, **8**, 2007-2010.
25. S. V. Chankeshwara and A. K. Chakraborti, *Org. Lett.*, 2006, **8**, 3259-3262.

26. R. K. Dieter, S. J. Li and N. Y. Chen, *J. Org. Chem.*, 2004, **69**, 2867-2870.
27. H. Kotsuki, H. Kuzume, T. Gohda, M. Fukuhara, M. Ochi, T. Oishi, M. Hirama and M. Shiro, *Tetrahedron: Asymmetry*, 1995, **6**, 2227-2236.
28. I. A. Rivero, S. Heredia and A. Ochoa, *Synth. Commun.*, 2001, **31**, 2169 - 2175.
29. A. Meinzer, A. Breckel, B. A. Thaher, N. Manicone and H.-H. Otto, *Helv. Chim. Acta*, 2004, **87**, 90-105.
30. E. A. A. Wallen, J. A. M. Christiaans, S. M. Saario, M. M. Forsberg, J. I. Venalainen, H. M. Paso, P. T. Mannisto and J. Gynther, *Biorg. Med. Chem.*, 2002, **10**, 2199-2206.
31. M. Cernerud, H. Adolfsson and C. Moberg, *Tetrahedron: Asymmetry*, 1997, **8**, 2655-2662.
32. G. Stones, R. Tripoli, C. L. McDavid, K. Roux-Duplatre, A. R. Kennedy, D. C. Sherrington and C. L. Gibson, *Org. Biomol. Chem.*, 2008, **6**, 374-384.
33. R. Herges, A. Dikmans, U. Jana, F. Kohler, P. G. Jones, I. Dix, T. Frike and B. Konig, *Eur. J. Org. Chem.*, 2002, 3004-3014.
34. K. Kawamura, H. Fukuzawa and M. Hayashi, *Org. Lett.*, 2008, **10**, 3509-3512.
35. W. Ye, D. Leow, S. L. M. Goh, C.-T. Tan, C.-H. Chian and C.-H. Tan, *Tetrahedron Lett.*, 2006, **47**, 1007-1010.
36. A. Winkel and R. Wilhelm, *Tetrahedron: Asymmetry*, 2009, **20**, 2344-2350.
37. R. H. Herpel, P. Vedantham, D. L. Flynn and P. R. Hanson, *Tetrahedron Lett.*, 2006, **47**, 6429-6432.
38. C.-T. Chen, J.-H. Kuo, V. D. Pawar, Y. S. Munot, S.-S. Weng, C.-H. Ku and C.-Y. Liu, *J. Org. Chem.*, 2005, **70**, 1188-1197.
39. K.-Y. Lee, Y.-H. Kim, M.-S. Park, C.-Y. Oh and W.-H. Ham, *J. Org. Chem.*, 1999, **64**, 9450-9458.
40. A. Lewanowicz, J. Lipinski, R. Siedlecka, J. Skarzewski and F. Baert, *Tetrahedron*, 1998, **54**, 6571-6586.
41. M. Largeron and M.-B. Fleury, *Org. Lett.*, 2009, **11**, 883-886.
42. D. Ok, M. H. Fisher, M. J. Wyvratt and P. T. Meinke, *Tetrahedron Lett.*, 1999, **40**, 3831-3834.
43. P. Garner and H. Ü. Kaniskan, *Tetrahedron Lett.*, 2005, **46**, 5181-5185.
44. Y. Turgut, E. Sahin, M. Togrul and H. Hosgören, *Tetrahedron: Asymmetry*, 2004, **15**, 1583-1588.
45. J. Christoffers and A. Mann, *Angew. Chem. Int. Ed.*, 2000, **39**, 2752-2754.
46. K. S. Ravikumar and S. Chandrasekaran, *J. Org. Chem.*, 1996, **61**, 826-830.

47. J. N. Hernandez, M. A. Ramirez and V. S. Martin, *J. Org.Chem.*, 2002, **68**, 743-746.
48. J. J. Posakony, J. R. Grierson and T. J. Tewson, *J. Org. Chem.*, 2002, **67**, 5164-5169.
49. S. J. Kim, H. B. Park, J. S. Lee, N. H. Jo, K. H. Yoo, D. Baek, B.-w. Kang, J.-H. Cho and C.-H. Oh, *Eur. J. Med. Chem.*, 2007, **42**, 1176-1183.
50. H. N. Nguyen and Z. J. Wang, *Tetrahedron Lett.*, 2007, **48**, 7460-7463.
51. A. J. Williams, S. Chakthong, D. Gray, R. M. Lawrence and T. Gallagher, *Org. Lett.*, 2003, **5**, 811-814.
52. D. Alker, K. J. Doyle, L. M. Harwood and A. Mcgregor, *Tetrahedron: Asymmetry*, 1990, **1**, 877-880.
53. J. E. Baldwin, A. C. Spivey and C. J. Schofield, *Tetrahedron: Asymmetry*, 1990, **1**, 877-880.
54. M. Kaik and J. Gawronski, *Tetrahedron: Asymmetry*, 2003, **14**, 1559-1563.
55. J. Christoffers, Y. Schulze and J. Pickardt, *Tetrahedron*, 2001, **57**, 1765-1769.
56. A. Murphy, A. Pace and T. D. P. Stack, *Org. Lett.*, 2004, **6**, 3119-3122.
57. H.-J. Cristau, P. P. Cellier, S. Hamada, J.-F. Spindler and M. Taillefer, *Org. Lett.*, 2004, **6**, 913-916.
58. W. Park, M. H. Shin, J. H. Chung, J. Park, M. S. Lah and D. Lim, *Tetrahedron Lett.*, 2006, **47**, 8841-8845.
59. M. M. Hammoud, J. J. McKamie, M. J. Heeg and J. J. Kodanko, *Dalton Trans.*, 2008, 4843-4845.
60. C. Betschart and D. Seebach, *Helv. Chim. Acta*, 1987, **70**, 2215-2231.
61. Y. L. Bennani and S. Hanessian, *Chem. Rev.*, 1997, **97**, 3161-3195.
62. Y. L. Bennani and S. Hanessian, *Tetrahedron*, 1996, **52**, 13837-13866.